# Development of novel mouse models to study the p53 tumour suppressor

Thesis presented in accordance with the University of Liverpool for the degree of Doctor in Philosophy (Ph.D.)

By

Kerryanne Crawford

September 2011

I wish to dedicate this thesis to the three father figures in my life,

Dad, Norman & Andy:

Ian David Crawford, Norman Roy Greer and Andrew Christopher Hargreaves,

*So what would you think of me now?*

*So lucky, so strong, so proud?*

*I never said thank you for that,*

*Now I'll never have a chance.*

*May angels lead you in.*

*Hear you me my friends.*

*On sleepless roads the sleepless go,*

*May angels lead you in.*

*"Hear you me." Lyrics by Jimmy Eat World.*

# Abstract

*TP53* is the most commonly mutated gene in all human cancers [Vogelstein, 1990] and co-ordinates many of the cellular responses to DNA damage. It is vitally important therefore that we gain a better understanding of the function and regulation of p53. Since a major consequence of p53 mutation is cancer, a disease of complex multicellular organisms, the best system to study the real complexities of p53 function and regulation is *in vivo*. Accordingly we have proposed to use gene targeting in ES cells to create genetically altered strains of mice to enable a range of studies of p53 regulation and function. Given the importance of p53 in human disease processes, it is perhaps surprising that there have been relatively few p53 reporter mouse strains described. Heretofore few p53 reporter mouse strains have been described and these have been based upon un-targeted, often artificial, repeated p53 response elements in constructs that integrate at random [Komarova et al., 1997, Gottlieb et al., 1997, Vasey et al., 2008, Briat and Vassaux, 2008]. Such random integration is known to be associated with loss of fidelity resulting from positional effects and thus it is unlikely that any of these provide authentic reporting of p53 activity. The ideal solution might be to target a p53 responsive gene using a knock-in approach, preferably in a gene that was exclusively activated by p53, eliciting a specific response program (cell cycle arrest/senescence/apoptosis) and which also does not display any haploinsufficiency. This project was based on such a strategy.

In order to study p53 activation and consequence(s) in the gastrointestinal tract we aim to generate novel transgenic mice which would contain fluorescent reporters in the downstream target genes of p53 activation in both of p53s main responses to DNA damage (apoptosis and cell cycle arrest). The resulting dual apoptosis/cell cycle arrest p53-reporter mice would allow a unique opportunity to visualise not only that p53 was activated but what responses p53 had induced. Furthermore, as visual technology advances these mice, or second generation mice with newer fluorescent proteins with improved bioimaging properties (such as increased tissue penetration and brightness), could also be used in real-time analyses of p53 responses to DNA damage or other stimuli, as well as for long term monitoring of gene-regulation during cancer development.

In addition, we aim to address fundamental questions regarding the regulation of p53 again using such gene targeting technology for *in vivo* studies. Importantly it is not yet known whether the

p53-mediated up-regulation of its essential negative regulator *Mdm2* is absolutely required for viability. Therefore we intend to make two transgenic mouse strains which lack either the *Mdm2* P1 (constitutive) promoter or the p53 RE sites within the *Mdm2* P2 (inducible) promoter. Studies of these mice are likely to have a profound impact on the field of cancer biology and normal development.

# Acknowledgements

I would like to express my utmost gratitude to my supervisors Dr. Nikolina Vlatković and Dr. Mark Boyd, for giving me the fantastic opportunity to work in their research group for the last four years. Without your support and encouragement this thesis would not have been possible. I would also like to thank Prof. Alastair Watson, for enlightening me in the ways of the gastrointestinal tract in the early days of this project. A big thanks to all the past and present members of the Boyd lab and the GI group for your support, friendship and willingness to help, including my Ph.D. comrade – sister in arms – (newly Dr.) Anna Behrendt, Dr. Carlos Rubbi and Dr. Carrie Duckworth. I would also like to express my appreciation to all those who have helped me on my scientific journey including, Dr. Antonius (Toni) Plagge (for much cloning advice and yeast), Dr. Bryony Lloyd (for stats and QRTPCR analysis) and for the Beatson Institute experience – Dr. Owen Sansom, Dr. Alicia Cole and Dr. Dimitris Athineos. I am extremely grateful to *Cancer Research UK* for full financial support of my studies, without which I would simply have been unable to perform any of this research. An extra special thanks to my dear friend Dr. Maria Maguire – it would be impossible to express just how much you've helped me these last few years, scientifically, professionally and personally – so a simple thank you will have to suffice! And to my lovely housemates Kelly Smith, Kristine Dahl and Sabrina Ramsey – for providing me with comedy banter, nacho tables and importantly, a healthy balance between research and life – I am honoured that you let me share this experience with you! And last, but by no means least – to my Mum and L'il Brother Kyle – for your unwavering belief in me love and support – without you, I honestly don't think I would ever have got so far – I say Thankee!

# Declaration of originality

This thesis is a result of my own work performed during the course of my studies in the Division of Surgery and Oncology, University of Liverpool, between October 2007 and September 2011. The material contained in this thesis has not been presented, nor is currently being presented, either wholly or in part for any degree or qualification. All work described was performed by me except where clearly indicated. The thesis was written wholly by me under guidance of my supervisors Dr. N. Vlatković and Dr. M. Boyd.

K. Crawford

September 2011

# Contents

# List of tables

# List of figures

# List of abbreviations

| | |
|---|---|
| 5'RACE | 5' rapid amplification of cDNA ends |
| 5'UTR | 5' un-translated region |
| AD | activation domain(s) |
| Apaf-1 | apoptotic protease activating factor |
| APC | adenomatous polyposis coli |
| ARF | alternative reading frame |
| ASPP | apoptosis stimulating protein of p53 |
| ATM | ataxia telangiectasia mutated |
| ATR | ATM-rad3-related |
| BAC | bacterial artificial chromosomes |
| Bax | Bcl-2-associated X protein |
| Bcl-2 | B-cell leukemia/lymphoma 2 |
| BH | Bcl-2 like homology region |
| Bid | BH3 interacting death agonist |
| BLAST | basic local alignment search tool |
| BNF | β-naphthoflavone |
| CARD | caspase recruitment domains |
| CBC | crypt base columnar |
| CDIP | cell death involved p53-target |
| Cdk | cyclin-dependent kinase |
| CDKN1a (p21) | cyclin-dependent kinase inhibitor 1a |
| d.*p.c* | days post coitum |
| DAB | 3,3'-Diaminobenzidine |
| DCC | deleted in colon cancer |
| DICD | detachment induced cell death |
| DISC | death-inducing-signalling-complex |
| DMEM | dulbecco's modified eagle medium |

| | |
|---|---|
| DNA-PK | DNA-dependent protein kinase |
| Dox | Doxorubicin (a drug) |
| ES | embryonic stem (cells) |
| FADD | fas-associated death domain protein |
| FAP | familial adenomatous polyposis |
| GADD45 | growth arrest and DNA damage-inducible protein 45 |
| GI | gastrointestinal (tract) |
| GSK-3 | glycogen synthase kinase 3 |
| Gy | gray (unit of irradiation) |
| HIF | hypoxic-inducible factor |
| HRP | horseradish peroxidise |
| IARC | international agency for research on cancer |
| IGTC | international gene-trap consortium |
| IHC | Immunohistochemistry |
| IMS | inter-membrane space |
| Lgr5 | leucine-rich-repeat-containing G-protein-coupled receptor 5 |
| LOH | loss of heterozygosity |
| Mdm2 | transformed mouse 3T3 cell double minute 2 |
| Mdm4/Mdmx | transformed mouse 3T3 cell double minute 4 |
| MEFs | mouse embryonic fibroblasts |
| MMRRC | mutant mouse regional resource centre |
| MOM | mitochondrial outer membrane |
| MOMP | mitochondrial outer membrane permeabilization |
| NES | nuclear exclusion signal |
| NK | Natural killer (cells) |
| NLS | nuclear localisation signal |
| NoLS | nucleolar localisation signal |
| p53-RE(s) | p53 responsive element(s) |
| PCR | polymerase chain reaction |

| | |
|---|---|
| PI3-K | phosphoinositide 3-kinases |
| PTEN | phosphatase and tensin homolog deleted from chromosome 10 |
| Puma | p53 upregulated modulator of apoptosis |
| Rb | Retinoblastoma |
| ROS | reactive oxygen species |
| RS | replicative senescence |
| RT | room temperature |
| SIGTR | sanger institute gene trap resource |
| SIS | stress induced senescence |
| tBid | truncated Bid |
| TNF-R | tumour necrosis factor receptor |
| TNF-β | transforming growth factor β |
| TRAIL | TNF-related apoptosis inducing ligand |
| TSG | tumour suppressor gene(s) |
| β-gal | β-galactosidase |
| HAUSP | Herpesvirus-associated ubiquitin-specific protease |
| TFBS | Transcription factor binding sites |
| F-MuLV | Friend Murine Leukemia Virus |
| IFN | Interferon |
| IRF8 | IFN regulatory factor 8 |
| DSB | DNA double strand breaks |
| IECS | IRF/Ets composite site |
| GC | germinal centre (B cells) |
| AP | activator protein family |
| Est | E26 transformation-specific transcription factor family |
| uORFs | upstream open reading frames |
| CVA | Crypt-villus-axis |
| TUNEL | terminal deoxynucleotidyl transferase dUTP-mediated nick end labelling |
| TK | Thymidine kinase |

| | |
|---|---|
| ESQ | ES cell grade quality |
| MCS | Multiple cloning site |
| Neo | Neomycin phosphotransferase |
| Poly A | Poly adenylation signal |
| tACE | Testis specific angiotensin-converting enzyme |
| gDNA | Genomic DNA |
| Luc | Luciferase |
| WT | Wild-type |
| Tg | Trans-gene |
| GTG | Genetic technology grade |
| RA | Recombinogenic arms |

# 1 Introduction

## 1.1 Introduction to p53

The *TP53* tumour suppressor gene is a critical part of the damage control pathways that prevent the development of cancer. The importance of p53 is highlighted by the fact that *TP53* has the greatest number of cancer-associated mutations of any known gene and is mutated directly in approximately half of all human cancers [Vogelstein, 1990, Hollstein et al., 1991]. Furthermore, in many cancers that retain wild-type *p53*, *p53* is inactivated indirectly by up-regulation of genes (such as MDM2 – see Section 1.4.1) whose products play a part in p53 regulation [Vogelstein et al., 2000, Lane, 1992, Oliner et al., 1992].

Of the known p53 mutations 27,580 are somatic mutations and 597 are germline mutations (IARC TP53 DATABASE, publicly available at http://www-p53.iarc.fr/) and see [Petitjean et al., 2007]. Mutations in *p53* have an unusual bias towards missense mutations (amino acid substitutions) totalling >73% of all *p53* mutations. This differs when compared with other tumour suppressor genes such as *Rb* and *APC*; in which the most frequent types of mutations are deletions, insertions and nonsense mutations [Hussain and Harris, 2006, Vousden and Lu, 2002]. The missense mutations in *p53* might lead to a gain of function mutant p53 protein being produced which switches the tumour suppressor effect of p53 to oncogenic [Lane and Benchimol, 1990, Hussain and Harris, 2006]. Some examples of an oncogenic gain of function in p53 are the p53His175 and p53Gly281 mutants which attenuate p53's transcriptional activation of p73 (another tumour suppressor gene) [Strano et al., 2000].

*p53* is highly conserved between a variety of species which allows easy extrapolation of data gathered from animals. Further, many of the mutations of the p53 protein are in residues that are also highly conserved between diverse species [Hollstein et al., 1991]. In fact 28% of mutations affect only six residues [Vousden and Lu, 2002], all of which occur in the sequence specific DNA binding domain and thus prevent p53 from acting as a transcriptional activator in the wild-type manner (see Figure 1.1.1). Mutants in p53 are thought to further hinder wild-type p53 by behaving in a dominant-negative manner when the functional tetramer of p53 is formed [de Vries et al., 2002, Petitjean et al., 2007]. However many tumours that harbour point mutations in p53 also show loss of heterozygosity (LOH) (common in other tumour suppressor genes such as *Rb*) where the wild-type allele is

completely deleted, implying that the dominant-negative effect is incomplete and further mutations are required for the tumour to progress [Vousden and Lu, 2002].

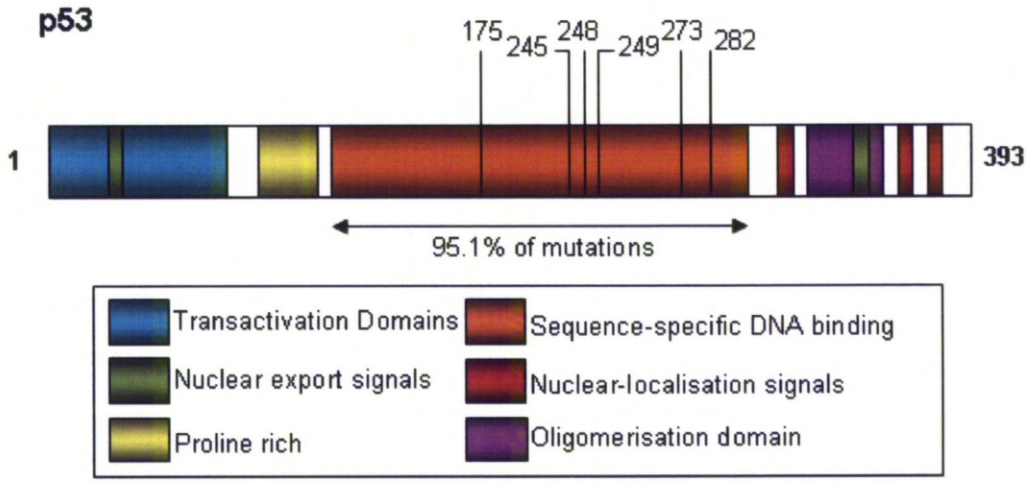


***Figure 1.1.1: p53 structure and location of tumour-associated mutations.***

*Taken from [Vousden and Lu, 2002]. Almost all point mutations in p53 occur in the sequence-specific DNA binding domain (shown in orange) and 28% of these mutations occur in the 6 highlighted residues. The transactivation domain (blue) has two activation domains, AD1 residues 1-42, and AD2 residues 43-63 [Zhu et al., 2000].*

Since it was first described in 1979 [Linzer and Levine, 1979, Lane and Crawford, 1979] p53 has been widely investigated with almost 60,000 papers published to date, however despite considerable advances in knowledge there are still gaps in this competitive field of cancer research. This project proposes to investigate novel areas of p53 regulation, activation, function and consequences with particular reference to the intestinal gut epithelium and to generate novel tools with which to do this. Therefore, the normal intestinal epithelium will be introduced next.

## 1.2 The normal intestine

### 1.2.1 Structure – crypt architecture

The epithelia of the small intestine are arranged into multiple deep folds inside the gut wall with finger like protrusions penetrating the gut lumen. These invaginations are called crypts and the protrusions are called villi and several crypts provide cells for one villus. Unlike the small intestine, only crypts are present in the colon [Yen and Wright, 2006] (see Figure 1.2.1 & Figure 1.2.2). These differences reflect the roles of the small and large intestine; the villi provide a large surface area suitable for secretion of enzymes that aid digestion and for absorption of nutrients, while the large intestine is the last part of the digestive system and acts to store solid waste and absorb the remaining water (discussed briefly in [Nicholl et al., 1985] and [Sarna and Otterson, 1989]). Cells migrate from the crypt base to the villus tip where they are shed into the gut lumen and die due to detachment-induced-apoptosis (also called anoikis). This process takes 2-3 days to complete in the mouse and is the source of one of the most rapid turnover rates in mammalian tissues [Tsubouchi, 1983, Watson and Pritchard, 2000, Brittan and Wright, 2004].

Epithelial stem cells (located at the base of the crypts) are pluripotent and can continually divide to provide new cells to re-populate the gut surface [Marshman et al., 2002, van der Flier and Clevers, 2009] (see Figure 1.2.1 & 1.2.2). Daughter cells migrate up towards the luminal surface and undergo further divisions and differentiate into specialised cell types such as absorptive enterocytes, goblet cells and enteroendocrine cells [Marshman et al., 2002, Stamataki et al., 2011]. Enterocytes are simple columnar cells that represent the majority of cells in the intestinal lining; they have a glycocalyx surface coat and microvilli on their apical edge which increases the surface area [Marsh et al., 1971]. The main role of enterocytes is to help digestion and to absorb nutrients from the gut lumen. Goblet cells secrete mucus, a viscous material which protects the gut lining from mechanical damage, while enteroendocrine cells are very rare and secrete hormones [Sancho et al., 2004, Stamataki et al., 2011]. A fourth type of cell lineage in the small intestine, the paneth cells are

located among the stem cells and contribute to innate immunity by secreting antimicrobial peptides when exposed to bacteria [Ayabe et al., 2004].

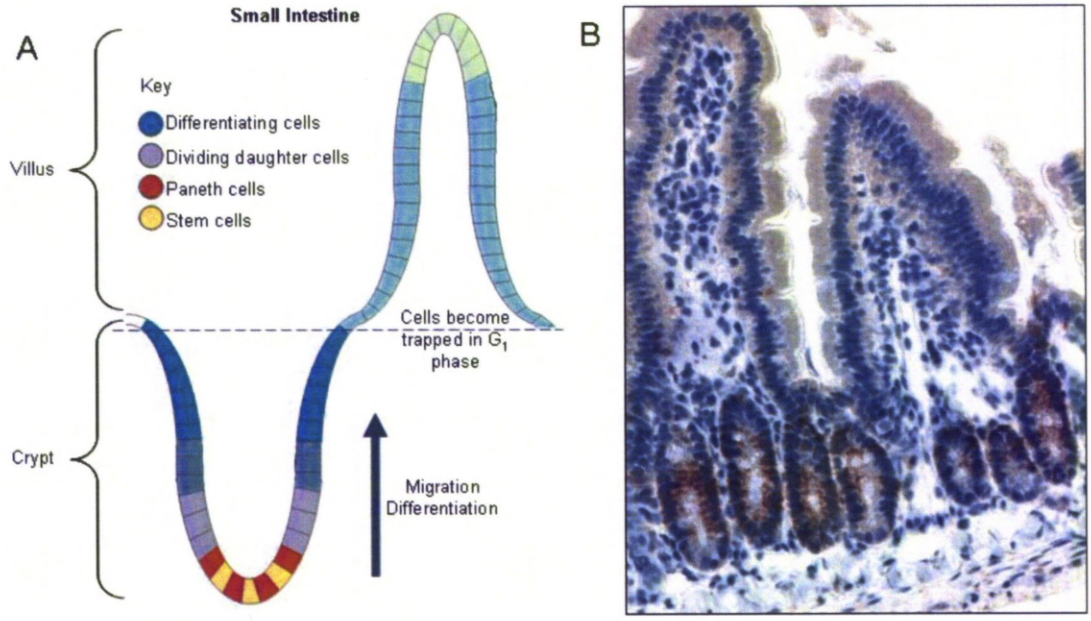


***Figure 1.2.1: The small intestine.***

*A) Schematic diagram of the small intestine illustrating the position of the stem cells amongst the paneth cells. Stem cells are thought to divide asymmetrically providing one replacement stem cell and one daughter cell to go on dividing and differentiating to populate the gut surface, with all the different cell types. B) Photo of mouse small intestine (x40 objective) to complement the schematic. Villi and crypts may appear differently, depending on how the tissue was cut.*

The well defined characteristics of this highly organised tissue make the gut an attractive model system to study. The position of a cell within a crypt (or villus) indicates its age, its proliferative capabilities and its lineage [Potten and Ellis, 2006]. Until very recently it was speculated that the stem cells were located towards the base of the crypts in cell positions 4-6 or 1-2 (small intestine and colon respectively – see Figure 1.2.1 & Figure 1.2.2) [Potten et al., 1997a]. However the position of these stem cells had been determined from indirect experimental evidence as there were no direct biochemical or molecular markers to accurately identify the position of the stem cells [Potten et al., 1997a, Watson and Pritchard,

2000]. In the search for this elusive *"stemness"* marker, Barker *et al.* hypothesised that since the Wnt signalling pathway played such an important role in both physiological and pathophysiological proliferation of the intestine, it could be reasoned that out of the 80 or so genes involved in this pathway a small subset might be solely expressed in the stem cells [Barker and Clevers, 2007]. Indeed, one of these, *Lgr5* (leucine-rich-repeat-containing G-protein-coupled receptor 5) was subsequently identified and shown to be expressed only in the crypt base columnar (CBC) cells of the small intestine and at the base of the colonic crypts [Barker et al., 2007]. Barker *et al.* then developed an elegant transgenic mouse system to determine whether the $Lgr5^+$ expressing cells could be self-renewing, long lasting and produce all the different cell types in the intestinal epithelium – three of the criteria for *"stemness"*. To demonstrate this, the mice generated had a Tamoxifen inducible *Cre* located in the *Lgr5* locus, and a *Rosa26-LacZ* with a stop sequence (between *loxP* sites) which prevented ubiquitous expression of *LacZ* in the absence of Cre recombinase [Soriano, 1999]. Upon administration of Tamoxifen, only Lgr5 expressing cells would produce *Cre* recombinase which would then excise the stop sequence and permanently switch on *LacZ* expression in those cells. LacZ expression allowed Barker *et al.* to perform lineage analysis which demonstrated that the $Lgr5^+$ cells were pluripotent and capable of self-renewal. The $Lgr5^+$ cells were also very long lasting, the pattern at 60 days post Tamoxifen treatment was the same as 5 days post treatment, illustrating that they were labelling genuine stem cells [Barker et al., 2008]. Similar genetic and phenotypic analysis was performed for another potential "*stemness*" marker gene, *Bmi1*, which demonstrated it to be another *bone fide* stem cell marker [Sangiorgi and Capecchi, 2008]. The Bmi1 positive cells were located underneath the traditional stem cell position, but above the *Lgr5* expressing cells indicating that there may be more than one pool of adult stem cells within the small intestine [Freeman, 2008]. These two sub-populations of intestinal stem cells may compensate for each other following exposure to genotoxic stress or other damage, allowing a mechanism for the intestine to replenish its stem cell population and recover from injury [Tian et al., 2011].

While morphologically similar there are major differences between the small and large intestine with respect to their ability to develop tumour. Cancers of the small intestine are rare, accounting for less than 5% of all gastrointestinal tumours [Haselkorn et al., 2005]. The

dramatic increase in colorectal cancer over small bowel tumours cannot be simply explained by size differences between the two organs since, the small intestine is much longer than the large intestine and has a larger absorptive area and yet the incidence of colorectal cancer is still higher than the incidence of the small bowel cancer. This may suggest that the cells in the colon are more prone to tumourigenesis and therefore it would be of importance to consider the difference(s) in p53 activity between the small and large bowel to examine whether this could account for the differences in tumour susceptibility.

Since we aim to generate transgenic reporter mice, henceforward the information in this report is directly relevant to the mouse gut, although due to the highly conserved nature of the p53 response it is possible to extrapolate data through to human responses.

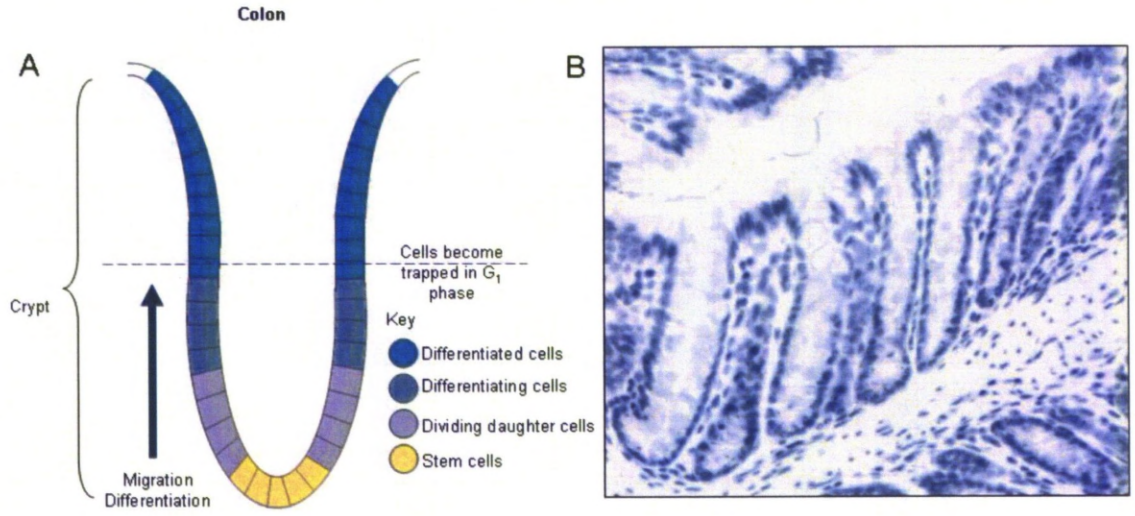


***Figure 1.2.2: The colon***

*A) Schematic representation of a colonic crypt, stem cells are shown in yellow at the base of the crypt. B) Photo of colon (x40 objective) to complement diagram. In the colon there are no villi, instead the crypts flatten off forming the crypt table, where cells will undergo anoikis.*

## 1.2.2 Development of the mouse gut

It takes about 18-21 days (varies depending on mouse strain) for a fertilised mouse egg to complete embryogenesis and become a viable neonate. During this time the egg must

divide, implant, undertake and complete gastrulation, neurolation, organogenesis and limb formation if it is to be successful in its bid to survive. One prominent developmental biologist, Lewis Wolpert, is commonly quoted as saying *'The most important event in your life is not birth, marriage, or death, but gastrulation'* [Wolpert, 1991]. Gastrulation is a particularly important stage of embryogenesis, because it dramatically alters the morphology of the embryo and creates all three germ layers of the embryo: ectoderm, mesoderm and endoderm, producing the first mesodermal cells (cells that will go on to induce and maintain neuronal development) [Tam and Beddington, 1987].

The main reference source of information for this section of the report is from a book by Kaufman and Bard [Kaufman and Bard, 1999]. Gut development begins at 6.5 d.*p.c.* (days *post coitum*) when the differentiating egg cylinder orientates itself, showing evidence of an embryonic axis as the primitive streak forms. Gastrulation continues as the primitive streak bulges and forms the amniotic bud (7 d.*p.c.*) and as the neural plate enlarges and forms head folds (7.5 d.*p.c.*). At this stage the foregut pocket begins to form and is clearly visible by 8 d.*p.c.* The hind-gut undergoes little development as the rest of the embryo takes shape. Later in embryogenesis (15 d.*p.c.*) the first evidence of villi and intestinal glands appear, however there is still little differentiation in the rectum. Cell proliferation is limited to the base of the invaginations that form during this stage [Sancho et al., 2004]. At 16 d.*p.c.* there is a large number of well formed villi and the mucosa begins to differentiate and there is early evidence of intestinal glands forming within the sub-mucosa. The small intestine also massively increases in size, so that by 17 d.*p.c.* there are gross changes in histological appearance although the hind-gut remains virtually unchanged. At 18 d.*p.c.* the mouse embryo is almost fully formed, long whiskers are visible and the morphology of the gut has become more reminiscent of an adult. The mucosal lining has differentiated; large numbers of goblet cells (filled with a homogenous eosinophilic material) have developed in the large intestine and the hind-gut. The duodenum has filiform projections (villi) which will develop more during postnatal development. By the time a mouse is born, all the basic tissue structure and cell types are present in the gastrointestinal tract, however the gut still must acquire post-natal immunity to its new environment (mucosal lining becomes populated with a

T-cell pool [Williams et al., 2006]) and continue to grow in order to digest adult food post-weaning.

In the first few weeks following birth the invaginations in the small intestine which contain the proliferative cells deepen into mature crypts, while the crypts in the colon deepen further [Sancho et al., 2004]. The crypts increase steadily in number as the gut develops into its final structure (see Figure 1.2.3).

The expression of p53 in the intestine during mouse embryogenesis has been previously examined by *in situ* hybridisation. Strong labelling of all cells in the stratified epithelium was detected at 14.5 d.*p.c* (before formation of villi), while by 16 d.*p.c.* the labelling was concentrated within the crypt (villi were formed). The cells of the submucosa had only low levels of p53 mRNA [Schmid et al., 1991]. The authors noted that while p53 is strongly expressed in all tissues early in embryogenesis, once organogenesis commences, varied tissue-specific p53 expression patterns can be observed. In general, in cells undergoing terminal differentiation (for example, those cells forming the villi), p53 mRNA expression declined [Schmid et al., 1991]. Could the absence of p53 expression along the length of the villi account for the differences observed between the crypt and the villus in response to whole body γ-radiation and other genotoxic stresses (as discussed in Section 1.2.6)?

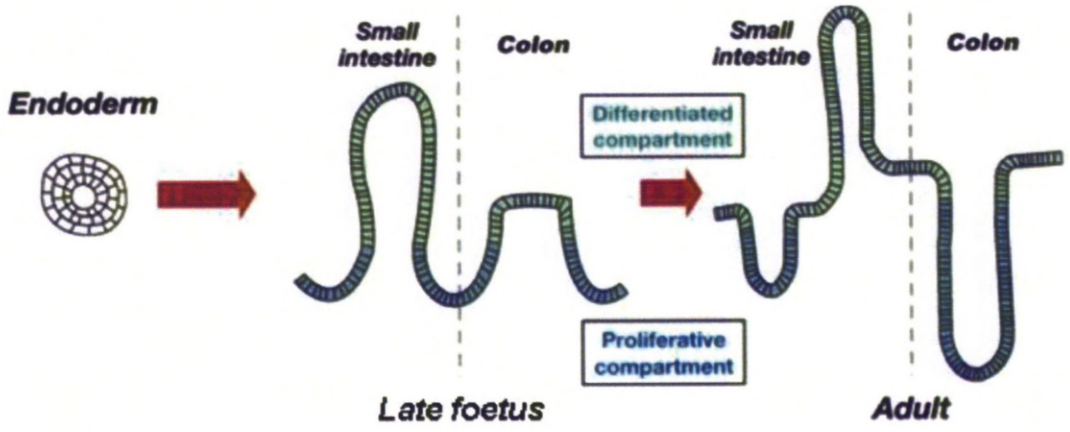


***Figure 1.2.3*: *Postnatal development of the gut*.**

*Taken from [Sancho et al., 2004] illustrating the progression into the final structure of the adult gut tissue, following invagination of the crypts and elongation of the villi.*

### 1.2.3 Cell cycle progression – in the intestine

Cell proliferation in the adult mouse (and human) is limited to within the intestinal crypts [Potten, 1998, Strater et al., 1995]. The stem cells were traditionally thought to divide asymmetrically, providing one replacement stem cell and one daughter cell to migrate up the crypt and differentiate, thus maintaining cell numbers [Marshman et al., 2002]. However, it has been demonstrated recently that this is not the case. In fact, most stem cell divisions are symmetrical and thus stem cell fate is not pre-determined [Snippert et al., 2010]. Also, the segregation of chromosomes in stem cells appears to be random [Escobar et al., 2011], adding weight to the theory of a dynamic stem cell niche whereby *"stemness"* is restricted to the cells at the base of the crypt and cell fate is arbitrarily assigned depending on the cell position [Simons and Clevers, 2011]. Therefore the stem cells within the intestinal crypts are intrinsically a clonal population which overtime results in the extinction of all cell lines except one (also know as clonal succession or neutral drift) [Kim and Shibata, 2002, Snippert et al., 2010]. This may have implications for cancer biology as clonal succession is usually a cancerous trait and therefore perhaps it allows an opportunity for *"silent"* mutations to accumulate.

Cell cycle progression does not occur outside the crypt. When migrating cells enter the villus they become trapped in the $G_1$ phase of the cell cycle because of down regulation of the growth promoters cyclin D1 and cyclin-dependent kinase 2 (Cdk2) [Chandrasekaran et al., 1996, Watson and Pritchard, 2000]. The cells remain in $G_1$ phase until they reach the tips of the villus and are then shed into the gut lumen. Proliferation never occurs in the normal villus, it is strictly confined to the crypt where it is carefully controlled and monitored for genetic mutations.

### 1.2.4 Apoptosis – unstressed intestine

Apoptosis is limited to within the crypt and villus tip. Very low levels of apoptosis occur normally in the proliferative region of the small intestine and apoptosis occurs even less frequently in the upper region of the colonic crypt (the intercrypt table – not associated with stem cells) [Potten, 1998, Merritt et al., 1994, Potten et al., 1997b]. This apoptosis, in

apparently normal tissue, is referred to as *"spontaneous"* since the identity of the true stimulus (if any) is unknown. Spontaneous apoptosis rates do not differ between wild-type and p53 null animals [Merritt et al., 1994, Potten et al., 1994], suggesting that the process is p53 independent.

The absence of spontaneous apoptosis in colonic stem cells has been investigated by generating *Bcl-2* null mice. *Bcl-2*$^{-/-}$ mice have similar levels of apoptosis inside the small intestine when compared to their wild-type counterparts, but greatly increased apoptosis in the large intestine [Merritt et al., 1995]. Furthermore, the increase in apoptosis was observed in the stem cell region of the colonic crypt (cell positions 0-2). Bcl-2 is an anti-apoptotic protein, which is conserved between diverse species (*C. elegans* homolog ced-9) and acts by interaction with other Bcl-2 family members such as pro-apoptotic Bax and Bak [Danial and Korsmeyer, 2004]. Indeed *Bak*$^{-/-}$ mice have reduced amounts of spontaneous apoptosis in the colonic intercrypt table and increased crypt cell number and levels of mitosis compared with the wild-type (deletion of *Bak* had no affect in the small intestine) [Duckworth and Pritchard, 2009]. However, *Bax*$^{-/-}$ mice show similar levels of apoptosis as wild-type mice in the crypt, indicating that *Bax* is not important in normal colonic epithelial homeostasis, whereas *Bcl-2* and *Bak* expression are ([Watson and Pritchard, 2000, Duckworth and Pritchard, 2009] and as discussed in detail in Section 1.4.5).

One theory attempting to explain the relatively high expression of Bcl-2 in the colonic crypts, but not in the small intestinal crypts, suggests that this favours repair of DNA damage in the event of a mutation rather than pushing cells to commit suicide. This cell survival strategy (instead of implementing apoptosis) may have evolved because the large bowel is exposed to more genotoxic molecules than the small bowel (due to a longer transit time) and thus it may be impractical (and risky since cell division can also induce mutations) to keep replacing damaged or mutated cells [Potten et al., 2002]. If colonic stem cells are allowed to accumulate genetic defects (by failed repair of DNA damage) then this provides one explanation for the increase in tumour malignancies in the colon.

The second kind of apoptosis seen in the unstressed gut is at the villus tip where terminally differentiated cells are shed into the lumen. This process is also called anoikis or detachment induced cell death DICD. Cells only appear morphologically apoptotic once they

have lost cell anchorage [Shibahara et al., 1995], however apoptosis is initiated once cells reach the luminal surface by activation of the *"executioners of apoptosis"* notably caspase-3 [Grossmann et al., 2002]. This priming of cells to apoptose may be due to a decrease in pro-survival proteins like Bcl-2 and an increase in pro-apoptotic Bcl-2 family members like Bax and Bak. Though studies where Bcl-2 was over expressed in villus epithelial cells indicated that there did not appear to be an effect on cell shedding [Watson and Pritchard, 2000, Coopersmith et al., 1999]. Other pro-apoptotic signals such as transforming growth factor β (TNF-β) are expressed and are known to induce apoptosis and detachment [Grossmann et al., 2002, Potten et al., 1997b]. Shedding appears to be p53 independent as it is a normal part of gastrointestinal homeostasis and is presumably unaltered in p53 null mice.

Apoptosis never occurs along the length of the villus in the normal unstressed intestine [Watson and Pritchard, 2000, Grossmann et al., 2002]. Cell death along the villus is associated with disease. Expression of a dominant negative N-cadherin (an adhesion molecule) along the entire crypt-villus axis causes spontaneous apoptosis along the length of the villus resulting in a Crohn's like inflammatory disease [Hermiston and Gordon, 1995]. Death is caused by anoikis from the loss of adhesion molecules [Hermiston and Gordon, 1995, Grossmann, 2002] indicating cells in the villi do contain the apoptotic machinery and are able to implement it. This does not tell us, however, if it is p53 dependent.

### 1.2.5 Stress induced apoptosis in the intestine

Apoptosis in response to stress (such as DNA damage) is limited to within the crypt. Shedding at the villus tip seems to be unaffected and there is no cell death along the villus length [Marshman et al., 2001, Watson and Pritchard, 2000].

Genotoxic damage induced by ionising radiation can result in massive cell death (even at relatively low doses of irradiation) in the small intestinal crypts and an attenuated apoptotic response in the colonic crypts [Merritt et al., 1994]. The acute apoptotic response (in the first few hours) was shown to be exclusively dependent on *p53*, since *p53* null mice had this response completely abrogated [Merritt et al., 1994]. However, deletion of *p53* actually sensitises cells to the later responses to γ-radiation, which occurred because of

catastrophic errors in mitosis 24 hours after exposure to higher doses of irradiation (>8 Gy) [Merritt et al., 1997, Kirsch et al., 2010].

A lower level of apoptosis in the colonic crypts may be due to the pro-survival actions of the anti-apoptotic protein Bcl-2. Bcl-2 was expressed in the stem cells of the colonic crypt (cell positions 0-2) but was absent from the small intestine, causing the colonic cells to be more resistant to spontaneous and stress induced apoptosis [Merritt et al., 1995]. When Bcl-$2^{-/-}$ mice and wild-type mice had their apoptotic levels compared following exposure to ionising-irradiation it was found that there was similar levels of apoptosis in the small intestine, but that the Bcl-$2^{-/-}$ mice had much higher levels of apoptosis in the colonic crypts [Coopersmith et al., 1999] indicating that Bcl-2 (an anti-apoptotic protein) is having a protective effect in the colon. Forced over-expression of Bcl-2 in the small intestine can in part counteract the p53-dependent apoptotic response to DNA damage, by delaying onset of apoptosis and reducing the total amount of apoptosis two-fold [Coopersmith et al., 1999].

*Bax*, a pro-apoptotic member of the Bcl-2 family appears to have redundant roles in the p53-dependent apoptotic response to DNA damage [Watson and Pritchard, 2000]. *Bax*$^{-/-}$ mice behaved indistinguishably from wild-type mice when administered with enterotoxin 5-fluorouracil (5FU- perturbs RNA metabolism including biosynthesis of deoxyribonucloetides by thymidylate synthase) or exposed to γ-radiation [Pritchard et al., 1999]. However, whilst there were no significant differences observed between the two mouse strains following genotoxic stress, the authors noted that there may be a general trend in the *Bax*$^{-/-}$ mice to have decreased apoptosis overall. Nonetheless, the data indicate that *Bax* only plays a minor role in the regulation of DNA damage induced apoptosis in the intestinal epithelium. On the other hand deletion of *Bak*, (another pro-apoptotic member of the Bcl-2 family) significantly reduced the amount of apoptosis in the colonic (but not small intestinal) epithelia when exposed to γ-radiation which indicates a non-redundant role for *Bak* in the DNA damage response in this tissue [Duckworth and Pritchard, 2009].

The only publication to date, which has shown stress-induced cell death along the entire length of the villus was Coopersmith *et al.* in 1999 who induced apoptosis by ischemia-reperfusion [Coopersmith et al., 1999]. Briefly; mice had their superior mesenteric artery clipped to occlude blood flow for 20 minutes and then the clip was removed to allow blood to

re-enter the intestines. The resulting apoptosis was greater in the differentiated, non-proliferating villi cells then the cycling, non-differentiated crypt cells, presumably because the cells along the villi are located further away from the submucosal blood vessels and hence suffer more from prolonged hypoxic effects. Indeed, reflecting this assumption, apoptotic levels where the highest in the upper region of the villi. Comparison with p53 null animals showed that ischemia-reperfusion-induced apoptosis was p53 independent [Coopersmith et al., 1999]. However, Puma (a pro-apoptotic protein that can be up-regulated by p53 [Nakano and Vousden, 2001]) knock-out mice had a significantly attenuated apoptotic response under the same experimental setting when compared to wild-type mice and p53-null mice [Wu et al., 2007]. Therefore Puma would appear to have a p53-independent role in detecting oxidative stress in the intestine and in initiating cell death.

### 1.2.6 Why don't some cells die?

Apoptosis does not occur along the length of the villi in response to radiation-induced DNA damage or as a result of many chemotherapeutic drugs or cytotoxic agents [Watson and Pritchard, 2000, Merritt et al., 1994]. One explanation for the lack of apoptosis might be that these cells do not proliferate however studies where enterocytes are forced back into the cell cycle by targeted expression of SV40 large T antigen does not appear to increase their radiosensitivity [Coopersmith and Gordon, 1997]. Although, the loss of p53 function as a consequence of the transforming ability of SV40 large T antigen confounds interpretation of these results. Another explanation for this might simply be that p53 is not induced – however as this report will go on to demonstrate even when p53 is induced in cells on the villi they remain refractory to apoptosis. So why don't cells along the villi die? The villus and crypt receive similar levels of radiation yet there is rarely any apoptosis observed in the intestinal villus cells [Marshman et al., 2001]. This bizarre biological phenomenon is part of the puzzle that will hopefully be explained by the use of transgenic mouse models (see Aims).

# 1.3 Cancer in the intestine

## 1.3.1 Colorectal tumourigenesis

In 2004 colorectal cancer had the second highest incidence in Europe (13.2%, after lung cancer at 13.3%) and was the second commonest cause of cancer related death (203,700 total deaths after lung at 341,800) [Boyle and Ferlay, 2005]. So any discoveries made that would help to understand the development of colorectal cancer would be of relevance to a large number of cancer patients.

Cancer progression is a multi-step process involving accumulation of aberrant genetic changes by which cells acquire dominant oncogenic properties and loose recessive tumour suppressive capabilities [Hanahan and Weinberg, 2000]. Clinicians use histopathological alterations to classify types and stages of the disease, for example small benign adenoma versus large metastatic cancers. Colorectal carcinomas arise from the epithelia of the colon and have the best documented histopathological progression of all human cancers (discussed in [Weinberg, 2006]). This is in part due to the large incidence of colorectal cancer in the western world and also to the relative accessibility of the colon through colonoscopy. The data suggests that most colorectal carcinomas originate from existing benign tumours which develop initially following the loss of a tumour suppressor gene, coupled with mutational activation of an oncogene. It takes a further four or five mutations or deletions of predominately tumour suppressor genes (such as *p53*) for the nascent tumour to then develop into a malignant cancer (see Figure 1.3.1) [Weinberg, 2006, Fearon and Vogelstein, 1990].

The use of linkage analysis and LOH studies on a small sub-population of individuals who suffered from a heritable colon cancer syndrome called familial adenomatous polyposis (FAP) enabled the discovery and cloning of the *APC* (adenomatous polyposis coli) gene in 1991 [Varesco, 2004, Groden et al., 1991, Vogelstein et al., 1989]. APC is a tumour suppressor gene (part of the Wnt signalling pathway), the loss of which is associated with the initiation of hyperplasic growth in the epithelium of the colon [Korinek et al., 1998].

Other consistent early events in colorectal tumourigenesis include; activation of the proto-oncogene K-*ras* (occurs in over one third of all human colorectal cancer cases, [Bos et al., 1987, Forrester et al., 1987]), loss of genetic stability (as identified by accumulation of ubiquitous somatic mutations in simple repeated sequences [Shibata et al., 1994]) and DNA hypomethylation [Goelz et al., 1985] (impacts on global gene expression which is important if it effects TSGs and thus perhaps further reduces genetic stability [Razin and Riggs, 1980]) .

Figure 1.3.1 illustrates a typical genetic model for colon carcinoma progression, although it is thought that the overall accumulation of mutations, rather than the order by which an individual acquires mutations, is more important for the development of cancer [Fearon and Vogelstein, 1990].

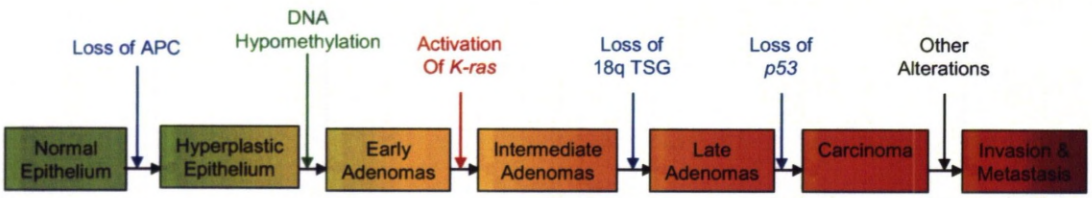


***Figure 1.3.1: Genetic model for colon carcinoma progression.***

*Adapted from [Fearon and Vogelstein, 1990]. Tissues from various stages of colorectal cancer had its DNA examined for loss of heterozygosity (LOH) at chromosomal markers [Vogelstein et al., 1989]. The chromosomal regions with frequent LOH were considered to be harbouring Tumour Suppressor Genes (blue text) and some of these have since been identified (APC and p53) while others remain unclear (18q TSG, also known as DCC (simply Deleted in Colon Cancer DCC – is separate from other TSGs in the 18q region such as SMAD2 and SMAD4 [Lassus et al., 2001])). DNA hypomethylation is thought to contribute to genetic instability while K-ras drives cell proliferation.*

# 1.4 Further introduction to p53

## 1.4.1 Activation of p53- an overview

p53 can become activated in response to a wide variety of stimuli including genotoxic stress, hypoxia and aberrant growth signalling [Vogelstein et al., 2000, Vousden, 2002]. Each of these stimuli inhibits the degradation of p53 leading to a rapid increase in p53 levels. In *"resting"* cells p53 is usually kept low in abundance and in an inactive form by the antagonising activities of Mdm2 and Mdmx (also known as Mdm4) [Blattner, 2008]. Mdm2 (Murine double-minute 2) is an E3 ubiquitin ligase which can bind to the transactivation domain of p53, hampering p53's ability to act as a transcription factor and can target p53 (and itself) for degradation by the proteasome [Brooks and Gu, 2006, Vousden, 2002]. The ability of Mdm2 to ubiquitylate p53 requires its RING finger domain to be intact [Honda et al., 1997]. Mdmx, a closely related protein, can also bind to and block the transactivation domain of p53 through the conserved p53-binding N-terminal region present on both MDM proteins [Shvarts et al., 1996] (and see Figure 1.4.1). Mdm2 and Mdmx also share homology with the RING finger domain (at the C-terminal), however, Mdmx lacks the E3 ubiquitin ligase activity of Mdm2 [Marine and Jochemsen, 2005]. Mdm2 and Mdmx are able to interact and form heterodimers through their mutual RING finger domains [Tanimura et al., 1999] which may contribute to Mdm2 stability by interfering with Mdm2 auto-ubiquitination and thus allows p53 to be efficiently degraded [Stad et al., 2001]. There are two main lines of thought regarding the outcome of the formation of Mdm2/Mdmx-p53 complexes; 1) Mdmx contributes to p53 degradation by stimulating ubiquitination [Linares et al., 2003] and 2) Mdmx prevents the Mdm2 mediated nuclear export of p53 thus preventing transport to the proteasome and the subsequent proteolysis [Jackson and Berberich, 2000]. The second theory would only appear to hold true in experimental settings when there is a massive excess of Mdmx over Mdm2, which could then compete for p53 binding [Marine and Jochemsen, 2005].

Interestingly – as Mdm2 mediates p53 degradation – Mdm2 is also a transcriptional target of p53, creating a negative feedback loop that ensures low levels of p53 are maintained in *"resting"* cells [Kubbutat and Vousden, 1998, Blattner, 2008, Harris and Levine, 2005].

Until very recently it was suggested that in contrast to Mdm2, Mdmx did not appear to have any p53 responsive elements (p53 REs) in its promoter region nor was it thought to be up-regulated by p53 [Marine and Jochemsen, 2005]. However it is now known that *HDMX* and the murine homolog *Mdmx* both have a consensus p53 binding site within the first intron (similar to Mdm2 – see Figure 1.4.3) which is responsive to p53 [Phillips et al., 2010, Li et al., 2010].

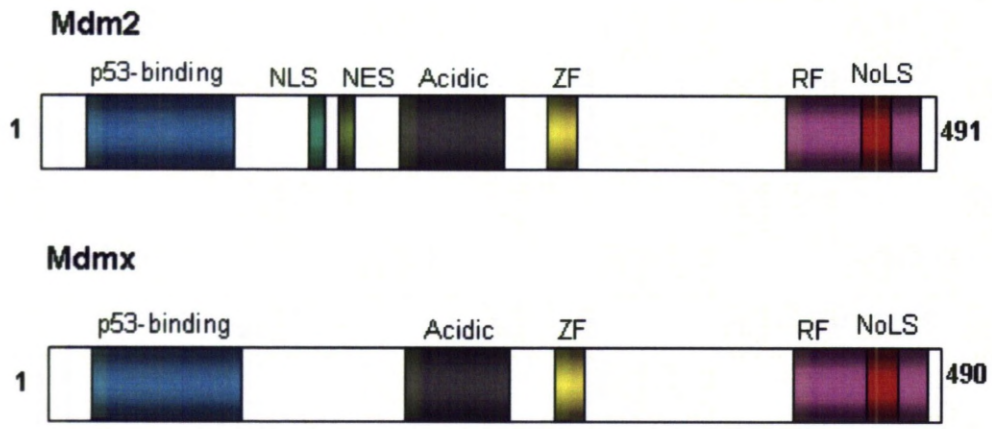


***Figure 1.4.1: Mdm2 (mouse or human) versus Mdmx (mouse) protein structure.***
*Adapted from an image available at http://p53.free.fr/p53_info/mdm_family.html information from [Marine and Jochemsen, 2005]. Blue is N-terminal p53-binding domain, NLS is nuclear localisation signal, NES nuclear exclusion signal, grey is the acidic region, yellow is the zinc finger domain, pink is the RING finger domain and red is the nucleolar localisation signal.*

The control of *p53* by *Mdm2* and *Mdmx* is essential for life. Deletion of *Mdm2* in mice causes them to die early in embryogenesis, and this phenotype is completely rescued on a *p53* null background [Montes de Oca Luna et al., 1995, Jones et al., 1995]. Similarly, *Mdmx* null mice also die early in embryogenesis (7.5 d.*p.c*) and this phenotype is also rescued through the deletion of *p53* [Parant et al., 2001]. Whilst *Mdm2*$^{-/-}$ mice die at 3 d.*p.c* from increased p53-dependent apoptosis, *Mdmx*$^{-/-}$ mice die at 7.5 d.*p.c* by aberrant p53-dependent growth arrest, thus demonstrating that deregulated *p53* activity appears to be the cause of death in these mice and suggests that *Mdm2* and *Mdmx* have distinct roles in the regulation of *p53*. Attempts have been made to delay embryo death in these *Mdm2*$^{-/-}$ or *Mdmx*$^{-/-}$ mice by

deleting downstream *p53* targets, such as *Bax* and *p21* [Chavez-Reyes et al., 2003]. On a *Bax* null background *Mdm2*$^{-/-}$ mice survived marginally longer (3 d.*p.c* to 6.5 d.*p.c*) and the mechanism of death switched from excessive apoptosis to growth arrest. *Mdmx*$^{-/-}$ mice did not have any increased survival following deletion of *p21*, however, the cause of death was initiated by apoptosis rather than cell cycle arrest. The different mechanisms of action and functional properties of *Mdm2* and *Mdmx* may become important in the intestinal gut epithelium; where there is a distinct difference in outcome of p53 activation along the crypt-villus axis (see Section 1.2.6).

In a stressed cell, following DNA damage, *p53* rapidly accumulates. This is attributed to *p53* rescue from proteasome degradation rather than *de novo* synthesis and is predominately due to disruption of the interaction between p53 and its negative regulators [Blattner, 2008]. Lesions in the DNA are thought to be recognised by members of the PI3-K kinsase family including; *ATM* (ataxia telangiectasia mutated), *ATR* (ATM-rad3-related) and *DNA-PK* (DNA-dependent protein kinase). *ATM* and *DNA-PK* appear activated following DNA double stranded breaks – as caused by ionising-radiation – whilst *ATR* is required for repair of stalled replication or DNA cross-links – as can be induced by UV-irradiation (reviewed in [Zhou and Elledge, 2000]). As discussed previously, *Mdm2* is a gene which is essential for the control of *p53* (at least during early development) and many of the responses to differing types of DNA lesion converge on Mdm2 as a means of liberating p53 [Blattner, 2008]. Indeed following their activation all three PI3-K kinases can phosphorylate Mdm2 in a way that causes its functional inactivation and/or destabilisation [Mayo et al., 1997, Maya et al., 2001, Shinozaki et al., 2003]. Destabilisation of the Mdm2 protein was initially speculated to be due to accelerated Mdm2 auto-ubiquitination [Stommel and Wahl, 2004] however later mouse models have demonstrated that auto-ubiquitination is not required for degradation of Mdm2 *in vivo* [Itahana et al., 2007]. Mdm2 degradation may instead be regulated by other E3 ligases (such as $SCF^{\beta\text{-}TRCP}$ [Inuzuka et al., 2010]) as well as the deubiquitinating enzyme HAUSP (Herpesvirus-associated ubiquitin-specific protease) [Meulmeester et al., 2005]. In addition, ATM and ATR can both phosphorylate p53 at serine 15 which blocks the ability of Mdm2 to bind to the transactivation domain of p53 [Lakin et al., 1999]. DNA-PK can also inactivate genes that would normally phosphorylate critical parts of the Mdm2 degradation

loop such as GSK-3 (glycogen synthase kinase 3) which further prevents p53 degradation [Blattner et al., 2002, Kulikov et al., 2005, Boehme et al., 2008] (see Figure 1.4.2).

Yet another mechanism for p53 stabilisation is the sequestration of Mdm2 into the nucleolus by a protein called ARF ($19^{ARF}$ in mice and $14^{ARF}$ in humans – based on the molecular weight of each protein) reviewed in [Zhang and Xiong, 2001]. ARF was discovered as an alternative reading frame in tumour suppressor gene $p16^{INK4A}$ (mouse and human) and becomes triggered in response to oncogenic activity [Sherr, 1998]. Each of the mechanisms described here allows the rapid accumulation of p53 without synthesising new protein. Transcriptional regulation of p53 would create a delay in the DNA-damage response pathways and there is also a high risk – as the DNA is damaged – of perhaps producing a mutated non-functional p53 protein [Blattner, 2008].

Following stabilisation, p53 is activated and regulated by post-translational modifications [Appella and Anderson, 2001, Olsson et al., 2007]. The outcome of p53 activation depends on a wide range of factors; the type of tissue, the state of the cell, if the cell has other oncogenic changes, the type and severity of the stress stimuli and the presence or absence of p53-independent death or survival signals that cooperate with p53 [Vousden, 2006]. p53 can inhibit tumour development by initiating a number of responses including reversible changes to induce cell cycle arrest and irreversible changes implementing apoptosis and cell senescence [Vousden and Lu, 2002]. What response p53 induces depends on which target genes it up regulates [Vousden, 2002]. p53 is thought to be able to control which downstream targets it up-regulates via promoter selection and binding with transcriptional co-activators (ASPP for example drives p53 to the induction of cell death [Samuels-Lev et al., 2001]). Promoter recognition and selection are controlled by a number of different mechanisms, one being post-translational modifications such as phosphorylation and acetylation [Vousden, 2002, Vousden, 2006]. The consensus DNA binding motif for p53 responsive elements (p53 REs) consists of a repeated 10bp 5'-PuPuPuC(A/T)(T/A)GPyPyPy-3' palindromic half site separated by 0-13bp [el-Deiry et al., 1992]. Genome wide searches for this motif using computer algorithms have suggested that more than 4000 genes contain a p53-binding site, while more recent studies using stress activation have placed a lower figure on this of approximately 1500 genes [Smeenk et al., 2008, Vousden, 2006].

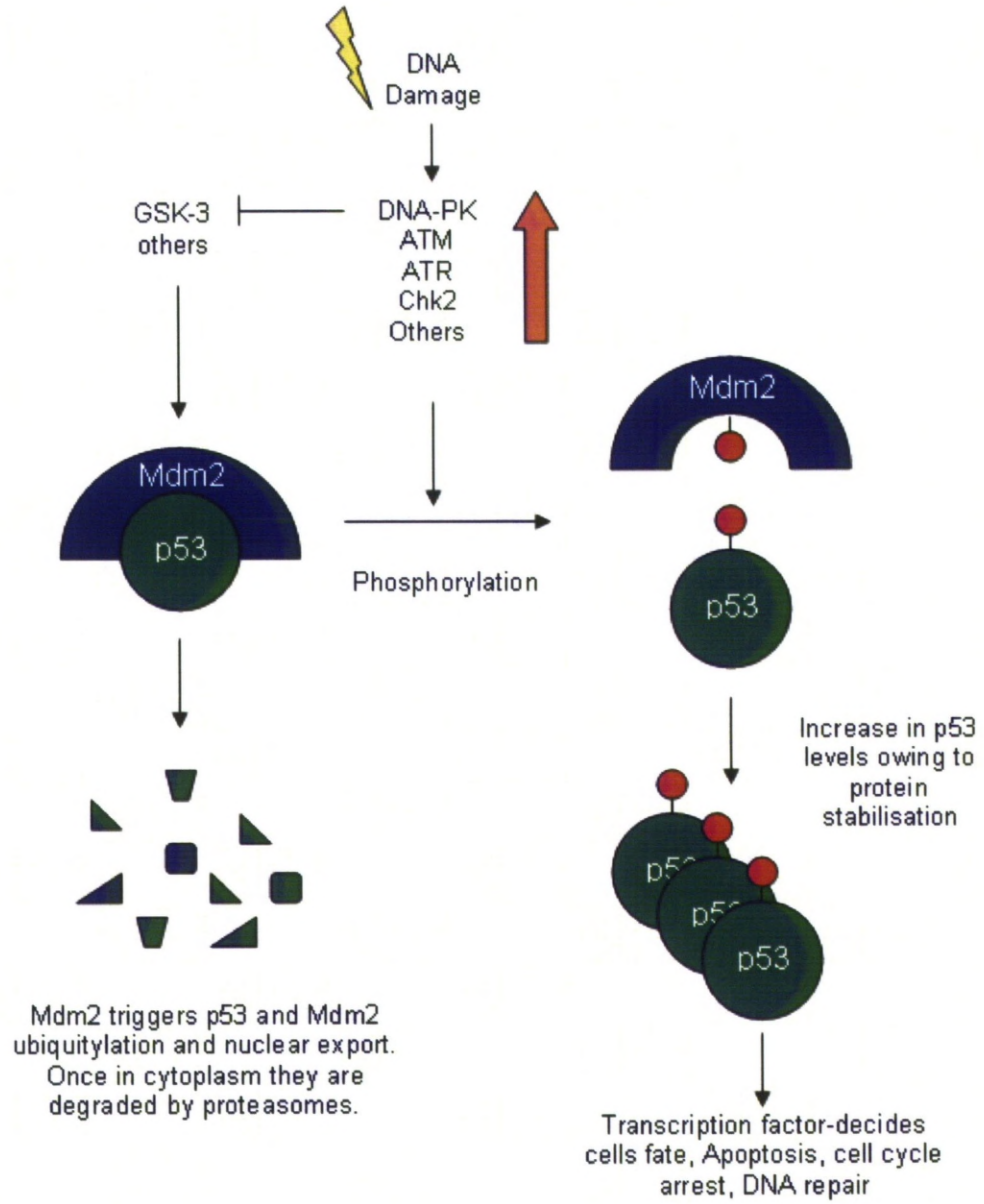


***Figure 1.4.2: Model of regulation of p53 stability.***

*Adapted from [Kubbutat and Vousden, 1998]. In response to DNA damage p53 is regulated by many pathways [Fisher, 2001]. Upstream genes such as DNA-PK (DNA-dependent protein kinase) and ATM (Ataxia Telangiectasia Mutated) sense specific DNA lesions and activate key players in the DNA damage response network, for example by phosphorylating p53 so it no longer binds to Mdm2 [Blattner, 2008]. Once liberated from its negative regulators, p53 levels rapidly accumulate in cells leading to p53-mediated cell cycle arrest or apoptosis [Vousden, 2006].*

Since so many genes have the potential to be involved in a p53 dependent DNA-damage response it is critical that we evaluate each of the major responses to p53 activation and determine which downstream p53 target genes are induced in our tissue of interest – the gastrointestinal tract. Below is an outline of the major responses to p53 activation, (regulation of p53 by Mdm2, senescence, cell cycle arrest and apoptosis) and in the case of cell cycle arrest and apoptosis a review of the downstream targets of p53 which could be used as a reporter in the intestinal gut epithelia.

### 1.4.2 Regulation of p53 by Mdm2: the P1, P2 conundrum

Mdm2 is an important proto-oncogene which is often up regulated in tumours where cells retain wild-type p53 [Oliner et al., 1992] and also in tumours lacking wild-type p53, illustrating Mdm2 has both p53-dependent and p53-independent functions [Ganguli and Wasylyk, 2003]. This is highlighted in the gene structure and promoter layout in Mdm2 (see Figure 1.4.3). Mdm2 has 12 exons that can create multiple splice variants and two promoter regions; P1 is located upstream of exon 1 and is responsible for basal expression while P2 is located in intron 1 just before exon 2 and has two p53 responsive elements (p53-REs). The P1 and P2 promoters produce different transcripts of Mdm2 but both promoters can produce both of the major isoforms of Mdm2 [Saucedo et al., 1999]. These are the full length $p90^{MDM2}$ which is capable of binding and inactivating p53, initiated from the first ATG in exon 3 and a shorter protein, $p76^{MDM2}$ initiated from the ATG in exon 4, which is missing part of the p53 binding domain. $p76^{MDM2}$ can act in a dominant negative manner to inhibit $p90^{MDM2}$ from degrading p53 (reviewed in [Iwakuma and Lozano, 2003]).

When transcripts from the P1 and P2 promoters were compared using a S1 nuclease protection assay, it was discovered that levels of RNA from P1 or P2 promoters did not change between p53 wild-type mice or p53 null mice [Mendrysa and Perry, 2000]. However when mice were exposed to 5 Gy of whole body γ-irradiation, there was a marked p53-dependent increase in the P2 promoter RNA levels; most dramatically there was a 32-fold increase of P2 transcripts in the spleen. Therefore p53 would appear to only up-regulate Mdm2 *in vivo* under conditions of stress – perhaps indicating that as cells in culture

continually produce Mdm2 from the P2 promoter that they are under some unidentified stress. Curiously, in *p53* null mice there was still some 10-30% of the total *Mdm2* RNA originating from the P2 promoter, indicating that other transcription factors must be able to bind to the P2 promoter [Mendrysa and Perry, 2000].

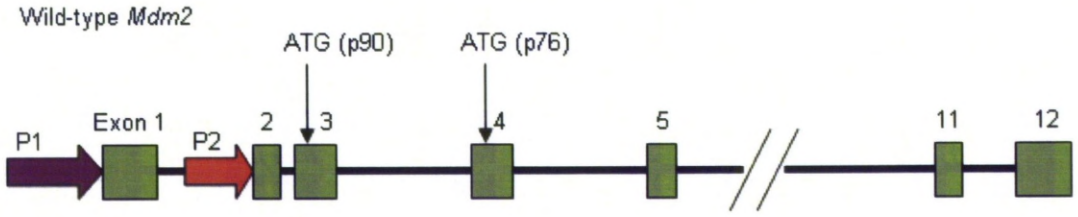


***Figure 1.4.3: Structure of Mdm2 (mouse and human) gene.***

*Adapted from [Chang et al., 2004] and [Iwakuma and Lozano, 2003]. Mdm2 has 12 exons (shown in green boxes) and two promoter regions (indicated by arrows; P2 has two p53 Responsive Elements). Transcripts from the human P1 promoter skip exon 2 – murine transcripts do not. The two start codons are also shown, the one in exon 3 codes for the long p90 isoform of Mdm2 while the one in exon 4 codes for the shorter protein p76. In MDM2 (the human gene) there is a third promoter region, called P3 in the third intron of this gene [Liang and Lunec, 2005]. It is thought p53 is able to bind to and down-regulate the P3 promoter expression when MDM2 levels are elevated, dampening levels of MDM2 and providing yet another feedback loop in this complex system.*

Indeed, transcription factor binding sites (TFBS) other than p53 have been reported within the P2 promoter region including; IECS, AP-1, Ets A, Ets B and AP-4 [Truong et al., 2005, Ku et al., 2009, Ries et al., 2000, Phelps et al., 2003, Zhou et al., 2009] and these are discussed next. The AP-1 and Ets sites have been shown to play a role in inducing Mdm2 through the Ras/Raf/MEK/MAP kinase pathways. In experiments where constitutively activated Ras is over-expressed in cultured cells there is a 5-8 fold increase in P2 promoter activity which is independent of p53 and completely abrogated in P2 promoters with mutations within either or the AP-1 or Ets B sites [Ries et al., 2000, Truong et al., 2005]. In addition, in breast cancer cell lines elevated HDM2 levels were also partly associated with this composite AP-1 Ets B site [Phelps et al., 2003]. Furthermore Fli-1 (an Ets transcription factor –

implicated in the progression of Friend Murine Leukemia Virus (F-MuLV)-induced erythroleukemia) was shown to bind to the Ets A site and up-regulate Mdm2 in a Ras/p53 independent fashion *in vivo* [Truong et al., 2005]. Mdm2 may also be induced by oxidative stress via the AP-1 site in cardiac myocytes, where Mdm2 is speculated to act as a cardioprotective agent [Pikkarainen et al., 2009].

Another p53-independent role for *Mdm2* has been suggested in the development of germinal centre (GC) B cells where *Mdm2* is up-regulated by IFN regulatory factor 8 (IRF8) [Zhou et al., 2009]. GC B cells are cells actively undergoing DNA double strand breaks (DSB) in order to rearrange immunoglobulin genes as part of gene diversification in the specific pathogen immune response – however despite undergoing DSB these cells do not up-regulate p53. IRF8, a transcription factor which is expressed in differentiating myeloid, dendritic and B cells, has been shown to bind to an IECS site within *Mdm2* intron 1. IRF8 binding allowed p53-independent up-regulation of *Mdm2* which is suggested to prevent p53 up-regulation and protect the GC B cells from p53 induced cell cycle arrest and/or apoptosis.

Another TFBS within the *Mdm2* P2 region is an AP-4 site located downstream of the second p53 RE site [Ku et al., 2009, Phelps et al., 2003]. AP-4 binding (with other cofactors) has been shown to down-regulate *MDM2* in human colorectal carcinoma cells [Ku et al., 2009].

The p53-independent TFBS within the P2 promoter may provide one explanation for the low level expression of *Mdm2* from the P2 promoter in *p53* null mice reported by [Mendrysa and Perry, 2000]. Indeed other research groups have also demonstrated that p53 is dispensable for low level expression from the P2 promoter in human astrocytic glioma cells [Dimitriadi et al., 2008]. P2 promoter transcripts are important as they are about 8 times more efficiently translated than transcripts from the constitutively active counterpart [Landers et al., 1997]. The reduction in translation efficiency of the P1 promoter is due in part to two upstream open reading frames (uORFs) present in transcripts which are inhibitory to downstream translation [Brown et al., 1999, Jin et al., 2003]. The induction of *Mdm2* by p53 results in accumulation of Mdm2 protein following genotoxic stress which may enable a rapid return to *"resting"* cell levels of p53 once the stress stimulus is removed [Blattner, 2008] which

could prevent further uncontrolled and perhaps deadly action from p53 [Stommel and Wahl, 2005] or for some other unknown function (discussed in Section 1.4.1).

The P1, P2 promoter layout in *Mdm2* does present an interesting biological question and a unique opportunity to discover more about the regulation of one of the most important tumour suppressor genes – p53. Would deletion of either the P1 or P2 promoter of *Mdm2* affect this complex regulatory loop and how would such affects be manifested/ ie what would the phenotype, if any, of such alterations be? Presumably a P2-Mutant mouse (which is unresponsive to p53) could develop normally as basal expression of Mdm2 would still be present; although it is likely that there will be occasional stresses even during normal development (such as ROS (reactive oxygen species) and oxidative stresses) which might require p53 induction. Assuming that the P2-Mutant mice survive embryogenesis, would basal expression of Mdm2 be enough to deal with genotoxic stress such as ionising-radiation or indeed just normal encounters with general stresses? Or would the mice be prone to tumour development? Or even might they be resistant to tumour formation? A P1-Null mouse might be even more interesting; would it develop normally or die in embryogenesis? And if it does survive to birth how would it deal with different cellular stresses? It may be important then that other tumour suppressor genes play a role in controlling levels of Mdm2. For example the PTEN (phosphatase and tensin homolog deleted from chromosome 10) tumour suppressor gene down-regulates Mdm2 expression through the P1 promoter in a p53-independent fashion [Chang et al., 2004], which could become even more important in a P2 deleted mouse.

To our knowledge, no such mice have yet been created. Part of this project then would be to create one or both of these mice. Data from these animals would be likely to have a significant impact in the field of cancer biology regardless of the phenotype of these mice.

### 1.4.3 Cellular senescence

Cellular senescence is when a cell irreversibly enters cell cycle arrest (reviewed in [Pazolli and Stewart, 2008] and [Funayama and Ishikawa, 2007]). Senescent cells are characterised by an enlarged and flattened morphology which is often accompanied by senescence-associated β-galactosidase (SA-β-gal) activity [Dimri et al., 1995]. Senescent cells may also have condensed chromatin [Funayama and Ishikawa, 2007]. Cells can enter senescence because of replicative stress (known as replicative senescence (RS)) or through other distinct stress signals such as oncogenic activity, loss of tumour suppressor genes, excessive DNA damage and oxidative stress (known as stress induced senescence (SIS)) [Pazolli and Stewart, 2008].

RS is triggered by telomere (a long repetitive region at the end of chromosomes) shortening as a result of repeated cell cycles. Cells have an *"internal clocking"* mechanism – the telomeres which protect the coding sections of the chromosome – thus they have a limit on the number of proliferation cycles they can undertake (50-70) [Hayflick and Moorhead, 1961]. Eventually, in cells which lack endogenous telomerase (an enzyme which can extend the telomeres) the telomeres become critically short, and the result is aberrant chromosome fusions in an attempt to repair the chromosomes. Such alterations are recognised as DNA damage which is detected by the kinases ATM and Chk2 [Serrano and Blasco, 2001]. ATM and Chk2, as discussed in Section 1.4.1 can stabilise and activate p53, which can in turn activate genes involved in the senescence response – namely p21 which goes on to induce Rb and ultimately senescence [Funayama and Ishikawa, 2007] (see Figure 1.4.4). Mice deficient in telomerase in their epithelial cells had a lower incidence of papillomas than wild-type mice, suggesting that telomere shortening and senescence can have a protective effect in tumourigenesis [Gonzalez-Suarez et al., 2000]. Conversely, a second line of thought is that senescent cells may actually promote tumourigenesis (in relation to aging) through interactions in the tissue microenvironment which promote growth of surrounding preneoplastic cells [Krtolica et al., 2001].

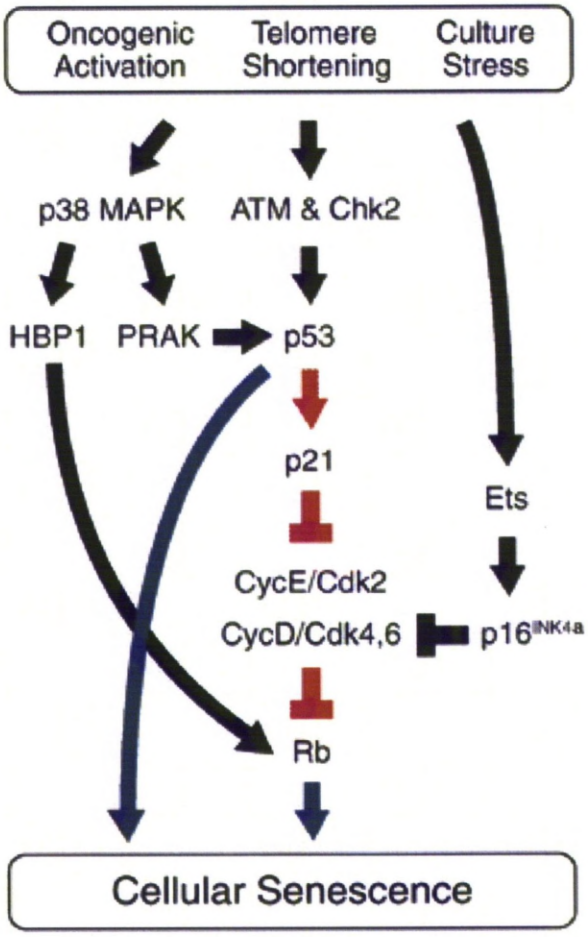


***Figure 1.4.4: The signalling pathways that lead to cellular senescence.***

*Taken from [Funayama and Ishikawa, 2007]. Whilst upstream changes are still undefined, downstream changes are usually dependent on tumour suppressor genes p53 and Rb. Inactivation of either gene appears to be sufficient for MEFs to evade cellular senescence [Harvey et al., 1993, Sage et al., 2000].*

### 1.4.4 Cell cycle arrest- *p21 (CDKN1a)*

*CDKN1a* (cyclin-dependent kinase inhibitor 1a) or $p21^{Cip1/Waf1}$ (from hereon referred to as *p21*) was the first p53 target gene discovered with a role in cell cycle arrest [el-Deiry et al., 1993]. It encodes a potent cyclin-dependent kinase inhibitor which represses cell cycle progression [Harper et al., 1993] and is involved in both the G1/S and G2/M checkpoint responses to DNA damage [Gartel and Tyner, 1999] (see Figure 1.4.5). Interestingly, whilst p21 does bind to and inhibit a wide range of cyclin and cdk (cyclin dependent kinases) complexes including; cyclin D1–Cdk4, cyclin E–Cdk2, cyclin A–Cdk2, and cyclin A–Cdc2, p21 may also act as an assembly factor for cyclin D1-Cdk4 at low concentrations [LaBaer et al., 1997]. At high concentrations of p21 (as would be induced upon p53 activation) the stimulatory effects are switched to inhibitory and thus prevent entry of the cell into the cell cycle [Zhang et al., 1994, Levine, 1997]. The paradoxical activity of cell cycle inhibitor p21 to also act a stimulator of early G1 phase of the cell cycle does not appear to be essential for normal cell function – as p21 null mice developed normally [Deng et al., 1995].

The ability of p53 to induce cell cycle arrest also lays with two other genes, *GADD45* (growth arrest and DNA damage-inducible protein 45) and *14-3-3σ* [Olsson et al., 2007]. 14-3-3σ sequesters cyclinB1-CDK1 complexes in the cytoplasm preventing their nuclear import, while GADD45 destabilises CDC2/cyclinB which ultimately induces G2/M arrest in cells with DNA damage [Olsson et al., 2007, Vogelstein et al., 2000].

p21 null mice developed normally and were fertile but were prone to renal failure [Deng et al., 1995] and eventually succumbed (average age 16 months) to spontaneous tumour development [Martin-Caballero et al., 2001]. There is also evidence of *p21* haploinsuffciency. Studies have shown that $p21^{-/-}$ and $p21^{+/-}$ mice developed more tumours and in a wider spectrum than $p21^{+/+}$ mice when exposed to a single 4 Gy dose of γ-irradiation at two weeks of age [Jackson et al., 2003]. $p21^{-/-}$ mice also had a much higher incidence of tumour metastasis, indicating p21 may function as an anti-metastatic agent. However, this phenotype is not nearly as severe as that displayed by p53-null mice (average age of tumour development 6 months [Donehower et al., 1992]) which thus argues that p21 is not responsible for all p53's tumour suppressor activity [Fisher, 2001]. Certainly lack of p21 does

not affect p53 dependent cell death in the intestine [Brugarolas et al., 1995], nor can loss of *p21* rescue *Mdm2* null lethality during embryogenesis [Montes de Oca Luna et al., 1997]. p21 deficiency does, however, compromise radiation-induced cell cycle arrest [Brugarolas et al., 1995].

p21 is induced in the colonic and small intestinal crypts in response to DNA damage. This process is p53-dependent as demonstrated by studies of p53 null mice in which no p21 induction occurs in response to ionising radiation [Wilson et al., 1998]. p21 was also induced in a p53-dependent manner in response to chemically induced DNA damage in the small intestine (using 5-fluorouracil, 5-FU) [Pritchard et al., 1998]. Since p21 is essential for p53-induced G1 cell cycle arrest, and p21's expression in the GI tract is dependent on p53, p21 appears to be an ideal downstream reporter for p53-mediated cell cycle arrest in the intestinal gut epithelia.

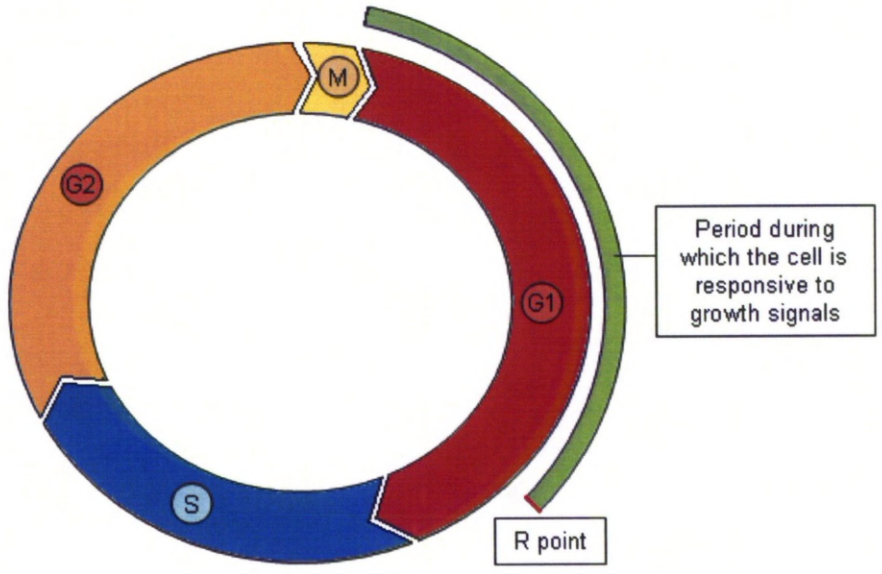


***Figure 1.4.5: The cell cycle clock.***

*Taken from [Weinberg, 2007] G1, S, G2 and M refer to first gap, DNA synthesis, second gap and mitosis. Restriction (R) point is the time when a cell must commit to continuing with DNA synthesis, it is also up to this point that a cell remains sensitive to mitogenic growth factors.*

Unlike p53, mutations in the p21 tumour suppressor protein are rare in human cancers [Shiohara et al., 1994], indicating that p21 may have redundant roles in the p53 response – for example p53 may up-regulate GADD45 and/or 14-3-3σ to compensate for loss of p21, or p53 may induce apoptosis instead – so that mutations in p53 itself are far more detrimental [Lozano and Zambetti, 2005]. In addition to p53, several other factors can activate the transcription of p21 (reviewed in [Gartel and Tyner, 1999]). However, since in response to DNA damage p53's main downstream target in cell cycle arrest seems to be p21 – and p21 appears to be essential for p53-depenedent G1 arrest (reviewed in [Levine, 1997]) – *p21* would appear to serve as an ideal p53-responsive reporter gene.

### 1.4.5 Apoptosis – an overview

Apoptosis, or programmed cell death, is a vital component of the maintenance of healthy multicellular organisms. Apoptosis occurs in response to a wide variety of stimuli including cellular stresses such as DNA damage or viral infection and is tightly controlled by a variety of pro- and anti-apoptotic proteins (reviewed in [Danial and Korsmeyer, 2004, Taylor et al., 2008]). A cell undergoing apoptosis has a very distinct morphology; the cell shrinks, its chromosomes condense, the nucleus fragments, the cellular membranes bleb and form small apoptotic bodies which are removed by phagocytes [Kerr et al., 1972]. It is the organised removal of cell debris and the prevention of an unwanted immune response that defines apoptosis from another type of cell death called necrosis [Savill and Fadok, 2000]. Apoptosis is a very rapid process and can be completed within a few hours after initiation which makes it particularly difficult to detect *in vivo* [Walker et al., 1988].

Apoptosis can be stimulated intracellularly or extracellularly but both pathways converge at the mitochondrial membrane where members of the Bcl-2 protein family compete to control the release of cytochrome *c* [Danial and Korsmeyer, 2004, Chipuk and Green, 2008]. The Bcl-2 protein family is divided into three subclasses based on their areas of Bcl-2 like homology (BH domains) (see Figure 1.4.6) [Willis and Adams, 2005, Puthalakath and Strasser, 2002]. The anti-apoptotic members (Bcl-2, Bcl-$_{XL}$ Mcl-1, A1 and others) contain all four areas of homology BH1-4, the "multidomain" pro-apoptotic members (Bax and Bak)

contain BH1-3 and finally the BH3-only pro-apoptotic members Puma and Noxa (among others) contain only BH3 domains [Huang and Strasser, 2000, Shibue and Taniguchi, 2006]. At the mitochondrial outer membrane (MOM), under normal conditions, the anti-apoptotic Bcl-2 family members such as Bcl-2 and Bcl-$_{XL}$ block apoptosis by preventing the oligomerisation of Bax and Bak. However, after receiving death signals from the BH3-only proteins, Bax or Bak migrate to the MOM where, following oligomerisation and the subsequent formation of homodimers, they can insert themselves into the membrane and create channels which allow the release of cytochrome *c*. It is thought to be the balance of Bcl-2 pro- versus anti-apoptotic family members on the MOM which determines whether to prevent or to allow release of inter-membrane space (IMS) proteins including cytochrome *c* [Chipuk and Green, 2008]. The release of IMS proteins from the mitochondria is called mitochondrial outer membrane permeabilization (MOMP) [Danial and Korsmeyer, 2004] and Bax or Bak are essential to inducing apoptosis in this way (also referred to as the intrinsic cell death pathway) [Cheng et al., 2001, Zong et al., 2001].

Following cytochrome *c* release, it is bound by Apaf-1 (apoptotic protease activating factor) through their mutual WD40 domains. The caspase recruitment domains (CARD) on Apaf-1 are usually bound by its WD40 domains, so once cytochrome *c* has bound to the WD40 domains the CARD sites become dislodged [Danial and Korsmeyer, 2004]. In the presence of ATP/dATP Apaf-1/cytochrome *c* can then recruit pro-caspase-9 through the CARD-CARD interactions between Apaf-1 and pro-caspase-9 [Li et al., 1997]. Pro-caspase-9, an initiator caspase, is able to auto-activate within the resulting structure, termed the *"the wheel of death"* but also known as the apoptosome [Chinnaiyan, 1999]. Activated caspase-9 can then go on to cleave and activate executioner caspase-3 which triggers the caspase cascade which will ultimately result in the death of the affected cell (see Figure 1.4.7) [Hill et al., 2003].

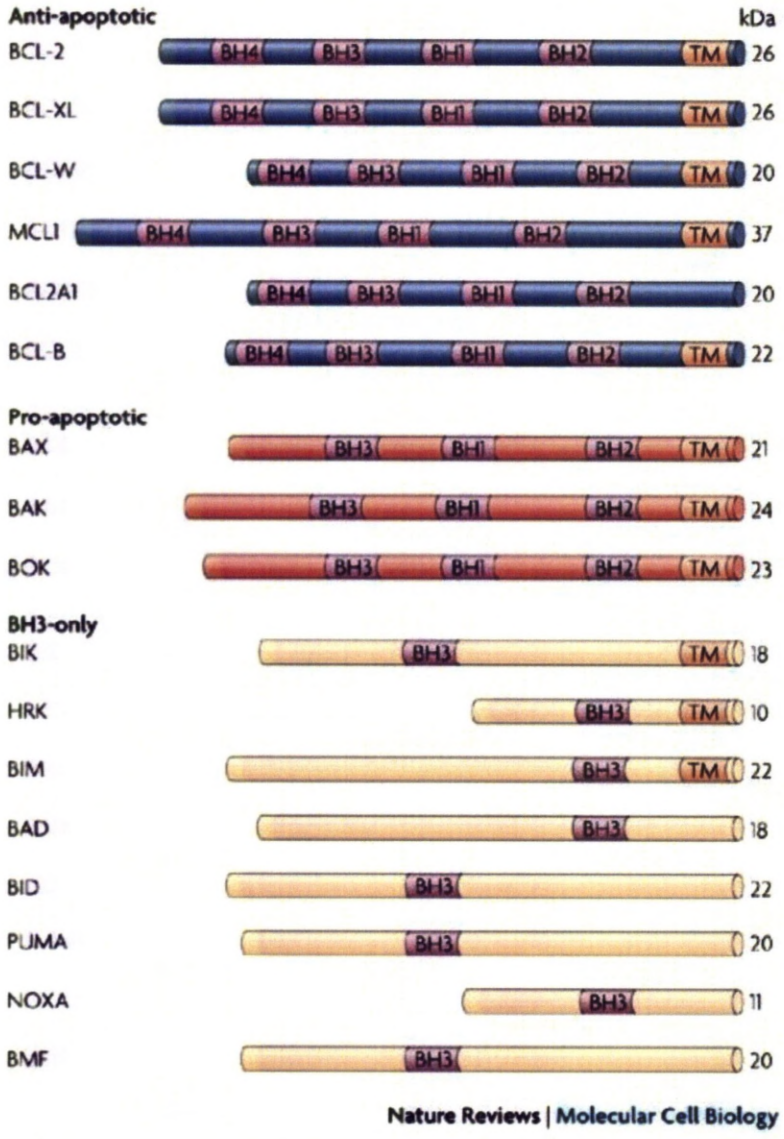


***Figure 1.4.6: The Bcl-2 family.***

*Image taken from [Taylor et al., 2008]. The B-cell lymphoma-2 (Bcl-2) family proteins have very important roles in the regulation of apoptosis and are divided into three groups; the anti-apoptotic proteins Bcl-2, Bcl-XL, Bcl-W, Mcl-1, Bcl2A1 and Bcl-B, the pro-apoptotic "multidomain" proteins Bax, Bak and Bok, and the pro-apoptotic BH3-only proteins Bik, Hrk, Bim, Bad, Bid, Puma, Noxa and Bmf (see text for further details).*

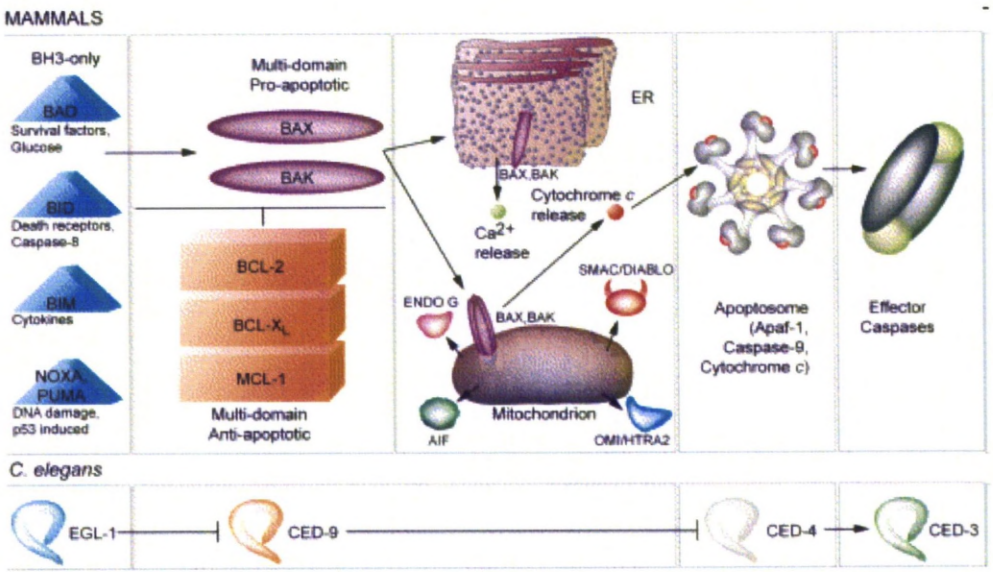


***Figure 1.4.7: The intrinsic apoptotic pathway.***

*Taken from [Danial and Korsmeyer, 2004] illustrating the similarities and divergence between C. elegans and the mammalian intrinsic death pathways. EGL-1 and a subset of the BH3-only proteins bind to and inactivate anti-apoptotic proteins CED-9 and Bcl-2. This leaves CED-4 free to activate CED-3 and Bax/Bak able to release cytochrome c from the mitochondria, allowing the formation of the apoptosome which activates the effector caspases. It is the effector caspases like caspase-3 (a homologue of CED-3) that trigger the caspase cascade and ultimately the death of the cell.*

The extrinsic death pathway is activated by so called death receptors including, the tumour necrosis factor receptor (TNF-R) family and Fas [Danial and Korsmeyer, 2004]. Both TNF-R and Fas have a common cytoplasmic region called the *"death domain"* and following binding with their ligands TNF-α and FasL respectively, the death domain binds and activates an associated protein termed FADD (Fas-associated death domain protein) [Boldin et al., 1996, Muzio et al., 1996]. The resulting complex, DISC (death-inducing-signalling-complex) activates the initiator caspases; pro-caspases -8 and -10 which then go on to activate the executioner caspases -3, -6 & -7 independently of the intrinsic mitochondrial pathway (see Figure 1.4.8). The executioner caspases trigger the caspase cascade which leads to the morphological changes associated with apoptosis [Taylor et al., 2008]. Caspase-8 also

catalyses Bid activation (a Bcl-2 BH3-only pro-apoptotic family member) which then translocates to the mitochondria [Gross et al., 1999] resulting in Bax/Bak activation and cytochrome *c* release [Willis and Adams, 2005]. Bid activation thus connects the death receptor pathway with the intrinsic mitochondrial apoptotic pathway and hence amplifies pro-apoptotic signals [Danial and Korsmeyer, 2004, Shelton et al., 2009].

A third pathway which activates the caspase cascade and apoptosis is the granzyme B pathway (See Figure 1.4.8) [Taylor et al., 2008]. T-cells and Natural killer (NK) cells can eliminate transformed tumour cells or cells infected with a virus by delivering granules, containing perforin and serine proteases called granzymes, to the cytosol of their targets [Martinvalet et al., 2008]. Perforin can form pores in the cells plasma membrane facilitating granzyme B entry into the cell. Granzyme B can cleave caspase-3 and BH3-only protein Bid (thus activating it) [Alimonti et al., 2001], whereupon this pathway converges with the other apoptotic pathways. Granzymes A and B can also induce caspase-independent death (not discussed in this report) [Danial and Korsmeyer, 2004].

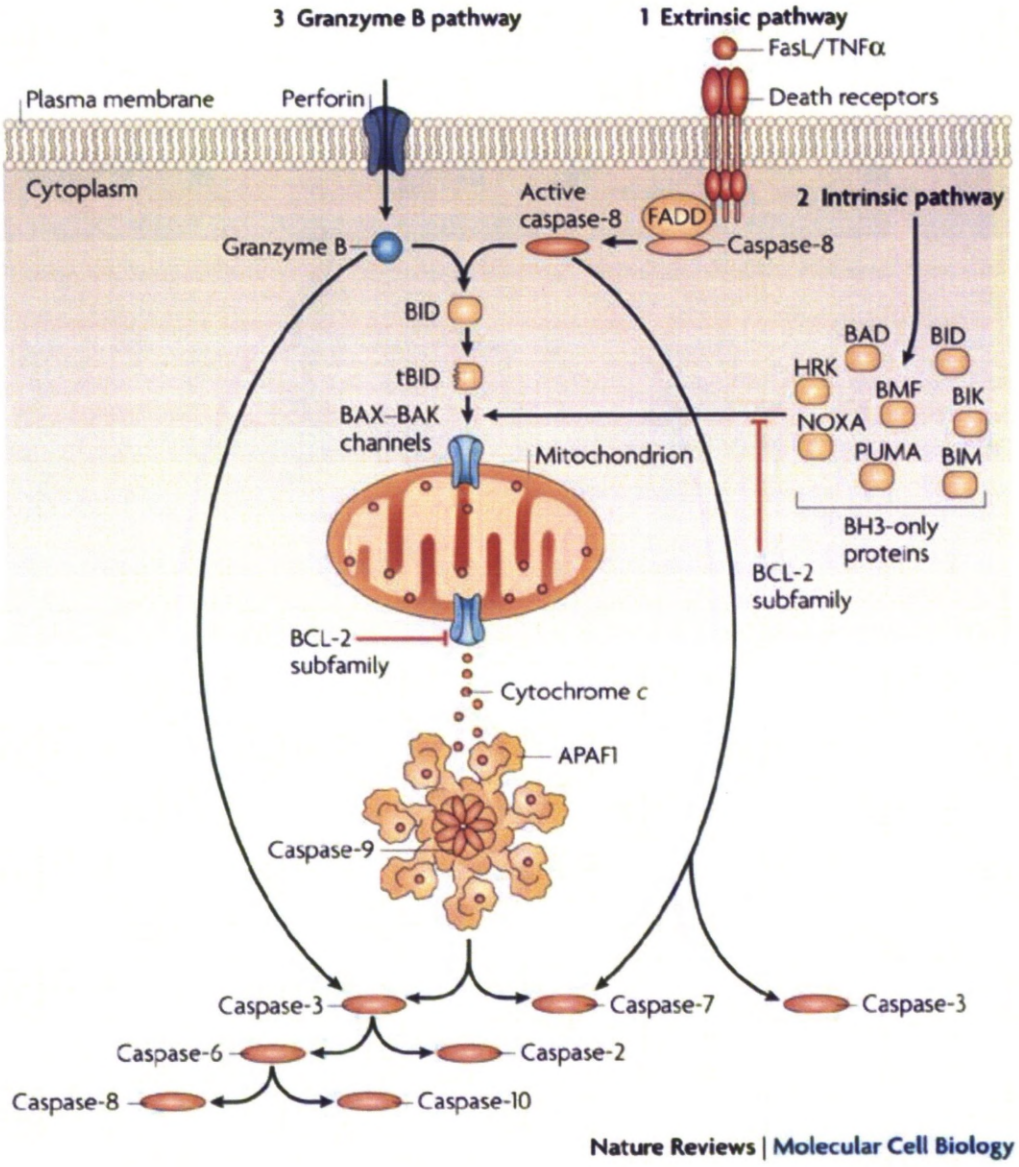


***Figure 1.4.8: Caspase activation pathways.***

*Image taken from [Taylor et al., 2008]. The caspase cascade and cell death can be triggered in three (not necessarily exclusive) ways. 1) The extrinsic pathway 2) the intrinsic pathway and 3) the granzyme B pathway (see text for details). Importantly the intrinsic pathway relies on Bax/Bak oligomerisation and the formation of channels in the mitochondrial membrane to allow the release of cytochrome c which then goes on to form the apoptosome and caspase 9 auto-activation, whereas the extrinsic pathway and granzyme B pathway can also activate the executioner caspases independently of the mitochondria.*

### *1.4.5.1 Apoptosis – downstream p53 targets*

The tumour suppressor gene *TP53* can initiate the intrinsic and extrinsic apoptotic pathways by up-regulating specific genes following its activation. For example p53 can up-regulate death receptor KILLER/DR5 in response to DNA damage induced by chemotherapeutic agents or by ionising radiation [Wu et al., 1999, Wu et al., 1997]. KILLER/DR5 activates the extrinsic death pathway once it is bound by its death ligand TRAIL (TNF-related apoptosis inducing ligand) in a similar manner to the Fas/TNF-R death receptors (see Section 1.4.5). p53 can also up-regulate CDIP (cell death involved p53-target), in response to genotoxic stress [Brown et al., 2007]. CDIP induces apoptosis in a caspase-8 dependent manner that implicates it in the extrinsic death pathway. In the mitochondrial intrinsic cell death pathway p53 can up-regulate key players such as; Bcl-2 pro-apoptotic protein family members Bax, Bid, Noxa and Puma in response to DNA damage.

The process of p53 induced apoptosis is far more complicated than just activating genes that promote apoptosis – as p53 does not always up-regulate the same pro-apoptotic target genes in every cell type or under every type of stimuli (for example DNA damage, hypoxia, oncogenic stress, UV light, free radicals etc) [Vousden, 2006]. p53, in fact, up-regulates a wide range of downstream target genes which often have redundant or cooperative roles in apoptosis. Since a large number of these target genes belong to the pro-apoptotic *"club"* and due to the complicated nature of how these gene interact under different conditions, there is not yet one p53 target gene that can account for the whole apoptotic response [Vousden and Lu, 2002]. In addition, p53 can act independently of transcription and initiate apoptosis by acting like a BH3-only protein in the cytoplasm of cells [Vousden, 2006]. In summary, the p53-dependent apoptotic pathways are very complex with tissue specific and stress specific responses which make it imperative that the unique properties of each candidate gene are examined when selecting between them to act as a reliable reporter for p53 activation in the gastrointestinal tract. Below the candidate genes Bax, Puma, Noxa and Bid are discussed.

### 1.4.5.2 The Multidomain Bcl-2 Proteins: Bax (and Bak)

**Bax** is a multidomain member of the Bcl-2 family [Cory et al., 2003, Danial and Korsmeyer, 2004] and is transcriptionally up-regulated by p53 [Wu and Deng, 2002] although, surprisingly (as expression of Bax (and Bak) is associated with apoptosis in rats and humans [Bowen et al., 2005]), it appears to play only a minor role in DNA damage induced apoptosis in the intestinal gut epithelia of mice [Pritchard et al., 1999, Watson and Pritchard, 2000]. Therefore, Bax would not appear to be the best candidate gene to act as a p53-responsive reporter gene in the gastrointestinal tract. Since the multidomain Bcl-2 proteins are required to create the pores in the outer mitochondrial membrane which initiates MOMP and cytochrome *c* release, the upstream BH3-only proteins cannot initiate apoptosis without them (the multidomain Bcl-2 family proteins) [Zong et al., 2001, Cheng et al., 2001, Wei et al., 2001]. Therefore, if Bax is not responsible for the induction of apoptosis in the intestinal gut epithelia then perhaps other Bcl-2 multidomain proteins are.

**Bak** – one potential candidate – is not thought to be, nor has it yet been identified as a transcriptional target of p53 [Cory et al., 2003] instead Bak is transcriptionally up-regulated by IFN-Gamma [Ossina et al., 1997] and thus would not be a good candidate as a reporter gene for p53 activation in the gut.

Bax and Bak are activated and controlled either directly or indirectly by BH3-only proteins [Fletcher and Huang, 2008, Willis and Adams, 2005, Willis et al., 2007]. Indirect activation occurs by displacement of Bak from Bcl-2 pro-survival members (Mcl-1 and Bcl-$_{xL}$) by BH3-only proteins such as Noxa [Willis et al., 2005]. Direct activation of Bax/Bak occurs in a two step process involving *"sensitizer"* BH3-only proteins like Bad, which bind to and inactivate the anti-apoptotic Bcl-2 members and *"activators"* (for example Bid) which bind Bax/Bak at the mitochondrial outer membrane to induce cell death [Willis and Adams, 2005, Zinkel, 2008]. Evidence also exists for protein-protein interactions between p53 and Bax/Bak in the cytoplasm of cells whereby p53 acts in a transcription-independent manner (similar to the BH3-only protein Bid) to initiate apoptosis [Chipuk et al., 2004, Pietsch et al., 2007].

To determine whether the roles of Bax and Bak are mutually exclusive, knock-out mice have been generated. Mice lacking either Bax or Bak develop normally with only minor

aberrations in apoptosis, whilst doubly deficient mice rarely survive to birth (only 10% survive embryogenesis) [Lindsten et al., 2000]. This indicates that Bax and Bak have overlapping (presumably partially redundant) roles in apoptosis during embryogenesis. Such studies seem to indicate that Bak may compensate in the absence of Bax in the intestine, and/or that Bax and Bak complement each other in their mechanism of action [Degli Esposti and Dive, 2003]. In a closely related tissue (the stomach) both Bax and Bak regulate ionising radiation induced apoptosis in proliferative regions of gastric epithelia [Przemeck et al., 2007]. This has yet to be investigated in detail in the epithelium of the gastrointestinal tract, but research into the endothelial cells shows Bax and Bak play non-redundant roles in response to ionising-radiation [Rotolo et al., 2008]. In summary the multidomain Bcl-2 family members do not appear to be good reporters of p53 activity. The next section of this report focuses on the BH3-only proteins which act upstream of Bax/Bak to induce apoptosis.

### *1.4.5.3 The BH3-Only Proteins: Puma, Noxa and Bid*

The BH3-only members of the Bcl-2 family are a diverse group of pro-apoptotic proteins, including: Bim, Bmf, Hrk, Bad, Puma, Noxa and Bid (among others see Figure 1.4.6). Characteristically, the only area of homology that BH3-only proteins share is the BH3 domain (see Section 1.4.5). The BH3 domain is a short 9-16 amino acid sequence that forms (with surrounding residues) an amphipathic helix capable of binding the anti-apoptotic Bcl-2 family members [Huang and Strasser, 2000].

BH3-only proteins are either absent or inactive in an unstressed cell. However, in response to various cellular stress stimuli, each BH3-only protein plays a unique role in inducing programmed cell death [Shibue and Taniguchi, 2006] (see Figure 1.4.9). Bim and Bmf, for example, are cytoskeletal proteins that contribute to anoikis when there is a disruption of the cytoskeleton [Puthalakath et al., 2001]. BH3-only proteins can be regulated by post-translational modifications, including phosphorylation. For example, Bad undergoes phosphorylation in the presence of growth factors [Zha et al., 1996, Bergmann, 2002] which renders it inactive. However upon de-phosphorylation (caused by the lack of appropriate growth factors) Bad becomes active and exerts its pro-apoptotic effects.

Puma, Noxa and Bid are a subset of BH3-only proteins up-regulated by tumour suppressor gene *TP53* in response to DNA damage [Wu and Deng, 2002, Sax et al., 2002]. Since *Puma, Noxa* and *Bid* are all transcriptional targets of p53; these genes are potential candidates to be used as a p53-responsive reporter gene. The suitability of Puma and Noxa as p53-reporter genes is discussed first; followed by Bid.

The role of **Puma** and **Noxa** in p53-mediated apoptosis is not fully understood. The reason(s) why p53 recruits either Puma or Noxa (or both) to instigate cell death remain(s) to be elucidated. Several lines of evidence collectively indicate that the contribution of Puma and Noxa to p53-mediated apoptosis is determined by cell type and cell state [Vousden, 2006]. Studies using Puma and Noxa knock-out mice have been used to further investigate the respective roles of each protein; these will be discussed below.

Mice lacking either Puma and/or Noxa were generated to test whether or not the p53-dependent roles of these two proteins in apoptosis overlap [Michalak et al., 2008]. These mice developed normally (with respect to their appearance, behaviour and health) and did not appear to be susceptible to tumour development (no tumours seen in mice up to a year old). In contrast, mice deficient in p53 developed a wide range of tumours and most had died by 6 months of age [Donehower et al., 1992] (and see Section 1.4.4). Mice doubly deficient in Puma and Noxa, whilst not susceptible to tumour formation, did however show an impaired apoptotic response in several tissues and cell types [Michalak et al., 2008]. In all of the cell types examined, Puma (rather than Noxa) consistently played a major role in inducing apoptosis. Indeed, following DNA damage in mature T and B cells in the spleen, Puma alone was responsible for inducing cell death in a p53-dependent manner. In other cell types, such as cultured thymocytes and mouse embryonic fibroblasts (MEFs) expressing oncogene E1A, Noxa also contributed to apoptosis [Shibue et al., 2006, Shibue et al., 2003]. Interestingly, MEFs lacking Puma (or both Puma and Noxa) and expressing oncogene E1A did not undergo apoptosis even at very high doses of γ-irradiation (50 Gy) whilst $p53^{-/-}$ MEFs were still vulnerable [Michalak et al., 2008]. Presumably this is because $p53^{-/-}$ MEFs cannot induce cell cycle arrest; hence the cells die later (24 hours after irradiation) from catastrophic errors in mitosis.

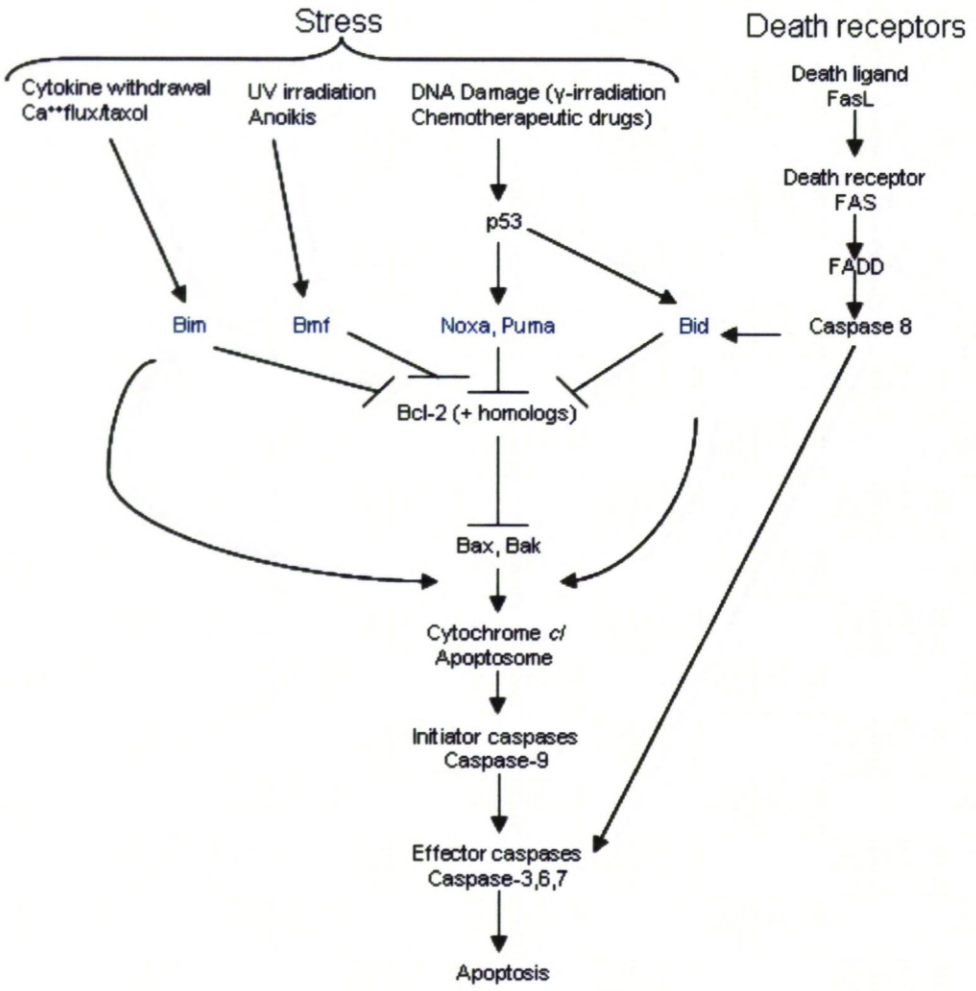


***Figure 1.4.9: Different stress conditions activate different BH3-only protein responses.*** *Adapted from [Puthalakath and Strasser, 2002] and [Cory et al., 2003]. BH3-only proteins are shown in blue text. Bim and Bid can activate Bax/Bak directly (as can Puma and p53) [Willis and Adams, 2005] and Bid has been shown to be up-regulated in some tissues by p53 (including the intestine) [Sax et al., 2002]. Bim and Bmf reside in separate cytoskeletal compartments and Bmf is released during anoikis [Puthalakath et al., 2001]. Noxa and Puma are up-regulated by tumour suppressor gene p53 [Wu and Deng, 2002].*

Deletion of both Puma and Noxa in some cell types (thymocytes and fibroblasts expressing oncogene E1A) completely recaptured a p53-null phenotype during the early apoptotic response to DNA damage; demonstrating their importance in p53-dependent cell

death [Michalak et al., 2008]. There are additional roles for p53 in the apoptotic response apart from inducing *Puma* and *Noxa*. For example, $p53^{-/-}$ mature B cells did not undergo any apoptosis in response to DNA damage whilst $Puma^{-/-}$ and $Noxa^{-/-}$ mature B cells still underwent some apoptosis. p53 must therefore have other unidentified target genes in mature B cells that play a role in apoptosis in these cells. Similarly, Puma and Noxa have apoptotic roles that don't rely on p53 activation and these p53-independent roles are discussed next.

Both Puma (p53 upregulated modulator of apoptosis) and Noxa (Latin for *damage* [Oda et al., 2000]) can act in a p53-dependent and independent manner to induce apoptosis [Jeffers et al., 2003]. It has been demonstrated that Puma plays a role in p53-independent cell death of primary thymocytes, including death induced by the addition of glucocorticoids (mechanism of death unknown [Wyllie, 1980]) or by serum deprivation [Jeffers et al., 2003, Han et al., 2001]. Puma also has p53-independent roles in inducing apoptosis as a result of ischaemia-reperfusion in the intestine [Wu et al., 2007] and in chronic colitis [Dirisina et al., 2011]. In contrast Noxa appears to only play a p53-independent role under hypoxic conditions. During hypoxia Noxa is up-regulated by hypoxic-inducible factor 1 α (HIF-1α) and contributes to cell death by generation of reactive oxygen species (ROS) [Kim et al., 2004].

Puma and Noxa, just like many other p53 inducible genes, have a consensus p53 REs in their promoter regions (see Section 1.4.1) that allow them to be transcribed by p53 [Oda et al., 2000, Nakano and Vousden, 2001]. However, Puma and Noxa differ in the mode of induction by p53. Whilst *Puma* requires both trans-activation domains of p53 to be intact for activation either domain seems to be sufficient for the induction of *Noxa* [Cregan et al., 2004]. The differential regulation of Puma and Noxa is thought to provide a mechanism for the differences observed in expression and activation of the two genes [Shibue and Taniguchi, 2006].

An important difference between Puma and Noxa is in their ability to bind to other Bcl-2 family members. Puma potently binds to all the Bcl-2 pro-survival family members whereas Noxa is more selective, binding only to Mcl-1 and (weakly) A1 [Fletcher and Huang, 2008, Chen et al., 2005] (see Figure 1.4.10). Puma may also directly activate Bax on the mitochondrial membrane to induce cytochrome *c* release [Cartron et al., 2004], however the

evidence for this remains controversial [Fletcher and Huang, 2008]. Noxa acts mainly through Bak (rather than Bax) but cannot directly activate either Bak or Bax [Letai et al., 2002]. Noxa can, however, displace Bak from Mcl-1, leaving Bak "*free*" (i.e. Bak which is no longer bound to its negative regulators Mcl-1 and Bcl-$x_L$) in the cell, ready to induce cell death upon a further stimulus [Willis et al., 2005].

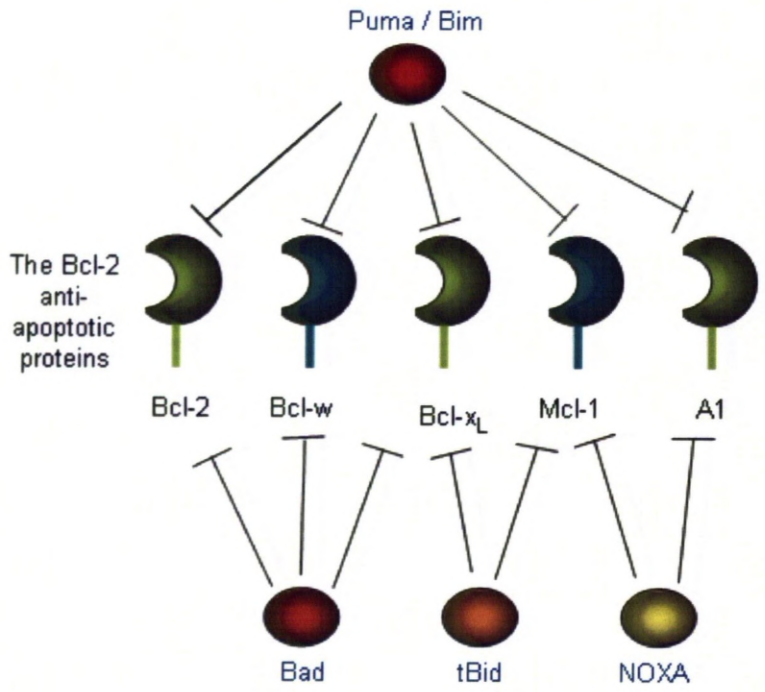


***Figure 1.4.10: BH3-only proteins can have selective or 'promiscuous' binding.***

*Adapted from [Fletcher and Huang, 2008]. BH3-only proteins are shown in blue text. Puma and Bim are "promiscuous", binding to and neutralising all pro-survival Bcl-2 family members. Bad, tBid and Noxa are more selective. Bad binds with Bcl-2, Bcl-w and Bcl-$x_L$, tBid binds Bcl-$x_L$ and Mcl-1 while Noxa neutralises Mcl-1 and A1.*

Puma and Noxa have different roles and mechanisms of action in the induction of apoptosis. Puma can be described as an *"effector"*, whereas Noxa is a *"sensitizer"* (see Section 1.4.5.2). Each of the unique properties of Puma and Noxa should be taken into consideration when choosing between the two genes to act as a reliable reporter for p53 activation in the gastrointestinal tract. For instance, since Puma has many p53-independent activities, its suitability as a true p53 reporter gene could be called into question. As Noxa acts as a sensitizer towards cell death, it may not be the gene of choice to be an accurate reporter of apoptosis. The role of Puma and Noxa in the gastrointestinal tract in response to DNA damage will now be discussed in an attempt to further evaluate their suitability as p53 reporter genes.

There is evidence that Noxa plays a role in p53-mediated apoptosis in the gastrointestinal tract based on the analysis of Noxa and p53 knockout animals [Shibue et al., 2003]. When wild-type mice, Noxa knockout mice and p53 knockout mice were each exposed to 10 Gy of x-ray-irradiation to induce DNA damage and had their jejunums harvested for analysis of apoptosis 6 hours later, it was observed that apoptosis was induced in the crypt region of the small intestine of the wild-type animals in the expected manner (see Section 1.2.5). Mice lacking Noxa showed a two-fold reduction of apoptosis, but in p53 knockout mice this acute apoptotic response in the small intestine was completely abrogated [Shibue et al., 2003]. Therefore, the apoptosis seen in the small intestine is completely p53-dependent (in agreement with previous studies [Merritt et al., 1994]), thus since Noxa only contributes to apoptosis in the small intestine when p53 is present, Noxa must have been induced, or otherwise activated by p53. However, Noxa cannot be the only target gene p53 up-regulates in response to DNA damage in the gastrointestinal tract as apoptosis still occurred in Noxa knockout mice. Noxa may share responsibility for inducing apoptosis with other genes [Nakajima and Tanaka, 2007, Fei et al., 2002] (such as *Puma* and *Bid*-discussed later in this section) and perhaps one of these would be better suited as a p53-responsive reporter gene. Noxa would not seem to be an ideal reporter gene for the apoptotic arm of the p53 response to DNA damage as the expression of Noxa does not always correlate with either p53 status or with the induction of apoptosis [Fei et al., 2002].

It has been demonstrated that Puma plays a major role in DNA damage induced apoptosis in the intestinal gut epithelium [Qiu et al., 2008]. Recent research into the regulators of gastrointestinal syndrome has implicated Puma as a key regulator of radiosensitivity. Radiotherapy is one commonly used method for treating cancer, however a major limitation in radiotherapy is gastrointestinal toxicity caused by the radiation. Mice that receive a γ-irradiation dose of greater than 14 Gy die at 7-10 days after treatment from damage to the small intestine [Komarova et al., 2004]. The lethal damage is initiated by a massive p53-dependent apoptotic response [Merritt et al., 1994] and cell death continues to occur later as a result of aberrations in cell division which are p53-independent [Merritt et al., 1997]. As Puma is a downstream apoptotic target of p53 activation [Nakano and Vousden, 2001], Puma knockout mice were generated to investigate whether Puma plays a role in the DNA damage induced apoptosis in the small intestine.

It has been shown in wild-type mice that Puma was rapidly up-regulated in response to a range of doses of γ-irradiation (8-18 Gy) in an exclusively p53-dependent manner [Qiu et al., 2008]. The induction of Puma (and p53) was contained within the crypt region of the small intestine, specifically in cell positions 0-6 (associated with the speculated stem cell position and progenitor cells [Potten et al., 1997a, Barker et al., 2007] – and see Section 1.2.1). As expected, Puma knockout mice underwent less irradiation induced apoptosis in the small intestine than the wild-type mice. At low doses of γ-irradiation (8 Gy) apoptosis was blocked to a similar degree between Puma knockout mice and p53 knockout mice during early stages (4 hours) after treatment. However, later on (24 hours) or when higher doses of γ-irradiation were used (>15 Gy), p53 knockout mice showed higher levels of apoptosis than the Puma knockout mice. One explanation for this difference in apoptotic rates between Puma knockout and p53 knockout mice could be that p53 knockout mice fail to activate the cell cycle arrest gene *p21*, hence there is a profound increase in cell proliferation in these mice. The increased cell proliferation accelerates the rate of gastrointestinal syndrome and consistent with this, p53 knockout mice die 3.5 days earlier than wild-type mice following exposure [Qiu et al., 2008, Komarova et al., 2004]. Puma knockout mice were, however, significantly protected against gastrointestinal syndrome, surviving approximately 50% longer than the wild-type mice. As Puma is up-regulated by p53 and is responsible for much of the

p53-dependent apoptotic response in the small intestine it would seem to be an ideal p53-responsive reporter gene.

One research group have already used p53 REs found in the *Puma* promoter region to examine the expression of p53/Puma *in vivo* [Briat and Vassaux, 2008]. Brait and Vassaux designed a construct that contained four copies of the human Puma p53 RE, upstream of a minimal promoter that drove the expression of the Firefly Luciferase (Luc) gene to generate the p53RE-Luc reporter mice. These mice were examined using bioluminescence imaging 24 hours prior to and 24 hours post administration of the chemotherapeutic drug, Doxorubicin (Dox), and it was found that luciferase activity was increased (by 4-fold) in the lower abdominal region in male (but not female) mice. Dox is thought to prevent DNA and RNA synthesis by interaction with nucleic acids [Momparler et al., 1976] making it a useful cancer therapy however Dox is also known to be very toxic to the testes [Yeh et al., 2009]. The p53RE-Luc transgenic mice provide a reliable indication of where p53/Puma is being activated in response to Dox testicular toxicity, which is thought to be caused by oxidative stress and cellular apoptosis (dependent on p53). Whilst the p53RE-Luc transgenic mice are a useful system to test drug toxicity, these mice do not report genuine endogenous Puma or p53 activity. The pro-nuclear injection method used to create these mice means that the p53RE-Luc construct has been randomly integrated into the host DNA and expression is thus subject to positional bias [Ittner and Gotz, 2007]. In addition, there are 4 REs, whilst in the endogenous Puma promoter only 2 are present [Nakano and Vousden, 2001]. One way of overcoming both of these problems is by generating a knock-in reporter mouse that would contain a reporter construct inside the actual *Puma* gene, thus reporting genuine *Puma* activation.

The third p53-inducible BH3-only gene we are examining for suitability as a p53-responsive reporter gene is Bid. Bid (BH3 interacting death agonist) is an interesting BH3-only gene as it is involved in both the intrinsic and the extrinsic cell death pathways (see Figure 1.4.9). Briefly, as described previously in Section 1.4.5, engagement of the death receptors Fas or TNF-R1 leads to the formation of DISC. DISC recruits caspase-8 through interaction with FADD [Boldin et al., 1996, Muzio et al., 1996]. Caspase-8 is rapidly activated (probably by autocatalysis within the protein complex [Cryns and Yuan, 1998]) and in turn

activates other caspases, triggering the caspase cascade. Activated caspase-8 also cleaves full length cytoplasmic Bid (p22) into a truncated active fragment known as tBid (p15) [Li et al., 1998]. tBid translocates to the mitochondria [Gross et al., 1999] where it can bind to and inactive Bcl-2 pro-survival family members Bcl-$x_L$ and Mcl-1 [Fletcher and Huang, 2008] as well as directly activate Bax/Bak [Willis and Adams, 2005, Walensky et al., 2006]. The balance of Bcl-2 family proteins, in this case, shifts towards pro-apoptotic Bcl-2 family members and consequently allows the release of cytochrome *c* from the inter-membrane space of the mitochondria [Danial and Korsmeyer, 2004]. tBid thus connects the activation of the death receptors Fas/TNF-R1 which is an essential part of the extrinsic apoptotic pathway with the rapid release of cytochrome *c* and hence activation of the intrinsic mitochondrial apoptotic pathway [Luo et al., 1998, Li et al., 1998].

*Bid* knockout mice were generated to examine the role of Bid in inducing apoptosis *in vivo*. *Bid* deficient mice developed normally, but whilst wild-type mice died within 4 hours following an injection with an antibody that binds Fas as a result of hepatic apoptosis and haemorrhagic necrosis, Bid null mice survived [Yin et al., 1999]. This suggests that Bid is critical for hepatocyte apoptosis induced by activation of the death receptors Fas/TNF-R1 [Yin, 2000]. Other cell types such as MEFs and thymocytes do not strictly require Bid to induce apoptosis in response to treatment in culture with an anti-Fas antibody [Yin et al., 1999]. However, Bid deficiency effectively delayed onset of apoptosis in MEFs and thymocytes (following activation of the Fas/TNF-R1 pathway) implying that whilst Bid is not essential in these cell types for initiation of apoptosis, it does contribute pro-apoptotic signals. It has been suggested that the activation of the mitochondrial pathway (and hence cleavage of Bid) following death receptor engagement is only essential in inducing apoptosis in certain cell types, also called type II cell lines [Scaffidi et al., 1998]. Hepatocytes might therefore belong to this class of cells [Yin et al., 1999].

Whilst Bid's involvement in the extrinsic death pathway in type II cells has been well characterised [Yin et al., 1999], its role in DNA damage induced apoptosis remains controversial. In some studies Bid deficient MEFs and myeloid progenitor cells (isolated from Bid knockout mice) were less susceptible to a variety of DNA damaging reagents than wild-type cells [Sax et al., 2002, Zinkel et al., 2005, Kamer et al., 2005], whereas another study

showed no role for Bid in DNA damage induced apoptosis [Kaufmann et al., 2007]. Nonetheless, Bid is up-regulated by p53 in response to γ-radiation in the colonic epithelium and in splenic red pulp [Sax et al., 2002]. Bid was also up-regulated in a p53 dependent manner in Campthothecin (a chemotherapy drug) treated neurones [Jacobs et al., 2007]. It is worth mentioning that although there may be a minor role for full length Bid in apoptosis [Goonesinghe et al., 2005], tBid is far more potent at inducing mitochondrial dysfunction and cytochrome *c* release [Li et al., 1998, Luo et al., 1998, Yin et al., 1999], therefore to induce apoptosis it is generally accepted that Bid has to be cleaved into tBid [Shelton et al., 2009].

In addition to Bid being cleaved by caspase-8 as part of the death receptor pathway [Li et al., 1998], Bid can also be cleaved by calpains, Granzyme B, cathepsins [Yin, 2006] and other executioner caspases (caspase-3 and caspase-2) [Bonzon et al., 2006, Shelton et al., 2009]. Bid, however, cannot be cleaved into tBid by p53 directly, so how Bid up-regulation by p53 contributes to the induction of apoptosis is uncertain. In neurones the death receptor pathway becomes activated as part of treatment with Campthothecin [Jacobs et al., 2007] thus caspase-8 is recruited and can readily go on to cleave and activate Bid. Therefore, in Campthothecin treated neurones Bid cleavage appears to be an upstream event in MOMP (mitochondrial outer membrane permeabilization see Section 1.4.5). In contrast, in the colonic epithelium there is no known death receptor activation during γ-radiation, therefore p53 up-regulated Bid can only be cleaved once executioner caspases are present implying that Bid cleavage is a downstream event. In the case of the colonic epithelium, Bid may act to amplify cell death signals, irreversibly committing cells to death in a *"feed forward"* loop [Shelton et al., 2009]. Whether Bid acts as an initiator of MOMP consistent with its role in the death receptor pathways or as a sensitizer which may be the case in the colon seems to depend on the cell type and the type of DNA damaging agent used.

Interestingly, an analysis of Bid expression by *in situ* hybridisation in wild-type mice and p53 null mice showed that Bid was induced in a p53-dependent manner in response to ionising radiation in the transverse colon, but not in the small intestine [Fei et al., 2002]. Bid was, however, constitutively expressed in $p53^{+/+}$ mice small intestine, but not in small intestine of $p53^{-/-}$ mice or in the colon. Since cells in the small intestine more readily undergo apoptosis than cells in the colon [Merritt et al., 1995], it is possible that Bid expression

contributes to the increased sensitivity in the small intestine. However, as Bid is expressed constitutively in the small intestine (albeit in a p53-dependent fashion) it cannot be used as an indication of p53 activation of apoptosis, which would be an essential property to any gene selected to be part of our p53-responsive reporter system. In addition, Bid may not be an ideal p53-responsive reporter gene as Bid is also a critical part of the death receptor pathway which may or may not be involved in the response to DNA damaging agents.

A final consideration, when deciding between Puma, Noxa and Bid as p53-responsive reporter genes, is to examine their status in colorectal cancer. If these genes are important in the development of cancer in the intestine it is likely they will be either mutated or have an altered expression pattern in the cancerous tissue when compared to healthy tissue. Indeed, Puma was highly expressed in human colorectal carcinomas when compared with normal tissue [Kim et al., 2007] and Bid was either over-expressed which was associated with good prognosis or lost altogether which when combined with over expression of Puma was associated with the worst prognosis for patient survival [Sinicrope et al., 2008]. Noxa expression did not have any association with the development of colorectal cancer [Jansson et al., 2003]. Since Puma and Bid can be over-expressed during tumour development in the intestine, this could appear to conflict with a positive role in apoptosis. However, it may also be interpreted as; the cancer has evolved to uncouple Puma and Bid from their apoptotic responses (perhaps via up-regulation of the pro-survival Bcl-2 family members) hence their levels become elevated to compensate. As Bid can also be lost altogether then this may indicate a further need for the cancer to bypass its apoptotic properties in order to progress. This data might suggest that Puma and Bid play a more important role in this tissue then Noxa – as they are manipulated during tumour development, whilst Noxa is not. However, as these types of studies are not directly related to the p53-dependent apoptotic response to DNA damage, it is unclear how relevant such data is when making a decision of which gene to use as a p53-responsive reporter.

Before selecting a downstream marker for p53-mediated apoptosis in the gut some of the discrepancies would need to be resolved. Puma expression, for example, when examined by two groups showed either no up-regulation [Fei et al., 2002] or rapid up-regulation [Qiu et al., 2008] in response to ionising radiation. Since both groups used *in situ*

hybridisation as a detection method and the mice used were on a C57BL/6 genetic background in both cases it is unclear how these two very different results arose. One explanation might be that Fei *et al* could have looked at the whole gut, including the sub-mucosa and endothelial cells (the literature does not specify what cells were examined for staining) whereas Qiu *et al* specifically focused on the epithelial crypt cells in the small intestine. Qiu *et al* also performed real-time PCR and western blotting to confirm that Puma expression which further supports their conclusions. In conclusion, therefore, it appears that Puma is the best candidate gene to compliment p21 in a dual cell cycle arrest/apoptosis p53-responsive reporter system.

# 1.5 Genetic manipulation

## 1.5.1 Gene-trapping: a public resource

Gene-trapping is a high-throughput approach to inserting mutations into genes. Gene-trap mutagenesis can be used to randomly generate loss-of-function genes in undifferentiated ES cells whilst simultaneously introducing a reporter to monitor endogenous gene expression [Skarnes et al., 2004]. Genes are *"trapped"* in ES cell lines by introduction of a vector (that contains a reporter gene (like *LacZ*) and a selectable marker (typically neomycin- which confers resistance to G418 an amino-glycoside antibiotic)) by either retroviral infection or electroporation [Stanford et al., 2001]. These cell lines are then screened using a PCR based technique called 5'RACE (5' rapid amplification of cDNA ends [Schramm et al., 2000]) which provides a sequence tag to BLAST (Basic Local Alignment Search Tool) and identify the gene affected (including novel genes) [Stryke et al., 2003]. Gene-trap mutagenesis overcomes some of the difficulties associated with more traditional mutation methods (such as x-ray, chemical mutation and gene-targeting) since it will only report endogenous gene expression and requires no previous knowledge of the genomic sequence. Gene-trapping can also be scaled up and used intensively to generate large libraries of gene-trapped ES cells [Skarnes et al., 2004].

These libraries can be searched through the IGTC (International Gene-Trap Consortium) website (http://www.genetrap.org/) [Nord et al., 2006] and cell lines are often available to the research community on a cost recovery basis from the MMRRC (Mutant Mouse Regional Resource Centers). The MMRRC acts as a repository for ES cell lines (and mouse strains), with many groups donating their mutated alleles (for example SIGTR, Sanger Institute Gene Trap Resource and BayGenomics) for use in creating transgenic mice [Stryke et al., 2003]. It is hoped that with use of multiple vectors (containing new designs to overcome insertion bias [Skarnes et al., 2004]) and different vector delivery methods (retroviral infection vs electroporation) that the genome will become saturated with gene-traps and thus there will eventually be an ES cell line available for almost every gene [Stanford et al., 2001].

There are three main gene-trap strategies exploiting different vector designs; the enhancer, promoter and gene-trap (see Figure 1.5.1) [Stanford et al., 2001]. As described above all vectors will have a reporter gene of some kind and a selectable marker, which can be the same thing, for example β-geo is a fusion protein between β-galactosidase (from *LacZ*) and neomycin [Friedrich and Soriano, 1991]. The enhancer-trap contains its own promoter which will, if it has inserted near to an enhancer region become active when the endogenous gene is activated. However, this does not always lead to the gene being disrupted (often genes can splice around the vector creating a truncated protein that may contain partial function) hence enhancer-traps often create hypomorphic mutations rather than nulls and as such are not widely used in the creation of knock-out mice [Stanford et al., 2001].

The promoter-trap has essentially the same structure as the enhancer-trap, except it is promoterless, which changes its functionality. For promoter traps to mutate a gene and successfully report that genes expression it must insert into an exon, thus creating a fusion transcript of the upstream endogenous gene with the vectors reporter. This has the advantage of almost always creating a mutation (usually null) but the disadvantage of low trapping frequency, as the probability of integrating in an exon is relatively low, since introns are generally much longer than exons [Stanford et al., 2001].

The last of these three strategies, utilising the gene-trap vector tries to overcome both these disadvantages. The gene-trap vector contains a splice acceptor upstream of a promoterless reporter and thus once integrated can be activated from the endogenous promoter from within the introns of genes. This design creates a fusion protein between the upstream coding region of the endogenous gene and the reporter (commonly β-geo) simultaneously interrupting the gene and reporting its expression (see Figure 1.5.2) [Stanford et al., 2001]. Gene-trap vectors have a relatively high trapping frequency and a high probability of causing a null mutation, especially if integrated towards the 5' ends of genes. There is a strong bias for gene-traps to insert in the 5' ends of genes with retroviral infection [Friedrich and Soriano, 1991]). A disadvantage of this kind of gene-trap is it requires the gene to be expressed in undifferentiated ES cells, meaning genes that are important later on in development will not be targeted.

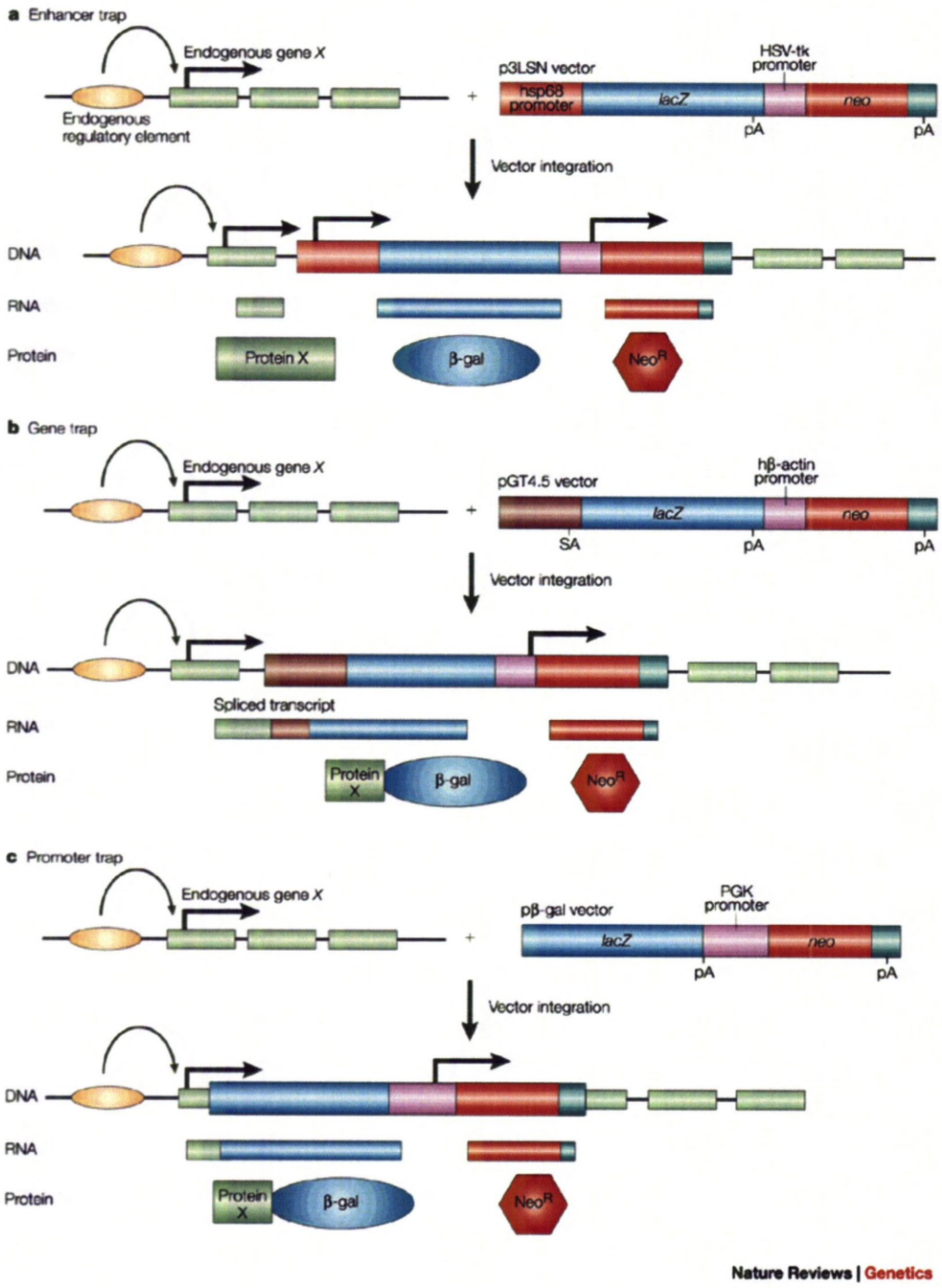


***Figure 1.5.1: The basic trap vectors.***

*Taken from [Stanford et al., 2001]. A) The enhancer-trap vector B) The gene-trap vector and C) The promoter-trap vector. See text for details.*

When generating transgenic animals one of the rate limiting steps is the development of a carefully planned targeting construct, since it requires in-depth knowledge of the gene's structure and sequence and is very labour intensive [Stanford et al., 2001]. Large libraries of gene-trapped ES cells have been developed and these enable researches to rapidly identify candidate ES cell clones with a gene-trap for their gene of interest. The idea being to provide the research community with low-cost, easily available, pre-targeted ES cell lines which can be used to produce knock-out mice [Skarnes et al., 2004, Stryke et al., 2003, Hansen et al., 2003]. Several research groups have used such gene-trapped ES cell clones and have demonstrated that this system can accurately report endogenous gene expression whilst simultaneously mutating the gene it has integrated into [Skarnes et al., 1992, Stoykova et al., 1998]. Our project would therefore use the public gene-trap libraries to identify ES cell lines with a gene-trap in the p53-responsive genes p21 and Puma to demonstrate in principle that this knock-in approach can report authentic expression of both these genes.

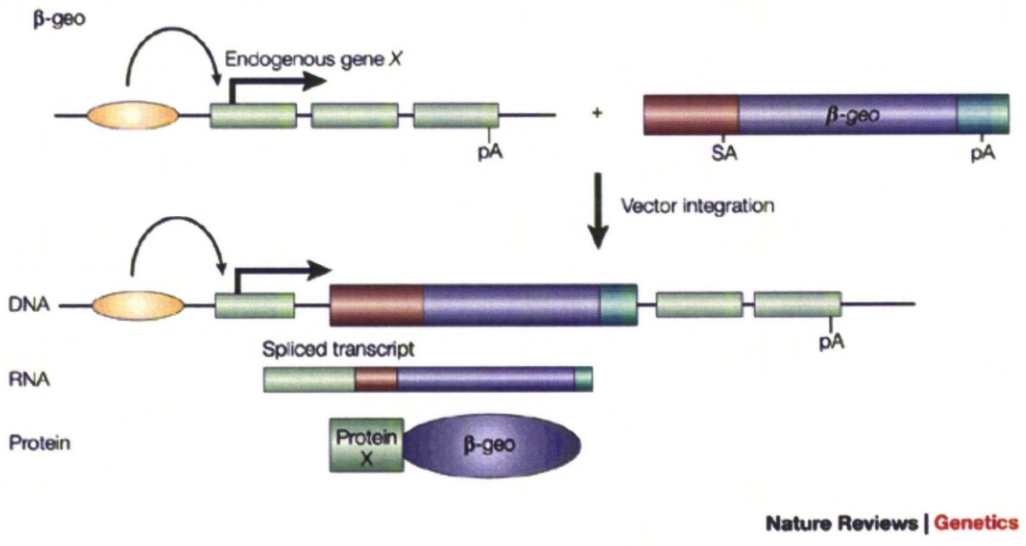


***Figure 1.5.2: β-geo gene-trap vector.***

*Taken from [Stanford et al., 2001]. The fusion transcript created by vector integration into a gene's intronic region generates a fusion protein consisting of a truncated protein from the endogenous gene X and β-geo (a fusion of the lacZ gene and neomycin phosphotransferase).*

Gene-trap technology cannot be used to insert subtle mutations, such as those required when creating either an *Mdm2 P1* or *P2* promoter-less mouse. Therefore the next section of this report discusses BAC clones and how (and why) we plan to use them as rich sources of DNA for generating the arms of homology and for sequencing the P2 region of Mdm2.

### 1.5.2 BAC clones

Bacterial Artificial Chromosomes or BAC Clones are large fragments of genomic DNA that have been spliced into a bacterial plasmid, such as F-Factor plasmids in *E.Coli* [O'Connor et al., 1989]. They can accept and maintain > 300Kb DNA fragments, acting as a method of storing and easy amplification of genomic DNA [Shizuya et al., 1992].

Gene-targeting in ES cells uses homologous recombination to target a specific locus, the efficiency of which can be determined by regions of homology in the targeting vector to genomic DNA. Identical sequences maximise the targeting efficiencies and different mouse strains can make a substantial difference to homologous recombination frequencies [te Riele et al., 1992]. Equally the construction of a vector to specifically target and mutate/delete either the P1 or the P2 locus of Mdm2, leaving the rest of the gene intact and functioning normally requires the exact sequence at and around these loci.

The mouse genome project was based on the C57BL/6J mouse strain while the first ES cells were derived from 129 strains leading to the majority of gene targeting being carried out in these substrains or from crosses between 129 mice and other inbred strains [Adams et al., 2005]. Thus it is important to have the exact sequence of Mdm2 and surrounding regions (+/- 5Kb) in the 129Sv mouse strain for a successful targeting event.

A 129Sv BAC library resource exists and is available to view alongside the C57BL/6J genome in Ensembl browser [Adams et al., 2005]. Three BAC clones span the Mdm2 region (see Figure 1.5.3) and the two larger fragments were selected to sequence the P2 region of Mdm2 and facilitate generation of a targeting vector. Following the same logic further BAC clones will be ordered to facilitate construction of the p21 and Puma knock-in reporter mice. These bMQ BAC clones (bMQ-305J12 and bMQ-81N13) were generated by partial digestion

of genomic DNA with Sau3A1 and cloned into a pBACe3.6 linearised (by BamHI) vector thus recreating a BamHI site at the point of integration (Clones and information ordered from GeneServices Ltd).

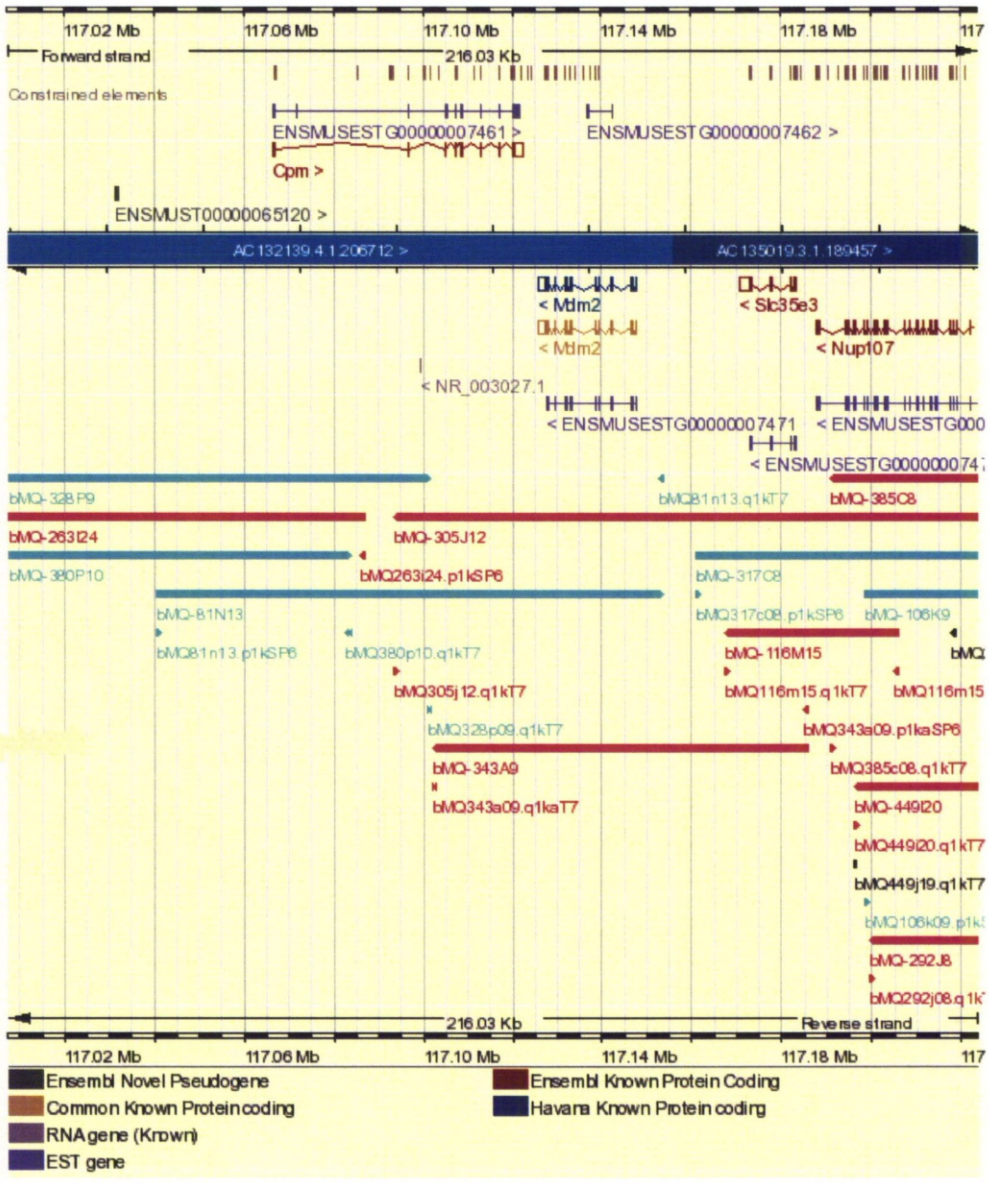


***Figure 1.5.3: Ensembl screen shot of AB2.2 129Sv DNA BAC clones available over the Mdm2 region.***

*Three clones cover Mdm2 and surrounding sequence, bMQ-305J12 (pink), bMQ-81N13 (green) and bMQ-343A9 (pink) colours indicate direction [Adams et al., 2005]. http://www.ensembl.org/Mus_musculus/contigview?region=10&vc_start=117007437&vc_end=117223468 website.*

### 1.5.3 Creation of transgenic mice: a brief overview

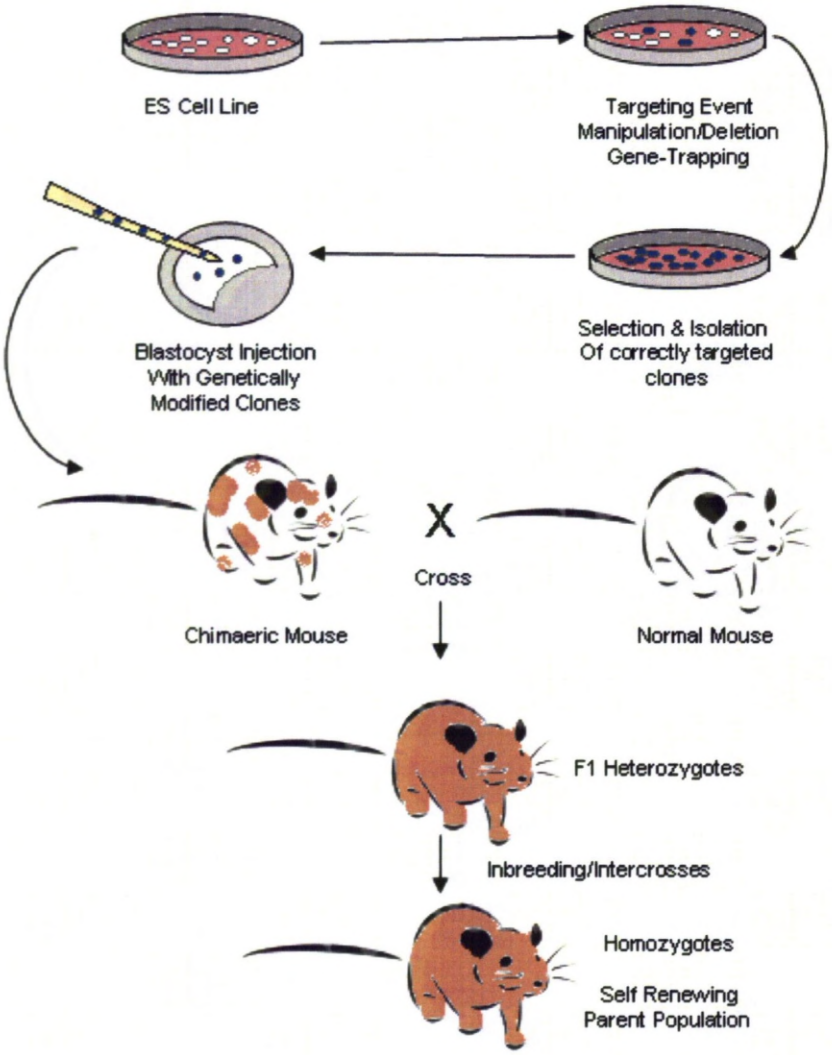


***Figure 1.5.4: Creation of transgenic mice from ES cells.***

*Adapted from [Babinet and Cohen-Tannoudji, 2001]. Mouse pictures adapted from www.istockphoto.com See text for details.*

Figure 1.5.4 illustrates the sequence of events leading to the generation of a self-renewing homozygous mutant mouse colony. ES cell lines (usually derived from a 129 strain of mice, which have an agouti coat [Adams et al., 2005]) are grown and kept in a pluripotent state and targeted through various means to genetically modify the cells, for example by retroviral infection with a vector containing a gene-trap or a point mutation. The successfully targeted cells are selected for and isolated (by means of selectable markers (resistance to

drugs) or other phenotypic screens (e.g. β-gal assay – targeted cells turn blue) which are then harvested and injected into a recipient blastocysts (of a different strain with a different coat colour – commonly C57BL/6J which are black). The blastocysts are implanted into a pseudo-pregnant surrogate mother and chimaeric mice are born containing two distinct genetic cell populations and hence, depending upon the ratios of the genetic contribution from each strain, may have patches of fur in different colours (black/brown). Chimaeras are mated with normal mice (of the recipient blastocyst genotype e.g. C57BL/6J) and genetic modifications that have entered the germ cells (i.e. ova or sperm cells) will produce heterozygous mice with all agouti coats (shown as brown in Figure 1.5.4). Heterozygotes are then inter-crossed to produce a homozygous population, known as the founder colony [Babinet and Cohen-Tannoudji, 2001].

# Aims

This project aims to examine the regulation of p53 function with a focus on the bowel and in particular on the small intestine. There are three components to this;

Firstly, p53 induces apoptosis in the crypt but not in the villi of the small intestine. In circumstances where p53 is induced on the villi, these cells do not apoptose (see Figure 3.1.7). Thus as the cells differentiate along the crypt villus axis, they become refractory to p53 mediated apoptosis. It is not clear whether this is because p53 is up-regulated but not activated or alternatively, p53 is up-regulated and activated BUT, p53 activity is suppressed (for example by expression of a negative regulatory gene such as MDM2 or MDMX). We therefore propose to characterise the expression of p53 target genes and regulatory genes along the crypt-villus axis *in vivo* in the presence and absence of apoptogenic stimuli.

Secondly, as stated above, to examine p53 activity and regulation we will be using surrogate indicators (target gene expression) to monitor p53 activity. Therefore we propose to develop a reporter mouse based upon a p53-responsive gene or genes to facilitate measurements of p53 activation *in vivo*.

Thirdly, we know that MDM2 is an essential negative regulator of p53 and that an autoregulatory feedback loop exists between these genes. In response to p53 activation by genotoxic and other stresses, p53 promotes up-regulation of MDM2 expression. We want to investigate whether and if so, to what extent, the ability of p53 to up-regulate MDM2 contributes to p53 regulation *in vivo*. To accomplish this we propose to generate two strains of transgenic mice which would contain either a deletion in the *Mdm2* constitutive (P1) promoter or mutate the p53 RE within the p53-responsive *Mdm2* (P2) promoter.

These aims will enable us to gain a better understanding of the regulation of p53 activity and we will use the tools we propose to generate to examine the bowel in the first instance. This is important in cancer since loss of p53 function is a critical event in carcinogenesis. Cells can compromise p53 partially or completely as part of the process of tumour development and progression. Our hypothesis is that cells in the bowel may be able to take advantage of an intrinsic ability displayed by villus cells to p53 expression.

The main emphasis, of this project, is on the development of a dual reporter system using *in vivo* technologies; as such the first task is to identify downstream targets of *p53* activation in both its apoptotic and cell cycle arrest functions with relevance to the intestine. Once suitable targets have been selected our second aim is to generate gene-trapped *LacZ* reporter mice by taking advantage of public gene-trap resources. The ultimate aim would be to develop a dual fluorescent apoptosis/cell cycle arrest *p53* reporter system which would have wide-reaching applications in cancer research and for studying normal development.

We envision using these mice in the first instance to define the long standing molecular phenomenon occurring in intestinal gut epithelium, in which cells on the villi display an uncoupling from the apoptotic actions of *p53*. Why is there this apparently black and white switch in the cells behaviour? This has implications for cancer progression, if cells have the ability at some point in their lifespan to resist the tumour suppressor activities of *p53*, a relapse into this state in a stem cell position would allow for easier tumour progression.

The last aim is to create the *Mdm2* P1-Null or P2-Mutant mouse strains. *Mdm2* is an essential negative regulator of *p53*, which is itself up-regulated by *p53* in response to stress (such as DNA damage). It has not yet been determined whether or not this regulation is critical to the action/s of p53 or indeed if it is critical *in vivo* during embryogenesis or normal physiological homeostasis. As the P2 promoter region is a p53 RE and a constitutive promoter (P1) is also present in the *Mdm2* gene this displays an exciting opportunity to define the regulation of one of the most important tumour suppressor genes; *p53*.

# 2 Materials and Methods

# 2.1 Bacteria

## 2.1.1 Strains used and basic maintenance

A table of all the bacterial strains used in this project is shown below, including details of each strain's genotype and general uses (see Table 2.1.1). For general cloning TOP10 bacteria were most frequently used, whilst different strains of bacteria were required for different/specialised purposes. For example when unmethylated DNA was required for downstream applications (such as a DNA digest with a Dcm sensitive restriction enzyme SexAI) a dam$^-$/dcm$^-$ competent *Escherichia coli* strain was used to generate the DNA. For more complex cloning exercises which included large DNA constructs (>20 kb) with very repetitive DNA MAX Efficiency® Stbl2 *E. coli* were the preferred option (since this strain had its recombination genes inactivated when grown at 30°C – hence the DNA was more stable). Some of the more common *E. coli* genotypes are explained in Table 2.1.2.

All bacterial work was carried out using aseptic techniques. *E. coli* were grown in Luria Broth (Sigma-Aldrich) liquid media that was prepared by adding 25 g/L of Luria Broth (formulation 10 g/L tryptone, 5 g/L yeast extract and 10 g/L $NaCl_2$) to distilled water and was sterilised by autoclaving at 122°C. Any appropriate antibiotics were added at their recommended working concentration (see Table 2.1.3) once the solution had cooled. Solid media was prepared using the same method and formulation but with the addition of 15 g/L of agar (Formedium – derived from seaweed) and antibiotics were added at ~ 50°C.

*E. coli* were initially propagated in small starter cultures and then diluted 1:100 for larger culture volumes. To set up a starter culture, an individual bacterial colony was picked from an LB-agar plate (containing either recombinant clones or known plasmids of interest), inoculated into small 5 ml liquid cultures (containing an appropriate antibiotic) in 14 ml sterile Falcon 2059 tubes and incubated overnight at 37°C with vigorous shaking (~230 rpm). Larger scale *E. coli* culture was inoculated into a conical flask that was at least five times the size of the culture volume (to ensure adequate aeration) and grown overnight at 37°C with vigorous shaking (~230 rpm).

***Table 2.1.1*: Complete table of all *Escherichia coli* strains used.**

| Strain | Source | Genotype | Uses |
|---|---|---|---|
| One Shot® TOP10 | Invitrogen #C4040 | F⁻ *mcr*A Δ(*mrr-hsd*RMS-*mcr*BC) φ80*lacZ*ΔM15 Δ*lac*X74 *rec*A1 *ara*D139 Δ(*ara-leu*) 7697 *gal*U *gal*K *rps*L ($Str^R$) *end*A1 *nup*G $\lambda^-$ | Routine cloning |
| DH5α | Invitrogen | F- φ80*lacZ*ΔM15 Δ(*lacZYA-argF*)U169 *rec*A1 *end*A1 *hsd*R17($r_k^-$, $m_k^+$) *pho*A *sup*E44 *thi*-1 *gyr*A96 *rel*A1 $\lambda^-$ | Routine cloning |
| XL1-Blue | Stratagene #200130 | *recA1 endA1 gyrA96 thi-1 hsdR17 supE44 relA1 lac* [F′ *proAB lacIqZΔM15* Tn*10* ($Tet^r$)]. | Routine cloning HQ DNA |
| SURE | Agilent Technologies | e14⁻ (*McrA*⁻) Δ(*mcrCB-hsdSMR-mrr*)171 *end*A1 *sup*E44 *thi*-1 *gyr*A96 *rel*A1 *lac rec*B *rec*J *sbc*C *umu*C::Tn5 ($Kan^r$) *uvr*C [F' *pro*AB $lacI^qZ\Delta M15$ Tn10 ($Tet^r$)] | Cloning DNA with non-standard structures |
| CopyCutter EPI400 | Epicenter Biotechnologies # C400CH10 | F⁻ *mcr*A Δ(*mrr-hsd*RMS-*mcr*BC) φ80d*lacZ*ΔM15 Δ*lac*X74 *rec*A1 *end*A1 *ara*D139 Δ(*ara, leu*)7697 *gal*U *gal*K $\lambda^-$ *rps*L *nup*G *ton*A Δ*pcnB dhfr.* | Cloning unstable DNA |
| MAX Efficiency® Stbl2 | Invitrogen #10268-019 | F⁻ *mcr*A Δ(*mcr*BC-hsdRMS-*mrr*) *rec*A1 *end*A1*lon gyr*A96 *thi sup*E44 *rel*A1 $\lambda^-$ Δ(*lac-pro*AB) | Cloning unstable DNA |
| dam⁻/dcm⁻ Competent *E. coli* "C2925s" | New England Biolabs #C2925 | *ara*-14 *leu*B6 *fhu*A31 *lac*Y1 *tsx*78 *gln*V44 *gal*K2 *gal*T22 *mcr*A *dcm*-6 *his*G4 *rfb*D1 *R(zgb*210::*Tn*10*)* $Tet^S$ *end*A1 *rsp*L136 ($Str^R$) *dam*13::*Tn*9 ($Cam^R$) *xyl*A-5 *mtl*-1 *thi*-1 *mcr*B1 *hsd*R2 | Cloning DNA free of Dam and Dcm methylation |

***Table 2.1.2*: Common *Escherichia coli* genotypes and their associated phenotypes.**

| Genotype | Phenotype |
|---|---|
| *hsd*R | Efficient transformation of unmethylated DNA from PCR amplifications |
| *mcr*A, mrr-sdRMSmcrBC | Restriction minus - efficient transformation of methylated DNA |
| *lac*ZΔM15 | For blue/white colour screening of recombinant clones |
| *end*A1 | *Endonuclease* deficient – increased plasmid yield and quality |
| *rec*A1 *rec*B *rec*J | *Recombination* deficient – increased DNA stability |
| *pcnB* | *Plasmid copy number* - modified version of the gene allows high copy number to be induced (CopyCutter EPI400) |

***Table 2.1.3*: Selective antibiotics.**

*Each antibiotic was prepared as a concentrated stock solution, which was sterilised by filtration and then aliquoted and stored at -20°C. *Except for the "C2925" strain where the final concentration used is 30 µg/µl.*

| Antibiotic | Source | Reconstituted in | Stock solution | Typical working concentration |
|---|---|---|---|---|
| Ampicillin | Sigma-Aldrich | $H_2O$ | x 1000 | 100 µg/µl |
| Kanamycin | Sigma-Aldrich | $H_2O$ | x 250 | 50 µg/µl* |
| Chloramphenicol | BDH biomedical | Ethanol | x 1000 | 20 µg/µl |

For long term storage of *E. coli* a freshly grown *"saturated"* overnight culture was mixed 1:1 with 50% glycerol and kept at -80°C. Frozen *E. coli* were revived by scraping off some of the frozen glycerol stock with an inoculation loop (without allowing the contents to thaw) and streaking this out onto an LB-agar plate which is then incubated overnight at 37°C or until individual colonies have become visible.

## 2.1.2 Introduction of plasmid DNA into bacterial cells

### *2.1.2.1 Transformation by heat shock in chemically competent bacteria*

Chemically competent *E. coli* strains were obtained from commercial sources (see Table 2.1.1) and were used according to manufacturer's guidelines. The basic method is outlined next (for One Shot® TOP10) followed by the strain-to-strain optimised variations.

One Shot® TOP10 *E. coli* were used for routine cloning. For each transformation reaction, 50 µl of chemically competent *E. coli* were thawed slowly on ice in a 2 ml screw cap tube. Once the cells had thawed either 10 pg of control plasmid such as pUC19 DNA or known plasmids of interest or 2-5 µl of a DNA ligation mixture was added. The transformation reaction was mixed by gentle swirling of the tube and/or gentle flicking (not by pipetting) and incubated on ice for 30 minutes. The transformation mix was then heat shocked at 42°C for exactly 30 seconds (without shaking) followed by a further incubation on ice for 2 minutes (it is this stage of the protocol which is often optimised depending on bacterial strain, vessel type, and reaction volume – see Table 2.1.4). 250 µl of SOC (Super Optimal broth with Catabolite repression – see Table 2.1.5 for formulation) medium was then added and the cells allowed to recover by incubation for 1 hour at 37°C with shaking (~230 rpm). The transformation mixture was then spread onto LB-agar plates containing selective antibiotics and incubated overnight at 37°C to allow the growth of transformants. In order to ensure the growth of individual colonies (for picking and screening of recombinant clones) typically 10% and 90% of the total transformation mixture volume were spread onto LB-agar plates. Transformation efficiency (colony forming units per µg of pUC19 DNA) was calculated to determine whether the transformation was performed satisfactorily (see Table 2.1.4 for the specified transformation efficiency of each strain used).

XL1-Blue cells were used when better quality and quantity of DNA was required for downstream applications (such as transfection into mammalian cells) and/or when the DNA to be transformed was a previously made plasmid (i.e. not DNA from ligation reactions). The XL1-Blue transformation protocol was essentially the same as the basic method detailed above for One Shot® TOP10 *E. coli* except only 10 µl of competent cells was used per transformation reaction and the heat shock was for 45 seconds.

***Table 2.1.4: Summary of Escherichia coli chemical transformation protocols.***

| Strain | Cell volume (µl) | Heat-shock @ 42°C (seconds) | Vessel (2 ml or 14 ml) | SOC medium volume (µl) | Outgrowth temperature | Transformation efficiency (cfu/ µg of pUC19 DNA) |
|---|---|---|---|---|---|---|
| One Shot® TOP10 | 50 | 30 | 2 ml | 250 | 37°C | $1 \times 10^9$ |
| XL1-Blue | 10 | 45 | 2 ml | 290 | 37°C | $1 \times 10^8$ |
| CopyCutter EPI400 | 50 | 30 | 2 ml | 250 | 37°C | $1 \times 10^7$ |
| MAX Efficiency® Stbl2 | 100 | 25 | 14 ml | 900 | 30°C | $1 \times 10^9$ |
| "C2925" | 50 | 30 | 2 ml | 950 | 37°C | $1\text{-}3 \times 10^8$ |

The CopyCutter EPI400 *E. coli* strain was used to transform unstable DNA constructs since it contains a modification which allows it to grow plasmid DNA at a low copy number (which can be induced to high copy number in liquid culture by 4 hour incubation in the presence of the CopyCutter Induction Solution). The transformation protocol was the same as for One Shot® TOP10 cells.

MAX Efficiency® Stbl2 cells were also used for cloning unstable or otherwise difficult to transform DNA constructs. The transformation protocol differs from the One Shot® TOP10 cells, most notably the cells are grown at 30°C to suppress recombination, including incubation of the LB-agar plates. For each transformation 100 µl of cells were gently pipetted into pre-chilled 14 ml Falcon 2059 tubes. Ligation reactions were diluted 1:5 in TE buffer (Qiagen, formulation 10 mM Tris (pH 8.0), 1 mM EDTA) and 1 µl of this was added gently to the cells. 50 pg of pUC19 DNA was used for the control reaction. Heat-shock (still at 42°C) was performed for only 25 seconds and 900 µl of SOC medium (pre-heated to 30°C) was added. Recovery was at 30°C for 90 minutes in a shaking incubator.

"C2925" a $dam^-/dcm^-$ competent *E. coli* strain were used to produce DNA free of Dam and Dcm methylation. The transformation protocol was almost the same as the One Shot® TOP10 cells, except 950 µl SOC media was used with more vigorous shaking during

recovery (~250 rpm). Note, the working concentration of kanamycin in this strain was 30 µg/µl (rather than 50 µg/µl listed in Table 2.1.3) and the LB-agar plates were made up accordingly.

### *2.1.2.2 Generation of electrocompetent bacteria*

Electrocompetent *E. coli* were prepared using aseptic technique by the following method. A single colony of the desired *E. coli* strain was inoculated into 5 ml LB medium (plus any appropriate antibiotic) and incubated overnight at 37°C, with shaking (300 rpm). 2.5 ml of this starter culture was then inoculated into 500 ml of LB medium and incubated at 37°C, with shaking at 300 rpm, until an OD600 nm of 0.5 to 0.7 was reached which typically takes 3-4 hours. Cells were then chilled in an ice water bath for 10-15 minutes before proceeding with harvesting. From this point on all centrifugation steps were performed at 2°C and all reagents/equipment were kept pre-chilled on ice. Cells were harvested in a 500 ml centrifuge bottle in a Sorvall RC 5C *Plus* (Du Pont) Centrifuge at 3000 *x g* for 20 minutes. The supernatant was poured off immediately and the cells washed with 500 ml of ice-cold water by re-suspending initially with 5 ml (to ensure a single cell suspension), then the remaining water was added. The cell suspension was mixed well before being harvested as before. The wash with 500 ml of ice cold water was repeated once more then the cells were re-suspended in 40 ml of 10% (v/v) glycerol. The cell suspension was transferred into a narrow bottom 50 ml Falcon tube and was harvested in an Eppendorf Centrifuge 5804R at 3000 *x g* for 10 minutes. The supernatant was promptly poured off and the cells re-suspended 1:1 with 10% glycerol (the volume of the pellet was estimated by eye – usually around 500 µl). The electrocompetent *E. coli* were then aliquoted 50 µl/1.5 ml micro-centrifuge tube and rapidly frozen either on dry ice (preferable, when available) or snap frozen in liquid nitrogen. The cells were stored at -80°C until needed.

### 2.1.2.3 Transformation by electroporation

Electro-transformation of *E. coli* by high voltage was performed using a Bio-Rad Gene Pulser II. Electroporation cuvettes (Bio-Rad) had a 0.1 or 0.2 cm gap and were recycled by a simple washing protocol between transformations (see below). SOC media was prepared in advance and was sterilised by autoclaving (see Table 2.1.5). The electro-transformation procedure was performed as follows; competent cells were thawed on ice and 1-2 µl of pre-chilled ligation mixture was added (or 10 pg of pUC19 control plasmid DNA). The transformation reaction was then carefully transferred to avoid air bubbles into an ice-cold electro-cuvette. The outside of the cuvette was wiped to be free of condensed moisture before being placed into the Bio-Rad Gene Pulser II and a single pulse was delivered (see Table 2.1.6 for specifications). Immediately following pulse delivery, 1 ml of chilled SOC medium was added to the cuvette and the transformation mix was gently re-suspended before being transferred to a chilled 2 ml screw cap tube. The cell suspension was then incubated for an hour at 37°C (or 90 minutes at 30°C for MAX Efficiency® Stbl2 cells) with shaking (~230 rpm). The transformation mixture was then plated out onto LB-agar plates, as with the chemically competent *E. coli* transformation protocol. Using this protocol cells typically produced transformation efficiencies of > 1 x $10^{8-9}$ cfu/µg pUC19 DNA.

Washing of the electro-cuvettes was performed by five complete rinses with $H_2O$ an acid soak in 0.2 M HCl for 10 minutes, then a further five complete rinses with 70% ethanol. Following a final rinse with 70% ethanol, the liquid was decanted under a sterile hood and allowed to air dry for about an hour. The cap of the cuvette was replaced and the electro-cuvette was ready to use again.

***Table 2.1.5*: *Formulation of Super Optimal broth with Catabolite repression (SOC) medium.***

| **SOC medium** | **/L** | **Source** |
|---|---|---|
| 0.5% Yeast Extract | 5 g | BD Biosciences |
| 2% Tryptone | 20 g | BD Biosciences |
| 10 mM NaCl | 2 ml of 5 M | BHD AnalaR |
| 2.5 mM KCl | 2.5 ml of 1 M | AnalaR NORMAPUR |
| 10 mM $MgCl_2$ | 10 ml of 1 M | BDH AnalaR |
| 10 mM $MgSO_4$ | 10 ml of 1 M | BDH AnalaR |
| 20 mM Glucose | 20 ml of 1 M | Formedium |

***Table 2.1.6*: *Specifications for Electroporation.***

| **Gap size (cm)** | 0.1 | 0.2 |
|---|---|---|
| **Capacitance (μF)** | 25 | 25 |
| **Resistance (Ω)** | 200 | 200 |
| **Voltage (kV)** | 1.5 | 2.4 |
| **Pulse (kV/cm)** | 15 | 12 |
| **Expected time constant (ms)** | 4.6 | 4.6 |

# 2.2 Yeast

## 2.2.1 Strain used and basic maintenance

The *Saccharomyces cerevisiae* strain YPH501 was used for cloning in this project to take advantage of the homologous recombination machinery in yeast. YPH501 (kindly provided by Dr Antonius Plagge, the University of Liverpool) is a diploid strain and its genotype is *ura*3-52, *lys*2-801amber, *ade*2-101ochre, *trp*1-delta63, *his*3-delta200, *leu*2-delta1. All yeast work was carried out using aseptic techniques.

Yeast were grown in either rich or minimal media depending on the experimental requirements. For convenience, stock solutions of each of the major components of the media were prepared in $H_2O$ and sterilised separately, see Table 2.2.1.

***Table 2.2.1*: Yeast media components.**

*YEP broth and glucose solutions were sterilised by autoclaving at 122°C. The YNB-AA, adenosine and the amino acids were sterilised by filtration.*

| Media component | Source | Stock solution | Working concentration |
|---|---|---|---|
| YEP broth | Formedium | X 5 | 30 g/L |
| Glucose | Formedium | X 10 | 2% (w/v) |
| YNB-AA | Formedium | X 10 | 6.9 g/L |
| Adenosine (hemisulfate salt) | Sigma-Aldrich | X 125 | 40 µg/µl |
| L-histidine | Formedium | X 120 | 20 µg/µl |
| L-leucine | Formedium | X 120 | 60 µg/µl |
| L-lysine | Formedium | X 120 | 30 µg/µl |

Rich media YPD (yeast extract, peptone, dextrose) was used to grow *S. cerevisiae* when there was no need for selection (for example during preparation of LiAc competent cells for transformation – see Section 2.2.2. Liquid media was prepared by diluting the x5 YEP broth (formulation 10 g/L yeast extract, 20 g/L peptone) and x10 glucose to x1 working

concentration in water. YPD-agar was prepared by autoclaving 2% agar (in water) in 85% of the total final volume. Once the agar solution had cooled to ~50°C the x5 YEP broth and x10 glucose stock solutions added, mixed thoroughly and poured into Petri dishes.

Minimal media used to select for recombined plasmids was composed of YNB-AA (yeast nitrous base without amino acids) supplemented with glucose and x1 nutrients. In order for the YPH501 strain to grow in minimal media it must be supplemented with the nutrients adenosine, L-histidine, L-leucine, L-lysine, L-tryptophan and uracil (see Table 2.2.1). However, since our selection protocol relied upon the reintroduction of both a functional *URA3* and *trp1* gene, uracil and L-tryptophan were not included (sometimes known as Ura/Trp-dropout media/plates). Liquid minimal media was prepared as follows; the x10 YNB-AA, the x10 glucose and appropriate stock amino acids solutions were added together to a suitable container (typically a 50 ml Falcon tube) and then the solution was diluted to x1 working concentration with sterile water and mixed well before use. The minimal-agar plates were prepared as follows; 2% agar in water was autoclaved in 80% of the total final volume and allowed to cool to ~50°C. Once cooled the concentrated YNB-AA, glucose and amino acids solutions were added to a final concentration of x1 and the minimal-agar mixed thoroughly before pouring.

*S. cerevisiae* were propagated using similar microbiological techniques as for *E. coli* (see Section 2.1.1). Starter cultures, each in 5 ml of liquid media (either rich or minimal), were inoculated with individual yeast clones from an agar plate and incubated at 30°C with shaking (230rpm). *S. cerevisiae* that were grown in rich media would typically reach stationary during an overnight culture (12-16 hours) however yeast cells that were grown in minimal media generally took longer (2-3 days).

For long term storage of yeast strains, *S. cerevisiae* were grown to late-log or early-stationary phase of growth and 1 ml placed into a sterile 1.5 ml screw cap micro-centrifuge tube. 80 µl of DMSO (dimethyl sulphoxide) was added (8% v/v) and the solution mixed and frozen at -80°C. Recovery from frozen stocks was essentially the same as for *E. coli* strains, a small volume of yeast cells were scraped from the frozen stock (without allowing the contents to thaw) and re-streaked onto an appropriate agar plate.

## 2.2.2 Co- transformation of yeast with lithium acetate

Competent *S. cerevisiae* cells were generated for co-transformation as follows; an overnight yeast culture was diluted into 50 ml of YPD-media to an OD600 nm of 0.2 and incubated at 30°C with shaking (~230 rpm) until an OD600 of 0.5-1 was reached which typically takes 3-4 hours. The cells were then transferred into a 50 ml Falcon tube and harvested by centrifugation at 1500 *x g* for 10 minutes at room temperature (RT). The supernatant was discarded and the pellet re-suspended in 10 ml of water and harvested as before. This wash step was followed by a further wash in 10 ml of 100 mM lithium acetate (LiAc (BD biosciences, Clontech)), before the cells were finally re-suspended in 250 µl 100 mM LiAc. These cells were then competent and ready to use immediately (although they could be stored on ice for a few hours).

The other components of the co-transformation shown in Table 2.2.2, were then prepared. The herring testes carrier DNA (BD biosciences, Clontech) was denatured just before use by performing two rounds of boiling (100°C for 5 minutes) and rapid cooling (in ice water for a few minutes). The shuttle vector DNA and donor DNA were prepared in advance (see Sections 2.3.9, 2.6.1 & 3.3.5.6 for details) and the PEG solution was prepared on the day of use by diluting a 50% PEG solution (BD biosciences, Clontech) with 1 M LiAc and water.

***Table 2.2.2: Co-transformation mix components.***

| Component | Amount | Source |
|---|---|---|
| Competent yeast cells | 50 µl | See above |
| 10mg/ml Herring testes carrier DNA (denatured) | 5 µl | BD biosciences, Clontech |
| Shuttle vector DNA | 500 ng | To be generated by user, unique to each reaction. |
| Donor DNA | 500 ng | |
| PEG solution (100 mM LiAc, 40% PEG) | 300 µl | BD biosciences, Clontech |

Once ready, all components of the co-transformation reaction were placed together in a 1.5 ml screw cap micro-centrifuge tube and vortexed briefly prior to incubation at 30°C for 30 minutes (with shaking ~230 rpm). The cell mixture was then heat shocked for exactly 15

minutes at 42°C with gentle vortexing every 3 minutes. 100 µl of the transformation mix was then spread onto Ura/Trp-dropout agar plates and incubated at 30°C for 2-3 days until individual yeast clones were visible.

# 2.3 DNA extraction methods

## 2.3.1 Basic small scale isolation of plasmid DNA using alkaline lysis and PCI

The plasmid DNA extracted using the low-cost/low-quality-DNA method detailed below, was used to screen recombinant clones (not for sequencing) and typically yielded between 30-50 µg DNA from a 4 ml liquid culture, of adequate quality for analysis by restriction digest (see Section 2.6.1 for details). This basic protocol has the benefit of being capable of isolating DNA quickly from many clones at once, allowing for rapid screening. All reagents were prepared in advance (see Table 2.3.1) and for ease and speed were dispensed during the protocol using a multi-pipetter (multipette®*plus*, Eppendorf). All DNA, regardless of the method used to generate it, was stored at -20°C.

Plasmid DNA isolation was performed as follows; *E. coli* overnight cultures were harvested in 2 ml micro-centrifuge tubes in an Eppendorf centrifuge *5415* at 6800 *x g* for 5 minutes at RT (4 ml of liquid culture per pellet). The cell pellet was re-suspended in 200 µl of GTE solution by vortexing, and then 200 µl of lysis buffer was dispensed into each tube, followed in quick succession by 200 µl of $K^+Ac^-$ solution and 500 µl of PCI (24:25:1). The tubes were sealed and mixed manually by inversion for 5 minutes and then centrifuged at maximum speed for 10 minutes. The aqueous phase was promptly transferred into a fresh 1.5 ml micro-centrifuge tube containing 500 µl of isopropanol (VWR) and mixed well before being incubated at RT for 5 minutes. The precipitated DNA was then harvested by centrifugation at maximum speed for 10 minutes. DNA pellets were washed thoroughly by adding approximately 1 ml of 70% ethanol and vortexing to ensure that the pellet was dislodged and moving freely in the solution. The samples were centrifuged briefly and the supernatant carefully decanted. The pellet was air-dried for 5-10 minutes (or until the white pellet became clear/translucent in appearance) and the DNA was re-suspended in 20 µl of TE buffer + RNase A. Optionally, to help the DNA dissolve, the DNA solution could be incubated for 30-60 minutes in a 37°C water-bath, with occasional vortexing. In general 2 µl of a 1:10 diluted (in $H_2O$) DNA solution was sufficient for analysis.

***Table 2.3.1*: Composition of buffers for basic plasmid DNA isolation**

*GTE, lysis buffer and $K^+Ac^-$ solution were stored at RT. The lysis buffer was heated up in a 37°C water-bath before use to dissolve any precipitated SDS. PCI (24:25:1) was stored at -20°C and defrosted in a 37°C water-bath before use. TE buffer + RNase A was stored at 4-8°C.*

| Solution | Composition | Source |
|---|---|---|
| GTE (re-suspension buffer) | 50 mM Glucose<br>25 mM tris (pH 7.4)<br>1 mM EDTA (pH 8.0) | AnalaR<br>Calbiochem<br>Sigma-Aldrich |
| Lysis buffer (AKA buffer P2) | 1% SDS (w/v)<br>200 mM NaOH | VWR<br>VWR |
| $K^+Ac^-$ solution (neutralisation buffer) | 3 M KAc<br>11.5% Glacial acetic acid (v/v) | BDH Biochemical<br>MERCK |
| PCI (24:25:1) | 24: Phenol<br>25: Chloroform<br>1: Isoamylalcohol | VWR<br>VWR<br>VWR |
| TE buffer + RNase A | 10 mM Tris.Cl (pH 8.0), 1 mM EDTA<br>10 µg/ml RNase A | QIAGEN<br>Sigma |

## 2.3.2 Small scale, high quality preparation of plasmid DNA

When small quantities of high quality, clean DNA were required for downstream applications (such as for DNA sequencing), the QIAprep spin Miniprep kit (QIAGEN) was used to isolate plasmid DNA. The kit is based on alkaline lysis (similar to the previous method – see Section 2.3.1), but DNA is extracted by binding in high salt to a silica membrane. The silica membrane is held within a column (QIAprep spin column), has a detachable collection tube (called a catch-tube) and is optimised for use in a standard bench-top centrifuge. Plasmid DNA isolation was performed according to the manufacturer's guidelines and typically yielded 5-20 µg DNA from 4 ml of an overnight *E. coli* culture.

Table 2.3.2 lists the reagents provided by all the QIAGEN plasmid DNA preparation kits used in this project.

Briefly, the protocol was as follows; after harvesting the bacterial cells in a 2 ml micro-centrifuge tube by centrifugation at 6800 *x g* for 5 minutes at RT, the pellet was re-suspended in 250 µl of buffer P1. 250 µl of buffer P2 was added to the cell suspension and mixed thoroughly by inverting the tube 4-6 times to lyse the bacterial cells. 350 µl of buffer N3 was added to neutralise the reaction (within 5 minutes) and the samples were centrifuged for 10 minutes at maximum speed at RT. The supernatant (cleared lysate) was then applied to a QIAprep spin column and centrifuged for 30-60 seconds. The flow through was discarded and 500 µl of buffer PB was added to the column and centrifuged for 30-60 seconds. The flow through was discarded and the column washed by adding 750 µl of buffer PE and centrifuging for 30-60 seconds. The flow through was discarded and the column was centrifuged again for 1 minute to remove any residual wash buffer. The QIAprep spin column was then placed into a fresh 1.5 ml micro-centrifuge tube and 30-50 µl of $H_2O$, or X 0.1 TE buffer was added carefully directly to the silica membrane. The column was left to stand for 1-5 minutes and then centrifuged for 1 minute. The concentration of DNA and its purity was determined using a UV spectrophotometer (see Section 2.4.1).

### 2.3.3 Medium scale, high quality preparation of plasmid DNA

The QIAGEN-tip 100 kit (QIAGEN) was used to isolate larger quantities (75-100 µg) of high quality plasmid DNA. The basis of the kit was briefly as follows; a modified alkaline lysis procedure was used on the bacterial cells followed by clearing the lysate by centrifugation. The cleared lysate was then applied to a single use QIAGEN anion-exchange resin (in a gravity-flow column) which bound the DNA under low salt and appropriate pH conditions. The resin was then washed to remove contaminants, such as RNA and proteins, and the DNA was eluted from the resin in a high-salt buffer. To concentrate and de-salt the DNA, DNA was precipitated with isopropanol and then washed in 70% ethanol. The plasmid DNA prepared by this midiprep protocol was of high quality and could be used to transfect mammalian cells.

***Table 2.3.2: Composition of buffers from QIAGEN Plasmid DNA preparation kits...***

*... used in this project, including QIAprep spin miniprep kit, QIAGEN-tip 100 kit (midiprep) and QIAGEN-tip 2500 EndoFree Plasmid Mega kit.*

| **Solution** | **Composition** |
|---|---|
| Buffer P1 (re-suspension buffer) | 50 mM Tris.Cl (pH 8.0), 10 mM EDTA (pH 8.0), 100 µg/ml RNase A |
| Buffer P2 (lysis buffer) | 1% SDS (w/v), 200 mM NaOH |
| Buffer P3 (neutralisation buffer) | 3 M potassium acetate (pH 5.5) |
| Buffer N3 (neutralisation buffer) | Confidential – proprietary component of kit |
| Buffer PB (binding buffer) | Confidential – proprietary component of kit |
| Buffer PE (wash buffer) | Confidential – proprietary component of kit |
| Buffer FWB2 (QIAfilter wash buffer) | 1 M potassium acetate (pH 5.0) |
| Buffer ER (endotoxin removal buffer) | Confidential – proprietary component of kit |
| Buffer QC (wash buffer) | 1 M NaCl, 50 mM MOPS (pH 7.0), 15% isopropanol (v/v) |
| Buffer QF (elution buffer) | 1.25 M NaCl, 50 mM Tris.Cl (pH 8.5), 15 % isopropanol (v/v) |
| Buffer QN (elution buffer) | 1.6 M NaCl, 50 mM MOPS (pH 7.0), 15% isopropanol (v/v) |
| TE buffer | 10 mM Tris.Cl (pH 8.0), 1 mM EDTA |

Plasmid DNA was prepared according to the manufacturers guidelines, albeit with some minor modifications as detailed below. A 25 ml culture of *E. coli* was grown overnight from a starter culture (see Section 2.1.1) and was harvested by centrifugation at 4500 *x g*, 4°C for 60 minutes (different from handbook). The bacterial cell pellet could be frozen at this point at -20°C indefinitely, or could be processed directly with the protocol as follows; the pellet was re-suspended with 4 ml of buffer P1. 4 ml of buffer P2 was added and the cell suspension mixed thoroughly by inverting the sealed tube 4-6 times. The lysis reaction was performed for 5 minutes at RT before neutralisation by adding 4 ml of chilled buffer P3. This

was mixed immediately by inverting the sealed tube 4-6 times and then left to incubate on ice for 15 minutes. The lysate was then centrifuged at 20,000 *x g* for 30 minutes at 4°C. The supernatant was removed promptly into a fresh centrifuge tube, before being mixed and centrifuged again. A QIAGEN-tip 100 resin column was equilibrated by adding 4 ml of buffer QBT and once the centrifugation steps were complete the supernatant was applied to the column and allowed to enter the resin by gravity flow. The QIAGEN-tip 100 containing the bound plasmid DNA was then washed twice with 10 ml buffer QC before the DNA was eluted with 5 ml buffer QF (which was heated to 65°C when larger constructs were being prepared – 40-50 kb). The plasmid DNA was precipitated by adding 3.5 ml of RT isopropanol. The following steps differ from the handbook; the 8.5 ml isopropanol/DNA solution was mixed well and then divided up into 1.5 ml micro-centrifuge tubes and harvested by centrifugation at 14,000 *x g* for 30 minutes at 4°C. The pellets were washed with 70% ethanol (at RT) before being pooled together and centrifuged at 13,000 x *g* for 10 minutes. The ethanol was carefully decanted and DNA pellets air dried for 5-10 minutes before being re-suspended in 50-75 µl of X 0.1 TE buffer. The concentration of DNA and its purity was determined using a UV spectrophotometer (see Section 2.4.1).

### 2.3.4 Medium scale preparation of DNA from very low copy number plasmid

The QIAGEN-tip 100 kit could also be used to isolate high quality plasmid DNA from very low copy number plasmids (such as BAC clones, which typically only have one copy per cell). The basis of the procedure is basically the same as for the previous method, except larger volumes are used and there is an additional precipitation with isopropanol prior to loading the QIAGEN-tip 100. The plasmid DNA was prepared using the manufacturer's guidelines, with some minor modifications and typically yielded 20-100 µg DNA.

Plasmid DNA isolation was as follows; for very low-copy number plasmids a 500 ml LB culture was grown overnight from a starter culture (see Section 2.1.1) and was harvested by centrifugation in a 500 ml centrifuge bottle at 6000 *x g* for 15 minutes at 4°C. The pellet of bacterial cells was re-suspended in 20 ml of buffer P1, then mixed (by inverting the sealed tube) with 20 ml buffer P2 and left for 5 minutes at RT. 20 ml of chilled buffer P3 was added

and mixed immediately by inverting tube 4-6 times to neutralise the lysis reaction followed by incubation on ice for 30 minutes. The mixture was then centrifuged at 4500 x *g* for 1 hour at 4°C (modified from handbook) and the supernatant (containing plasmid DNA) was promptly and carefully removed. The DNA was precipitated by mixing the supernatant with 42 ml of RT isopropanol and the DNA pellet was harvested by centrifugation as before. The DNA pellet was re-suspended in approximately 500 µl of TE buffer and brought to a final volume of 5 ml with buffer QBT. At this point the QIAGEN-tip 100 was equilibrated with 4 ml of buffer QBT and the protocol continued as for the normal midiprep method (see Section 2.3.3).

### 2.3.5 Large scale, high quality preparation plasmid DNA (with endotoxin removal)

When large quantities of high quality, ultra-pure transfection grade DNA were required, then a QIAGEN-tip 2500 EndoFree Megaprep kit was used to isolate the plasmid DNA. This kit was based on the same principles as the QIAGEN-tip 100 kit, except the bacterial cell lysate was cleared by filtration (not centrifugation). The procedure was performed according to the manufacture's guidelines, with some minor modifications and typically yielded 1.5-2.5 mg DNA.

Plasmid DNA was isolated as follows; a 500 ml LB culture was grown overnight from a starter culture (see Section 2.1.1) and was harvested by centrifugation in a 500 ml centrifuge bottle at 6000 *x g* for 15 minutes at 4°C. The pellet of bacterial cells was re-suspended in 50 ml of buffer P1, then mixed (by inverting the sealed tube) with 50 ml P2 buffer and left for 5 minutes at RT. The lysis reaction was neutralised by adding 50 ml of chilled buffer P3 followed by vigorously inverting the tube 4-6 times. There was no incubation on ice, instead the lysate was poured straight onto a QIAfilter Mega-Giga cartridge (which was already screwed into a 500 ml glass bottle and connected to a vacuum source) and allowed to incubate at RT for 10 minutes. The vacuum source was then switched on until all the liquid had been pulled through the filter. 50 ml of buffer FWB2 was then added to the QIAfilter and stirred gently with a spatula. The vacuum source was switched back on, until the liquid had been pulled through completely. Once the lysate had been filtered, 12.5 ml of

buffer ER was added to the 500 ml glass bottle and mixed by inverting the bottle approximately 10 times. The endotoxin removal reaction was then incubated on ice for 30 minutes, during which time, a QIAGEN-tip 2500 was equilibrated by adding 35 ml of buffer QBT. The filtered lysate was then applied to the column and allowed to enter by gravity flow. The column was washed with 200 ml total of buffer QC. The remainder of the protocol was modified from the handbook and continued as follows; the DNA was collected in a 50 ml Falcon tube by eluting with 30 ml of buffer QN. The DNA was then precipitated by adding 21 ml of RT isopropanol, mixed well and harvested by centrifugation at 4500 x *g* for 1 hour at 4°C. The supernatant was carefully decanted and the pellet re-suspended in 7 ml of endotoxin-free RT 70% ethanol. The DNA and ethanol solution was then aliquoted out between 1.5 ml sterile screw cap micro-centrifuge tubes, and centrifuged at 13,000 *x g* for 10 minutes at RT. Following centrifugation the pellets were pooled together in one tube and centrifuged again at maximum speed for 1 minute. The supernatant was removed, without disturbing the pellet and allowed to air-dry for 10-20 minutes. The DNA was then re-dissolved into a suitable volume of TE buffer. The concentration of DNA and its purity was determined using a UV spectrophotometer (see Section 2.4.1).

### 2.3.6 Fast, small scale isolation of yeast/plasmid DNA by mechanical lysis

Very small amounts (~ pg) of plasmid DNA were isolated from yeast cells (along with contaminating genomic DNA) using the rapid mechanical lysis protocol detailed below. The DNA extracted was suitable for PCR and transformation of bacterial cells.

5 ml starter cultures of individual yeast clones were grown in selective media for 2-3 days as described in Section 2.2.1. 1.5 ml of this yeast culture was then harvested in a 1.5 ml micro-centrifuge tube by centrifugation at 13,000 *x g* for 10 seconds (at RT). The supernatant was decanted and the pellet re-dissolved in the remaining liquid. To the sample 200 µl of YLB (yeast lysis buffer – see Table 2.3.3 for formulation) and 200 µl of PCI (24:25:1) were added. Small acid-washed glass beads (Sigma-Aldrich) were also added up to the interface (~ 0.3 g). The tubes were sealed and the samples vortexed vigorously for 2 minutes. Following mechanical lysis, the samples were centrifuged at 13,000 *x g* for 5 minutes at RT.

100 µl of the aqueous phase was retained and stored at -20°C while another 100 µl of the aqueous phase was transferred to a fresh pre-chilled 1.5 ml tube and the DNA was precipitated by adding 30 µl of 3 M sodium acetate (pH 5.2) and 200 µl of ice-cold 100% ethanol. The solution was mixed and left to stand in a -20°C freezer for at least an hour (could be left overnight) and then was centrifuged for 10 minutes at maximum speed (13,000 *x g*). The supernatant was decanted and the pellet washed in 200 µl of ice-cold 70% ethanol. The sample was briefly centrifuged again and the supernatant removed, allowing the pellet to air dry for 2-5 minutes before re-suspending in 20 µl of TE buffer + RNase A. The DNA was then checked by PCR and/or transformed into *E. coli*.

***Table 2.3.3: Formulation of (YLB) yeast-lysis-buffer.***

*YLB was prepared by dissolving the Tris.Cl in 80 ml $H_2O$ and then the pH was adjusted to pH 8.0 with HCl. The remaining components were added and the solution was mixed well using a stir bar, with heating to 37°C. YLB was stored at RT, but was heated to 37°C and mixed again before each use.*

| **Component** | **/100 ml** | **Source** |
|---|---|---|
| 10 mM Tris.Cl (pH 8.0) | 0.1211 g | Calbiochem |
| 1 mM EDTA (pH 8.0) | 200 µl of 0.5 M | Sigma-Aldrich |
| 100 mM NaCl | 0.5844 g | VWR |
| 1% SDS (w/v) | 5 ml of 20% (w/v) | VWR |
| 2% Triton X 100 (v/v) | 2 ml of 100% (v/v) | Sigma-Aldrich |

## 2.3.7 Isolation of genomic DNA from whole animal tissue

The protocol is essentially as described in Sambrook [Sambrook et al., 2000]. Briefly, frozen liver from a *129SvEv* mouse strain was ground with a pestle and mortar then aliquoted (approximately 0.2 g per tube) and placed in 500 µl of genomic DNA preparation lysis buffer (50 mM Tris (pH 8.0), 100 mM EDTA and 0.5% SDS (w/v)) with 250 µg proteinase K (Sigma-Aldrich) (final concentration 5 µg/µl) and left overnight at 55°C. The next day, DNA was extracted using an organic solvent-based extraction method. The cell lysate was mixed with

500 µl phenol and left for an hour with gentle shaking. Following centrifugation (5 minutes, 13,000 x *g*) the aqueous phase was transferred to a fresh tube and mixed with 500 µl PCI (24:25:1) for 5 minutes by inverting the tubes (without vortexing) then centrifuged again as before. The aqueous phase was transferred into a fresh tube and the DNA was precipitated by adding 50 µl 3 M sodium acetate (pH 6.0) and 500 µl of 100% ethanol to each tube. This was mixed (by inverting the tubes) for 1 minute then centrifuged for 10 minutes (13,000 x *g*). The supernatant was removed and the pellet was washed with 70% ethanol. The DNA pellet was re-suspended in TE buffer + RNase A. The concentration of DNA and its purity was determined using a UV spectrophotometer (see Section 2.4.1).

### 2.3.8 Isolation of genomic DNA from mammalian cells

Genomic DNA was isolated from mammalian tissue cultured cells by using essentially the same protocol as described above in Section 2.3.7. The only major difference was that cells in culture were harvested initially from their plastic tissue culture flasks using trypsin as described in Section 2.9.1. A cell pellet of about 5 x $10^6$ cells was typically re-suspended in 500 µl of the genomic DNA preparation lysis buffer with 5 µg/µl of proteinase K, where upon this method rejoins the previous protocol.

### 2.3.9 Extraction of DNA from agarose gels

DNA products were extracted from agarose gels using the GENECLEAN *Turbo* Kit (Qbiogene) according to the manufacturer's instructions. The DNA yield from the kit was typically 70-90% for DNA products 1-8 kb in length, but could be markedly less for larger or smaller DNA products. The DNA isolated using the GENECLEAN kit was suitable for many downstream applications including sequencing and molecular cloning.

DNA extraction was performed as follows; appropriate DNA bands were excised from the agarose gel and agarose gel plugs were placed in 1.5 ml micro-centrifuge tubes with 100 µl of GENECLEAN *turbo* salt solution per 0.1 g of agarose gel. This was then incubated in a water bath set to 55°C for ~ 10 minutes, until the agarose gel had melted completely. A cartridge with a glass-milk membrane was placed inside a second tube which was used to

collect the flow through (called a catch-tube) and the DNA/gel/salt solution was then applied over the membrane (no more than 600 µl at a time) and centrifuged for 10 seconds. The flow through was run over the membrane a second time, along with any remaining DNA/gel/salt solution. The liquid was then discarded since the DNA was bound to the membrane. The membrane was washed by adding 500 µl of GENECLEAN *turbo* wash solution over the column then centrifuged for 10 seconds. Flow-through was discarded and then the column was centrifuged for a further 4 minutes at 13,000 x *g* (to dry the membrane). The column, containing the DNA was then put into a fresh 1.5 ml micro-centrifuge tube with a detachable lid (provided in the kit) and 20 µl of $H_2O$ was applied directly to the membrane, incubated for 5 minutes at RT and then centrifuged for 1 min at 13,000 x *g*. The final eluate contains the purified DNA fragment. In order to estimate the yield, 10% of the eluted sample was analysed on another agarose gel (see Section 2.4.2 for further details).

### 2.3.10 Purification of DNA from enzymatic reactions

The GENECLEAN *Turbo* kit could also be used to purify DNA after enzymatic reactions. For example, during cloning exercises where two restriction enzymes were required to cut a particular DNA fragment, but which had incompatible buffers; a faster, liquid version of the GENECLEAN reaction was performed. This protocol is much the same as described previously in Section 2.3.9 except the DNA reaction to be cleaned had X 5 (v/v) GENECLEAN *turbo* salt solution added to it, prior to loading onto a GENECLEAN column.

Larger quantities of DNA (> 10 µg) were purified by a phenol/chloroform extraction as follows; an equal volume of PCI (24:25:1) was added to the DNA containing solution and mixed thoroughly. The DNA/PCI mixture was then centrifuged at maximum speed (~ 13,000 *x g*) for 30 seconds at RT. The aqueous phase was promptly transferred to a fresh 1.5 ml sterile screw cap micro-centrifuge tube. An equal volume of TE buffer (QIAGEN) was added to the organic phase and mixed thoroughly and then centrifuged as before. The aqueous phases were combined together and an equal volume of chloroform was added and mixed. The DNA/chloroform solution was centrifuged as before and the aqueous phase was transferred into another fresh 1.5 sterile screw cap micro-centrifuge tube. The DNA was then

precipitated by adding 2.4 volumes of 100% absolute (molecular biology grade) ethanol (Sigma-Aldrich). The sample was mixed and centrifuged at maximum speed for 10 minutes. The supernatant was removed under a sterile hood (if required), and the DNA pellet allowed to air dry for 5-10 minutes (or until the pellet became colourless/transparent) before being re-suspended in an appropriate buffer, at an appropriate concentration. The purity and yield of the DNA was either examined by UV spectroscopy or by agarose gel electrophoresis (see Section 2.4).

### 2.3.11 Purification of DNA sequencing reactions (genCLEAN 96 Well)

DNA sequencing reactions for use on the MegaBACE capillary sequencer were cleaned up to remove contaminating excess dyes by using the genCLEAN 96 Well Dye Terminator Removal Kit (Genetix). The procedure was performed according to a slightly modified version of the manufacturer's guidelines as follows; the genCLEAN plate was equilibrated to RT and once warmed, the buffer was removed by placing the genCLEAN plate onto a wash plate and then centrifuging it in a Sorvall Legend RT+ centrifuge at 910 *x g* for 5 minutes. The wells were then washed twice with 100 µl of $H_2O$ by loading the water with a multi-channel pipetter (Eppendorf) and centrifuging as before. The genCLEAN plate was then placed onto the collection plate and the DNA samples were loaded carefully into the wells directly onto the gel matrix. Any unused wells were loaded with water to prevent drying during centrifugation. The samples were then collected by a final centrifugation step, for 6 minutes at 1000 *x g*. The unused wells were loaded with 100 µl water and the genCLEAN plate was stored in the fridge for use later. These samples were then ready for analysis on the MegaBACE capillary sequencer – see Section 2.7.2.6 for further details.

### 2.3.12 Extraction of DNA from 96-well plates

DNA was extracted from ES cells in 96-well plates in order to screen for positive clones by mini-Southern blot analysis or PCR. The method briefly utilised freeze/thaw technique to crack open the cellular membranes, followed by an overnight digestion with proteinase K to remove proteins and cellular debris. The DNA was then precipitated with ice-

cold ethanol, washed 2-3 times in 70% ethanol, dried and re-suspended in a restriction digest cocktail. The yield using this method was variable (1-15 µg), but was usually sufficient for analysis by mini-Southern blot.

DNA was extracted in detail as follows; one duplicate ES cell plate (see Section 2.9.2.2.5) was taken from the -80°C freezer (after being frozen for at least 3 hours) and allowed to warm up to RT for 5 minutes. Once defrosted 50 µl of mini-Southern lysis buffer (MSLB – see Table 2.3.4) was added per well using a multi-channel pipette. The plate was then sealed using masking tape (Tessa) and was placed into a Tupperware box with a well fitting lid and wet paper towels to reduce evaporation whilst it was incubated overnight at 60°C.

***Table 2.3.4*: Formulation of Mini-Southern lysis buffer (MSLB).**

*MSLB without proteinase K was frozen at -20°C in 5.4 ml aliquots (sufficient for x1 96-well plate). Proteinase K was prepared as a 10 mg/ml (x 10) stock solution and also frozen at -20°C in 0.7 ml aliquots. For use, 0.6 ml of Proteinase K was added fresh to the rest of the MSLB once defrosted.*

| **Component** | **/50 ml** | **Source** |
|---|---|---|
| 10 mM Tris (pH 7.8) | 500 µl of 1 M | Calbiochem |
| 10 mM EDTA (pH 8.0) | 1 ml of 0.5 M | Sigma-Aldrich |
| 10 mM NaCl | 100 µl of 5 M | VWR |
| 0.5% Sarcosyl | 5 ml of 5% | BDH |
| $H_2O$ | 45 ml | - |
| 1 mg/ml proteinase K **[ADD FRESHLY]** | 0.6 ml of 10 mg/ml | Sigma-Aldrich |

The following day the plate was removed from the incubator and was centrifuged briefly to remove the condensation form the lid. At this stage if PCR was to be performed on the samples, 5 µl was removed and placed into another duplicate 96-well PCR plate. The PCR-duplicate plate was then sealed with an adhesive sticker and the proteinase K heat-inactivated by boiling the samples at 95°C for 10 minutes. Once boiled the PCR-duplicate plate was labelled and stored at -20°C until required. Continuing with the main DNA

extraction protocol; DNA was precipitated by gently adding 100 µl of ice-cold 100% molecular biology grade, 200 proof, ethanol (Sigma-Aldrich) per well. The plate was then incubated at RT for 30 minutes. Precipitated DNA adhered to the polystyrene wells of the tissue culture vessel, therefore after 30 minutes the plate was gently inverted onto layers of blue roll towel and allowed to drain. The DNA was then washed 2-3 times with 100 µl of 70% ethanol. After the final wash the plate was left to dry completely as any residual ethanol could impede the restriction digest reaction. In order to help the ethanol dry from the plate (typically this requires 15-30 minutes) the lid was removed and the plate placed into a 37°C bacterial incubator.

***Table 2.3.5*: Restriction reaction cocktail.**

*40 µl was required per sample. A master mix was prepared for all the samples by multiplying the 40 µl reaction by n, where n = number of samples + 10. For example a 96-well plate would be x 106.*

| **Component** | **/40 µl** | **Source** |
|---|---|---|
| X 1 NEBuffer | 4 µl of x 10 | NEB |
| 100 µg/ml BSA | 0.4 µl of x 100 | NEB |
| 1 mM Spermidine | 0.04 µl of 1 M | Sigma-Aldrich |
| 50 µg/ml RNase (DNase-free) | 0.2 µl of 10 mg/ml | Sigma-Aldrish |
| 15-20 units restriction enzyme | Varies | NEB |
| $H_2O$ | Up to final volume | - |

Whilst the ethanol was evaporating from the wells the restriction digest cocktail was prepared (see Table 2.3.5). Once the plate was completely dry, 35 µl of restriction digest cocktail was added to each well using a multi-channel pipette and the contents of each well was mixed by pipetting up and down ~ 10 times. Tips were changed between each row to avoid cross-contamination. The plate was sealed with tape and incubated overnight at the appropriate temperature for the restriction enzyme being used in a Tupperware box with wet paper towels. Once the digestion was complete the plate could be stored at -20°C until required.

## 2.4 Analysis of DNA

### 2.4.1 Determining the purity and concentration of DNA/RNA by UV spectroscopy

DNA concentration and purity were determined using a UV spectrophotometer (BioPhotometer, Eppendorf) as follows; 1 µl of sample was diluted 1:100 with DNA re-suspension buffer (usually water or X 0.1 TE buffer), mixed well and transferred into UV cuvette (Eppendorf). Re-suspension buffer without any DNA added was used as a blank. The BioPhotometer determines the concentration of the DNA using the equation; *Concentration (µg/ml) = ($A_{260}$ reading – $A_{320}$ reading) x dilution factor x 50 µg/ml*, since a DNA solution of 50 µg/ml has an absorbance of 1 at $A_{260}$ (this is adjusted for turbidity - $A_{320}$). Total yield was determined as; *Yield (µg) = Concentration (µg/µl) x total volume (µl)*. The purity of DNA was estimated from the $A_{260}$/ $A_{280}$ ratio, where pure DNA has a value of 1.8, though values from 1.7-2 are accepted as high quality DNA. A value of less than 1.8 is indicative of protein contamination and a value of 2.0 is thought to be pure RNA (see http://www.promega.com/paguide/chap9.htm#title1.g).

The concentration and purity of RNA was determined using a similar method. 2 µl of sample was diluted 1:30 with water and mixed well. High quality RNA should have an $A_{260}$/ $A_{280}$ ratio of 2.0, however it was also necessary to run an agarose gel to qualitatively assess the RNA quality – see below.

### 2.4.2 Agarose gel electrophoresis

Agarose gel electrophoresis was used to separate, purify and estimate the yield of DNA fragments ranging from 100 bp to 15-20 kb. An agarose gel was prepared to an appropriate concentration (see Table 2.4.1) in TAE buffer (40 mM Tris-Base, 1 mM EDTA (pH 8.0) 1.142% Glacial acetic acid). Gensieve LE agarose (Flowgen) was typically used, unless the DNA fragment of interest was to be extracted later for molecular cloning exercises (see Section 2.3.9), in which case SeaKem®GTG® agarose (Lonza) was used instead. The

agarose solution was melted in a standard microwave oven, on full power for 2-4 minutes with occasional swirling. Once fully dissolved the agarose solution was then allowed to cool to ~ 50°C before being supplemented with 0.5 µg/ml ethidium bromide (Roche) and poured into a sealed gel cast, with comb, to set. Once set, the comb and sealing tape were gently and carefully removed and the gel (in the supporting cast) was submerged (~ 1 mm over the surface of the gel) in TAE buffer inside a suitably sized electrophoresis tank. All DNA samples to be run were supplemented with 10% (v/v) orange G loading buffer (50% glycerol with sufficient orange G dye (BDH) to produce a bright orange colour) and were loaded carefully into the wells along with a DNA marker (either 100 bp DNA ladder (NEB) or 1 kb DNA ladder (Invitrogen) – as stated).

***Table 2.4.1: Appropriate concentration of agarose gels for different sized DNA fragments.***

| % agarose (w/v) | Effective resolution of DNA fragments (kb) |
|---|---|
| 0.5 | > 12 |
| 0.7 | 1-12 |
| 1.0 | 0.5-8 |
| 1.2 | 0.2-5 |
| 2 | 1 < |

Electrophoresis was run in horizontal gel units (Scie-Plas) by applying a voltage of 1-10 V/cm across the gel until the desired band separation had taken place. Since ethidium bromide was included in the agarose gel, DNA bands could be visualised as the samples were being run by placing the gel onto a High Performance UV-transilluminator (UVP). A picture was recorded digitally using a Kodak EDAS 290 and edited in Adobe Photoshop.

The yield of DNA fragments was estimated from the agarose gel, by comparing the intensity of the band of interest with the intensity of a band of known amount of DNA. The lower limit of what DNA could be visualised by eithidium bromide under a UV light was ~ 5-10 ng of DNA, whilst the upper limit to accurately predict the yield was ~ 200-500 ng. Estimating

DNA yield using this method was helpful when low concentration of DNA were expected, such as after a GENECLEAN (see Sections 2.3.9 & 2.3.10), since a UV spectrophotometer was not accurate at those ranges.

Agarose gel electrophoresis was also used to qualitatively assess the quality of RNA samples. The method was essentially the same as described above with the exception that the electrophoresis tank, gel cast and gel comb were soaked in 1 M HCl for an hour and then washed with copious amounts of RNase/DNase free water before use. A 1% general purpose agarose gel was prepared and run with 200-500 ng of each RNA sample (supplemented with Orange G loading buffer) including the 1 kb DNA marker. A digital photograph was taken and the RNA quality was assessed based on the presence and ratios of the two rRNA subunit bands, 28S and 18S. The large subunit (28S) should contain approximately twice as much double stranded RNA than the smaller subunit (18S); therefore in an un-degraded RNA sample there should be two sharp bands at ~ 2:1 ratio. In a degraded, or partially degraded RNA sample there is usually a shift in the 2:1 ratio towards a 1:1 ratio (since the larger subunit degraded faster) and other non-specific bands, or even a smear might be present on a gel. The presence of a separate smear towards the top of the gel is usually indicative of genomic DNA contamination.

### 2.4.3 Southern blotting

Southern blotting was used for screening of ES cell colonies in order to identify a successful targeting event. Briefly; DNA was extracted from the potential clones and was digested overnight with a restriction endonuclease enzyme (see Section 2.3.12) which would produce a digest pattern that could differentiate between wild-type and correctly targeted DNA. The digested DNA was run on an agarose gel (described above) and then the DNA was transferred by capillary action onto a nitrocellulose membrane, where it was immobilised by UV irradiation. The membrane was then probed with a short (300-700 bp) radioactively labelled DNA sequence unique to the fragment of interest. The probed membrane was then exposed to X-ray film in order to detect any radioactive signal. A correctly targeted ES cell

colony would show both the wild-type and the expected recombined size shift in the DNA digest pattern and would therefore be worth investigating further.

The Southern blotting protocol described here was based on [Sambrook et al., 2000]. Following DNA extraction and digestion from the ES cell colonies in the duplicate 96-well plates, samples were run on a 0.7% agarose gel. Included with the samples was the 1 kb DNA ladder, a wild-type control (10 µg of genomic DNA, digested with the same restriction enzyme as the samples) and an equivalent of a 0.1 and 0.01 copy number of the gene of interest used as positive control (from the linearised plasmid containing the DNA fragment corresponding to the probe DNA). Once the gel had been run a digital photograph was taken with a ruler on the UV transilluminator to record the ethidium bromide staining pattern (to determine whether there was complete digestion of DNA samples and approximate DNA yield).

The gel was prepared for transfer by several washes in buffers which denatured, depurinated and neutralised the DNA (see Table 2.4.2). The washes were performed as follows; 45 minute wash with agitation in denaturing buffer with buffer being replaced every 15 minutes, 5 minute wash in 0.2 N HCl with agitation, followed by brief rinse with water and finally 45 minute wash in 3 changes of neutralisation buffer. Meanwhile the DNA nitrocellulose membrane (HyClone), Whatman papers and paper towels were cut to the appropriate size. The nitrocellulose membrane was soaked for at least 20 minutes in $H_2O$, followed by soaking in 10 X SSC prior to use. Once the washes were complete the gel was placed briefly into 10 X SSC whilst the transfer apparatus was assembled. The Southern blot transfer apparatus was set up as shown in Figure 2.4.1. Once set up the apparatus was wrapped in cling-film to provide stability and reduce evaporation. Transfer was performed for 16 – 24 hours overnight.

***Table 2.4.2: Composition of Southern blotting buffers.***

| Buffer | Composition | Source |
|---|---|---|
| Denaturing buffer | 1.5 M NaCl | VWR |
| | 0.5 N NaOH | VWR |
| Neutralisation buffer | 1 M Tris (pH 7.4) | Calbiochem |
| | 1.5 M NaCl | VWR |
| 20 X SSC (pH 7.0) | 3 M NaCl | VWR |
| | 0.3 M Sodium citrate | Sigma-Aldrich |
| Pre-hybridisation mixture | 1 M NaCl | VWR |
| | 10% Dextran sulphate | PKChemicals |
| | 1% SDS | VWR |

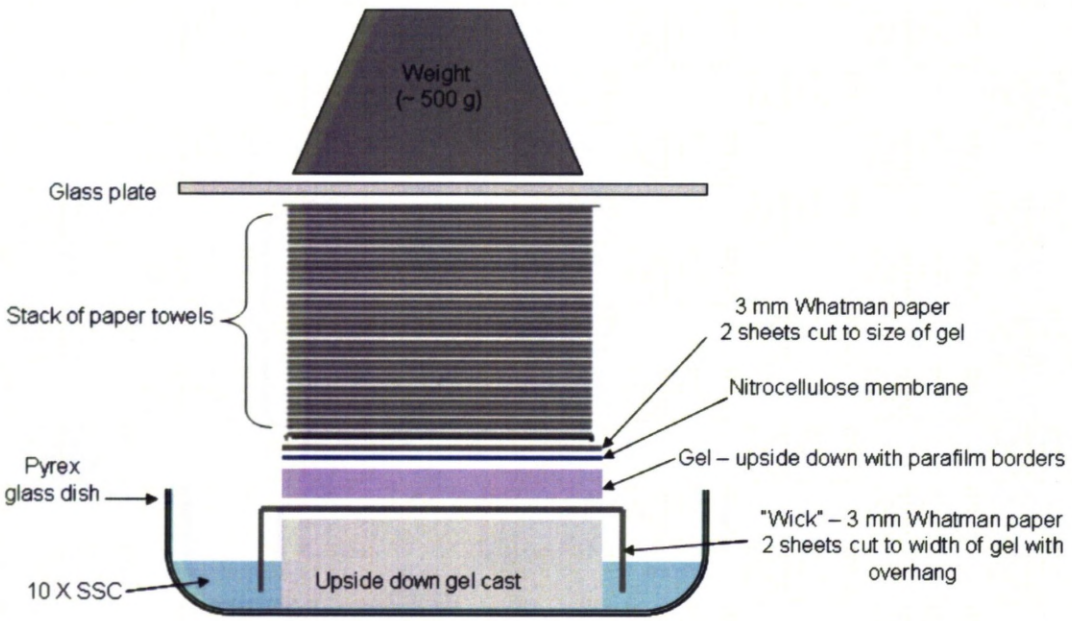


***Figure 2.4.1: Southern blot transfer apparatus.***

Once the transfer was complete the apparatus was disassembled and the back of each nitrocellulose membrane was marked to indicate which gel it was and where the first well was. If desired, to check the efficiency of the DNA transfer, the old agarose gel could be re-stained with ethidium bromide and photographed with UV light for comparison. Re-staining was performed by immersing the gel in a 0.5 µg/ml solution of ethidium bromide for 30

minutes with agitation; the gel was rinsed briefly in water to remove any excess ethidium bromide before examination. The nitrocellulose membranes were air-dried on a clean sheet of Whatman paper for 10-15 minutes and the DNA was then immobilised onto the nitrocellulose membrane by exposure to UV irradiation (using a UV cross-linker). The membranes at this point could be wrapped up in foil and stored for several months at 4°C. To continue with the protocol the dried membranes were soaked in 1 M NaCl for at least 30 minutes to ensure that the entire membrane had been completely wetted. In the meantime, the pre-hybridisation mixture (pre-hybe mix), hybridisation bottles, and hybridisation oven were all heated to 65°C. When ready, the nitrocellulose membranes were then transferred into the hybridisation bottle with 25 ml of pre-hybe mix. Two membranes could be placed into one chamber by using special mesh screens to separate them. The membranes were incubated in pre-hybe mix at 65°C with circular turning for at least 3 hours – typically this was performed overnight.

Ahead of commencing the screening experiments the probe sequence had been carefully designed and tested. For most screens the probe sequence was 300-700 bp long and was designed outside of the DNA targeting construct to prevent detecting false positive results. A draw back of this strategy, however, was that it would not detect random integration events and therefore a second screen was planned on any promising clones to address this. The probe itself was generated by PCR using primers designed by primer-BLAST (see Section 2.7.1) and was cloned by TA-cloning into vector pCR2.1 (see Section 2.6.6.1) and checked by sequencing (see Section 2.7.2.7). The probe was then liberated from vector pCR2.1 by performing a restriction digest (see Section 2.6.1) which was run on an agarose gel (see Section 2.4.2) and then the correct DNA fragment was extracted from the agarose gel by using the GENEclean *turbo* kit (see Section 2.3.9). 10% of the gene-cleaned product was run on another agarose gel to determine the concentration. The probe was then ready to be radioactively labelled.

The probe was radioactively labelled using the Amersham Megaprime DNA Labelling System RPN1604 according to the manufacturer's instructions as follows; in a 0.2 ml PCR tube 50 ng of probe DNA was added to 5 µl of primer mix and was brought to a final volume of 26 µl with $H_2O$. The mixture was boiled in a PCR machine for 5 minutes, allowed to cool to

RT and centrifuged briefly. Next the following components were added, 4 µl of dATP, 4 µl of dTTP, 4 µl of dGTP and 5 µl of reaction buffer. Then in the radiation room, behind the Perspex radiation screen 5 µl of $^{32}P$ labelled dCTP (Easy Tides Deoxycytidine 5'-triphosphate, [$\alpha$-$^{32}P$] 250 µCi (9.25 mBq) in 25 µl from Perkin Elmer) is was added, followed by 2 µl of Klenow (a DNA polymerase). The reaction was mixed by gentle pipetting and was then incubated at 37°C for 45 minutes. Whilst the reaction was taking place the G-50 sephadex separation column was prepared using a glass Pasteur pipette , which had been partly obstructed with a small amount of siliconised glass wool (Sigma-Aldrich) and filled with swollen G-50 sephadex beads (~50% (w/v) G-50 sephadex in water). Once the labelling reaction had finished the tubes were placed briefly on ice (at least 2 minutes) before being prepared for the column.

The radioactive labelling reaction was prepared for column purification by adding 20 µl of Orange G and 20 µl of dextran blue (HWM ≥ 2 MD). The solution was mixed by careful pipetting and was then loaded drop-wise onto the column. The eluate was collected in a 1.5 ml micro-centrifuge tube. Water was then added drop-wise (in 200 µl increments) and the blue droplets (containing the probe) were collected (typically 400 µl) in a separate screw cap top tube. A 2 µl aliquot of the probe was then used to measure the radioactivity in a liquid scintillation counter (PACKARD, 1500 TRI-CARB)). The specific activity (dpm/µg) of the probe was determined in order to calculate the volume necessary to achieve 1 x $10^6$ dpm/ml (a total of 2.5 x $10^7$ dpm was required for 25 ml). Salmon sperm DNA (Sigma-Aldrich) at a final concentration of 100 µg/ml was then added to the probe and the tube was boiled for 10 minutes, promptly incubated on ice for at least 5 minutes prior to being added to the pre-hybe mix with the nitrocellulose membranes. The hybridisation reaction was performed overnight in gently rotating hybridisation bottle(s) placed in hybridisation oven at 65°C.

The following morning the membranes were removed from the hybridisation bottle(s) and two quick washes in 2 X SSC were performed, followed by two 15 minute washes in 2 X SSC on a rocker at RT. The next two washes were in 2 X SSC, 0.1% SDS buffer and were performed inside a sealed Tupperware box in a shaking (60 rpm) 65°C water-bath (buffer was pre-heated). The final washes were in 0.1 X SSC at RT for 5 minutes on the rocker. The membranes were wrapped in cling-film and exposed to X-ray film (Kodak Biomax MS Film) in

a cassette with an intensifying screen at -80°C for 3-4 days. All reagents for radioactive labelling, unless otherwise stated were from Amersham. All film related paraphernalia was made by Kodak but sourced from Sigma-Aldrich.

## 2.5 Plasmids and Bacterial Artificial Chromosomes (BAC)

***Table 2.5.1: Plasmids.***

| Name | Description (Accession #) | Source |
|---|---|---|
| pACN | Contained a self-excision neomycin cassette (AF169416) | Dr Antonius Plagge |
| pBluescript II SK(+) | Basic cloning vector | Fermentas |
| pcDNA3 | Basic mammalian expression vector | Invitrogen |
| pcDNA3-WTp53 | Murine wild-type p53 cDNA cloned into pcDNA3 | Dr Lorna Warnock |
| pCR2.1 | TA-cloning vector – for cloning *Taq* amplified PCR products | Invitrogen |
| pCR-XL-TOPO | TA-cloning vector – for cloning long (3-10 kb) *Taq* amplified PCR products | Invitrogen |
| pE2-Crimson-N1 | Encodes for far-red fluorescent protein E2-Crimson | Clontech |
| pEGFP-N1 | Encodes red-shifted variant of GFP – suitable for N-fusions (U55762) | Clontech |
| pGL4.11 | Promoter-less luciferase reporter | Promega |
| pKO Scrambler NTKV-1902 | Contained negative selectable marker Thymidine kinase. | Stratagene |
| pmCherry | Source of pmCherry cDNA | Clontech |
| pRAY-Cre | Contains self-excision cassette with neomycin and URA3 (AJ627603) | Dr Antonius Plagge |
| pRS414 | Yeast-*E. coli* shuttle vector with TRP1 marker (U03448) | Dr Antonius Plagge |
| pUC19 | Control plasmid | Invitrogen |

***Table 2.5.2: Bacterial Artificial Chromosomes (BAC).***

*All BAC clones were sourced from Geneservice Ltd and contained segments of 129Sv/Ev genomic DNA, in vector pBACe3.6. These BAC clones carried resistance to chloramphenical.*

| Name | Gene of Interest | Size (bp) | Chromosome | Start | Finish |
|---|---|---|---|---|---|
| bMQ-305J12 | Mdm2 | 164210 | 10 | 117059258 | 117223468 |
| bMQ-81N13 | Mdm2 | 112123 | 10 | 117007437 | 117119560 |
| bMQ-262p22 | p21 | 102673 | 17 | 29198745 | 29301418 |
| bMQ-44e41 | p21 | 99063 | 17 | 29194941 | 29294004 |
| bMQ-397h22 | Puma | 118745 | 7 | 16837560 | 16956305 |
| bMQ-207e13 | Puma | 163875 | 7 | 16879773 | 17043648 |

# 2.6 Enzymatic manipulation of DNA

## 2.6.1 Restriction endonuclease digestion

Digestion of DNA was performed with restriction endonucleases, according to the manufacturer's instructions. All restriction endonucleases and buffers were purchased from New England Biolabs (NEB), unless otherwise stated. Plasmid DNA was digested either for diagnostic purposes (to identify correctly targeted recombinant clones) or for cloning exercises (i.e. for ligation reactions). Typically, for diagnostic digests, 0.5-1 µg of plasmid DNA was digested in a 20 µl volume containing 5-10 units of restriction enzyme supplemented with an appropriate X 1 buffer and if necessary X 1 BSA (final concentration of 100 µg/ml) – see Table 2.6.1 for reaction components. The digestion was incubated for at least 2 hours (generally 3-4 hours) at the manufacturers recommended temperature (usually 37°C). The DNA digest patterns were then analysed by agarose gel electrophoresis (see Section 2.4.2).

When DNA was prepared for ligation reactions, the same basic set-up as described above was applied, however, to ensure that there was sufficient DNA for the ligation reactions, (especially for DNA inserts < 300bp) up to 10 µg of plasmid DNA was digested. The digestion reaction was typically performed in a larger reaction volume (30-500 µl), with a longer incubation time (3 hours to overnight) and with X 10 excess enzyme (10 U/µg) to allow for complete digestion of the DNA. It was the volume of the enzyme which determined the final reaction volume since the enzyme content was not permitted to exceed 10% (v/v) (no more then 5% (v/v) glycerol) to reduce non-specific cutting (also called star activity). The digested DNA was then usually subjected to further enzymatic manipulation (de-phosphatising reaction – see Section 2.6.2, and/or blunting reaction – see Section 2.6.3) before being run on a GTG® (genetic technology grade) agarose gel and purified – see Section 2.4.2 & Section 2.3.9.

When a double digest was required (i.e. digestion with two restriction enzymes) the most suitable compatible buffer was chosen according to the manufacturer's guidelines to allow both enzymes a minimal activity of 75%. In the cases where no suitable compatible

buffer was available, the sequential digestion was performed by extracting the DNA after the first restriction digest using the liquid GENECLEAN protocol as described in Section 2.3.10 followed by the second restriction digest..

***Table 2.6.1: Components of a restriction endonuclease reaction.***

| Reaction component | Concentration/Amount |
|---|---|
| Plasmid DNA | ~ 0.5-10 µg |
| NEBuffer | X 1 |
| BSA | X 1 (100 µg/ml) |
| Restriction endonuclease | ~ 10 U/µg |
| Water | Up to the final volume |

## 2.6.2 Vector De-phosphorylation (Antarctic phosphatase reaction)

Antarctic phosphatase (NEB) was used to catalyse the removal of 5' phosphate groups from DNA and in doing so, reduce the probability of vector self-ligation and consequently the amount of vector background in cloning experiments. The procedure was performed according to the manufacturer's guidelines as follows; once the backbone vector DNA (1-5 µg) had been digested with the desired restriction enzyme (see Section 2.6.1) the reaction mix was supplemented with $1/10^{th}$ volume of X 10 Antarctic phosphatase buffer. 1 µl of Antarctic phosphatase (5 units) was then added and mixed by vortexing for 2-3 seconds. The sample was centrifuged briefly and incubated at 37°C for 15 minutes for 5' extensions or blunt-ends, or 60 minutes for 3' extensions. Antarctic phosphatase was inactivated by heating to 65°C for 5 minutes or alternatively by adding $1/10^{th}$ volume orange-G loading buffer and proceeding straight away with GTG® agarose gel electrophoresis (see Section 2.4.2).

### 2.6.3 Blunting DNA ends (with DNA polymerase I, large (Klenow) fragment)

DNA polymerase I, large (Klenow) fragment (NEB) was used to fill-in 5' overhangs and to remove 3' overhangs from DNA following restriction endonuclease reactions (see Section 2.6.1) to create a blunt-ended DNA product. Creating a blunt-ended DNA product was useful in some cloning exercises when there were no compatible cohesive end restriction sites available or when particular restriction sites needed to be removed for downstream cloning steps. The protocol was performed according to the manufacturer's instructions as follows; a 100 µl restriction enzyme reaction (in any X 1 buffer) was supplemented with 33 µM of each dNTP and 1 U of Klenow per µg DNA. The solution was mixed well by vortexing, briefly centrifuged and then was incubated at 25°C for 15 minutes. The reaction was promptly stopped by adding EDTA to a final concentration of 10 mM and incubating at 75°C for 20 minutes. The solution was then allowed to cool slowly before adding $1/10^{th}$ volume orange-G loading buffer and running the sample on a GTG® agarose gel (see Section 2.4.2).

### 2.6.4 Ligation of DNA fragments

DNA ligation reactions were performed with T4 DNA ligase (multiple sources, Ambion, Invitrogen, and NEB) according to the manufacturer's protocols. All T4 DNA ligases worked equally well, the choice of which enzyme to use was decided by availability at the time of the experiment. The Ambion T4 DNA ligase was routinely used for cloning in our laboratory, however this product was discontinued and our stock run out towards the end of this project. There was a small supply of the Invitrogen T4 DNA ligase available which was used before replacing and continuing with the NEB T4 DNA ligase.

The basic method of each ligation reaction remained relatively unchanged between each supplier and was set up as follows; the components of the ligation reaction were placed together in a 0.2 ml PCR tube (see Table 2.6.2) to a final volume of 10 µl (for Ambion and Invitrogen T4 DNA ligase) or 20 µl (for NEB T4 DNA ligase). The reaction was then mixed by vortexing for 2-3 seconds and centrifuged briefly before incubation at the appropriate temperature for overnight or longer. For cohesive end ligation reactions Ambion and Invitrogen supplied T4 DNA ligases were incubated at 14°C, whereas for blunt-end ligation

reactions they were incubated at 16°C. The NEB T4 DNA ligase was always incubated at 16°C and did not require additional supplementation with HCC and ATP for blunt-end DNA ligation reactions. Once the ligation reaction had been incubated sufficiently a small volume (1-5 µl) of the reaction was used in the transformation of competent *E. coli* – see Section 2.1.2.

***Table 2.6.2*: *Components of a ligation reaction.***

**Only added to blunt-end DNA ligation reactions with T4 DNA ligase from Ambion/Invitrogen.*

| **Component** | **Final concentration** |
|---|---|
| Vector DNA | 50 ng |
| X 10 ligase buffer | X 1 (could precipitate in storage so was warmed to 37°C before use and mixed well by vortexing) |
| Ligase | 1 unit |
| *Hexamine cobalt chloride (HCC) | 1.5 µM |
| *ATP | 0.5 mM |
| Insert DNA | At least 1:1 molar ratio of vector : insert DNA however typically aim for much higher insert concentration (1:3 – 1:10 ratio) |

In addition to the desired ligation reaction, two control reactions were also routinely performed. The control reactions included the vector DNA with and without T4 DNA ligase in the appropriate buffer with any supplements (e.g. HCC/ATP). Neither of the control reactions contained any insert DNA; hence neither of these control reactions should produce any bacterial colonies in a transformation reaction. The presence of bacterial colonies on the first control (with ligase) may indicate an inefficient de-phosphorylation reaction (see Section 2.6.2), whilst the presence of bacterial colonies on the second control (without ligase) might suggest an incomplete DNA digest (contamination with uncut plasmid DNA).

## 2.6.5 Annealing linkers and adaptors

Linkers and adaptors are short (8-14 bp) fragments of double stranded DNA that can be used to introduce new restriction endonuclease sites into a plasmid. Linkers are blunt ended whereas adaptors create cohesive ends. This project only used adaptor-oligonucleotides; however the principle behind both linkers and adaptors was the same. The first step was to pick a suitable restriction enzyme site to adapt and then carefully design the oligonucleotide sequences to introduce the desired new restriction enzyme site (see Figure 2.6.1). The oligonucleotides were obtained from Eurofin MWG Operon with a 5' phosphate modification which allows for the formation of phosphodiester bonds between the de-phosphorylated backbone vector and the adaptor.

The adaptors were annealed by mixing the two oligonucleotides together (0.2 µg each) in 0.1 X TE buffer in a 1.5 ml micro-centrifuge tube to final volume of 25 µl. The tube containing the reaction was centrifuged briefly and placed into recently boiled water ~ 90°C. The water (and reaction) was allowed to cool slowly down to RT, before being moved into a fridge to cool further to ~ 4-8°C. The oligonucleotides would have annealed during the temperature gradient and 2 µl was then used in a ligation reaction.

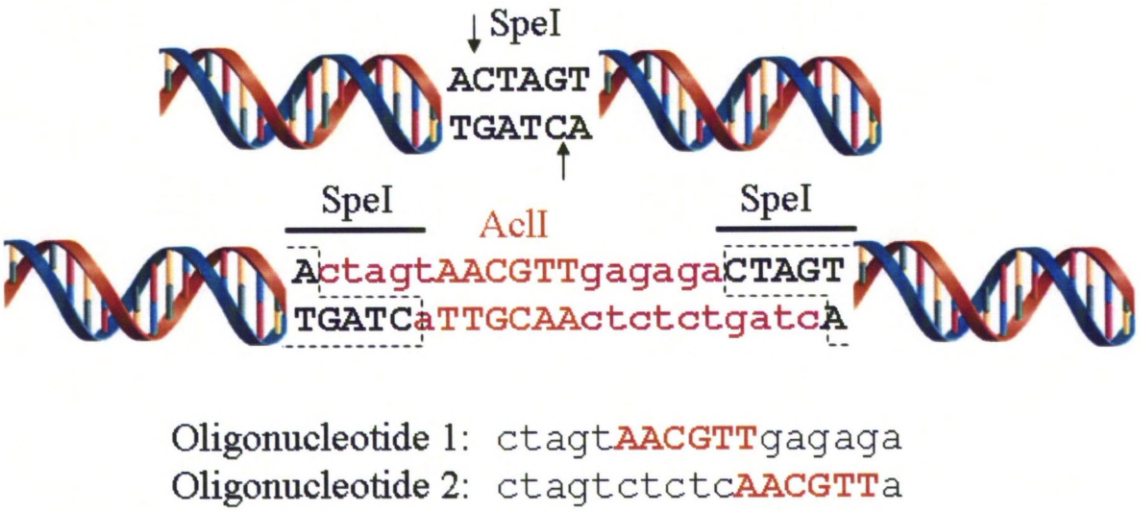


***Figure 2.6.1*: *An example of a design of adaptor oligonucleotides.***

*The SpeI site was chosen to be adapted to an AclI site. The adaptor was designed to complement the 5' overhang left by digestion with restriction endonuclease SpeI. The AclI site is introduced (shown in orange font) and non-specific bases are added to increase the amount of homology between the two oligonucleotides (in this case there will be 13 bp of overlapping double stranded DNA sequence). In this example the SpeI site was maintained, however the SpeI site could have been destroyed by designing the oligonucleotides differently.*

## 2.6.6 TA-cloning

### *2.6.6.1 A-tailing reaction (for cloning into pCR2.1 & pCR-XL-TOPO)*

Cloning into the vectors pCR2.1 or pCR-XL-TOPO (Invitrogen) is based upon the 3' A-tail overhang created by *Taq* DNA polymerase during a PCR reaction (see Section 2.7) for successful ligation (called TA-cloning). Therefore, it was necessary to add this 3' A-tail overhang to the blunt-ended PCR products created by Phusion DNA polymerase. Briefly, the first step of the A-tailing reaction was to remove or inactivate any remaining Phusion DNA polymerase. This was because Phusion had 3' to 5' exonuclease activity and hence any residual enzyme would continue to remove the desired A-tail. The next step was incubation (in a suitable buffer) with excess dATPs and *Taq* DNA polymerase to attach the 3' A-tails.

There were three different methods for achieving the first important step of reducing the activity of Phusion; the first two protocols simply allowed the enzyme to become less efficient at removing the A-tails which fresh *Taq* DNA polymerase enzyme adds either by leaving the initial Phusion DNA polymerase PCR reaction overnight at 4°C or by heat-treating the reaction instead. The third method removed the Phusion DNA polymerase completely. Heat-treating was performed by incubating the Phusion PCR reaction at 98°C for 20 minutes immediately after completion of the PCR reaction. The reaction was then allowed to cool slowly before proceeding with the A-tailing reaction. Alternatively Phusion could be removed completely from the PCR reaction by performing a liquid GENECLEAN for purification of DNA (see Section 2.3.10). This third method was the most robust and was therefore the preferred option when multiple samples were being prepared simultaneously. However for successful ligations this required a high PCR product yield due to loss of PCR product during multiple purification steps (recovery rate was typically 70-90%).

The A-tailing reaction was then performed as follows; to the old PCR reaction (typically in 50 µl) 1 µl of 10 mM dATPs and 1 µl of *Taq* DNA polymerase (10 units) were added, mixed well and centrifuged briefly before incubation at 72°C for 20 minutes. When the DNA had been purified by liquid GENECLEAN, the reaction was performed as described above, except the reaction needed to be supplemented with X 1 *Taq* DNA polymerase buffer. Once the A-tailing reaction was completed the PCR products were then run on a GTG® agarose gel, and the DNA extracted for downstream cloning steps.

### *2.6.6.2 Topoisomerase reaction (cloning into pCR-XL-TOPO)*

The TOPO® XL PCR cloning kit was purchased from Invitrogen and was used to clone long (3-10 kb) PCR products into the pCR®-XL-TOPO vector. The pCR®-XL-TOPO vector was supplied linearised with single 3' T overhangs for TA-cloning and was also covalently bound to topoisomerase, which catalysed the ligation of DNA fragments. The reaction was performed according to the manufacturer's instructions as follows; 4 µl of gel purified PCR product (DNA concentration was between 2-40 ng/µl – estimated by agarose gel electrophoresis see Section 2.4.2) was added to 1 µl of linearised pCR®-XL-TOPO vector

and mixed gently. After 5 minutes of incubation at RT, 1 µl of the 6 X TOPO® Cloning Stop Solution was added and mixed gently. The tube containing the reaction was then briefly centrifuged and placed on ice. 1-2 µl of the topoisomerase reaction was then used immediately in the transformation of competent *E. coli*.

# 2.7 Amplification of DNA by Polymerase Chain Reaction (PCR)

## 2.7.1 Standard Procedures and Optimisation

DNA fragments of interest were amplified using two suitable primers and a thermostable DNA polymerase (such as *Taq* or Phusion). A standard reaction (in 25 µl) contained an enzyme at the manufacturer's recommended working concentration with the supplied buffer, 800 µM dNTPs (GE Healthcare), 0.05 µg of each primer and the appropriate amount of template DNA (typically 10 ng of BAC clone or 0.1 µg of genomic DNA) (see Table 2.7.1). Once all components of a PCR reaction were mixed they were placed in a thermal cycler (Px2 Thermal Cycler, Thermo. Electron Corporation) and appropriate cycle conditions were used (see Table 2.7.2). Following a number of cycles (typically 30) the specific DNA of interest was amplified sufficiently for visualisation by UV light once stained with ethidium bromide in an agarose gel (see Section 2.4.2). In PCR reactions where the DNA product was to be used in molecular cloning, additional optimisation was required to increase specificity and reduce the introduction of random mutations. This was accomplished in two stages; i) a temperature gradient was performed for the annealing temperature and ii) the number of cycles performed was reduced to the minimum required.

For standard, relatively short PCR products (up to 2 kb), A-Tailing reactions (see Section 2.6.6.1) and for screening bacterial colonies (see Section 2.7.2.4) *Taq* DNA polymerase (NEB) was used. Alternatively, when screening was performed on genomic DNA, JumpStart *Taq* DNA polymerase (Sigma-Aldrich) was used. The use of JumpStart *Taq* DNA polymerase markedly reduced non-specific products because the enzyme was only activated once heated to its optimal temperature (heat-denaturing antibody hot start).

***Table 2.7.1: Standard components of a PCR reaction.***

| **Component** | **/25 µl** |
|---|---|
| Standard buffer | X1 |
| dNTPs | 200 µM each |
| Primers | 0.05 µg each |
| DNA polymerase | 0.5-1 units |
| DMSO (optional) | 3% |
| Template DNA | 50-250 ng of high complexity DNA (genomic)<br>1 pg-10 ng of low complexity DNA (plasmids) |

***Table 2.7.2: Standard cycle conditions for DNA polymerases Phusion and Taq.***

| | Phusion High-Fidelity DNA polymerase | | *Taq* DNA polymerase (NEB) | | JumpStart *Taq* DNA polymerase | |
|---|---|---|---|---|---|---|
| Initial denaturisation | 98°C | 30 sec | 95°C | 30 s | 94°C | 2 minutes |
| **15-35 cycles** | | | | | | |
| Denaturisation | 98°C | 10 s | 95°C | 30 s | 94°C | 30 s |
| Anneal | 50-65°C | 30 s | 50-65°C | 30 s | 55-68°C | 30 s |
| Extend | 72°C | 15-30 s/kb | 68°C | 60 s/kb | 72°C | 2 minutes |
| Final extension | 72°C | 5-10 minutes | 68°C | 5 minutes | 72°C | 5 minutes |
| Hold | 4°C | | 4°C | | 4°C | |

For all molecular cloning or on longer more difficult to amplify DNA templates, PCR reactions were performed with Phusion (Hot Start) High-Fidelity DNA polymerase (NEB). Phusion was supplied with two buffers, a high-fidelity standard buffer and a second buffer for use with GC-rich or difficult to amplify DNA templates. A standard procedure was implemented such that, if a PCR reaction failed using the standard reaction buffer, the GC-rich buffer was used instead with a further addition of 3% DMSO if the reaction continued to

fail. PCR reactions which failed even after supplementation with DMSO were abandoned or new primers were designed.

Primers were designed using Primer3 (http://frodo.wi.mit.edu/primer3/) or Primer-BLAST (http://www.ncbi.nlm.nih.gov/tools/primer-blast/index.cgi?LINK_LOC=BlastHome) and were usually 18-25 nt in length, with a GC content between 40-70% and a melting temperature (Tm) close to 60°C. When Primer3 could not find suitable primers or when specific mutations/start sites were required the oligonucleotides were designed manually and analysed on Primer3 to check their properties. All oligonuleotides were synthesised by Eurofins MWG Operon (http://www.eurofinsdna.com/home.html) and were reconstituted in $H_2O$.

## 2.7.2 Specialised PCR techniques

### *2.7.2.1 PCR-mediated mutagenesis*

PCR was used to introduce useful sequences (such as unique restriction sites, point mutations and nuclear localisation signals) at the ends of PCR products. The desired sequence (up to a maximum of ~80 bp) was added to the 5' end of oligonuleotides and would, provided that there was sufficient homology at the 3' end of the primer to perform the reaction, be incorporated into the new PCR fragment see Figure 2.7.1. The appendage of additional sequence to the 5' end of primers does not affect the properties of the original PCR reaction – hence all site-directed mutagenesis PCR reactions were optimised as described previously in Section 2.7.1. A 5'-GAGA cap was also included in the primer design in order to protect the integrity of the desired sequence.

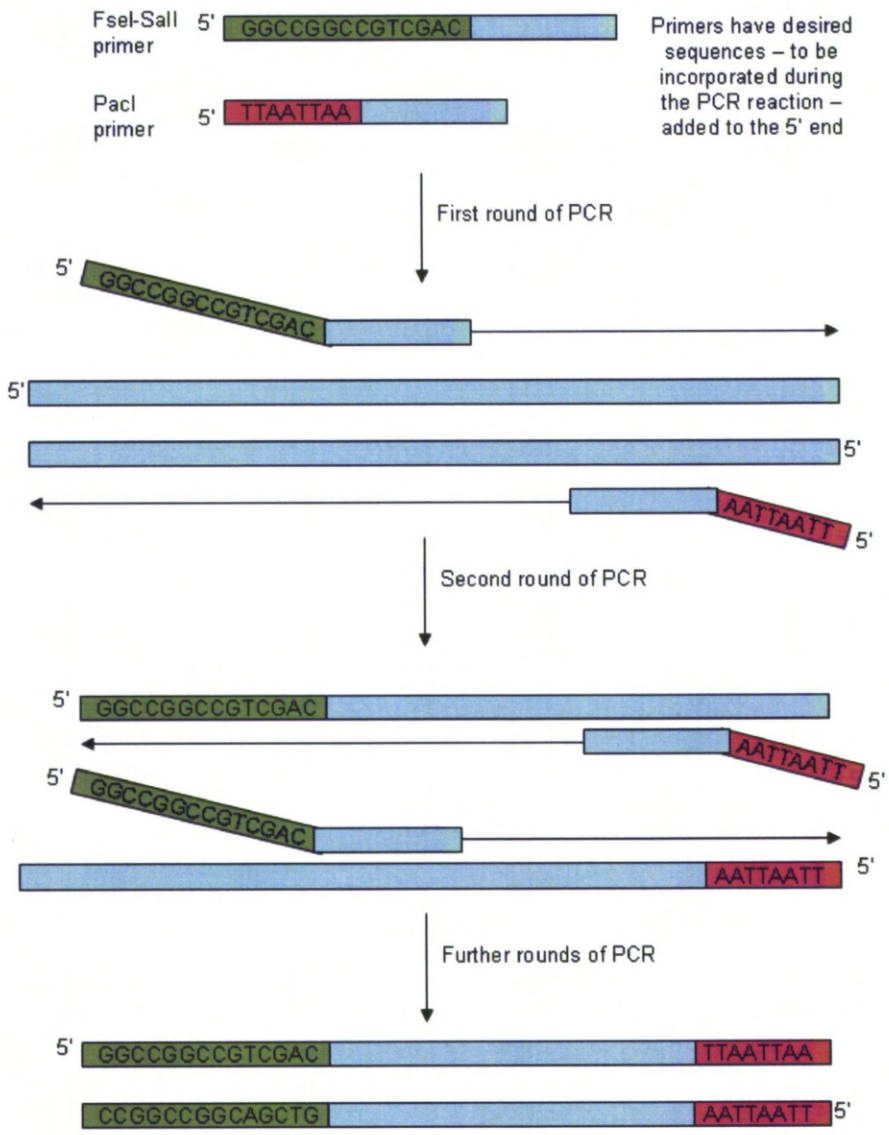


***Figure 2.7.1: Schematic diagram of an example of PCR-mediated mutagenesis.***

*Adapted from [Watson et al., 2007]. The addition of the restriction enzymes sites FseI-SalI, and PacI to the PCR product was achieved as follows. Primers were designed to include 18-25 nt of complementary sequence to the template DNA and the desired sequences were included on the 5' end of the primers (as well as a 5'-GAGA protective cap, not shown here). The PCR reaction was carried out as described in Section 2.7.1 and following further rounds of PCR the final product contained the new modifications, in this case the restriction enzyme sites FseI-SalI and PacI.*

### 2.7.2.2 *Fusion PCR*

Fusion (or overlap extension) PCR is a technique which enables the accurate joining of two individual PCR products to produce one larger combined PCR product. In order to 'fuse' the two PCR products together they must have a short (~15-40 bp) overlapping DNA sequence at the relevant 5' or 3' end of the PCR fragment. The overlapping sequence can either exist within the DNA template or be added on through PCR-mediated mutagenesis (see Section 2.7.2.1). The procedure is carried out in two stages, briefly the first stage amplifies and purifies the two starter PCR products individually and the second stage mixes these two templates together for a further round of PCR – which creates the fused product (see Figure 2.7.2).

A typical fusion PCR reaction was performed as follows; after careful planning, and primer design the two initial PCR reactions were optimised and performed as described in Section 2.7.1. The products from these PCR reactions were then separated and purified by agarose gel electrophoresis (see Section 2.4.2) and DNA gel extraction (Section 2.3.9). 10% of the gel-purified DNA product was run on another agarose gel to estimate the concentration of the DNA. The two DNA products were mixed at a 1:1 molar ratio and this DNA mixture was then used as the template DNA for the final round of PCR.

***Table 2.7.3: Standard components of a fusion PCR reaction.***

| **Component** | **/50 µl** |
|---|---|
| HF or GC-rich buffer | X1 |
| dNTPs | 400 µM each |
| Very end primers | 0.1 µg each |
| Phusion DNA polymerase | 1 units |
| DMSO (optional) | 3% |
| Template DNA | 25-37.5 µl of DNA mixture (~20-200 ng) |

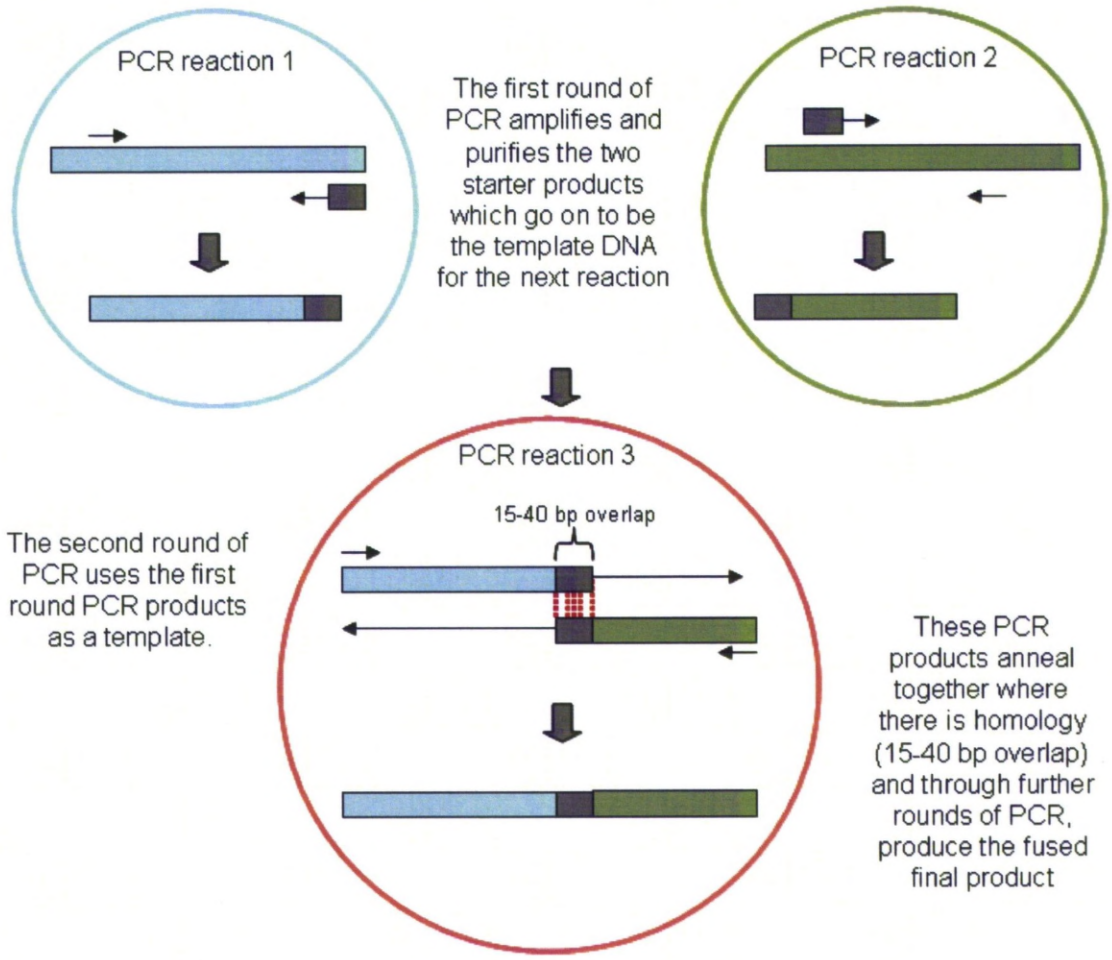


***Figure 2.7.2: A schematic diagram of fusion PCR***

*In the first round of PCR the two starter products which are to be joined together are amplified separately. In this example the overlap region (shown in grey) is added on to each starter product by PCR-mediated mutagenesis (see Section 2.7.2.1). Once purified the two starter PCR products are mixed together in a 1:1 molar ratio and become the template DNA for the next PCR reaction. The two templates anneal together where there is overlapping sequence homology (shown as dotted red lines) and act as primers from the join region, to begin to create the desired fused PCR product. The very end primers are also included and after several more cycles of PCR (typically 20-30) the full length fused PCR product is produced.*

The final round of PCR was performed in 50 µl and unlike normal PCR reactions the template DNA contributed to 50-75% of the total reaction volume (see Table 2.7.3). The PCR reaction was performed according to the Phusion DNA polymerase specifications listed in Table 2.7.2, typically 20-30 cycles of PCR were required to generate the full length PCR product. Fusion PCR was used to join together DNA fragments from different templates, to introduce specific site mutations and to overcome difficulties in amplifying large PCR products from problematic regions of DNA.

### *2.7.2.3 Manual hot start PCR*

Hot start PCR is used to minimise contamination with non-specific DNA products and to reduce the formation of primer dimers. Non-specific products could be a particular problem when genomic DNA was used as a template, or when the primers were designed in a repetitive region of DNA. Non-specific products are often result of non-specific priming at lower temperatures and one method to reduce this background is to only add the DNA polymerase once the PCR reaction has been heated to its denaturisation temperature (typically 95°C or 98°C) – called a hot start PCR.

Most commercially available DNA polymerases can be supplied bound to an antibody which prevented the non-specific activity of the polymerase at lower temperatures until the antibody becomes denatured (for example JumpStart *Taq* DNA polymerase). However, these hot start enzymes are more expensive and so in some cases it was preferred to perform a manual hot start. A manual hot-start was performed by mixing all the components of the PCR reaction together, except for the DNA polymerase, and heating the mixture to the denaturisation temperature optimised for that DNA polymerase (in the case of *Taq* DNA polymerase from NEB, this temperature was 95°C). Once heated the tubes are quickly supplemented with 0.5 units of DNA polymerase (the stock enzyme was diluted to a suitable concentration, for example 0.5 units/µl to simplify the task of pipetting). The reaction then continued as for a normal PCR reaction.

### 2.7.2.4 Bacterial colony PCR

PCR was used to screen bacterial colonies from LB agar plates directly using a technique called bacterial colony PCR. Briefly, bacterial colonies were selected and dipped into a pre-prepared tube containing the PCR reaction. The remaining bacteria (still attached to the inoculation loop) were then inoculated into a 5 ml LB starter culture and grown at 37°C overnight with shaking for expansion and DNA mini-prep. This technique requires a robust PCR reaction for successful screening, with a good positive control, which has been optimised as described in Section 2.7.1 in advance of screening.

Bacterial colony PCR was performed as follows; a PCR master mix was prepared for the number of colonies to be screened (plus a positive and negative control) assuming that the bacterial colony would take up approximately 1 µl volume, using *Taq* DNA polymerase (NEB). The PCR master mix was then aliquoted into labelled PCR tubes and kept chilled on ice whilst separate tubes containing 5 ml LB (plus appropriate antibiotic) were prepared and labelled. Next, one bacterial colony was selected from the LB-agar plate (containing the recombinant clones to be screened), and was picked using an inoculation loop and aseptic technique. The loop, with the bacteria attached, was then dipped 2-3 times very carefully into the PCR reaction tube before being shaken much more vigorously into the LB starter culture tube. The PCR reaction was then performed as described in Section 2.7.1 and analysed by agarose gel electrophoresis (see Section 2.4.2).

### 2.7.2.5 Yeast Colony PCR

PCR was performed on yeast cells to screen for positive recombinant clones. The method was very similar to the bacterial colony PCR described above, except for an additional initial heat denaturisation step. The protocol was performed as follows; 2-3 days previously a master yeast plate was generated by spreading individual yeast clones onto another minimal yeast agar plate with a grid. One master yeast plate containing 20-30 colonies was usually sufficient for screening, since the majority of clones were expected to be positive due to the double selection protocol (see Section 2.2). Once the yeast colonies had grown into thick patches a sterile toothpick was used to gently scrape the surface of each

patch. The toothpick was then transferred to a 0.2 ml PCR tube containing 10 µl of $H_2O$ and shaken to dislodge the yeast cells. The yeast cell mixture was then heated to 90°C for 10 minutes; in the meantime a PCR master mix was prepared using Phusion Hot Start DNA polymerase as described in Section 2.7.1. The PCR reaction was then aliquoted into PCR tubes and kept on ice. After the 10 minute incubation the yeast/$H_2O$ mixture was vortexed well and 1 µl was transferred into each PCR reaction. Yeast colony PCR reactions were mixed by pipetting since the samples could not be centrifuged once the yeast cells had been added. The PCR was performed as described in Section 2.7.1 for 30 cycles and then analysed by agarose gel electrophoresis (see Section 2.4.2).

### *2.7.2.6 Sequencing reaction (MegaBACE)*

The DYEnamic™ ET dye terminator cycle sequencing kit (MegaBACE™) was used to perform short sequencing reactions (150-400 nt in length) when there were many different clones to screen and multiple reactions to perform. The sequencing reaction was performed according to a slightly modified version of the manufacturer's instructions as follows; the plasmid DNA to be sequenced was diluted to a concentration of 1 µg / 11 µl in $H_2O$ (not TE buffer since the EDTA could sequester important metal cofactors). Master mixes were then prepared for each primer (see Table 2.7.4 for reaction components) and were aliquoted into the wells of a 96-well plate. 0.5 µg of the desired template DNA in 5.5 µl was then added to each corresponding well. Once all the reagents had been prepared the 96-well plate was sealed and the cycling programme described in Table 2.7.5 was performed.

***Table 2.7.4: Components of a standard MegaBACE sequencing reaction.***

| **Component** | **/10 µl** |
|---|---|
| DYEnamic ET reagent premix | 4 µl |
| Primer (5 µM) | 0.5 µl |
| DNA template | 5.5 µl (0.5 µg) |

***Table 2.7.5: Standard cycling parameters of a MegaBACE sequencing reaction.***

| **25 cycles** | | |
|---|---|---|
| Denaturisation | 95°C | 20 s |
| Anneal | 50°C | 15 s |
| Extend | 60°C | 1 minute |

Following completion of the sequencing reaction excess dye and other contaminants were removed from the reaction mixture by using a genCLEAN 96 Well Dye Terminator Removal Kit (Genetix) – see Section 2.3.11 for details. The sequence details were obtained by using the Cimarrun 3.12 software within the MegaBACE sequence analyser and were exported as a text document in FASTA format.

### *2.7.2.7 Sequencing (Eurofins MWG Operon/GATC)*

For longer, higher quality DNA sequencing reads (up to 1100 nt) DNA samples were outsourced for sequencing. The two companies used in this project to perform this service were Eurofins MWG Operon and GATC Biotech. The DNA samples were prepared for sequencing following instructions on the company websites summarised in Table 2.7.6.

***Table 2.7.6: DNA sample preparation for sequencing at Eurofins MWG Operon and GATC Biotech.***

*The information in this table was taken directly from the company websites.*

| | **Eurofins MWG Operon** | **GATC Biotech** |
|---|---|---|
| Purified plasmid DNA | 50-100 ng/µl in minimum volume of 15 µl (per reaction) | 30-100 ng/µl in 20 µl (sufficient for 8 reactions) |
| Primers | 15 pmol, sent pre-mixed with template DNA | 10 pmol/µl in 20 µl (sufficient for 8 reactions) |
| Purified PCR product | 2-10 ng/µl in minimum volume of 15 µl (per reaction) | 10-50 ng/µl in 20 µl (sufficient for 8 reactions) |

## 2.8 Bioinformatics

### 2.8.1 Basic Local Alignment Search Tool (BLAST)

BLAST is a search tool hosted by the National Center for Biotechnology Information (NCBI), used to align nucleotide or protein sequences and to statistically analyse how similar they are. In this project BLAST was generally used to compare data from DNA sequencing against either a database (for example the mouse genomic plus transcript database) or my own input material (for example vector DNA sequences). Specialised BLAST tools, such as primer-BLAST were also used to help design primers – see Section 2.7.1.

Website: http://blast.ncbi.nlm.nih.gov/Blast.cgi?CMD=Web&PAGE_TYPE=BlastHome

### 2.8.2 Identification of transcription factor binding sites (MAPPER)

MAPPER (Multi-genome Analysis of Positions and Patterns of Elements of Regulation) is an online search engine used to identify putative transcription factor binding sites (TFBS) within a DNA sequence [Marinescu et al., 2005]. It had extensive TFBS databases for several species including human and mouse and matches were displayed with straightforward access to the recognition model, statistical alignment scores and binding factor information (including the organism and structural class).

Part of this thesis was to design a mutated version of the *Mdm2* P2 promoter region so that the P2-mutant would lose its ability to be bound and up-regulated by p53, but would be unaffected at any other, validated or speculated, TFBS. The MAPPER resource was used to help design the specific base changes in the P2 promoter region by monitoring for the deletion or introduction of TFBS as well as to verify that the p53 REs were no longer detectable. Briefly the task was performed as follows; the wild-type *Mdm2* p53 RE DNA sequence +/- 40 bp was searched for putative TFBS, which were then recorded by exporting the graphical display and data summary sheet. Next, based on the consensus binding site for p53, various positions along each of the *Mdm2* p53 REs were mutated in order to disrupt them. The modified sequence (at first only containing 2 nucleotide substitutions) was then

run through the MAPPER search engine to confirm whether or not the p53 REs were still present. The number of nucleotide substitutions was steadily increased, starting with the most conserved positions (to be more effective at disrupting the p53 consensus binding sites), until the minimum number of base alterations that would theoretically prevent p53 binding was discovered. Attention was then focused on reducing non-specific effects such as deletion/introduction of other TFBS within the region that could potentially lead to confounding variables and make the results difficult to interpret. This was accomplished through systematically altering each base substitution to minimise its local effects. MAPPER was used to search for TFBS between each round of mutations and through a process of trial and error, combined with some educated deduction from using the recognition models available on MAPPER, the optimum sequence was derived. That is, the sequence that had the smallest number of mutations, which successfully prevented p53 binding whilst altering as few other TFBS within the region as possible.

Since the P2-mutant sequence was to be ultimately used in the generation of a transgenic mouse line, one final consideration to be included in the designing process was to introduce a restriction endonuclease site (or delete one) for screening purposes. Therefore once the optimum sequence had been defined, the sequence was further analysed (using NEBcutter – see Section 2.8.6) to see if any restriction enzyme sites had been introduced by chance, and if not, whether one could be incorporated without compromising any of the previously optimised features.

Website: http://mapper.chip.org

### 2.8.3 Splice site prediction tool

The splice site prediction tool was used to identify putative splice acceptor sites within a given DNA sequence [Reese et al., 1997]. Specifically, for this thesis, this tool was used to determine whether the point mutations designed for the disruption of the p53-REs within the *Mdm2* P2 promoter region had introduced any additional splice acceptor sites (compared with the wild-type *Mdm2* P2 promoter region).

Website: http://www.fruitfly.org/seq_tools/splice.html

### 2.8.4 Translation tool (ExPASy)

The ExPASy translation tool is hosted by the Swiss Institute of Bioinformatics (SIB) and was used to translate nucleotide sequences into their corresponding amino acid code. The tool was particularly helpful when checking whether a fused DNA sequence was in-frame and also for determining whether or not an unwanted DNA mutation was silent, that is the change in DNA sequence did not result in an altered protein sequence.

Website: http://web.expasy.org/translate/

### 2.8.5 Reverse complement

The reverse complement tool was used to convert DNA sequences into their reverse complement counterparts, which was helpful for many basic DNA sequence manipulation exercises, such as reversing primers and compiling vector DNA sequences. Another useful aspect of the reverse complement programme, although not its intended purpose, was that the tool removed all document formatting. Document formatting such as paragraphing and the inclusion of numbers or spaces was often present in downloaded DNA sequences and was a nuisance since it made searching for a particular DNA sequence (for example a primer or the start of a gene) within a sequence in Microsoft Word almost impossible. Formatting was removed using this tool as follows; the desired formatted version of the DNA sequence was entered and run through the reverse complement tool twice. The first round was sufficient to remove the formatting however the sequence will be its reverse complement; therefore a second round was performed on the output of the first round to revert the DNA sequence back to its original 'forward' configuration.

Website: http://www.bioinformatics.org/sms/rev_comp.html

### 2.8.6 Restriction site mapping (NEBcutter)

The NEBcutter, restriction site mapping tool was used to analyse DNA sequences for the presence (and absence) of restriction enzyme sites [Vincze et al., 2003]. NEBcutter was essential when designing DNA cloning strategies to check for available restriction sites and to determine which restriction endonucleases should be avoided (for example if they cut elsewhere in a critical region of the DNA). Restriction mapping was also important for designing screening strategies, for example during routine recombinant clone diagnostic digests (see Section 2.6.1) and Southern blotting (see Section 2.4.3)

Website: http://tools.neb.com/NEBcutter2/

### 2.8.7 Chromatogram analysis (Sequence Scanner)

The Sequence Scanner Software v1.0 was downloaded from Applied Biosystems and was used to open chromatogram files with the extension .ab1 from sequencing reactions performed by GATC Biotech. The software contained a helpful search function and adjustable scale bars which enabled fast and detailed inspection of the sequencing reactions' raw format. These features were helpful when there was an apparent mutation in a DNA sequence, since the 'mutated' nucleotide could be located quickly (using the Find option and pasting in the aligned sequence just prior to the mutation – sequences were aligned in BLAST– see Section 2.8.1) and were examined closely by adjusting the scale to determine whether the mutation was real or just a base miscall. Confirmed mutations were dealt with on a case by case basis to decide what impact the mutation might have (if any).

# 2.9 Mammalian Cells

## 2.9.1 Cell lines used and cell culture

Cell culture was carried out in Class II safety cabinets using aseptic technique. Cells were grown at 37°C, in 5% $CO_2$ in a humidified incubator and all reagents were pre-warmed to 37°C. A summary of the cell lines used in this project and their growth medium is listed in Table 2.9.1. A detailed description of each cell line and its maintenance is provided next.

H1299 is an immortalised, p53 null, human non-small cell lung carcinoma cell line. H1299s were routinely passaged 1:10 at 100% confluency. Subculture of cells was performed as follows. Once cells reached the desired confluency (typically took 2-3 days) the old media was removed and the cells washed with Dulbecco's phosphate buffered saline (DPBS – Sigma-Aldrich) see Table 2.9.2 for appropriate volumes. Trypsin-EDTA (Sigma-Aldrich) solution was then applied evenly to the cells, by gentle tilting of the culture vessel to ensure adequate coverage, and the cells returned to the incubator for 2-5 minutes. Once the cells were becoming detached from the cell culture vessel, confirmed by microscopy, the trypsin was inactivated by adding at least x1 volume of growth media. The cells were then pipetted vigorously to ensure a single cell suspension and replaced into fresh culture vessel/s at the appropriate cell density with new media.

H1299 cells were frozen for long term storage in liquid nitrogen as follows; once the cells were in a single cell suspension (see above) the cells were then harvested by centrifugation at 300 x *g* for 5 minutes at RT. The cell pellet was then gently re-suspended in x 1 freezing media (see Table 2.9.3) at 1-2 x $10^6$ cells/ml and dispensed in 0.5 ml aliquots into cryovials. The cryovials were then packaged into polystyrene containers and placed into a -80°C freezer, to freeze slowly. After at least 24 hours the cryovials were moved into liquid nitrogen storage.

***Table 2.9.1*: Summary of cell lines used and the composition of each cell lines' growth medium.**

**These cell lines required high quality (HQ) FBS – see text for details. β-mercaptoethanol (Sigma-Aldrich #M6250) was prepared as a x 100 stock solution in ESQ-PBS which was sterilised by filtration and stored at 4°C. ESGRO® LIF (Millipore #ESG1107) was prepared as a x 1000 stock solution in ES cell media and stored at 4°C in aliquots.*

| Cell line | Source | Base medium | Supplements |
|---|---|---|---|
| H1299 | Laboratory stock | RPMI-1640 (Sigma-Aldrich) | 10% FBS (Sigma-Aldrich) |
| Wild-type MEF | Laboratory stock | DMEM HEPES modification (Sigma-Aldrich #D6171) | 10% FBS (Sigma-Aldrich)<br>2 mM L-glutamine (Invitrogen) |
| p53 null MEF | Laboratory stock | As above | As above |
| Double null MEF | Laboratory stock | As above | As above |
| *SNL76/7 | The Wellcome Trust Sanger Institute | KnockOut DMEM (Invitrogen #10829018) | 7% HQ FBS (HyClone/Invitrogen)<br>2 mM L-glutamine |
| *AB2.2 | The Wellcome Trust Sanger Institute | As above | 15% HQ FBS (Invitrogen)<br>2 mM L-glutamine<br>1 x $10^{-4}$ M β-Mercaptoethanol<br>1000 units/ml LIF |
| *AM0998 | IGTC | As above | 15% HQ FBS (HyClone)<br>2 mM L-glutamine<br>1 x $10^{-4}$ M β-mercaptoethanol |

***Table 2.9.2: Appropriate volumes of DPBS, trypsin, gelatin and media to add to each culture vessel.***

| Culture Vessel | | Volume of DPBS (ml) | Volume of Trypsin | Volume of gelatin | Volume of media |
|---|---|---|---|---|---|
| Multiwell plates | 96-well | 0.1 | 25 µl | 70 µl | 200 µl |
| | 48-well | 0.3 | 100 µl | 200 µl | 300 µl |
| | 24-well | 0.5 | 250 µl | 500 µl | 1 ml |
| | 6-well | 5 | 0.5 ml | 3 ml | 5 ml |
| Dishes | 6 cm | 5 | 0.5 ml | 3 ml | 5 ml |
| | 10 cm | 5 | 1 ml | 7 ml | 10 ml |
| | 15 cm | 10 | 3 ml | 12 ml | 12 ml |
| Flasks | T25 | 5 | 1ml | 3ml | 5 ml |
| | T75 | 10 | 2 ml | 10 ml | 10 ml |
| | T175 | 10 | 3 ml | 15 ml | 25 ml |

***Table 2.9.3: Formulation of the freezing media used in this project.***

| Cell line/s | Freezing media components | Source |
|---|---|---|
| H1299, wild-type MEF, p53 null MEF, double null MEF | *x 1 freezing media*<br>90% FBS<br>10% DMSO | <br>Sigma-Aldrich #F9665<br>Sigma-Aldrich #D5879 |
| SNL76/7, AM0998, AB2.2 | *x 2 freezing media*<br>80% high quality (HQ) FBS<br>20% HQ DMSO | <br>HyClone/Invitrogen<br>Sigma-Aldrich #D2650 |
| 96-well plates of ES cells | *x 2 freezing media*<br>40% ES cell media<br>40% HQ FBS<br>20% HQ DMSO | <br>See Table 2.9.1<br>Invitrogen<br>Sigma-Aldrich #D2650 |

Frozen cell lines were thawed and growth re-established as follows; the cryovial/s containing the desired cell line were removed from liquid nitrogen storage and the caps of the cryovials were loosened slightly (to prevent the vials from exploding). These vials were then placed into a 37°C water bath to defrost. Once all the ice inside the cryovial had melted the contents of the tube was transferred into a 15 ml Falcon tube and 10 ml of media was added drop-wise in order to slowly acclimatise the cells. The cell solution was then centrifuged at 300 x *g*, for 5 minutes and the old media (containing DMSO) was removed. The cell pellet was gently re-suspended in an appropriate volume of growth media and transferred into a fresh cell culture vessel.

Mouse embryonic fibroblasts (MEFs) had been previously generated by our laboratory. Three different genotypes of MEFs were used in this project, including wild-type MEFs, p53 null MEFs and double null MEFs ($p53^{-/-}$, $Mdm2^{-/-}$). MEFs were split at 80-90% confluence at varying split ratios, reflecting their relative growth rates. Wild-type MEFs generally grew slower than either of the mutant cell lines and were only split 1:4, whereas the mutant cell lines (particularly the double nulls) grew very fast and could be split 1:12. Subculture, freezing and thawing of MEFs was performed as for H1299s.

SNL76/7 mouse embryonic fibroblasts were obtained from The Wellcome Trust Sanger Institute and were used as a feeder layer for embryonic stem (ES) cells. SNL 76/7 cells are used because they produce Leukemia inhibitory factor (LIF) which maintains the ES cells in a pluripotent state [Williams et al., 1988] and also these cells contain a neomycin cassette and hence are resistant to drug selection by G418. SNL76/7 cells were grown on pre-gelatinised cell plates. Cell culture vessels were pre-gelatinised by coating the cell culture surface area with an appropriate amount of 0.1% gelatin solution (see Table 2.9.2 for volumes) for 2 hours, the 0.1% gelatin solution was then aspirated just before use. 0.1% gelatin solution was prepared by adding 0.5 g of porcine gelatin (Sigma-Aldrich #G1890) to 500 ml of $H_2O$ with enough phenol red (BHD) to create a bright yellow colour. The 0.1% gelatin solution was sterilised by autoclaving and was stored at RT.

SNL76/7 cells required a high quality fetal bovine serum (FBS) for the best results. Serum quality had been determined previously by The Wellcome Trust Sanger Institute, who kindly provided us with the batch numbers of the highest quality serum. For our early

experiments (growing ES cell line AM0998) HQ FBS was purchased from HyClone, whereas for the later experiments HQ FBS was sourced from Invitrogen. SNL76/7 cells were passaged at 80% confluence and split 1:10. The method of sub-culture was as for H1299 cells with the exception that SNL76/7 cells were washed twice with DPBS (rather than only once) with an ES cell optimised formulation of DPBS (HyClone #SH30850.02) and different 0.25% trypsin-EDTA solution (Sigma-Aldrich #T4049). From hereon ES cell quality (ESQ) DPBS and 0.25% trypsin-EDTA solution will be referred to as ESQ-PBS and ESQ-trypsin respectively. Freezing and thawing SNL76/7 cells was performed as for H1299 cells except SNL76/7 cells were frozen 1:1 feeder cell medium to x 2 freezing medium (see Table 2.9.3).

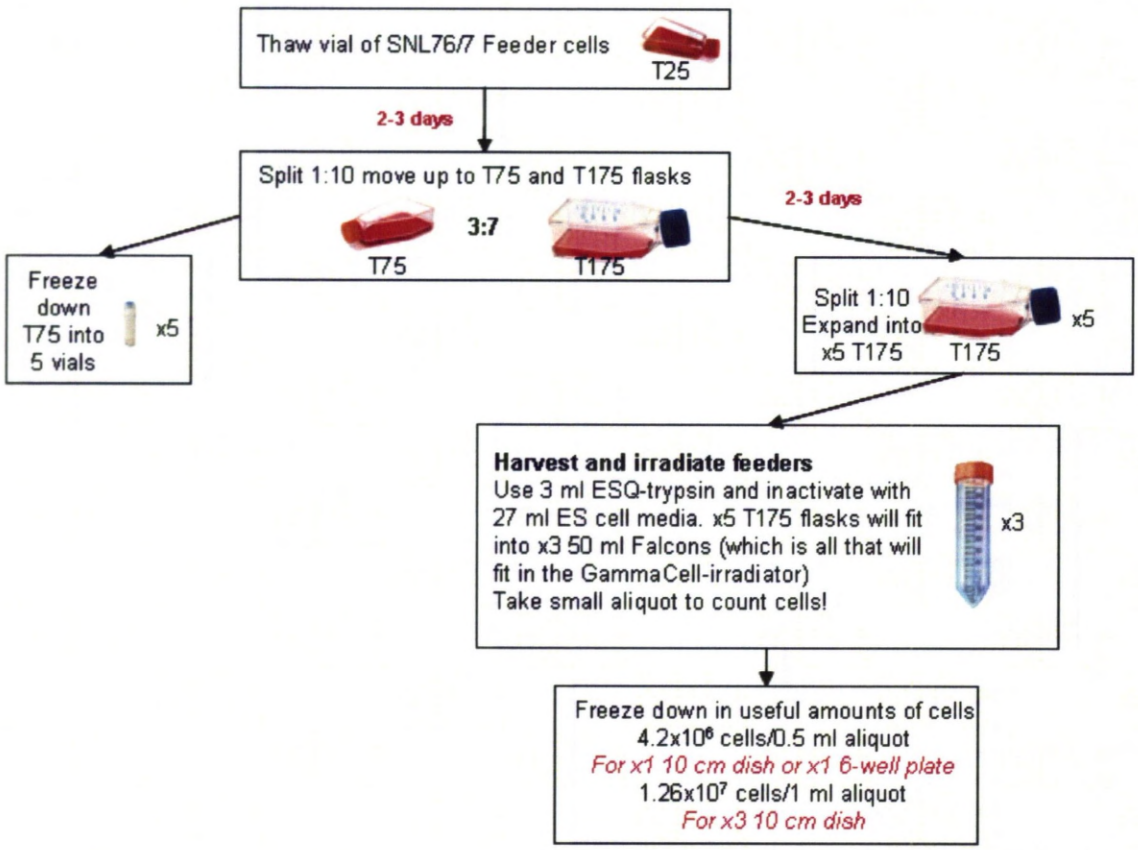


***Figure 2.9.1: Flow diagram of the method used to generate large batches of mitotically inactivated feeder layers.***

*See text for further details.*

In order to act as a feeder layer for the ES cells, SNL76/7 cells were required to be mitotically inactivated; this was performed by exposing the cells to very high doses of γ-radiation and this next section describes how the feeder layers were prepared. Feeder layers were prepared in batches as follows; x 5 T175 flasks of 80% confluence SNL76/7 cells were harvested as described previously, with the exception that the ESQ-trypsin solution was inactivated in x 10 feeder layer cell media (see Figure 2.9.1). Once harvested, the cells were pooled together in x 3 50 ml Falcons and were exposed to 60 Gy γ-radiation (GammaCell irradiator with a $^{137}$Cs source dose rate 2.6 Gy/min). This mitotically inactivates the cells so that they can be used as feeder layers for the ES cells. A small aliquot of cells was taken to be counted. The irradiated feeder layer cells were then centrifuged at 300 x *g* for 5 minutes and were re-suspended in a suitable volume of feeder layer media to create useful aliquots of cells when frozen 1:1 feeder cell medium to x 2 freezing medium. For use with ES cells γ-SNL76/7 cells were plated onto pre-gelatinised plates at the densities listed in Table 2.9.4. The feeder layers were allowed to settle and attach to the culture vessels for at least 1 day prior to use with ES cells, although slightly older feeders were preferred (5-7 days old) since the cells should have flattened nicely and any contamination would be obvious. Feeders older than 10 days were not used. From this batch method, you would expect to generate approximately 10 cryovials with 1.26 x $10^7$ γ-SNL76/6 cells/vial which should be sufficient for one round of ES cell targeting.

***Table 2.9.4: Volumes and densities for plating irradiated feeder layers.***

| Cell culture vessel | | Volume | Density |
|---|---|---|---|
| Multiwell plates | 96-well (flat) | 200 µl | 1x$10^5$ cells/ml |
| | 24-well | 1 ml | 3.5x$10^5$ cells/ml |
| | 6-well | 2 ml | 3.5x$10^5$ cells/ml |
| Dishes | 6 cm | 4 ml | 3.5x$10^5$ cells/ml |
| | 10 cm | 12 ml | 3.5x$10^5$ cells/ml |

AM0998 was a p21 gene-trapped ES cell line generated by The Wellcome Trust Sanger Institute which we requested from the international gene-trap consortium (IGTC) and see Section 3.2.1. AB2.2 is an untargeted, undifferentiated ES cell line with a 129*SvEv* genetic background which is available upon request from The Wellcome Trust Sanger Institute. ES cells were grown on mitotically inactivated feeder layers (see above for preparation of feeder layers) and consequently growth of ES cells must always be well co-ordinated with the availability of high quality feeder layers. Therefore before embarking on ES cell growth it is essential to determine when and what feeder layers will be required and to have them prepared at least a day in advance. ES cells were routinely sub-cultured every other day and their media was changed on alternate days, thus ES cells required daily attention. Since we intended to use these ES cells to generate transgenic mouse lines it was extremely important to maintain the ES cells in an undifferentiated state. Reflecting the importance of maintaining our ES cells in a pluripotent state, in our later experiments the media was also supplemented with exogenous LIF at 1000 U/ml. Subculture of ES cells was performed as for SNL76/7 cells, with the notable difference that the ES cell media was changed 3-4 hours prior to passaging.

ES cell lines were frozen in a similar manner to the SNL76/7 cells except instead of being frozen in polystyrene boxes the cryovials were frozen in an isopropanol container. The isopropanol container was initially at RT when the cells were placed inside, then it was transferred to the -80°C freezer. The isopropanol controlled the rate at which the temperature dropped, which allowed the cells temperature to drop slower (than the polystyrene box method) at approximately 1°C per minute and was hence better for acclimatising the cells and maintaining cell viability. For long term storage the cells were transferred to liquid nitrogen. The method of thawing ES cells was essentially the same, with the minor provision that thawing of ES cells was always performed at the end of the day and the media was always changed first thing in the morning. This was to limit the detrimental effects of any residual DMSO in the media.

## 2.9.2 Introduction of DNA into mammalian cells

### *2.9.2.1 Transfection using GeneJuice*

GeneJuice™ (Novagen) was used to transiently transfect mammalian cells with plasmid DNA. GeneJuice contains a non-toxic cellular protein and novel polyamine which allows for highly efficient non-toxic entry of DNA into treated cells. Transfection was performed on 50-60% confluent H1299 or p53 null MEF cells in triplicate wells of a 48-well plate. The procedure was performed according to the manufacturer's instructions essentially as follows; the DNA was pipetted and mixed together first in sterile 1.5 ml screw-cap micro-centrifuge tubes (one tube per condition). Next the GeneJuice, which was used at a 3:1 ratio with the DNA (3 µl of GeneJuice to 1 µg of DNA), was added to the serum free media and mixed by vortexing, then left to incubate at RT for 5 minutes. After incubation the GeneJuice/serum free media was added carefully to the DNA mixture and the reaction components were mixed well by flicking the tubes. Once mixed the tubes were centrifuged briefly and left to incubate at RT for 20 minutes. The contents of each tube were then very gently pipetted up and down and 15 µl was added drop-wise across the surface of the well being treated. Once all the wells had been treated the 48-well plate was then tilted back and forth and side to side (not by swirling) in order to aid distribution of the transfection reagents within the media. The transfected cells were then left in the tissue culture incubator for at least 24 hours before continuing with analysis (for example performing a luciferase assay see Section 2.13.8).

### *2.9.2.2 Stable transfection of embryonic stem cells using electroporation*

There are four major steps involved in the successful targeting of ES cells. These are DNA preparation; cell preparation, the electroporation itself and the subsequent selection and expansion of positive clones and these are described below.

2.9.2.2.1 Preparation of DNA

Each electroporation required approximately 15-25 µg of targeting DNA, therefore to guarantee sufficient DNA for at least two attempts 60 µg of targeting construct DNA was digested overnight as described previously in Section 2.6.1 in order to linearise it. In the morning, 500 ng of the digested DNA was analysed on an agarose gel alongside 500 ng of the uncut DNA to confirm that complete digestion had taken place. The DNA was then extracted using the phenol/chloroform method described in Section 2.3.10 with precautions taken to ensure that the DNA was kept sterile once it was precipitated. The DNA was re-suspended in 60 µl of sterile ESQ-PBS (approximately 1 µg/µl) and the DNA concentration and quality was checked by using a UV spectrophotometer. One final check on the DNA was performed by running a further 500 ng sample of the precipitated DNA on an agarose gel (with an uncut control) to confirm that everything appeared as expected. Preparation of the DNA was usually performed a few days ahead of the planned ES cell electroporation to allow time for all the quality control checks to be made. DNA was stored at -20°C until required, although storage for more than a few days was avoided.

2.9.2.2.2 Preparation of cells

Figure 2.9.2 provides an overview to the ES cell targeting strategy, including expected cell culture times, amount of feeder layers required and screening/expansion plans. Prior to the day of electroporation, the ES cell population was expanded from the initial thawed vial of AB2.2 cells, on three 10 cm dishes. One of these dishes was frozen (see Section 2.9.1) for use in future targeting events whilst the remaining two dishes (at 80% confluence) were utilised for the electroporation as follows; 3-4 hours before electroporation the ES cells media was changed to fresh ES cell medium. The media on the nine 10 cm feeder layer dishes, where the targeted ES cells were to be seeded post-electroporation, was also changed to ES cell media. The ES cells were then harvested as described in Section 2.9.1 and the cells from two 10 cm dishes were combined into a single 15 ml tube (10 ml total). A 500 µl aliquot of cells was taken to be counted before the cells were centrifuged at 300 x *g* for 5 minutes. The old media was removed and the cell pellet was gently re-suspended in a suitable volume of ESQ-PBS to achieve a density of $1.1 \times 10^7$ cells/ml (two 10

cm dishes typically yielded enough AB2.2 cells for 2-3 electroporations). The cells were then ready to be electroporated.

2.9.2.2.3 Electroporation of ES cells

Electroporation of mammalian cells was performed using a Bio-Rad Gene Pulser II with Capacitance Extender. The electrode chamber was connected to the output jack on the Gene Pulser II Unit Control Panel which was the main panel – not to the Pulse Controller II Front Panel which was used for high voltage transformation of bacterial cells. Single use 0.4 cm gap electroporation cuvettes were prepared by adding 0.9 ml of cells ($1 \times 10^7$ cells) and ~ 25 µl of DNA solution (25 µg of DNA as prepared above). The cuvette was placed into the electrode chamber, the Gene Pulser II was set at 230 V, 500 µF and a single pulse was delivered. Following exposure to a single pulse, the cuvettes were incubated at RT for 5 minutes and then the cells were transferred from the cuvettes into a 15 ml Falcon tube. The cuvettes were washed out 2-3 times with more ESQ-PBS and contents collected together in the 15 ml Falcon tube. The total volume in the tube was then brought up to 9 ml with ESQ-PBS and the cells were very gently pipetted up and down before 1 ml was placed into each 10 cm feeder layer dish. Each dish was then gently swirled in a figure of eight pattern to evenly distribute the cells, before being returned to the incubator. Electroporation was generally performed late in the evening so that selection protocols could be commenced in the morning of day 2 (36 hours post-electroporation) since this allowed maximum time for the ES cells to settle and attach before changing the media.

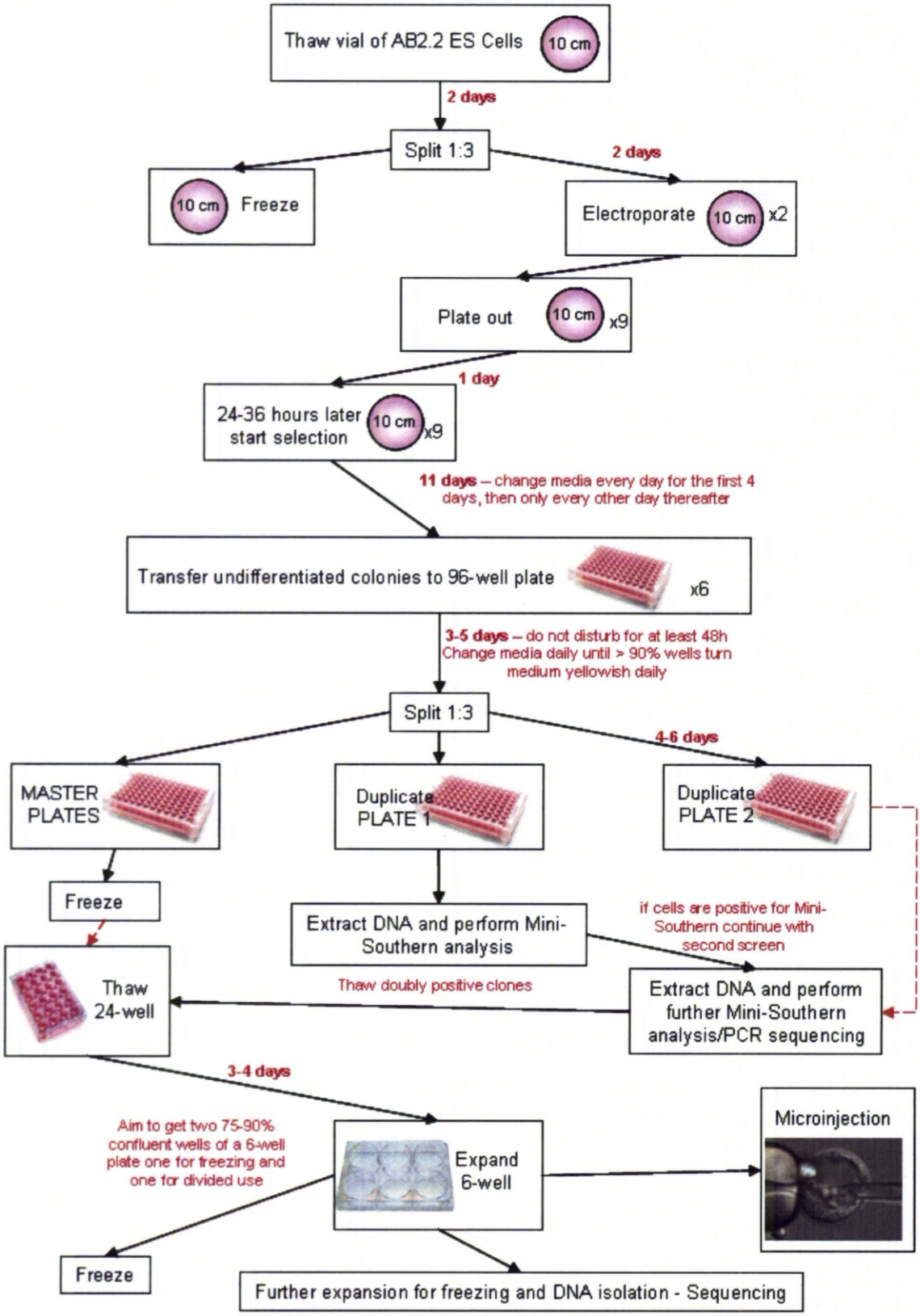


***Figure 2.9.2: Flow diagram for ES cell targeting strategy.***

2.9.2.2.4 Selection of positive clones

Selection of recombinant clones was started 36 hours post electroporation once the majority of the ES cells had settled and attached to the feeder layers. Since correctly targeted homologous recombination events are relatively rare, both positive and negative selections were used to increase the probability of selecting correctly targeted clones. Positive selection was based on resistance to G418 (Calbiochem), an aminoglycoside antibiotic, to which resistance is conferred after integration of the neomycin cassette (the positive selection marker). However, positive selection alone does not discriminate against random recombination events (integration at non-specific loci) therefore negative selection was also used and was based on the presence of the viral protein thymidine kinase (TK - the negative selectable marker) that renders ES cells sensitive to Ganciclovir (Sigma-Aldrich) an antiviral drug. Ganciclovir is a harmless nucleoside analogue unless it is phosphorylated by the viral protein thymidine kinase whereupon it becomes incorporated into replicating DNA and causes cell cycle arrest and eventual death of the affected cells.

For convenience both selection agents were prepared as concentrated stock solutions and were diluted into the ES cell media just before use. G418 was used at a working concentration of 300 µg/ml and was prepared as a X 100 stock solution in ESQ-PBS. Ganciclovir was used at a working concentration of 2 µM and was prepared as a X 1000 stock solution. Initially Ganciclovir powder was dissolved in a small volume (10%) of 0.1 M HCl before being brought to the final desired volume (to create a X 1000 stock) with ESQ-PBS. Both solutions were sterilised by filtration and stored at 4°C.

Selection was performed over a 10-11 day period as follows; plates were re-fed daily with fresh ES cell media plus G418 and Ganciclovir for the first four days, then only every other day thereafter. Colonies became visible around days 5-7 and most of the debris from dead cells was gone by day 10. In our experience each 10 cm plate had 100 + colonies and most appeared undifferentiated when examined briefly under a microscope. Picking of colonies was started on day 10 of selection and usually continued for 2-3 days. 1-2 hours before picking colonies the old feeder layer medium on the 6 x 96-well feeder layer plates was removed and replenished with 100 µl of fresh ES cell media (it was not necessary to maintain selection once colonies had been picked). Just prior to commencing picking 30 µl of ESQ-

trypsin was added per well of a 96-well round bottom sterile tissue culture plate. Picking ES cell colonies was then performed as follows; working with one plate at a time, the ES cells were washed twice with 5 ml ESQ-PBS and then the plate was flooded with 8 ml of ESQ-PBS. A p20 pipette was set to 10 µl and a fresh box of sterile 1-10 µl pipette tips was used, so that each tip corresponded to a well of the 96-well plate. ES cell colonies were picked off the feeder layer one at a time and tips were changed between colonies to keep track of which wells had been used and to avoid cross-contamination (I typically picked 72 colonies/30 minutes).

Once all the desired colonies had been picked (often not from a full plate to select only the best colonies from each of the 9 x 10 cm plates) they were returned to the incubator to trypsinize for a further 15 minutes. The trypsin was then inactivated by adding 70 µl of ES cell media to each well by using a multichannel pipette. The colonies were broken up into a single cell suspension by triturating the contents of each well with 35-40 pipette strokes. Tips were changed between each row to prevent cell line cross-contamination. The single cell suspensions were then transferred onto a new 96-well feeder layer plate and returned to the incubator for 48 hours before the media was changed. Following the initial 48 hours, which allowed the ES cells to settle and attach to their new feeder layer, the media was changed on the ES cells daily until more than 90% of the wells were turning the media yellow overnight (this typically took 3 days). When the majority of the wells appeared ready, the next step was to generate a master plate which would be frozen to preserve the cell lines and to create two duplicate plates for DNA screening purposes.

2.9.2.2.5 Generation of master plates and expansion of ES cells for DNA

A master plate was generated as follows: 3-4 hours prior to freezing/expansion the ES cells were re-fed with fresh ES cell media. Two gelatin coated plates were also prepared to create the duplicate plates. Feeder layers were not required for the duplicate plates since those cells were only to be used for DNA extraction and screening purposes therefore it did not matter if they became differentiated. Working with one plate at a time, each row was washed twice with 100 µl of ESQ-PBS, and then 25 µl of ESQ-trypsin was added. Once all the rows in the plate had been prepared the plate was returned to the incubator for 15 minutes. While the cells were trypsinising, 150 µl of ES cell media was added to the gelatin

coated plates. Following incubation, 25 µl of ES cell medium was added per well and pipetted up and down for 35-40 strokes to triturate the cells. 50 µl of 96-well plate x 2 freezing medium (see Table 2.9.3 for formulation) was then added per well and pipetted a further 5-10 strokes. 20 µl of the ES cell suspension was then transferred into each corresponding well of the duplicate plates before returning the plates to the incubator. The media was changed on the duplicates after 48 hours and then daily (or more frequently if required) until more than 90% of the wells turned the medium yellow overnight.

Meanwhile the master plate was prepared by gently pipetting 100 µl of sterile mineral oil (Sigma-Aldrich) overlay on to the remaining cell suspension in the original 96-well plate. The master plate was then sealed carefully with extreme-temperature resistant tape (Tessa) and packed into a polystyrene box before being transferred to a -80°C freezer. Cells should be viable at -80°C for several months, although for long term storage plates should be transferred to the gas phase of liquid nitrogen.

The duplicate plates were also frozen once the majority of wells (> 90%) were confluent (this typically took 3 days). This was performed as follows; duplicate plates were removed from the incubator and wells washed twice with 100 µl of ESQ-PBS before sealing the plates with tape and freezing at -80°C. These cells were used for DNA extraction, using the protocol described in Section 2.3.12.

### 2.9.3 Exposure of mammalian cells to γ-irradiation

Mammalian cells were exposed to γ-irradiation for two purposes in this thesis; to generate feeder layers (described previously in Section 2.9.1) and to induce p53 up-regulation in cells to examine the subsequent protein expression. In the latter case, cells were grown to approximately 90-100% confluence in T25 flasks and then were exposed to 6, 20 or 60 Gy of γ-irradiation (or mock treated) in a GammaCell irradiator (dose rate 2.6 Gy/minute). T25 flasks were used since three could fit inside the GammaCell irradiator when standing upright. Cells were mock treated by simply standing their T25 flasks upright for the same length of time as the cells that were irradiated. When cells received a 60 Gy dose, because of the technical complication (T25 flasks only fitted inside the machine whilst upright)

irradiation was delivered in 5 minute pulses with a 5 minute recovery time in-between. Following treatment cells were then either stained for expression of β-galactosidase (β-gal) (Section 2.13.7) or were harvested for analysis by western blotting (Section 2.10).

# 2.10 Protein extraction and analysis

## 2.10.1 Protein sample preparation and quantification (Bradford assay)

Protein samples were prepared from tissue culture cell pellets as follows; the desired cell pellets were harvested as described previously in Section 2.9.1. Once the cell pellets had been collected they were washed twice with DPBS before being centrifuged (300 x *g*, 5 minutes, RT) and the DPBS removed. Cell pellets could be processed straight away, or stored at -80°C and defrosted on ice before use.

Protein was extracted from the cell pellets as follows; once the pellets had defrosted cells were then re-suspended on ice in the appropriate amount of SLIP buffer supplemented with protease inhibitors (see Table 2.10.1 for composition of SLIP buffer and Table 2.10.2 for information on protease inhibitors), lysed on ice for 10 minutes and centrifuged at maximum speed (16,000 x *g*) at 4°C for 10 minutes. The supernatant was transferred to a fresh pre-chilled 1.5 ml micro-centrifuge and kept on ice.

In the meantime protein standards were prepared by dissolving bovine serum albumin (BSA) in SLIP buffer to create the following dilutions; 20, 10, 5, 2.5, 1.25, 0.625, 0.3125 mg/ml. 2 µl of standard or sample was added to 1 ml of Bradford reagent (BioRad – diluted 1 in 5 in water before use) and vortexed briefly. The addition of protein to the Bradford reagent results in a colour change in the dye, Coomasie Brilliant Blue G-250, which can be measured by a shift in the absorbance at 595 nm. The absorbance of the known protein standards was measured first using the BioPhotometer (Eppendorf) to create a standard curve and protein concentration of samples determined based on the calibrated spectrophotometer and recorded. Samples were then prepared to a concentration of 25 µg/20 µl in sample buffer (see Table 2.10.1) and stored at -80°C.

An alternative version of the Bradford assay, a micro-Bradford assay, was performed when low protein yields were expected, for example for a luciferase assay (see Section 2.13.8). A micro-Bradford assay was essentially the same as the regular assay described above except the following protein standards were created in the passive lysis buffer (PLB - Strategene); 5, 2.5, 1.25, 0.625, 0.3125, 0.156, 0.078 mg/ml and 5 µl of standards/samples

was added to 1 ml of Bradford reagent. Once the spectrophotometer (Eppendorf Biophotometer) was calibrated the samples were then measured and the protein concentration estimated as before. For a luciferase assay, protein samples did not need to be prepared in sample buffer.

***Table 2.10.1: Composition of protein buffers.***

| **Solution** | **Composition** | **Source** |
|---|---|---|
| Standard lysis and immunoprecipitation Buffer (SLIP buffer) | 50 mM HEPES (pH 7.5) | Calbiochem |
| | 150 mM sodium chloride | VWR |
| | 10% glycerol | Sigma-Aldrich |
| | 0.1% triton X-100 | Sigma-Aldrich |
| | 0.5 mg/ml bovine serum albumin | Fluka |
| Protein sample buffer | 0.25 M Tris (pH 6.8) | Calbiochem |
| | 8% sodium dodecyl sulphate (SDS) | VWR |
| | 40% glycerol | Sigma-Aldrich |
| | 4 mg/ml bromophenol blue | Sigma-Aldrich |
| | 1% *β-mercaptoethanol* | Sigma-Aldrich |
| Tris-glycine electrophoresis buffer (running buffer) | 25 mM Tris | Calbiochem |
| | 220 mM glycine | Fisher |
| | 0.1% SDS | VWR |
| Transfer buffer | 25 mM Tris | Calbiochem |
| | 192 mM glycine | Fisher |
| | 20% methanol | BHD |
| PBS/Tween | 0.065 M $Na_2HPO_4$ | Sigma-Aldrich |
| | 0.015 M $NaH_2PO_4xH_2O$ | Sigma-Aldrich |
| | 0.075 M NaCl | VWR |
| | 0.1% Tween 20 | Sigma-Aldrich |

***Table 2.10.2: Protease inhibitors.***

*All protease inhibitors except PMSF (Fluka) were purchased from Roche and were stored in aliquots at -80°C. PMSF was prepared fresh on the day.*

| Protease inhibitor | Reconstituted in | Stock solution | Working concentration |
|---|---|---|---|
| Aprotinin (A) | $H_2O$ | X 1000 | 2 µg/ml |
| Leupeptin (L) | $H_2O$ | X 1000 | 0.5 µg/ml |
| Pepstatin (P) | Methanol | X 1000 | 1 µg/ml |
| Soybean Trypsin Inhibitor (STI) | $H_2O$ | X 1000 | 100 µg/ml |
| Phenylmethylsulphonyl fluoride (PMSF) | Ethanol | X 100 | 1 mM |

## 2.10.2 Western blotting

Western blotting is used to identify and quantitate specific proteins using specific antibodies. Briefly, protein samples are first resolved by SDS-PAGE (sodium dodecyl sulphate polyacrylamide gel electrophoresis) using the Mini-PROTEAN®-3 system (BioRad). Once resolved the protein samples were transferred onto a Hybond ECL nitrocellulose membrane (GE Healthcare) which could then be probed with an antibody specific for the protein of interest.

SDS-PAGE was performed as follows; the resolving gel mixture (see Table 2.10.3) was prepared at an appropriate percentage and poured into a glass cassette sandwich and allowed to set for approximately 40 minutes. In order to prevent the gel from drying out, remove bubbles and to ensure a flat surface, 1 ml of water was added immediately to the top of the glass cassette once the gel had been poured. After the gel had set, the water was shaken off and the stacking gel applied. The stacking gel comb was then gently and quickly inserted into the stacking gel and checked for air bubbles which might appear under the wells. The stacking gel was then left to polymerise for a further 40 minutes.

***Table 2.10.3: Components of SDS-PAGE gels.***

*The percentage of acrylamide can be varied to produce different densities of resolving gel. Low percentage gels (6%) were for resolving high molecular weight proteins such as β-geo (150 kDa) whereas high percentage gels (12%) were for resolving low molecular weight proteins such as p21 (21 kDa).*

| Component | Source | SDS-PAGE resolving gel | | SDS-PAGE stacking gel |
|---|---|---|---|---|
| | | 6% | 12% | |
| $H_2O$ | - | 5.8 ml | 4.3 ml | 7.225 ml |
| 40% acrylamide mix | VWR | 1.5 ml | 3 ml | 1.275 ml |
| 1.5 M Tris (pH 8.8) | Calbiochem | 2.5 ml | 2.5 ml | - |
| 1 M Tris (pH 6.8) | Calbiochem | - | - | 1.25 ml |
| 10% SDS | VWR | 0.1 ml | 0.1 ml | 0.1 ml |
| 10% ammonium peroxosulfate | BDH | 0.1 ml | 0.1 ml | 0.1 ml |
| 10% TEMED (N,N,N',N'-tetramethylethylenediamine ) | VWR | 8 µl | 8 µl | 10 µl |

Following polymerisation, the gel comb was gently removed and the glass cassette containing the gel was set up inside the vertical gel electrophoresis tank. The gel tank was filled with running buffer (see Table 2.10.1) and was then ready for the protein samples to be loaded. Protein samples (including pre-stained protein marker - NEB) were prepared for SDS-PAGE by being defrosted on ice and then boiled at 100°C for 5 minutes. The samples were then vortexed briefly before being centrifuged at 4°C for 4 minutes at 16,000 x *g*. The samples were kept briefly on ice before being promptly loaded into the wells of the polyacrylamide gel. The gel was run at 200 V for approximately 1 hour.

The next step was transfer the separated proteins from the polyacrlamide gel onto a nitrocellulose membrane using the Mini-PROTEAN®-3 system (BioRad) following the manufacturer's instructions, typically for 1 hr at 100 V.

Once the transfer was complete, the membrane was stained with Ponceau S solution (0.1% (w/v) in 5% acetic acid - Sigma-Aldrich) for visualisation of proteins and to check whether the protein loading and transfer were even. The membrane was then incubated in

PBS/Tween with 5% non-fat dry milk (BioRad) typically overnight at 4°C, or at least for 1 hr at RT before continuing with the immuno-blot. The membranes (with or without overnight storage in the fridge) were then blocked in the 5% milk solution with shaking (~ 60 rpm) at RT for at least 1 hour. In the meantime the primary antibodies were prepared in the 5% milk solution (see Table 2.10.4). Some antibodies did not tolerate freeze/thawing and therefore they were prepared fresh each time, whilst others could be frozen at -80°C and re-used. Once blocking was complete, the membranes were incubated with the appropriate primary antibody for 1 hour at RT with gentle agitation. Following incubation with the primary antibodies, the membranes were washed in PBS/Tween for 3 x 10 minutes. The membranes were then incubated with the appropriate secondary antibody for 1 hour at RT with shaking. Secondary antibodies (from Amersham/GE Healthcare) conjugated to horseradish peroxidise (HRP) were diluted in 5% milk solution as follows; 1:5,000 for anti-rabbit-HRP antibody and 1:2,500 for anti-mouse-HRP antibody. After incubation with the secondary antibody, the membranes were washed again in 3 x 10 minutes with PBS/Tween.

Once all the washes were completed the membrane was then ready to be treated with the Western lightning chemiluminescence reagent plus (ECL reagent – Perkin Elmer). The ECL reagent was prepared by mixing the enhanced luminol reagent and oxidizing reagent together at a 1:1 ratio (require 0.1 ml per 1 $cm^2$) and this was then pipetted over the membrane and allowed to incubate for 1 minute. Excess ECL reagent was dabbed off the membrane using a clean soft tissue on the edge of the membrane and then the membrane was arranged between two sheets of acetate. The luminescence signal was detected using a Kodak IS4000MM image station.

*Table 2.10.4: Primary antibodies used in this project for Western blotting*

| Protein | Antibody | Source | Raised in | Working concentration |
|---|---|---|---|---|
| p21 | M19 | Santa Cruz | Rabbit polyclonal | 1:200 |
| p53 | CM5 | Novacastra | Rabbit polyclonal | 1:1000 |
| β-gal | OBO2 | Calbiochem | Mouse monoclonal | 3 µg/ml |
| Actin | C-2 | Santa Cruz | Mouse monoclonal | 3 µg/ml |

# 2.11 RNA extraction methods

## 2.11.1 Preservation of RNA integrity by RNA*later* stabilisation solution

RNA*later* solution was purchased from Applied Biosystems and was used to prevent the degradation of RNA inside animal tissues. A major technical problem when isolating RNA from tissues is the presence of ribonucleases (RNases) that catalyse the breakdown of RNA and therefore need to be inhibited.

RNA*later* solution was used on freshly isolated mouse gut samples to preserve the integrity of RNA as follows; freshly isolated mouse gut samples (5 cm in length) were placed into 5 ml universal tubes which had been pre-filled with RNA*later* solution and incubated overnight at 4°C to ensure that the RNA*later* solution had permeated all the cells in the sample. The sample was then frozen and stored at -80°C whereupon the RNA should be preserved indefinitely.

To isolate RNA from a tissue preserved in RNA*later*, the tissue sample was removed from the -80°C freezer and allowed to defrost at 4°C overnight. The following day, once the RNA*later* solution had thawed completely, the tissue could be removed and utilised. Samples preserved in RNA*later* could be freeze/thawed multiple times without affecting the quality of RNA, therefore routinely, a small portion of the tissue (0.3 g) was removed for RNA isolation and the remaining tissue was returned to the RNA*later* solution and re-frozen. The next section describes RNA isolation from whole animal tissue with the QIAGEN RNeasy Mini kit.

## 2.11.2 Isolation of RNA from whole animal tissue

The QIAGEN RNeasy Mini kit was used to isolate RNA from whole animal tissues using a variation of the guanidine extraction method. Briefly; the samples were lysed in a buffer that contains guanidine thiocyanate (a powerful protein denaturant) to ensure immediate inactivation of RNases. Once lysed the samples are loaded onto a silica-based membrane within the RNeasy spin column (similar to QIAprep spin Miniprep kit used for isolation of plasmid DNA – see Section 2.3.2). Under the appropriate binding conditions (high salt and presence of ethanol) the silica-based membrane binds to the RNA. Once bound to

the RNeasy spin column the RNA can be washed to remove any contaminants and then eluted in RNase-free water. The yield using this kit could vary depending on the starting material but typically produced 70-100 µg of high quality RNA.

The RNeasy Mini kit was used to isolate RNA according to the manufacturer's guidelines essentially as follows; 30 mg of fresh tissue or 15-20 mg of RNA*later* stabilised tissue (since RNA*later* partially dehydrated the sample) was disrupted by using a pestle and mortar, with liquid nitrogen to facilitate the grinding. The liquid nitrogen was allowed to evaporate and 600 µl of buffer RLT was added to lyse the cells. The cell lysate was collected and transferred into a pre-cooled (in liquid nitrogen) 2 ml micro-centrifuge tube. The lysate was then homogenised by passing it through a 20-gauge (0.9 mm) needle at least 5-10 times. Once the lysate appeared homogenous it was then centrifuged for 3 minutes at maximum speed (16,000 x *g*) in a bench top centrifuge. The supernatant was promptly transferred to a fresh tube and 1 volume of 70% ethanol was added to the cleared lysate and the sample was mixed by pipetting (ethanol was added to promote binding of the RNA to the silica-based membrane). Addition of ethanol sometimes produced a precipitate which was ignored in the subsequent steps, since it did not affect the efficiency of RNA isolation. Up to 700 µl of the sample was loaded onto the RNeasy spin column which was placed inside a 2 ml collection tube. The RNeasy spin column was then centrifuged for 15 seconds at > 8000 x *g* and the flow-through was discarded. Samples which had a volume greater than 700 µl were simply loaded onto the same spin column, and centrifuged as before in successive aliquots. 700 µl of buffer RW1 was then applied and centrifuged as before. The flow-through was discarded and 500 µl of buffer RPE was added to the column and centrifuged as before. The flow-through was discarded and another 500 µl of buffer RPE was applied to the RNeasy spin column. This time the RNeasy spin column was centrifuged at > 8000 x *g*, for 2 minutes to both wash and dry the membrane. To avoid transfer of residual ethanol (from wash buffer RPE) the RNeasy spin column was placed into a fresh 2 ml collection tube and centrifuged for a further 1 minute. The RNeasy spin column was then transferred into a fresh 1.5 ml collection tube and 30-50 µl of RNase-free water was applied directly to the silica-based membrane. The RNA was then eluted by centrifuging the spin column for 1 minute (> 8000 x *g*). The quantity of RNA was estimated by using a UV spectrophotometer (taking readings at

230, 260 and 280nm) and the quality was assessed by running the samples on a non-denaturing agarose gel (see Section 2.4).

### 2.11.3 Isolation of RNA from intestinal epithelial cell extraction

RNA was isolated from cell pellets which had been collected using the intestinal epithelial extraction protocol described in Section 2.13.4 by using a basic chloroform extraction/isopropanol precipitation protocol. The cell pellets were re-suspended 1:1 with TRIZOL reagent to preserve the integrity of RNA (TRIZOL reagent contains guanidine isothiocyanate – which inhibits the activity of RNases) and frozen prior to commencing this procedure.

RNA was extracted from cell pellets frozen in TRIZOL as follows; the cell pellets in TRIZOL were defrosted on ice and homogenised by pipetting the samples through decreasing diameters of needles. Once the samples were homogenous they were centrifuged at maximum speed (16,000 x *g*) at 4°C for 10 minutes. The supernatant was promptly transferred to a fresh pre-chilled tubes and 200 µl of chloroform was added and mixed by inversion. The RNA extraction reaction was performed for 15 minutes on ice, with occasional inversion of the tube to mix. The samples were centrifuged as before and then the aqueous phase was transferred to a fresh tube containing 600 µl of isopropanol. The samples were mixed again by inversion and then were incubated on ice for at least 1 hour while the RNA precipitated. After the RNA had precipitated, the samples were centrifuged as before and the supernatant was carefully removed (RNA forms a pellet at base of tube). The RNA pellet was washed with 500 µl of pre-chilled 70% ethanol and then the pellet was allowed to air dry for 5-10 minutes. RNA was re-suspended in 100 µl of nuclease-free water and the quantity/quality checked by using a UV spectrophotometer (Section 2.4.1).

The RNA samples were then cleaned up to be of high enough quality for RNA microarray analysis as follows; 50 µl of each sample was treated with DNase I and cleaned up using the QIAGEN RNeasy Mini kit (Section 2.11.4). A PCR was then performed to check for any residual contaminating genomic DNA. The DNase I treatment, column purification

and subsequent PCR check was kindly performed by Dr Dimitris Athineos (The Beatson Institute Glasgow).

### 2.11.4 Removal of contaminating DNA from RNA – treatment with DNase I

RNA samples which were contaminated with genomic DNA were treated with DNase I (QIAGEN) according to the manufacturer's instructions. Once the DNA was digested the sample was reloaded onto an RNeasy spin column for RNA purification.

DNase I stock solution prepared in advance as follows; the lyophilized form of DNase I was re-suspended in RNase-free water and mixed by inversion (not vortexing – since DNase I is sensitive to mechanical stress) and then aliquoted and stored at -20°C. The DNase I treatment was then performed. The reaction components in Table 2.11.1 were mixed together and left to incubate at RT for 10 minutes.

***Table 2.11.1: DNase I reaction components***

| Amount | Components |
|---|---|
| 87.5 µl | RNA solution (contaminated with genomic DNA) |
| 10 µl | Buffer RDD |
| 2.5 µl | DNase I stock solution |

RNA from the 100 µl DNase I reaction was then recovered using a modified version of the RNeasy Mini kit protocol as follows; to the 100 µl reaction 350 µl of buffer RLT was added and mixed well. 250 µl of 96-100% ethanol was then added and mixed well by pipetting. This 700 µl solution was then transferred to an RNeasy spin column with a 2 ml collection tube attached. The RNeasy spin column was centrifuged for 15 seconds at > 8000 x *g* and the flow-through discarded. 500 µl of buffer RPE was applied to column and centrifuged as before. From here the protocol proceeds as for isolation from whole animal tissue RNeasy protocol (see Section 2.11.2).

# 2.12 RNA microarray

## 2.12.1 Reverse-Transcriptase reaction for generation of cDNA

RNA samples were reverse-transcribed into cDNA (complementary DNA) using the RNA-directed DNA polymerase Moloney Murine Leukemia Virus (M-MuLV) reverse transcriptase (RT) from NEB. cDNA was synthesised according to the manufacturer's instructions essentially as follows; in a sterile, nuclease free, 0.2 ml PCR tube (or for multiple samples a 96-well PCR plate was used) the initial reaction components were mixed together (see Table 2.12.1). The initial reaction components were then heated to 80°C for 5 minutes and placed promptly onto ice. The remaining reaction components were then added to the tube/s (for multiple reactions a master mix was prepared for ease of addition) and the reaction was performed at 42°C for 1 hour. A control reaction, without M-MuLV RT (known as minus RT), was also performed for each sample. The enzymes were then heat-inactivated by incubation at 90°C for 10 minutes and cDNA samples were stored at -20°C until required.

***Table 2.12.1: Reverse-transcriptase reaction components.***

*Initial reaction contains heat-insensitive reagents, whereas final reaction contains the buffers and enzymes.*

| Component | Amount | Source |
|---|---|---|
| *The following Initial reaction components were mixed together and heat-denatured* | | |
| RNA solution | 0.5-2 µg | Own material – used 0.5 µg |
| Primer: oligo dT | 40 µM | MWG Eurofins |
| dNTPs | 2.5 mM each | GE Healthcare |
| Nuclease-free water | Up to 16 µl | With M-MuLV Kit |
| *Final reaction components were then added and RT reaction performed* | | |
| X 10 RT buffer | 2 µl | With M-MuLV kit |
| 10 U/ µl RNase inhibitor | 1 µl | NEB |
| M-MuLV reverse-transcriptase | 1 µl | NEB |

## 2.12.2 Quantitative Real-Time PCR (QRTPCR)

Quantitative Real-Time PCR (QRTPCR) was performed on cDNA samples using the iQ™ SYBR® Green Supermix and iQ5 multicolor real time PCR detection system (BioRad). QRTPCR was used to determine whether the villus/crypt enrichment procedure, as performed in the small intestine epithelial extraction protocol (see Section 2.13.4), was successful. That is, would villus-specific genes be up-regulated in the 'mostly villus' fraction over the 'mostly crypt' fraction and vice-versa. To accomplish this, three different genes were examined, a villus specific gene (*Max*), a crypt specific gene (*Lgr5*) and a house-keeping gene to standardise the data (*Hprt1*).

QRTPCR was performed according a slightly modified version of the manufacturer's guidelines as follows; working with one high profile, clear 96-well PCR plate at a time, a master mix containing all reaction components except for the template DNA (see Table 2.12.2) was prepared for *n* reactions (*n* = number of reactions + 5). 15 µl of master mix was then pipetted into each assigned well using a multipipette® (Eppendorf) for speed and consistency. Once the master mix was dispensed, the 96-well PCR plate was sealed with a temporary plate sticker and placed to one side whilst the template cDNA and DNA standards were prepared.

***Table 2.12.2: Standard components of a QRTPCR reaction.***

| **Component** | **/20 µl** |
|---|---|
| X 2 iQ SYBR Green Supermix | 10 µl |
| Forward primer (0.1 µg/µl) | 0.4 µl |
| Reverse primer (0.1 µg/µl) | 0.4 µl |
| $H_2O$ | 4.2 µl |
| Template DNA | 5 µl |

The template cDNA was prepared by diluting the cDNA synthesised from the reverse transcriptase reaction (described previously in Section 2.12.1) 1 in 20 with $H_2O$. If cDNA samples were not already in a 96-well PCR plate they were transferred into one to simplify

pipetting and storage. The DNA standards used were seven serial dilutions of known concentration of plasmid DNA which contained the PCR fragment being amplified (fragment was typically cloned into a TA vector such as pCR2.1). The starting dilution was 1000 amol (1 attomol = 1 x $10^{-18}$ M) in 5 µl and this was diluted 1 in 10 until 1 zmol (1 zmol = 1 x $10^{-21}$ M) was reached and see Table 2.12.3. The DNA standard serial dilutions were prepared fresh on the day in 1.5 ml micro-centrifuge tubes (10 µl into 90 µl $H_2O$) but were transferred into the wells of a 96-well PCR plate so a multichannel pipette could be used. The cDNA template and DNA standard reactions were each performed in triplicate, the minus-RT (negative control) was only performed in duplicate.

***Table 2.12.3: Concentration of DNA standards for QRTPCR.***

| DNA Standard | Amount in 5 µl |
|---|---|
| 1 | 1000 amol |
| 2 | 100 amol |
| 3 | 10 amol |
| 4 | 1 amol |
| 5 | 100 zmol |
| 6 | 10 zmol |
| 7 | 1 zmol |

Once the template DNA was ready, 5 µl of standard or sample was transferred into its corresponding well in the original 96-well PCR plate which contained the master mix. A multichannel pipette was used when possible for speed and consistency. Following addition of DNA, the reaction plate was sealed with an appropriate adhesive sticker (Microseal® 'B' film - BioRad) and plate sealer tool (to avoid marking the top of the plate). The plate was then centrifuged briefly to ensure that the contents was at the base of each well, before being placed into the iQ5 multicolor real time PCR detection system for the QRTPCR reaction to be run.

The QRTPCR reaction, including plate layout, was set up using the workshop in the BioRad iQ5 software. The standard cycling parameters of a QRTPCR is shown in Table

2.12.4. Once a run was complete the results could be briefly analysed in the data analysis section, however for a more detailed analysis, the files were saved and sent to Dr Bryony Lloyd (The University of Liverpool).

***Table 2.12.4: Standard cycling parameters of a QRTPCR***

| | | |
|---|---|---|
| Initial Denaturisation | 95°C | 3 minutes |
| **40 cycles** | | |
| Denaturisation | 95°C | 30 s |
| Anneal | Primer specific | 45 s |
| Melt curve | 95°C → 50°C | 1°C per 10 s |

# 2.13 Phenotype analysis

## 2.13.1 Animals

c-Rel$^{-/-}$ knock-out mice (on a *C57BL/6* genetic background) were obtained from Dr J.C. Caamano from the University of Birmingham as described in [Mason et al., 2002]. These mice retain wild-type p53 and thus have intact apoptotic responses and since these were readily available they were used to optimise conditions for immunohistochemistry (IHC). Conditionally floxed Mdm2 null mice were a kind gift from Dr O.J. Sansom, Beatson Institute, Glasgow, UK. These mice contain a *cre* gene under the control of the gastrointestinal specific promoter CYP1A1, which can be switched on by administrating lipophilic xenobiotics (such as β-naphthoflavone) [Campbell et al., 1996]. A summary of the experiments performed in this thesis can be found in Table 2.13.1. All experiments were conducted under the authority of a valid UK Home Office project licence.

## 2.13.2 Exposure of animals to γ-irradiation

12-13 week old female mice (c-Rel$^{-/-}$) were exposed to 8 Gy γ-radiation (Gammacell irradiator with a $^{137}$Cs source dose rate 2.6 Gy/min) and sacrificed at 4.5 hours by cervical dislocation. 8-10 week old Mdm2$^{flox/flox}$ or wild-type male mice were exposed to 14 Gy γ-irradiation using a cobalt-60 source at the Beatson Institute and sacrificed at 6 hours by cervical dislocation.

## 2.13.3 Cre-mediated recombination by β-naphthoflavone (BNF)

Various doses of β-naphthoflavone (BNF) (Sigma, Dorset, UK) dissolved in corn oil were administered by gavage and/or injection to induce expression of cre. Note that since BNF is broken down by exposure to light it is necessary to dissolve BNF in an amber bottle and to freeze it in aliquots in amber bottles. BNF and corn oil were heated in a water bath set to 99.9°C. Large pieces of BNF were crushed using a glass rod and then the whole amber bottle was transferred to a heated stirrer set at 100°C and stirred for about 10 minutes. This

process was continued (water bath to stirrer) until all the BNF has dissolved (takes about an hour). The BNF is then aliquoted and frozen. After 3 freeze-thaw cycles the remaining BNF is discarded. Following gavage with BNF mice were sacrificed either on day 1 or day 2 by cervical dislocation, or exposed to 14 Gy γ-irradiation and then sacrificed see for Table 2.13.1 Table 2.13.1details.

***Table 2.13.1: Summary of in vivo experiments***

| Experiment | Animals | Treatment | Other details |
|---|---|---|---|
| Liverpool 2007 | 6 x c-Rel$^{-/-}$ (♀) | +/- 8 Gy γ-irradiation sacrificed 4.5 hours | Small and large intestine for paraffin blocks |
| Glasgow 2008 | 6 x Mdm2$^{flox/flox}$ 6 x Wild-type (♂) | **Day 0** – 1 x 80 mg/kg dose of BNF (gavage) **Day 1** – sacrifice 3 x Mdm2$^{flox/flox}$ & 3 x wild-type **Day 2** – sacrifice 3 x Mdm2$^{flox/flox}$ & 3 x wild-type | Small intestine and liver for paraffin blocks |
| Glasgow 2009 | 6 x Mdm2$^{flox/flox}$ 6 x Wild-type (♂) | **Day 0** – 3 x 80 mg/kg dose of BNF (IP injections at 9am, 12pm and 5pm) + additional 1 x 80 mg/kg BNF (gavage 12pm) **Day 1** – +/- 14 Gy γ-irradiation sacrificed 6 hours | Small intestine and liver for paraffin blocks Small intestine frozen in RNA*later* |
| Glasgow 2010 | 3 x Mdm2$^{flox/flox}$ 6 x Wild-type (♂) | **Day 0** – 3 x 80 mg/kg dose of BNF (IP injections at 9am, 12pm and 5pm) + additional 1 x 80 mg/kg BNF (gavage 12pm) **Day 1** – 3 x wild-type + 14 Gy γ-irradiation sacrificed 6 hours. Remaining animals also sacrificed | Performed intestinal epithelial extraction – collected 2 fractions 'mostly villus' and 'mostly crypt' – were frozen in TRIZOL reagent |

### 2.13.4 Isolation of epithelial cells from mouse gut

The epithelial extraction protocol described here is based on [Weiser, 1973]. During the procedure two cell fractions were collected; the first fraction was said to be 'mostly villus' whilst the second was said to be 'mostly crypt'. For this experiment, a custom made piece of equipment was necessary – a 0.5 mm diameter spiral glass rod (made using a glass blower). The experiment was performed as follows; mice were sacrificed by cervical dislocation and their small intestine was promptly removed. The first 5 cm (from the stomach) was discarded and the next 10-20 cm was used for extraction. The gut was flushed with water then a suture was used to tie off ~ 1 cm of intestine. This ~ 1 cm of intestine was carefully threaded onto the curved end of the custom made helical glass rod so that the tie was flush with the tip of the glass rod. The remaining gut was then forced back over itself so that the intestine was inverted on the helical glass rod. The glass rod was then wedged inside the pipetteaid and lowered into a 50 ml Falcon tube containing 25 ml of 10 mM EDTA in HBSS (Ca and Mg free Gibco #14170-088). The 50 ml Falcon and EDTA/HBSS were pre-warmed to 37°C and were kept at 37°C for the duration of the extraction procedure. The pipetteaid was held in a retort stand and its expel button was taped down to create a gentle vibration which dislodges the cells from the intestine (see Figure 2.13.1). The first fraction was collected for 15 minutes, after which the glass rod with the inverted intestine was removed from the pipetteaid and given a quick shake (to dislodge loose cells and any remaining mucus) into the EDTA/HBSS. The glass rod was then reinserted into the pipette aide and was lowered into a fresh 50 ml Falcon with another 25 ml EDTA/HBSS to collect the second fraction. The second fraction was collected for 15 minutes and once finished; the glass rod was again shaken firmly to remove any remaining cells. The collected fractions were stored on ice until all the mice had been sacrificed.

When all the samples had been collected they were centrifuged at 3000 x *g* for 15 minutes to pellet the cells. The supernatant was very carefully poured off and the cells re-suspended in 1 ml TRIZOL reagent. The cells/TRIZOL suspension were transferred into a nuclease free 1.5 ml micro-centrifuge tube and frozen at -80°C until commencing RNA work (see Section 2.11.3).

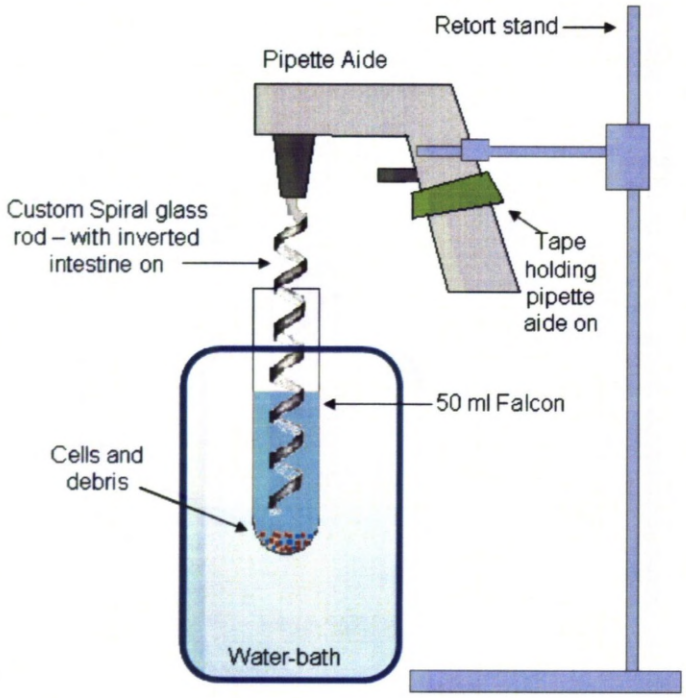


***Figure 2.13.1: Intestinal epithelial extraction apparatus.***

## 2.13.5 Immunohistochemistry (IHC)

IHC was performed on formalin-fixed paraffin-embedded mouse intestinal tissue as described in [Wilson et al., 1998]. Sections were cut in series on a microtome at 4 μm thickness and stained for Noxa (1:200) (rabbit polyclonal anti-Noxa, Anaspec), p21 (1:900) (rabbit polyclonal anti-p21 (M-19) Santa Cruz) and p53 (1:500) (rabbit polyclonal anti-p53 protein (CM5) Novocastra).

Following de-waxing in xylene and hydration through 100%, 90% and 70% ethanol baths, the endogenous peroxidase activity in sections was blocked in buffer (1% $H_2O_2$ in methanol) for 12 minutes at room temperature (RT). Sections were then washed for 5 minutes in distilled water. Antigen retrieval was carried out by boiling sections in 10mM citric acid buffer (pH 6.0) for 20 minutes in a microwave and then allowing them to cool for a further 20 minutes. All antibodies were incubated for 2 hours at room temperature followed by a 30 minute incubation with a horseradish peroxidise (HRP) labelled polymer which is conjugated with secondary antibodies (DAKO Envision Rabbit-Primary kit). 10 minute washes were carried out between each stage using TBS-Tween (0.05 M Tris-base, 0.15 M NaCl and 0.1%

Tween 20). Staining was visualised with DAB (10 minutes) and counterstained with Gill's haematoxylin (Vector Laboratories). Sections were dehydrated and clarified in xylene then mounted using VectaMount permanent mounting media.

## 2.13.6 Cell scoring

Normal cells, apoptotic cells and mitotic cells were distinguished based on their morphological characteristics (see Section 1.4.5.1 and Figure 2.13.2) and scored based on their cell position from the bottom of the crypt [Ijiri and Potten, 1983]. 50 half crypts were counted from each mouse and the data was recorded and analysed using the WinScore programme [Roberts, 1996]. Mitotic cells can be differentiated from apoptotic cells by the absence of apoptotic bodies and in addition they appear displaced towards the gut lumen [Wilson et al., 1998].

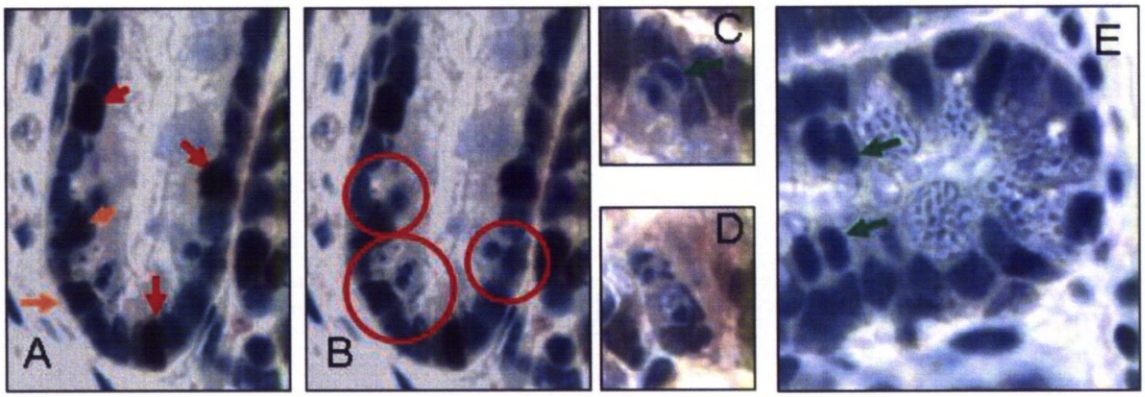


***Figure 2.13.2: Examples of cell scoring.***

*A) Base of a colonic crypt, the red arrows show strong immunoreactivity while the orange arrows show weak-to-moderate cell staining. B) The same colonic crypt, the red circles illustrate the apoptotic cells. C) & E) Photos of mitotic cells (green arrows) and D) Photo of an apoptotic cell.*

Immunoreactivity for Noxa, p21 and p53 was classified based on signal intensity (weak-to-moderate versus strong) and scored using the same counting method as above. This approach, while subject to observer bias, has been shown to be both robust and

reproducible [Wilson et al., 1998]. An equal number of crypts were counted from at least three circumferences of intestine to avoid bias where there might be areas of patchy staining.

A slightly different scoring protocol was used for scoring cells on the villi. Rather than scoring cells based on their absolute position (as for crypts), the total number of positive cells were recorded based on their general location (lower villus, mid-section and villus 'tip'). This was because the villi are much longer than crypts and therefore are more difficult to cross-section accurately. 25 villi were scored from each mouse.

## 2.13.7 β-galactosidase staining assay

In order to detect expression of β-geo (a fusion protein of β-galactosidase and neomycin) in the p21 gene-trapped ES cell line AM0998, a β-galactosidase (β-gal) X-gal staining assay was performed. In this assay X-gal (5-bromo-3-indoyl-β-D-galactopyranoside) substrate is cleaved by β-geo which has β-galactosidase activity fused to a neomycin resistance gene (see Figure 2.13.3) generating a product that when oxidised forms an insoluble blue product which can be observed inside cells.

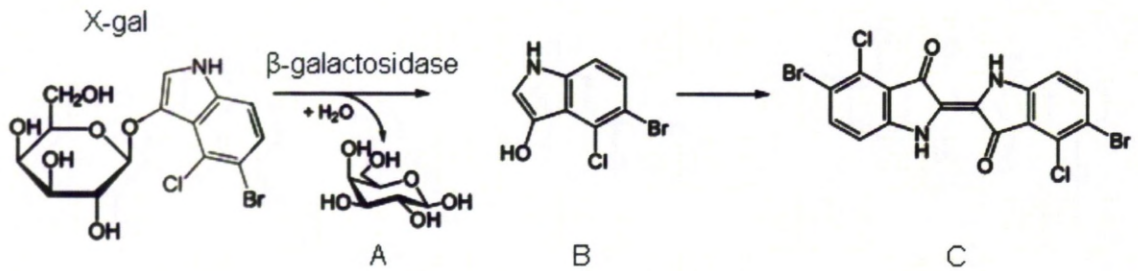


***Figure 2.13.3: X-gal reaction***

*X-gal is cleaved by β-galactosidase into A) galactose and B) 5-bromo-4-chloro-3-hydroxyindole. B) Becomes oxidised over time to produce C) 5,5'-dibromo-4,4'-dichloro-indigo which is responsible for the blue colour observed. Image was adapted from http://en.wikipedia.org/wiki/X-gal.*

The β-gal staining assay was performed on cells as follows; the old media was removed from the tissue culture vessel and the cell monolayer was washed twice with 2 ml

DPBS and incubated with 2 ml of fixing buffer (see Table 2.13.2 for composition – buffers were prepared fresh on the day) for 15 minutes at RT. Following incubation, the fixing buffer was removed and the cells were washed twice with DPBS. 4 ml of substrate buffer was added to the flask which was then returned to the 37°C, tissue culture incubator for at least 2.5 hours (was routinely left overnight) in order to let the blue colour develop. Once the reaction appeared complete, the substrate buffer was removed and the cells were washed twice with $H_2O$ and the flasks were inverted to dry. The colour (if any) could be photographed on a light microscope. The volumes above are suitable for a T25 flask, and should be scaled up or down accordingly for other tissue culture vessels.

***Table 2.13.2: Composition of β-Galactosidase assay buffers.***

| Buffer | Composition | Source |
|---|---|---|
| Fixing buffer | 2% glutaraldehyde | BDH |
| | In DPBS | Sigma-Aldrich |
| Substrate buffer | 3 mM potassium ferrocyanide | BDH |
| | 3 mM potassium ferricyanide | BDH |
| | 1 mM magnesium chloride | BDH AnalaR |
| | 0.5 mg/ml X-Gal | Sigma-Aldrich |
| | In DPBS | Sigma-Aldrich |

## 2.13.8 Luciferase assay

The Dual-Luciferase® Reporter Assay System from Promega was used to detect expression of firefly and *Renilla* luciferase constructs which had been transfected into mammalian cells (See Section 2.9.2.1). Firefly (*Photinus pyralis*) luciferase is an enzyme which catalyses the oxidation of luciferin to produce oxyluciferin and light, whilst *Renilla* luciferase catalyses the oxidation of coelenterazin to produce coelenteramide and light (see Figure 2.13.4). Thus firefly and *Renilla* (*Renilla reniformis*, a sea pansy) luciferases utilise two distinct chemical pathways which both generate bioluminescence. The dual-luciferase reporter assay system exploits these two different biological pathways so that the activities of

each enzyme can be measured in turn from a single sample. Briefly, cell lysates are first examined with LAR II (luciferase assay reagent II) to detect the activity of firefly luciferase. Then, once the luminescence had been measured, a second reagent is added and the luminescence measured again. The second reagent contains both a quencher (Stop+Glo reagent) to stop the luminescence generated by firefly luciferase and the *Renilla* substrate to initiate the second bioluminescence reaction. The protein concentration (to normalise the data) is also determined using a micro-Bradford assay (see Section 2.10.1).

The luciferase assay was performed according to a scaled down version of the manufacturer's guidelines as follows; cells in a 48-well plate which had been transfected with luciferase constructs at least 24 hours prior had the old media removed and were washed with 300 µl of DPBS twice. 150 µl of passive lysis buffer (PLB – diluted 1 in 5 in $H_2O$ before use) was then added to each well and left to incubate for 10 minutes at RT with agitation (on a rocking table). The cell lysates were transferred into 1.5 ml micro-centrifuge tubes (one for each well) and centrifuged at maximum speed for 1 minute. The supernatant was transferred into a fresh 1.5 ml micro-centrifuge tube and examined for luciferase activity.

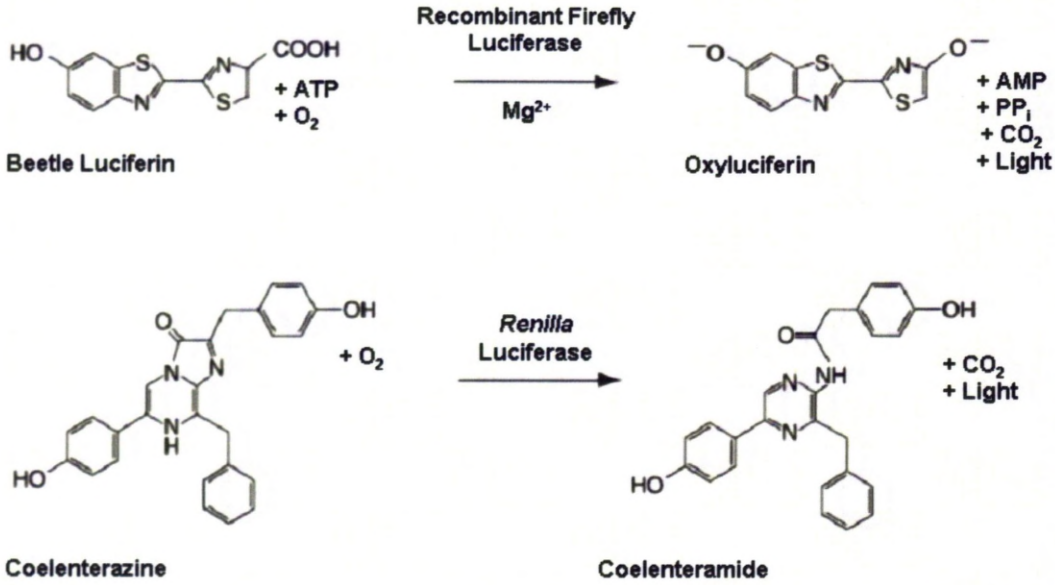


***Figure 2.13.4: The firefly and Renilla luciferase bioluminescence reactions.***

Firefly luciferase activity was measured first as follows; 30 µl of LAR II reagent was pipetted into a fresh 1.5 ml micro-centrifuge tube (Eppendorf). To the tube 6 µl of cell lysate was added and vortexed for exactly 1 second (without closing the lid) then placed into the luminometer and measured. When measuring the luminescence of the samples it was important to move at a steady speed to minimise variability. The luminometer (GloMax® 20/20 Luminometer) was set to have no time delay prior to reading and an integration time of 10 seconds. Whilst the sample luminescence was being measured 30 µl of the *Renilla* substrate/Stop+Glo reagent was taken up into a pipette tip ready for when the firefly luciferase reading was finished. Immediately upon completion of the reading the tube was removed from the machine and the second reagent added. This was then vortexed for exactly 5 seconds before being returned to the luminometer and measured again. The luminescence readings were recorded and the steps repeated for any remaining samples. The *Renilla* substrate/Stop+Glo reagent was prepared fresh on the day by diluting the *Renilla* substrate 1 in 50 into the Stop+Glo reagent.

In order to normalise the results a micro-Bradford assay was then performed in the cell lysates – see Section 2.10.1.

# 3 Results

# 3.1 Investigating cell death in the mouse intestinal epithelium

## 3.1.1 γ-irradiation of mice (cRel$^{-/-}$)

### *3.1.1.1 Immunohistochemistry*

To determine whether p21 and Noxa levels reliably indicated a p53 response in the gastro-intestinal tract, mice were exposed to an 8 Gy dose of whole body ionising radiation to induce DNA damage and serial sections of the colon and small intestine were examined for p53, p21 and Noxa by IHC (Figure 3.1.1 & Figure 3.1.2 respectively). We used c-Rel$^{-/-}$ mice for these studies because these were readily available and according to results from all of our available analyses they behaved indistinguishably from wild-type mice. The staining in the crypts was then compared to control mice that had not received whole body γ-radiation. p53 and p21 were up-regulated in intestinal cells as a result of whole body γ-radiation as shown in Figure 3.1.1 and Figure 3.1.2 (and see (Pritchard et al., 1999)). Noxa appeared up-regulated as a result of ionising radiation in the colon; however its expression was relatively high regardless of irradiation status in the small intestine (see Figure 3.1.3).

p53 and p21-specific antibodies stained the nucleus of cells in a uniform pattern across the section, whereas Noxa staining was cytoplasmic, punctuated and often heterogenous across different gut circumferences within the section (see Figure 3.1.3). The observed pattern of expression is expected since p53 is a transcription factor that acts on DNA in the nucleus (Vousden, 2006), and p21 is also localised in the nucleus, where upon activation it binds to cyclin dependent kinases (CDKs) and induces cell cycle arrest (Coqueret, 2003). However Noxa is found in the cytoplasm of the cells, since it interacts with anti-apoptotic protein Mcl-1 at the mitochondrial surface (Willis and Adams, 2005). The pattern of dotted staining for Noxa matches that of other mitochondrial proteins such as cytochrome *c* (Payne et al., 2005).

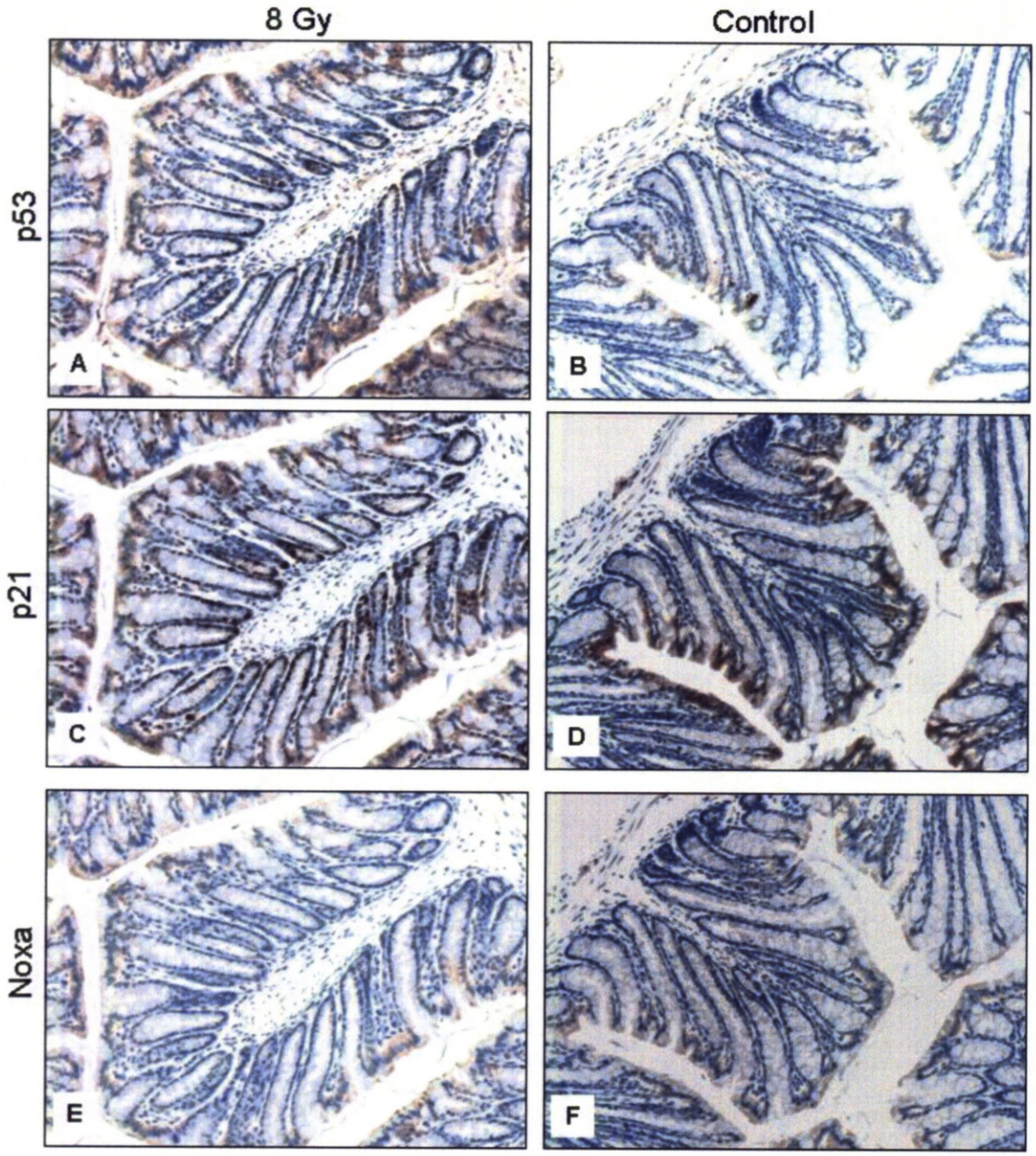


***Figure 3.1.1: Immunoreactivity of p53, p21 and Noxa in mouse colon.***

*Colon was harvested from c-Rel$^{-/-}$ (p53 wild-type) mice 4.5 hours post ± 8 Gy γ-irradiation. Serial sections were probed with antibodies against p53, p21 and Noxa. Digital photographs were taken with x 20 objective. p53 and p21 expression (A, B, C and D) was increased upon irradiation, whilst there was no staining for Noxa (E and F) in this series. There was little or no staining for p53, p21 or Noxa in the colonic crypts of non-irradiated mice demonstrating that the response was dependent on γ-radiation.*

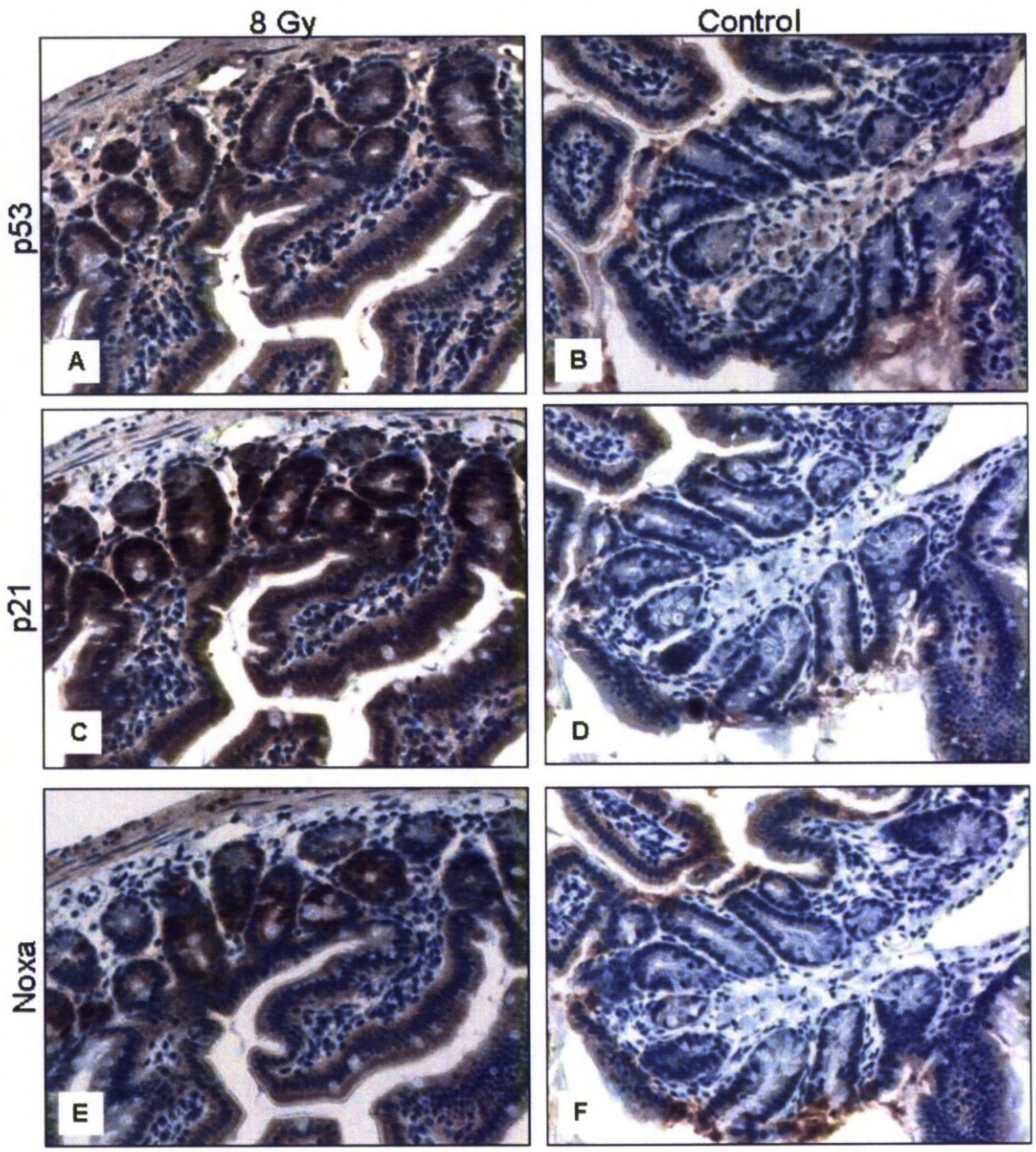


***Figure 3.1.2: Immunoreactivity of p53, p21 and Noxa in the small intestine.***

*Small intestine was harvested from c-Rel$^{-/-}$ (p53 wild-type) mice 4.5 hours post ± 8 Gy γ-irradiation. Serial sections were probed with antibodies against p53, p21 and Noxa. Digital photographs were taken with x 40 objective. p53, p21 and Noxa all appear to be up-regulated in response to ionising radiation, however Noxa staining was inconsistent and non-irradiated tissue also shows some areas of very strong staining. See also Figure 3.1.3.*

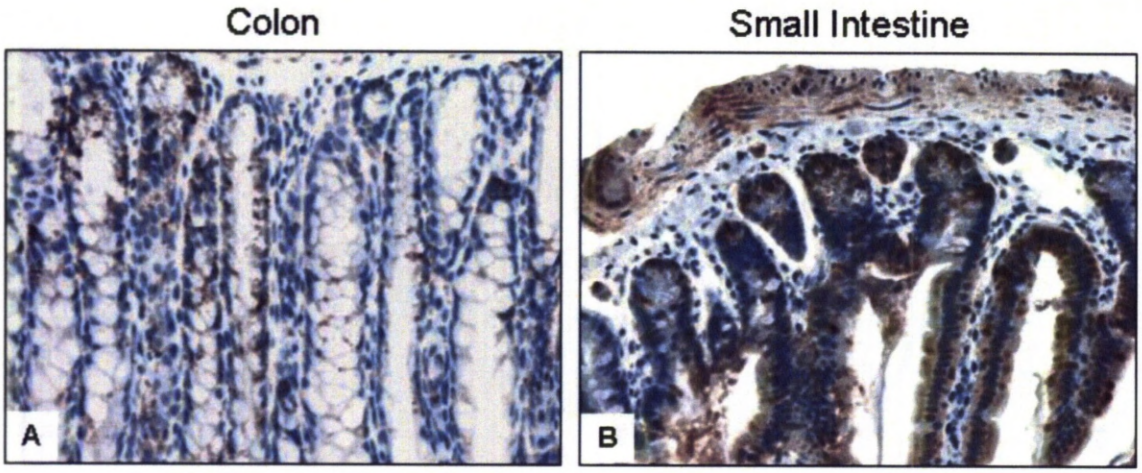


***Figure 3.1.3: Comparison of Noxa staining in c-Rel$^{-/-}$ mice.***

*A) Staining of Noxa in part of an irradiated mouse colon. Noxa staining appeared ubiquitously in this section of colon, however other areas were completely unstained (compare with Figure 3.1.1). B) Noxa staining in non-irradiated small intestine; crypt and villi cells were both stained as strongly as irradiated animals (see Figure 3.1.2) despite a lack of stimulus.*

The specificity of the p53 (CM5) (Botchkarev et al., 2001, Midgley et al., 1995) and p21 (M-19) antibodies has been well documented (Canman et al., 1995, Chang et al., 2011). Relatively little, however, was known about the specificity of Anaspec anti-Noxa antibody.

### *3.1.1.2 Crypt cell scoring data*

Cells in the crypt were scored for apoptosis and immunoreactivity to p53, p21 and Noxa in the serial gut sections prepared above. Apoptosis was characteristically high at the base of the crypt in both the large and small intestine 4.5 hours after 8 Gy of γ-radiation (cell positions 0-5). This apoptosis peak was matched in the colon with high immunoreactivity for p53, p21 and Noxa. Of these proteins, p21 had the widest response and its up-regulation was significant until approximately half way up the crypt (cell position 33 - see Figure 3.1.4). In the small intestine only the p53 immunoreactivity matched the apoptosis peak, as p21 and Noxa had a more bell shaped distribution peaking at around position 15 (as opposed to 0-5). Noxa had a relatively high background in non-irradiated animals (see Figure 3.1.5), whilst p21 was expressed towards the top (lumen) end of the crypt in non-irradiated mice. This mini-peak of p21 expression coincided with migrating cells entering $G_1$ phase cell cycle arrest (el-Deiry et al., 1995) and was, most likely, associated with differentiation and maturation of intestinal cells (Yang et al., 2001).

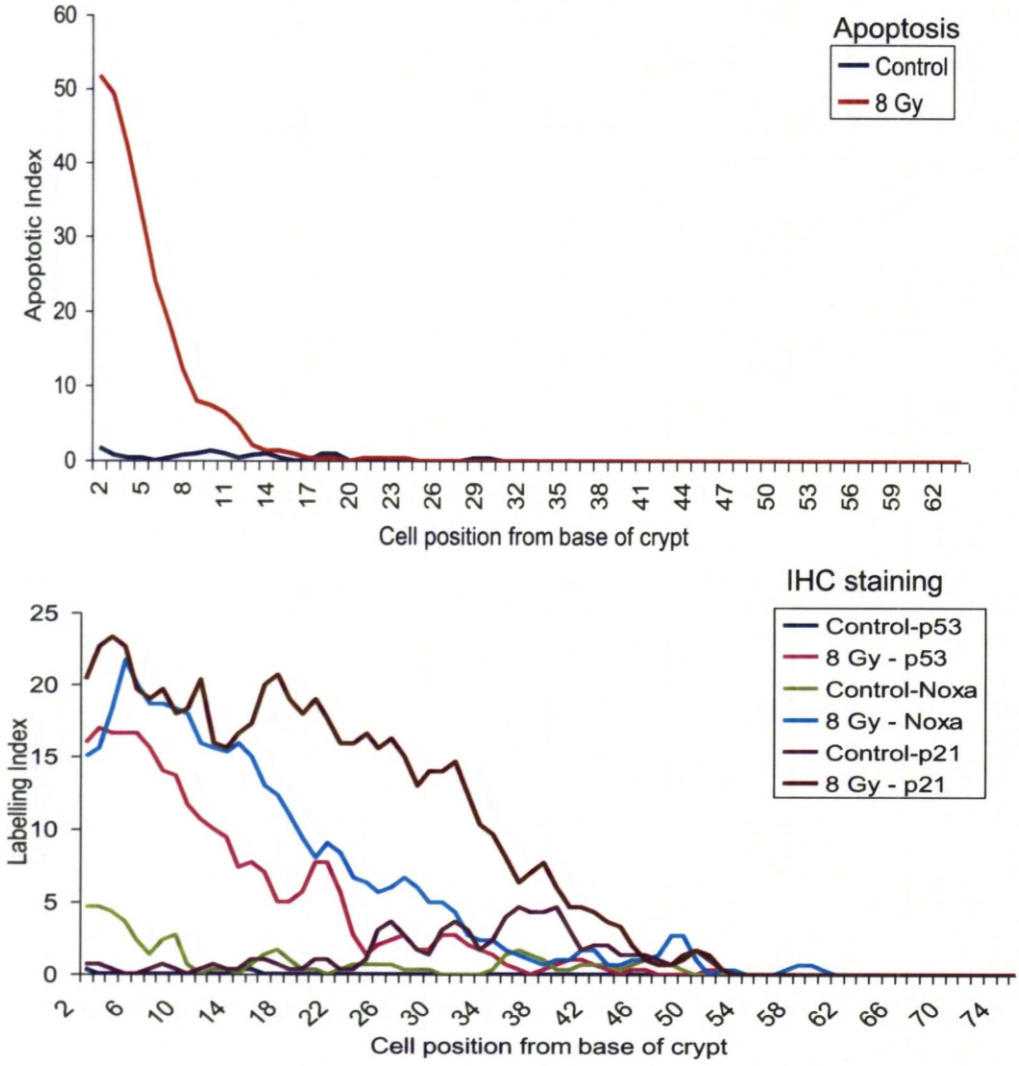


***Figure 3.1.4: Cell scoring data for the colonic crypts of c-Rel-/- mice.***

*Apoptosis (top) and immunoreactivity of p53, p21 and Noxa (bottom) in irradiated and non-irradiated c-Rel$^{-/-}$ mouse colon. Apoptosis is significantly induced by whole body irradiation (significant up to cell position 12) as is p53, p21 and Noxa expression (significant up to cell position 32, 33 and 29 respectively).*

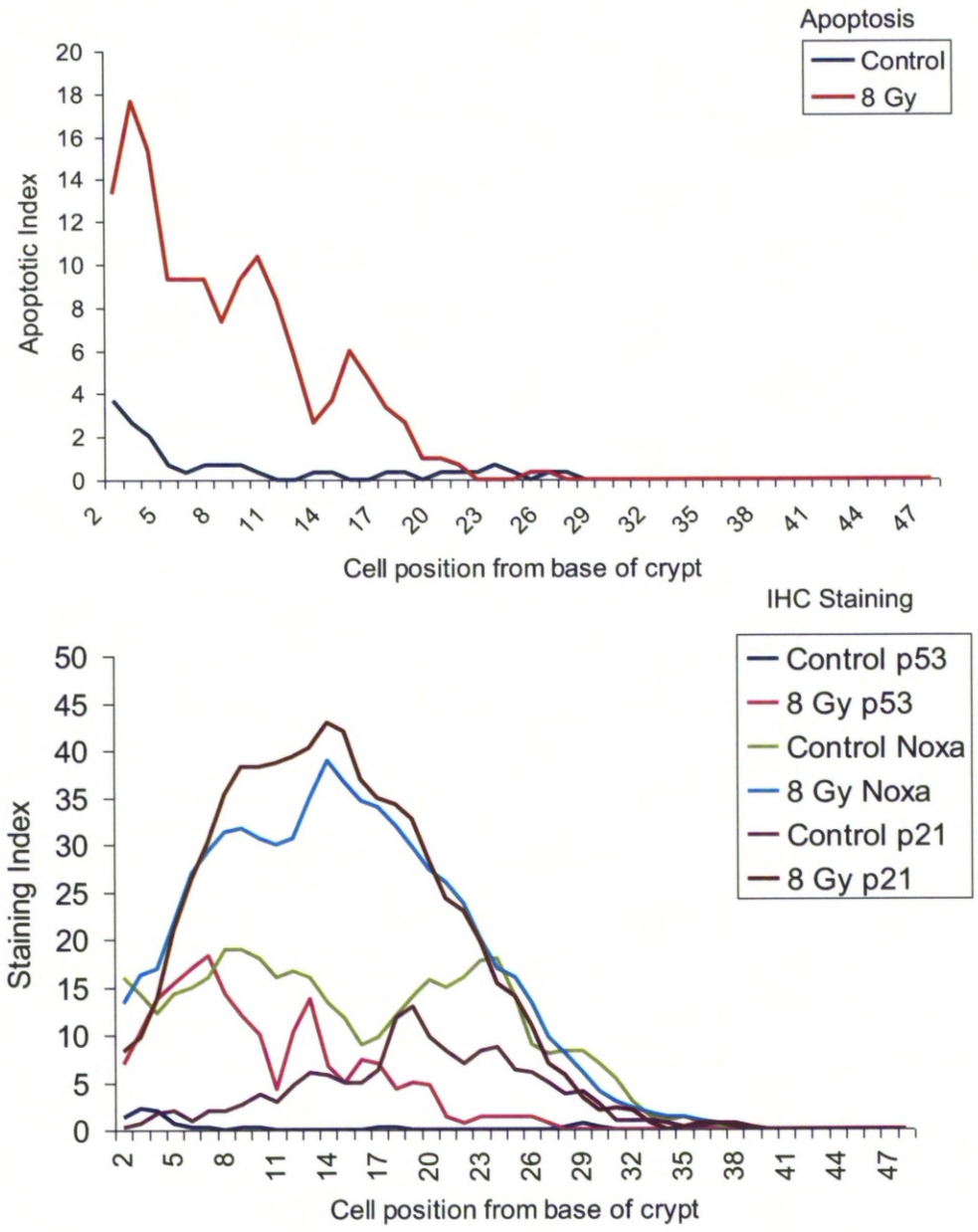


***Figure 3.1.5: Cell scoring data for the small intestine of c-Rel-/- mice.***

*Apoptosis (top) and immunoreactivity of p53, p21 and Noxa (bottom) in irradiated and non-irradiated c-Rel$^{-/-}$ mouse small intestine. Apoptosis is significantly induced by whole body irradiation (significant up to cell position 17) as is p53, p21 and Noxa expression (significant up to cell position 23 (p53), and between 10-20 & 11-19 (p21 & Noxa respectively)).*

## 3.1.2 Conditionally floxed Mdm2 null mice

### *3.1.2.1 Immunohistochemistry*

To examine whether p53 and its downstream targets p21 and Noxa would be up-regulated following loss of *Mdm2* (an essential negative-regulator of p53 (Jones et al., 1995)) in the small intestine, we took advantage of conditionally floxed *Mdm2* null mouse strain: $Mdm2^{flox/flox}$. Activation of Cre recombinase upon addition of BNF (β-naphthoflavone) to these animals leads to conditional knockout of *Mdm2* only in the small intestine (and liver). For these experiments, $Mdm2^{flox/flox}$ and wild-type mice were both administered with 1 x 80 mg/kg of BNF by gavage. Serial sections of small intestine from both groups were stained for p53, p21 and Noxa at day 1 and day 2 following treatment (see Figure 3.1.6).

p53 was strongly expressed in the crypt compartment of the small intestine at 24 hours following loss of *Mdm2*, but less so at 48 hours. Indeed, p53 levels had returned to approximately wild-type levels in the crypt cells by day two. p21 up-regulation was less obvious in this system, since p21 staining appeared in both wild-type and $Mdm2^{flox/flox}$ animals and background staining was generally high. Nonetheless p21 staining did appear to be more intense on day 1 following knockout of *Mdm2*. Noxa expression appeared to be up-regulated as a result of the gavage treatment itself, rather then as a consequence of loss of *Mdm2* and the subsequent up-regulation of tumour suppressor gene *p53*, since all day 1 sections stained equally strongly for Noxa regardless of genotype.

Interestingly, p53 protein up-regulation was not limited just to cells within the crypts. Following conditional knockdown of *Mdm2*, p53 was also up-regulated in epithelial cells on the villi, an observation that has been previously reported (see Figure 3.1.7. and (Valentin-Vega et al., 2008)). The observed p53 expression pattern on the villi was only present in $Mdm2^{flox/flox}$ animals and was thought to be genuine, not an artefact or a consequence of the migration of crypt cells onto the villus. We thought this for several reasons; the staining occurred in the nucleus of the cells as expected for a transcription factor such as p53 and therefore the pattern of staining appeared specific. In this experiment the first time point was 24 hours which does not allow sufficient time for the whole intestinal gut epithelia to turnover (typically takes 2-7 days (Brittan and Wright, 2004)), therefore the crypt-to-villus migration of

cells can not account for all of the p53 positive cells – which occurred along the entire length of the villi (not just at the base or crypt-villus shoulder). Perhaps most convincingly, *p21*, a downstream target gene of p53, was also up-regulated on the villi of the *Mdm2*$^{flox/flox}$ animals but not in wild-type animals. The up-regulation of p21 in cells on the villi was unambiguous since background staining was low and, unlike the cells within the crypt region, p21 positive cells rarely occurred on the villi of wild-type animals. p21 expression along the length of the villus indicated that not only was p53 present in cells on the villus, but that it was actively transcribing at least one of its downstream target genes – *p21*. Despite p53 up-regulation, however, there was still no apoptosis observed in cells on the villi

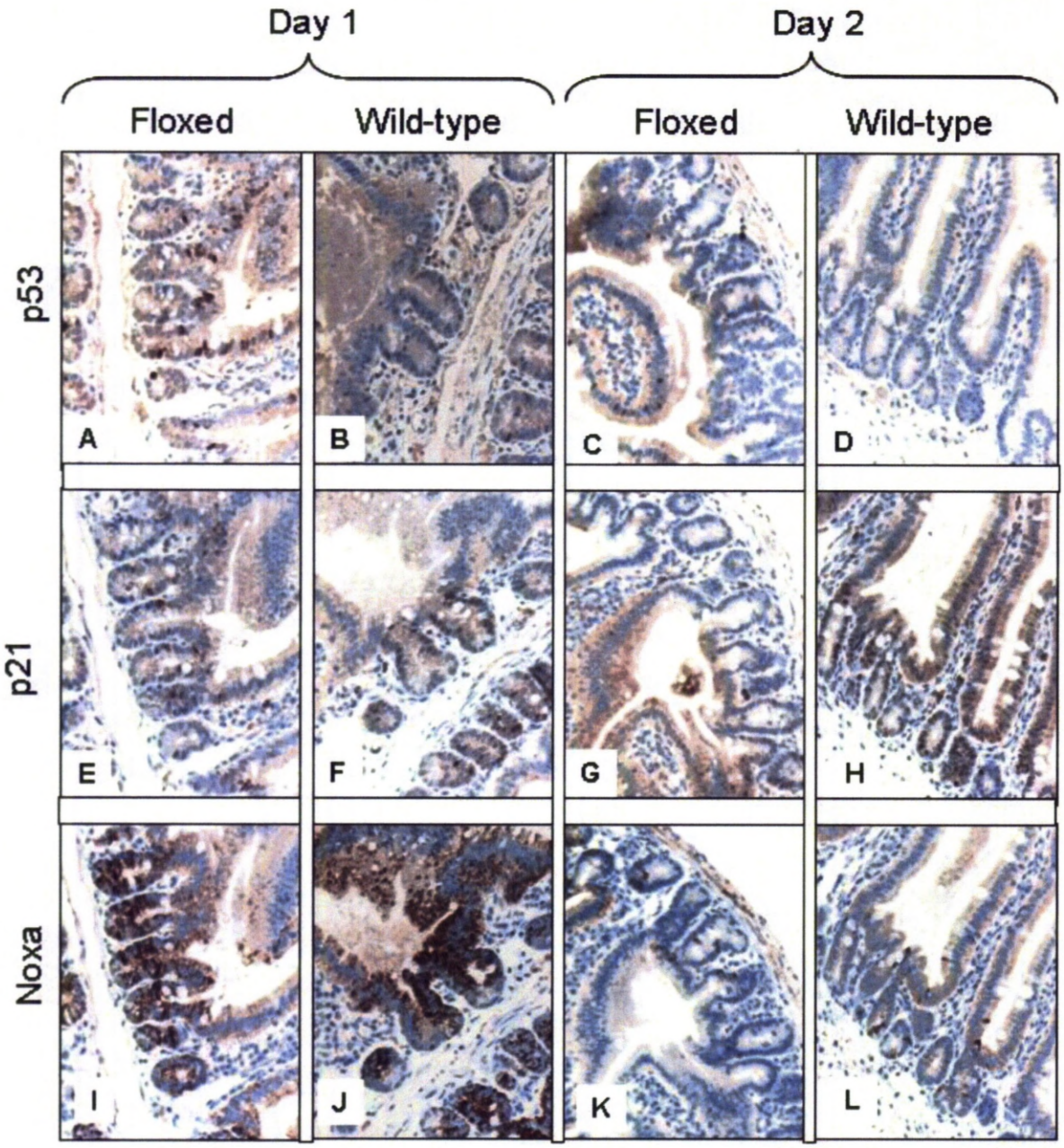


***Figure 3.1.6: Immunohistochemical analysis of time course following administration of β-naphthoflavone (BNF) in the small intestine of wild-type & Mdm2$^{flox/flox}$ mice.***

*Mdm2 conditionally null mice and wild-type mice both received 1 x 80 mg/kg of BNF by gavage on day 0. Staining for p53, p21 and Noxa was carried out on serial sections 24 and 48 hrs following treatment. Photos were taken at x 40 magnification. p53 was very strongly expressed on day 1 but less so on day 2. p21 appeared up-regulated in all animals and time points, though perhaps the staining was more intense on day 1 (see Figure 3.1.10). Noxa expression was patchy and very strong in some sections (I & J), but was independent of Mdm2 status.*

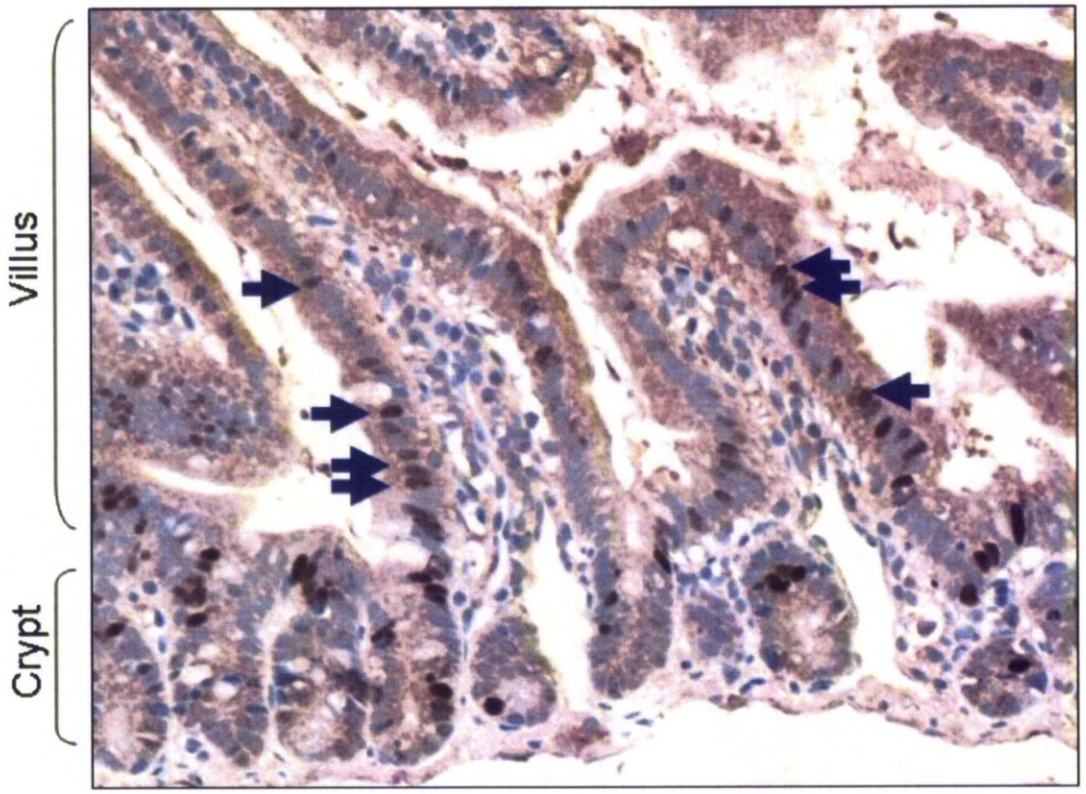


***Figure 3.1.7: Immunohistochemical analysis of p53 expression on villi.***

*IHC using p53-specific antibody of a conditionally floxed Mdm2 null mouse small intestine 24 hours post administration of 1 x 80 mg/kg BNF by gavage. Blue arrows indicate p53 positive cells. Since only 24 hours had passed from the administration of BNF, crypt to villus cell migration does not account for the presence of these p53 positive cells on the villi.*

### *3.1.2.2 Crypt cell scoring data*

Cell scoring was performed as described in Section 2.13.6 for the experiment described above in order to quantify the IHC results. There was an unambiguous marked increase in both apoptotic and p53 levels 24 hours after loss of *Mdm2*, which had returned to basal levels by 48 hours (see Figure 3.1.8). The apoptosis level peaked at the base of the crypt, with p53 expression peaking further along from the base of the crypt at cell position 16. p53 up-regulation was coincident with the expression peak of p21 (also at approximately cell position 16 – see Figure 3.1.9), although the interpretation of p21 expression was less clear since there was much higher background staining present (also seen in IHC photos see Figure 3.1.6). This uncertainty was resolved when only the very strong staining levels were compared (see Figure 3.1.10). p21 was clearly up-regulated in a similar manner to p53 and the background was completely eliminated. There was no difference in Noxa expression between wild-type and floxed mice even when only strong immunoreactivity was compared. In addition, high background staining for Noxa made interpreting results quite difficult. Noxa up-regulation appeared instead to be temporally regulated, with expression on day 1 being considerably higher than that observed on day 2 in both wild-type and floxed animals. This may be a side effect of the gavage technique or an indication of a problem with the specificity of the antibody, which as discussed previously was unknown.

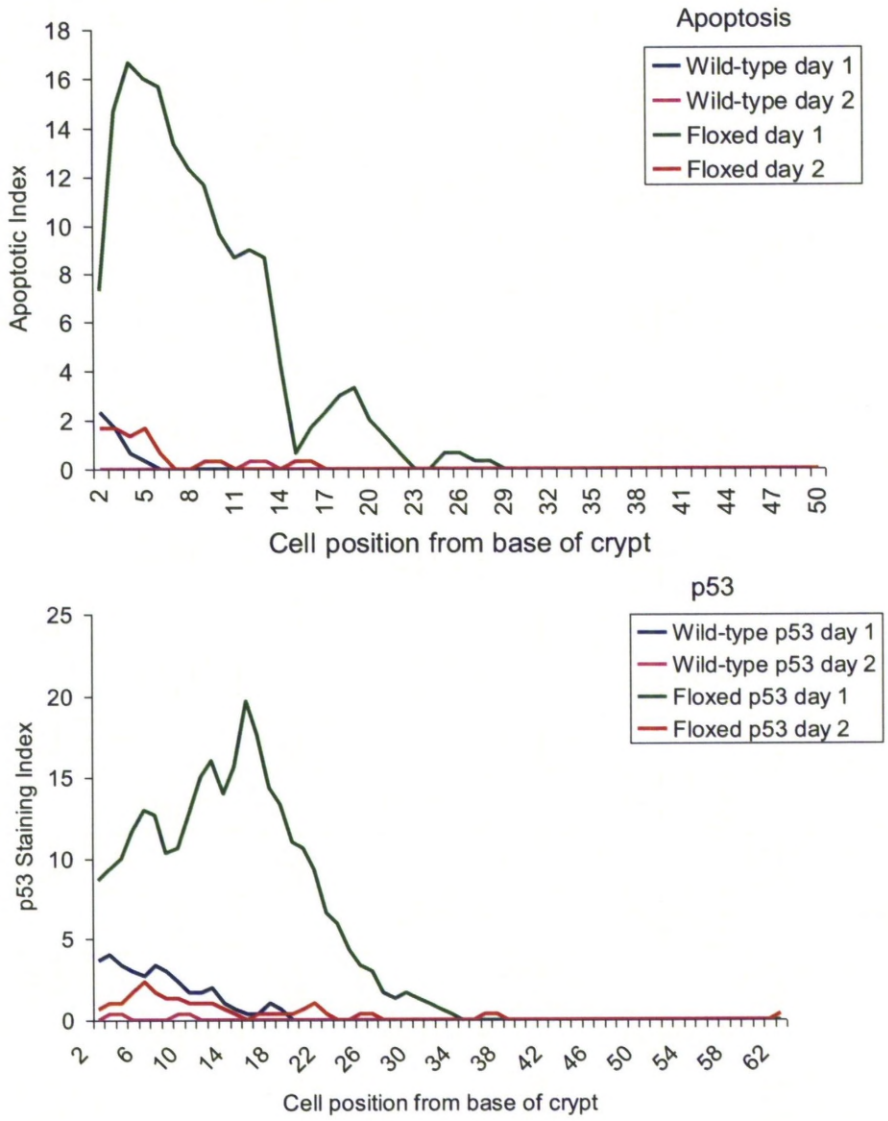


***Figure 3.1.8: Crypt cell scoring data for apoptosis and p53***

*Apoptosis (top) and p53 (bottom) levels on day 1 and day 2 after administration of 1 x 80 mg/kg BNF by gavage to either conditionally floxed Mdm2 null or wild-type mice. Floxed day 1 mice have an increased apoptotic response (significant up to cell position 21) and increased p53 expression (significant up to cell position 29).*

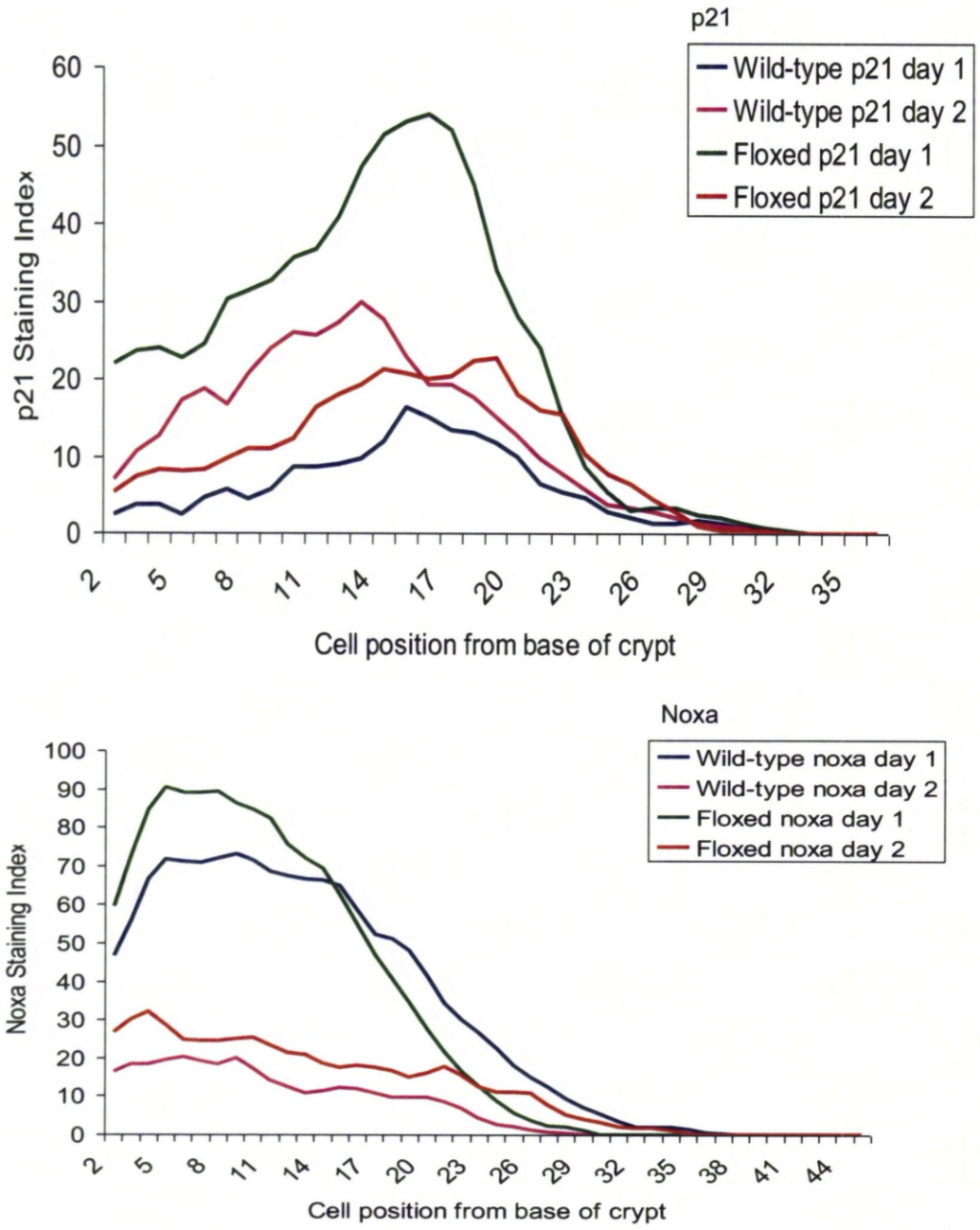


***Figure 3.1.9: Crypt cell scoring data for p21 and Noxa.***

*p21 (top) and Noxa (bottom) protein levels on day 1 and day 2 after administration of 1 x 80 mg/kg of BNF by gavage to either conditionally floxed Mdm2 null or wild-type mice. p21 protein levels on day 1 only appeared marginally increased following knockout of Mdm2 (high background staining made analysis difficult). Noxa expression appears to be independent of Mdm2 status, but depended on time from treatment by gavage.*

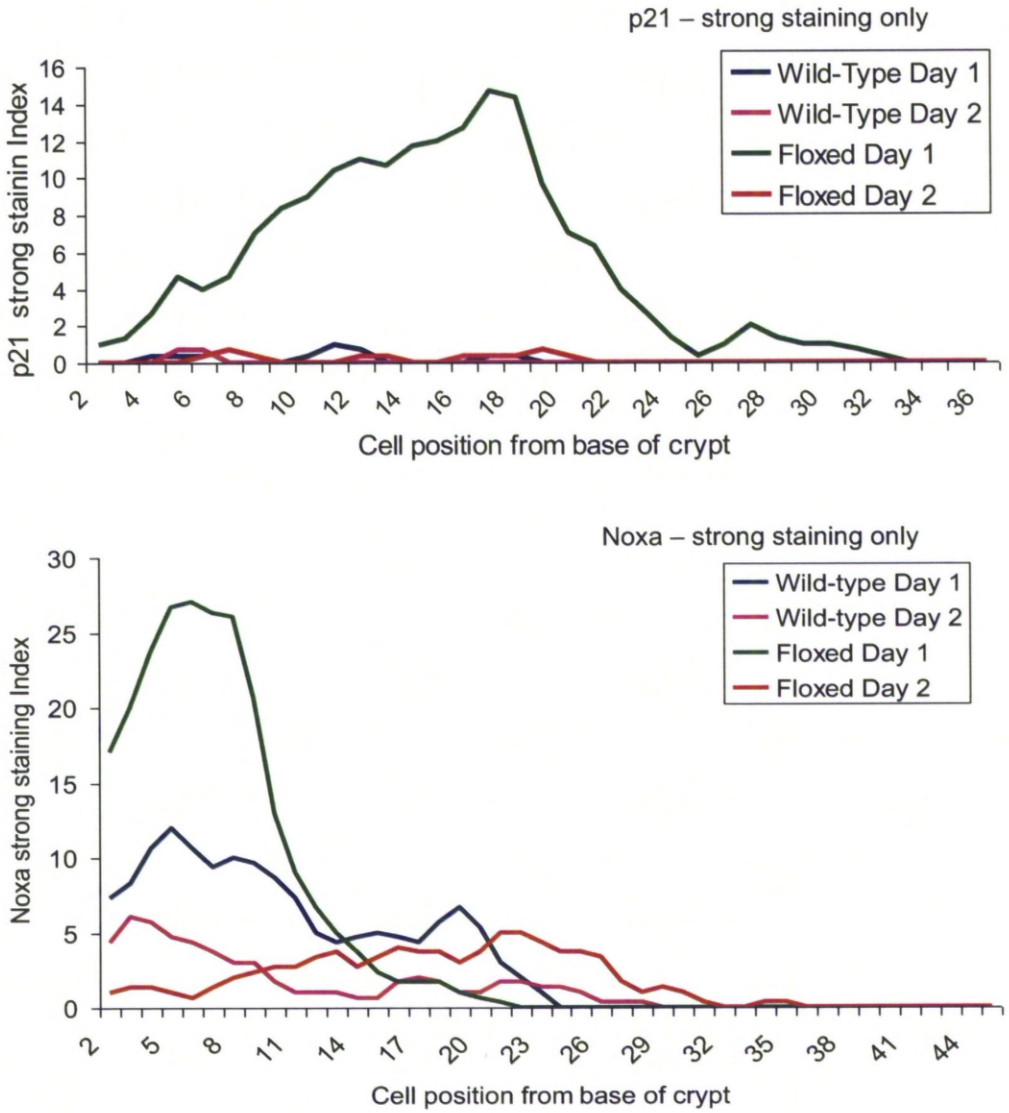


***Figure 3.1.10: Crypts cell scoring data of strong staining only for p21 and Noxa.***

*Examination of strong staining only for p21 (top) and Noxa (bottom) on day 1 and day 2 after administration of 1 x 80 mg/kg BNF by gavage to either conditionally floxed Mdm2 null or wild-type mice. Strong immunoreactivity only occurs in floxed animals 24 hours after Mdm2 loss for p21, eliminating the background when weak-to-moderate and very strong staining were pooled together. Noxa may be reacting to Mdm2 loss as the peak for floxed day 1 appears considerably higher than wild-type day 1 but the back ground is still very high (note the scale on the Y axis).*

### *3.1.2.3 Villus cell counting data*

In order to quantify the unusual cell staining observed on the villi for p53 and p21 proteins, positive cells were counted and compared for the different treatments as described in Section 2.13.6. Whilst p53 or p21 positive cells were rarely observed in wild-type animals (average 0 – 2 positive cells per villi), they were frequently seen in *Mdm2*$^{flox/flox}$ animals (average 8 – 15 positive cells per villi) as shown in Figure 3.1.11. This was only statistically significant for p21 staining on day 1 (p-value = 0.006), because by day two p21 levels returned to wild-type levels. Presumably, the p53 staining was not significant due to the wide variability in cell count data. For example; the total number of p53 positive cells on day 1 in each floxed animal was 117, 278 and 718 compared with the three individual wild-type animals which was 0, 0 & 1 (p-value = 0.094). The observed variability could be a problem with the nature of scoring villi because getting a full cross section of the entire length of any one villi is extremely difficult and therefore quite often only part of a villus was scored. This may inadvertently lead to some bias in scoring, although since p21 staining was consistent and statistically significant it may also be a problem with p53 antibody optimisation. Regardless, whilst p53 immunoreactivity on the villi was not statistically significant there was still an obvious trend which requires further investigation, especially since, despite p53 up-regulation there was still no apoptosis observed on the villi.

Noxa immunoreactivity was also scored on the villi and compared for the different treatments (see Figure 3.1.11). Noxa positive cells appeared across all treatment groups, however there was significantly more staining on day one compared with day two (p-value = 0.001). This villus scoring data concurs with the previous IHC and crypt scoring data, showing that Noxa staining appears higher as a result of administrating BNF rather than because of the knockout of *Mdm2*. Noxa generally appears to be an unreliable reporter of p53 apoptotic activity, since it is often up-regulated without stimulus and its up-regulation does not always lead to apoptosis.

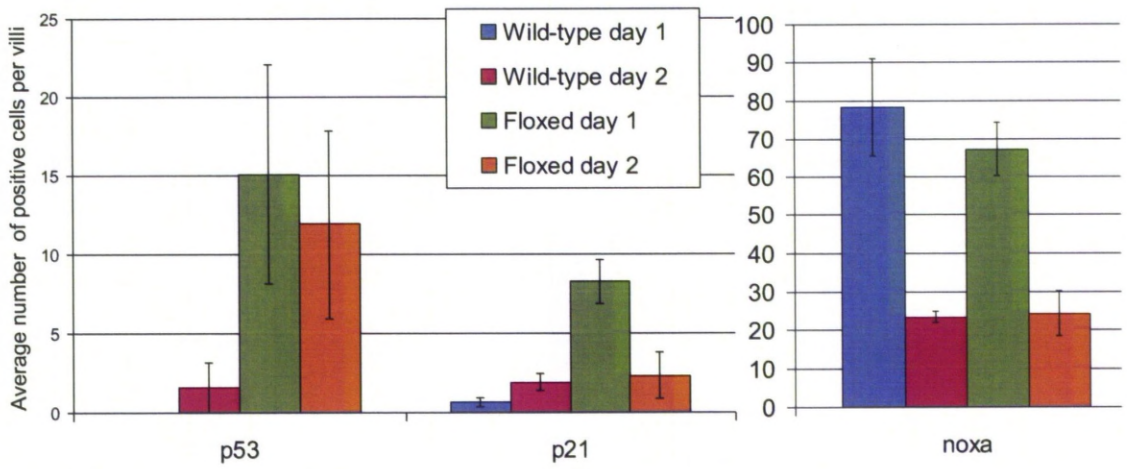


***Figure 3.1.11: Villi cell scoring data in conditionally floxed Mdm2 null mice.***

*Bar chart plots of p53, p21 and Noxa immunoreactivity on the villus on day 1 and day 2 after administration of 1 x 80 mg/kg BNF by gavage to either conditionally floxed Mdm2 null or wild-type mice. p53 and p21 levels both increase following knockout of Mdm2 but start to decrease again by 48 hours. Noxa levels appear unaffected by knockout of Mdm2 but instead appear to be a side effect of treatment by gavage. 25 villi were scored from each animal, 3 animals per group the error bars are the SEM.*

### 3.1.3 γ-irradiation of conditionally floxed *Mdm2* null mice

As demonstrated in the above section, using the conditionally floxed *Mdm2* null system, it was possible to induce p53 expression in cells on the villus. These p53 positive cells were able to up-regulate *p21*; a downstream target gene of p53 involved in the cell cycle arrest response to genotoxic stress, but still appeared unable to undergo apoptosis. The absence of an apoptotic response in villi cells has been well documented (Grossmann et al., 2002, Marshman et al., 2001, Watson and Pritchard, 2000); however previously it could have been argued that this was due merely to lack of p53 up-regulation. Obviously this was not entirely the case, since now even with p53 present on the villi there was still no apoptosis observed. We thought to try and induce apoptosis in these p53 positive cells on the villi by adding an additional stimulus in the form of whole body ionising radiation. Would the additional genotoxic stress signal finally induce apoptosis in cells on villi? We attempted to address this question with the experiment described next.

BNF was administered to 6 Wild-type and 6 *Mdm2*$^{flox/flox}$ mice on day 0. The dosing system was slightly different to the previous experiment, here the mice received 3 x 80 mg/kg of BNF by three IP injections (given at 9am, 12pm and 5pm) and at 12pm mice also received an additional 80 mg/kg of BNF by gavage. This more intense dosing plan was used to ensure maximum induction of the Cre-recombinase gene and hence better knockout of *Mdm2*. In the morning of day 1, 3 Wild-type and 3 *Mdm2*$^{flox/flox}$ mice were each exposed to 14 Gy of whole body ionising radiation. In the afternoon, 6 hours post-irradiation, all the animals were sacrificed and the small intestine was taken for IHC and cell scoring analysis of the crypts and villus which is described next.

### 3.1.3.1 Crypt cell scoring data

Cells in the crypt were scored for apoptosis and immunoreactivity to p53 and p21 for the experiment described above. Apoptosis was characteristically high at the base of the crypt (up to cell position 9) for the 'floxed', 'floxed + 14 Gy' and the 'wild-type + 14 Gy' treatment groups (see Figure 3.1.12). Apoptosis was induced to similar levels between these three treatment groups which demonstrated that knockout of *Mdm2* alone or treatment with whole body γ-irradiation alone was sufficient to induce a full apoptotic response. On the other hand, mitosis was only observed in the unstressed 'wild-type' treatment group as might be expected when p53 is up-regulated (Merritt et al., 1997, Pritchard et al., 1998). In concurrence with this observation, immunoreactivity for p53 was high at the base of the crypt for the 'floxed', 'floxed + 14 Gy' and the 'wild-type + 14 Gy' treatment groups but not in the 'wild-type' control group as shown in Figure 3.1.13. Unlike the apoptotic levels, however, (which remained similar regardless of the stress stimulus) p53 staining was more intense and occurred further up the crypt in the 'floxed' and 'floxed +14 Gy' treatment groups when compared to the 'wild-type + 14 Gy' treatment group. The increased levels of p53 expression in the $Mdm2^{flox/flox}$ mice was most striking when only very strong staining was analysed (see Figure 3.1.13 – bottom panel). The 'wild-type + 14 Gy' treatment group had negligible p53 'strong' staining (comparable to 'wild-type' treatment group) whilst the 'floxed' and 'floxed + 14 Gy' treatment groups had significantly increased p53 'strong' straining (p53 up-regulation was significant up to cell positions 12 and 18 for 'floxed' and 'floxed + 14 Gy' respectitively).

The increased levels and wider range of p53 expression in the $Mdm2^{flox/flox}$ mice, with whole body ionising radiation treatment alone, was not completely unexpected since it is well documented that p53 up-regulation in response to ionising radiation is limited to the proliferative compartment of the crypt (Merritt et al., 1994, Pritchard et al., 1999). The conditional knockout of *Mdm2,* however, relied upon successful activation of Cre-recombinase and hence on delivery of BNF which was therefore not limited to a particular cellular compartment. Thus p53 expression could (and did) occur further up the crypt and indeed even on the villus (discussed in Section 3.1.3.2). The up-regulation of p21 is examined next.

In accordance with our previous observations p21 expression appeared normally distributed with a bell shaped curve in the 'floxed', 'floxed + 14 Gy' and the 'wild-type + 14 Gy' treatment groups (see Figure 3.1.14). The peak of these expression curves was around cell position 9-10 for all three treatment groups. There were no statistically significant differences between these curves, nor did p21 staining appear more intense for any particular treatment. This raised some interesting questions since the observed increase in p53 expression in the floxed animals was not matched with either an increase in apoptosis or p21 expression. Perhaps this was due to the fact that p21 expression was already very high (85% at the peak of the curve) and therefore p21 could not physically be expressed any more then it already was. These results would also indicate that despite p53 not being induced as strongly in the wild-type mice when exposed to irradiation, the p53 present was sufficient to produce all the normal physiological responses – or rather extra p53 does not contribute any additional responses, (at least not in the crypt).

One last observation was the characteristic mini-peak of p21 expression towards the crypt-villus boarder (seen also in Figure 3.1.5 & Figure 3.1.9), observed in the control group (wild-type mice which had been administered with BNF but had not been exposed to γ-irradiation). As discussed previously this p21 mini-peak was in part a result of exit of cells from the proliferative compartment and also of normal differentiation signals (Yang et al., 2001, el-Deiry et al., 1995). The expression of p53 and p21 was also examined on the villi.

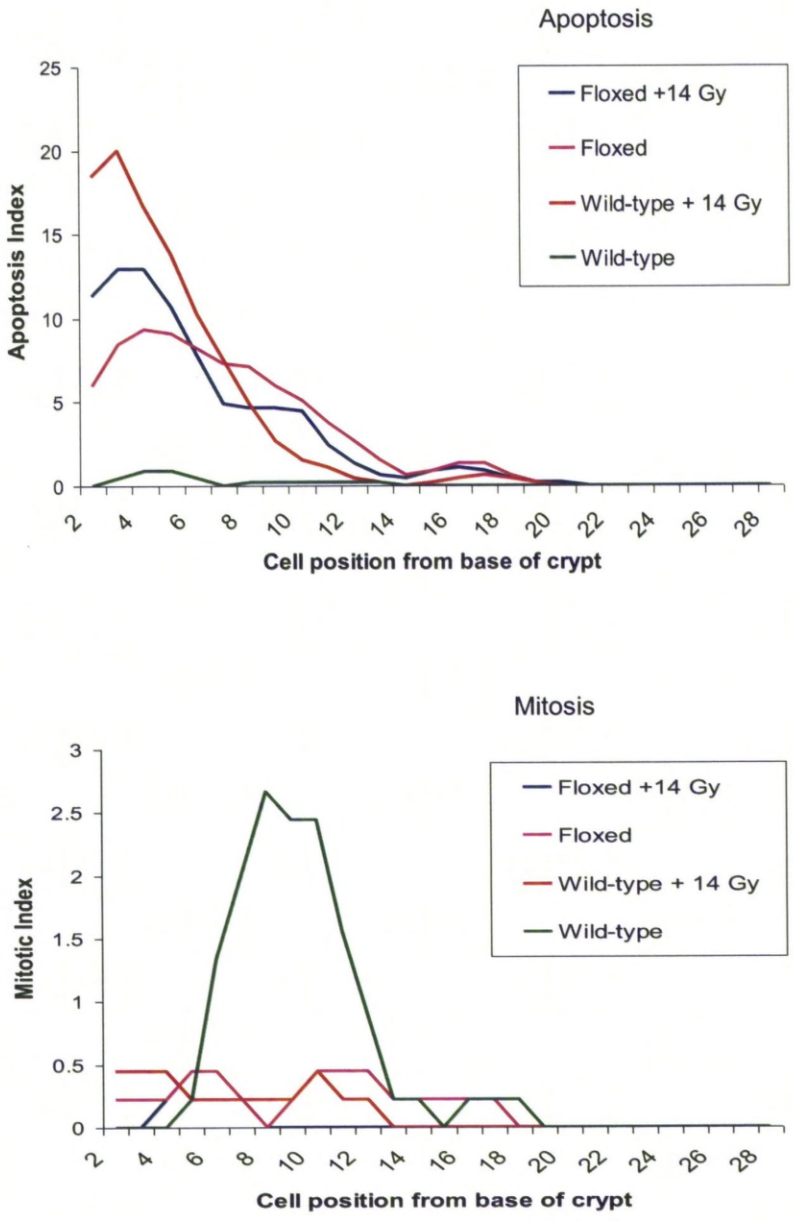


***Figure 3.1.12: Cell scoring data for apoptosis and mitosis.***

*Apoptosis (top) and mitosis (bottom) levels were examined in the small intestine of 24 hours post induction of Cre-recombinase in either conditionally floxed Mdm2 null or wild-type mice ± 14 Gy of ionising irradiation. Apoptosis is characteristically high at the base of the crypt in both groups of conditionally floxed Mdm2 null animals and in the irradiated wild-type control group (significant up to position 9). There were no statistically significant differences between the apoptotic rates in these animals. As expected only wild-type non-irradiated animals had cells undergoing mitosis. Cre-recombinase was induced by administrating 3 x 80 mg/kg of BNF by IP injections plus 1 x 80 mg/kg of BNF by gavage.*

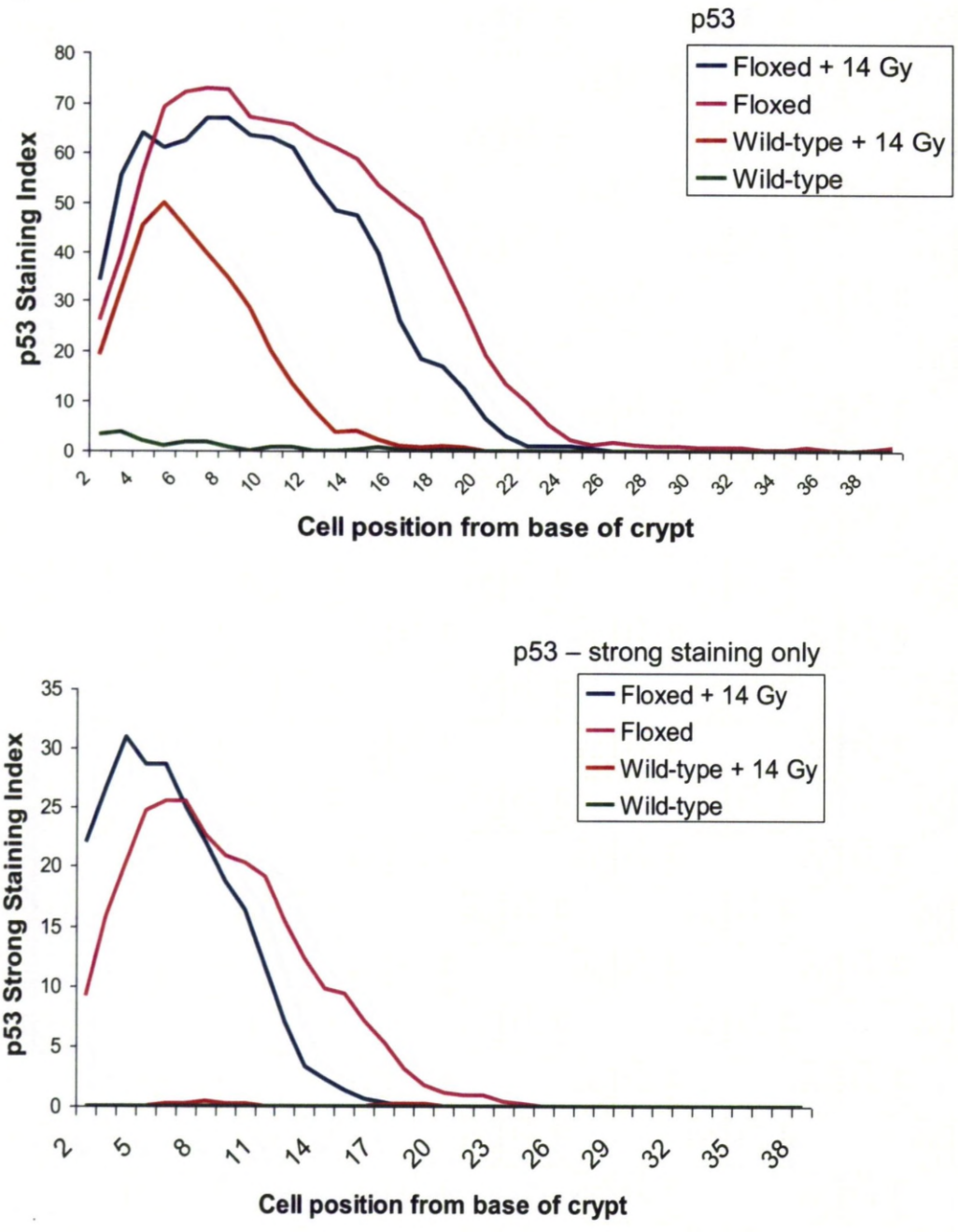


***Figure 3.1.13: Cell scoring data for p53.***

*Comparison between all staining (top) and only very strong staining (bottom) of p53 in the small intestine, 24 hours post induction of Cre-recombinase in either conditionally floxed Mdm2 null or wild-type mice ± 14 Gy of ionising irradiation (sacrificed 6 hours later). Up-regulation of p53 was significant up to cell position 22, 25 & 14 for floxed + 14 Gy, floxed & wild-type + 14 Gy treatment groups respectively – with the strongest and widest responses from the floxed animal groups. Cre-recombinase was induced by administrating 3 x 80 mg/kg of BNF by IP injections plus 1 x 80 mg/kg of BNF by gavage.*

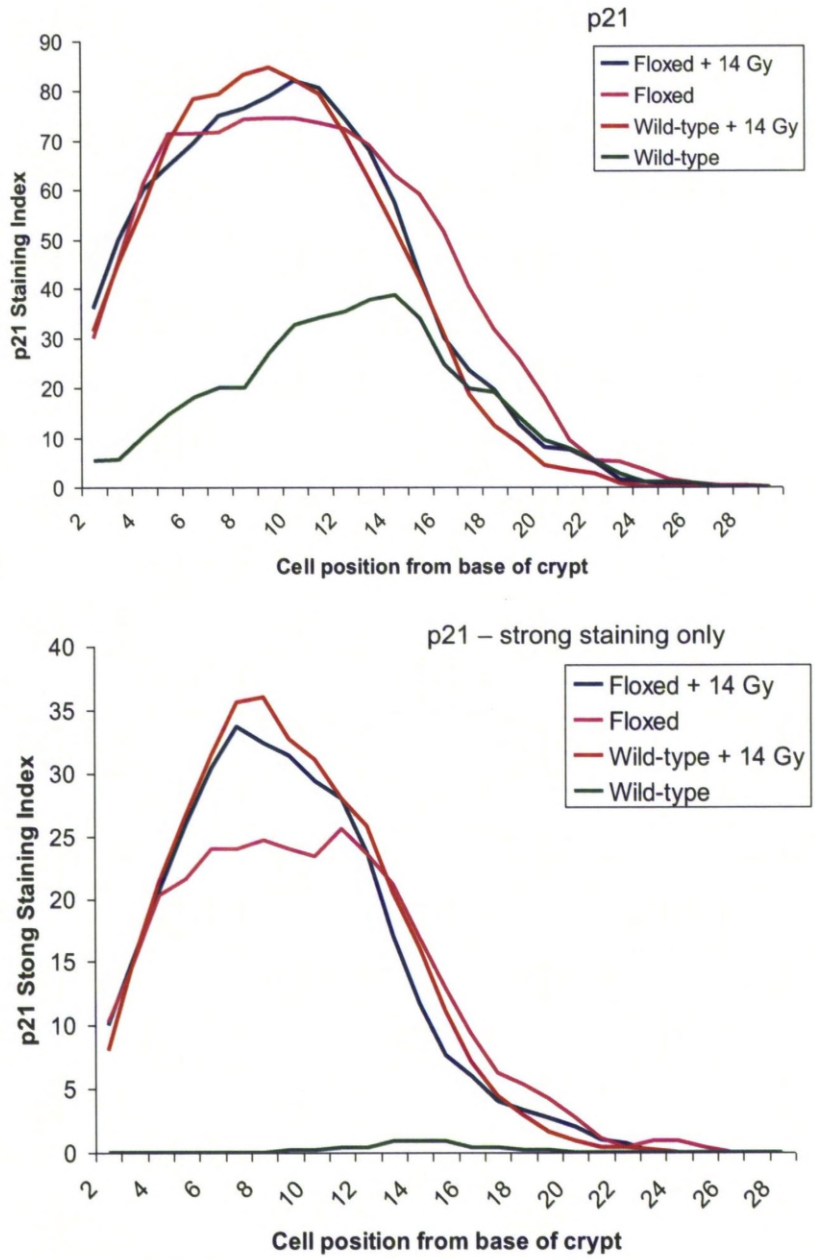


***Figure 3.1.14: Cell scoring data for p21.***

*Comparison between all staining (top) and only very strong staining (bottom) of p21 in the small intestine, 24 hours post induction of Cre-recombinase in either conditionally floxed Mdm2 null or wild-type mice ± 14 Gy of ionising irradiation (sacrificed 6 hours later). Up-regulation of p21 occurred in a bell-shaped distribution which peaked at cell position 9-10 for both the floxed groups and the wild-type + 14 Gy control group. There were no significant differences between these groups. The non-irradiated wild-type group had the characteristic mini-peak at cell position 13 towards the crypt-villus shoulder. Cre-recombinase was induced by administrating 3 x 80 mg/kg of BNF by IP injections plus 1 x 80 mg/kg of BNF by gavage.*

### *3.1.3.2 Villus cell counting data*

To investigate the effect of whole body γ-irradiation, as an additional stress, on p53 and p21 immunoreactivity on the villi, positive cells were counted and compared between wild-type and *Mdm2*$^{flox/flox}$ animals. As observed with our previous experiment, there were relatively few p53 or p21 positive cells observed in wild-type mice (average 0 – 1 positive cell per villi), whilst *Mdm2*$^{flox/flox}$ mice frequently had p53 and p21 positive cells (average 18 – 25 positive cells per villi) (see Figure 3.1.15). These differences were statistically significant for both p53 and p21 (p-values = < 0.001), even though there was considerable variability in cell scoring counts. One animal in particular seemed to contribute to the very wide error bars in the 'Floxed + 14 Gy' treatment group, since the IHC staining pattern observed was clearly uneven across the gut circumference. In this outlier the crypts were stained very strongly, whilst the villi were stained only very faintly. This may have also been a technical problem, perhaps due to the samples drying out during IHC or the section not being completely de-waxed when IHC was commenced. Regardless of these problems, the results still demonstrated that p53 and p21 were up-regulated in this animal.

When the irradiation status was taken into consideration, there did not appear to be any additional up-regulation of p53 or its downstream target p21 on the villi in the *Mdm2*$^{flox/flox}$ mice. In other words, the additional DNA damage did not induce any extra p53 protein. This may not be completely unexpected since p53 protein is not normally up-regulated on the villi in response to genotoxic stress (Merritt et al., 1994, Pritchard et al., 1998, Leibowitz et al., 2011). We were very interested, however, in whether the cells on the villi which were expressing p53 were then more prone to undergoing apoptosis. No convincing apoptosis was observed along the length of the villi, even when the animals were exposed to 14 Gy of γ-irradiation. Apoptosis was defined by the characteristic appearance of cell shrinkage, membrane blebbing and the formation of nuclear bodies (Kerr et al., 1972). During the scoring of villi for this thesis no cells on the villi have ever completely matched this description, although some cells displayed some of the phenotypic features of apoptosis. For example there were occasional cells which were simply missing nuclei, or they had darkly stained circular bodies within their cytoplasm (nucleus was intact) or there were cell sized gaps in the epithelial lining of the villi. The occasional apoptotic cell on the villus tip could be

explained by the normal physiological process of cell shedding. Apoptosis was probably not more commonly observed on the villus tip purely because the likelihood of getting an entire cross section of a single villus, all the way to the 'real' villus tip, was relatively small (Marshman et al., 2001). The occasional apoptotic cell near the crypt-villus join region could perhaps be explained by an awkward cross section of a crypt. Only 5 cells were potentially apoptotic in the middle of a villus for all the animals examined in both wild-type (1 'cell') and floxed mice (4 'cells'). None of these 'apparently apoptotic' cells appeared to entirely fit the profile of an apoptotic cell. Therefore, since none of these cells completely matched our definition of an apoptotic cell and since there were so few of them in both the wild-type and floxed animals, we concluded that there was no apoptosis along the length of the villi – even with the additional stress stimulus.

The immunoreactivity for p53 and p21 on the villi was then compared between the two conditionally floxed *Mdm2* null experiments since a different BNF treatment regime was used for each. As shown in Figure 3.1.16, higher p53 and p21 cell positivity was observed following the more intense BNF dosing protocol. This was statistically significant for p21 between the 'floxed day 1' and 'floxed' treatment groups (p-value = 0.012). Therefore, in order to achieve maximum induction of Cre-recombinase and hence better knockout of *Mdm2* and up-regulation of p53/p21, the higher dose of BNF was chosen for any future experiments.

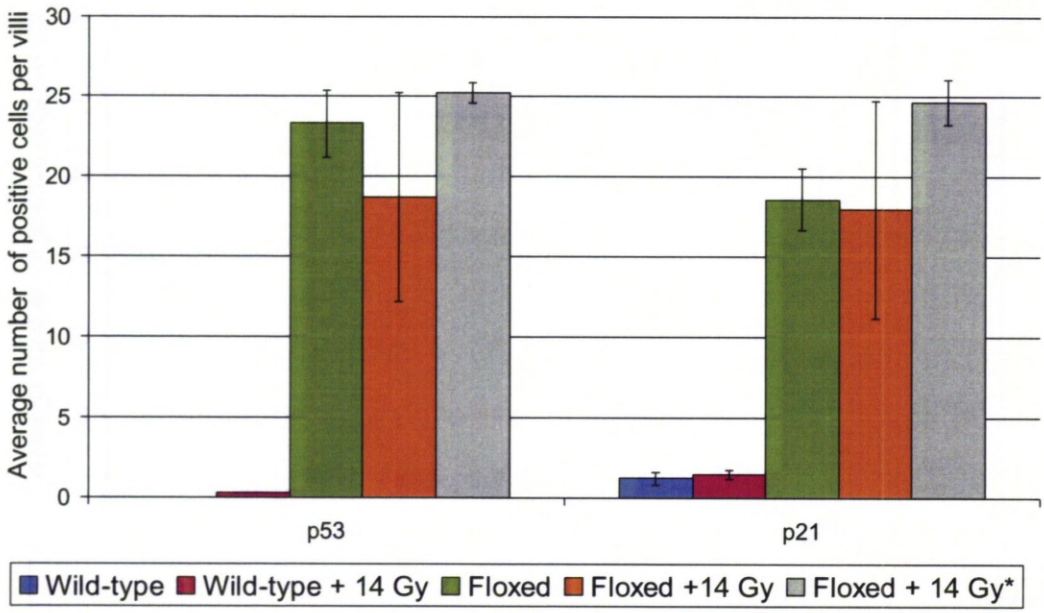


***Figure 3.1.15: Villi cell scoring data for p53 and p21.***

*Bar chart plots of p53 and p21 immunoreactivity on the villus, 24 hours post induction of Cre-recombinase in either conditionally floxed Mdm2 null or wild-type mice ± 14 Gy of ionising irradiation (sacrificed 6 hours later). *One animal in the "Floxed + 14 Gy" group displayed a very strong staining in the crypt region but did not stain very well in the villus region, therefore results with and without this outlier were included for comparison. p53 and p21 protein levels increase following Mdm2 knockout. Additional treatment with 14 Gy ionising radiation does not appear to increase the number of positive cells. Cre-recombinase was induced by administrating 3 x 80 mg/kg of BNF by IP injections plus 1 x 80 mg/kg of BNF by gavage. 25 villi were scored from each animal, 3 animals per group (with the exception noted above) the error bars are the SEM.*

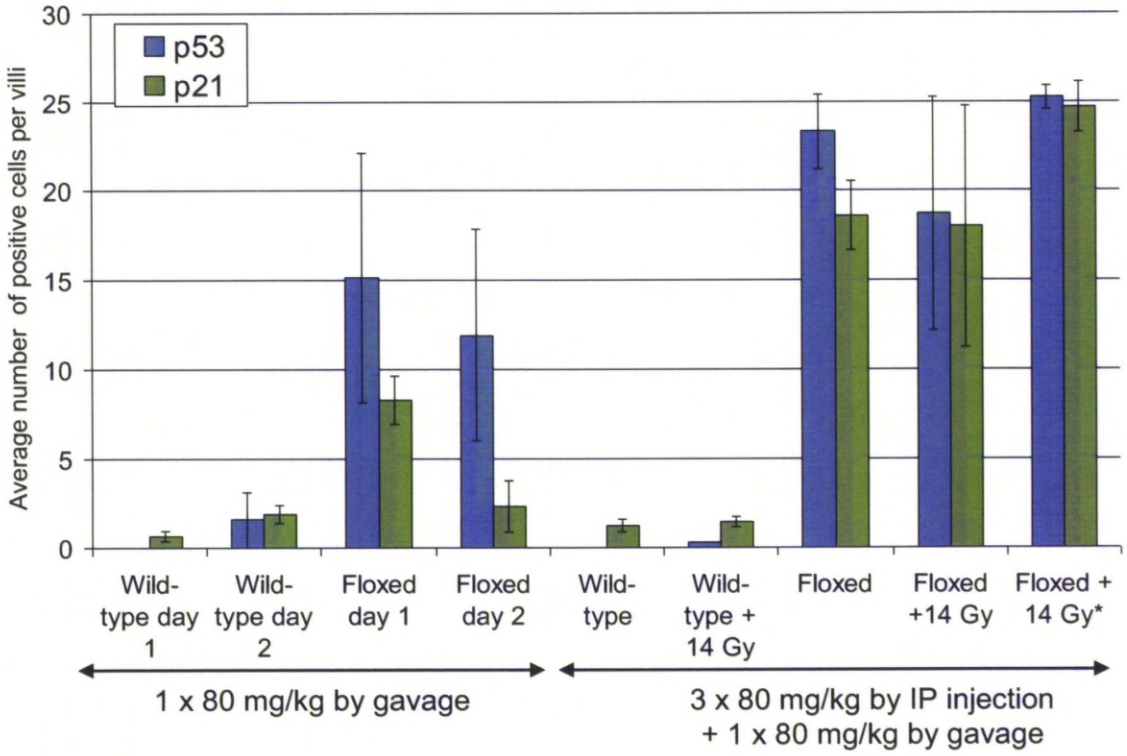


***Figure 3.1.16: Comparison of p53 and p21 positivity on the villi.***

*Wild-type animals (regardless of irradiation status) have relatively low staining for p21 and p53 (1 or 2 positive cells per villi) whilst conditionally floxed mdm2 null animals have relatively high staining for p21 and p53 (up to 25 positive cells per villi). *One animal from the "Floxed + 14 Gy" group was obviously less intensely stained than the others so results with and without this animal were included for comparison. The stronger BNF dosing regime appears to induce higher cell staining positivity. 25 villi were scored from each animal, 3 animals per group (with the exception noted above) the error bars are the SEM.*

### 3.1.4 Quality control of RNA samples extracted from epithelial cells

In order to investigate the differences in p53 up-regulation and activation along the crypt-villus axis in mice, an RNA expression array analysis experiment was designed (see Figure 3.1.17). The RNA was collected for micro-array analysis as follows; on day 0, six wild-type mice and three $Mdm2^{flox/flox}$ mice were each administered with high dose of BNF (see Section 3.1.3.2). In the morning of day 1, three of the wild-type mice were exposed to 14 Gy of γ-irradiation and then in the afternoon, 6 hours post-irradiation all the animals were sacrificed. Epithelial extractions were performed on the small intestine (as described in Section 2.13.4) which provided a "villus enriched" sample and "crypt enriched" sample from which the RNA was extracted (see Section 2.11.3).

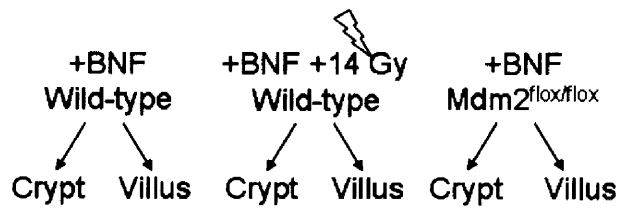


***Figure 3.1.17: Schematic diagram of RNA expression array experiment***

*See text for further details*

Prior to sending this RNA for micro-array analysis, it was necessary to first check the purity and quality of the RNA and to check whether the crypt/villus enrichment process was efficient. In the first instance, the 260/280 ratio of the RNA was examined (results in Table 3.1.1) and a small (200 – 500 ng) aliquot of the RNA was run on an agarose gel (see Figure 3.1.18) to assess the purity and quality of the RNA isolated. From the UV spectrophotometer analysis (shown in Table 3.1.1) the RNA quality and purity appeared good since the OD 260/280 and 260/230 ratios were around 2.0 for the majority of samples. The quality of the RNA samples was then further examined by agarose gel electrophoresis. RNA quality was assessed based on the presence and ratio of the two rRNA subunit fragments, 28S and 18S (which should appear as two sharp bands at a ~ 2:1 ratio in un-degraded RNA – see Section 2.4.2). In the RNA samples examined here there was a shift in the 2:1 ratio towards 1:1 (see Figure 3.1.18) which is indicative of partial degradation. One possible explanation for the

slight RNA degradation observed might be that, due to the tedious nature of the tissue collection protocol, the extracted cells were not placed immediately into TRIZOL reagent (an RNase inhibitor) and hence there was a relatively long delay before RNA degradation was prevented. Part of the delay was because of the epithelial extraction protocol itself (see Section 2.13.4) during which two cellular fractions were collected from whole gut by incubation in buffer with gentle agitation for 15 minutes (30 minutes in total). RNA, however, would begin to degrade from the moment the animal was sacrificed thus RNases would have the opportunity to degrade the samples during cell collection. On top of this, because of space limitations, only two animals could be processed at a time which meant that between the first and last animal 2-3 hours would have elapsed. This unavoidable delay presented a challenge when attempting to preserve the integrity of the RNA and hence these RNA samples can not be expected to appear as perfect as RNA extracted following other protocols, such as RNA extracted from whole gut tissue preserved in RNA*later* reagent for example.

On a more optimistic note the RNA samples were not contaminated with genomic DNA (which would appear as a high molecular weight smear on the agarose gel), nor was there any evidence of complete degradation of the RNA samples present (see Figure 3.1.18). If the RNA samples were completely degraded the two subunit bands would appear as a smear (if present at all) and there would also be an additional low molecular weight smear on the agarose gel. Therefore, the RNA was considered of good enough quality to continue with the validation experiment which is described next.

***Table 3.1.1: RNA samples extracted for micro-array analysis.***

*Sample ID identifies the mouse genotype, flox = Mdm2$^{flox/flox}$ mouse, WT = wild-type, the animal number (1-6) and the extraction fraction V = mostly villus & C = mostly crypt cells. High quality RNA should have an OD 260/280 ratio of 1.8 – 2.0 and an OD 260/230 ratio of 1.8 or greater. Most of the RNA samples in this table meet those standards.*

| Sample ID | ng/µl | 260/280 | 260/230 | Additional information |
|---|---|---|---|---|
| **Flox1_V** | 929.16 | 2.04 | 1.34 | 3 x Mdm2$^{flox/flox}$ mice |
| **Flox1_C** | 1089.54 | 2.03 | 1.84 | Day 0 = administered with |
| **Flox2_V** | 2089.94 | 1.98 | 2.02 | 3 x 80 mg/kg BNF by IP injection |
| **Flox2_C** | 1436.37 | 1.98 | 1.59 | + 1 x 80 mg/kg BNF by gavage |
| **Flox3_V** | 1020.31 | 2.02 | 1.83 | Sacrificed day 1 |
| **Flox3_C** | 2149.62 | 2.01 | 2.03 | |
| **WT1_V** | 1188.85 | 2.03 | 1.87 | 3 x Wild-type mice |
| **WT1_C** | 1818.34 | 2.00 | 1.93 | Day 0 = administered with |
| **WT2_V** | 1370.45 | 2.02 | 2.06 | 3 x 80 mg/kg BNF by IP injection |
| **WT2_C** | 1927.61 | 2.02 | 2.00 | + 1 x 80 mg/kg BNF by gavage |
| **WT3_V** | 1094.12 | 2.04 | 1.96 | Sacrificed day 1 |
| **WT3_C** | 317.17 | 2.00 | 1.77 | |
| **WT4_V** | 1189.52 | 2.03 | 1.9 | 3 x Wild-type mice |
| **WT4_C** | 1499.88 | 2.03 | 2.05 | Day 0 = administered with |
| **WT5_V** | 304.73 | 2.00 | 1.23 | 3 x 80 mg/kg BNF by IP injection |
| **WT5_C** | 843.65 | 2.04 | 1.97 | + 1 x 80 mg/kg BNF by gavage |
| **WT6_V** | 2124.99 | 2.01 | 1.95 | Day 1 = exposed to 14 Gy γ-radiation |
| **WT6_C** | 1702.98 | 2.01 | 1.63 | Sacrificed 6 hours later |

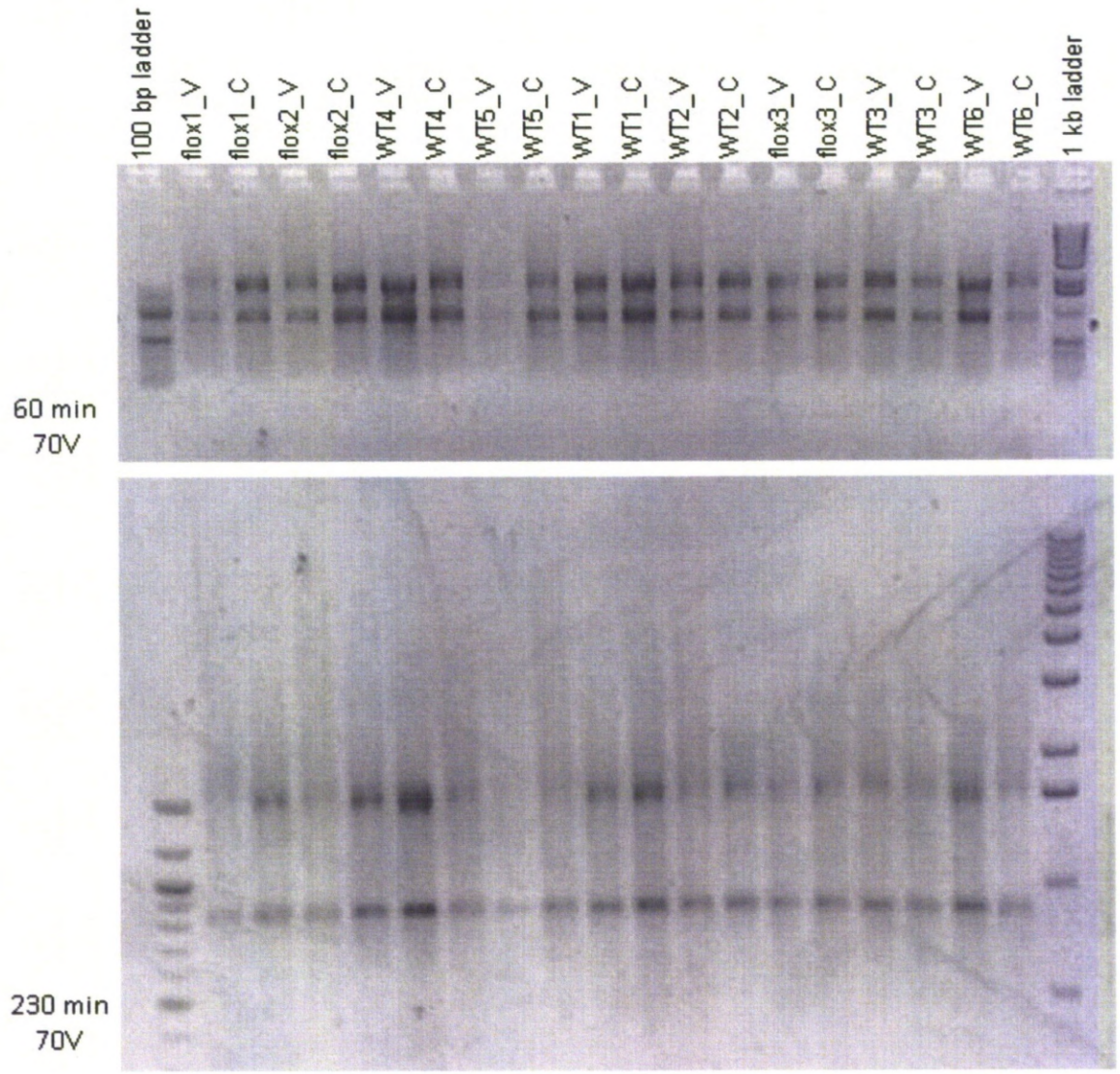


***Figure 3.1.18: Agarose gel electrophoresis of RNA samples extracted for micro-array analysis.***

*RNA samples (200 – 500 ng) were run on a 1% agarose gel initially for 1 hour at 70 V (top) then permitted to run for longer (bottom). The RNA samples in this gel do not appear to be of the highest quality since the two ribosomal subunit fragments do not appear at an ~ 2:1 ratio and the bands appear a little fuzzy. However there is no genomic DNA contamination and it was unreasonable to expect that a very high quality RNA would be isolated due to the nature of the extraction process. Since the two bands are still clearly present in all the RNA samples and there are no low molecular weight smears (which would indicate mass degradation), the RNA quality was assessed as good enough for proposed experiments.*

### 3.1.5 Validation of crypt versus villus enrichment by QRTPCR

QRTPCR was performed on the RNA samples extracted for micro-array analysis to assess how efficient the enrichment for crypt/villus cells had been. To examine this, QRTPCR was performed for a crypt specific gene (*Lgr5*), a villus specific gene (*Max*) and a house-keeping gene to normalise the data (*Hprt1*) – see Appendix C.1. I performed the QRTPCR reactions; however all the analysis of data, including the figures was kindly performed by Dr Bryony Lloyd (Applied Cancer Biology Research Group, The University of Liverpool).

Figure 3.1.19 shows the *Hprt1* normalised transcript expression levels of *Lgr5* (top) or *Max* (bottom) for the 'mostly villus' or 'mostly crypt' cell fractions from each animal. Analysis revealed that the villus specific gene *Max* was indeed enriched within the villi cell fraction (p-value = 0.01) as expected however, surprisingly, stem cell marker gene *Lgr5* was also enriched in the 'villus' cell fraction (p-value = 0.017). Since *Lgr5* had previously been validated as a crypt specific marker by QRTPCR (von Furstenberg et al., 2010) it seemed likely that our enrichment protocol had failed.

In one last attempt to make sense of the contradictory *Lgr5* expression levels, a box and whisker plot analysis was also performed (Figure 3.1.20). We hypothesised that because the 'Flox' and 'WT + 14 Gy' treatment groups would have incurred p53-mediated cell death within the crypt compartment (particularly in the highly proliferative *Lgr5* positive stem cells) that perhaps the *Lgr5* villus:crypt ratio would be higher in these treatment groups (as compared to WT). Whilst there was a slight indication that this may be true for the Flox group this was not statistically significant. In addition, this explanation does not satisfactorily clarify why *Lgr5* was not enriched in the intact crypts of the WT group. In conclusion, since these RNA samples are not sufficiently enriched for crypt or villus specific genes we decided not to examine them further.

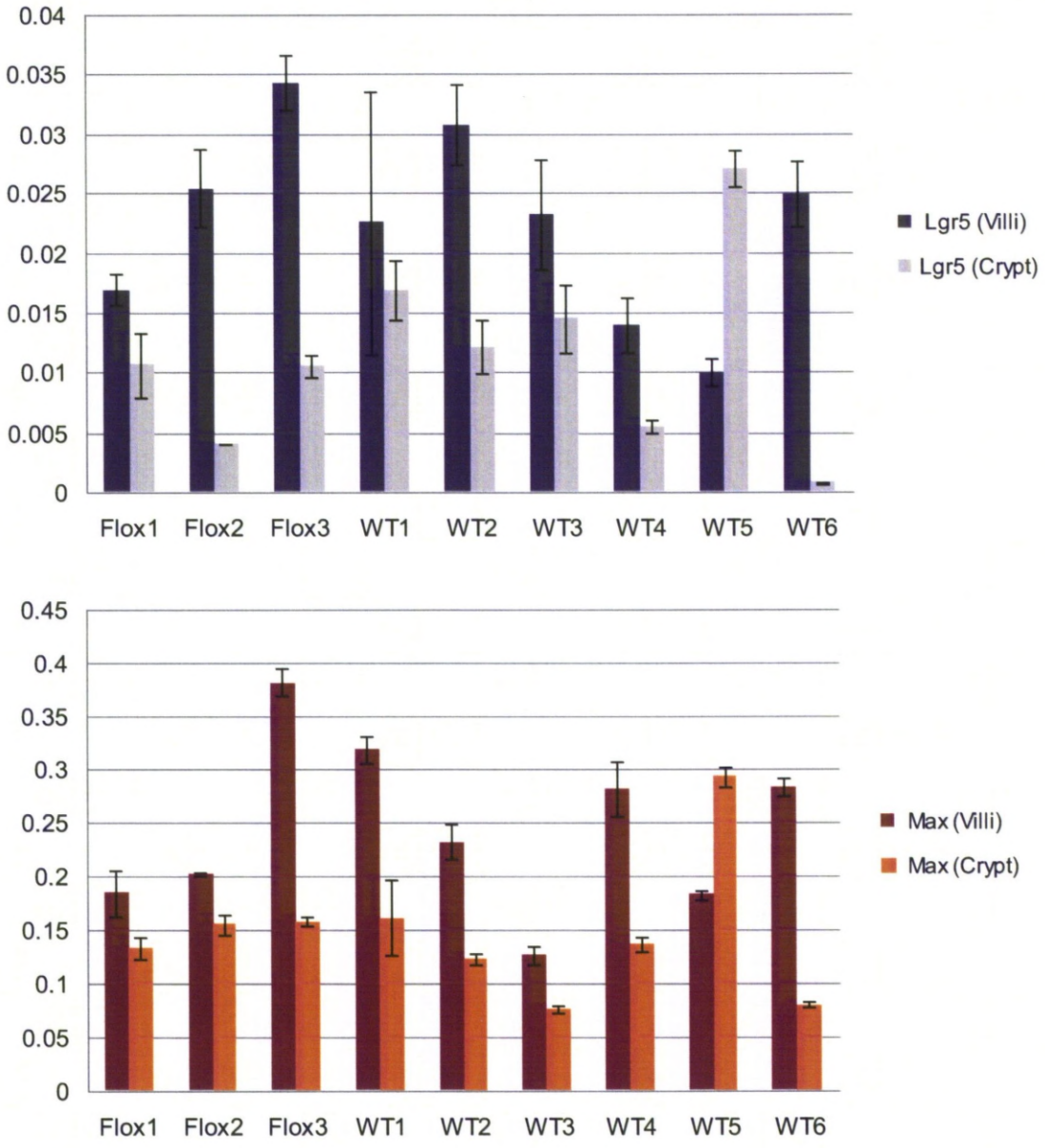


***Figure 3.1.19: Transcript expression for Lgr5 and Max (normalised to Hprt1) in the small intestine.***

*Top panel: Lgr5 (stem cell marker gene) transcript expression on the villi and in the crypt (normalised to Hprt1) in the 9 animals. All samples were collected 24 hours post administration of BNF in Mdm2$^{flox/flox}$ (Flox) or WT mice. WT animals 4-6 also received 14 Gy of γ-irradiation 6 hours pre-harvesting. QRTPCR was performed in triplicate, error bars are the SEM. Bottom panel: As above except for Max (villus specific gene marker). Both Lgr5 and Max appeared enriched in the 'mostly villus' cell fraction (p-values = 0.017 & 0.01 respectively). Performed by Dr Bryony Lloyd.*

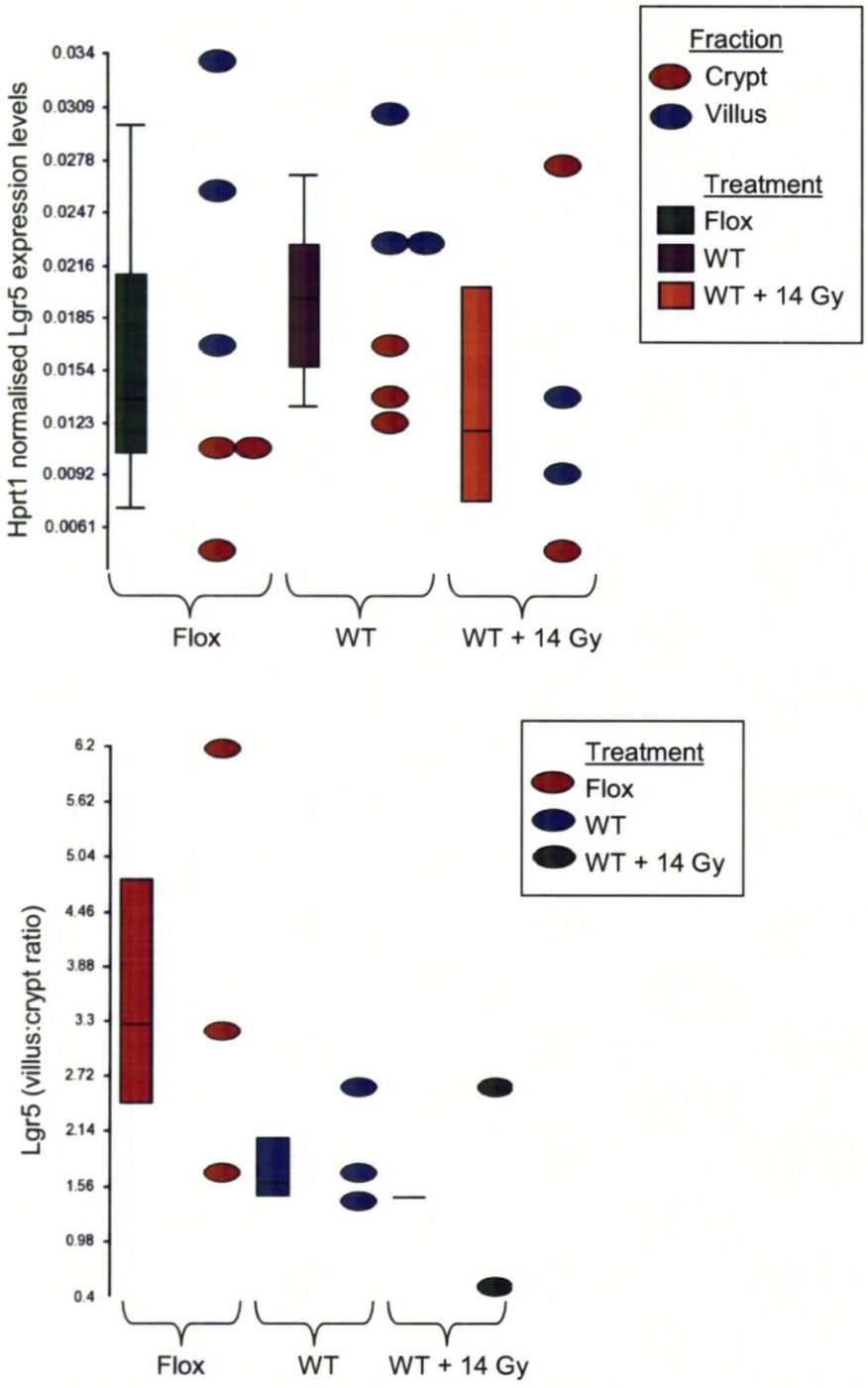


***Figure 3.1.20: Box and whisker plots of Hprt1 normalised Lgr5 expression levels.***

*Top panel: Box and whisker plot of Hprt1 normalised Lgr5 expression levels. Bottom panel: Box and whisker plot of Lgr5 villus:crypt ratio. The coloured ovals are the individual data points. The outlier animal WT5 was omitted from these analysis. The Flox treatment group may have an indication of decreased Lgr5 expression in the crypt as compared to WT, although this is not significant. Performed by Dr Bryony Lloyd.*

# 3.2 Gene-Trapping

## 3.2.1 p21

### *3.2.1.1 Evaluation and selection of gene-trapped ES cell lines*

Three p21 gene-trapped ES cell lines were identified using the search tool (key word *"p21"*) on the IGTC website (http://www.genetrap.org/ and see Table 3.2.1). These cell lines had been screened and localised to *p21* by matching the sequence tag generated by 5'RACE to *p21* exon/s. 5'RACE is a PCR based technique which enables sequencing of unknown 5' termini from specific cDNA clones obtained from mRNA [Schramm et al., 2000, Methods, 2005]. Briefly it was employed as follows: RNA was extracted from the ES cells and reverse-transcribed into cDNA using an anti-sense primer which was specific to the gene-trapping vector (within β-geo). The enzyme terminal transferase was then used to add on a homopolymeric tail onto the 3' end of the cDNA clones (upstream of the unknown 5' DNA sequence). PCR was then performed using a universal primer which annealed within the 3' homopolymeric tail and a second anti-sense primer specific to the gene-trapping vector. The resulting PCR fragments were cloned and sequenced to give rise to the sequence tag. 5'RACE is a useful initial screening method since it simultaneously localises the gene-trapping vector and demonstrates that it is being transcribed – this does not, however, demonstrate that the β-geo transcript is also translated into a functional protein.

***Table 3.2.1: Cell lines targeting p21 available on the IGTC website.***

*Identification status refers to what information is available on each cell line regarding the genomic localisation of the gene-trap vector. Localised data: sequence tag matched to a single genomic locus. Transcript data: full-length mRNA transcript for a single genomic locus.*

| Cell Line ID | Identification Status | Source | Vector |
|---|---|---|---|
| AM0998 | Localised & Transcript | SIGTR | pGT01xr |
| PST004 | Localised & Transcript | BayGenomics | pGT0TMp |
| YTC584 | Localised & Transcript | BayGenomics | pGT0Lxf |

Since all three ES cell lines identified had sequence tags which aligned to exon/s within *p21* (see Figure 3.2.1), there did not appear to be any distinguishing features, at this stage, to select one clone in preference to another. There were difficulties, however, with gathering further information on the two ES cell clones which had been generated as part of the BayGenomics project. Information was difficult to obtain because the BayGenomics Project had closed. AM0998, the cell line generated by SIGTR was therefore selected since information regarding this cell line, including vector sequences and growth maintenance protocols, was readily available.

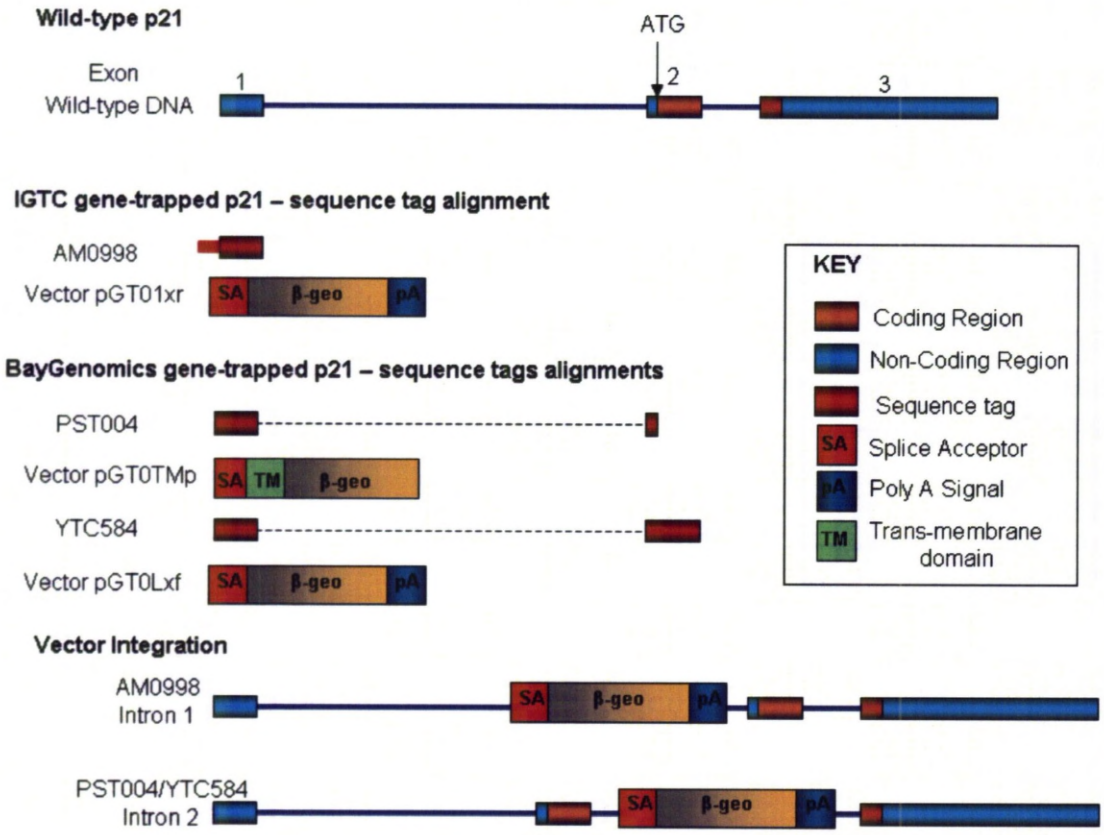


***Figure 3.2.1: Gene-trapped p21.***

*Schematic diagram illustrating the wild-type gene structure of p21 and the gene-trapped locus of p21 following vector integration. p21 has three exons with the ATG start codon located in exon 2. The sequence tag of AM0998, which was generated by 5'RACE aligned with exon 1 – indicating that the β-geo had integrated into intron 1. Cell lines PST004 and YTC584 had sequence tags which aligned with exons 1 & 2 indicating that in those cell lines the gene-trap vectors had integrated within intron 2.*

### 3.2.1.2 *Verification of the identity and functionality of the p21 gene-trapped ES cell line AM0998*

Upon receipt of the AM0998 ES cell line it was important to verify the genotype and test the expression of β-geo. The genotype was confirmed by using a PCR screen and by sequencing the integration sites. The expression of β-geo was confirmed initially by growing the cells under G418 selection (hence neomycin resistant genes must be present) and then by testing for expression of β-gal using an X-gal assay. Expression of β-gal was also tested by western blotting. Testing and confirmation of expression of β-gal in the cell line was important as some 10% of gene-trapped ES cell lines do not show β-galactosidase activity *in vivo* so pre-screening *in vitro* can help identify this potential problem [Voss et al., 1998]. Following successful identification and confirmation of the expression pattern (p21 is inducible following γ-irradiation) it would then be appropriate to proceed to use the clone to create gene-trapped reporter mice. The PCR screen and sequencing results are described first followed by the phenotypic analysis of AM0998 cells.

#### 3.2.1.2.1 PCR screen & sequencing

The sequence tag generated by 5'RACE in the ES cell line AM0998 indicated that the targeting vector pGT01xr had integrated into *p21* within the first 4.5 kb intron (see Figure 3.2.1). A PCR screen was used to help localise pGT01xr within the 4.5 kb intronic region as follows; *p21* specific PCR primers were designed approximately every 1 kb along the length of the *p21* intron 1, in both the forward and reverse directions. These *p21* specific primers were then paired with vector specific primers (1stPCR and 2ndPCR designed by the SIGTR centre) in order to pinpoint the vector's integration site. PCR was performed on genomic DNA isolated from AM0998 ES cells and on wild-type genomic DNA, which acted as a control to identify non-specific products. Several screening PCR reactions were performed (see Appendix B) until the presence of an AM0998 specific PCR fragment was identified (see Figure 3.2.2).

The vector integration site was localised to the fourth kilobase of intron 1 when PCR reaction D (from Figure 3.2.2), which used the primer pair 2ndPCR & p21In1+4kbR, produced

a PCR fragment of ~ 200 bp. Additional primers were designed within *p21* intron 1 and pGT01xr to confirm the 5' integration site (see Figure 3.2.3). PCR was performed and the AM0998 specific DNA fragments were sent for sequencing.

Sequencing results revealed that the vector pGT01xr had inserted at a position 4186 bp into *p21* intron 1. There were some minor rearrangements within the integration sites which are described next (and see Table 3.2.2). Within the vector there were small 13 & 11 bp deletions at the 5' and 3' ends respectively. In addition to the small deletions in the vector there was also a small deletion of the *p21* intron (10 bp – CCACGCCCGG) at the 3' insertion site. At the 5' integration site there were 4 bp of random DNA (TTTA) inserted between the upstream *p21* intronic DNA sequence and downstream vector sequence. There was also a duplication of 15 bp of *p21* intronic DNA at both the 5' and 3' integration sites. No major deletions or rearrangements were detected therefore the AM0998 ES cell line appeared to be as expected from its sequence tag. Next the AM0998 ES cell line was examined phenotypically by β-galatosidase assay and western blotting to determine the expression of β-geo.

***Table 3.2.2: DNA sequence of the integration sites of gene-trapping vector pGT01xr into intron 1 of gene p21.***

| **KEY:** BLUE TEXT = *p21* genomic DNA, GREEN TEXT = random inserted DNA, PURPLE TEXT = pGT01xr DNA, * = site where genomic DNA was deleted (CCACGCCCGG) | |
|---|---|
| 5' integration site | AGTGCTGGGATTAAAGGCGTGTGCCTTTAatgggaagag |
| 3' integration site | tgtaaaacgaTTAAAGGCGTGTGCCAC*TGTCCAGGGT |

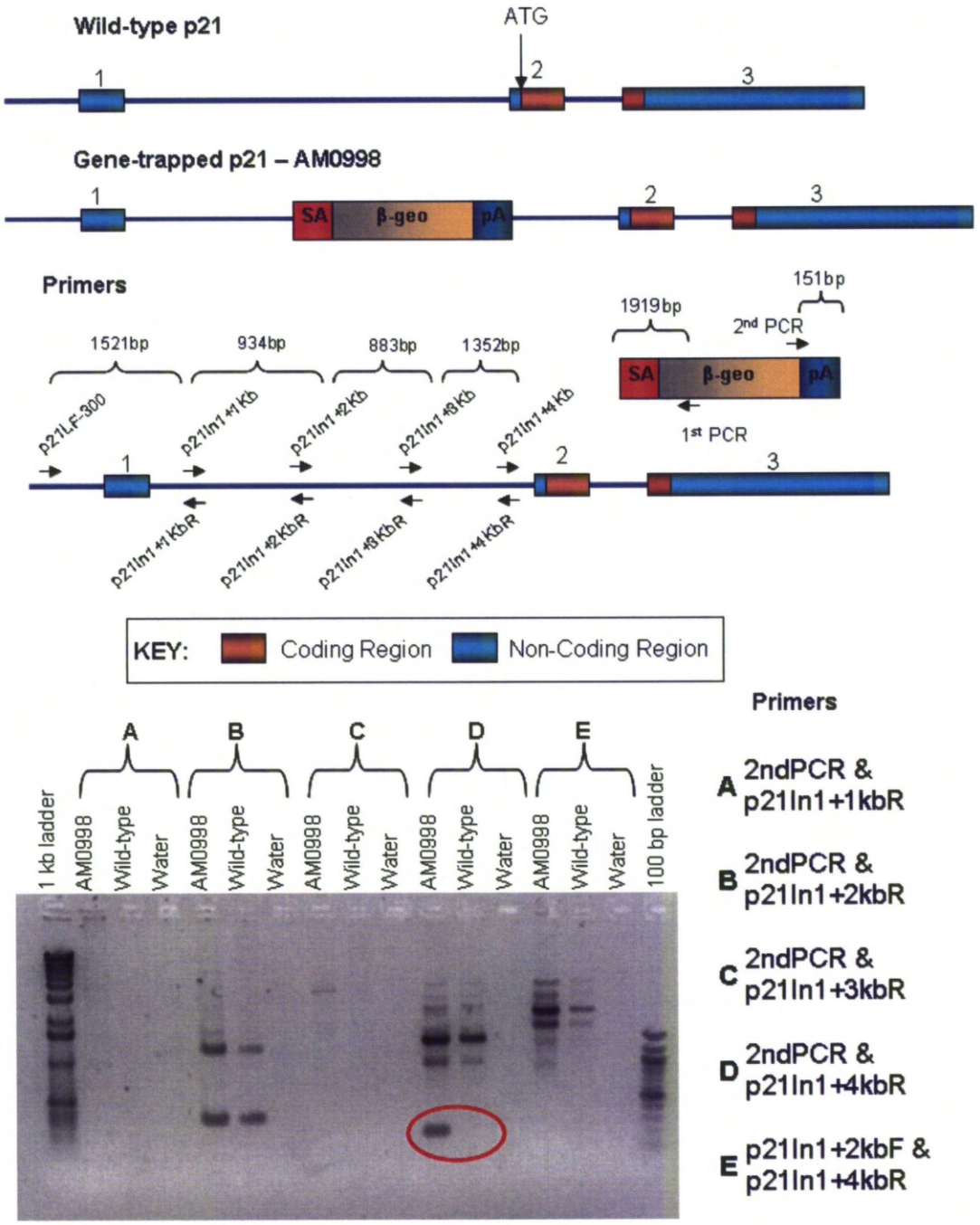


***Figure 3.2.2*: Confirmation of the identity of the p21 gene-trapped ES cell line AM0998 by PCR.**

*The top panel shows a schematic diagram of the wild-type p21 locus versus its gene-trapped counterpart. The PCR primers and their locations within p21/vector are shown next, followed by a photograph of an agarose gel displaying the results of PCR analyses. PCR reaction D using primers 2ndPCR & p21In1+4kbR produced an AM0998 specific DNA fragment of ~ 200 bp – localising the gene-targeting vector to the fourth kilobase of p21 intron 1.*

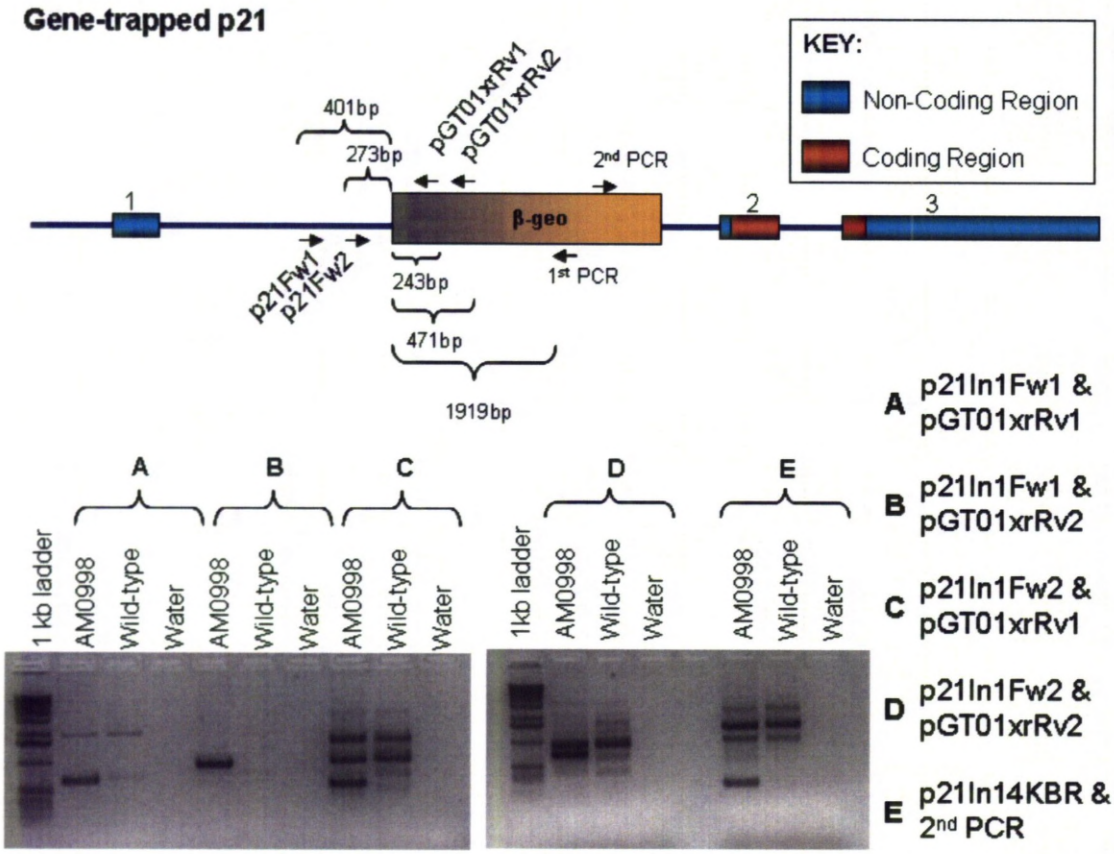


***Figure 3.2.3*: Sequencing of gene-trapped p21.**

*The top panel shows a schematic diagram of the primers designed to identify the 5' integration site. PCR was performed and the reactions were run on an agarose gel (bottom panel). AM0998 specific DNA fragments were excised from the agarose gel and sent for sequencing.*

3.2.1.2.2 β-galatosidase & western blotting

The second important task, prior to using the ES cell line AM0998 to generate a transgenic mouse was to test expression of the reporter construct – β-geo. Initially this was confirmed by growing the cell line in the presence of G418 (150 μg/ml) since only cells which had a functional neomycin resistant gene should survive. Next the expression pattern of β-geo was examined using a β-galatosidase assay. One aliquot of the AM0998 ES cell line was grown on gelatin only plates (without a MEF feeder layer) for several passages to allow the ES cells to differentiate. ES cells were allowed to differentiate for several reasons. First, there was no obvious benefit in maintaining the ES cells used for screening purposes in an undifferentiated state since these cells were only to be harvested for DNA/protein or fixed and stained, therefore growing those ES cells on MEF feeder layers would only waste the feeder layers. Another consideration was that the presence of feeder layers could make results difficult to interpret since they would contaminate the ES cell population and finally there was some ambiguity over whether undifferentiated ES cells express/respond to p53 induction [Aladjem et al., 1998]. The following experiments were therefore performed on differentiated ES cells. Differentiated ES cells were identifiable from undifferentiated cells by characteristic changes in morphology, such as loss of smooth cellular edges and better adherence to the culture vessel surface (see Figure 3.2.4).

Differentiated AM0998 ES cells (and a differentiated 'wild-type' ES cell line B6-C2 – described later in this section) were exposed to several doses of γ-irradiation (6, 20 & 60 Gy) to induce p53 activation and were then fixed and stained using the X-gal assay at several time points (8, 24, 36 & 48 hours). A wide range of irradiation doses and time points were used in order ensure induction of p53 and sufficient time for production of β-geo. Disappointingly however, none of these conditions appeared to produce any positive cells. The lack of positive cells was not a fundamental problem with the reagents or staining protocol since positive cells could be identified with a *LacZ* transfected control plate. The expression of β-geo was then investigated further using western blotting.

Western blotting was performed on four cell lines AM0998, B6-C2, wild-type MEFs and p53 null MEFs. B6-C2 is an ES cell line selected from the laboratory cryostore of archived ES cell clones which had been previously cultured and expanded (in 2002) as part of

other experiments, but which does not contain a p21 targeting event and thus can be used as a wild-type control for this screening experiment. Wild-type MEFs were included to act as a positive control for p53 induction and antibody reactivity, whilst p53 null MEFs were used to identify non-specific p53 antibody binding.

The cell lines either received 6 Gy of ionising radiation or were mock treated. Cells were harvested at 24 and 48 hours post-irradiation (to allow enough time for β-gal expression). Western blotting was performed to check for expression of p53, p21, β-actin and β-gal. It was hoped that this screen would determine whether or not p53 was induced in the ES cells, and whether activated p53 was up-regulating p21. If p21 was up-regulated then the obvious test would be to see whether or not β-geo could also be detected in the AM0998 ES cell line. Unfortunately this screen did not resolve any of the outstanding issues since the controls did not respond as expected (p53 null MEFs, which had previously been confirmed genetically to contain the p53 targeting event appeared to have a band at c. 53kD – data not shown). However, rather than investing more time and effort on these experiments to work we instead re-investigated how the ES cell line AM0998 was generated – specifically we wanted to determine whether it might be possible for the gene-trapped cells to have a functional neomycin gene and yet fail to express β-gal.

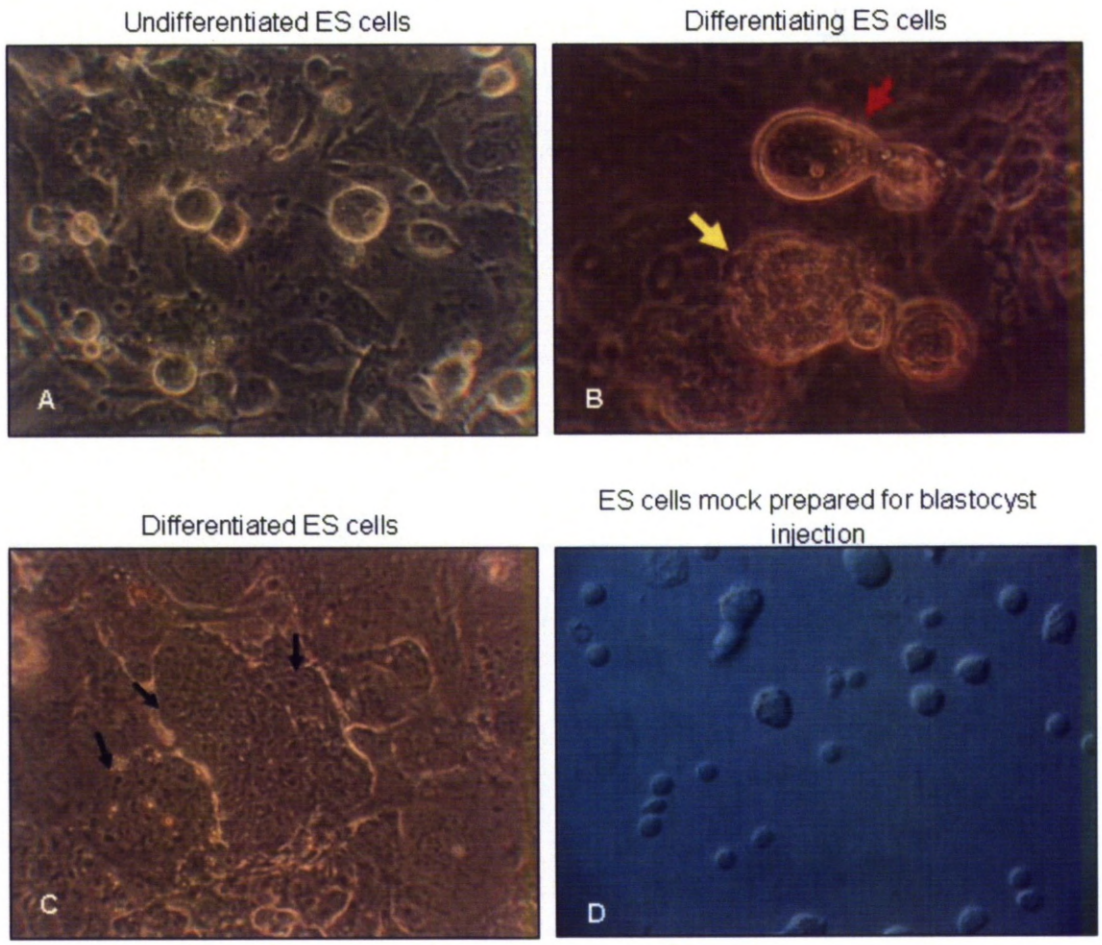


***Figure 3.2.4: Photomicrographs of embryonic stem cells growing in culture and when prepared for a mock blastocyst injection.***

*(A-C) Shows ES cells growing in culture, photos were taken using the x40 objective on a phase contrast microscope, however B has had the magnification increased 33% compared to A&C. The different colours are a reflection of the colour of the media. A) Undifferentiated ES cells are circular with a shiny nimbus around them and smooth edges. B) As ES cells begin to differentiate they lose their shape and the edges become scalloped (see top cell just beginning to differentiate (red arrow) vs the bottom cell that has very bubbly edges and is therefore more differentiated (yellow arrow)). C) Once completely differentiated the ES cell colonies spread outwards and small individual nuclei become visible (dark spots in the large colony as indicated by black arrows). D) Shows ES cells which were prepared for a mock blastocyst injection. ES cells were trypsinised and then the trypsin was inactivated in 10x the amount of media, the ES cells were then photographed. ES cells are small and round whereas feeder layers (MEFs) are large and amorphous. ES cells shown here appear to be of the quality required for blastocyst injection.*

3.2.1.2.3 The p21 gene-trap vector is integrated upstream of the endogenous ATG

When multiple attempts to detect expression of β-geo *in vitro* appeared negative we investigated why this might be. The initial screening method, 5'RACE, generated a sequence tag from the mRNA, hence β-geo was being actively transcribed in the AM0998 p21 gene-trapped ES cells. Also, AM0998 cells were resistant to G418 drug selection providing evidence that this transcript was being successfully translated into protein. However, despite this we could still not detect β-gal activity *in vitro*. What was happening then to the β-gal portion of β-geo? To answer this question we examined the layout of the gene-trapping vector pGT01xr, specifically how were β-gal and neomycin fused together and could this explain why AM0998 cells were resistant to G418 but did not display any detectable levels of β-gal activity?

We discovered that β-gal and neomycin were fused together in that order and that essentially there was no upstream ATG to commence translation for the entire length of the β-geo cassette. Within the β-geo cassette there were several in-frame ATG sites which could potentially initiate the translation for the latter half of this fused transcript (hence cells were still resistant to G418). We had already sequenced the 5' integration site therefore we knew that an ATG had not been introduced by chance. The first in-frame ATG site excluded the first 84 amino acids of the β-gal protein and it would appear that if that ATG site was used those first 84 amino acids were essential to β-gal activity. In conclusion the p21 gene-trapped ES cell line AM0998 could not be used for our purpose of generating a transgenic reporter mouse since it did not express any detectable levels of β-gal and, since this was not the endogenous ATG site it was unlikely to provide an authentic report of p21 activation.

At this point, the direction of this project changed from creating gene-trapped mice to generating our own DNA targeting constructs and targeting our own ES cells. The plan for the DNA targeting constructs was to return to the original concept – a dual fluorescent reporter system for p53 activation. However, for completeness an evaluation of the *Puma* gene-trapped ES cell lines is included in the next section.

### 3.2.2 Puma – evaluation of gene-trapped ES cell lines

There were eight ES cell lines localised to *Puma* (Bbc3) available to view on the IGTC website see Table 3.2.3 search performed on the IGTC website using the key word *"Bbc3"* http://www.genetrap.org/)). However upon further investigation none of these ES cell lines were suitable for the generation of transgenic mice, for reasons discussed briefly below. The TIGM (Texas Institute for Genomic Medicine) ES cell lines did not contain a vector in the correct orientation and the ESDB (ES Cells- Mammalian Functional Genomics Centre) cell lines used the vector U3NeoSV1 which did not contain a reporter construct [Hicks et al., 1997].

A further two ES cell lines were identified on the MGI (Mouse Genome Informatics) website from Lexicon Genetics OST197510 & OST364098 (see Figure 3.2.5). These cell lines contained a gene-trapping vector with β-geo and a second cassette which was used to generate sequence tags by 3'RACE. 3'RACE is essentially the same as 5'RACE (see Section 3.2.1.1) except it identifies unknown flanking DNA sequences at the 3' termini. This means that 3'RACE can take advantage of the poly A tail present on all mRNAs to anchor its universal primer for PCR - rather than synthetically adding a homopolymeric tail as used in 5'RACE. The sequence tags were analysed by BLAST to confirm the location of the gene-trapping vector within the *Puma* locus (intron 2 and intron 3 respectively – downstream of the internal ATG site – and see Table 3.2.4). These ES cell lines were deemed suitable to use in the generation of transgenic mice, however, at a cost of $9500 (US dollars) per project we decided to design and create our own targeting DNA construct.

***Table 3.2.3*: Cell lines localised to the Puma locus available to view on the IGTC website.**

*Identification status refers to what information is available on each cell line regarding the genomic localisation of the gene-trap vector. Localised data: sequence tag matched to a single genomic locus.*

| Cell Line ID | Identification Status | Source | Vector |
|---|---|---|---|
| IST11193F7HMF1 | Localised only | TIGM | Not specified |
| IST11317F12HMF1 | Localised only | TIGM | Not specified |
| PST1671-1 | Localised only | ESDB | U3NeoSV1 |
| PST418-1 | Localised only | ESDB | U3NeoSV1 |
| PST418-3 | Localised only | ESDB | U3NeoSV1 |
| PST50-3 | Localised only | ESDB | U3NeoSV1 |
| PST908-3 | Localised only | ESDB | U3NeoSV1 |
| PST953-2 | Localised only | ESDB | U3NeoSV1 |

***Table 3.2.4: The sequence tags of the two Lexicon PUMA gene-trapped ES cell lines.***

*Red highlight indicates a mismatch, an asterisk * shows a missing base, while bright green and grey highlighting illustrate exon 3 and 4 respectively.*

| Clone | Sequence Tag |
|---|---|
| OST197510 | Gacgtctggggagctcctgcattaagtcagactgaggtcctcagccctccctgtcaccagcccagcagca<br>cttatagtcgcccgtgcccagcgccccggaggccctggcaggaggccccacccaagctgccccgggagtg<br>ctgtgtggaggaggaggagtgggcccagggagatcngnngcccagctgnggaggatggcnggacaanctn<br>aacgcgcagtacgagccggcggaaacaanaagagcagcatctacaccgaccctcaccctggagggncatg<br>tacantctcttcatgggactcctcccctttacccnnggatcctggagccccanaaatggagcccaactant<br>gtgcctacacccgcccgggggacgtnggagacttnggggggcaggacccccctncgtcttctgacancctgg<br>ccagcgcgggggga |
| OST364098 | ccct*accctggagggt*atgtacaatctcttcatgggactcctcccccttacccagggatcctggagccc<br>cagaaatggagcccaactaggtgcctacacccgcccgggggacgtcggagacttgggggggcaggacccccc<br>tccgccttctgacaccctggccagcgcgggggacttttttctgcaccatgtagcatactnggactgccagc<br>cttgcccgtcccaggggcaggcaagggatgccactcgagcccgggcagnctgggtgcactgatggagata<br>cggacttgggggggaccctggcctcccgaaagccagggaagggagggctgatgaaaaaaaaaa |

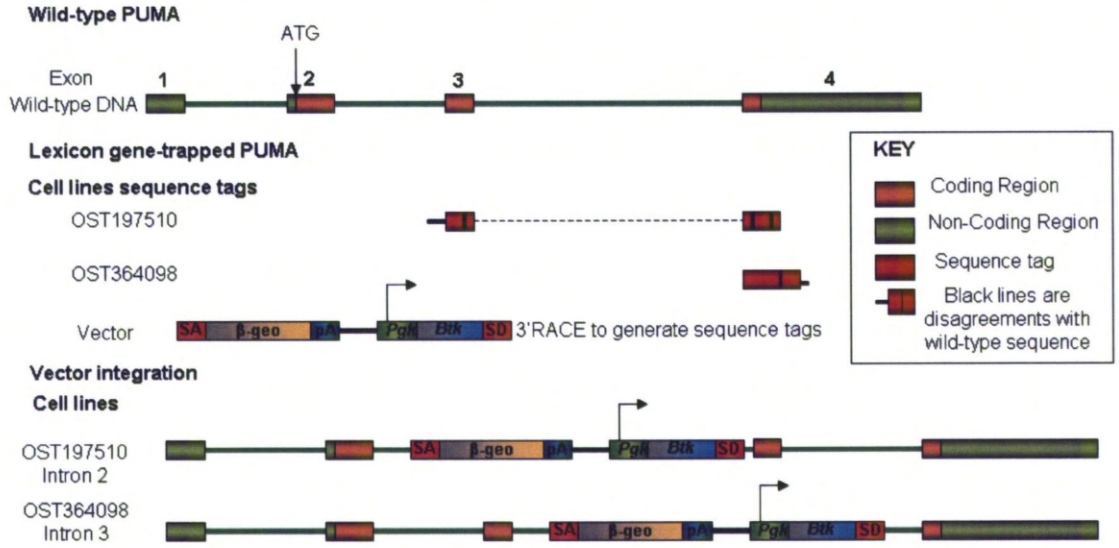


***Figure 3.2.5: Gene-trapped Puma.***

*Schematic diagram of the wild-type gene structure of Puma and the gene-trapped structure of Puma in the ES cell lines OST197510 and OST364098. Puma has four exons and the coding region starts in exon 2. The gene-trapping vector contains a β-geo fusion gene with upstream splice acceptor (SA) and downstream poly-A signal (pA) for simultaneous selection and report of targeted genes. The gene-trapping vector also contains a second cassette which has a ubiquitous murine ES cell promoter (such as Pgk – phosphoglycerate kinase) which expresses the first exon of Btk (Bruton agammaglobulinemia tyrosine kinase) followed by a splice donor site (SD). The second cassette is used to generate sequence tags by 3'RACE. Clone OST197510 is inserted into intron 2 whilst OST364098 is inserted into intron 3. There are areas of discrepancies between the sequence tags and the genome which were examined further in Table 3.2.4.*

## 3.3 Generation of DNA targeting constructs

### 3.3.1 Brief overview

This project aimed to generate four different transgenic mouse strains by homologous recombination – also known as gene targeting. These strains were;

- *p21*-mCherry knock-in reporter
- *Puma*-E2Crimson knock-in reporter
- *Mdm2* P2-mutant
- *Mdm2* P1-null

The first stage of gene targeting was to design and create a DNA targeting construct for each desired transgenic mouse strain. Each DNA targeting construct was to contain a negative selectable marker, a positive selectable marker, a left and right arm of homology and the desired mutation (see Figure 3.3.1). Positive and negative selection was used to enrich for cells containing the desired recombination event [Mansour et al, 1988] and see Section 2.9.2.2.4. The arms of homology were to be 4 – 5 kb in length and were made using isogenic DNA to improve homologous recombination frequencies [te Riele et al, 1992] and see Section 1.5.2. The desired mutations were unique to each targeting construct and included variously knock-in of fluorescent proteins or more subtle specific point mutations. Completed DNA targeting constructs were then used to target undifferentiated embryonic stem (ES) cells (see Figure 3.3.2).

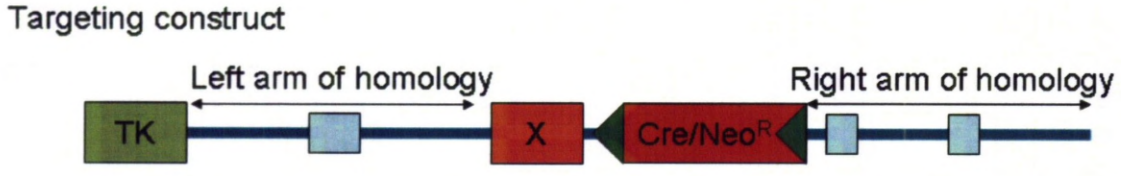


***Figure 3.3.1: General plan of a DNA targeting construct.***

*The targeting construct contains a negative selectable marker (thymidine kinase – TK), a left and right arm of homology (4 – 5 kb of wild-type genomic DNA) either side of the desired mutation (shown here in an orange box with an X) and positive selectable marker (self excision neomycin cassette (shown in red with green arrows)).*

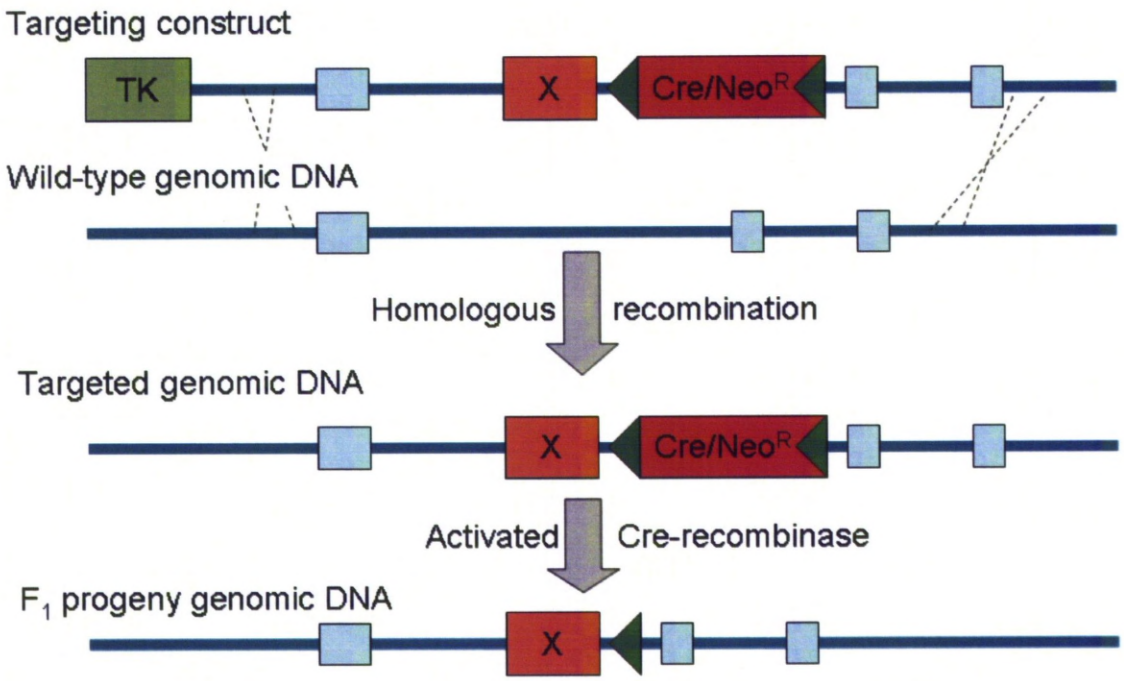


***Figure 3.3.2: Schematic diagram of gene targeting events.***

*Following a successful homologous recombination event the desired mutation X (orange box) had become incorporated into the genomic DNA of targeted ES cells. The self-excision neomycin cassette (shown in red box with green arrows) is then removed by activated Cre-recombinase in the first generation ($F_1$) of the heterozygous mice. Cre-recombinase is up-regulated from within the self excision neo cassette by a testis specific promoter (tACE) and thus becomes active in the testis of the chimeras. Recombination promoted by the Cre-recombinase results in removal of DNA located between the two LoxP sites (green arrows) – leaving behind only a single copy of the LoxP site (34 bp of foreign DNA). It is important to remove the positive selectable marker to avoid confounding the results that might arise as a consequence of a large independent expression cassette being inserted into the gene.*

One of the major obstacles in the process of generation of transgenic mice is often the creation of the complex DNA targeting constructs. One major reason for this in the present project was that DNA targeting vectors contained large pieces of genomic DNA which were often repetitive and/or filled with complex secondary structures which made propagating the DNA in bacteria difficult and PCR virtually impossible (such as during cloning of the *p21* right arm of homology and the *Puma* left arm of homology – see Sections 3.3.3.7 and Section

3.3.4.1). Another reason why generation of large DNA targeting vectors took a relatively long time was that there were many steps (see cloning overview in Figure 3.3.4 and Figure 3.3.44) which required sequential assembly – if a single cloning step was unsuccessful then it halted progression of the construct/project until it was completed (or redesigned to overcome the obstacle). Much of the work described in this thesis has consequently been concerned with overcoming these difficulties to successfully prepare DNA for targeting of ES cells. This results chapter describes how the four gene targeting vectors were finally successfully constructed. *p21*-mCherry and *Puma*-E2Crimson are discussed first including the selection of fluorescent proteins; followed by *Mdm2* P2-mutant and *Mdm2* P1-null.

## 3.3.2 Selecting the optimum fluorescent proteins

Different fluorescent proteins were examined to determine which two would be the most appropriate to use in a dual fluorescent reporter system for p53 activation *in vivo*. The small animal imaging system (The FMT 2500™ LX quantitative tomography system – referred to as the FMT system) at the University of Liverpool contains two lasers which excite at 635 nm and 750 nm. Originally, when it was not yet clear which imaging system would become available, we had planned to use a monomeric variant of Ds Red, mCherry (excitation peak 587 nm) to replace one p21 allele and a red-shifted GFP protein, EGFP (excitation peak 488 nm) to replace Puma [Shaner et al., 2005]. However it became obvious when the FMT imaging system was purchased towards the end of this project that we needed to re-evaluate those choices, especially for EGFP (since this fluorescent protein would in all probability not be detectable in the FMT system).

Several important factors were considered prior to selecting the fluorescent proteins, including the feasibility of swapping proteins part-way through a cloning exercise. The ideal pair of fluorescent proteins would have limited toxicity in mammalian cells, be bright enough to overcome auto-fluorescence of tissues, have high photostability (for imaging), mature quickly and efficiently, have minimal cross-talk between the two proteins and possess two distinct emission spectra (to differentiate between the proteins) (reviewed in [Shaner et al., 2005]). mCherry and EGFP were chosen initially since they appeared to meet these criteria,

however once the FMT system was purchased there was an additional criteria to meet; the fluorescent proteins selected must have sufficient brightness when excited at 635 nm. On this decisive factor EGFP failed completely and mCherry was only capable of emitting at < 2% of its maximum brightness (however subsequent studies with mCherry expressing cells have confirmed that the FMT does detect mCherry in xenografted cells). Therefore, a literature review was performed to determine whether other, possibly newer, far-red fluorescent proteins could be identified which might meet these requirements.

The far-red fluorescent proteins mKate, TagRFP657, E2Crimson and eqFP670 were identified and examined for suitability. The properties of each protein are summarised in Table 3.3.1 and their relative brightness is compared in Figure 3.3.3. mKate (and mKate2) is a monomeric version of Katushka but is only slightly brighter than mCherry when excited at 635 nm (1.7 fold) [Shcherbo et al., 2009]. TagRFP657 was developed from mKate and is further red-shifted (excitation peak 611 nm) and hence found to be brighter than both mCherry and mKate when excited at 635 nm (7.7 fold brighter than mCherry). The maturation time of TagRFP657 however, was the longest out of all those examined (125 minutes) [Morozova et al., 2010] and at the time of this study TagRFP657 was not commercially available. eqFP670 is a dimeric far-red shifted fluorescent protein which was found to be 4.3 fold brighter then mCherry when excited at 635 nm [Shcherbo et al., 2010]. eqFP670 was derived from Katushka-9-5, a variant of Katushka with lower cytotoxicity but was also not available commercially. The brightest far-red fluorescent protein in this comparison and also with the fastest maturation time (26 minutes) was E2Crimson. E2Crimson was 30 fold brighter than mCherry and 3.9 fold brighter then the next brightest protein (TagRFP657) when excited at 635 nm [Strack et al., 2009]. E2Crimson is a tetrameric protein developed from DSRed-Express2 and is supposedly non-cytotoxic to bacterial and mammalian cells [Strack et al., 2009]. One disadvantage of the tetrameric structure of E2Crimson is that we could not risk tagging it with a NLS (Nuclear Localisation Signal) since this may inadvertently interfere with tetramerisation which might reduce the sensitivity when observing single cells [Strack et al., 2009]. E2Crimson also had a second bright blue peak within its emission spectra – although this should not interfere with detection in whole animals using the FMT system. Therefore, because E2Crimson was considerably brighter than all the

other fluorescent proteins examined, it was deemed the most suitable candidate to replace EGFP.

It was decided to keep mCherry as the fluorescent protein for the *p21* construct since the molecular cloning had already progressed past the point when it would be trivial to change plans. Also despite mCherry only able to be excited at < 2% of its maximal efficiency, preliminary work by other members of our research group demonstrated that mCherry could be detected *in vivo* (data not shown). However, since the emission spectra of mCherry and E2Crimson overlapped it would not be possible to differentiate between them at this stage. Although this development was not ideal and would prevent our ultimate aim of simultaneous detection of *p21* and *Puma* up-regulation *in vivo* (for now), the proposed transgenic strains (*p21*-mCherry and *Puma*-E2Crimson) are still likely to provide useful tools with which to study *p53* activation individually (discussed in detail in Section 4.4).

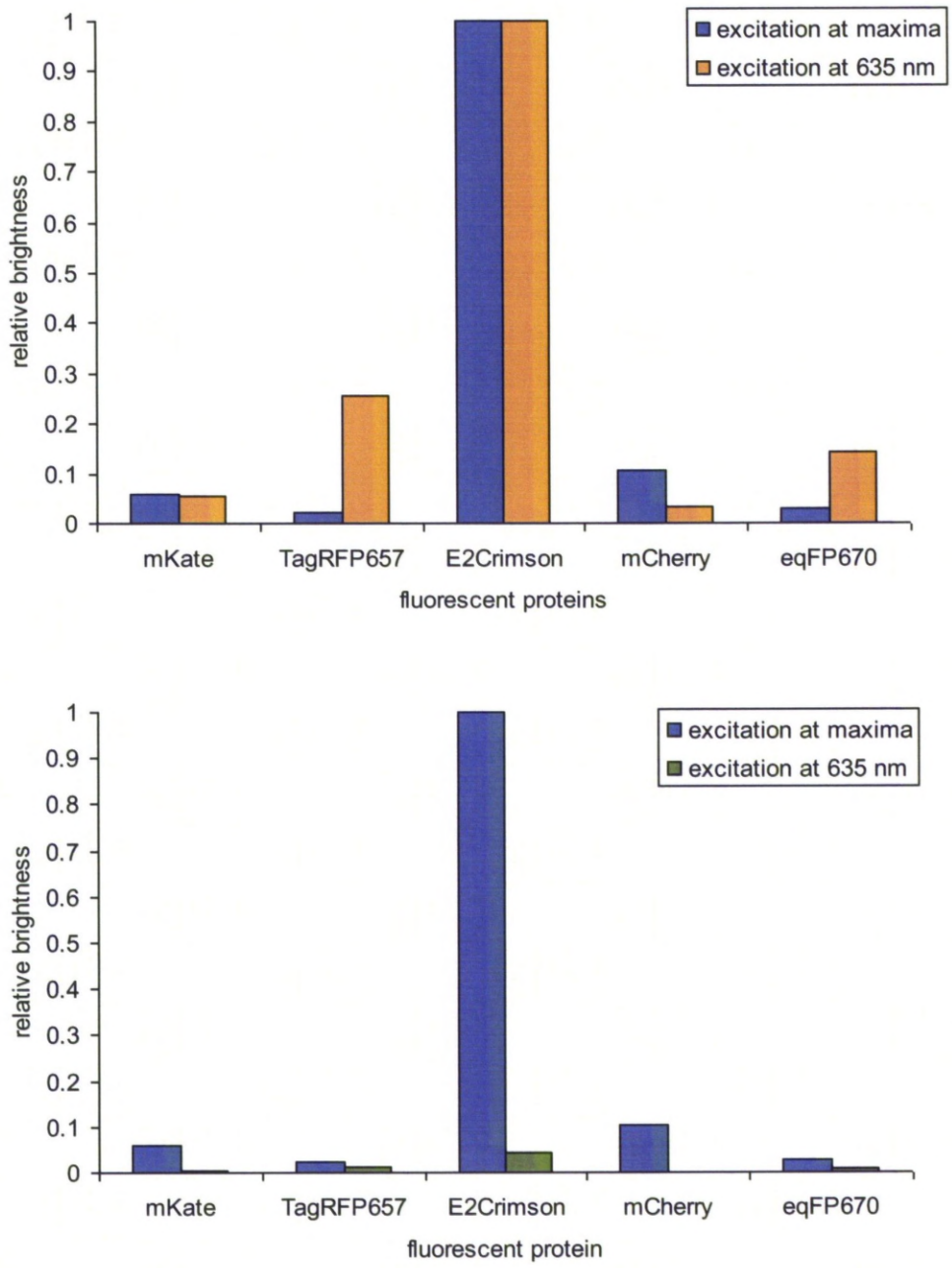


***Figure 3.3.3: Relative brightness of various far-red fluorescent proteins.***

*Values shown are relative to the brightness (BR) of E2Crimson at either its excitation maxima or to its excitation at 635 (the wavelength of the laser in our small animal imager). Top panel: Each data series is relative to either BR at the excitation maxima (blue bars) or BR at 635 nm (orange bars). Bottom panel: All data is shown relative to BR at maxima. Data was generated using the modest assessment of E2Crimson's quantum yield (QY = 0.12). E2Crimson was considerably brighter then all the other far-red proteins compared here, including mKate and mCherry, at both the excitation maximums and at 635 nm. When excited at 635 nm all of the proteins fluoresce at only a fraction of their potential. See also Table 3.3.1.*

***Table 3.3.1: Properties of different far-red fluorescent proteins.***

*Quantum yield (QY) is the ratio of absorbed light to released light. The extinction coefficient (EC) is the quantity of light absorbed by a protein therefore brightness (BR) = QY x EC.*

| **Fluorescent protein** | **Excitation maxima (nm)** | **Emission maxima (nm)** | **Maturation time (minutes)** | **Quantum Yield (QY)** | **Extinction coefficient (EC) ($M^{-1} cm^{-1}$) at maxima** | **Extinction coefficient (EC) ($M^{-1} cm^{-1}$) at 633-635 nm** | **Brightness (BR) at maxima** | **Brightness (BR) at 633-635 nm** | **References** |
|---|---|---|---|---|---|---|---|---|---|
| mKate | 588 | 635 | 75 | 0.28 | 31500 | 1300 | 8820 | 364 | [Shcherbo et al., 2009] |
| TagRFP657 | 611 | 657 | 125 | 0.1 | 34500 | 17000 | 3450 | 1700 | [Morozova et al., 2010] |
| E2-Crimsom | 611 | 646 | 26 | 0.12<br>0.23 | 1260000 | 55400 | 151200<br>289800 | 6648<br>12742 | [Shcherbo et al., 2010]<br>[Strack et al., 2009] |
| mCherry | 587 | 610 | 40 | 0.22 | 72000 | 1000 | 15840 | 220 | [Shaner et al., 2004] |
| eqFP670 | 605 | 670 | ND | 0.06 | 70000 | 15700 | 4200 | 942 | [Shcherbo et al., 2010] |

## 3.3.3 p21- mCherry

### *3.3.3.1 Cloning strategy*

Figure 3.3.4 shows the basic cloning plan for generation of the *p21*-mCherry and *Puma*-EGFP DNA targeting constructs. This plan relies upon PCR techniques to create the initial vectors (vectors 1-3 in Figure 3.3.4) and then on four unique restriction sites which would be used assemble the penultimate and ultimate vectors. These unique restriction sites would ideally be the same for *p21*-mCherry and *Puma*-EGFP (EGFP was later switched to E2Crimson – Section 3.3.2) so that some of the vectors and intermediate steps could be shared between the two cloning exercises, thus simplify the task of cloning. Whilst this was not completely achievable (sequences examined on NEBcutter tool – see Section 2.8.6), three suitable enzyme sites were identified as FseI (GGCCGGCC), SalI (GTCGAC) and PacI (TTAATTAA). A further two restriction enzymes were identified that were suitable except for the fact that they cut somewhere in the other gene's arms of homology. These were AseI (ATTAAT) for *p21*-mCherry and AscI (GGCGCGCC) for *Puma*-EGFP.

The selected restriction enzymes were then allocated to the planned unique restriction sites A-D in Figure 3.3.4 as follows; A, B & C were FseI, SalI and PacI respectively which enabled vector 1 (the negative selectable marker) to be shared between the *p21*-mCherry and *Puma*-EGFP cloning exercises. D was AseI or AscI depending on the gene. FseI/PacI and SalI/AseI were paired together for the restriction digests since they had compatible buffers. Once the restriction enzymes had been chosen the primers for the numerous planned PCR reactions were designed and ordered.

There now follows a detailed description in Section 3.3.3 to Section 3.3.4.6 of how each component of the targeting vector was generated. As mentioned in the overview, whilst undertaking the task of generating multiple DNA targeting constructs we encountered many challenges and many modifications to this basic plan had to be made in order to complete the vectors. Despite this, the basic strategy outlined below provides an essentially correct summary of the planned sequence of events.

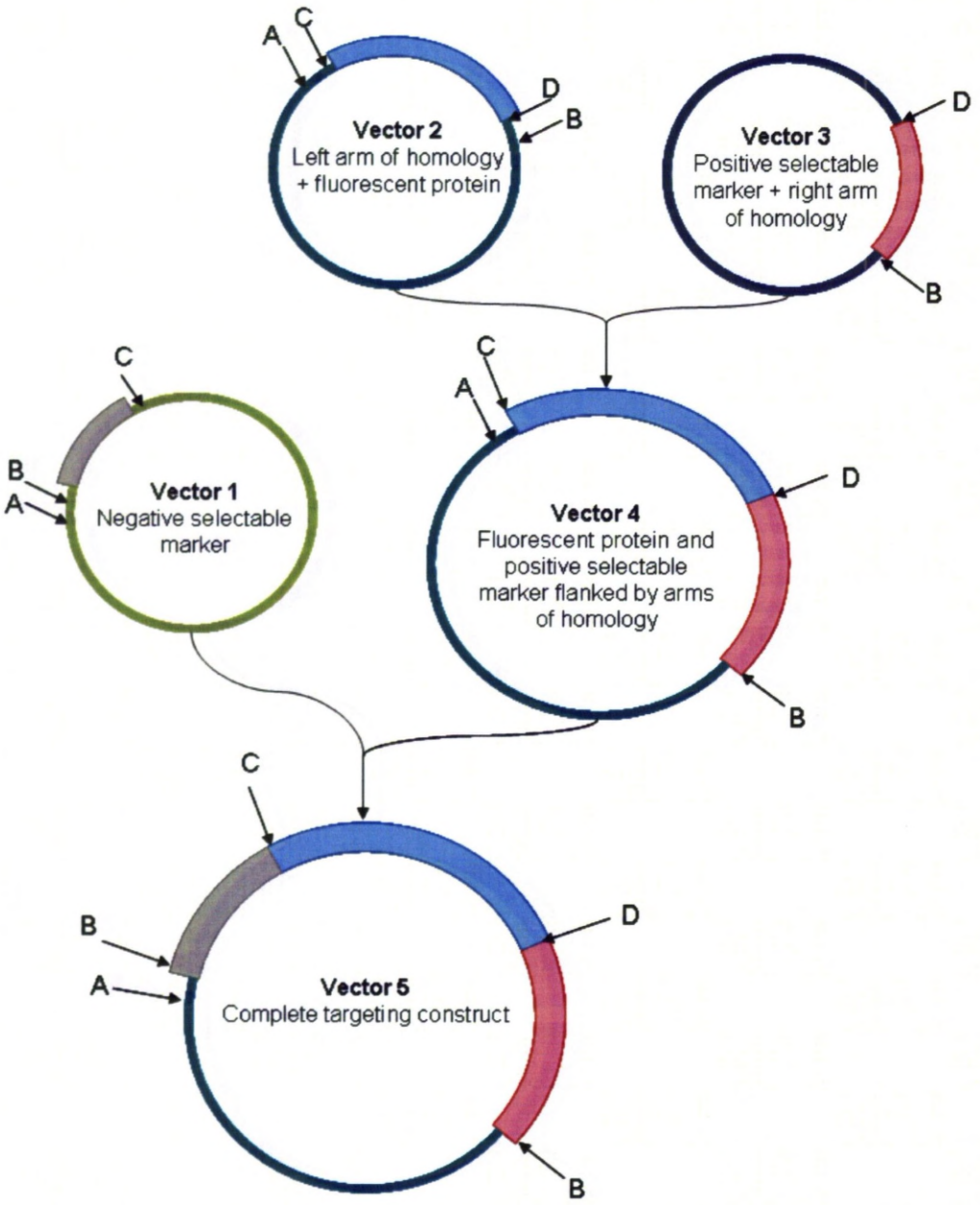


***Figure 3.3.4: Basic cloning strategy for the DNA targeting constructs p21-mCherry & Puma-EGFP.***

*Flow diagram of the construction of the targeting constructs. Vectors 1-3 were planned to be generated by various PCR techniques including PCR-mediated mutagenesis and fusion PCR. The final targeting vector would then be assembled using the unique restriction endonuclease sites (shown as letters A-D). A, B & C were FseI, SalI & PacI respectively whilst D was AseI for p21-mCherry or AscI for Puma-EGFP.*

### 3.3.3.2 Negative selectable marker

A negative selectable marker was included in the design of our DNA targeting constructs since, when negative and positive selection are used in combination, they greatly enrich for positive clones [Mansour et al., 1988]. The basis for negative selection is that integration of a negative selectable marker into cells confers sensitivity to a particular treatment. In this project, the viral protein thymidine kinase (TK) was used as the negative selectable marker for all four DNA targeting constructs. TK sensitises mammalian cells to treatment with the antiviral drug Ganciclovir [Cannon et al., 1999] (see Section 2.9.2.2.4). TK was placed at one end of the targeting vectors (outside the arms of homology) so that during a targeted homologous recombination event TK would not be incorporated into the genome (see Figure 3.3.2). In the case of random recombination however, TK is more likely retained in the genome and hence those cells could be eliminated in the presence of Ganciclovir.

Cloning of the negative selectable marker (TK) is described next and an outline of the strategy is provided in Figure 3.3.5. The TK cassette containing the TK gene with poly A signal under the control of the MCI promoter was obtained from the pKO Scrambler NTKV-1902 vector by PCR-mediated mutagenesis (see Section 2.7.2.1) which added 5' FseI-SalI and 3' PacI restriction sites for use in subsequent cloning steps. The PCR product was TA-cloned into vector pCR2.1 and the recombinant clones were screened for successful insertion of the TK fragment by an EcoRI digest (see Figure 3.3.5 – C). 9/10 clones appeared positive and two clones (TK1 & TK2) were sent for sequencing. Two clones were sent for sequencing because there were mismatches in the sequence alignment for the first clone (TK1). The second clone (TK2) also had the same mismatches so in order to confirm whether these differences were present in the original template sequence; this region of the parental plasmid DNA (pKO Scrambler NTKV-1902) was also sequenced. All three sequences (TK1, TK2 & pKO Scrambler NTKV-1902) were in agreement which does not match the published sequence. There were 9 mismatches in total (see Appendix D.1) of which 2 caused a missense mutation in TK (T133A & T232A), however since these mutations were not caused by PCR and the pKO Scrambler NTKV-1902 vector had been used previously in our laboratory for a different gene targeting experiment (which had been successful – manuscript in preparation) the clones TK1 & TK2 were deemed suitable for use.

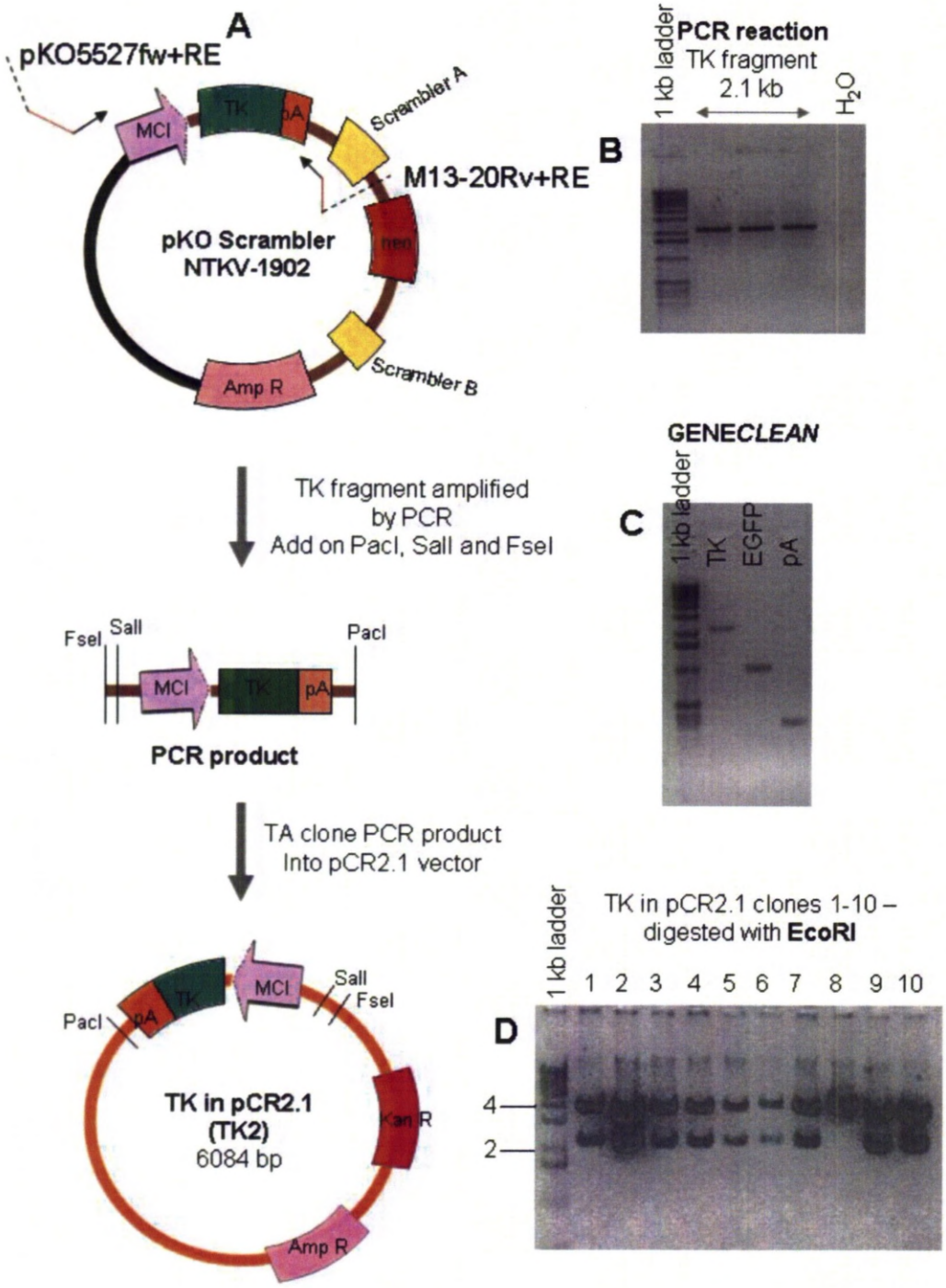


***Figure 3.3.5: Cloning of the negative selectable marker – thymidine kinase (TK).***

*A) Flow diagram of the cloning strategy. 5' FseI-SalI & 3' PacI restriction sites were added onto the TK fragment by PCR then cloned by TA-cloning into pCR2.1. B) The PCR product was run on an agarose gel to confirm it was the correct size (2.1 kb). C) The concentration of the DNA was determined following extraction from the previous gel. 10% of the total product was run. D) EcoRI digest of DNA extracted from bacterial clones transformed with the TK in pCR2.1 vector. Positive clones should have two fragments 2.1 & 3.9 kb in size.*

### 3.3.3.3 *p21 left arm of homology*

The *p21* left arm of homology is 4.3 kb in length with the endogenous translational initiation codon (ATG) at the 3' end followed by an inserted nuclear localisation signal (NLS). The NLS was added to localise mCherry expression within a cellular compartment to increase the local concentration of fluorescent protein and hence increase sensitivity when imaging cells [Fujii et al., 1999, Toby et al., 1998, Hadjantonakis et al., 2003].

Prior to successfully generating the *p21* left arm of homology we had attempted to proceed directly from the BAC clone DNA to the second product (B in Figure 3.3.6), but this resulted in an unexpected complication. After sequencing one of these clones (p21NLS3) it was discovered that 72 bp were deleted from the region between 3 and 4 kb of *p21* intron 1. A further 6 clones were sequenced all of which contained the same 72 bp deletion. In addition, a second problem emerged in which the incorporation of the NLS signal was not always 100% accurate and the primer region was frequently mutated – discussed in more detail later in this section. Since sequencing was relatively expensive and time consuming, a PCR screen was designed to distinguish the wild-type (811 bp) and mutated (739 bp) DNA (see Figure 3.3.7). This PCR reaction proved robust and could be used for PCR from bacterial colonies. 32 bacterial colonies were screened in total but none of these appeared to be wild-type. At this point it was decided to return to the BAC clone DNA and amplify the p21 gene fragment in two rounds.

The *p21* left arm of homology including the desired modifications (5' FseI-PacI and 3' NLS) was eventually generated by two steps of PCR (see Figure 3.3.6). The initial round of PCR amplified the *p21* fragment only (no modifications) and used BAC clone bmQ-262p22 as a template. BAC clone DNA was used in preference to genomic DNA since the DNA used to create the BAC library from which the bmQ-262p22 plasmid was obtained, was derived from 129*SvEv* mice (and so was isogenic to the AB2.2 ES cells we planned to use for gene targeting), but was only 102.6 kb in size (versus 3 x $10^6$ kb) and therefore provided an enriched source of the *p21* locus. The product from the first round of PCR (A in Figure 3.3.6) was TA-cloned into vector pCR-XL-TOPO and recombinant clones were screened for insertion of the correct sized product by MluI/NotI digest (see Figure 3.3.7). 10/10 clones appeared positive and one (p21LA2) was sent for sequencing. The sequencing results

matched the genomic sequence 100% (aligned using BLAST) and so this clone was used as the template DNA for the second round of PCR.

The second round of PCR was used to append the desired modifications, a 5' FseI-PacI for downstream cloning steps and the 3' NLS sequence. The template DNA was the previously described and sequenced clone p21LA2. The resulting PCR product (B in Figure 3.3.6) was then cloned into pCR-XL-TOPO and screened first by a MluI/NotI digest (13/13 appeared positive – see Figure 3.3.7) and then by the PCR screen described above to determine if these clones contained the 72 bp region which had been previously deleted (7/13 appeared wild-type – see Figure 3.3.7). I sequenced all 7 PCR positive clones using the MegaBACE method (see Section 2.7.2.6) at the 5' and 3' ends using the primers M13F, M13R and p21In1+4kbF to check for successful incorporation of the restriction enzyme sites and the NLS. This screen was performed since previously we had encountered problems with the incorporation of these sequences. Of the 7 clones only 1 (p21NLS8b) had both the 5' FseI-PacI and 3' NLS sequences added correctly (the other clones either had confirmed mutations or reads were too short to confirm either way). Therefore this clone (p21NLS8b) was sent away for complete sequencing. The sequencing results for clone p21NLS8b matched the genomic DNA 100% except for a deleted T within the 5' primer region (not part of the FseI-PacI region). Since this mutation was at location 16 bp of the *p21* left arm of homology and therefore would probably not be incorporated into the genome during homologous recombination, it was decided that this clone was suitable to use for the next cloning stages (fusion PCR reaction with mCherry).

The 5' oligonucleotide mutation described in clone p21NLS8b was unexpected since it was within the 40 bp p21In1LA-Fw+RE primer region and therefore could only be mutated if the primer itself contained a mutation. This high mutation frequency (5/12) issue was brought to the attention of Eurofin MWG Operon (who synthesised all primers used during this project) and as a result another synthesis of this primer was sent to us for use in the next stage of cloning.

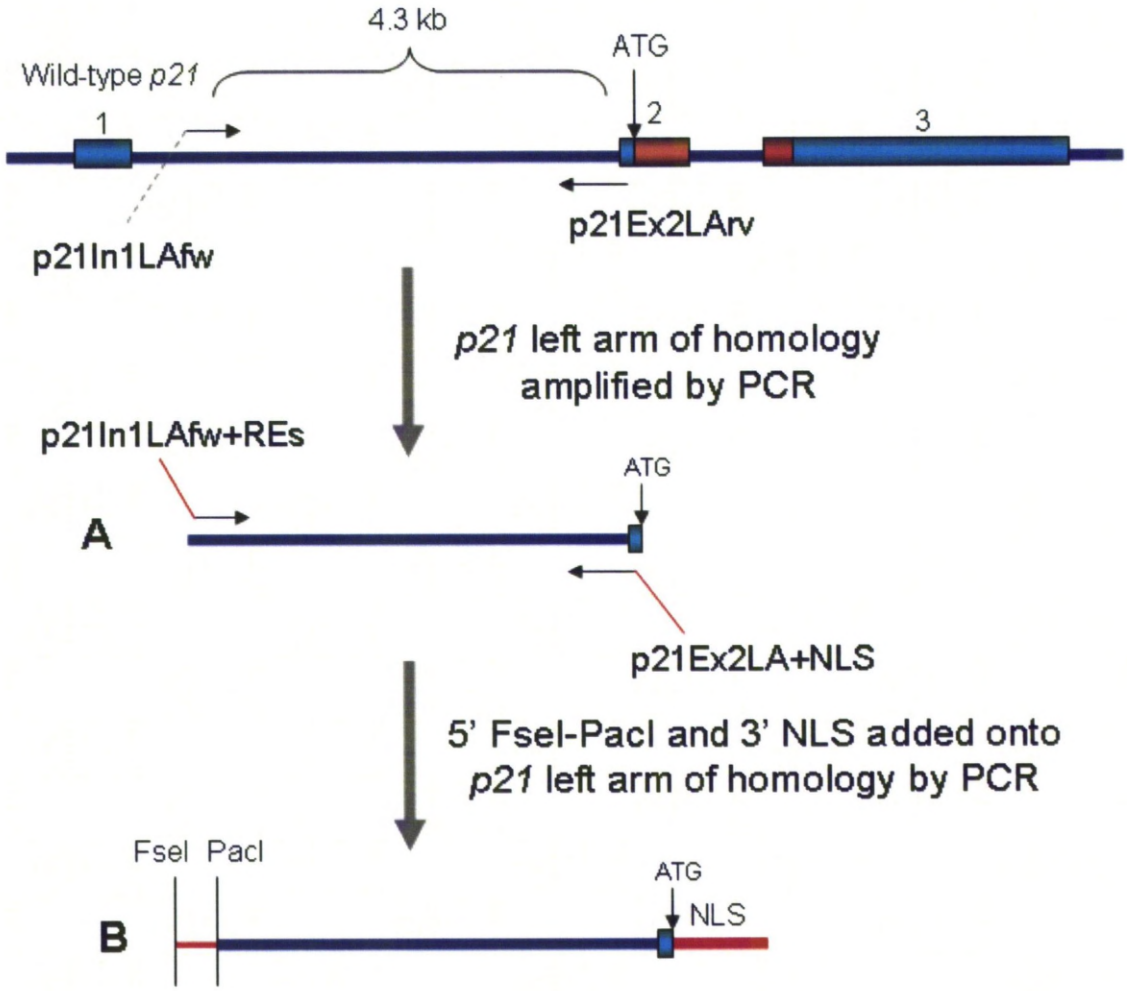


***Figure 3.3.6: Flow diagram for cloning of the p21 left arm of homology.***

*The 4.3 kb DNA fragment of p21 (immediately upstream of the endogenous ATG site) was amplified from the BAC clone bmQ-262p22 by PCR. This product (A) was TA-cloned into vector pCR-XL-TOPO and sequenced. Once the correct sequence was confirmed 5' FseI-PacI & 3' NLS (nuclear localisation signal) sequences were added by PCR-mediated mutagenesis to produce PCR product B. B was then TA-cloned into vector pCR-XL-TOPO and sequenced.*

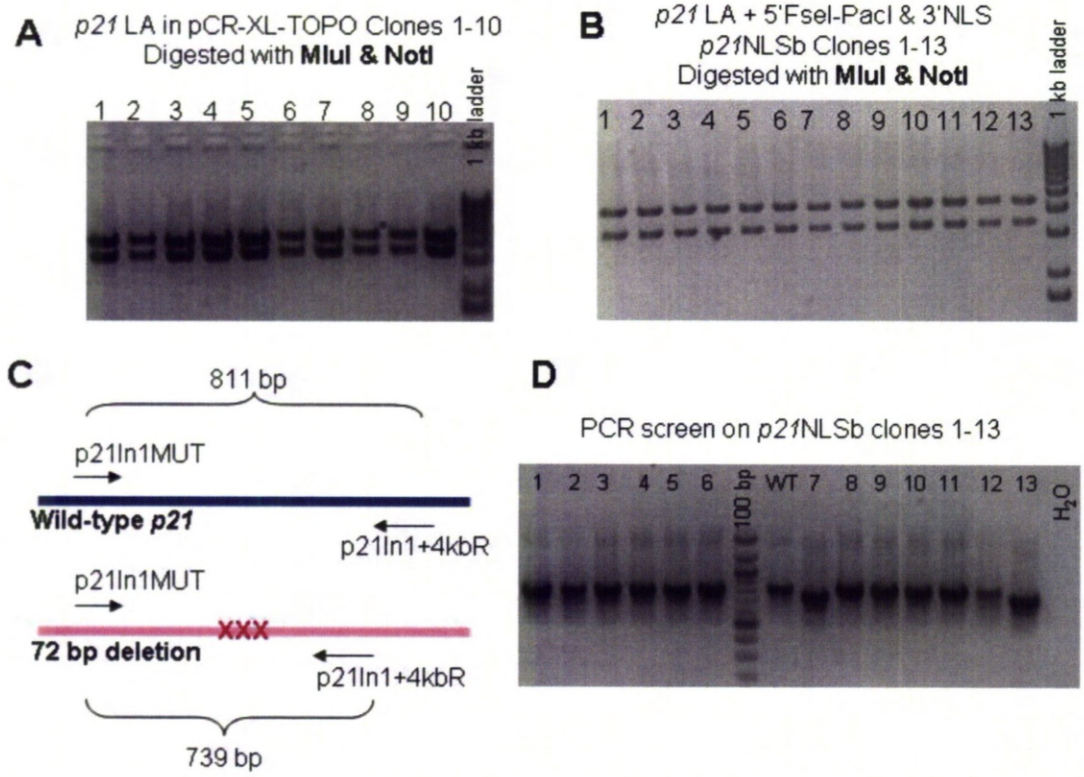


***Figure 3.3.7: Cloning of the p21 left arm of homology.***

*A & B) Recombinant clones were digested with restriction enzymes MluI and NotI to liberate the 4.3 kb genomic fragment of p21 from the vector pCR-XL-TOPO (backbone 3.5 kb). All clones here appeared positive. C) A schematic diagram of the PCR screen used to identify bacterial clones with wild-type p21 (primers p21In1MUT & p21In1+4kbR). D) Example agarose gel of the PCR results. Wild-type (WT) DNA produced an 811 bp product whilst mutated DNA produced a smaller product ~ 740 bp. The PCR results shown here demonstrate that clones 1-6 and clone 8 (7/13) appeared to retain the wild-type sequence.*

### 3.3.3.4 *mCherry*

*mCherry* was selected to be the fluorescent reporter gene for *p21* activation *in vivo*. In order to capture authentic expression we planned to replace one copy of *p21* with *mCherry*, so that the endogenous *p21* ATG translational initiation site would represent the start of *mCherry* coding. An NLS sequence was also included (see Section 3.3.3.3) so that the mCherry protein would concentrate in the nuclei of cells to increase detection sensitivity [Hadjantonakis et al., 2003].

Figure 3.3.8 provides an overview of the cloning steps required to prepare the mCherry cassette before it could be fused with the p21 left arm of homology. The parental plasmid (pmCherry) did not contain a poly A signal therefore before any downstream cloning could take place a poly A signal needed to be added. The SV40 poly A signal from pEGFP-N1 was amplified (with the addition of 5' EcoRI and 3' SpeI sites) by PCR and TA-cloned into vector pCR2.1. Recombinant clones were screened with an EcoRI/SpeI digest to check for successful insertion of the 299 bp PCR product. 8/10 clones were positive and clone 5 (polyA-5) was sequenced. The sequencing results were identical to the expected sequence.

Once the sequence of the SV40 poly A signal was confirmed it was digested and sub-cloned into pmCherry using the common EcoRI/SpeI sites. Positive clones were confirmed initially by restriction digest with enzymes HindIII/SpeI which resulted in a shift in the digest pattern from the parental clone 2500 & 844 bp to a targeted clone 2500 & 1085 bp. All 10 clones appeared positive, but because the agarose gel had some additional bands present (which sometimes occurred when DNA quality was low) this positive result was further examined by digesting one clone (mCh-polyA1) with EcoRI/SpeI (see Figure 3.3.9).

Clone mCh-polyA1 was then used as the template DNA for PCR-mediated mutagenesis which added the desired 5' NLS & 3' AseI-SalI sequences. The PCR product (B in Figure 3.3.8) was TA-cloned into pCR2.1 and positive clones were confirmed by digest with EcoRI (see Figure 3.3.9). One clone was selected for sequencing (mChNLS1), however the sequencing results indicated that there was a single T deletion within the NLS. The second clone (mChNLS2) was then sent for sequencing and fortunately was found to be identical to the expected sequence. Clone mChNLS2 was therefore selected for the downstream cloning steps which would fuse the p21 left arm of homology in-frame with mCherry.

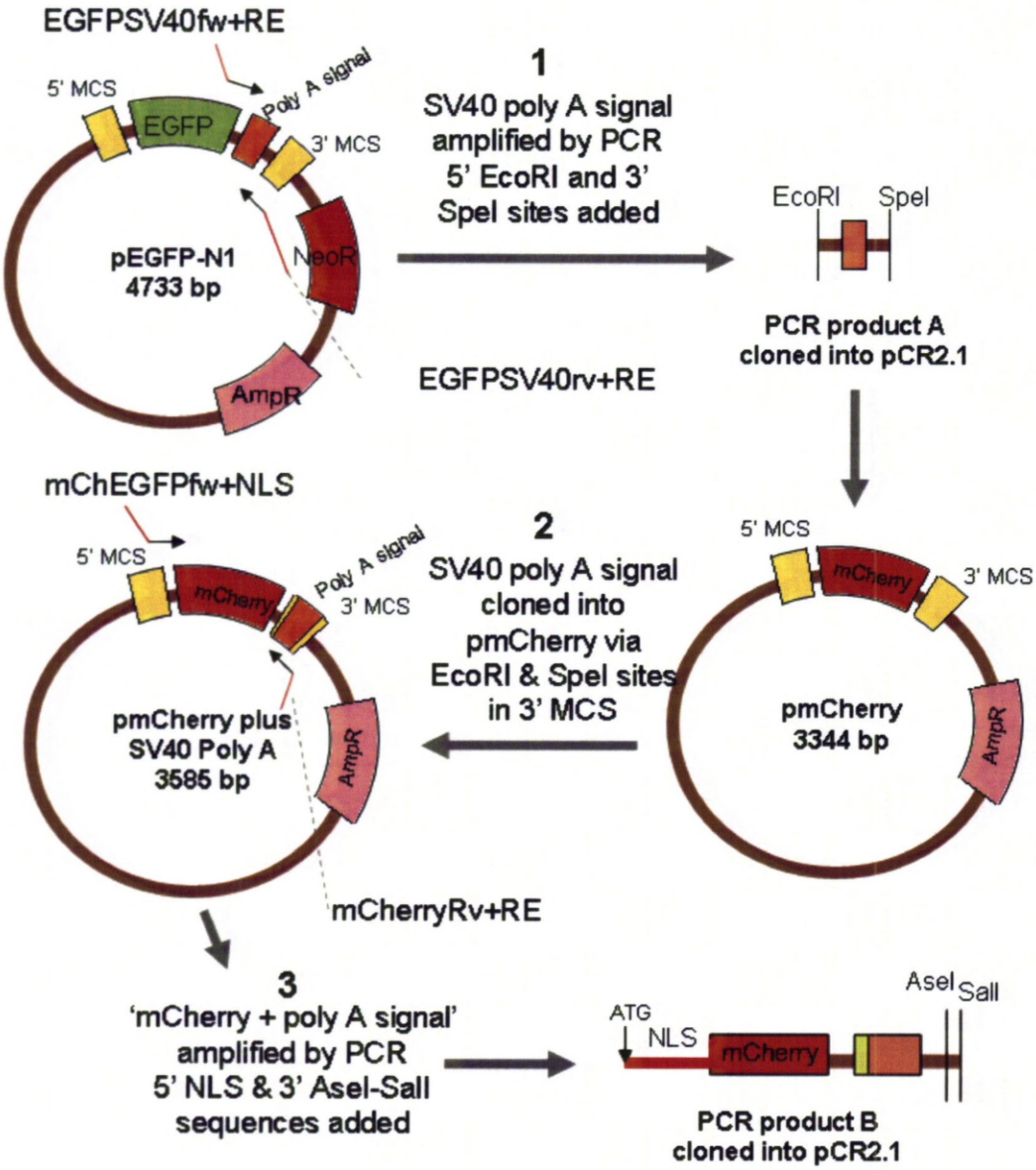


***Figure 3.3.8: Flow diagram for cloning of mCherry.***

*1. Since the plasmid pmCherry did not contain a poly adenylation (poly A) signal the SV40 poly A signal was amplified from pEGFP-N1 (with additional 5' EcoRI and 3' SpeI restriction sites) by PCR. This short PCR product (299 bp – A) was TA-cloned into vector pCR2.1 and sequenced. 2. Once the sequence had been confirmed the SV40 poly A signal was excised from pCR2.1 using the restriction sites EcoR1 and SpeI and cloned into the 3' MCS (multiple cloning site) of pmCherry using the same sites. 3. Once a positive clone had been identified another round of PCR was performed to append 5' NLS and 3' AseI-SalI sequences to mCherry+pA. The resulting PCR product (B) was then TA-cloned into pCR2.1 and sequenced.*

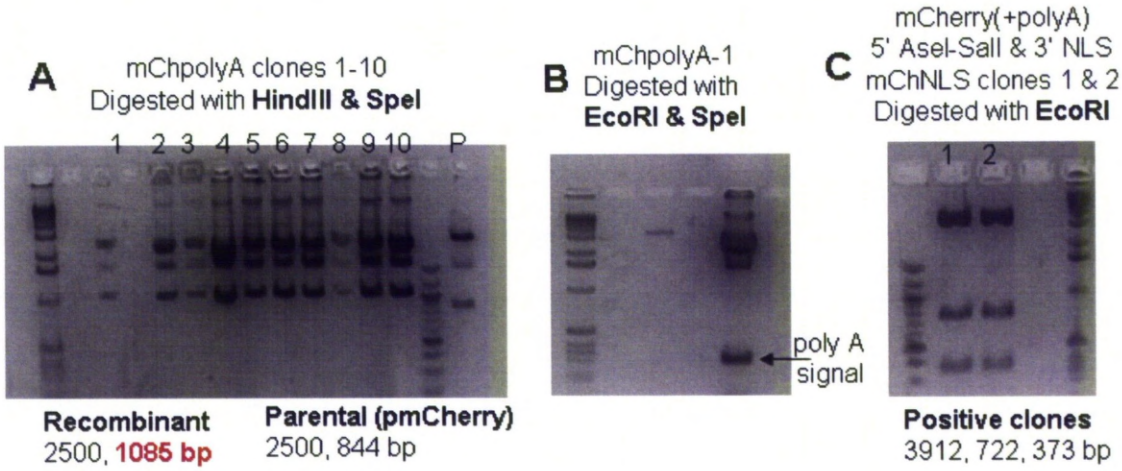


***Figure 3.3.9: Cloning of mCherry.***

*Restriction digests analysis to confirm positive clones. A) 10/10 clones appear positive for the size shift from the parental clone to recombinant clones (844 → 1085 bp). B) The poly A signal was excised from the plasmid to further confirm clone mChpolyA-1. C) mChNLS clones 1 & 2 both appear positive following digestion with restriction enzyme EcoRI.*

### *3.3.3.5 Fusing the p21 left arm of homology with mCherry*

The p21 left arm of homology was fused in-frame with mCherry by using the overlapping NLS sequence as the anchor for fusion PCR (described in Section 2..7.2.2) and see Figure 3.3.10). Since there had been difficulties with appending the NLS sequence to the ends of both the previous PCR stages, shorter primers were designed to attempt to prevent such a high mutation rate (which might have been associated with the length of the oligonucleotide). These primers were used in the two initial PCR reactions (PCR reaction 1 & 2 in Figure 3.3.10) in combination with the previous end primers, that is p21In1LAfw+RE (re-synthesised by Eurofins MWG Operon – see Section 3.3.3.3) and mCherryRv+RE. The two initial PCR products were then used as the template DNA in PCR reaction 3 (see Figure 3.3.10).

The final PCR product (see Figure 3.3.11) was TA-cloned into vector pCR-XL-TOPO and the resulting bacterial colonies were screened using the bacterial colony PCR described in Figure 3.3.7 to identify clones which had retained the ~ 70 bp region within *p21* intron 1. 6/56 clones appeared positive (p21mCh clones 10, 15, 42, 51-53) and I then sequenced these clones using the MegaBACE 1000 sequencer with the primers M13F, M13R, p21In1+4kbF to check for successful incorporation of the desired modifications 5' FseI-PacI and 3' AseI-SalI as well as the p21 → mCherry join region. This screen was performed since previously we had encountered problems with the incorporation of these sequences.

Clone p21mCh10 was sent away for complete sequencing since our sequencing screen indicated it had successfully incorporated all the desired 5' and 3' restriction enzyme sites and the p21 → mCherry join region. However, further sequencing revealed that the p21mCh10 clone matched <u>almost</u> 100% with the expected sequence except for a long A homopolymeric run within the 3 – 4 kb region of *p21* intron 1. This poly A run was 38 nt in the wild-type DNA (and indeed in our two previous clones p21LA2 & p21NLS8b) however in p21mCh10 this poly A run was only 36 nt. On the chromatogram these 36 A's appeared as discrete peaks, evenly spaced without any "noise" that might be associated with polymerase slippage during the sequencing reaction (see Figure 3.3.11) we therefore had to conclude that this was a real difference. The remaining clones were then sequenced to attempt to identify a

clone with the wild-type sequence. Of the six clones sequenced, three had 36 As, two had 37 As and one had 40 As, none had the wild-type 38 As. In each case the differences appeared real when the chromatogram was examined, therefore, time being a factor the clone p21mCh10 with 36 A's was selected as a compromise to continue with the cloning exercise.

Once the p21mCh10 clone had been selected there were still two additional cloning steps to be performed on the vector prior to its use in the final construct assembly (see Figure 3.3.12). These two cloning steps removed un-wanted AseI and FseI sites from the pCR-XL-TOPO backbone which would otherwise complicate downstream cloning steps. The two AseI sites were located between the pUC origin of replication and the 3' end of p21/mCherry sequence and the FseI site was located in the Zeomycin resistance cassette. The AseI sites were removed first by digesting p21mCh10 DNA with MluI and PciI. The DNA ends were then blunted (see Section 2.6.3) and the gel purified product was re-ligated to create a small (377 bp) deletion in the plasmid backbone. Positive clones were identified by two restriction digests which checked for an intact MluI or PciI site (see Figure 3.3.12– A & B).

Next, the FseI site was removed from the $Zeo^R$ cassette by performing a partial digest with FseI. A blunting reaction was performed (see Figure 3.3.12 – C) and the linearised 8.6 kb DNA fragment was extracted from the gel and re-ligated so that the resulting plasmid should only have one intact FseI site. To identify positive clones, which had the correct FseI site destroyed, a restriction digest was performed on recombinant clones with FseI and AseI (see Figure 3.3.12 – D). Perhaps surprisingly all 8/8 clones appeared positive for correct FseI site deletion. These clones were then ready for the next downstream cloning step.

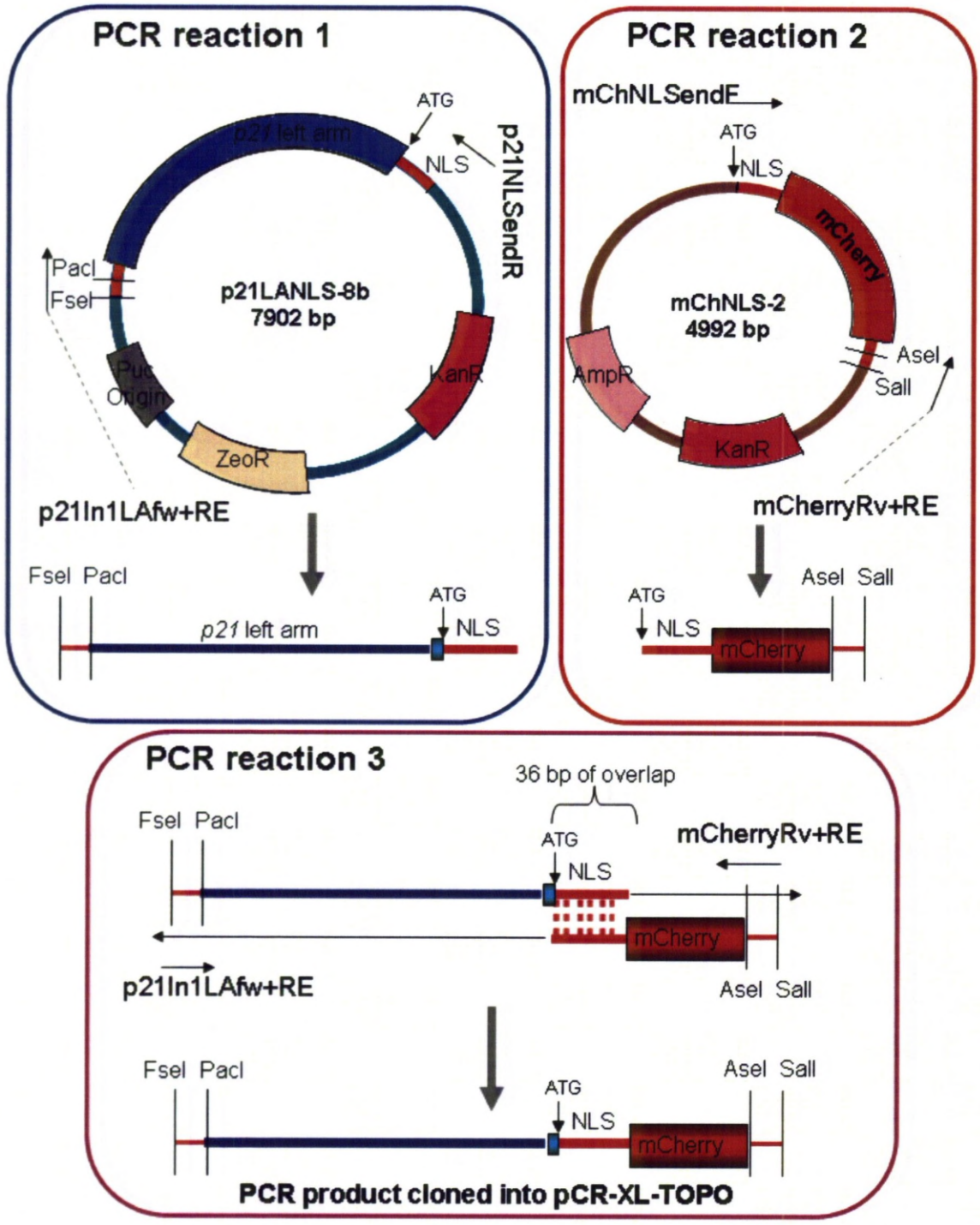


***Figure 3.3.10: Schematic diagram for the fusion of the p21 left arm of homology in-frame with mCherry.***

*Fusion PCR was performed as described in Section 2.7.2.1. The 4.3 kb genomic fragment of p21 was fused to the 1 kb mCherry fragment so that the endogenous ATG was followed by a 36 bp NLS then an in-frame mCherry coding sequence. The final product was cloned into pCR-XL-TOPO.*

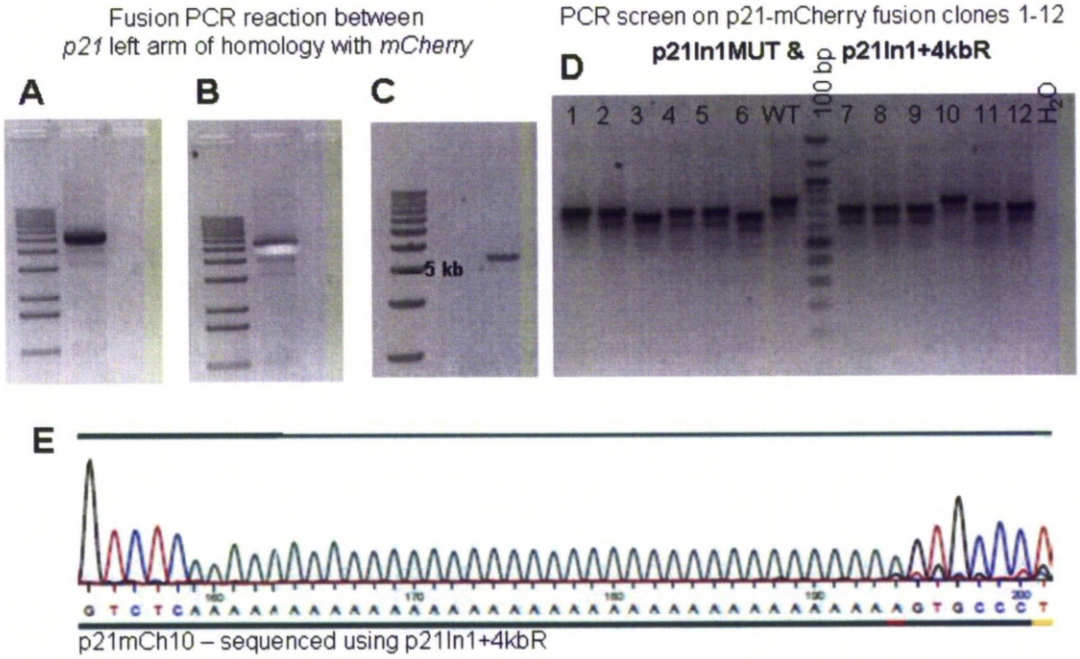


***Figure 3.3.11: Fusion PCR reaction for p21 left arm of homology and mCherry.***

*A) The fusion PCR product (~ 5.3 kb) was recovered from the gel (B) and (C) 10% was analysed to estimate the concentration. D) Example PCR screen (described in Figure 3.3.7) to identify recombinant clones which retained wild-type (WT) p21 sequence – clone 10 appeared positive. E) Part of p21mCh10 sequencing chromatogram to illustrate the poly A run (36 nt).*

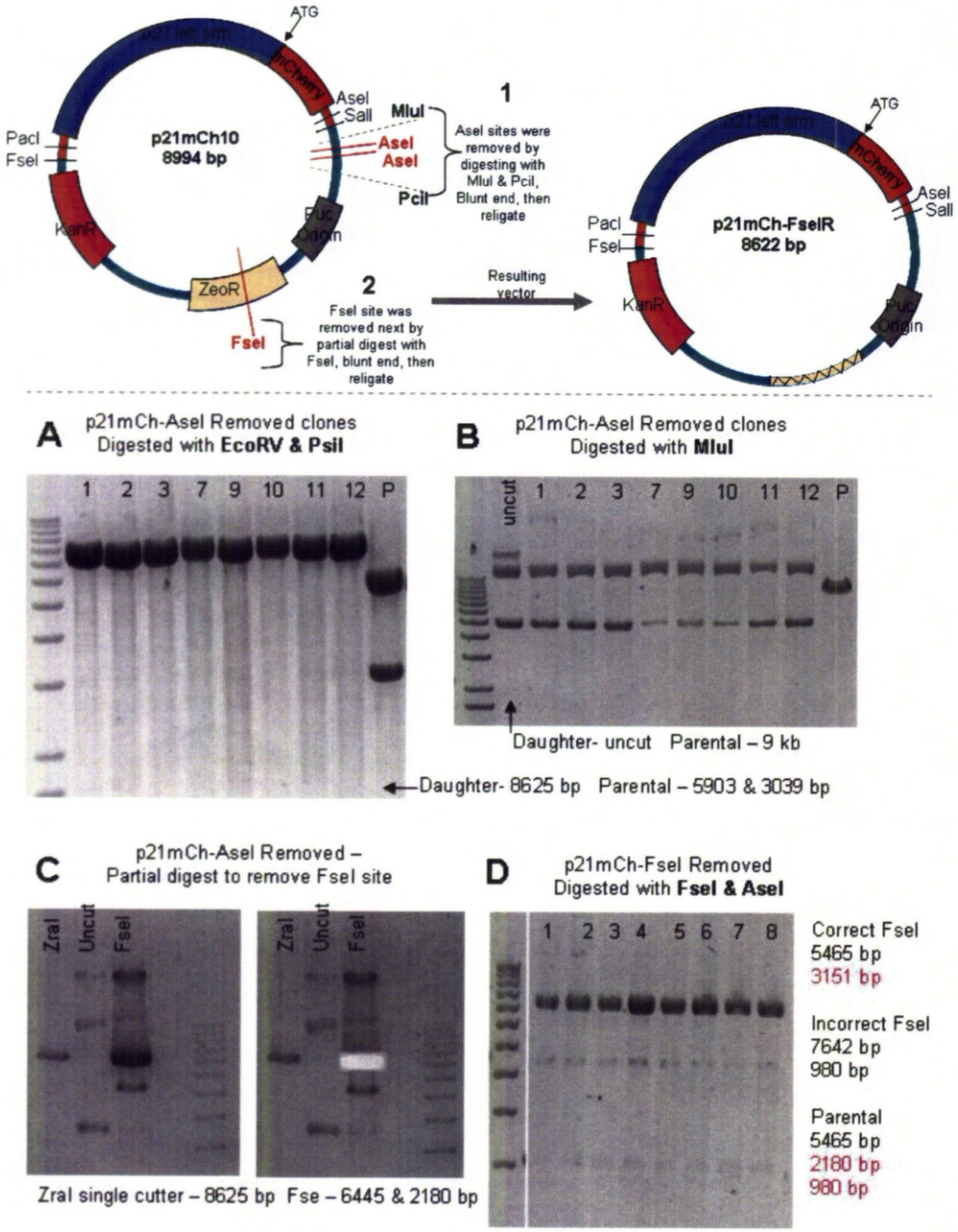


***Figure 3.3.12: Removing additional AseI/FseI sites from the p21mCh10 clone***

*Top panel: schematic diagram of the cloning strategy used to remove the unwanted AseI and FseI restriction sites from the pCR-XL-TOPO backbone. Bottom panel: A & B restriction digest analysis on the p21mCh10 clones with the MluI-PciI fragment deleted (and hence the two AseI sites were also removed). All clones appeared positive. C) The partial FseI digest of a p21mCh10-AseI removed clone* (optimised as 5 µg of DNA, with 5 U of FseI, in 30 µl for 30 minutes at 37°C). *ZraI a single cutter (for linearised plasmid) and uncut DNA were included for comparison. D) Restriction digest analysis on bacterial colonies from the FseI site removed ligation. Although the digest was quite inefficient (a lot of linearised plasmid is present at ~ 8.6 kb) the correct fragments were still visible. All 8 clones appear positive for the desired FseI site deletion.*

### 3.3.3.6 Positive selectable marker

The positive selectable marker used in the generation of both the *p21*-mCherry and *Puma*-E2Crimson DNA targeting constructs was the self excision neomycin cassette from the pACN vector (see Figure 3.3.13). This positive selectable marker has the benefit of catalysing its own excision from the genome and thus there would be no need for additional ES cell selection protocols [Gu et al., 1993] or time consuming animal crosses [Schwenk et al., 1995] to remove the neomycin resistance genes [Bunting et al., 1999]. Residual positive selectable markers in the genome can have unpredictable effects *in vivo* and hence should be removed to avoid confounding the interpretation of results. This occurs because the expression of selection cassettes is usually driven by strong constitutive promoters/enhancers which may interfere with the neighbouring genes' regulation [Olson et al., 1996] or effect the targeted allele itself [Meyers et al., 1998].

The cloning of the positive selectable marker (Cre/Neo$^R$) was essentially the same for both *p21*-mCherry and *Puma*-E2Crimson therefore the generation of both these vectors is described in this section. The Cre/Neo$^R$ fragment was amplified by PCR to add either a 5' AseI (*p21*) or AscI (*Puma*) restriction enzyme site for downstream cloning steps (see Figure 3.3.13). The PCR products were then TA-cloned into vector pCR-XL-TOPO and bacterial colonies were screened for positive clones using a HindIII digest. 7/10 clones appeared positive for both cloning exercises and two clones (NeoA6 & NeoB3) were sequenced.

The sequencing results of clones NeoA6 & NeoB3 showed three mismatches within the Pol II promoter region, which were identical between both clones. Since the probability of two separate PCR reactions both incorporating identical errors would be extremely low it seemed logical to conclude that these 'mismatches' were present in the parental plasmid (pACN). Indeed, when we aligned the DNA sequencing results for our clones (NeoA6 and NeoB3) against the mouse genomic DNA the supposed mismatches were no longer apparent, indicating that the error probably lies within the published sequence for pACN rather than the plasmids. Therefore both these sequenced clones were suitable to use in downstream cloning experiments.

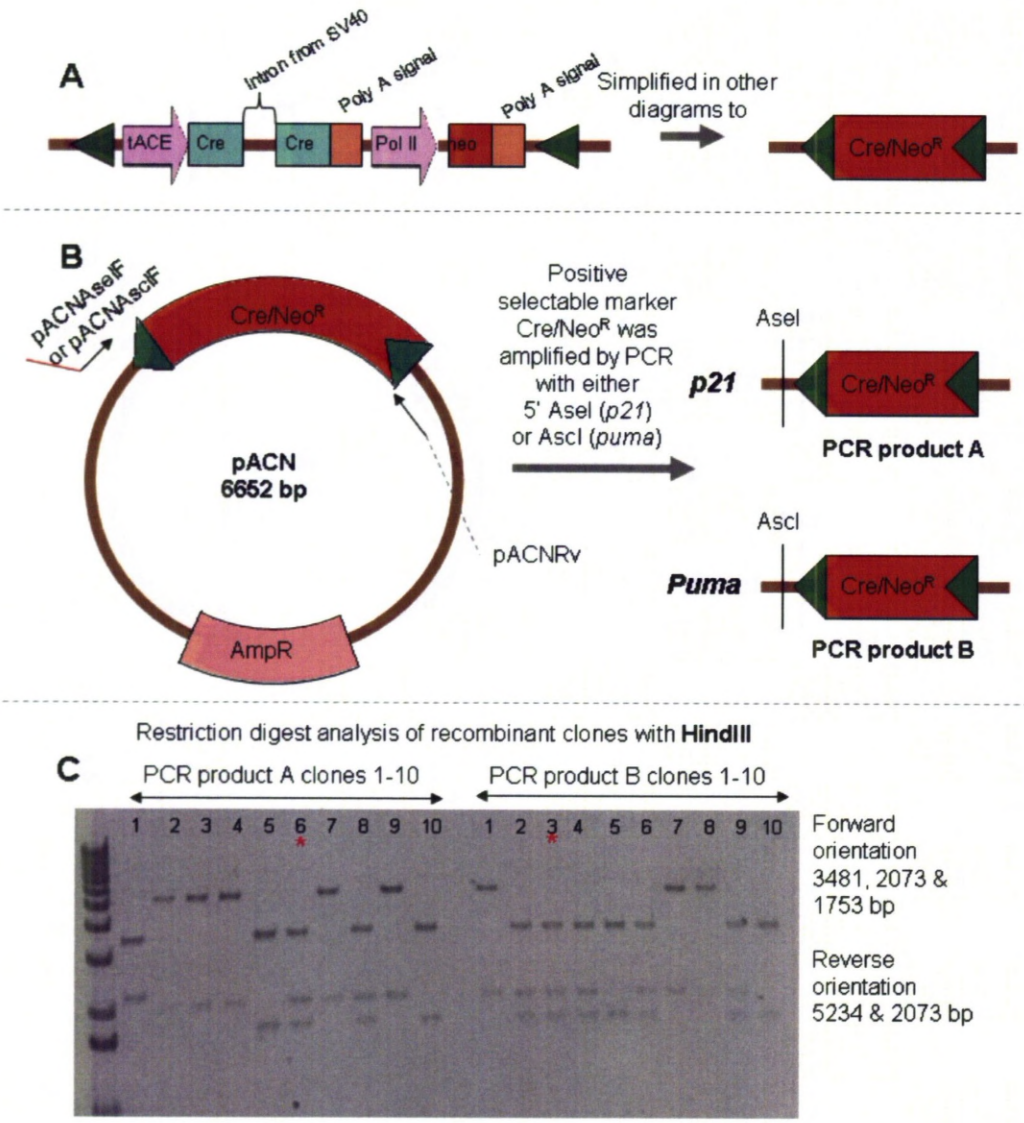


***Figure 3.3.13: Cloning of the positive selectable marker.***

*A) Schematic diagram of the self excision neomycin cassette. Image adapted from [Bunting et al., 1999]. The plasmid pACN contains the neomycin phosphotransferase cDNA driven by the RNA polymerase II large subunit promoter and Cre recombinase with nuclear localisation sequence and an intron from SV40 t-antigen. The cassette was flanked with two 34 bp loxP sites (green arrow heads in diagram). Cre recombinase is under the control of testis specific angiotensin-converting enzyme promoter (tACE) – hence upon passing through the germ line of male mice the entire 3.8 kb cassette would be removed leaving behind only a single loxP site at the targeted locus. B) Cloning strategy: The 3.8 kb PCR product was amplified from the pACN vector using either primer pair pACNAseIF & pACNRv (p21) or pACNAscIF & pACNRv (Puma). The resulting PCR products either contained a 5' AseI or AscI site respectively. C) These PCR products were cloned into pCR-XL-TOPO and recombinant clones were screened for successful insertion by HindIII digest. *Clones A6 & B3 were sequenced.*

### 3.3.3.7 *p21 right arm of homology*

The *p21* right arm of homology was designed to be 4 – 5 kb in length downstream of the coding region (~ 200 nt into *p21* exon 3). The original plan for the generation this fragment was to use PCR-based techniques to amplify the genomic DNA region of interest from a BAC DNA clone (employing a similar strategy to that used to generate the left arm of homology). However following several attempts at performing this PCR with multiple primer pairs and under various reaction conditions (including touch-down PCR, a technique whereby the annealing temperature was the same as the extension temperature) it became obvious that there was a problem in amplifying DNA from this region since PCR products from these reactions always appeared as a smear when separated by agarose gel electrophoresis.

Upon closer examination it was revealed that the DNA sequence immediately downstream of the *p21* gene was extremely repetitive. The repetitive region was comprised of several slight variations of a short (10-20 nt) sequence repeated in tandem which stretched on for approximately 12 kb (according to the C57BL/6 genomic reference assembly database). At approximately 5 kb into this repetitive region there was a slight lapse in the repetitive elements, where the Primer3 program selected several sequences as suitable for PCR primers, however if even if these primers were annealing correctly there was still apparently a problem with polymerase slippage during the DNA replication step of the PCR.

Since the repetitive region of DNA commenced immediately downstream of exon 3 (the end of *p21*) this only left 1.3 kb of genomic DNA sequence to use for the right arm of homology if PCR was to be used. Considering the wealth of literature advising against short arms of homology for gene targeting experiments [Hasty et al., 1991, Deng and Capecchi, 1992] the possibility of extracting a suitably sized fragment using the BAC clone DNA was investigated.

A suitable BAC fragment would be greater then 4 kb in length, would not contain any of the unique restriction sites required for construct assembly (FseI, PacI, SalI or AseI) and should also ideally be readily distinguishable from other BAC restriction fragments following digestion. Following sequence analysis of the p21 right arm region and BAC clone 262p22 DNA using the NEBcutter tool only one DNA restriction fragment met these requirements; an EcoRV-HindIII fragment of predicted size 12,054 bp. In order to differentiate the EcoRV-

HindIII fragment from other contaminating bands an additional restriction enzyme was used in the digest (NsiI). The final cloning strategy and identification of positive clones is shown in Figure 3.3.14, however prior to achieving this several other strategies and rounds of cloning had been attempted. These failed attempts are detailed briefly in Appendix C.2

Cloning of the p21 left arm of homology was eventually achieved following digestion of BAC clone bmQ-262p22 DNA with EcoRV, HindII and NsiI. The top band (~10 kb) was cloned into vector pBluescript II SK+ via the SmaI (blunt) and HindIII sites within the multiple cloning site (MCS). When this ligation reaction was initially transformed into TOP10 *E. coli* (a routine cloning strain) the DNA extracted from the resulting bacterial colonies appeared to have undergone recombination since the digest patterns were apparently random. However, when the same ligation reaction was transformed into MAXstbl.2 *E. coli* (a bacterial strain for growing unstable DNA sequences), the DNA extracted from the resulting bacteria behaved as might be expected (the backbone was at least present at the correct size). 10/24 colonies appeared positive and two of these clones (p21RASK+ 23 & 24) were sequenced using primers T7 & M13R to confirm the 5' and 3' ends.

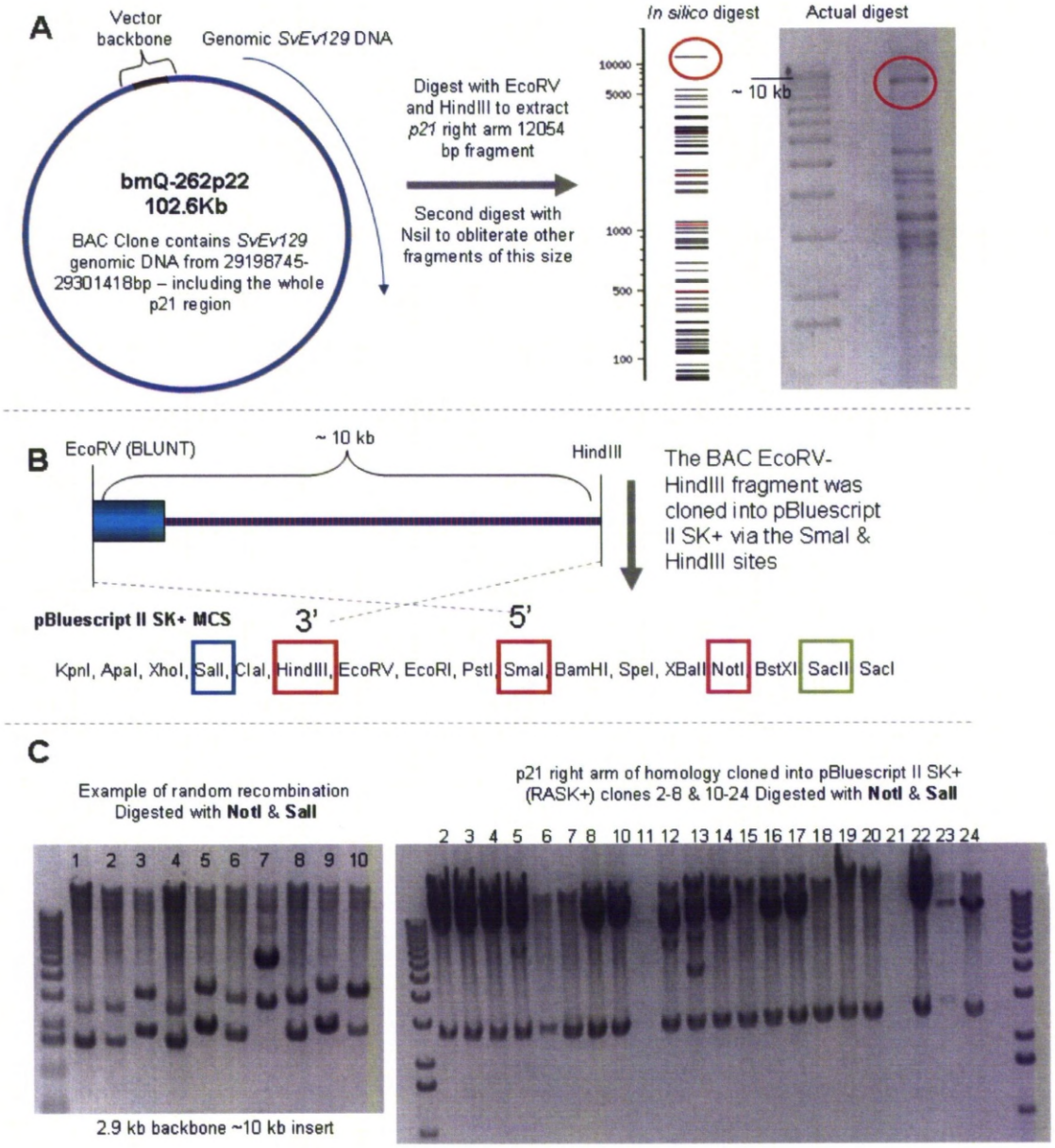


***Figure 3.3.14: Cloning of the p21 right arm of homology.***

*A) BAC clone bmQ-262p22 was digested in silico to determine whether restriction fragments containing the p21 right arm (red circle) would be distinguishable from other fragments, followed by a restriction digest of the BAC DNA to confirm in silico predictions. NB. The apparently 12 kb fragment resolved at ~ 10 kb. B) The p21 right arm fragment was cloned into vector pBluescript II SK+ via the SmaI and HindIII sites. The MCS also had a 3' SalI and two additional unique sites (NotI and SacII) which were utilised during assembly of the p21 right arm with the neo cassette. C) Initial cloning of the p21 right arm resulted in strange digest patterns in which even the backbone was re-arranged, typical of recombination. Once the ligation reaction was transformed into MaxStbl.2 E. Coli the diagnostic digest was performed again and despite several lanes being overloaded the expected digest pattern was observed. Clones 23 & 24 were apparently positive.*

### *3.3.3.8 Fusing the positive selectable marker to the p21 right arm of homology.*

In order to join the Cre/Neo$^R$ cassette with the p21 right arm of homology without using PCR as originally planned (since the p21 right arm of homology was extremely repetitive and unable, in our hands, to be amplified) the cloning strategy had to be revised. The new cloning plan was based on the availability of unique restriction sites in pBluescript II SK+, that is the availability of restriction endonuclease recognition sites that did not cut within the p21 right arm or the within Cre/Neo$^R$ cassette. pBluescript II SK+ is a commonly used cloning vector and was chosen since it enabled directional cloning of the ~10 kb EcoRV-HindIII BAC digest DNA fragment into its SmaI and HindIII sites and left a downstream SalI site required for final assembly of the DNA targeting construct (see Figure 3.3.4 & Figure 3.3.14). The pBluescript II SK+ MCS also had a further two unique restriction sites (SacII and NotI) upstream which were used to insert the Cre/Neo$^R$ cassette into the p21RASK+24 plasmid (see Figure 3.3.15).

Inserting the positive selectable marker into the p21 right arm of homology vector was performed in two stages. The first stage added the necessary SacII site to the NeoA6 plasmid whilst the second stage assembled the DNA fragments together in the correct orientation. Since the NeoA6 vector did not contain a SacII site, a pair of adaptor oligonucleotides were designed to convert the 5' KpnI site. 1/17 bacterial colonies were identified as containing the SacII site by restriction digest with SacII (clone A610). The Cre/Neo$^R$ cassette was then cloned into p21RASK+24 using the now mutual SacII and NotI sites. Note that the backbone of clone A610 was 3.5 kb whilst the insert was 3.8 kb therefore to successfully separate these fragments agarose gel electrophoresis was performed slowly for a relatively long time. Contamination with the backbone however was not a major concern since the parental vector pCR-XL-TOPO contains a Kanamycin resistance gene rather than Ampicillin used for selection of pBluescript II SK+ plasmid. Following transformation of the ligation reaction into MAXstbI.2 *E. coli,* colonies were screened for successful insertion of the 3.8 kb Cre/Neo$^R$ cassette by SacII and NotI digest. 1/5 clones appeared positive, out of the negative clones two contained the correct insert size (3.8 kb) however the backbone

(containing the ~10 kb of repetitive DNA) size varied – demonstrating that this DNA was unstable. No additional sequencing was required because no PCR had been performed and therefore this clone (2410-5) was ready for the next stage of cloning – final assembly of the vectors.

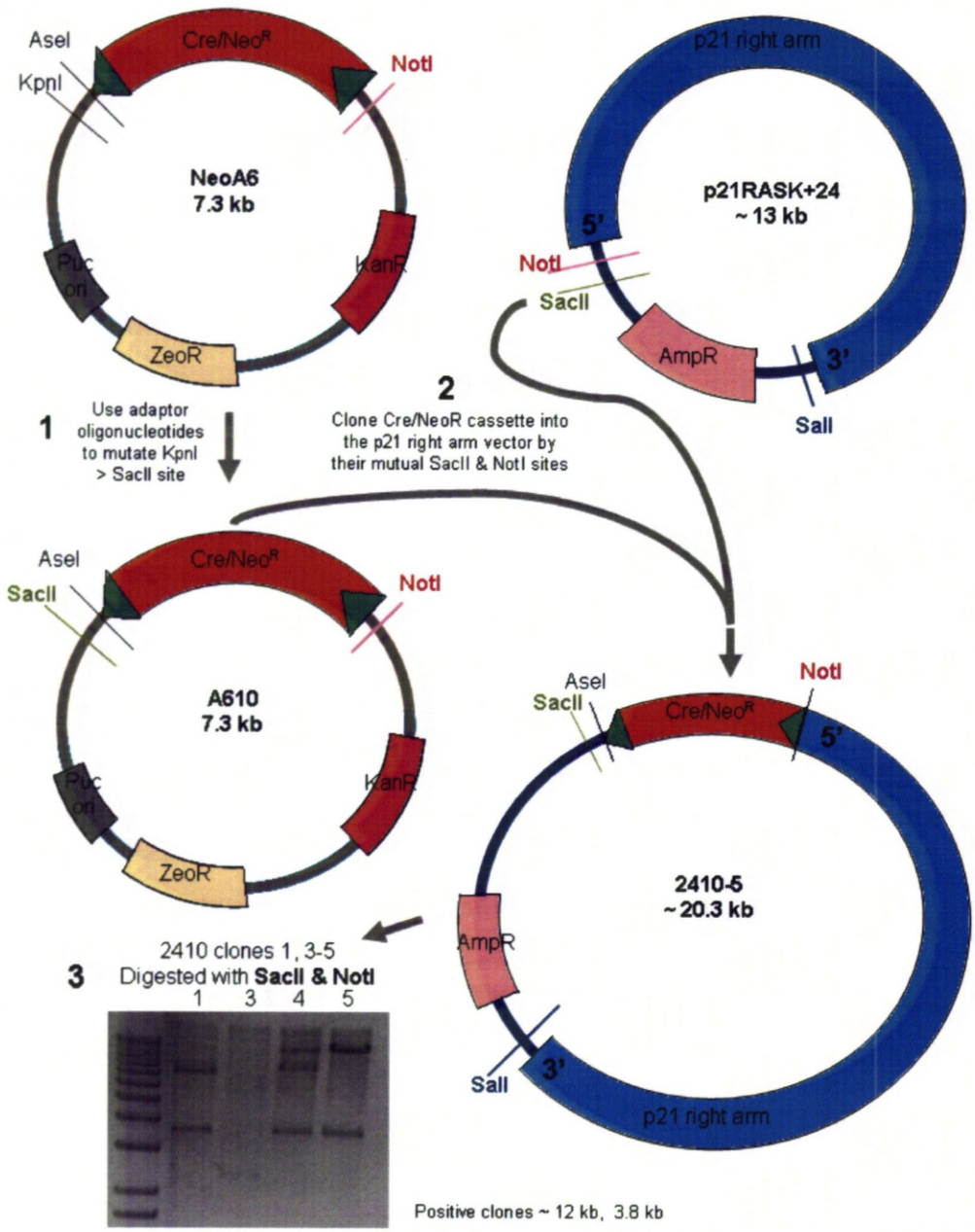


***Figure 3.3.15: Cloning the Cre/Neo$^R$ cassette into the p21 right arm of homology***

*1. The 5' KpnI site in NeoA6 was mutated to create a SacII site. 2. This allowed directional cloning of the Cre/Neo$^R$ cassette into p21RASK+24 via their now mutual NotI & SacII sites. The ligation reaction was transformed into MAXstbl.2 bacteria since the DNA was known to be unstable. 3. One positive clone was identified (2410-5) when the DNA from bacterial clones was screened by SacII & NotI restriction digest.*

### 3.3.3.9 *Final construct assembly*

Assembly of the penultimate and ultimate cloning vectors was performed as originally planned (see Figure 3.3.4 and Figure 3.3.16) – albeit with some difficulty. The penultimate step combined the *p21* left arm of homology-mCherry with the Cre/Neo$^R$-*p21* right arm of homology to create Vector 4. The last step of cloning then inserted the TK cassette into Vector 4 to generate the final DNA targeting construct (Vector 5). The first of these two final steps progressed as expected, however the final step of cloning took several attempts to complete. The main reason for this was probably because of the very repetitive region of DNA within the *p21* right arm of homology – discussed in detail later in this section. Cloning of Vector 4 is described first followed by the generation of the evasive Vector 5.

Vector 4 was generated by inserting the ~13.9 kb AseI-SalI DNA fragment from "Vector 3" (2410-5) into the AseI and SalI sites in "Vector 2" (p21mCh-FseIR). This moved the 'Cre/Neo$^R$-*p21* right arm' DNA fragment into "Vector 2" in the correct orientation for gene targeting. The ligation reaction was transformed into MAXstbl.2 *E. coli* because of the known unstable DNA elements within the *p21* right arm of homology. 2/6 of the resulting colonies appeared positive by an initial test digest with restriction endonucleases AseI and SalI which excised the ~13.9 kb insert (Figure 3.3.17 – A). The positivity of these clones (V4-1 and 3) was then further confirmed by three additional restriction digests with EcoRV, EcoRI and XhoI (Figure 3.3.17 – B). Since all the DNA fragments appeared at their expected size and stoichiometric ratios, at this stage both clones V4-1 and V4-3 were deemed suitable for use in the final stage of cloning.

The final stage of cloning the *p21*-mCherry DNA targeting construct was to insert the 2.1 kb TK negative selectable marker cassette into the main construct (Vector 4) via their common FseI and PacI restriction sites. As alluded to earlier, this proved challenging since *E. coli*, even the MAXstbl.2 strain (which was optimised to grow unstable DNA), struggled to stably propagate the very repetitive region of DNA within the *p21* right arm of homology. In fact even previously positive clones such as V4-3 could (and would) frequently "lose" varying amounts of this repetitive arm during overnight culture. Cloning of the ultimate vector then, was not entirely straightforward and is described in detail in Appendix C.3.

The problem with the maintenance of the unstable DNA in the *p21* right arm of homology was never completely resolved however, eventually, following advice from Invitrogen (who supplied the MAXstbl.2 strain) to grow the *E. coli* at 27°C (rather then 30°C) some (3/24) apparently positive clones were identified as shown in Figure 3.3.18. Upon further examination (and additional overnight culture) by restriction digest analysis with XhoI, SmaI, AleI and BsrGI one of these clones had already "lost" part of the repetitive region. The other two clones however (V5h-7 and V5h-21) retained the region (see Figure 3.3.19) and these were prepared as a midi-prep (see Section 2.3.3) in order to have sufficient DNA for 1 – 2 attempts at gene targeting. One clone was selected (V5h-21) and sent for further sequencing which confirmed the DNA sequences at the cloning junctions between the assembly vectors and at important locations such as the *p21* left arm of homology into *mCherry*. We also sequenced parts of the *p21* right arm of homology (where primers would anneal) and compared it with p21RASK+24 DNA sequence (since this was our first clone to successfully maintain the repetitive DNA region) to be confident that the DNA appeared as expected. The clone V5h-21 was therefore determined to be, to the best of our knowledge, a whole and accurate DNA targeting construct for the generation of a *p21*-mCherry knock-in transgenic reporter mice and was deemed suitable for use in gene targeting of ES cells.

This should have been the end of this cloning exercise however, since the first *p21* gene targeting experiment was unsuccessful (discussed in Section 3.4.1) more DNA needed to be generated. Unfortunately re-growing the *E. coli* from glycerol stocks was plagued with the same recombination issue as described previously – namely that the ~10 kb repetitive DNA region in the *p21* right arm of homology was lost to varying degrees between clones. 20/20 clones had lost the part of the region and this deletion occurred typically within the first 5 kb (since the 4.5 kb fragment which should have been generated by a BsrGI digest frequently appeared missing in these clones). The desired DNA was eventually regenerated by retransformation of MAXstbl.2 *E. coli* with V5h-21 DNA (see Figure 3.3.20). 6/10 colonies were apparently positive for the *p21* right arm region and two of these clones (V5h-21-25 and V5h-21-30) were selected for additional confirmation digests (see Figure 3.3.21). Since all the digests appeared as expected clone V5h-21-25 was then prepared as a Mega-prep. This DNA was then used for the second round of ES cell gene targeting for *p21*.

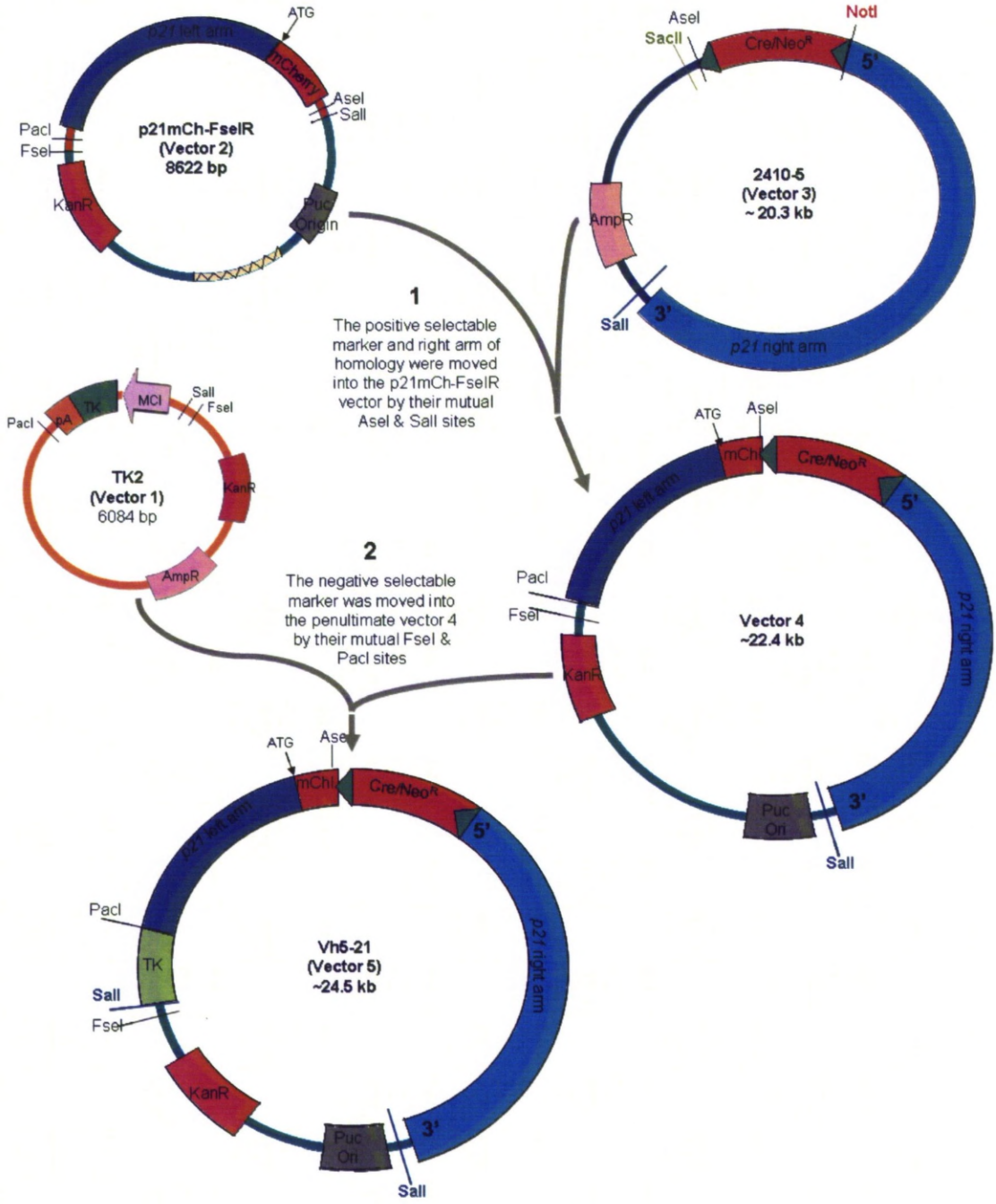


***Figure 3.3.16: Final assembly of p21-mCherry DNA targeting vector.***

*1. The positive selectable marker and p21 right arm of homology was inserted in to the vector containing the p21 left arm of homology and mCherry by their mutual AseI and SalI restriction sites. 2. Next, the negative selectable marker was added to the resulting vector (Vector 4) using the FseI and PacI sites.*

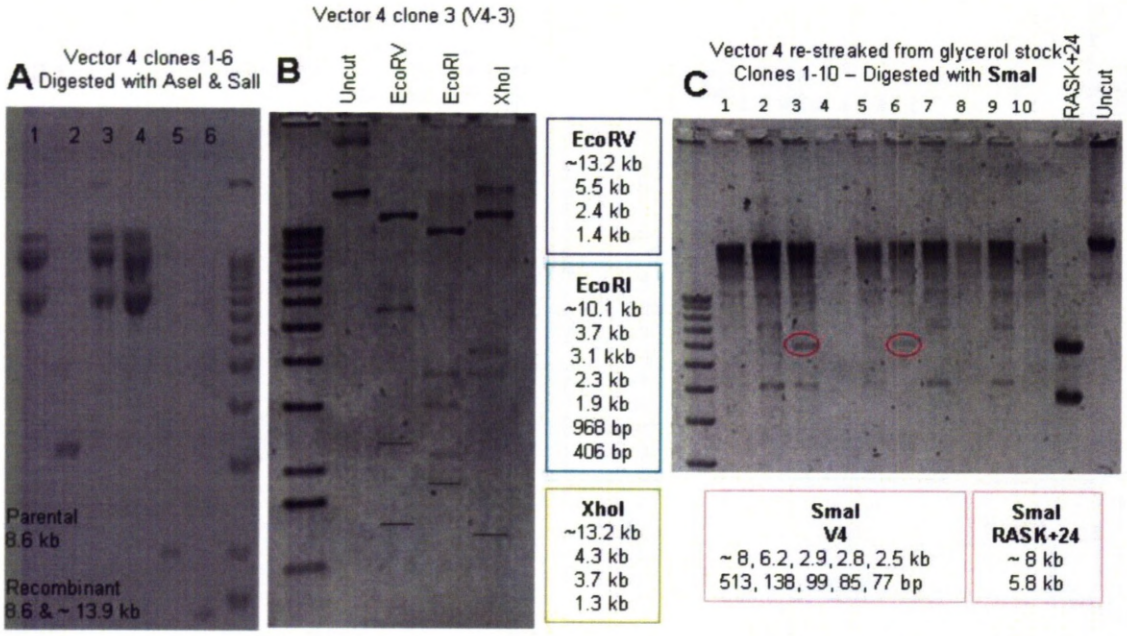


***Figure 3.3.17: Cloning of the penultimate p21-mCherry vector (vector 4)***

*A) Initial screen of vector 4 transformants was performed by restriction analysis with AseI and SalI. 2/6 clones appeared to contain the ~ 13.9 kb insert DNA. B) Further analysis of vector 4 clone 3 (V4-3) with additional digests including restriction enzymes EcoRV, EcoRI and XhoI. The digest patterns appear at the expected sizes. (The lower molecular weight bands have been digitally enhanced in this figure to make them easier to identify). C) The glycerol stock for V4-3 was re-streaked onto a fresh LB-Agar (Kan) plate and the resulting colonies were screened by SmaI digest. Only 2/10 colonies appear to have kept the repetitive region (clones 3 and 6 – circled region) compared to the original p21 right arm clone (p21RASK+24 – see Figure 3.3.14).*

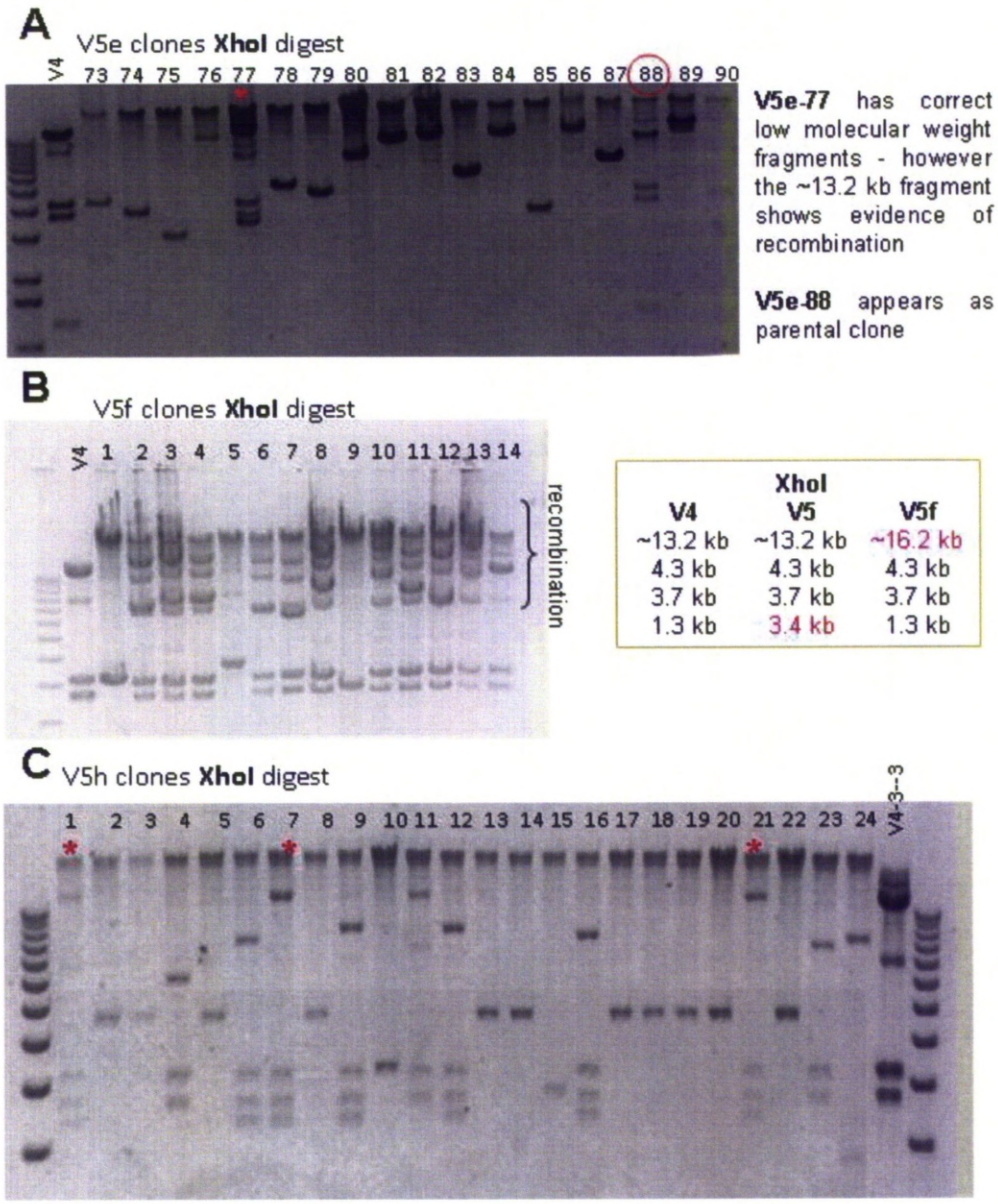


***Figure 3.3.18: Cloning of the p21-mCherry final DNA targeting construct.***

*Restriction digestion analysis of potential clones from various cloning experiments. A) An example of an unsuccessful attempt (V5e). Most DNA digestion patterns appear as random single fragments with a high molecular weight smear (probably bacterial genomic DNA). One clone (V5e-77) displays the correct low molecular weight fragments however the high molecular weight fragment appears lower than expected – indicating that some of the DNA is missing. B) Another unsuccessful cloning attempt (V5f) with clear evidence of loss of the large DNA fragment. Instead of there being one discrete large molecular weight band – multiple bands appear at various sizes. C) Successful cloning attempt (V5h) clones 1, 7 and 21 appear positive.*

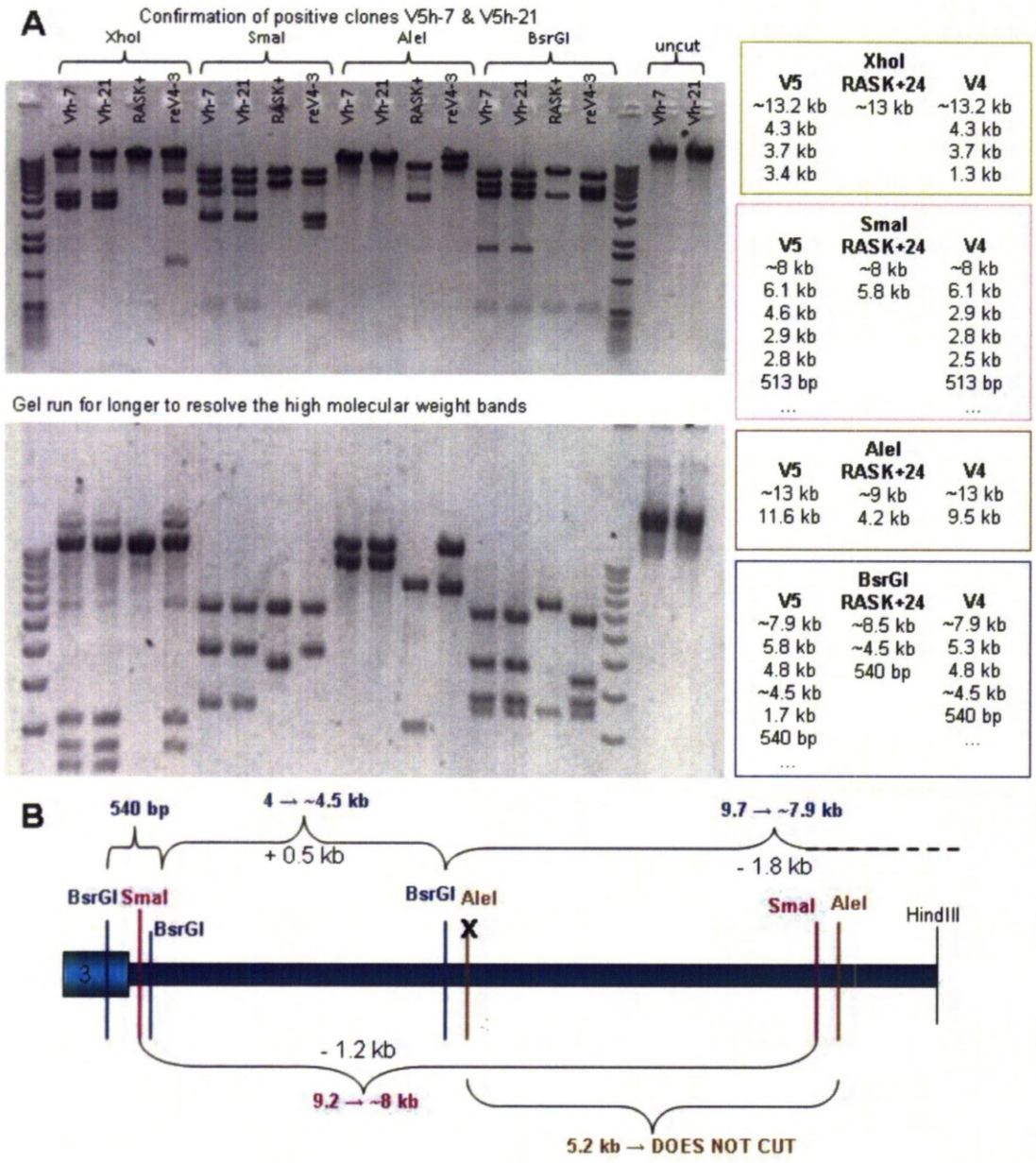


***Figure 3.3.19: Confirmation digests of positive clones V5h-7 & 21.***

*A) p21-mCherry DNA targeting constructs V5h-7 & 21 were digested with multiple enzymes to identify any unwanted recombination events – specifically those which might affect the length of the very repetitive region of DNA within the p21 right arm of homology. Digest patterns appeared as expected for both clones when compared to previous clones – therefore one clone (V5h-21) was selected for sequencing. B) Schematic diagram of the restriction digest fragments for the p21 right arm of homology. The predicted sizes of the DNA fragments based on C57BL/6 genomic DNA are shown first followed by the actual approximate size of the fragment (129SvEv strain) as determined by the experimental digests.*

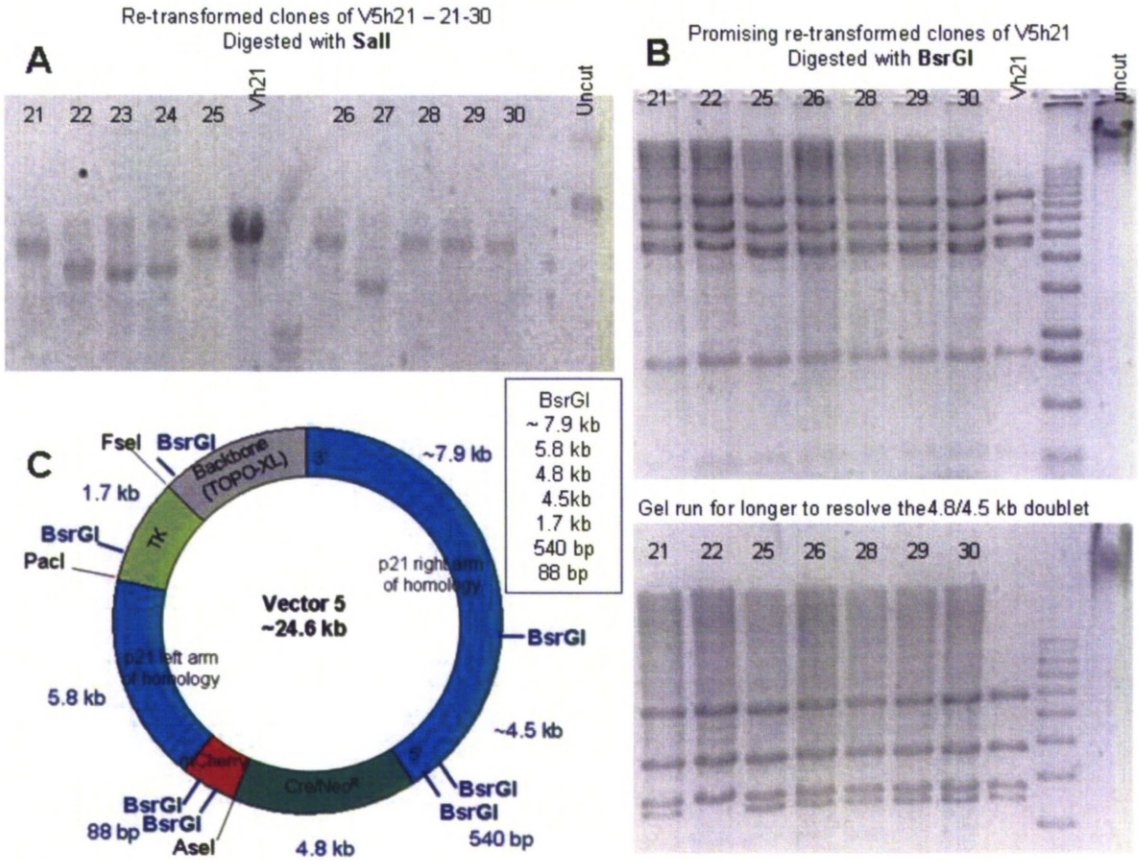


***Figure 3.3.20: Re cloning the p21-mCherry DNA targeting construct.***

*Following re-transformation of the original positive clone (V5h21) into MaxStbl.2 E. coli the resulting clones (21-30) were then examined for retention of the repetitive DNA fragment present in the p21 right arm of homology. A) SalI digest releases the gene targeting construct from the pCR-XL-TOPO backbone. DNA fragment sizes were compared to the original DNA (V5h21). B) The most promising clones (21, 25, 26, 28, 29 & 30) were then digested with BsrGI which cuts the vector within the repetitive region and hence is diagnostic for where recombination is taking place. Since all the clones (with the exception of 22, included for comparison only) contain the doublet at 4.8/4.5 kb all would be suitable for further growth and digests. Clones 25 and 30 were selected for further growth and analysis. C) Schematic diagram showing BsrGI sites in Vector 5 and expected fragment sizes.*

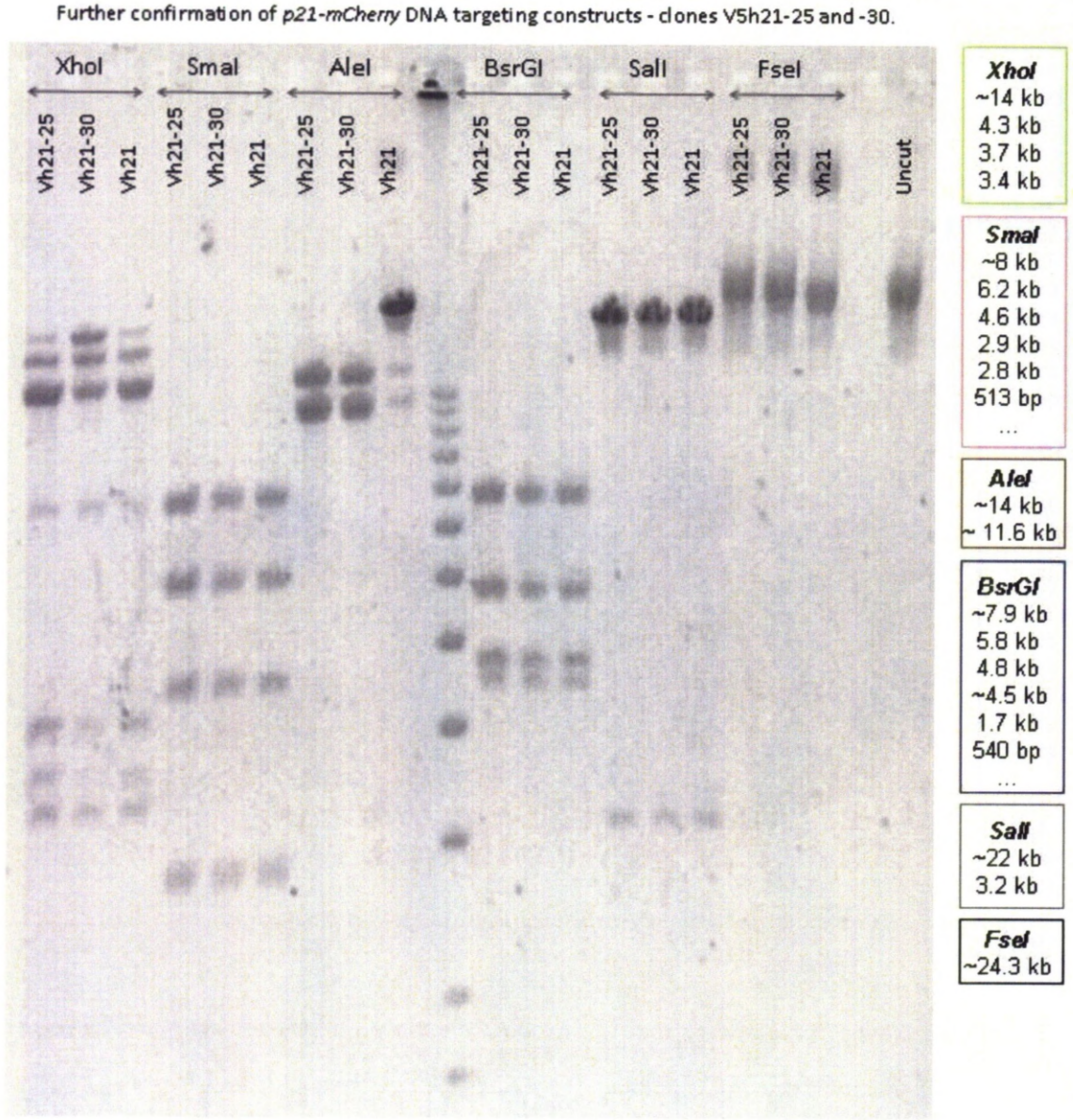


***Figure 3.3.21: Confirmation of re cloned p21-mCherry DNA targeting constructs.***

*Re-transformed clones V5h21 -25 & -30 were compared side by side with the original p21-mCherry DNA targeting construct V5h21 to examine the size and stoichiometry of the restriction fragments when the samples were digested with multiple restriction enzymes. With the exception of the AleI digest, all restriction digests appeared very similar (if not identical). The reason(s) why V5h21 did not cut as well when digested with AleI is not obvious, since previously AleI was able to digest this DNA (see Figure 3.3.19).*

## 3.3.4 Puma-E2Crimson

### *3.3.4.1 Puma left arm of homology*

The *Puma* left arm of homology was designed to contain 4 – 5 kb of *129SvEv* genomic DNA immediately upstream of the endogenous start codon (ATG). We initially aimed to generate this genomic DNA fragment by two rounds of PCR, similar to the method used to generate the *p21* left arm of homology (see Section 3.3.3.3). However despite several attempts to optimise this PCR reaction (as described in Section 2.7.1 and see Appendix B) no satisfactory results were achieved – that is, we observed either no product, wrongly sized product and/or multiple bands of an incorrect size (see Figure 3.3.22). The reason or reasons for the failure of PCR to amplify this region was or were unclear. We were confident that the template DNA (either BAC clone bmQ-397h22 or bmQ-207e13) contained at least part of the *Puma* locus and was an appropriate template to use for PCR since PCR of the *Puma* right arm of homology had been successful (see Section 3.3.4.4). We reasoned that given the size of the average BAC clone (100-300 kb) it seemed highly probable that the rest of the *Puma* locus should be present since the regions were only separated by ~ 2 kb. In addition, other than being slightly GC rich (~60%) and containing a few microsatellite repeats there did not appear to be any inherent problems with the primary DNA sequence (unlike the *p21* right arm of homology – see Section 3.3.3.7). Whatever the reason(s), because PCR was problematic we decided to investigate the possibility of isolating a suitable DNA fragment by restriction digestion of the BAC clone DNA (as for the *p21* right arm of homology – see Section 3.3.3.7).

Following sequence analysis of the *Puma* left arm region and BAC clone bmQ-397h22 DNA using the NEBcutter tool an NcoI-NcoI fragment with an expected size of 5865 bp was identified. This 5865 bp fragment was considered suitable for our purpose since it was > 4 kb and did not contain the restriction sites FseI, PacI, SalI or AscI - also discussed in Section 3.3.3.7. The desired NcoI-NcoI fragment was distinguishable from other contaminating digest fragments *in silico* due to the presence of two additional restriction enzymes sites, EcoRI and HindIII, however when this triple digest was performed the restriction fragments did not match the expected sizes, nor were the anticipated stoichiometric

ratios of bands observed (see Figure 3.3.23). For example, the highest molecular weight fragment should have been 7.1 kb however in the triple digest there were two DNA bands clearly visible at approximately 10 and 12 kb. The individual digest patterns for EcoRI, HindII and NcoI were also analysed, but as seen in the triple digest, whilst there might have been some identifiable fragments (for example the triplet at ~5 kb in the NcoI digest), the majority of these patterns did not match the predicted patterns of bands. The same digest analysis was performed on the other '*Puma*' BAC clone (bmQ-207e13) with similar results. At this point the idea to use the 5.9 kb NcoI-NcoI BAC restriction digest fragment as the Puma left arm of homology was abandoned in favour of returning to a PCR-based strategy.

In order to establish whether the *Puma* left arm region was present within either of the '*Puma*' BAC clones, several additional primers were designed. These additional primers would be expected to produce smaller PCR products (< 1 kb) and hence the PCR reactions should be more efficient and the products easier to amplify. Indeed it was possible to detect a few correctly sized PCR products using these new primers; however some regions (including the central 1.4 kb) still failed to amplify products of the expected size (see Figure 3.3.24). We therefore designed additional primers in order to break up the problematic section of DNA into easier to manage smaller sections, with the ultimate aim being to 'stitch' (ligate) the smaller DNA products together by fusion PCR and recreate the required 4 – 5 kb for the arm of homology.

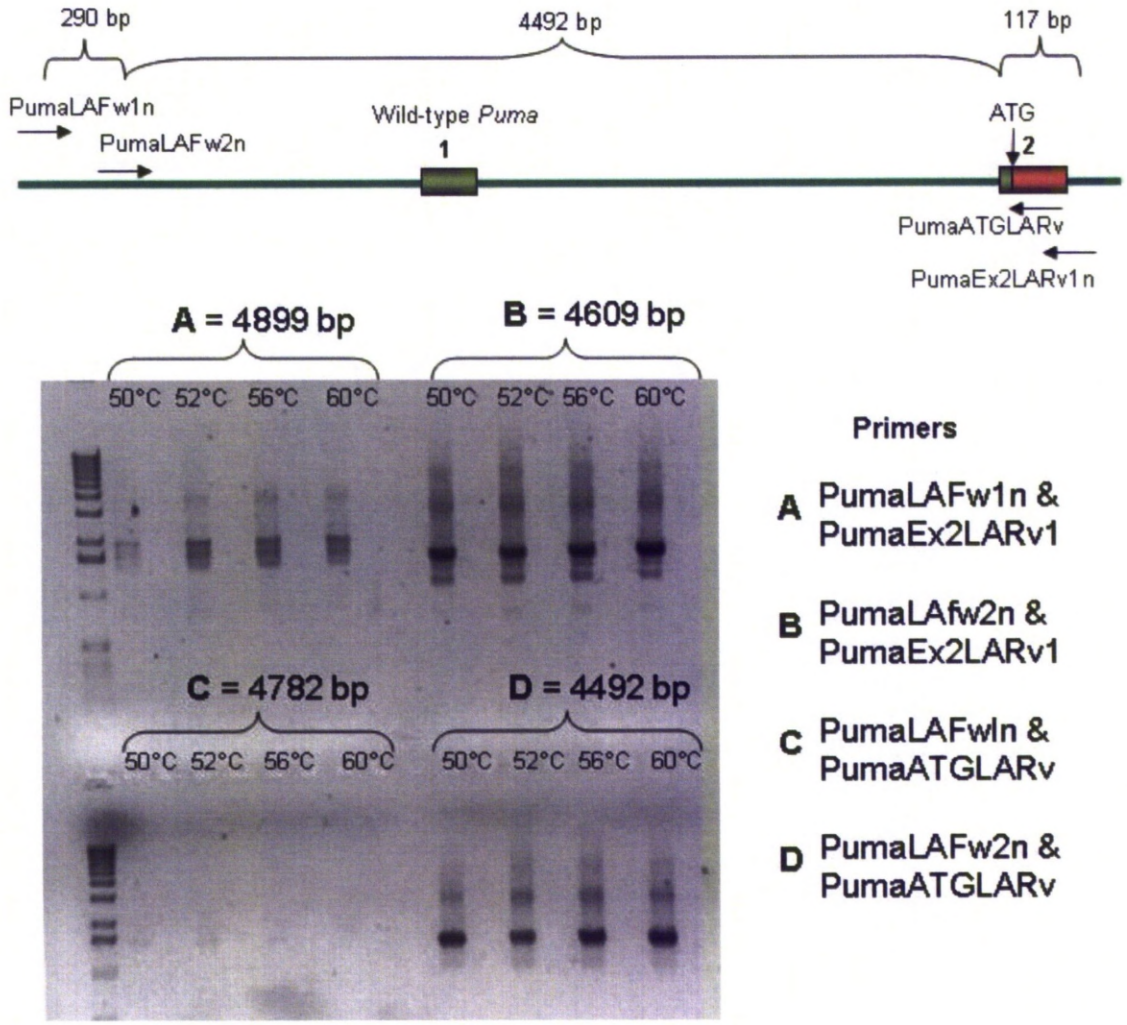


***Figure 3.3.22: Long range PCR of the Puma left arm of homology.***

*Top panel shows a schematic diagram of the Puma left arm of homology and the primer annealing sites. Bottom panel shows the PCR results. Agarose gel lanes were loaded from PCR reactions +/- template DNA (bmQ-397h22) for each annealing temperature (50-60°C). None of the PCR reactions attempted here (A-D) showed products of the expected size. PCR reactions shown here were performed using Phusion (Hot Start) DNA polymerase and the GC rich buffer, for 30 cycles.*

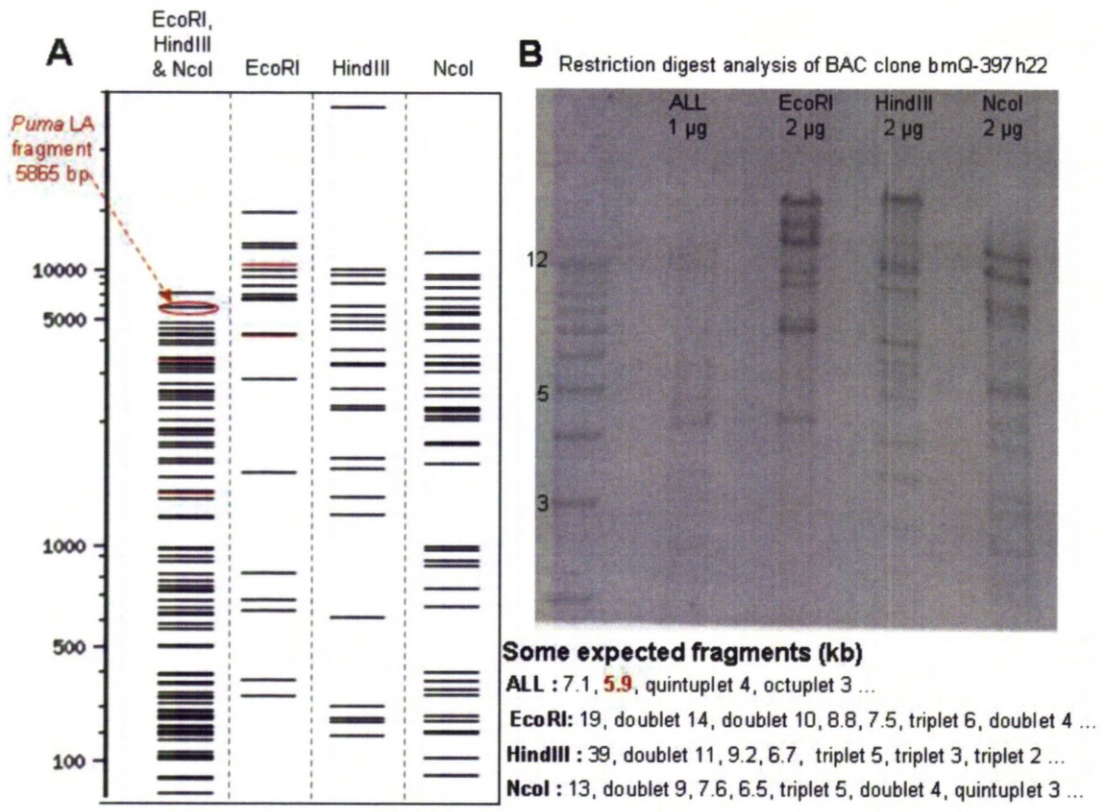


***Figure 3.3.23: Puma BAC clone bmQ-397h22 restriction digests analysis***

*A) In silico digest of the 119 kb BAC clone DNA for restriction enzymes EcoRI, HindIII and NcoI. B) Actual digest pattern observed for the same restriction enzymes when 1 or 2 µg of BAC clone DNA was digested overnight and resolved slowly by agarose gel electrophoresis. It was hoped to be able to identify the 5.9 kb NcoI-NcoI fragment to use as the Puma left arm of homology however the digest patterns did not appear as expected.*

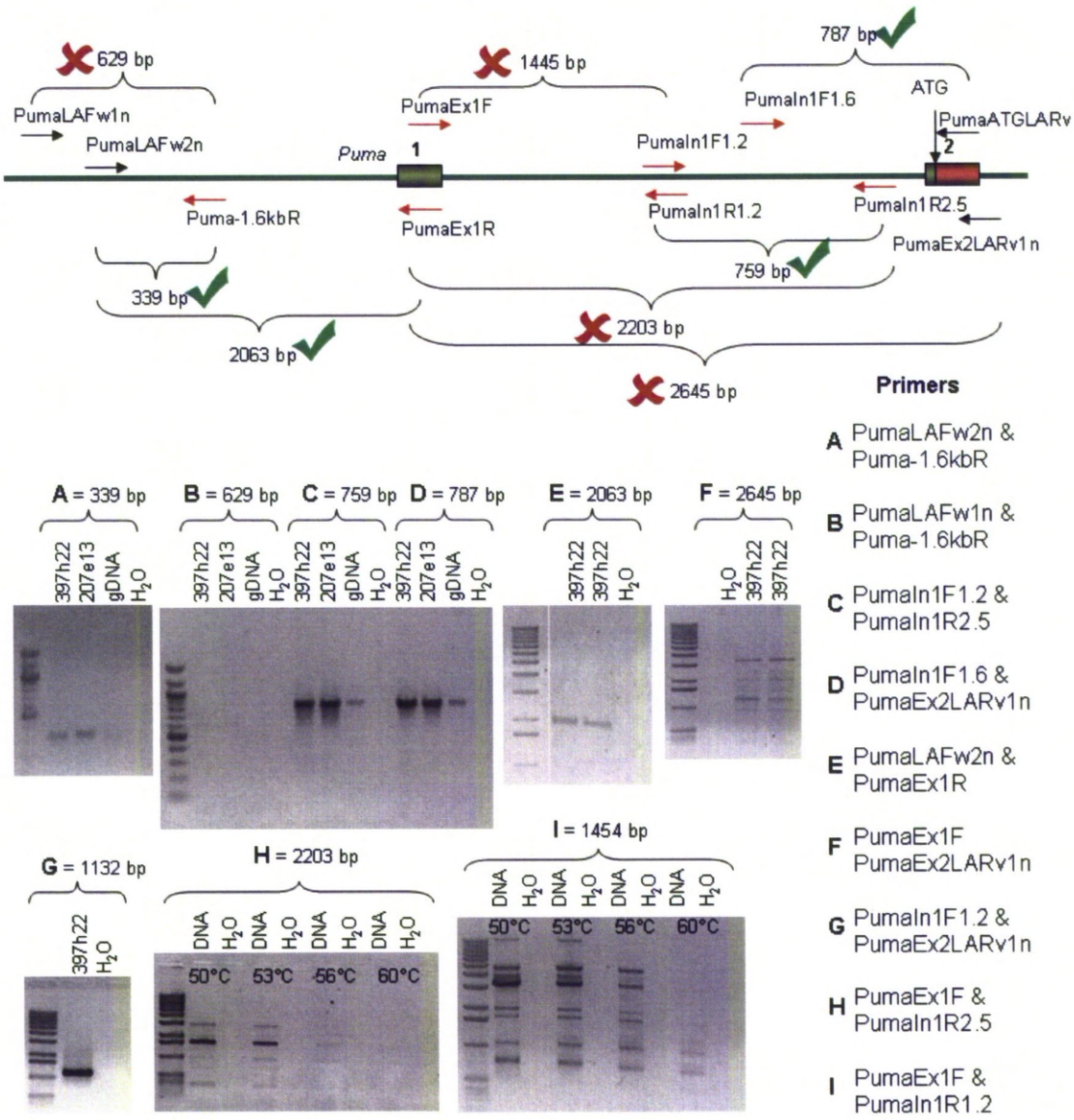


***Figure 3.3.24: PCR of the Puma left arm of homology – 1***

*Top panel: Schematic diagram of the Puma left arm of homology region, with primer alignments. New primers (red arrows) were designed in order to amplify smaller PCR products (< 1 kb) to determine if PCR within the Puma left arm region was possible (since previous long range PCR had failed). Ticks and crosses indicate whether that primer pair produced a correctly sized product. Bottom panel: PCR results, example agarose gels for the 9 PCR reactions (A-I). Successful PCR reactions (A, C, D, E & G) amplified a single DNA fragment of the correct size. Unsuccessful PCR reactions (B, F, H & J) either produced no product or multiple non-specific fragments. PCR reactions were performed with either BAC clones bmQ-397h22, bmQ207e13, genomic DNA (gDNA) or $H_2O$.*

The difficult to PCR, 1.4 kb DNA region situated immediately downstream of *Puma* exon 1, was eventually amplified by dividing the region into three smaller sections as shown in Figure 3.3.25. The trickiest PCR product to obtain was the middle 355 bp region. This 355 bp fragment required very strict PCR reaction conditions in order to produce the correct sized product with a reasonable yield and without too many non-specific bands contaminating the agarose gel (see Figure 3.3.25 – C and Appendix B for reaction conditions). One reason for the difficulty in amplifying DNA from the *Puma* left arm region may be the increased GC content (for the 355 bp section the GC content was 76%). High GC content can cause problems during PCR because of formation of secondary structures (such as hairpins) which may result in non-specific truncated products [Frey et al., 2008]. With the whole *Puma* left arm region now able to be amplified by PCR in sections the task of fusing all the separate PCR fragments together could now be completed.

Fusion PCR was performed according to the reaction scheme detailed in Figure 3.3.26. For the most part this proceeded as expected however there were some minor complications which are detailed next. The first potentially problematic observation was that the sequencing data for the *Puma* locus did not match with the C57BL/6 genomic DNA database. There were 52 mutations in the non-coding DNA sequence, including 28 base pair substitutions, 9 deletions, 9 insertions and 6 changes at microsatellite regions. This relatively frequent variability in the DNA sequence was also observed when we sequenced the 4.5 kb *Puma* right arm of homology. In the *Puma* right arm of homology there were 53 mutations in the non-coding DNA sequence including 27 base pair substitutions, 6 deletions, 12 insertions and 8 changes at microsatellite regions. These observed differences might be explained by mouse strain variation since we used *129SvEv* genomic DNA and not C57BL/6 which was the strain the reference assembly database was based on. To provide more convincing evidence that that was indeed the case, multiple clones for each PCR product were sequenced (typically 2-3). Therefore, since sequence analysis from multiple clones agreed with the observed changes we concluded that these differences were genuine for the *129SvEv* mouse strain and were not introduced by PCR. The amended *129SvEv* consensus genomic DNA sequence for both the *Puma* left and right arm of homology is included in Appendix D.3 & D.4.

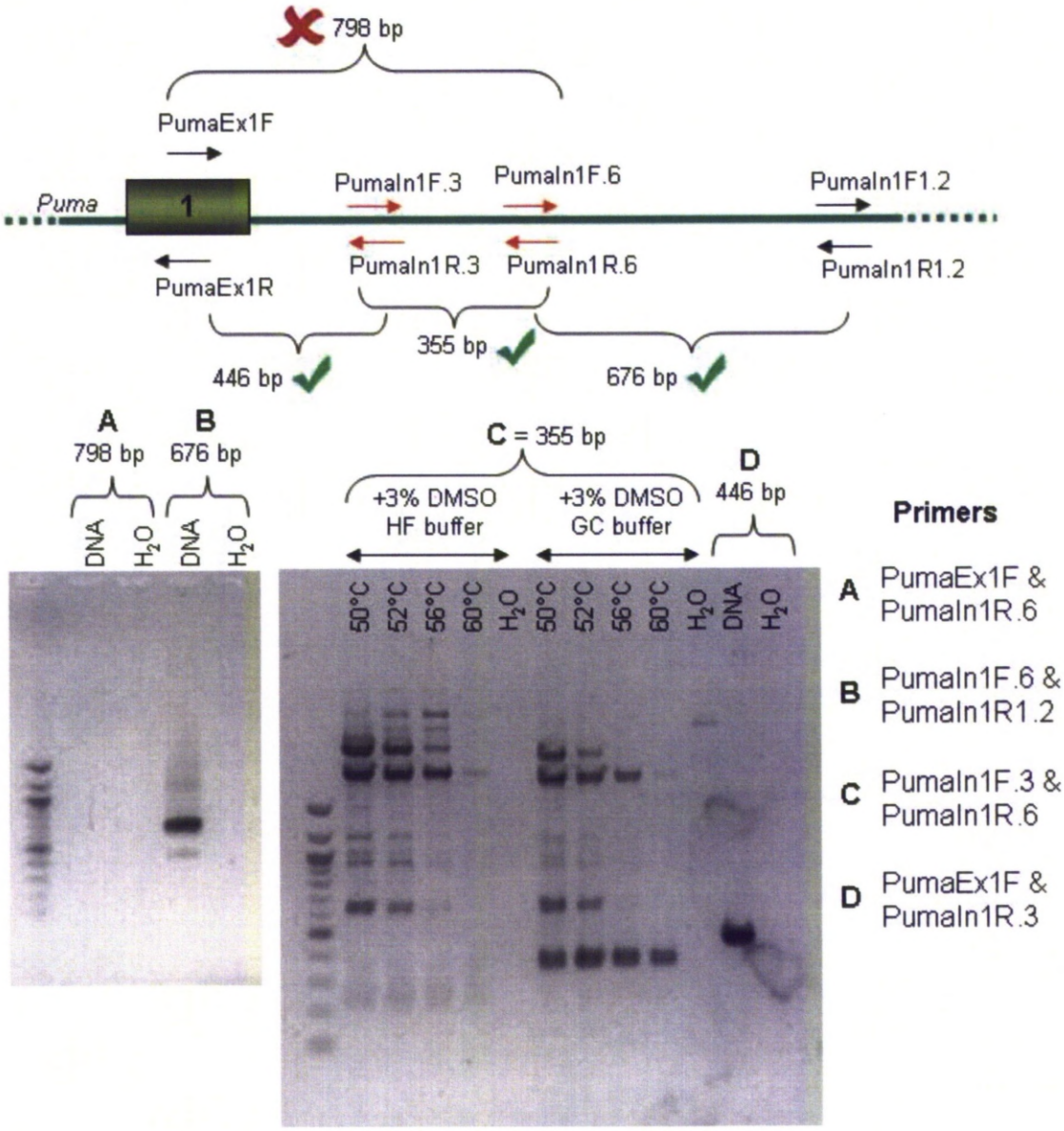


***Figure 3.3.25: PCR of the Puma left arm of homology – 2***

*Top panel: Schematic diagram of the 1.4 kb DNA region immediately downstream of Puma Exon 1, with primer alignments. Since previous primers (black arrows) had been unable to amplify this difficult region, new primers (red arrows) were designed in order to break it into easier to manage smaller sections. Bottom panel: PCR results, example agarose gels for the 4 primer pairs (A-D). Primer pair A failed to product a correct sized product so the 5' 798 bp region was further divided into two smaller fragments of 446 & 355 bp (D & C respectively). D produced a single DNA fragment of the expected size whilst C required additional optimisation (use of GC rich buffer + 3% DMSO) to generate the desired fragment. PCR Reactions were performed with BAC clone bmQ-397h22 DNA.*

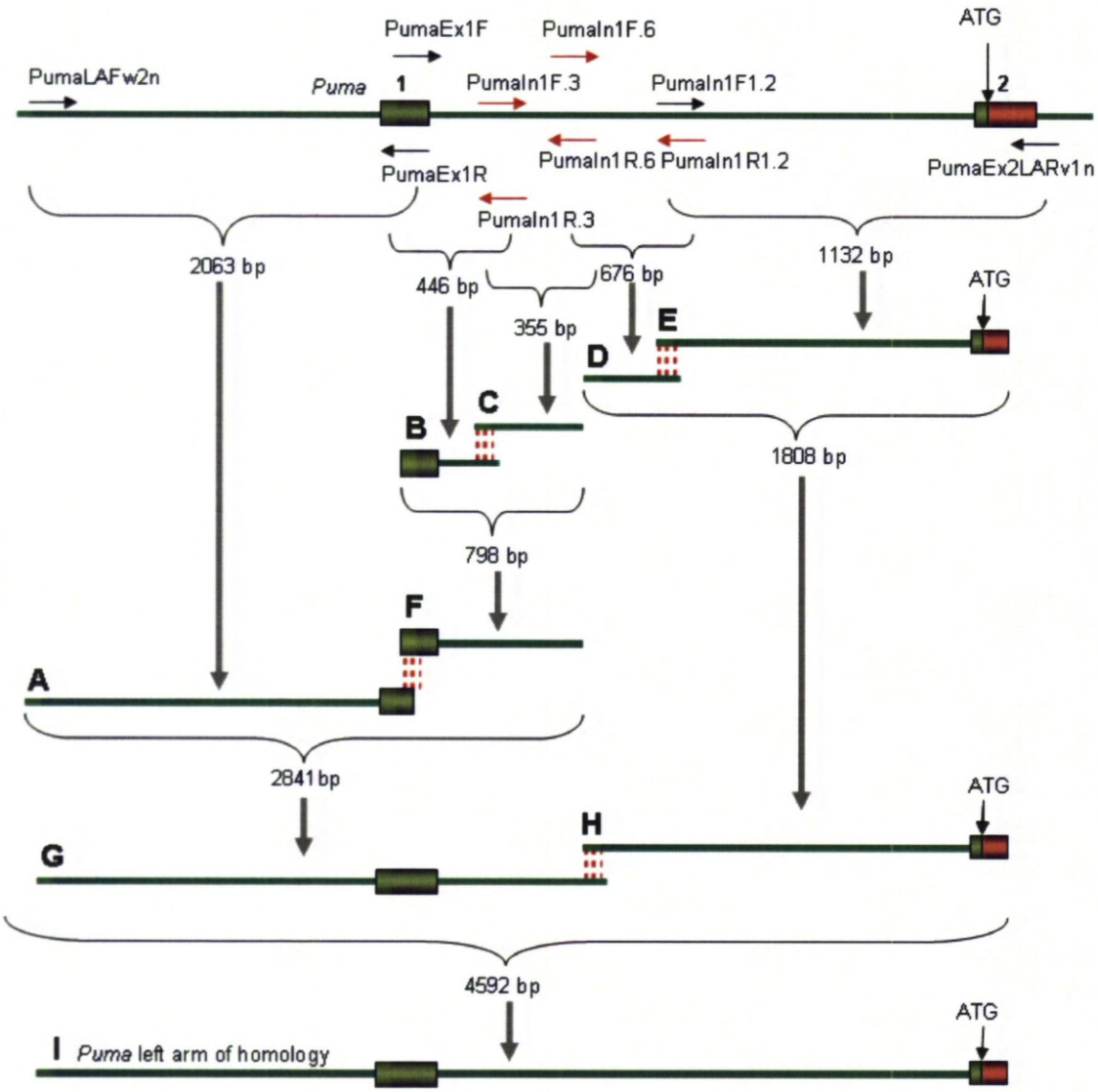


***Figure 3.3.26: Fusion PCR of the Puma left arm of homology.***

*Schematic diagram of each individual PCR reaction performed to construct the 4.6 kb Puma left arm of homology. Almost all PCR products were TA-cloned into either pCR2.1 (product < 2.1 kb) or pCR-XL-TOPO (product > 2.1 kb) and then sequenced, before being used as the template DNA for their next round of PCR. The exceptions to this were the PCR products B & C which were gel purified and used immediately as DNA templates in the fusion PCR reaction which produced PCR product F. Product F was then cloned and sequenced as for the other products. Dotted red lines indicate areas of sequence overlap (typically 20 bp) which were used as the anchors for fusion PCR. Bacterial colonies were screened initially by restriction digest with EcoRV & SpeI, which excised the PCR product from the vector backbone, and then by sequencing.*

The other minor complication during fusion PCR of the *Puma* left arm of homology was a 30 – 100 bp deletion which was detected when the PCR products A and F were fused together to generate PCR product G (see the overview in Figure 3.3.26). The deletion was present in the *Puma* promoter region just upstream of exon 1, where the p53 REs are situated. Since the first cloning attempt only produced two bacterial colonies, both of which contained deletions in this region (50 bp and 100 bp), this fusion PCR step was repeated. On the second attempt, more colonies were generated (60 +) and 10 of these were screened by restriction digest with EcoRV and SpeI to excise the 2841 bp PCR product G. Resolution of these restriction fragments was facilitated by extended agarose gel electrophoresis in order to distinguish between clones which might have a deletion (see Figure 3.3.27). Using this screen 3/10 clones appeared to contain a larger insert fragment and so these clones were sent for sequencing. Whilst one of these clones contained a 30 bp deletion the other two appeared correct therefore one of these was used as the template DNA for the final fusion PCR reaction which successfully generated the full 4.6 kb *Puma* left arm of homology (see Figure 3.3.28).

Once the *Puma* left arm of homology had been cloned into pCR-XL-TOPO and its sequence confirmed, there was one last additional cloning step to make this vector ready for assembly with E2Crimson. Fortuitously, the *Puma* start codon and the E2Crimson start codon, both contain NcoI (CCATGG) sites. We therefore intended to assemble the *Puma* left arm of homology in frame with E2Crimson without performing any additional fusion PCR. However since both vector backbones pCR-XL-TOPO and pCR2.1 (into which E2Crimon would be cloned – see Section 3.3.4.2) contained several NcoI sites a different vector would be needed. pBluescriot II SK+ was chosen since it did not contain any NcoI sites and had other restriction sites suitable for vector assembly. The 4.6 kb *Puma* left arm of homology was then moved from pCR-XL-TOPO into pBluescript II SK+ via using mutual EcoRV and HindIII sites (see Figure 3.3.29). 10/10 bacterial colonies were positive by EcoRV and HindIII restriction digest analysis. These vectors (PumaLASK+) were all suitable for use in the next downstream cloning step.

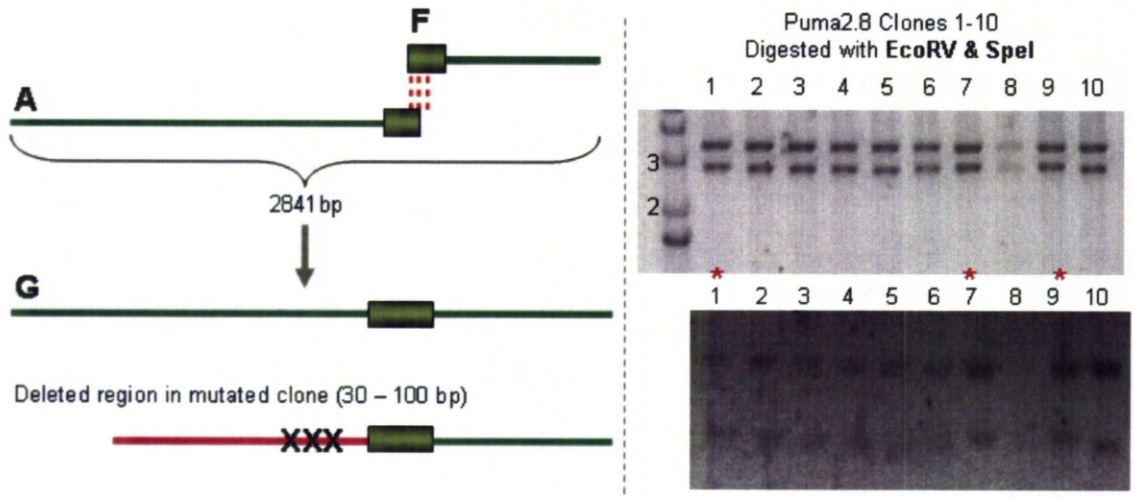


***Figure 3.3.27: Penultimate fusion PCR step for the Puma left arm of homology.***

*Left panel: Schematic diagram of the penultimate fusion PCR reaction. Previous PCR products A and F were amplified together (with appropriate end primers – not shown here) to generate the 2841 bp PCR product G – taken from the overview in Figure 3.3.26. Right panel: Since there was a known problem with a 30 -100 bp deletion within PCR product G, recombinant clones were screened by restriction digest with EcoRV & SpeI and the fragments were allowed to separate until a difference in the size of the insert fragment was noticeable. *These clones were sent for sequencing.*

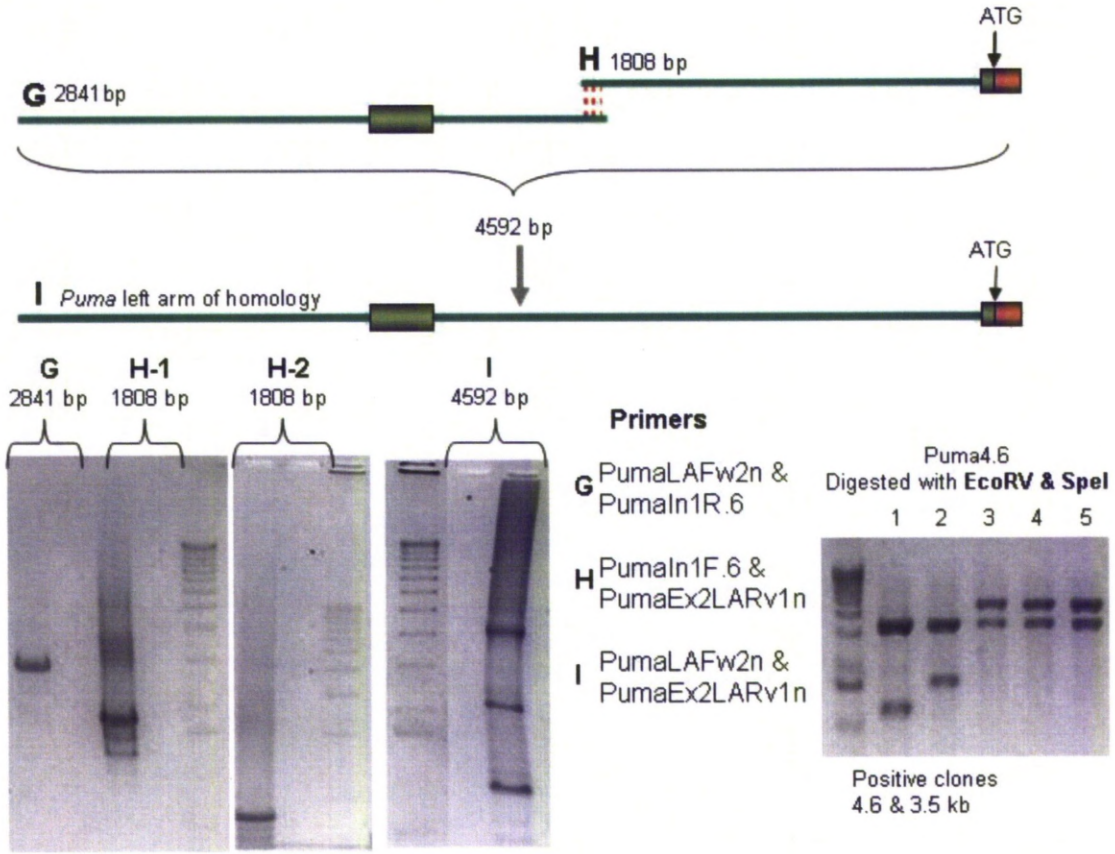


***Figure 3.3.28: Ultimate fusion PCR step for the Puma left arm of homology***

*Top panel: Schematic diagram of the ultimate fusion PCR step to generate the Puma left arm of homology. Bottom panel (left): PCR reactions for the two starter products G and H (as annotated in Figure 3.3.26). Since there were some non-specific products contaminating H, this reaction was separated by agarose gel electrophoresis until the contaminating lower molecular weight DNA fragments had been run off the bottom of the gel (H-2). I, the final round PCR product also had some non-specific products; however the desired 4.6 kb was also present. Bottom panel (right): Gel purified PCR product I was then TA-cloned into pCR-XL-TOPO and the resulting colonies were screened by restriction digest with EcoRV and SpeI. 3/5 products appeared positive and one was selected for sequencing (Puma4.6-5).*

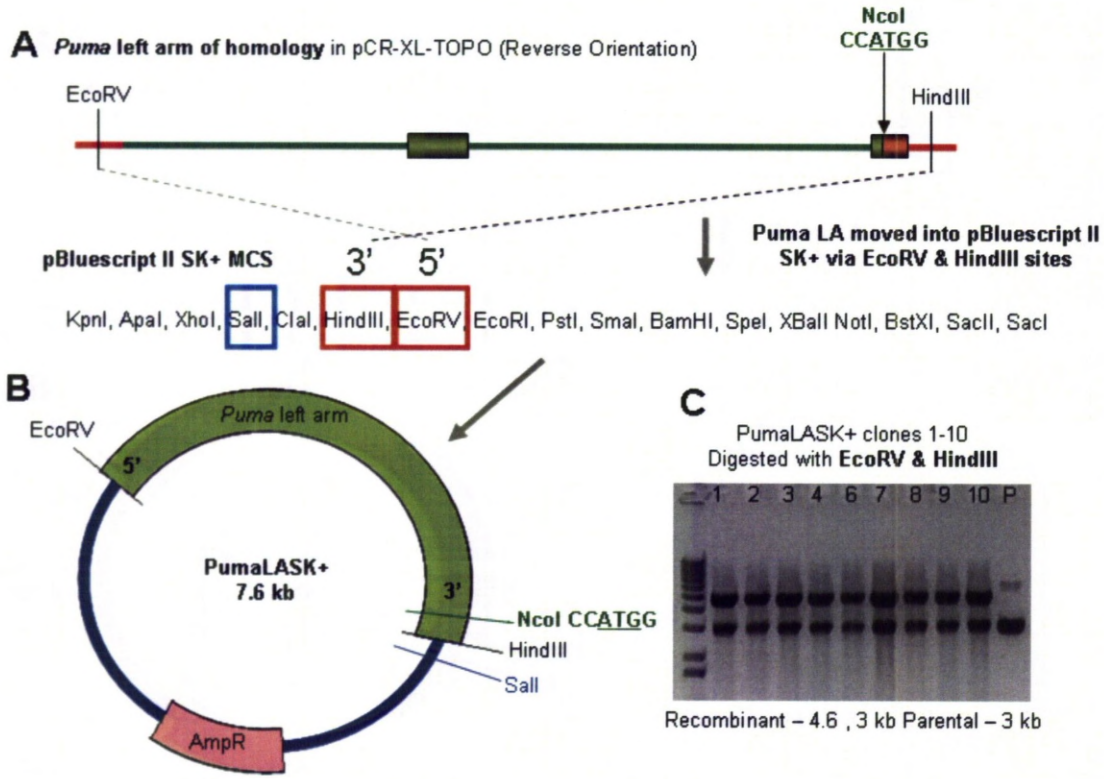


***Figure 3.3.29: Cloning of the Puma left arm of homology into pBluescript II SK+.***

*A) Schematic diagram of the Puma left arm of homology and the multiple cloning site of pBluescript II SK+. The 4.3 kb Puma left arm region was moved from its pCR-XL-TOPO backbone into pBluescript II SK+ via their mutual EcoRV and HindIII sites. There was also a downstream SalI site for the subsequent cloning steps. B) The resulting vector PumaLASK+ and C) restriction digest analysis of bacterial clones. 10/10 clones appeared positive by digestion with EcoRV and HindIII.*

### 3.3.4.2 *E2Crimson*

Cloning of *E2Crimson* for the *Puma*-E2Crimson DNA targeting construct was relatively straightforward since the template DNA already contained a poly A signal (unlike mCherry – see Section 3.3.3.4) and a 5' NcoI site for in-frame fusion with the upstream *Puma* sequence. Therefore only the 3' AscI-SalI restriction sites needed to be appended onto E2Crimson before it could be used in the final construct assembly. This was performed by PCR mutagenesis using the pE2-CrimsonN1 vector as the template DNA and the primers CrimsonF and CrimR+AscI-SalI (see Figure 3.3.30). The resulting 1 kb PCR product was then TA-cloned into pCR2.1 and recombinant bacterial clones were screened by restriction digest analysis with EcoRV and HindIII. 6/10 clones appeared positive and one (Crim9) was sent for sequencing. The sequencing results matched 100% with the expected sequence and therefore this clone was ready for the next stage of cloning.

### 3.3.4.3 *Fusing the Puma left arm of homology in frame with E2Crimson*

In order to avoid an additional round of fusion PCR which would require optimisation and then further sequencing, we instead planned to take advantage of the naturally occurring NcoI site at both the start codons of *Puma* and *E2Crimson* to combine the cloned products in these vectors. E2Crimson was therefore inserted into PumaLASK+ via their mutual NcoI and SalI sites to create the vector PumaLACrimSK+. The resulting recombinant clones were screened for successful introduction of E2Crimson by restriction digest with NcoI and SalI. 10/10 colonies appeared positive and any one of these would be suitable for the next stage of cloning.

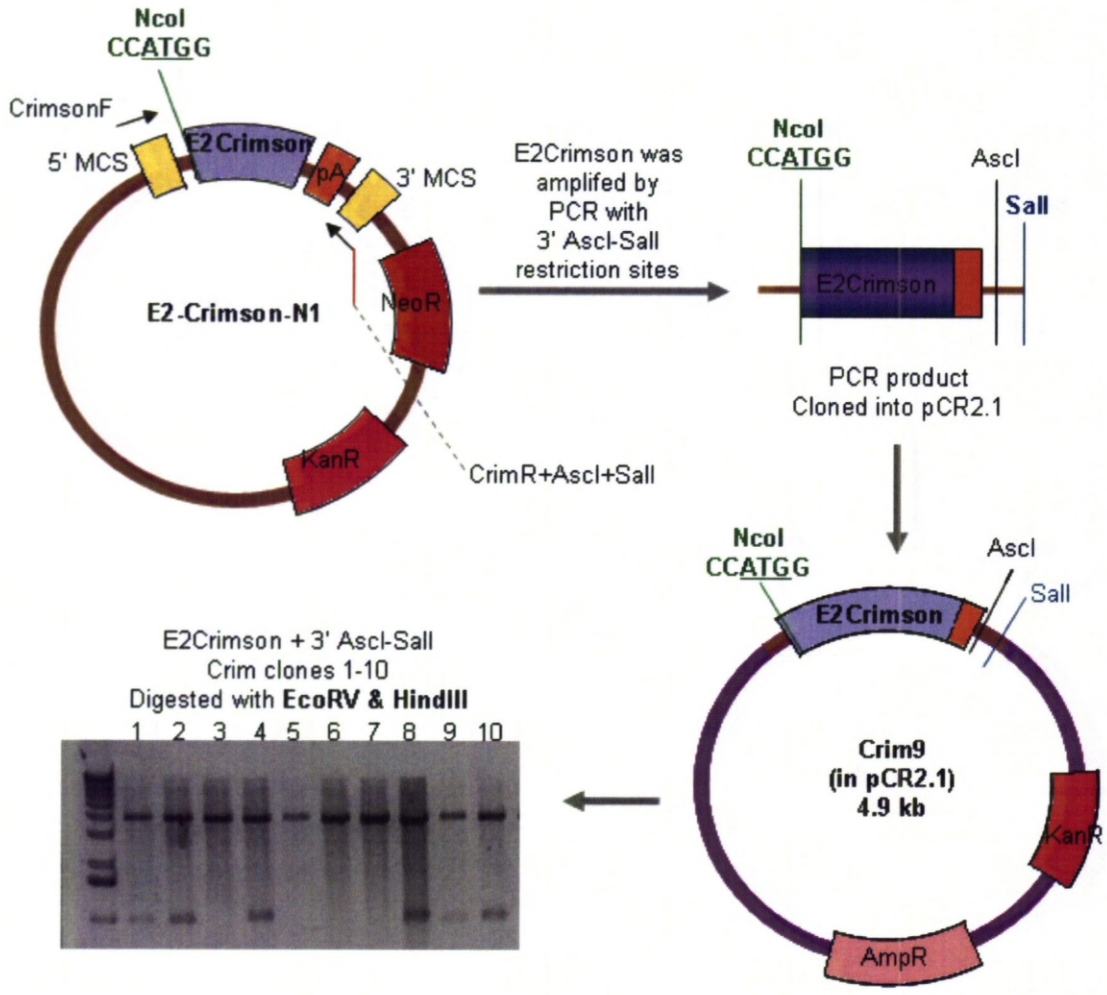


***Figure 3.3.30: Cloning of E2Crimson.***

*Schematic diagram of the cloning plan for E2Crimson: 3' AscI-SalI restriction sites were appended to the 3' end by PCR mutagenesis and the resulting PCR product was TA-cloned into pCR2.1. Bacterial transformants were screened for the 1 kb E2Crimson insert by restriction digest with EcoRV and HindIII. 6/10 clones appeared positive (Crim- 1-2, 4, 8-10) and one of these was sent for sequence analysis (Crim9).*

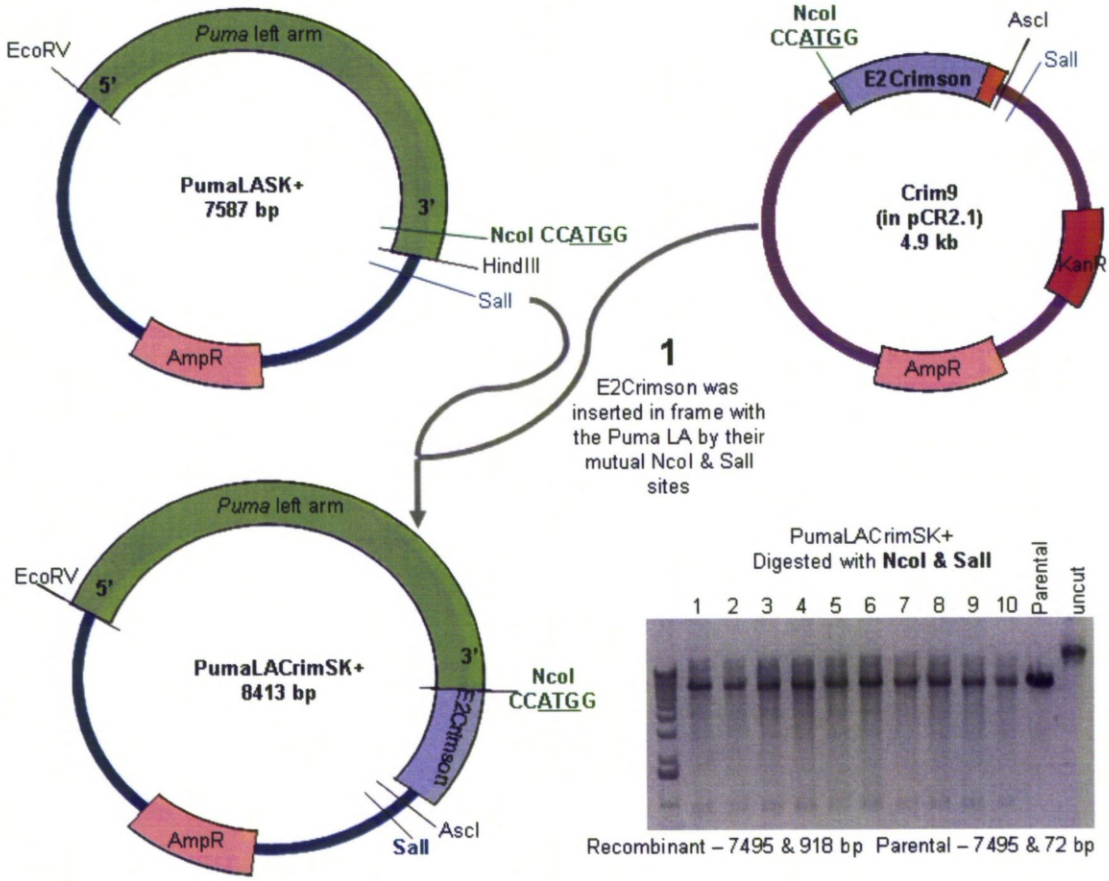


***Figure 3.3.31: Cloning E2Crimson in-frame into the Puma left arm of homology.***

*E2Crimson was cloned in-frame with the endogenous ATG site in Puma exon 2 by taking advantage of the naturally occurring NcoI site in the initiation codons of both of these genes. The 1 kb NcoI-SalI DNA fragment from Crim9 was cloned into the same sites in PumaLASK+. Positive clones were identified by a restriction digest with NcoI and SalI. All clones shown here appeared positive.*

### 3.3.4.4 *Puma* right arm of homology

The *Puma* right arm of homology contained 4.5 kb of *129SvEv* genomic DNA which commenced 719 bp into *Puma* intron 3 and ended 788 bp downstream of *Puma* exon 4 (see Figure 3.3.32). This region was cloned by two rounds of PCR similar to the method used to generate the *p21* left arm of homology (see Section 3.3.3.3). The resulting vector (PumaRA+SalI2) contained the 4.5 kb region of homology and 5' 20 bp of sequence overlap with the NeoB3 vector (containing the Cre/Neo$^R$ cassette – described in Section3.3.3.6) and a 3' SalI site. The 20 bp of Cre/Neo$^R$ overlap was included since originally we had planned to join the *Puma* right arm of homology with the Cre/Neo$^R$ by fusion PCR. This original plan was later amended to avoid unnecessary PCR steps and is discussed in the next section. Cloning of the *Puma* right arm of homology was quite straightforward and progressed smoothly with only one minor issue concerning high sequence variation from the C57BL/6 genomic database which was resolved following sequencing of additional clones (discussed in detail in Section 3.3.4.1).

### 3.3.4.5 *Fusing the positive selectable marker (Cre/Neo$^R$) with the Puma right arm of homology*

The Cre/Neo$^R$ cassette from vector NeoB3 (described in Section 3.3.3.6) was inserted into the 5' EcoRV site in the vector PumaRA+SalI-2 by blunt ended cloning (see Figure 3.3.33). Since the *Puma* right arm of homology (clone PumaRA+SalI-2) had recombined into pCR-XL-TOPO in the reverse orientation this meant the EcoRV site in the vector backbone was at the 5' end of the cloned sequence and hence could be used to insert the Cre/Neo$^R$ cassette upstream. In order to excise the 3.8 kb Cre/Neo$^R$ cassette from NeoB3, a triple digest was performed with KpnI, NotI and ZraI. KpnI and NotI were sufficient to excise the positive selectable marker however since the backbone was a similar size at 3.5 kb contamination was a likely problem. Therefore, ZraI was also included in the digest since this enzyme cleaved the pCR-XL-TOPO backbone approximately in half and hence would allow better resolution of these fragments during agarose gel electrophoresis.

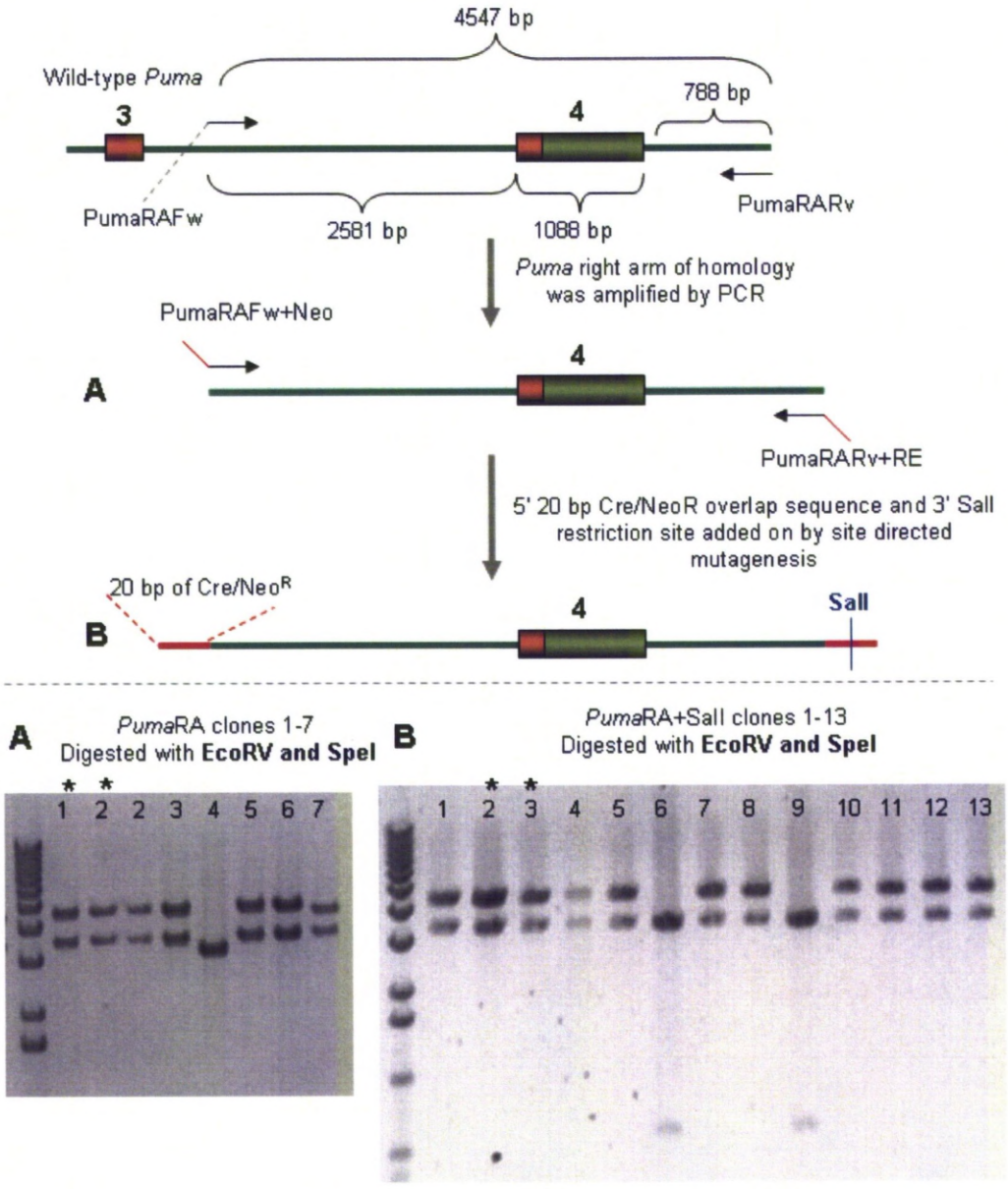


***Figure 3.3.32: Cloning of the Puma right arm of homology.***

*Top panel: Flow diagram for cloning the 4.5 kb DNA fragment of the Puma right arm of homology by PCR. PCR was performed using the BAC clone bmQ-397h22 DNA as a template. The first stage amplified the Puma right arm only. This product (A) was TA-cloned into vector pCR-XL-TOPO, screened by restriction digestion and then sequenced. Once the sequence was confirmed in two separate bacterial clones the second round of PCR was performed. The second round of PCR annealed 5' '20 bp overlap sequence to Cre/Neo$^{R}$' & 3' SalI restriction site to generate PCR product B. B was then TA-cloned into vector pCR-XL-TOPO, screened by restriction digest and sequenced. Bottom panel: corresponding restriction digests. *These clones were sent for sequencing.*

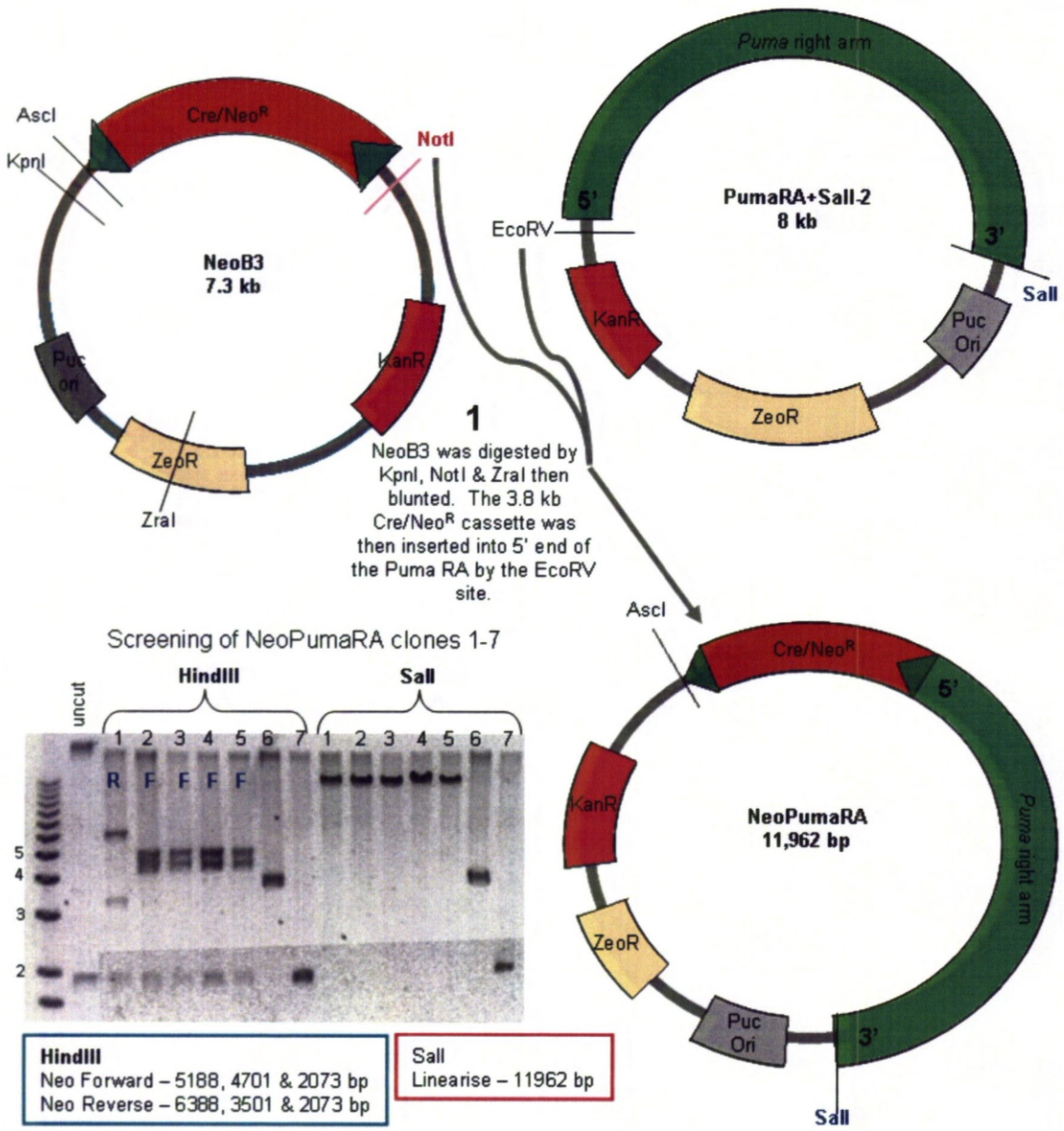


***Figure 3.3.33: Cloning the Cre/Neo$^R$ cassette into the Puma right arm of homology.***

*The Cre/Neo$^R$ cassette was inserted into the EcoRV site in the PumaRA+SalI-2 vector by blunt end cloning. The resulting bacterial clones were screened by restriction digest analysis with HindIII – which could determine the orientation of Cre/Neo$^R$ (see blue box for expected restriction digest fragment sizes). 4/7 clones contained the Cre/Neo$^R$ cassette in the correct (forward) orientation. A second digest with SalI was also performed to confirm the vector size.*

Since blunt ended cloning was used, insertion of the Cre/Neo$^R$ cassette into the *Puma* right arm of homology could occur in either orientation, however for downstream cloning steps we required only the forward orientation. The resulting bacterial clones therefore were screened with HindIII which could determine the orientation (see Figure 3.3.33). 4/7 clones were positive for Cre/Neo$^R$ in the correct (forward) orientation and one (NeoPumaRA-4) was selected for the final construct assembly.

### *3.3.4.6 Final construct assembly*

Assembly of the penultimate and ultimate *Puma*-E2Crimson cloning vectors was performed according to a slightly altered version of the original cloning plan (see Figure 3.3.4). In the new cloning plan, shown in Figure 3.3.34, the TK cassette was inserted into vector PumaLACrimSK+ first, rather than last and by blunt end cloning rather than directional cloning using FseI and PacI restriction sites. This was done because we had forgone an additional round of PCR which would have also appended 5' FseI-PacI sites to the *Puma* left arm of homology. Since the 5' FseI-PacI unique restriction sites were absent we utilised the 5' EcoRV site present in the pBluescript II SK+ backbone (see Figure 3.3.29) to insert the blunted TK cassette. The TK cassette had to be inserted prior to adding the Cre/Neo$^R$-*Puma* right arm of homology fragment because the Cre/Neo$^R$ cassette contained an EcoRV restriction site which would otherwise disrupt the cloning. Once the TK cassette was added, the 'Cre/Neo$^R$-*Puma* right arm of homology' fragment from vector NeoPumaRA was then inserted using the mutual AscI and SalI sites.

The TK cassette was excised from TK2 (Vector 1 see Figure 3.3.34) by digestion with restriction enzymes PacI and SalI. The digested TK fragment was then blunted and inserted into the EcoRV site in vector PumaLACrimSK+. SalI was used instead of FseI so that the SalI recognition sequence would be destroyed during cloning, thus maintaining the unique SalI site (3' to E2Crimson) required for the final stage of cloning. Orientation of TK should not matter for the purposes of gene targeting, however the only positive clone was in the forward orientation when screened by NcoI restriction digest and so this clone was used in the final cloning step.

The final cloning step for generation of the *Puma*-E2Crimson DNA targeting construct inserted the 'Cre/Neo$^R$-Puma right arm' fragment from NeoPumaRA (*Puma* Vector 3) into the TKPumaLACrim vector by their mutual AscI and SalI sites. The resulting bacterial clones were screened by both NcoI and NotI restriction digests to doubly confirm positive clones (see Figure 3.3.35). 5/10 colonies appeared positive and one of these (PumaU-6) was sent for further sequencing to confirm the DNA sequences at the cloning junctions between the assembly vectors and at important locations such as the *Puma* left arm of homology into *E2Crimson*. The clone PumaU-6 was confirmed in this way to represent a full and accurate DNA targeting construct for the generation of a *Puma*-E2Crimson knock-in transgenic reporter mouse suitable for use in gene targeting of ES cells.

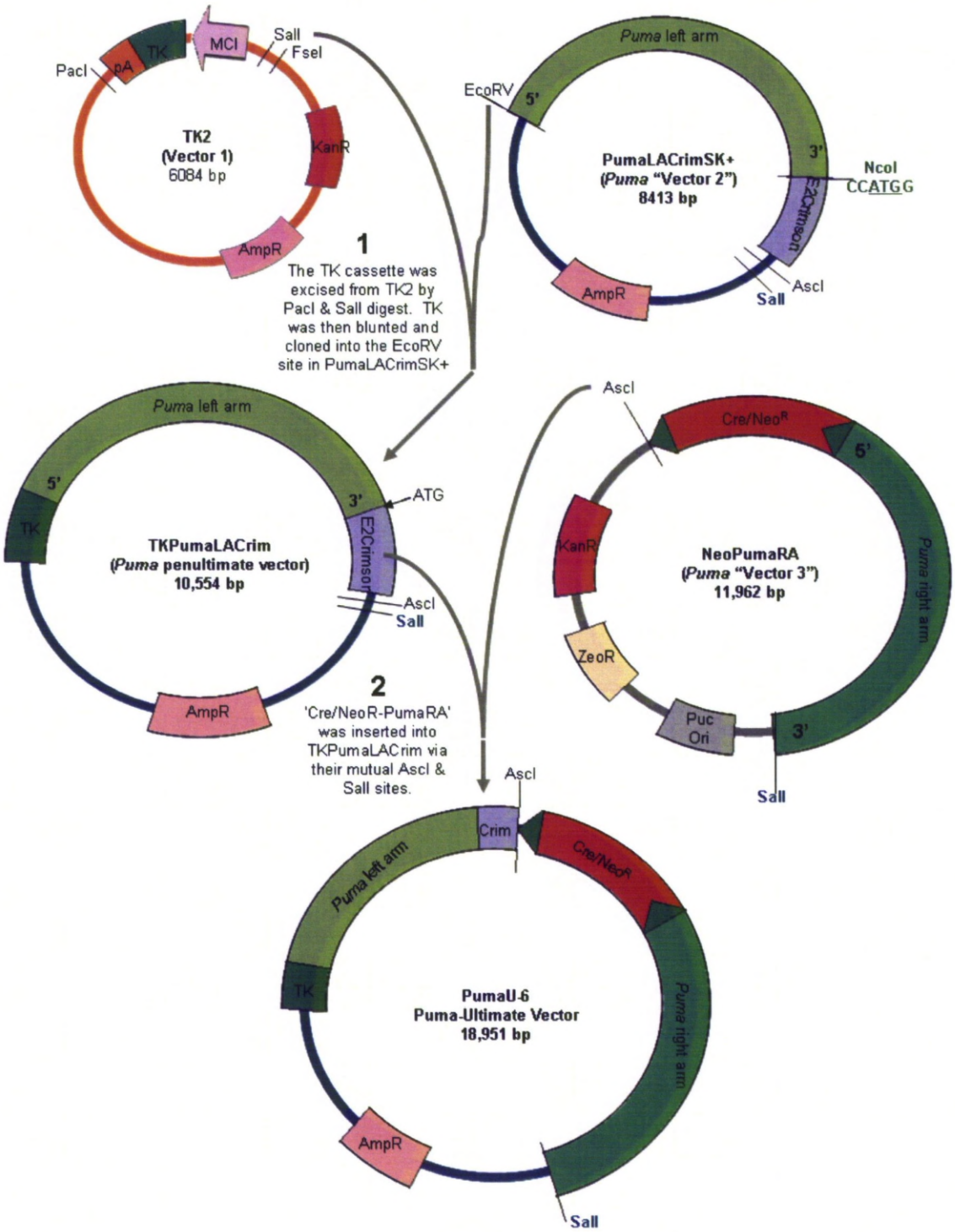


***Figure 3.3.34: Final assembly of the Puma-E2Crimson DNA targeting vector.***

*1. The negative selectable marker (TK) was inserted into the 5' EcoRV site in PumaLACrimSK+ by blunt end cloning. 2. Lastly the 'Cre/Neo$^R$-Puma right arm' fragment was inserted into the resulting vector TKPumaLACrim using the mutual AscI and SalI sites.*

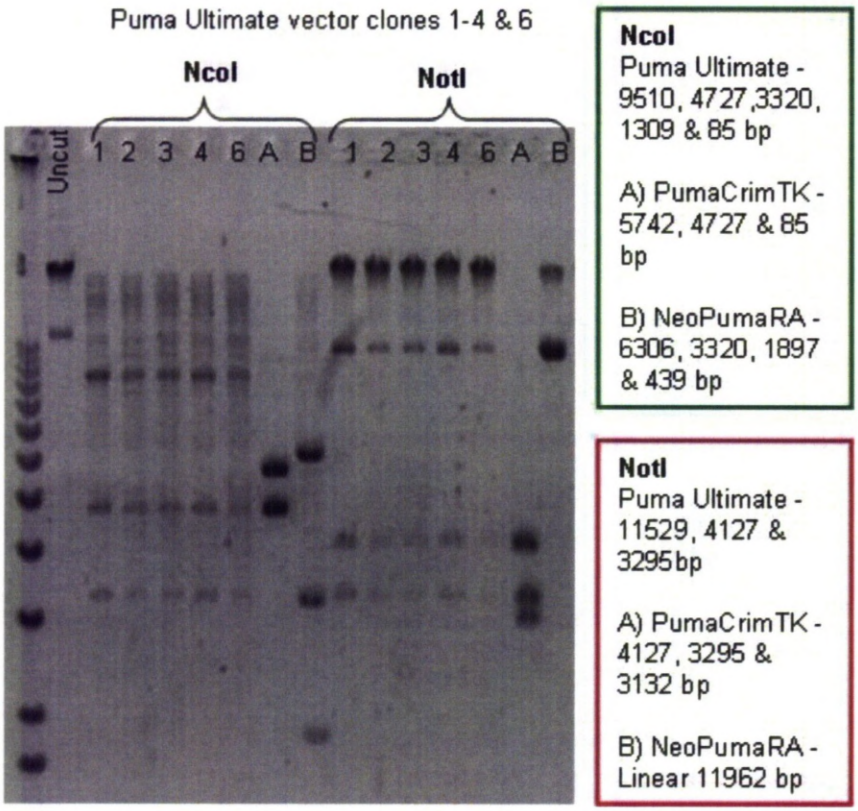


***Figure 3.3.35: Cloning of the ultimate Puma-E2Crimson DNA targeting construct.***

*Restriction digest analysis of potential clones by NcoI and NotI. 5/5 appeared positive for insertion of the Cre/Neo$^R$ cassette. Lanes A & B correspond to the parental plasmids TKPumaLACrim and NeoPumaRA respectively.*

## 3.3.5 Mdm2 Constructs

In order to address fundamental questions regarding the regulation of *p53* and *Mdm2* *in vivo*, we proposed to generate two strains of transgenic mice which would contain either a deletion in the *Mdm2* constitutive (P1) promoter or mutate the p53 RE within the p53-responsive *Mdm2* (P2) promoter (as discussed in Section 1.4.2). The first of these strains (*Mdm2* P1-Null) will determine if constitutive/p53-independent up-regulation of *Mdm2* is essential for viability whilst the second strain (*Mdm2* P2-Mutant) will determine if inducible/p53-dependent up-regulation of *Mdm2* is essential for viability. In other words can the deletion of either one of these promoter regions be rescued/compensated for by the remaining promoter region? Additional studies of these strains would also reveal (if viable) the contributions of these processes, p53-dependent and p53-independent, with regards to the role(s) of *Mdm2* in normal development, tumour susceptibility and in response to a wide variety of cellular stresses. This results chapter describes the design and *in vitro* testing of each of these mutations followed by a description of the strategy that led to the successful cloning of the gene targeting constructs required for generation of the proposed transgenic mouse lines.

### *3.3.5.1 Design of Mdm2 promoter region mutations*

*Mdm2* is an important proto-oncogene, with both p53-dependent [Oliner et al., 1992] and p53-independent [Ganguli and Wasylyk, 2003] roles in carcinogenesis. Reflecting this, *Mdm2* has two promoter regions, including an upstream constitutive promoter (P1) and a p53-inducible (P2) promoter which is situated in intron 1 (as discussed in Section 1.4.2 and see Figure 3.3.37). Part of the work for this thesis then, was to investigate the relative contributions of each of these promoters to the regulation of *Mdm2* and in turn, on the Mdm2 negative regulation of p53. To accomplish this, we designed and created two DNA targeting constructs which would either delete the P1 region or mutate the p53 RE sequences in P2 to abrogate their p53 responsiveness. The design and *in vitro* testing of these mutations is described next.

During the *Mdm2* P1/P2 mutation design process, several important factors needed to be considered in order to generate the optimum mutational sequences – that is to introduce mutations which would effectively disrupt the desired promoter whilst leaving other features (such as other transcription factor binding sites) within the locus unaffected. The first consideration was whether there were any other genes (validated or hypothetical) at the *Mdm2* locus which might be affected by the planned introduction of mutations to the region. Disruption of genes other than *Mdm2* could confound interpretation of the results due to unintended non-specific affects. Originally when this project started in 2007, there was indeed a small (612 bp) hypothetical gene, EG668154, on the positive strand (*Mdm2* is on the negative strand) which overlapped with the *Mdm2* P2 promoter region. EG668154 had a predicted translation initiation codon within the p53 RE region and the predicted transcript ran until part way through *Mdm2* exon 1. The presence of this hypothetical gene greatly complicated the design of mutations within the P2 region since only base pair changes which did not affect the hypothetical amino acid sequence could be used. Fortunately however, part way through this project, the EG668154 gene record was withdrawn from the MGI and RefSeq databases. EG668154 had been originally identified by a computational analysis however during the process of curation of such hypothetical genes the judgement was made that EG668154 was not a gene and the record was discontinued in 2009 [email communication with MGI]. Therefore, since *Mdm2* did not appear to have any other *bona fide* overlapping genes and the nearest upstream gene was ~ 23 kb away we were fairly confident that any mutations we introduced would only affect the *Mdm2* gene (see Figure 3.3.36). The P1/P2 specific design aspects are discussed next.

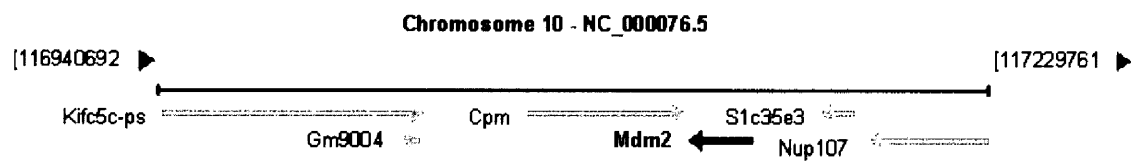


***Figure 3.3.36: The genomic context of Mdm2.***

*Section of chromosome 10 with the alignment of Mdm2 and other genes. No other genes overlap with Mdm2 and the closest 5' gene (S1c35e3) is ~ 23 kb upstream of Mdm2 exon 1. Image was exported from the NCBI website http://www.ncbi.nlm.nih.gov/gene/17246.*

Deletion of the *Mdm2* P1 promoter region was relatively simple in design (compared to the *Mdm2* P2-Mutant – discussed later in this section), since we intended to completely eliminate the functionality of P1 and were not concerned about retaining any specific features in this region. Therefore, to ensure maximum disruption of P1, the entire minimal essential region was deleted as well as the first 22 bp of *Mdm2* exon 1 (163 bp in total) (see Figure 3.3.37). This deletion would remove many of the conserved features between the mouse and human P1 promoter region including several GC rich regions, putative transcription factor binding sites and a CCAAT box [Phillips et al., 2006]. Since the transcriptional initiation site was also removed, even if there was somehow residual activity of the P1 promoter this should not be transcribed into mRNA. The P1 promoter region would be deleted by replacing the 163 bp region with a self-excision positive selectable marker (described in Section 3.3.5.3), therefore in the $F_1$ heterozygote mice (and all subsequent progeny) the P1 region will be replaced with 132 bp of spacer DNA which will include a single *LoxP* site (see Figure 3.3.38). The activity of the *Mdm2* P1-Null region was also assessed *in vitro* to confirm reduction in P1 activity and to check that deletion of P1 did not affect p53-dependent induction of the *Mdm2* P2 promoter (discussed in further detail in Section 3.3.5.2).

Disruption of the p53 responsive elements within the *Mdm2* P2 promoter region was slightly more complex, owing to the additional known and putative TFBS within the region (see Figure 3.3.39 and Figure 3.3.41). In order to create a P2-Mutant which was unresponsive to p53 but otherwise unaffected at the other TFBS, subtle point mutations were introduced. These point mutations, typically affecting the most conserved residues of the p53 consensus binding sequence, were analysed using the online MAPPER tool to help determine the optimum sequence (method described in Section 2.8.2). The optimum sequence (that is, the sequence that had the smallest number of mutations, which successfully prevented p53 binding whilst altering as few other TFBS within the region as possible) was derived and is shown in Figure 3.3.40. Whilst creating a P2 mutated sequence that did not introduce any changes other than deletion of the p53 RE was not completely achievable, the optimum sequence derived for this thesis only introduced 6 alterations and only 2 of these were in mammalian TFBS (see Table 3.3.2 and Figure 3.3.41). The two alterations in the mammalian TFBS were addition of an NFKB1 (also known as p50) site and

deletion of an ELK1 site. It would be theoretically possible to test the functionality of these sites by performing co-transfection experiments with the promoter regions ± murine *Nfkb1* or *Elk1* however since these predicted TFBS did not have a high alignment score and were from the human sequence models, rather than mouse, it seems unlikely to impact on the promoter region.

One final design consideration with the *Mdm2* P2-Mutant sequence is the incorporation of a restriction endonuclease site (or deletion of one) for screening purposes. Indeed, it was possible to introduce an NcoI site within the 13 bp spacer region between the two p53 RE sites, without compromising any of the previously optimised features (see Figure 3.3.40). The inclusion of an NcoI site, however does raise its own concerns, namely that creating an NcoI site (CCATGG) introduces an ATG site which aligns well with the Kozak consensus sequence (ACCATGG) [Kozak, 1978] and therefore it may potentially act as a translational initiation site. However, upon further consideration, this concern would appear to be unfounded since the NcoI site is within intron 1 and will be spliced out during mRNA processing. The *Mdm2* P2-Mutant sequence was also analysed by a splice site predictor tool (see Section 2.8.3) to ensure that we had not inadvertently simultaneously introduced a splice acceptor site which might enable alternative splicing of *Mdm2* and hence create an alternative transcript where the ATG introduced by the NcoI site could feasibly be utilised. Importantly, the only splice acceptor site recognised by either the wild-type or P2-Mutant *Mdm2* promoter region was the endogenous AG at the *Mdm2* intron 1 – exon 2 boundary. Therefore to the best of our knowledge *in silico* the *Mdm2* P2-Mutant promoter region effectively abrogates p53-responsiveness with minimal impact on the surrounding features. The activity of the *Mdm2* P2-Mutant promoter region was then examined *in vitro* along with the previously designed *Mdm2* P1-Null promoter region.

***Table 3.3.2: Alterations in the putative transcription factor binding sites (TFBS)...***

***...between the wild-type and mutant p53 RE region of the Mdm2 gene (+/- 40 bp).*** *Oryza sativa is Asian rice and Triticum aestivum is common wheat. The score value is a statistical measurement of how well the model matches the actual DNA sequence (the higher the value the higher the significance). The E (expect) value is a measure of how often it might be expected to see this sequence purely by chance hence the higher the value the lower the significance – compare with the genuine murine p53 RE sites.*

| Inserted or deleted? | Model | Factor | Strand | Start | End | Score | E-value | Species (gene) |
|---|---|---|---|---|---|---|---|---|
| Deleted | T01806 | p53 | + | 41 | 60 | 9.9 | 0.6 | *Mus musculus* |
| Inserted | MA0105 | NFKB1 | + | 50 | 60 | 2.9 | 7 | *Homo sapiens* (p50) |
| Inserted | MA0023 | DI_2 | - | 50 | 59 | 0.8 | 19 | *Drosophila melanogaster* (Dorsal_2) |
| Inserted | MA0105 | NFKB1 | - | 50 | 60 | 2.7 | 7.8 | *Homo sapiens* (p50) |
| Deleted | M00507 | TRAB1 | - | 50 | 59 | 3.1 | 7.7 | *Oryza sativa* |
| Deleted | T01098 | EmBP-1b | - | 54 | 59 | 2.4 | 20 | *Triticum aestivum* |
| Deleted | MA0028 | ELK1 | - | 56 | 62 | 2.2 | 14 | *Homo sapiens* |
| Deleted | T01806 | p53 | + | 79 | 98 | 8.9 | 1.2 | *Mus musculus* |

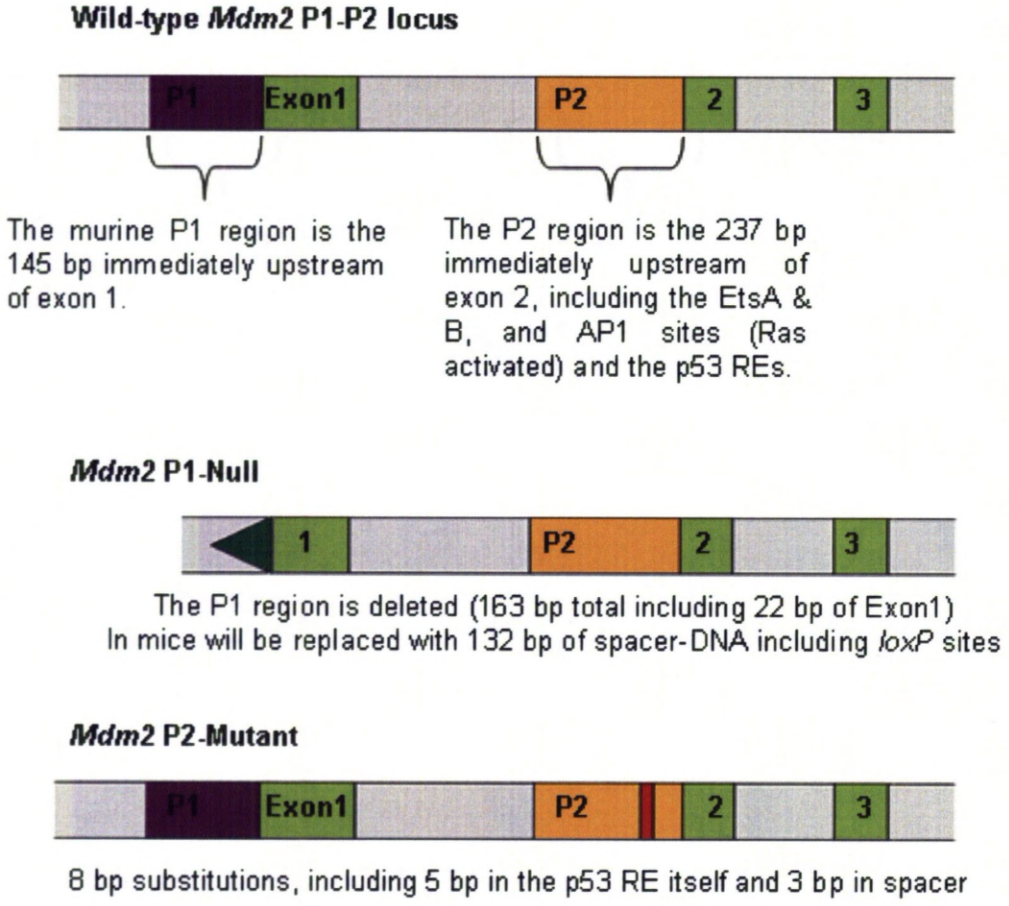


***Figure 3.3.37: Design of the Mdm2 promoter mutations.***

*Schematic diagrams of the wild-type, P1-Null & P2-Mutant Mdm2 promoter regions. The details of each region are described underneath each one. The Lox P site is shown as a green arrow head. The red stripe in the P2 region in the Mdm2 P2-Mutant represents the mutated p53 REs. The sequence detail and alignment of specific features of the wild-type, P1-Null and P2-Mutant promoter regions are shown in Figure 3.3.39, Figure 3.3.38 & Figure 3.3.40 respectively.*

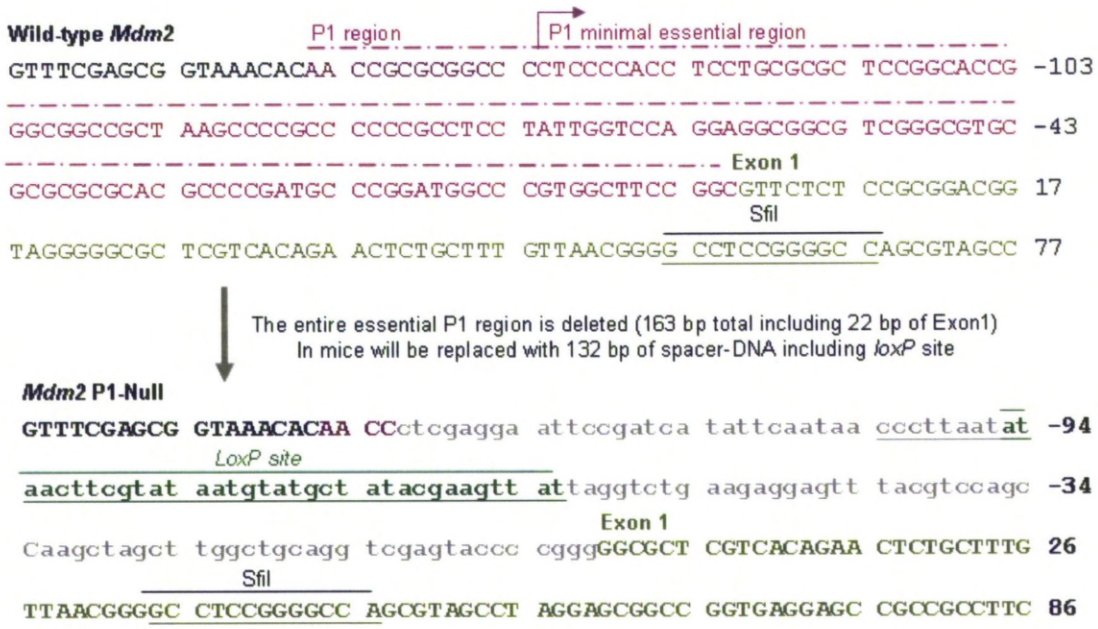


***Figure 3.3.38: Sequence detail following deletion of the Mdm2 P1 promoter.***

*Top panel: The wild-type Mdm2 P1 promoter region is the 145 bp upstream of exon 1 shown in purple text as defined by [Chang et al., 2004]. The P1 minimal essential region was inferred from the conserved features between human and mouse Mdm2 [Phillips et al., 2006]. Bottom panel: The predicted DNA sequence at the P1 region following deletion in transgenic mice. The P1 minimal essential region will be replaced with 132 bp of spacer DNA, leaving only 4 residual bp of the original promoter region.*

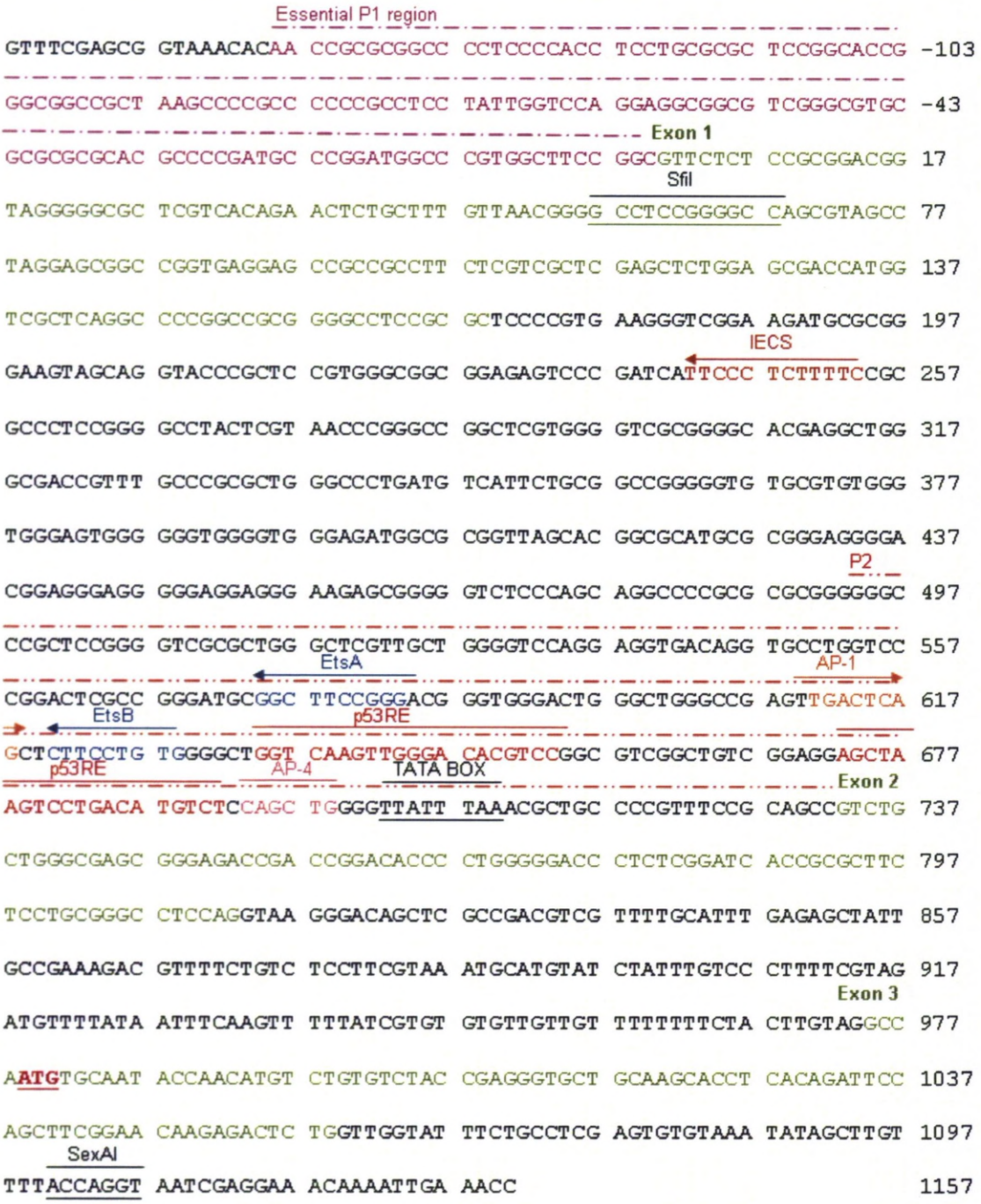


***Figure 3.3.39: Sequence detail and features at the Mdm2 P1 – P2 locus.***

*Based on [Phelps et al., 2003]. The 1294 nt Mdm2 DNA sequence including the 145 nt upstream of exon 1 which contains the essential region for the Mdm2 P1 promoter (purple text) and the 273 nt P2 region (dashed red line). Exons are shown in green text, the p53 REs (red text) and other features are also shown including IECS (Brown), EtsA, EtsB (blue) AP-1 (orange), AP-4 (pink) and putative TATA BOX. The ATG translational initiation site is within exon 3.*

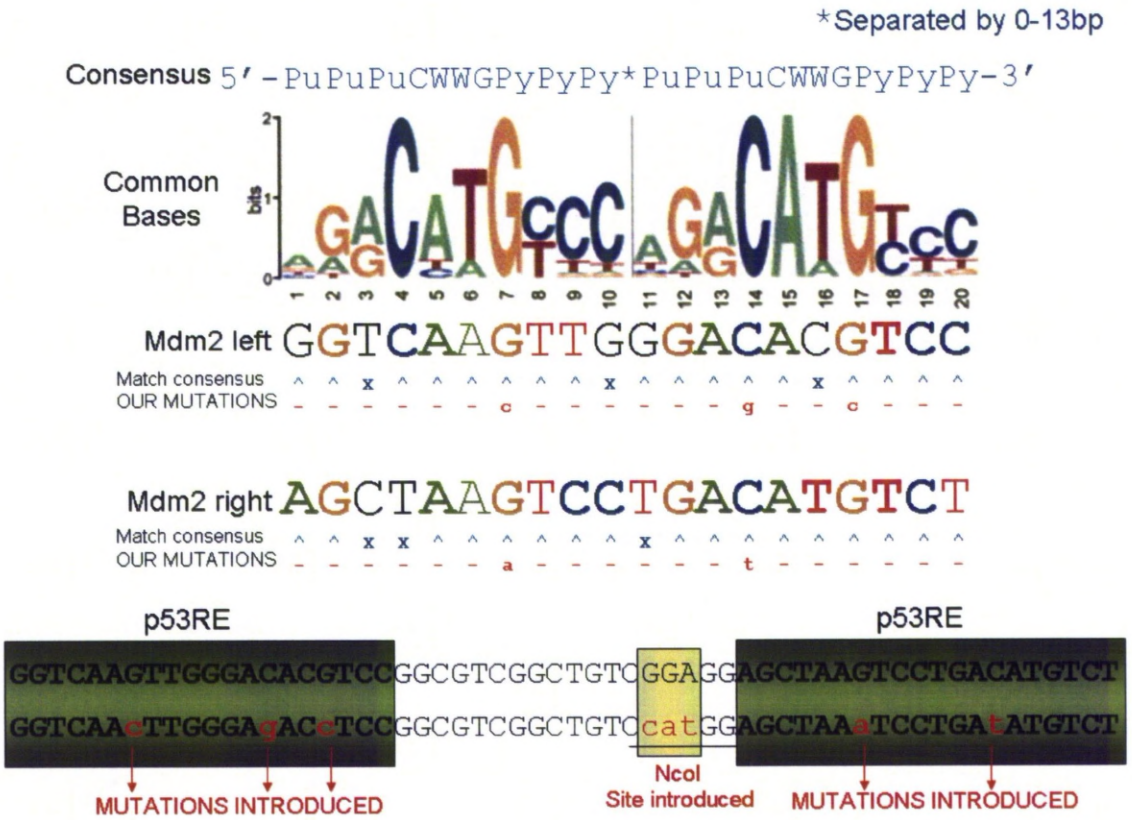


***Figure 3.3.40: Specific point mutations introduced to Mdm2 to create the P2-Mutant.***

*Figure based loosely on [Wei et al., 2006]. From the top line down: the consensus p53 RE site followed by the most common bases and then the actual Mdm2 p53 RE sequences (left then right). Mutations were systematically introduced in order to render the p53 RE sites inactive, starting with the most conserved bases (see methods Section 2.8.2). 8 base pair mutations were introduced in total; 5 bp substitutions were introduced to the p53 RE site and a further 3 mutations were placed in the spacer region (to create an NcoI site for screening targeted ES cells/transgenic mice).*

*KEY Pu = purine (A/G), Py = Pyrimidine (C/T), W = Weak (A/T).*

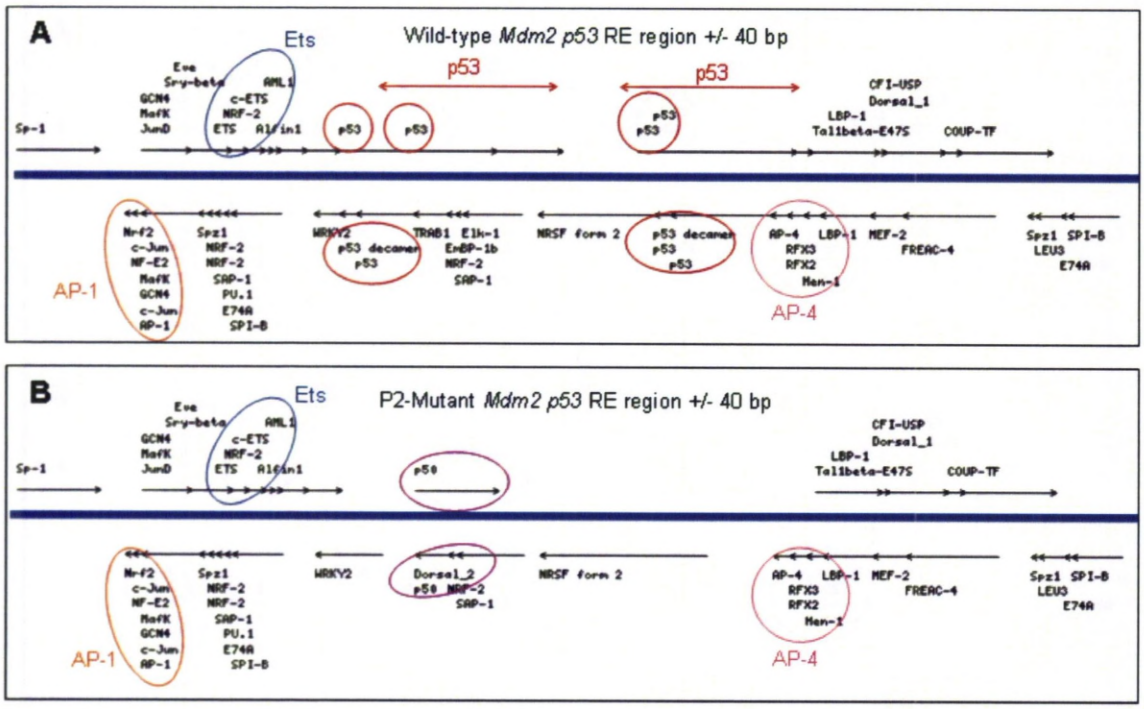


***Figure 3.3.41: Putative transcription binding sites at the Mdm2 P2 locus***

*The Mdm2 p53 RE sites +/- 40 nt were analysed by MAPPER to identify putative transcription factor binding sites (TFBS) [Marinescu et al., 2005]. This figure shows the graphical output from these searches, arrows are indicative of a predicted binding site. A) The wild-type Mdm2 p53 RE region and B) The mutated Mdm2 p53 RE region generated for this thesis. The P2-mutant sequence has lost its p53 REs but still contains the known upstream TFBS Ets and AP-1 and downstream AP-4. The TFBS p50 and Dorsal-2 have been added whilst the TFBS TRAB1, EmBP-1b and Elk-1 have been deleted, summarised in Table 3.3.2.*

### 3.3.5.2 *In vitro validation of the Mdm2 promoter region mutations*

To determine whether the previously described mutations (see Section 3.3.5.1) introduced to the *Mdm2* P1/P2 promoters had significantly impacted on the activity of these promoters an *in vitro* luciferase assay was performed. To perform this analysis the whole P1-P2 promoter region (~1600 bp including 300-400 bp of upstream and downstream sequence) was cloned into pGL4.11 (a simple promoterless luciferase plasmid) and transfected into p53 null cells with and without murine p53. The cloning of these vectors is described in Appendix C.4. The luciferase assay was performed in p53 null human non-small cell lung carcinoma cell line H1299 and p53 null MEF in triplicate wells of a 48-well plate as described in Section 2.13.8 and the results are shown in Figure 3.3.42 and Figure 3.3.43.

Following co-transfection with murine p53, the WT (wild-type) and P1-Null luciferase plasmids both had a massive increase in luminescence in both H1299 (45 and 83 fold, p-values = 0.009 and 0.003 respectively) and p53 null MEFs (5.5 and 18 fold, p-value = 0.004 and < 0.001 respectively). On the other hand, the *Mdm2* P2-Mutant promoter had its p53-dependent response completely abrogated in both H1299 and p53 null MEF cells (p-value = 0.009 and 0.002). There was a trend for the P2-Mutant to also have slightly lower basal luminescence (without co-transfection with murine p53) although this was not significant (p-values = 0.051 (H1299) and 0.104 (p53 null MEF)). Importantly, for generation of the *Mdm2* P1-Null mouse, there were no significant differences between the p53-dependent expression values of the WT and P1-Null plasmids (p-value = 0.695 (H1299) and 0.918 (p53 null MEF)). This indicates that the absence of *Mdm2* P1 promoter does not interfere with the p53 dependent up-regulation from the *Mdm2* P2 promoter.

The positive control plasmid pp53-TA-Luc, was also induced following co-transfection with murine p53. The increase in luciferase expression was less than the WT or P1-Null constructs in both H1299 (~ 14 fold reduction) and p53 null MEFs (~ 7 fold reduction) which may be due to the slightly different luciferase genes. pp53-TA-Luc contains the standard *Luciferase* gene, whereas pGL4.11 contains *Luc2,* a mammalian codon optimised version of *Luciferase* for more efficient translation and expression in mammalian cells.

As might be expected the effects of deleting of the *Mdm2* P1 promoter were more subtle however these differences were significant. The *Mdm2* P1-Null had a 1.6 and 3.1 fold reduction in luciferase compared to WT in H1299 (p-value = 0.015) and p53 null MEF (p-value = 0.015) respectively. When the P1-Null basal luminescence levels were compared with the P2-Mutant this was also significantly different in the murine system (p-values = 0.643 (H1299) and 0.002 (p53 null MEF)). The murine system is probably more sensitive since we are using the murine *Mdm2* promoter regions which may be associated with more efficient up-regulation of the WT *Mdm2* P1 promoter in mouse cells due to increased specificity of mouse-mouse transcription factor DNA binding interactions. The relatively higher basal luminescence in murine cells provides one explanation as to why the fold changes in the p53-dependent up-regulation of luciferase appeared greater in the human H1299 cells (45-80 fold compared with 5-18 fold increase).

In conclusion, since the *Mdm2* P2-Mutant was not p53 responsive and had comparable baseline expression, this indicates that the mutations designed are ideal to use in a transgenic model to study the p53-dependent up-regulation of *Mdm2*. Also, since the *Mdm2* P1-Null had compromised basal expression but still had comparable p53-dependent induction of expression, this too indicates that the P1 promoter deletion has worked as designed and would therefore be suitable to use in a transgenic model to study the p53-independent up-regulation of *Mdm2*. This thesis will now go on to describe how the two DNA targeting constructs for each of the *Mdm2* promoter mutant mice were generated.

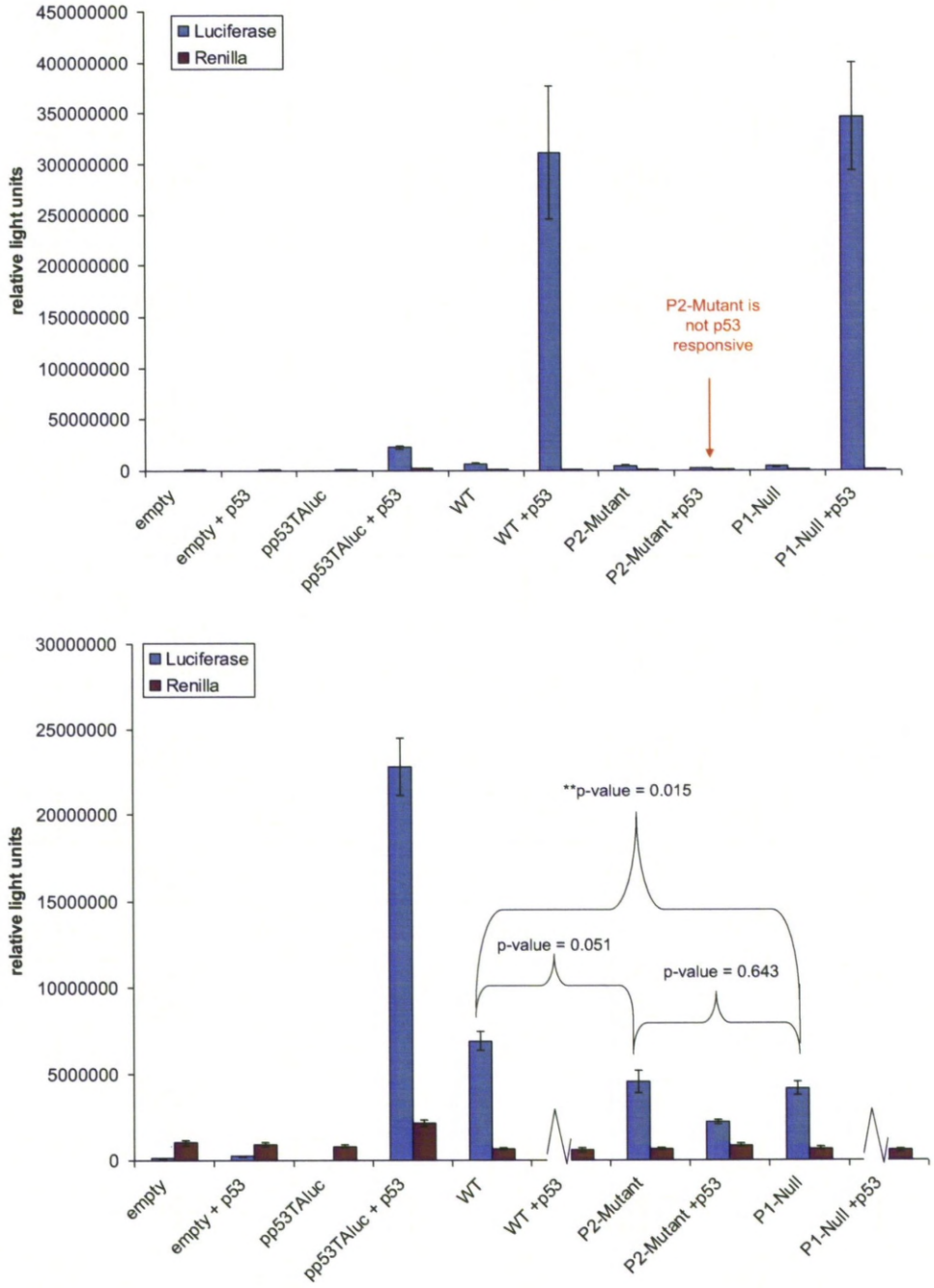


***Figure 3.3.42: In vitro testing of the Mdm2 promoter mutations.***

*A luciferase assay was performed on H1299 cells transfected with the indicated plasmids. Empty vector is the pGL4.11 plasmid (negative control) and pp53-TA-Luc is a luciferase gene under the control of a consensus p53 binding site [Komarova et al., 1997] (positive control). WT, P2-Mutant and P1-Null are the various promoter regions cloned into promoterless luciferase plasmid pGL4.11. +p53 indicates co-transfection with murine p53. Values shown here are luminescence corrected for protein concentration. Readings were obtained from triplicate wells of a 48-well plate and Error bars are the SEM. The bottom panel shows the same data without the 'WT +p53' and 'P1-Null +p53' treatment groups in order to expand the scale for better comparison.*

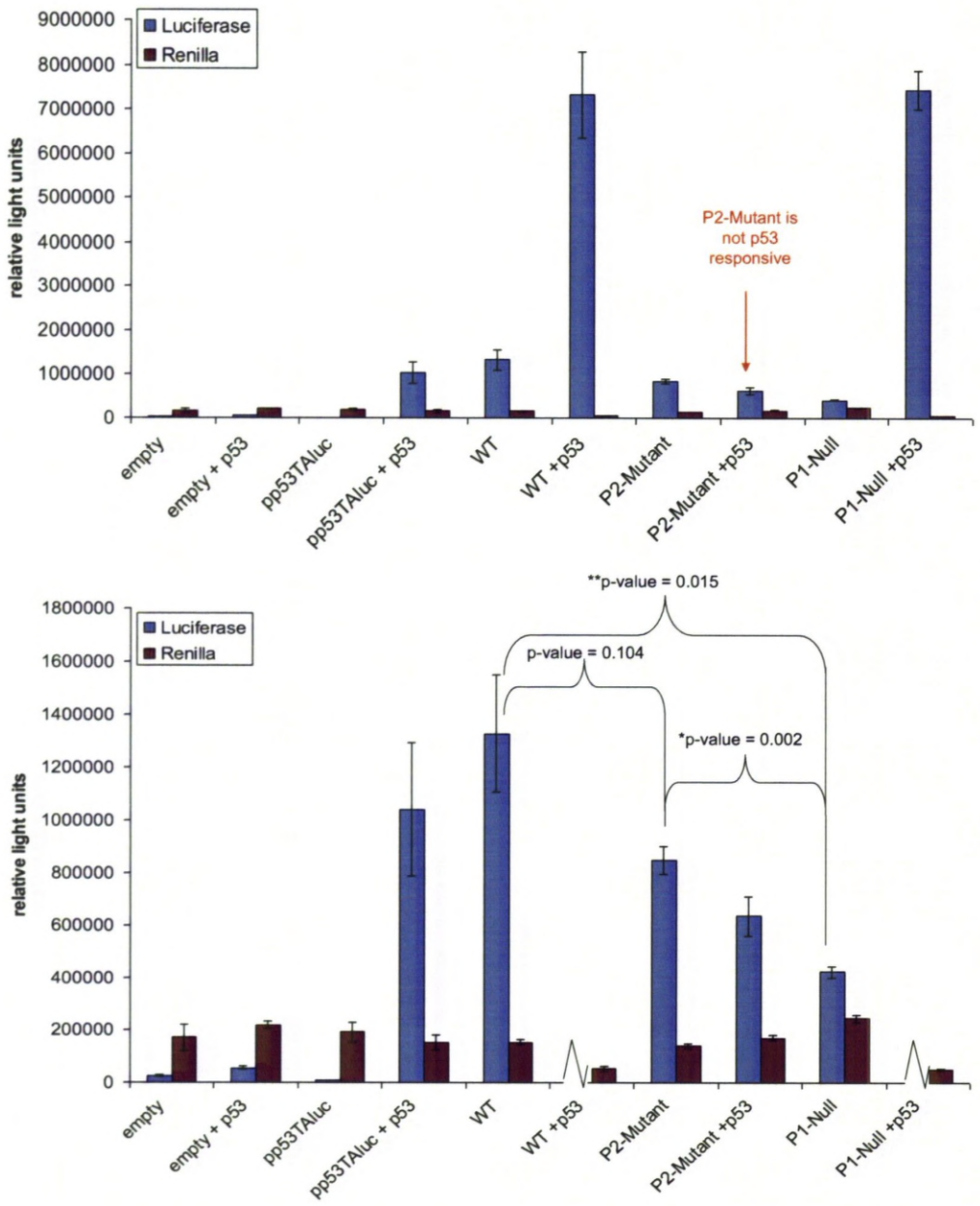


***Figure 3.3.43: In vitro testing of the Mdm2 promoter regions***

*A luciferase assay was performed on p53 null MEF cells transfected with the indicated plasmids, as detailed in Figure 3.3.42.*

### 3.3.5.3 Cloning strategy

Figure 3.3.44 shows the basic cloning plan for the generation of the *Mdm2* P1-Null and *Mdm2* P2-Mutant DNA targeting constructs. This plan utilises the natural ability of yeast cells to perform high efficiency homologous recombination between relatively short (200-400 bp) regions of identical DNA [Storck et al., 1996]. Short recombinogenic arms (RA) are inserted either side of a yeast/mammalian positive selectable marker which when excised from its bacterial plasmid backbone (pRAY-Cre) acts as the donor DNA. The donor DNA recombines precisely in yeast cells where there is sequence overlap with the shuttle vector to introduce the positive selectable marker (pRAYNeo$^R$). The shuttle vector contains 11 kb of genomic DNA around the *Mdm2* promoter region, so that following insertion of the positive selectable marker, the resulting vector will contain two 4-6 kb arms of homology and could be used as the gene targeting vector. The genomic DNA would be obtained from a suitable BAC clone restriction digest and cloned immediately into the vector containing the negative selectable marker (TK2 – see Section 3.3.3.2), therefore, this method does not involve the labour intensive steps to generate the arms of homology as the previous method for p21-mCherry and Puma-E2Crimson did (see Section 3.3.3.7 and Section 3.3.4.1).

For generation of the *Mdm2* P1-Null DNA targeting construct, the plan was to simply replace the P1 promoter region with the positive selectable marker. This could be effectively accomplished in just a few steps of cloning by selecting RAs either side of the P1 region since any DNA between the two RAs would be deleted [Storck et al., 1996]. For the *Mdm2* P2-Mutant DNA targeting construct the point mutations were added to the shuttle vector first, by reconstructing the region through PCR-based techniques (see Figure 3.3.49). The pRAYNeo$^R$ cassette was then introduced ~700 bp downstream through homologous recombination in yeast. The construction of these vectors is described next.

### 3.3.5.4 Shuttle vector construction

The shuttle vector was required to contain an 8-15 kb section of *129SvEv* genomic DNA isolated from a suitable restriction digest fragment from a BAC clone. A suitable DNA fragment would contain the *Mdm2* P1-P2 promoter region and sufficient DNA sequence

upstream and downstream to create at least two c. 4 kb arms of homology. The BAC restriction digest fragment would also ideally contain two unique restriction sites around the *Mdm2* P2 site (or one restriction site twice) so that the region could be manipulated more easily. The BAC fragment should also be distinguishable by *in silico* digestion and ideally be cloned immediately into the negative selectable marker plasmid (TK2 – see Section 3.3.3.2) to avoid additional rounds of cloning.

Following sequence analysis of the '*Mdm2*' BAC clone bmQ-305J12 DNA using the NEBcutter tool a 10,994 bp PacI-AclI restriction digest fragment was identified (see Figure 3.3.45). This PacI-AclI fragment was cloned into a modified version of vector TK2 (named TK-AclI) as shown in Figure 3.3.46. The TK2 vector was modified to remove the two AclI sites in the Ampicillin$^R$ cassette and to introduce a new AclI site just downstream of the PacI site. The removal/addition of the AclI sites in TK2 allowed the 11 kb PacI-AclI BAC restriction digest fragment to be cloned directly into the negative selectable marker (TK-AclI). The transformation reaction was performed using the bacterial strain MAXstbl.2 to avoid any potential problems that might arise in association with cloning a large section of genomic DNA (such as DNA instability as seen with the p21 right arm of homology – see Section 3.3.3.7). 4/39 colonies appeared positive through a NotI & SalI digest and *Mdm2* specific PCR screen (see Figure 3.3.47). The positivity of these 4 promising clones (Mdm2TK-16, 22, 25 & 31) was then further confirmed by three additional restriction digests with KpnI, SacI and XhoI (see Figure 3.3.47 – C). Since all the DNA fragments appeared at their expected size and stoichiometric ratios, at this stage all the clones were deemed suitable for use in the next stage of cloning.

The next stage of cloning was to move the 13.1 kb TK-*Mdm2* DNA fragment into the yeast-*E. coli* shuttle vector pRS414 via their common SalI and SpeI sites. This cloning took four attempts to complete without obvious reasons for failure (detailed in Appendix C.5). The cloning was finally accomplished by using the TOP10 bacterial strain (rather than the MAXstbl.2 strain). 5/5 colonies appeared positive when bacterial colonies were screened by restriction digestion with SalI and NotI (see Figure 3.3.48). The positivity of two of these clones (pRSmdm2TK) was then further confirmed by two additional digests with KpnI and SacI. At this stage these clones (pRSmdm2TK-2 and 5) were both considered suitable for the

next round of cloning. In the case of the *Mdm2* P1-Null DNA cloning exercise, this DNA (pRSmdm2TK-2 or 5) could be used immediately in co-transformation in yeast cells; however for the *Mdm2* P2-Mutant additional rounds of cloning in bacteria were required first. The additional rounds of cloning were required to reconstruct the P2 region to include our desired point mutations. As alluded to earlier, there are two unique restriction sites around the *Mdm2* P2 region, SfiI and SexAI, which define a 1024 bp DNA fragment (see Figure 3.3.39). This ~1 kb DNA fragment was amplified by PCR to introduce the desired point mutations as outlined in Figure 3.3.49. Briefly, the DNA fragment was amplified in two sections which separated the p53 RE sites and allowed the mutations to be introduced by use of specially designed 'mutating' primers. These two initial PCR products A and B in Figure 3.3.49 were TA-cloned into pCR2.1, screened by restriction digest with EcoRV and SpeI, then sequenced to ensure successful incorporation of the desired base pair substitutions. Once the DNA sequences had been confirmed, a further round of PCR was performed to fuse these two sections together. The resulting PCR product (C in Figure 3.3.49) was then also TA-cloned into pCR2.1 and screened by EcoRV and SpeI restriction digest (see Figure 3.3.48 – C). 10/10 clones appeared positive for the P2-Mutant region and one clone (10) was sent for sequencing. The DNA sequencing results were identical to the expected sequence and therefore this clone was used in the next step of cloning the P2-Mutant shuttle vector.

In order to create the *Mdm2* P2-Mutant shuttle vector, the P2-Mutant SfiI-SexAI DNA fragment was then inserted into the pRSMdm2TK shuttle vector, however since the restriction enzyme SexAI was blocked by overlapping Dcm methylation the two vectors were first retransformed into Dcm/Dam negative bacterial strain "C2925" (see Figure 3.3.50 for an overview). The Mdm2 P2-Mutant region was then inserted into the shuttle vector by using their common SfiI and SexAI sites. 3/3 clones were positive when screened using an NcoI and NheI restriction digest (see Figure 3.3.48 – D) and of these one was selected (pRSm-P2-1) for co-transformation in yeast cells. This report will now go on to describe the cloning of the *Mdm2* P1-Null and P2-Mutant donor DNA.

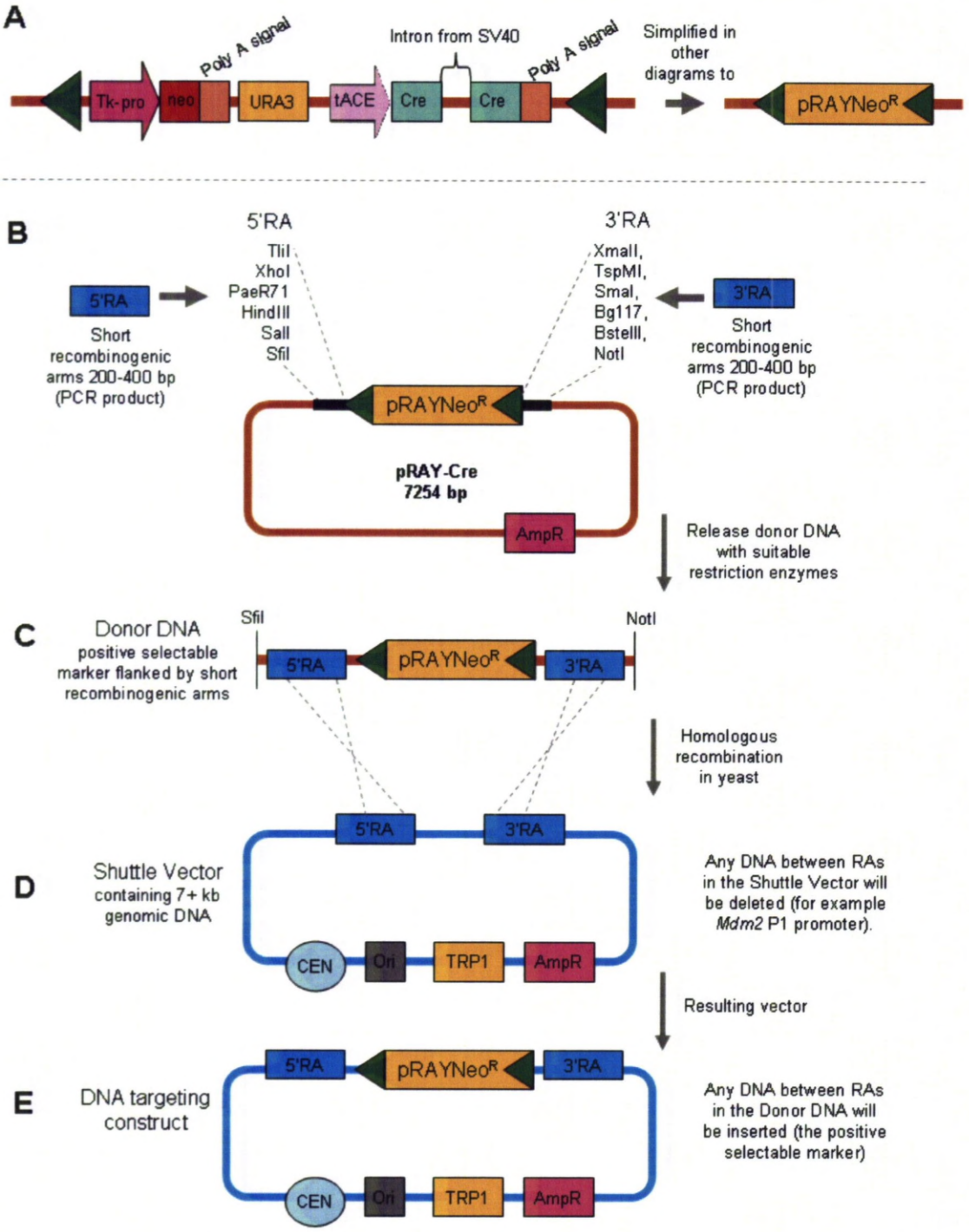


***Figure 3.3.44: Basic cloning strategy for the DNA targeting constructs Mdm2 P1-Null and Mdm2 P2-Mutant.***

*A) Schematic diagram of the yeast/mammalian self excision positive selectable marker pRAYNeo$^R$. pRAYNeo$^R$ contains the neomycin phosphotransferase cDNA driven by the Tk promoter, yeast selectable marker URA3 and the Cre recombinase gene as described in Figure 3.3.13 and [Bunting et al., 1999]. The cassette was flanked with two 34 bp Lox P sites (green arrow heads in diagram). B) Schematic diagram of the pRAY-Cre vector adapted from [Storck et al., 1996]. pRAY-Cre contains the pRAYNeo$^R$ cassette with two multiple cloning sites either side which are used to introduce the recombinogenic arms. C) The donor DNA and D) The shuttle vector are co-transformed into yeast cells and homologous recombination occurs where there is sequence overlap. E) The resulting vector.*

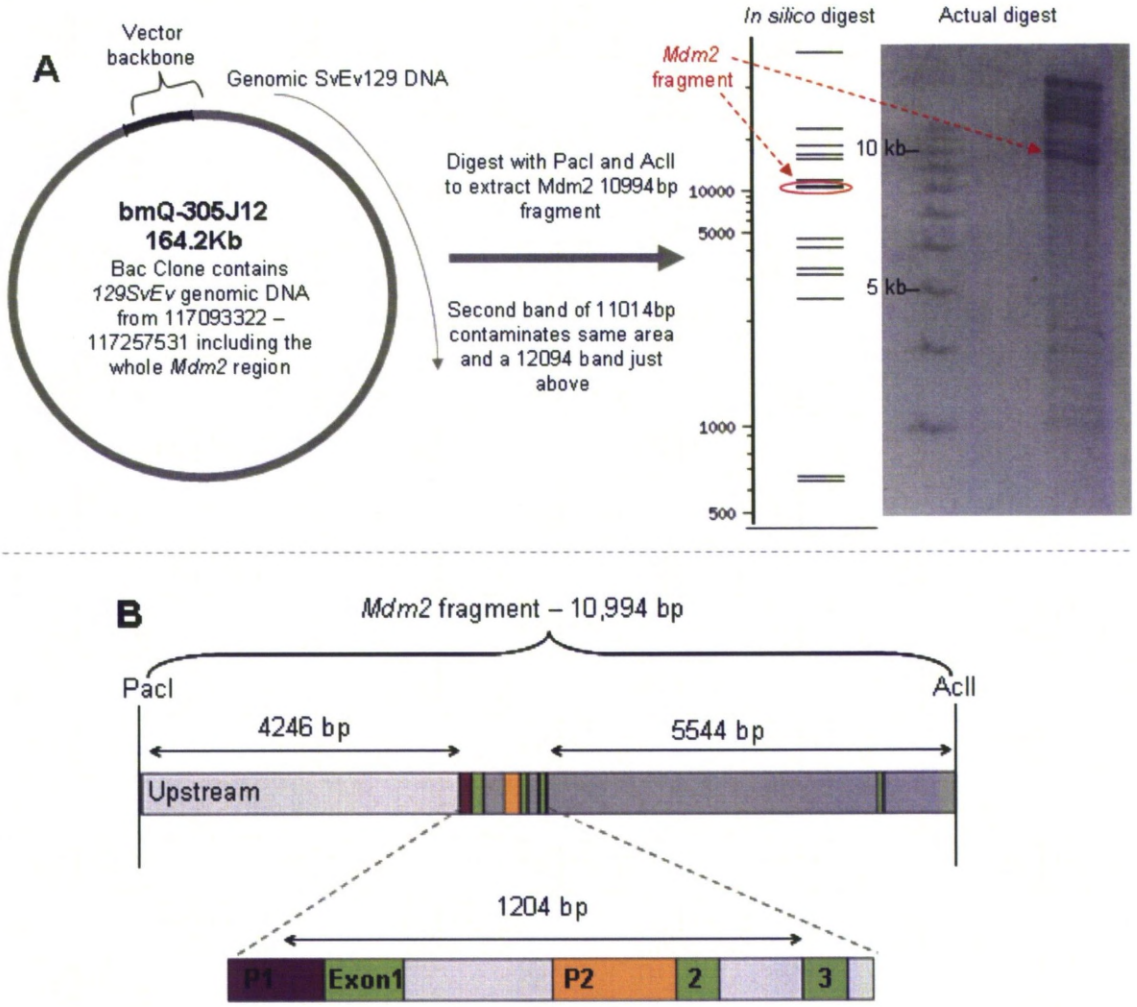


***Figure 3.3.45: Cloning the Mdm2 genomic DNA fragment.***

*A) BAC clone bmQ-305J12 was digested in silico to determine whether the restriction fragment containing the 11 kb Mdm2 fragment (red circle) would be distinguishable from other fragments, followed by an actual digest to confirm. The actual restriction digest pattern appears to accurately resemble the results predicted in the virtual gel. B) Schematic diagram of the 11 kb PacI-AclI Mdm2 fragment. Since the regions of interest, the Mdm2 promoters P1 (purple box) and P2 (orange box), are located approximately in the centre of this genomic DNA fragment, this provides two substantial flanking regions to act as the arms of homology for gene targeting (4.2 – 6.7 kb).*

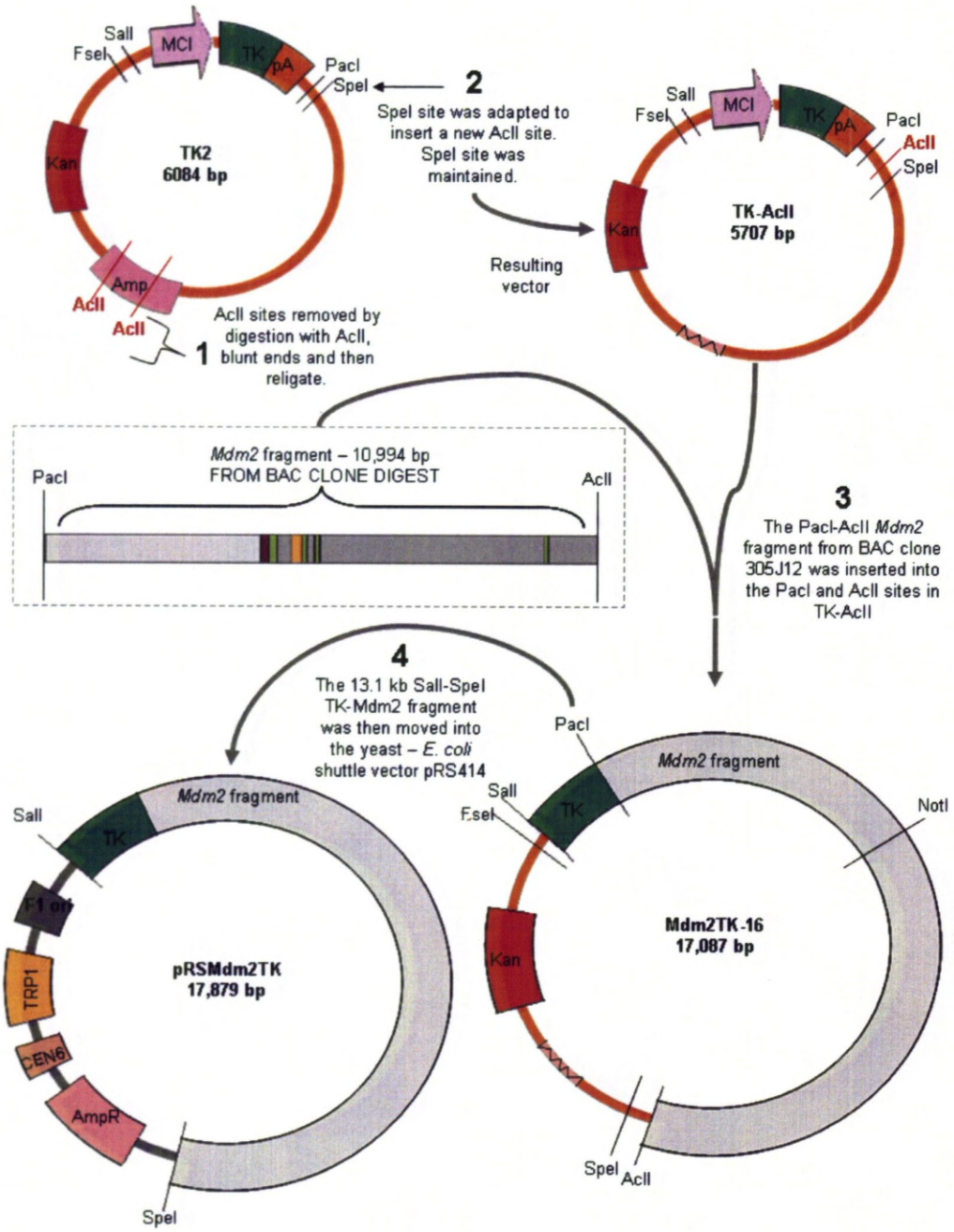


***Figure 3.3.46: Flow diagram for the cloning of the Mdm2 shuttle vectors.***

*1. The 2 AclI sites in Amp$^R$ were removed from TK2 by digestion with AclI, followed by blunting and religation. 2. The resulting vector then had a new AclI site introduced at the unique SpeI site. The SpeI site was maintained for downstream cloning. 3. The 11 kb PacI-AclI BAC digest fragment was inserted into the vector TK-AclI using the mutual PacI & AclI sites. 4. The whole negative selectable marker (TK) and Mdm2 genomic region were then transferred into the yeast-E. coli shuttle vector, pRS414, via their mutual SalI & SpeI sites. This shuttle vector (pRSMdm2TK) was then ready for use in co-transfection experiments in yeast to generate the P1-Null DNA targeting construct (P2-Mutant required additional cloning steps – see Figure 3.3.50).*

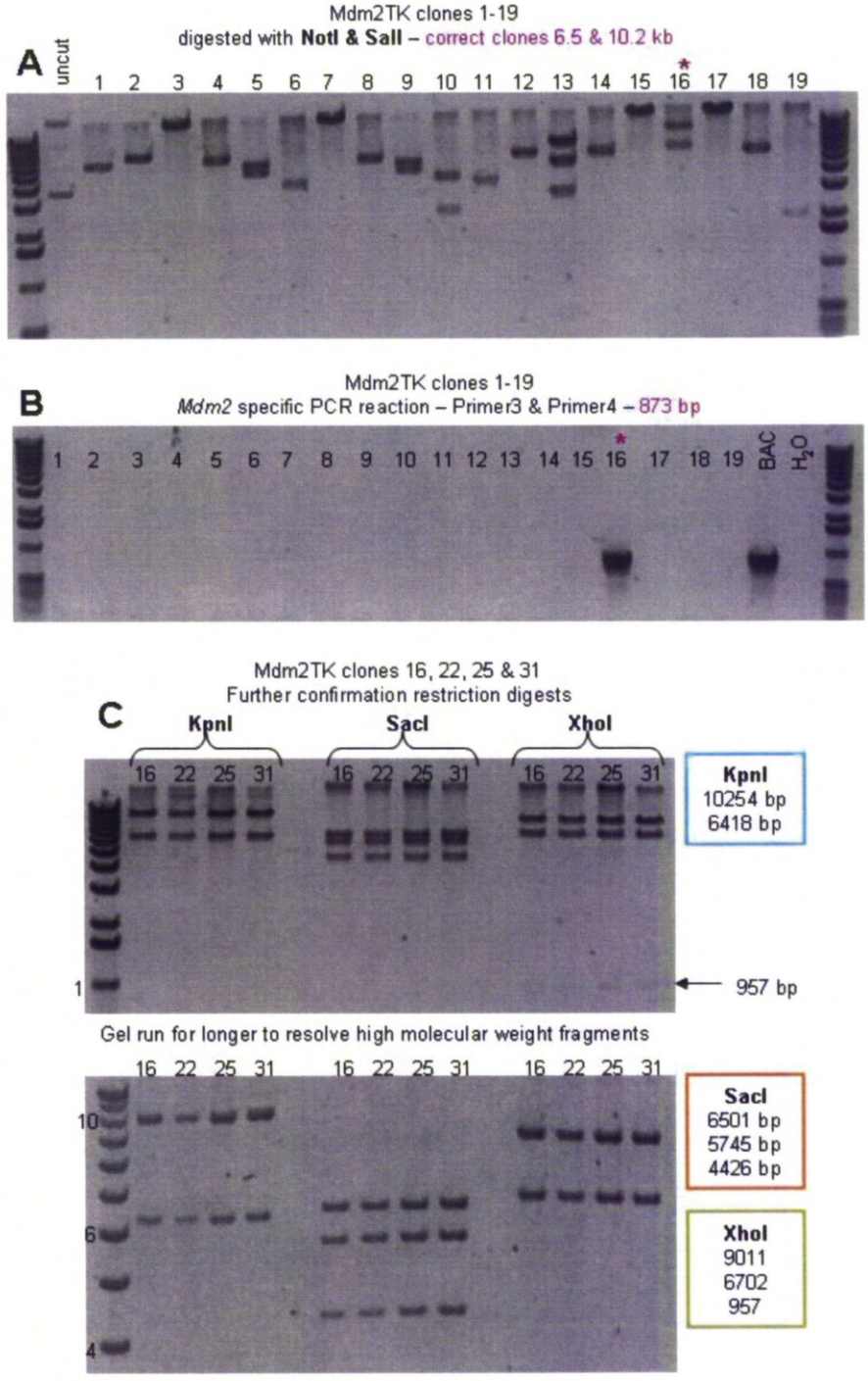


***Figure 3.3.47: Confirmation of positive Mdm2TK clones.***

*A) Restriction digest analysis of Mdm2TK clones 1-19 with NotI & SalI. B) PCR screen with Mdm2 specific primers – BAC clone 305J12 DNA was included as a positive control. *Clone 16 appeared doubly positive (for restriction digest and PCR). C) The 4/39 doubly positive promising clones were then examined further by additional restriction digest analysis with KpnI, SacI and XhoI. All four clones tested (16, 22, 25 & 31) had restriction fragments at the correct sizes therefore all four would be suitable for the next stage of cloning.*

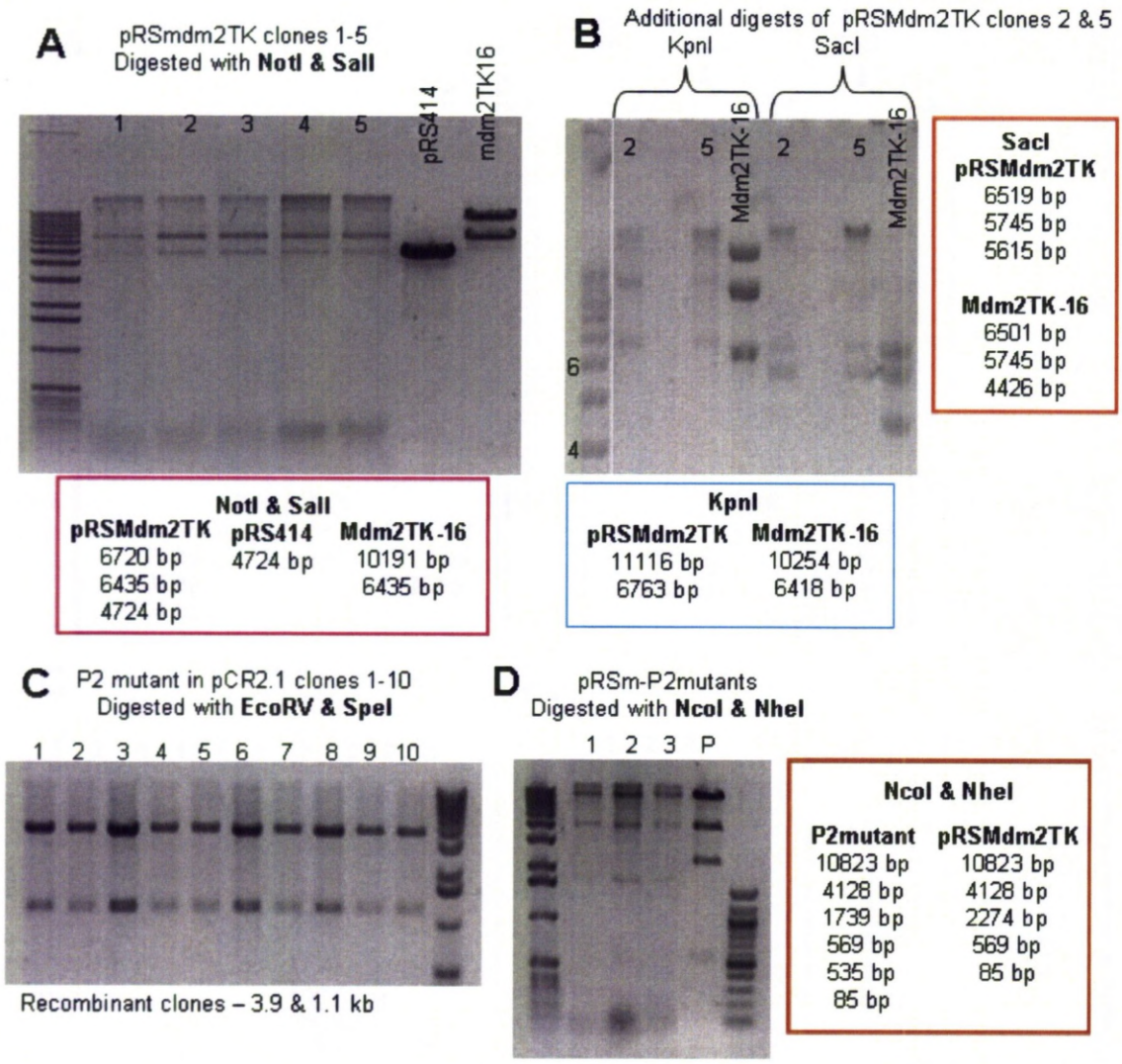


***Figure 3.3.48: Cloning of the Mdm2 shuttle vector.***

*Restriction digestion analysis of pRSMdm2TK clones. A) Initial test digest with SalI and NotI. 5/5 clones appear positive. B) Further digests on clones 2 & 5 with KpnI and SacI. All DNA fragments appeared at the expected sizes and stoichiometric ratios. C) The mutated Mdm2 P2 promoter region was TA-cloned into pCR2.1 (see Figure 3.3.49). 10/10 clones were positive when screened with EcoRV and SpeI. D) The P2-Mutant region was then inserted into the shuttle vector pRSMdm2TK. 3/3 clones appeared positive by restriction digest with NcoI and NheI. Expected sizes of DNA restriction digest fragments are shown in boxes.*

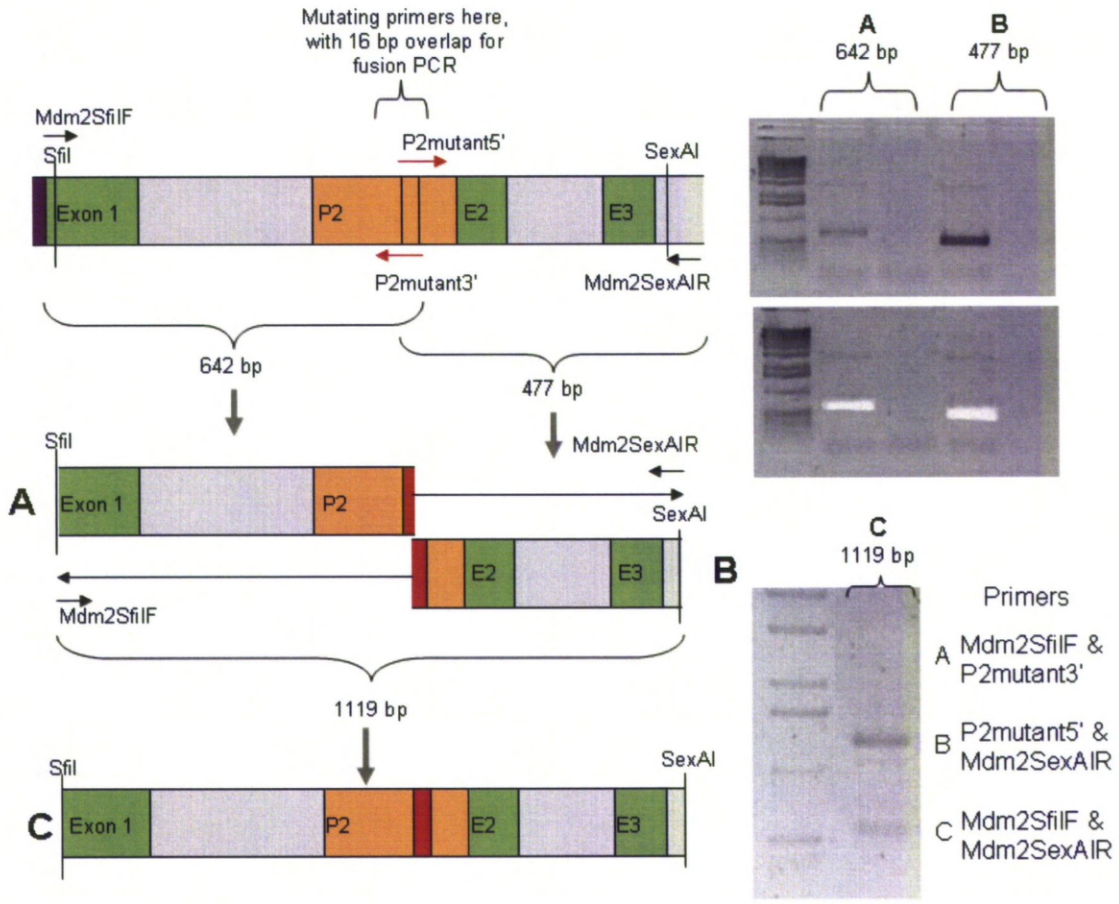


***Figure 3.3.49: Generating the Mdm2 P2-Mutant promoter region by fusion PCR.***

*Right panel: Schematic diagram of the fusion PCR steps to create the Mdm2 P2-Mutant region. PCR products A and B were TA-cloned into pCR2.1 and sequenced prior to use in the next round of PCR to create PCR product C. The primers P2Mutant5' and P2Mutant3' contained the desired point mutations which would be introduced following the first round of PCR. Left panel: Corresponding agarose gel photographs.*

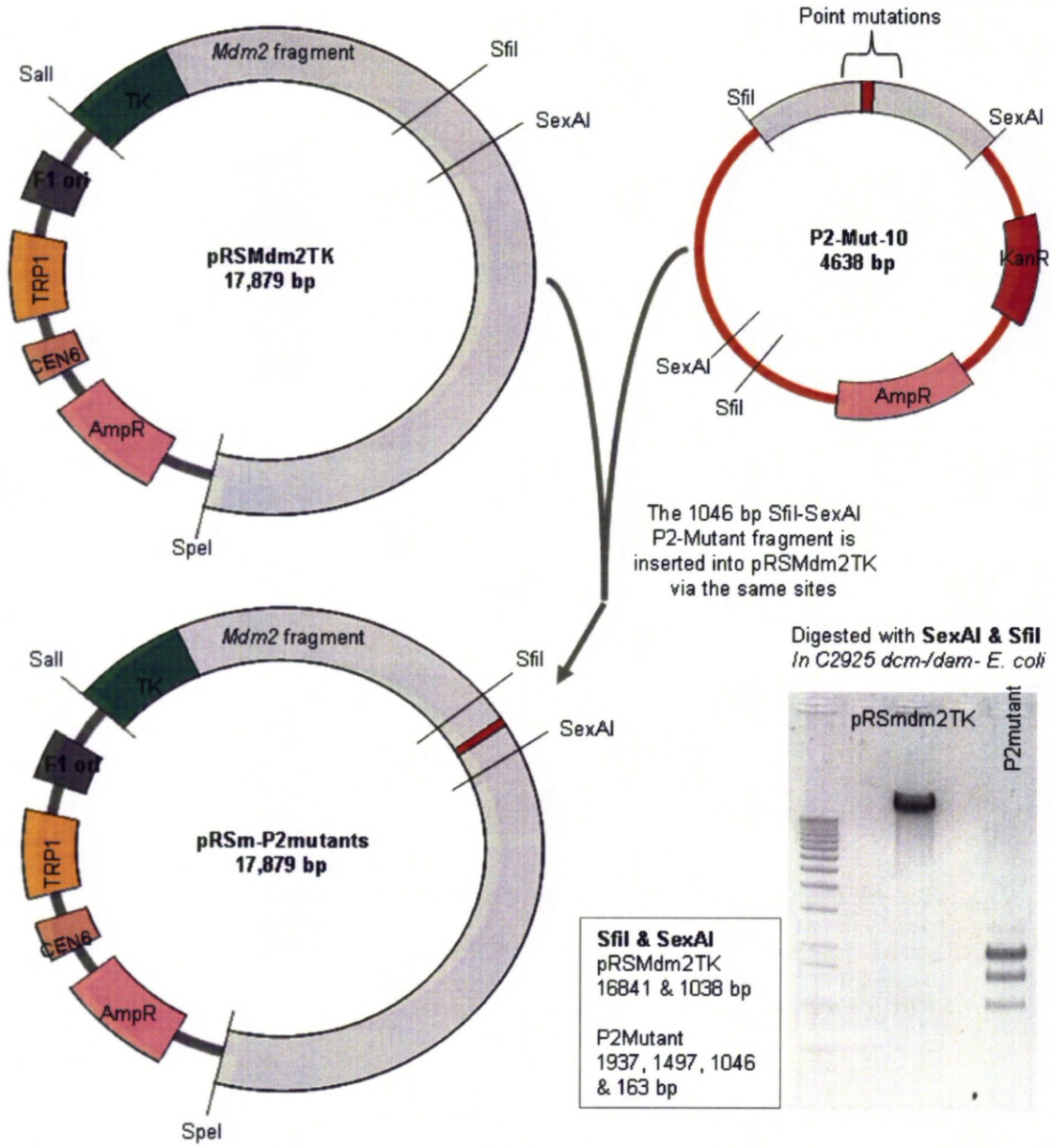


***Figure 3.3.50: Flow diagram of the cloning the Mdm2 P2-Mutant shuttle vector.***

*The plasmids pRSMdm2TK and P2-Mut-10 were retransformed into Dcm⁻/Dam⁻ C2925 E. coli to allow the methylation sensitive restriction enzyme SexAI to cleave the DNA. The Mdm2 P2-Mutant region was then inserted into pRSMdm2TK via their common SfiI and SexAI sites. Bottom left corner, the agarose gel which resolved the backbone (pRSMdm2TK ~ 17 kb) and insert (P2-Mutant ~1 kb) DNA.*

### 3.3.5.5 Donor DNA construction

The donor DNA was designed to contain the yeast/mammalian self-excision positive selectable marker pRAYNeo$^R$ flanked by two short (200-400 bp) genomic DNA fragments known as recombinogenic arms (RAs). These RAs were generated by PCR and were inserted into the relevant multiple cloning site of the plasmid pRAY-Cre (see Figure 3.3.44). In the case of the *Mdm2* P1-Null cloning exercise, these RAs would determine which section of the P1 promoter and *Mdm2* exon 1 would be deleted (see Figure 3.3.51). For the *Mdm2* P2-Mutant cloning exercise, the RAs would insert the pRAYNeo$^R$ cassette 715 bp downstream of the p53 RE point mutations (see Figure 3.3.52).

The cloning of the donor DNA plasmids was performed according to the cloning plan detailed in Figure 3.3.51 (P1-Null) and Figure 3.3.52 (P2-Mutant). All PCR products were first TA-cloned into pCR2.1, screened by EcoRV and SpeI restriction digestion and then sequenced (see Figure 3.3.53 – A & B). Once the sequences were confirmed the RAs were then inserted sequentially into the pRAY-Cre vector using the indicated restriction enzymes. Positive clones were identified for successful integration of the RA by restriction digestion with various enzymes as shown in Figure 3.3.53 C-E. The exception to this was insertion of the P2 5' RA, since this was inserted using unidirectional cloning and therefore an addition PCR screen was performed to determine the orientation (see Figure 3.3.53 – F). The final donor DNA plasmids were P1B2-3 and P2C3-8 for the P1-Null and P2-Mutant cloning exercises respectively. These vectors were then prepared for co-transformation into yeast cells by releasing the donor DNA fragment from the backbone by restriction digestion with SalI and NotI. Identification of positive yeast colonies and re-transformation of the recombined DNA back into bacteria is described next.

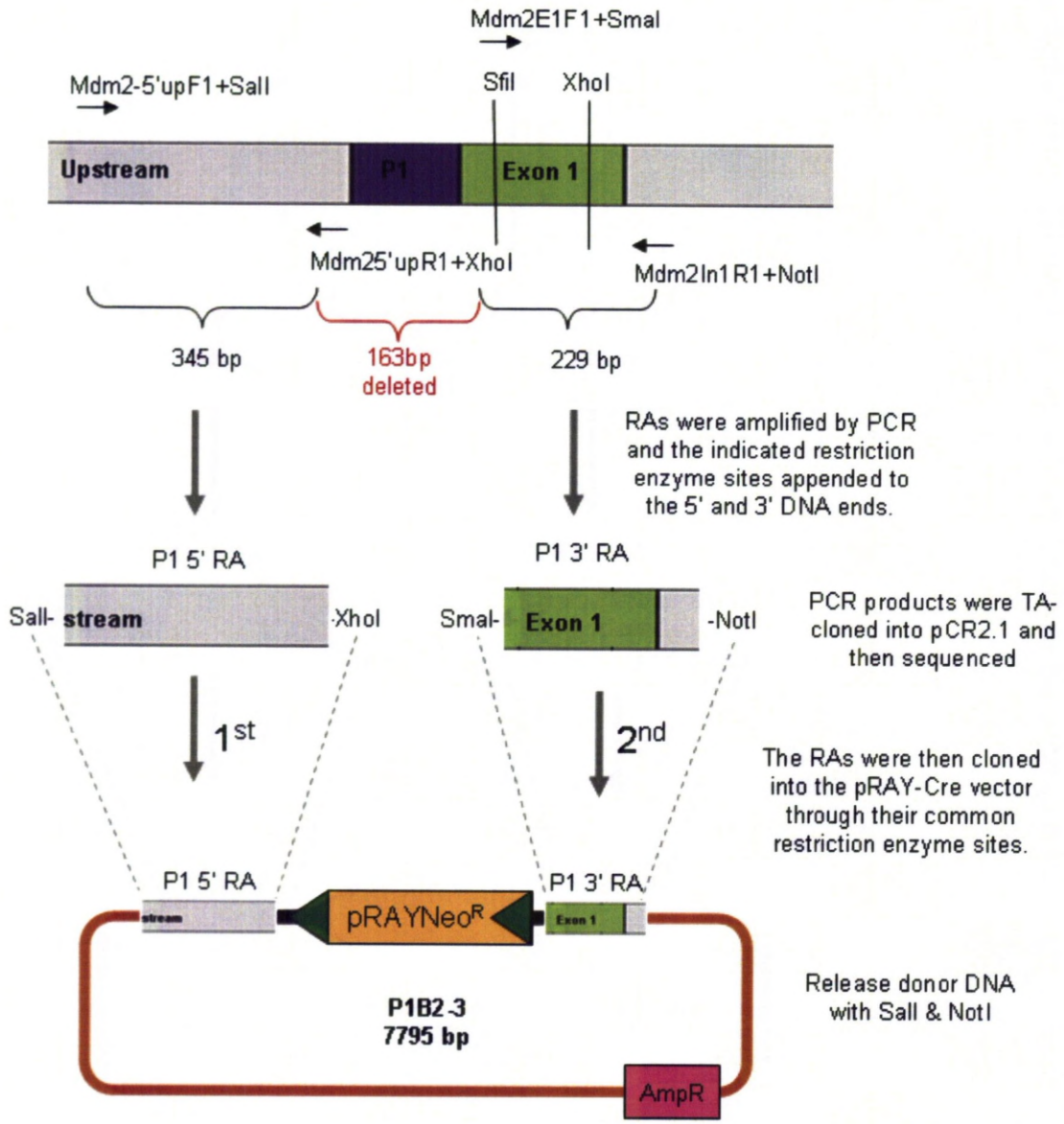


***Figure 3.3.51: Cloning of the Mdm2 P1-Null donor DNA.***

*The two RAs were amplified by PCR using the mdm2TK2-16 DNA as a template. Since the P1 region and first 22bp of Mdm2 exon 1 lie between the two RAs, this 163 bp region will be deleted during homologous recombination in yeast. The P1 5' RA was introduced to the pRAY-Cre vector first, followed by the P1 3' RA by the indicated common restriction sites. Once constructed, the donor DNA could be excised from its backbone plasmid P1B2-3 by restriction digestion with SalI and NotI.*

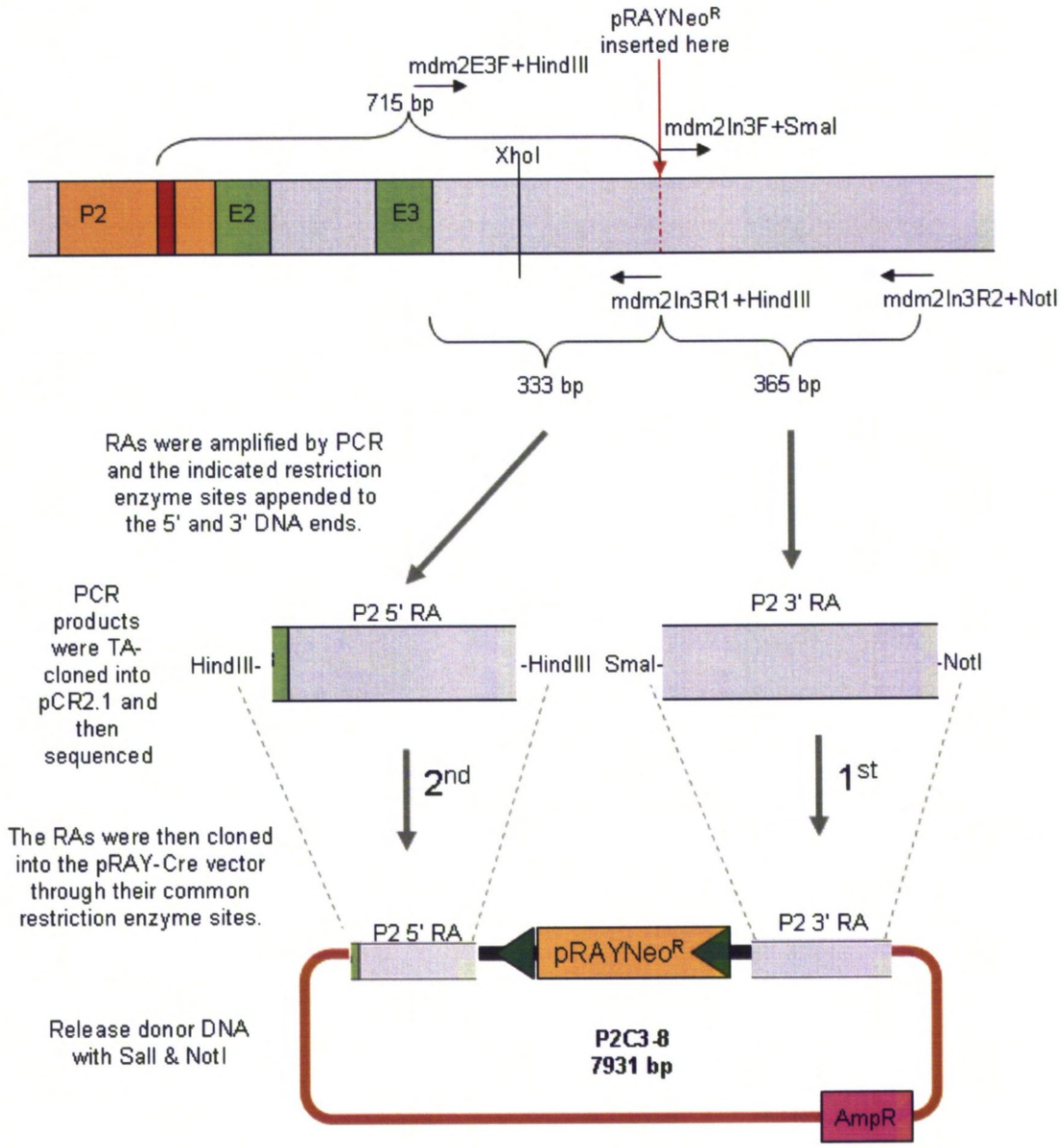


***Figure 3.3.52: Cloning of the Mdm2 P2-Mutant donor DNA.***

*The two P2 RAs were amplified by PCR using the mdm2TK2-16 DNA as a template. There is no gap between the two RAs, hence the only modification in the $F_1$ heterozygous mice should be the accumulation of ~ 100 bp of spacer DNA (including 34 bp LoxP stie) in Mdm2 intron 3. The pRAYNeo$^R$ cassette is 715 bp downstream of our P2-Mutated sequence since we did not wish to disrupt the promoter region other than in the p53 RE sites. Once constructed, the donor DNA could be excised from its backbone plasmid P2C3-8 by restriction digestion with SalI and NotI.*

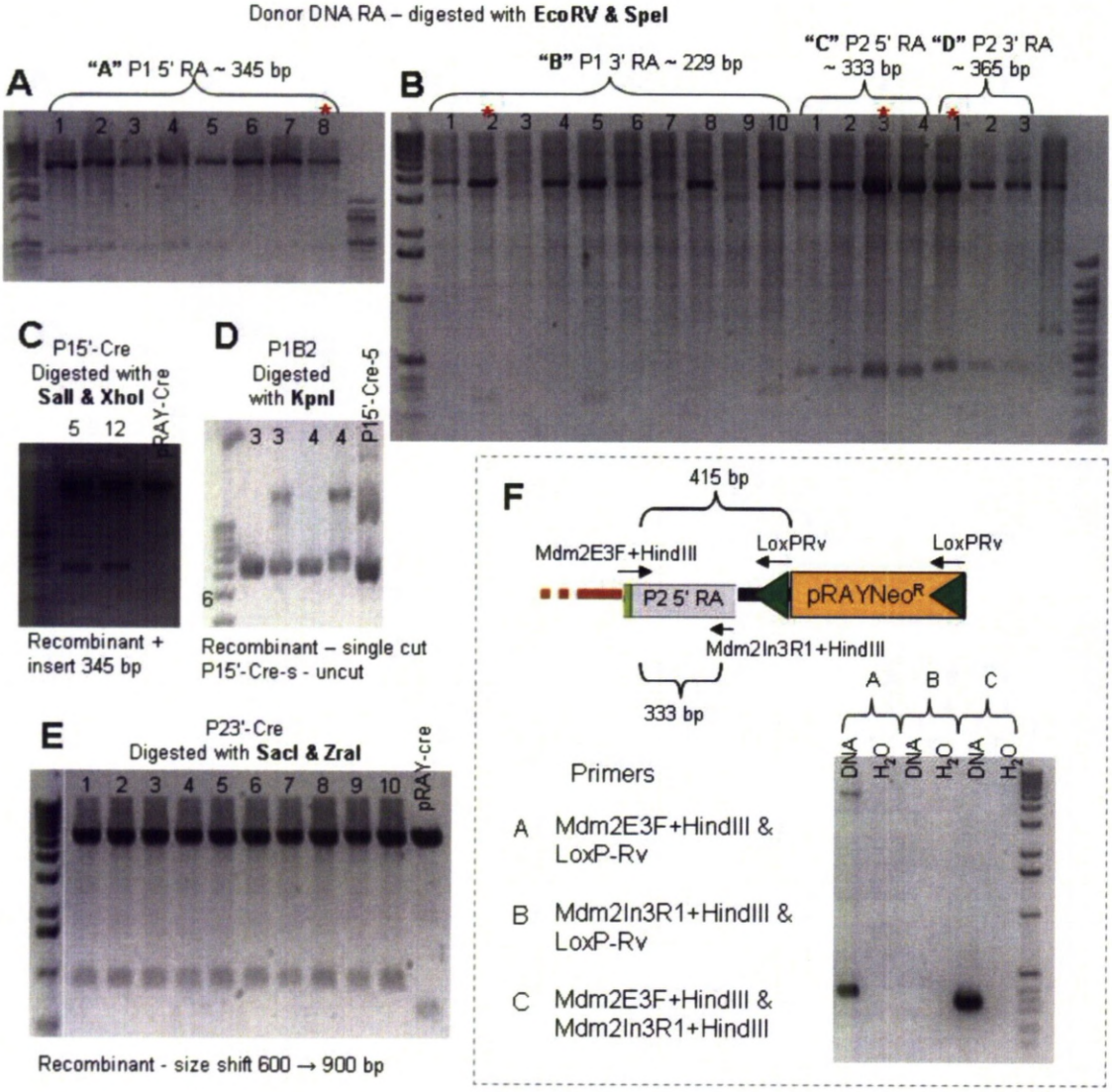


***Figure 3.3.53: Cloning of the Mdm2 donor DNA.***

*The RAs were amplified by PCR and TA-cloned into pCR2.1. A-B) Restriction digestion analysis with EcoRV and SpeI to screen for positive clones (expected DNA fragment size is indicated at top of gel). *These clones were sent for sequencing. Once the sequence was confirmed the RAs were inserted into pRAY-Cre via their common restriction sites. C-E) Positive clones were identified by restriction digestion analysis with the indicated enzymes, expected DNA fragments are indicated underneath each gel. All clones shown here are positive. F) PCR reaction to determine the orientation of the P2 5'RA once inserted into P23'-Cre. Primer pair A indicates the correct orientation, whilst B is the incorrect orientation and C is the positive control reaction. The PCR reactions were tested using clone P2C3-8 and fortunately this clones was positive (no further clones screened).*

### 3.3.5.6 Assembly of final constructs

Final assembly of the *Mdm2* P1-Null and P2-Mutant DNA targeting constructs was intended to be performed by homologous recombination in yeast as described in Section 3.3.5.3 however, due to unforeseen complications several additional cloning steps (in *E. coli*) were required to successfully complete the cloning of these two DNA targeting constructs. The main reason for the initial failure of homologous recombination in yeast (or rather the retransformation of correctly recombined yeast DNA back into bacterial cells) was primarily because we did not take into account the presence of the TK promoter within the pRAYNeo$^{R}$ cassette. The TK promoter (which drives expression of the neomycin phosphotase cDNA) shares significant sequence homology with the MCI promoter (which drives expression of TK) within the shuttle vector DNA. In fact analysis of the MCI and TK promoters revealed that they were virtually identical, except that the MCI promoter also contains a polyoma enhancer [Thomas and Capecchi, 1987]. As a result there existed a 275 bp identical sequence overlap between the TK and MCI promoters which was potentially sufficient to allow the yeast cells to perform homologous recombination between these sequences. This unwanted recombination event was found to be not only a potential, but an actual problem since it simultaneously deleted the TK cassette and the 4-5 kb region intended to be the *Mdm2* left arm of homology and the resulting smaller vector was preferentially propagated when yeast DNA was retransformed into *E. coli*.

This cloning strategy setback was overcome in two different ways; therefore the cloning of the P1-Null and P2-Mutant DNA targeting constructs are discussed separately. Cloning of the *Mdm2* P2-Mutant DNA targeting construct is described first, since this was completed without amending the original P2-Mutant shuttle vector whilst the *Mdm2* P1-Null DNA targeting construct is discussed afterwards, since this cloning exercise (which took longer to complete), also required redesigning of the P1-Null shuttle vector (pRSMdm2TK).

3.3.5.6.1 *Mdm2* P2-Mutant

Following co-transformation of the P2 shuttle vector (pRSm-P2mutant) with the P2 donor DNA (excised from P2C3-8) in yeast, 100 + yeast colonies were obtained after 2-3 days of growth on $Trp^-/Ura^-$ ("drop out") plates (see Section 2.2.1). 10 of these colonies were screened for successful integration of the donor DNA (and hence the positive selectable marker $pRAYNeo^R$) by several PCR reactions (see Figure 3.3.54). Plasmid DNA isolated from the most promising yeast clones (P2Y1, P2Y5 & P2Y7) was then used to transform bacterial cells. This step, namely the transfer of the DNA targeting construct back into *E. coli* was required to generate sufficient quantities of high quality plasmid DNA for gene targeting experiments. It was also important to isolate individual plasmids since within a yeast cell multiple copies of the shuttle vector can be propagated and it is possible that not all copies will contain the correct homologous recombination event (or indeed any homologous recombination event).

The yeast DNA was initially transformed into TOP10 cells (since this was the strain in which the shuttle vector was maintained) however despite screening ~20 clones we did not obtain any restriction digest patterns which matched with either the desired DNA targeting construct or the shuttle vector (see Figure 3.3.55 – A & B). These restriction digest patterns contained DNA fragments with very uniform sizes which perhaps indicated contamination with some unknown vector DNA. At this point we did not consider there to be a problem with the yeast-*E. coli* plasmid DNA since all the PCR screens (which had been repeated on the DNA extracted from the yeast cells) indicated that the desired homologous recombination event had occurred. The yeast colonies were re-streaked and fresh DNA was extracted and transformed into bacteria again nevertheless the same uniform digest pattern was observed. To attempt to resolve this problem, which we speculated might be due to difficulty in propagating the relatively large DNA construct in TOP10s, various other *E. coli* strains were utilised including MaxStbl.2, CopyCutter, SURE, XL1-blue and DH5α. However the majority of restriction digestion patterns appeared much the same as for TOP10s except for the occasional bacterial colony which had either a random digest pattern or seemingly uncut DNA. One of these occasional rare bacterial colonies (P2Y1α2) appeared to have at least

some of the correctly sized DNA fragments and so was selected for further restriction digest analysis (see Figure 3.3.55 B & C).

Upon further analysis it emerged that the bacterial clone P2Y1α2 had somehow incorporated the pRAYNeo$^R$ cassette twice in the forward orientation. Fortuitously there is a unique restriction site (ClaI) within pRAYNeo$^R$ which was used to rescue the *Mdm2* P2-Mutant DNA targeting construct as outlined in Figure 3.3.56. The resulting plasmid (P2TClaI) was confirmed by multiple restriction digests (see Figure 3.3.55 – C) and then sequenced in its entirety. The sequencing results for P2TClaI were identical to the expected sequences, therefore this clone was determined to be, to the best of our knowledge, a whole and accurate DNA targeting construct for the generation of a *Mdm2* P2-Mutant transgenic mouse strain and was deemed suitable for use in gene targeting of ES cells (as described in Section 2.9.2.2).

It was during sequencing of this clone (P2TClaI) that the 275 bp sequence overlap between the TK and MCI promoter regions became apparent. This unwanted region of homology enabled yeast cells to perform a second homologous recombination event which would result in the loss of the TK cassette and *Mdm2* left arm region. Whilst the loss of this ~ 7 kb region, did not completely explain the uniform restriction digest patterns observed during screening of bacterial transformants it did indicate that we needed to redesign the cloning strategy to increase the probability of obtaining the desired homologous recombination event. This redesigned P1-Null cloning strategy is detailed next.

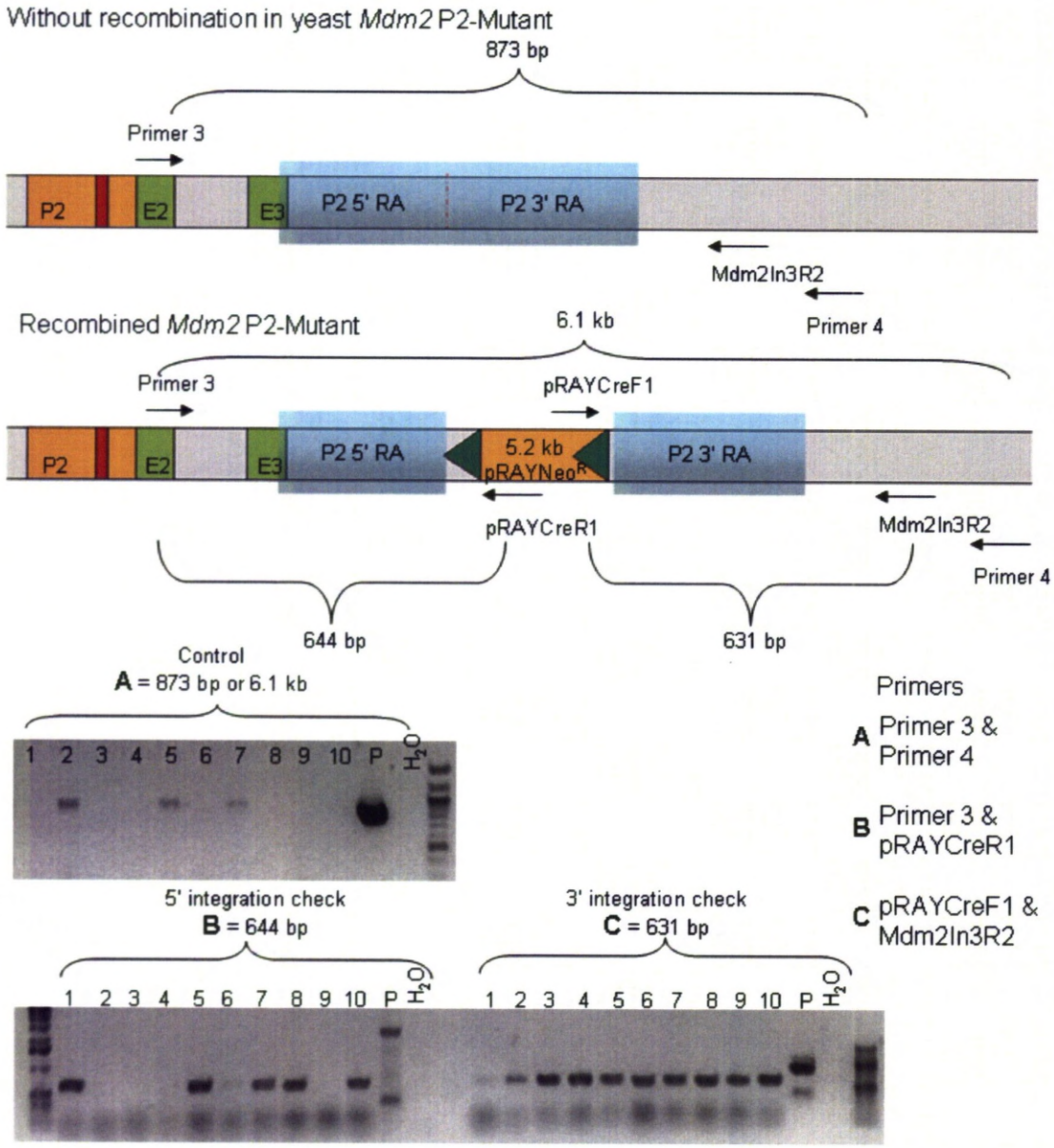


***Figure 3.3.54: Yeast colony PCR screen for Mdm2 P2-Mutant***

*Top panel: Schematic diagram of the un-recombined and recombined Mdm2 P2-Mutant region, with alignment of primers (black arrows). PCR reactions were performed to test for the successful incorporation of the 5.2 kb pRAYNeo$^R$ cassette by homologous recombination in yeast. Primers were designed outside of the RAs so that generation of a correctly sized PCR product only occurred following successful integration. Bottom panel: Example agarose gels for the indicated primer pairs. Yeast colony PCR was quite sensitive (indeed, the use of too many yeast cells easily inhibits the PCR reaction) therefore a negative result does not always reliably indicate the absence of the target DNA region. From these screens P2Y clones 1, 5 & 7 were selected for retransformation into E. coli.*

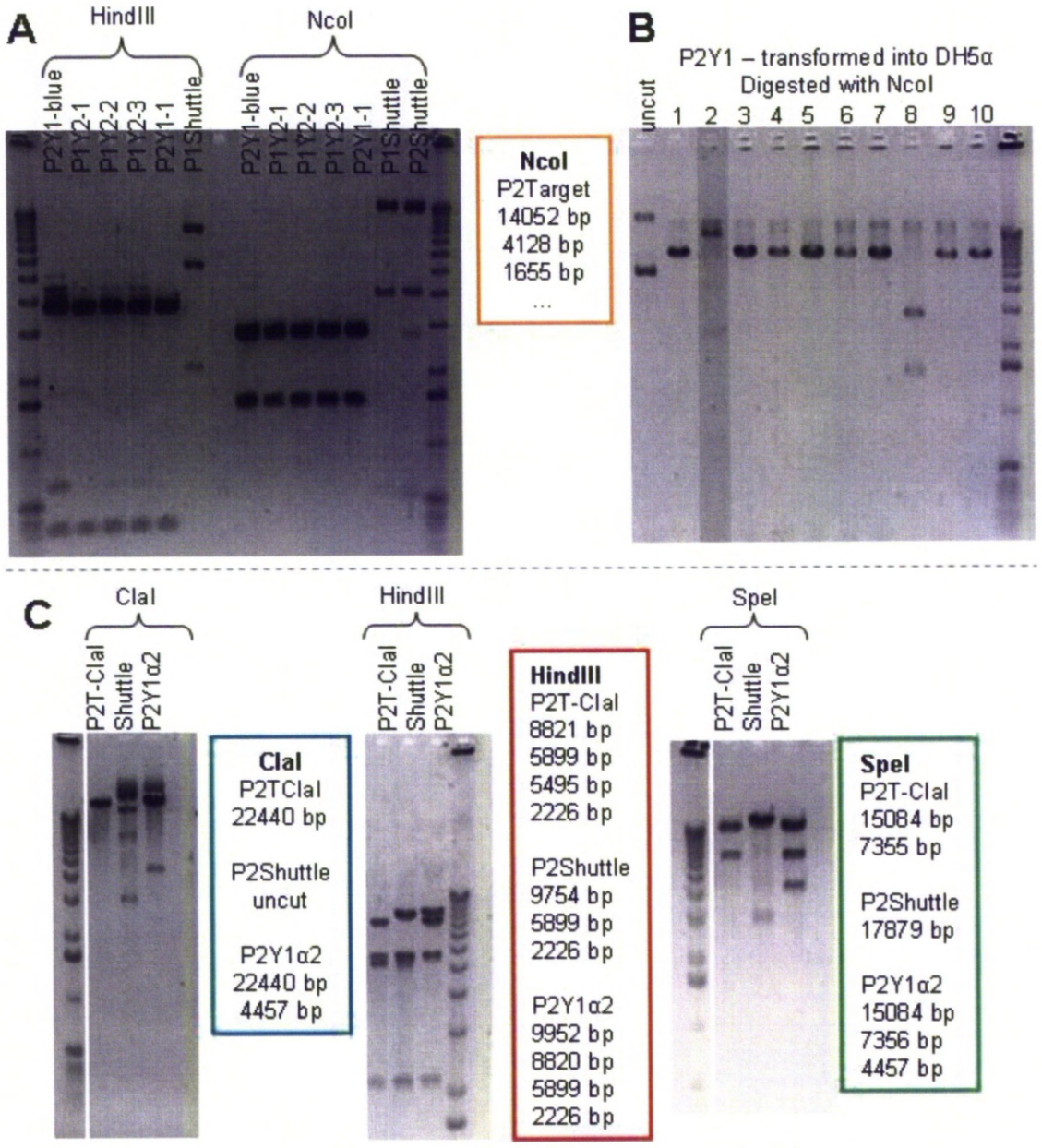


***Figure 3.3.55: Cloning the Mdm2 P2-Mutant DNA targeting construct.***

*A) Example of a typical restriction digest pattern observed when yeast DNA was retransformed into various strains of E. coli (XL1-blue and TOP10 shown here). B) Another restriction digest screen of retransformed yeast DNA, this time in DH5α. Only clone 2 (P2Y1α2) appears to contain some of the correct sized DNA fragments. C) Restriction digestion analysis of bacterial clones P2Y1α2, P2TClaI, and P2 shuttle vector (pRSm-P2mutant) with various enzymes as indicated to confirm the positivity of P2TClaI. All DNA restriction fragments appear at the expected sizes and stoichiometric ratios, therefore vector P2TClaI was sent for complete sequencing.*

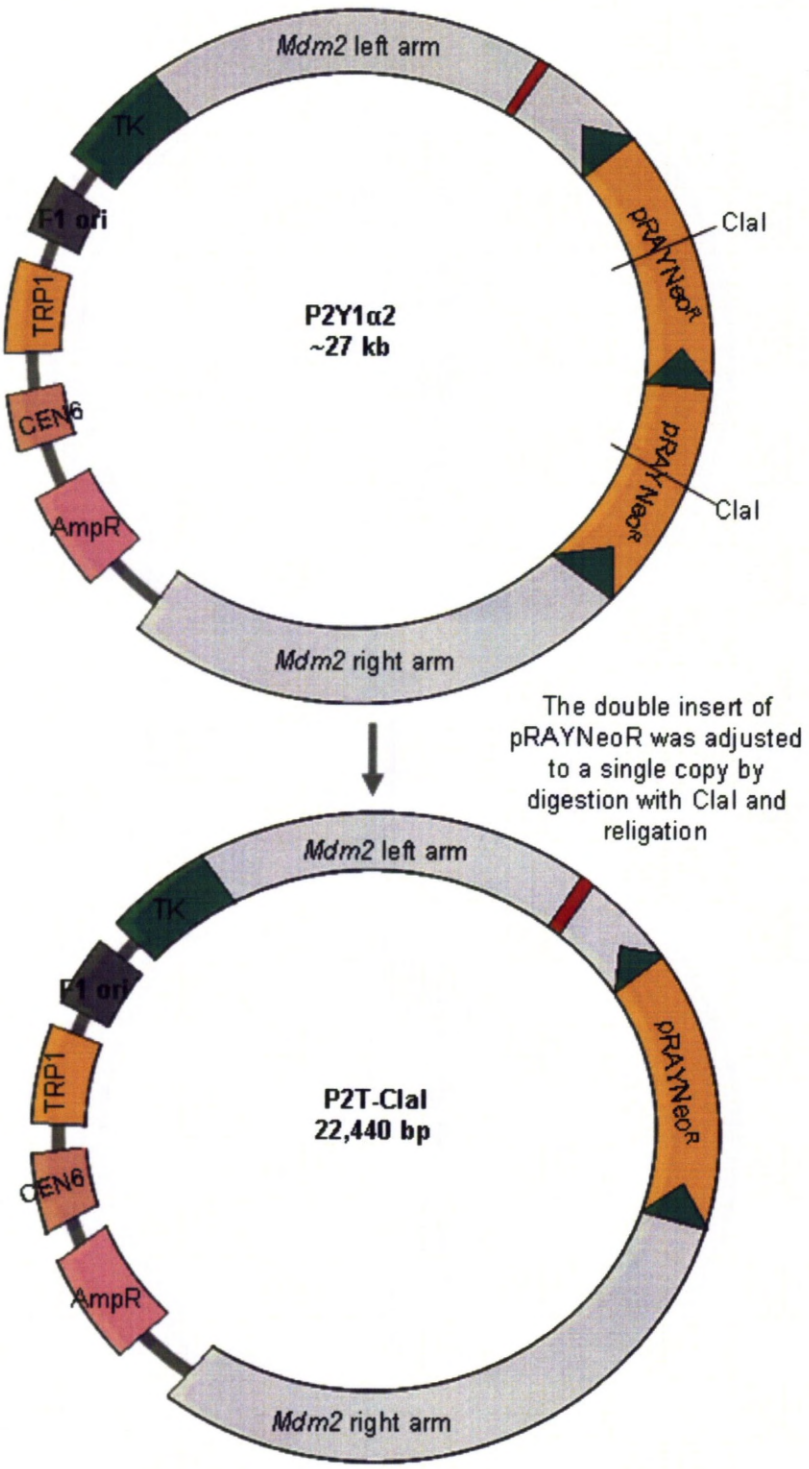


***Figure 3.3.56: Final assembly of the Mdm2 P2-Mutant DNA targeting construct.***

*Flow diagram for the final step in cloning the Mdm2 P2-Mutant DNA targeting vector. The double insertion of the pRAYNeo$^R$ cassette could be rescued by digesting with ClaI and re-ligating the 22.4 kb backbone.*

3.3.5.6.2 *Mdm2* P1-Null

Cloning of the *Mdm2* P1-Null DNA targeting construct had been previously hindered by the unintentional inclusion of an additional region of homology between the shuttle vector and donor DNA (discussed in Section 3.3.5.6). Therefore the cloning strategy was redesigned to remove the TK cassette (containing one of the unwanted regions of homology) from the shuttle vector before homologous recombination in yeast and then to reintroduce it afterwards (see Figure 3.3.57 and Figure 3.3.58).

The TK cassette was removed from the P1 shuttle vector (pRSMdm2TK) by digestion with restriction enzymes SalI and PacI, the DNA ends were then blunted and the vector religated to create a smaller plasmid (pRSm-TK). 4/4 bacterial transformants appeared positive for removal of the 2.1 kb TK region when screened by restriction digestion with KpnI and SacI (see Figure 3.3.57). One of these clones (pRSm-TK1) was selected to be the shuttle vector in a second round of homologous recombination in yeast.

Following co-transformation of the new shuttle vector (pRSm-TK1) and donor DNA (excised from P1B2-3) in yeast, 100 + yeast colonies were obtained. DNA was extracted from 12 yeast clones and screened for successful incorporation of the pRAYNeo$^R$ cassette by several PCR reactions as shown in Figure 3.3.59. The most promising clones (P1YB-5, 11 and 12) were then transformed into *E. coli* strain SURE. SURE bacteria were used since they were readily available and previously had demonstrated high transformation efficiency with DNA prepared from yeast cells (see Section 2.7.2.5 for method). 5/14 transformants appeared to contain the correct DNA fragments when screened by an initial test digest with HindIII. All five of these clones were from the transformation of yeast clone P1YB-5. Following additional restriction digests to further confirm the positivity of these clones with NcoI, NotI, KpnI and SacI (see Figure 3.3.60 – A & B) one clone (P1Target-1) was selected for the final stage of cloning.

The ultimate step in cloning the *Mdm2* P1-Null DNA targeting construct reintroduced the negative selectable marker to allow for double selection (positive and negative) during gene targeting in ES cells as discussed in Section 2.9.2.2.4. The TK cassette was excised from TK2 by double digestion with FseI and PacI, blunted and then inserted into the blunt SwaI site within the TRP1 gene of the P1Target-1 vector (see Figure 3.3.58). 1/5 of the

resulting colonies appeared positive for insertion of TK by restriction digestion with KpnI and SacI (see Figure 3.3.60) and this clone (P1Target+TK-3) was sent for sequencing to confirm the DNA sequences at the cloning junctions between the assembly vectors. The sequencing results for P1Target+TK-3 were identical to the expected sequences, therefore this clone was determined to be, to the best of our knowledge, a whole and accurate DNA targeting construct for the generation of a *Mdm2* P1-Null transgenic mouse strain and was deemed suitable for use in gene targeting of ES cells.

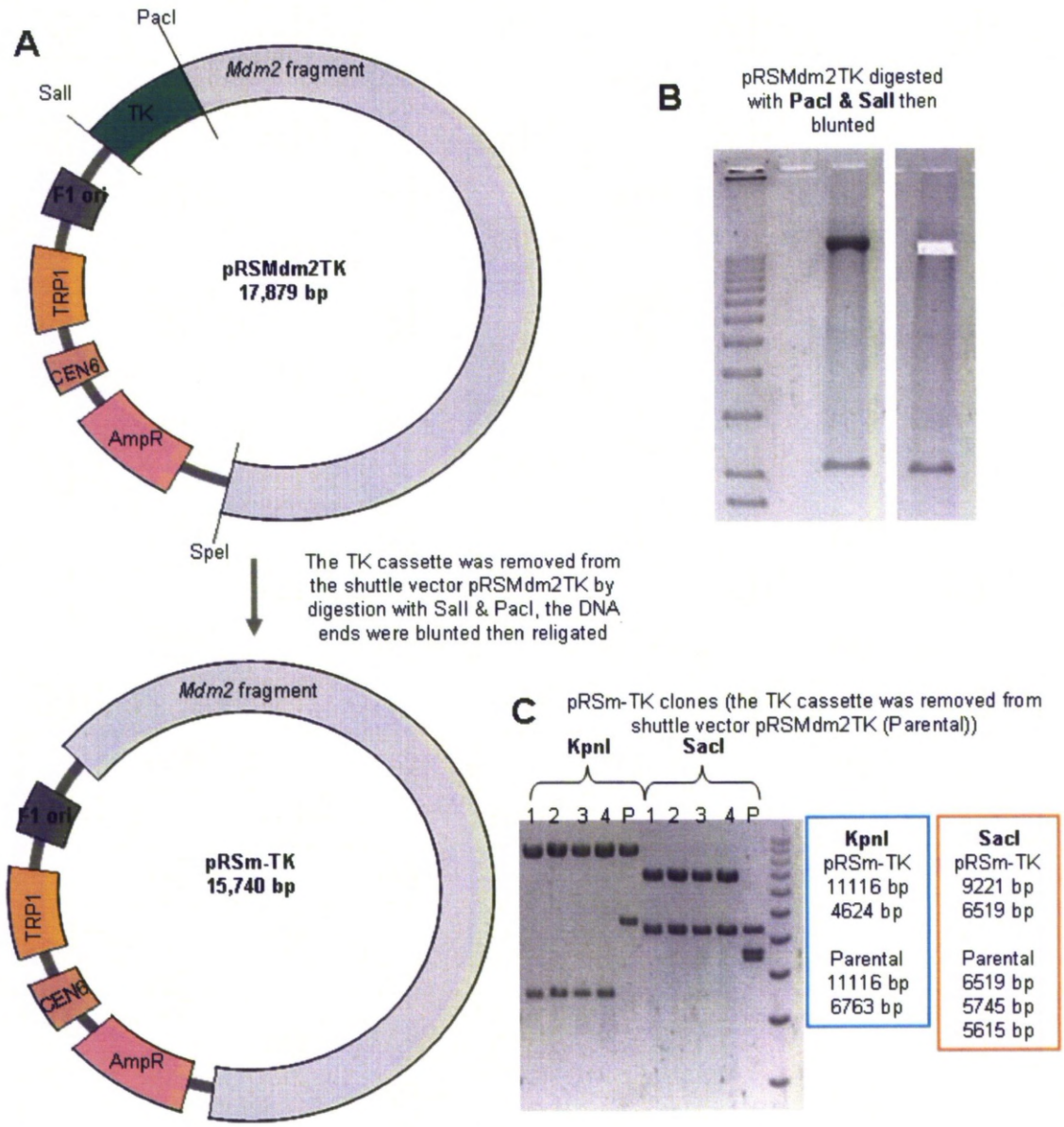


***Figure 3.3.57: Re-cloning of the Mdm2 P1-Null shuttle vector.***

*A) Flow diagram for the removal of the TK cassette from the original shuttle vector pRSMdm2TK. The 2.1 kb TK cassette was removed by digestion with SalI and PacI. The DNA ends were blunted then the plasmid was religated to form pRSm-TK. B) Restriction digestion of pRSMdm2TK. The 15.7 kb backbone DNA fragment was extracted from the gel for generation of the pRSm-TK vectors. C) 4/4 clones appeared positive when screened by two different restriction digests KpnI and SacI. P stands for the parental vector, in this case pRSMdm2TK.*

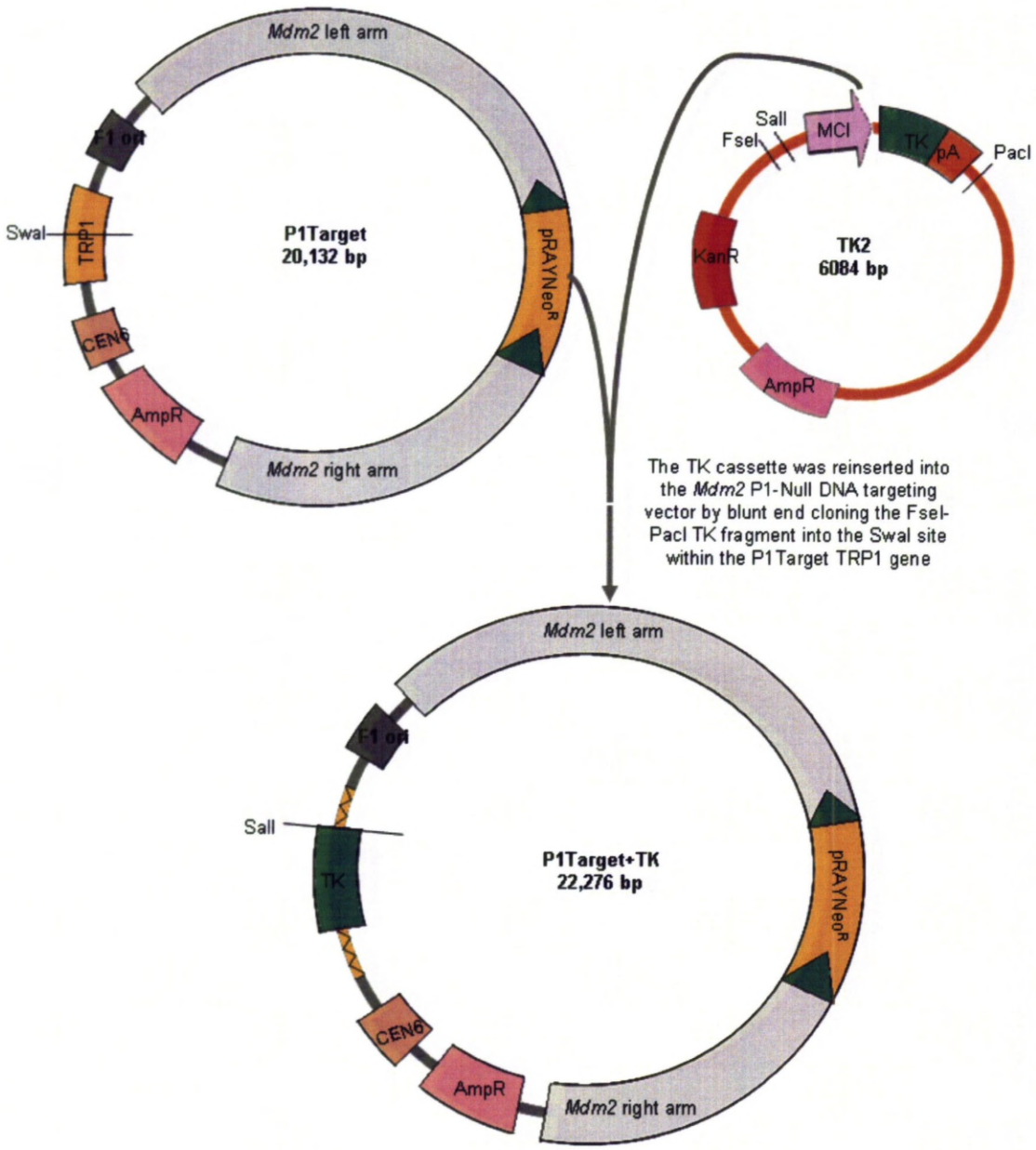


***Figure 3.3.58: Final assembly of the Mdm2 P1-Null DNA targeting construct.***

*Flow diagram of the ultimate step in cloning the Mdm2 P1-Null DNA targeting construct. The negative selectable marker (TK) was reintroduced to the targeting vector to enable both positive and negative selection during ES cell targeting experiments. The TK fragment released from TK2 by digestion with FseI and PacI, this was blunted and then inserted into the blunt site SwaI within the TRP1 gene (a yeast selectable marker) of the P1Target vector. The resulting vector P1Target+TK could be linearised by restriction digestion with SalI.*

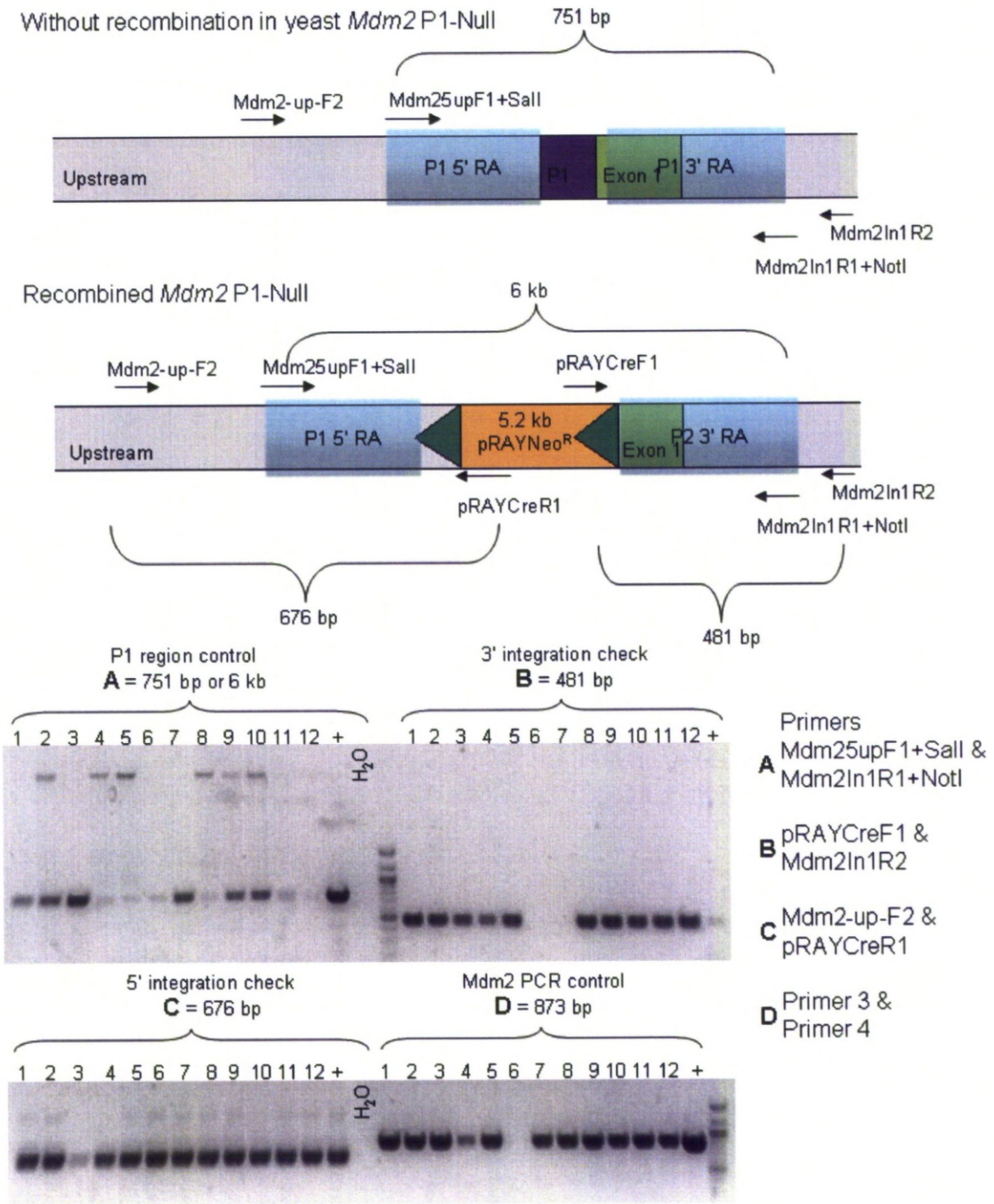


***Figure 3.3.59: Yeast DNA PCR screen for Mdm2 P1-Null.***

*Top panel: Schematic diagram of the un-recombined and recombined Mdm2 P1-Null region, with alignment of primers (black arrows). Bottom panel: Example agarose gels for the indicated primer pairs. PCR reactions were performed on DNA extracted from yeast clone liquid cultures. + indicates a positive control, the negative controls ($H_2O$) were combined post-PCR and run together. From these screens P1YB clones 5, 11 & 12 were selected for retransformation into E. coli (SURE strain).*

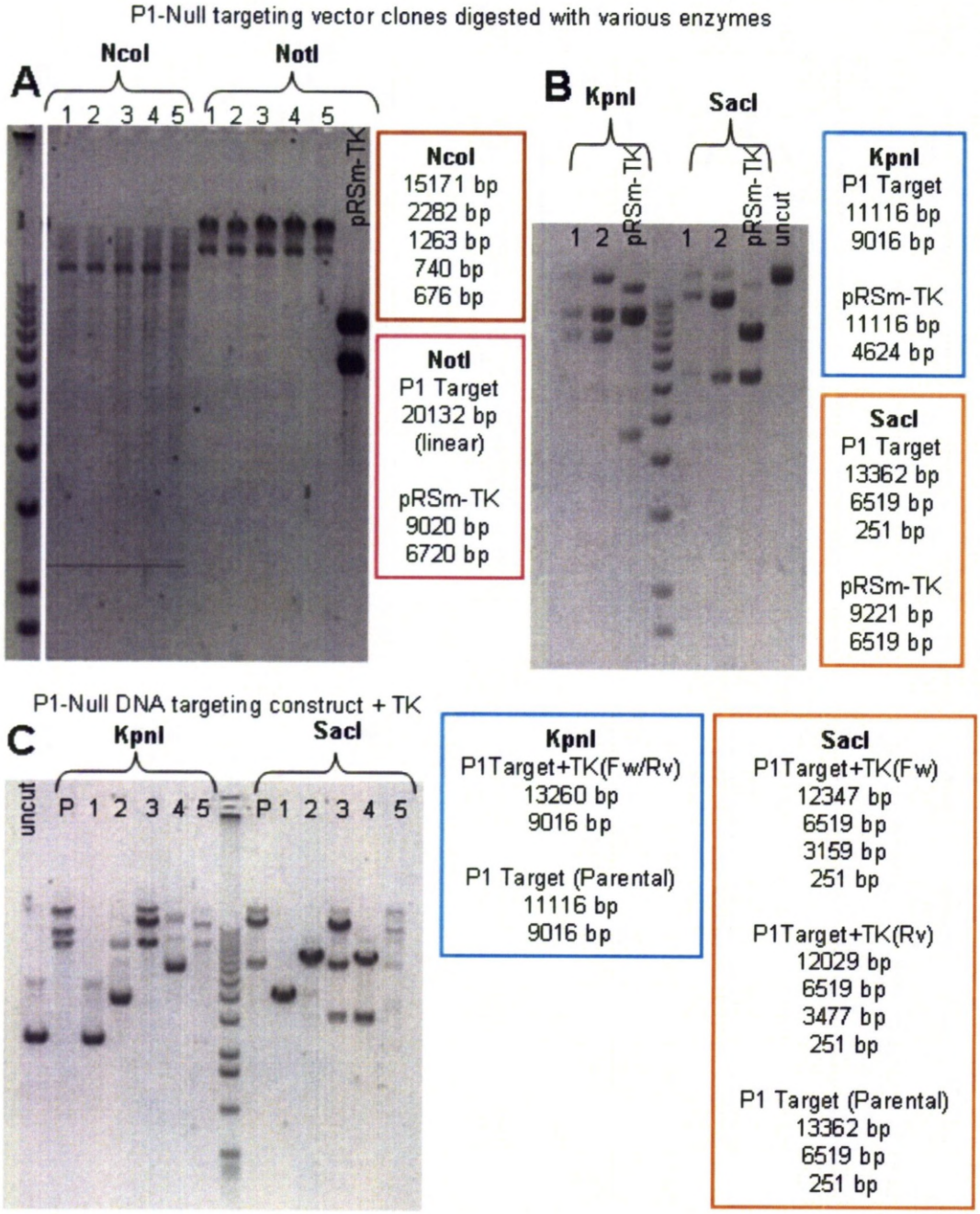


***Figure 3.3.60: Confirmation of positive Mdm2 P1-Null DNA targeting construct.***

*A) Further restriction digests identify positive clones for retransformation of the yeast DNA into E. coli with NcoI and NotI. Despite low concentration of DNA loaded into the agarose gel, the correct sized DNA fragments were just visible on the NcoI digest (the 2.3 kb band has been digitally enhanced to be visible in this figure). B) Further confirmation of the P1Target clones 1 & 2 by KpnI and SacI digests. C) The TK cassette was then reintroduced to the P1Target construct and 1/5 clones appeared positive when screened by restriction digestion with KpnI and SacI (P1Target+TK-3).*

# 3.4 ES cell gene targeting

## 3.4.1 p21-mCherry (1st attempt)

The first attempt at targeting ES cells with the p21-mCherry DNA targeting construct was unsuccessful. Following electroporation and selection protocols there were only a few, very small (only visible under a microscope) ES cell colonies to pick off of the dishes at day 11 of selection. These colonies grew very slowly, if at all. The reason or reasons for the slow ES cell growth was or were initially unclear since the preparation of the DNA targeting construct appeared to proceed as expected (see Figure 3.4.1) and the ES cells appeared healthy prior to electroporation. Further investigation, however, indicated that the failure of this first attempt at gene targeting might be due to the set-up of the GenePulser II during the electroporation since the actual recorded time constant (RC) was sub-optimal suggesting that the discharge might have been too rapid. Another factor that might have contributed to the slow growth of ES cells was the quality of our FBS. Although we were already using an ES cell approved FBS (HyClone), the batch that we used was only quality controlled by the supplier/manufacturer. Previous successful gene targeting had been performed using FBS from a batch tested and approved by the Bradley laboratory at the The Wellcome Trust Sanger Institute in Cambridge. According to their experts the batch-to-batch quality and ES cell suitability of FBS can vary tremendously [email communication with The Wellcome Trust Sanger Institute]. Fortuitously the The Wellcome Trust Sanger Institute had just finished batch testing a new lot of FBS (Invitrogen) which was of a high quality therefore it was decided to order fresh FBS from this batch and repeat the gene targeting experiment.

Southern blotting was necessary to locate where mCherry had integrated into the genome. Figure 3.4.2 contains an outline of the Southern blot strategy for identification of correctly targeted ES cells and genotyping the subsequent transgenic mice. However, initial testing of the 790 bp DNA fragment intended to act as the p21 Southern blot probe demonstrated that this probe was not specific enough. Instead of detecting a single DNA band this 790 bp probe detected a smear (see Appendix C.6). Therefore for future screening

this probe needs to be redesigned. We therefore, in the meantime attempted to screen these slow growing colonies by PCR.

Despite the slow growth some (51 out of 140 picked) ES cell colonies did eventually reach confluence and these were screened for insertion of mCherry by PCR (see Figure 3.4.3). 4/51 clones (20, 23, 34 & 36) appeared positive for insertion of mCherry however since these DNA bands were very faint when visualised by UV on an agarose gel we attempted to improve the PCR product yield (and perhaps identify other positive clones) by optimising the reaction conditions (see Figure 3.4.3 – C). Optimisation of the reaction conditions identified conditions using 2 µl of template DNA for 35 cycles. Unfortunately when the number of cycles was increased, this resulted in an unexpected and persistent contamination problem in the negative controls (the genomic DNA, the water, mCherry control) in both the mCherry specific and the positive control PCR reactions. The contamination was clearly on issue of technical competence since it was possible to generate clean controls. In the future it would be better to rely on Southern blotting (which is the better screen – since PCR is unable to localise an insert within the genome) to circumvent this problem.

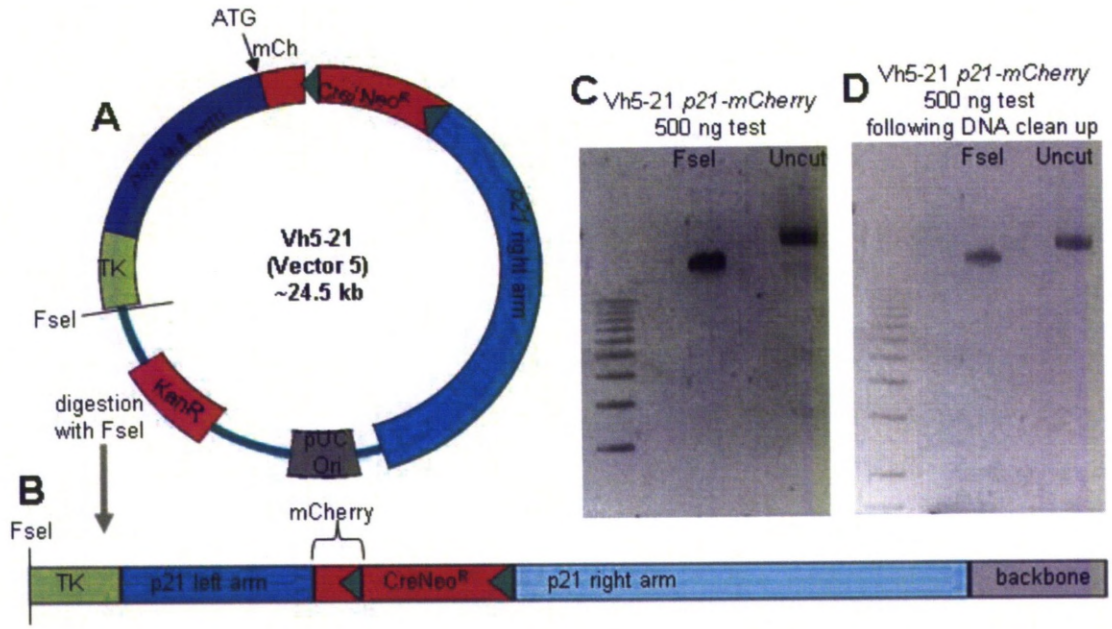


***Figure 3.4.1: Preparation of the gene targeting vector for ES cell electroporation.***

*A) 60 µg of the p21-mCherry DNA targeting construct (Vh5-21) was digested overnight with FseI to linearise it. B) Schematic diagram of the linearised gene targeting vector. C) Agarose gel electrophoresis was performed on 500 ng of the FseI cleaved Vh5-21 vector to check for complete digestion. D) A second 500 ng sample was examined by agarose gel electrophoresis post DNA clean up (by PCI extraction see Section 2.3.10) to confirm that everything appeared as expected. An uncut control sample was included for comparison.*

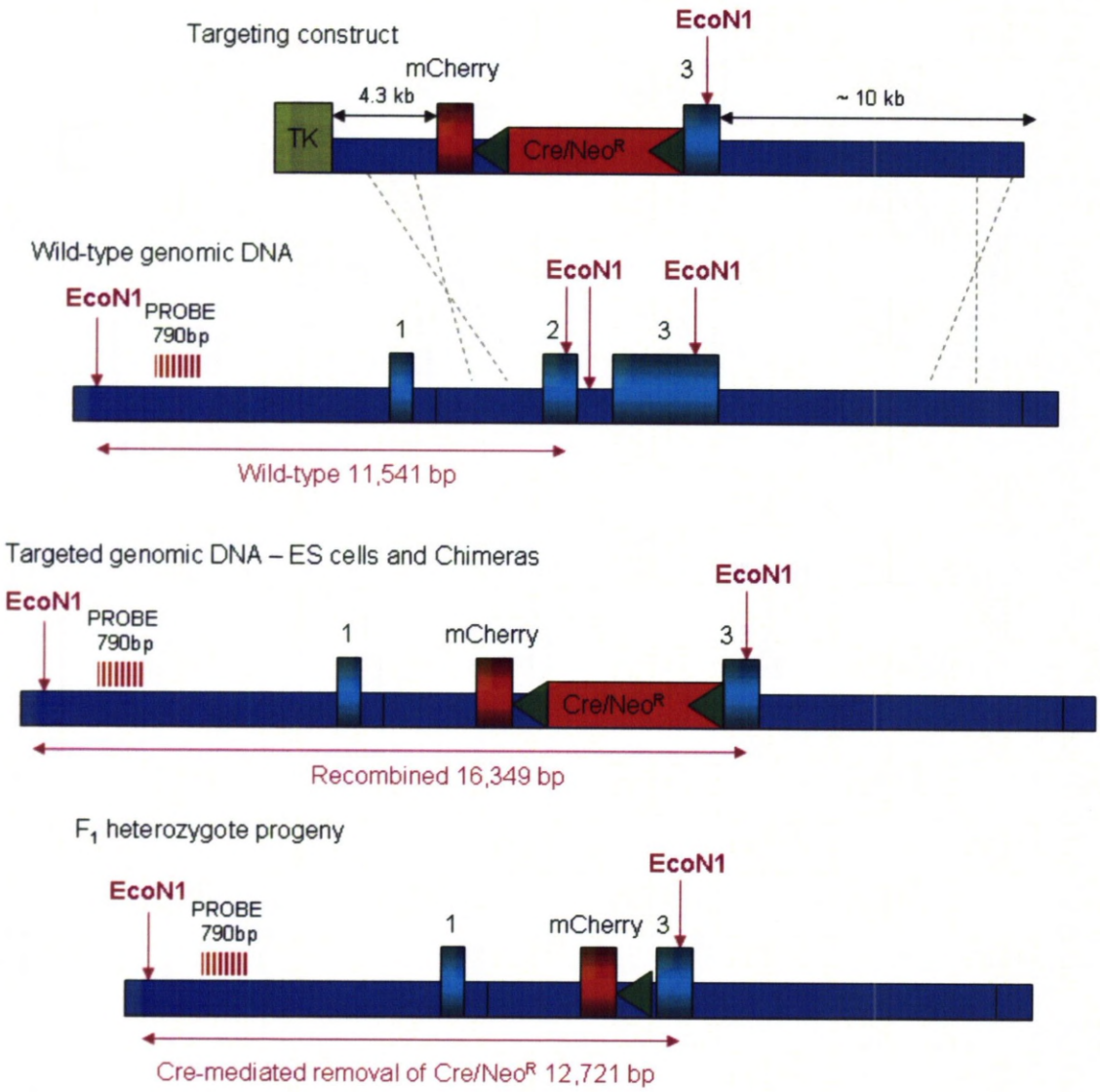


***Figure 3.4.2: Southern blot strategy for p21-mCherry.***

*Following a successful homologous recombination event in ES cells, the self-excision neomycin cassette (Cre/Neo$^R$ –shown in red with green arrows) is integrated into intron 1 of p21 (exons blue boxes shown numbered). The Southern strategy utilises restriction enzyme EcoN1 which cuts only once inside the targeting construct and relies on a specific upstream EcoN1 site to generate products of the expected size. Since the probe hybridises outside of the targeting construct (upstream of p21), the recombined fragment only occurs in the event of successful recombination. The same Southern blot strategy could potentially be used to genotype the first generation ($F_1$) mice following the removal of Cre/Neo$^R$ by Cre-recombinase (see Section 3.3.3.6).*

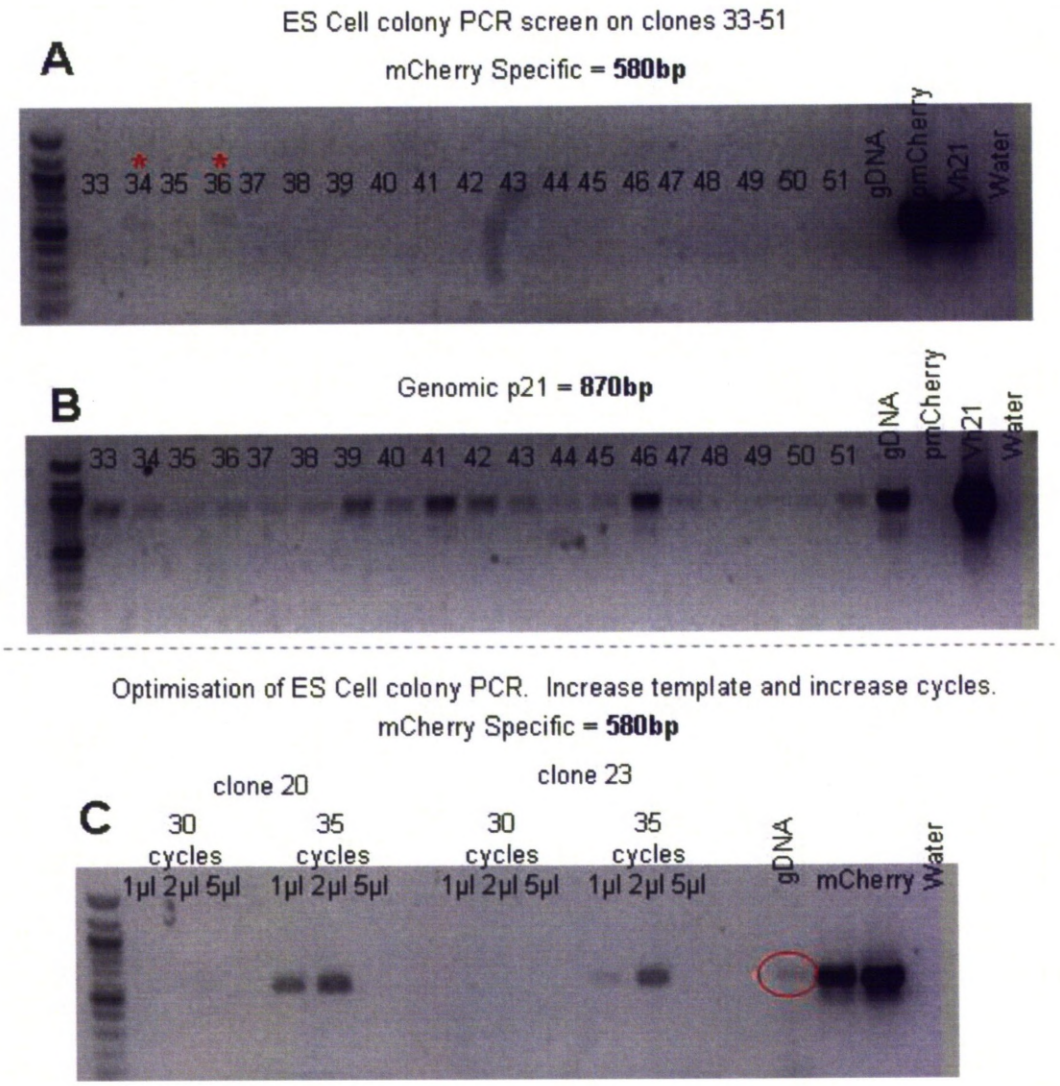


***Figure 3.4.3: ES cell colony PCR screen.***

*PCR results for p21-mCherry ES cell clones 33-51. A) mCherry specific PCR and B) positive control reaction (to determine if DNA was extracted and whether it was acceptable quality for PCR). *Clones 34 & 36 appeared positive although these bands were very faint. C) Optimisation of the ES cell colony mCherry specific PCR reaction to improve yields. Optimised PCR reaction conditions used 2 µl of template DNA (see Section 2.3.12 for DNA extraction method) for 35 cycles. However contamination was a problem when 35 cycles were used (wild-type genomic DNA also produced an apparent mCherry specific product- red circle). Primers were; pmChPROBEF & pmChPROBER for mCherry specific PCR reaction and p21In1+2kb & p21In1+3kbR for the control reaction.*

### 3.4.2 Mdm2 P2-Mutant

The second attempt at gene targeting was performed using the Mdm2 P2-Mutant DNA targeting construct. This round of ES cell targeting proceeded much more smoothly then the previous attempt and there were large numbers of easily visible ES cell colonies by day 9 of selection. Approximately 600 (6 x 96-well plates) ES cell colonies were picked for expansion and screening. Potential positive clones would be identified initially by using Southern blot analysis and then by sequencing of PCR products (to ensure successful incorporation of the point mutations within the P2 region).

Figure 3.4.4 shows the outline of the Southern blot strategy designed to screen for successful incorporation of the positive selectable marker (pRAYNeo$^R$) in targeted ES cells. Using this screen, 10/208 colonies have so far been identified as containing pRAYNeo$^R$ cassette correctly integrated at the *Mdm2* locus (see Figure 3.4.5). The homologous recombination efficiency in clones screened to date is ~ 4.8%. Whilst this is encouraging, it does not unequivocally demonstrate that the P2 mutation has been incorporated. This is because the positive selectable marker is ~ 700 bp downstream of the P2 point mutations therefore there is a small chance that the homologous recombination event has occurred within that region and if so, our desired mutations would not have been integrated into the genome. Also, even if the P2 point mutations have been successfully incorporated the aforementioned Southern blot strategy is unable to detect random recombination events which may have occurred simultaneously during ES cell targeting. These issues will need to be resolved prior to use the of these ES cell clones in micro-injection experiments for the generation of chimeras. These issues will be addressed in two separate ways which are discussed next.

In order to determine whether the P2 mutations have been incorporated into the genome the P2 region (of the ES cells clones which are positive by Southern blot analysis) will be amplified by PCR and sequenced. Since the template DNA will also contain the wild-type allele we will be looking for mixed peaks on the chromatogram at the expected mutated base pairs. Alternatively the P2 region PCR product could be cloned into pCR2.1 and transformed into *E. coli*, to enable single PCR products to be sequenced and reduce the ambiguity surrounding mixed peaks.

In the meantime the Southern blot screen will be repeated but instead of using a Southern probe that detects a region outside of the DNA targeting construct, we will use one designed to anneal within the pRAYNeo$^R$ cassette to create a single fragment of 12.7 kb. If non-specific bands appear during this Southern blot analysis it would be indicative of an additional unwanted random recombination event(s). This screen was not performed originally since without a probe based outside of the DNA targeting construct, an expected size shift alone does not guarantee integration at the correct loci (since the correct expected sizes could occur purely by chance). Due to time constraints these important controls have yet to be performed.

The restriction enzyme NcoI which was introduced by the P2 point mutations will be used to help genotype transgenic mice, rather than correctly targeted ES cells (see Figure 3.4.6).

In conclusion, since we already have 10 pRAYNeo$^R$ positive colonies, it is highly likely that one or more of these contains the correct homologous recombination event and therefore we are in an excellent position to continue on and make the *Mdm2* P2-Mutant transgenic mouse.

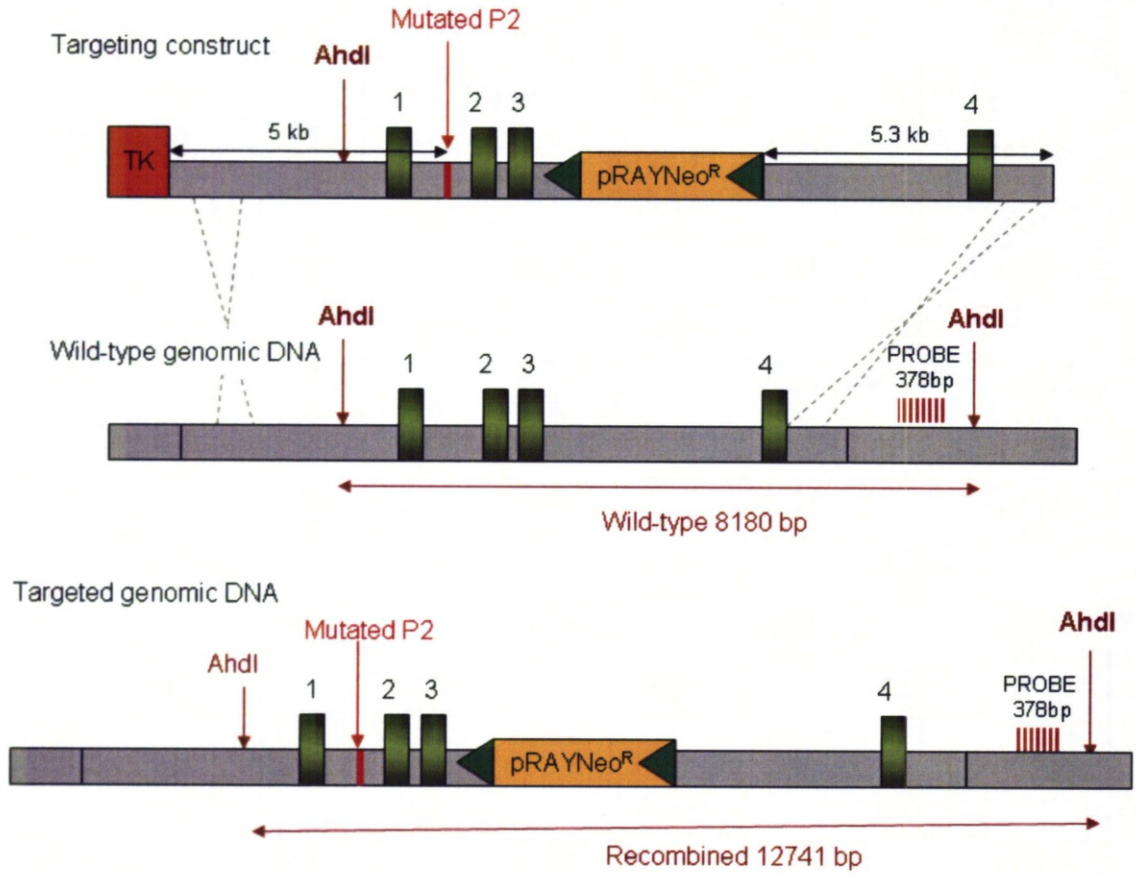


***Figure 3.4.4: Southern blot strategy for Mdm2 P2-Mutant – ES cells.***

*Following a successful recombination event, the self-excision neomycin cassette (pRAYNeoR shown in yellow with green arrows) is integrated into intron 3 of Mdm2 (exons green boxes shown numbered). The Southern strategy utilises restriction enzyme AhdI which cuts only once inside the targeting construct and relies on a specific downstream AhdI site to generate products of the expected size. Since the probe hybridises outside of the targeting construct (in intron 4 of Mdm2), the recombined fragment only occurs in the event of successful recombination.*

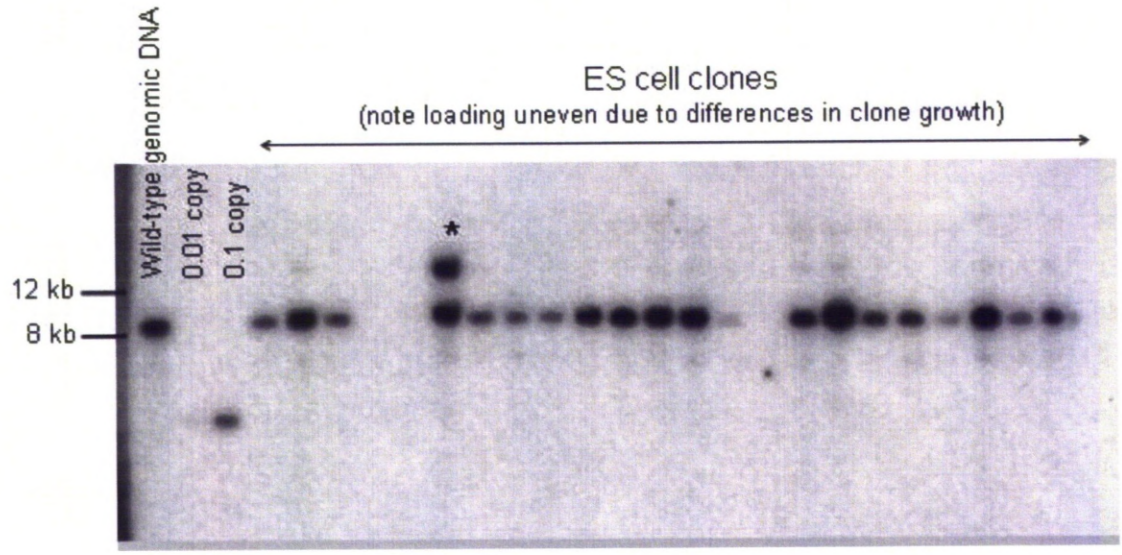


***Figure 3.4.5: Southern blot analysis of targeted ES cells.***

*Example Southern blot film following a 3 day exposure. Southern probe hybridises to genomic Mdm2 region (outside of the targeting construct). Wild-type genomic DNA should yield a band at 8180 bp, whereas a correctly targeted clone will have both an 8180 bp band and a larger recombined band at 12741 bp. *One clone shown here is positive. The signal of the recombined fragment should be detected at approximately a 1:1 ration with the un-recombined fragment band.*

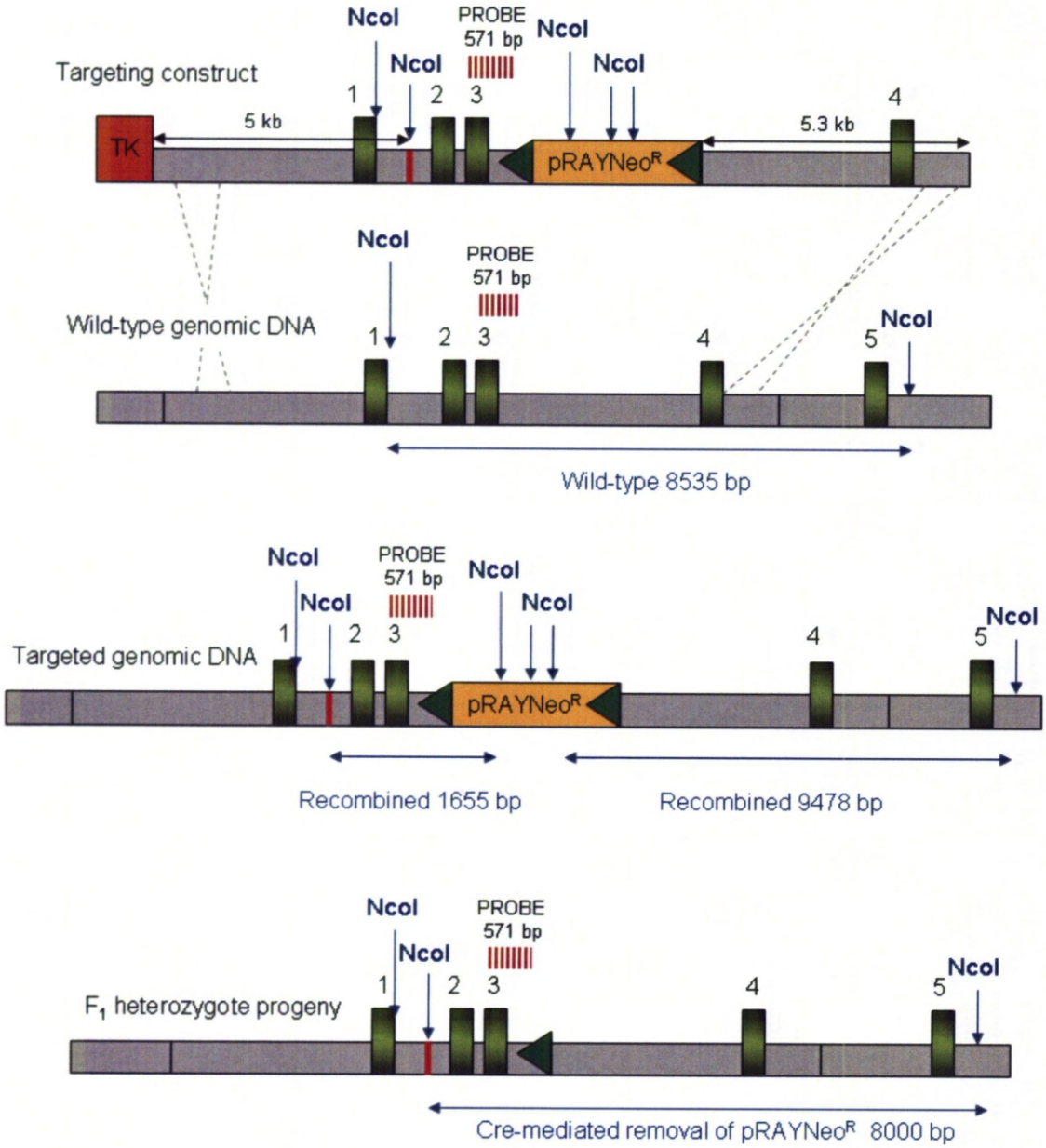


***Figure 3.4.6: Southern blot strategy for Mdm2 P2-Mutant – transgenic mice.***

*Following a successful recombination event, pRAYNeoR is integrated into intron 3 of Mdm2 (exons green boxes shown numbered). The Southern strategy utilises restriction enzyme NcoI which is introduced by the specific point mutations of the P2-Mutant and by the positive selectable marker. Since the 1655 bp recombined fragment near the P2 locus is also present within the DNA targeting construct, this screen was not suitable to identify correctly targeted ES cells. However, following Cre-mediated removal of pRAYNeoR the resulting DNA fragments can be distinguished. The NcoI screen will therefore be used to help genotype transgenic mice.*

### 3.4.3 p21-mCherry (2nd attempt)

The p21-mCherry gene targeting experiment was repeated as soon as new targeting construct DNA had been generated (see Section 2.3.5) and taking advantage of the, now proven, Sanger Institute ES cell –tested batch of FBS. This second attempt (the third ES cell targeting experiment) appeared much more successful than the first and like the *Mdm2* P2-Mutant gene targeting experiment there were many (100 + colonies per 10 cm dish); large, rapidly growing, undifferentiated ES cell colonies, visible by day 10 of selection. Approximately 600 ES cell colonies were picked (6 x 96-well plates) however, due to time restraints these ES cell colonies have yet to be screened. Nonetheless, given the high homologous recombination frequency observed for the *Mdm2* P2-Mutant construct we have every reason to believe it will be possible to isolate p21-mCherry positive clones.

# 4.1 Investigating cell death along the crypt-villus-axis (CVA)

In order to study key aspects of *p53* activation and regulation *in vivo* we examined the expression of p53 target genes *p21* and *Noxa* along the CVA in response to DNA damage and also changes in p53 levels by using conditionally floxed *Mdm2* null mice. We aimed to determine whether p21 and/or Noxa could be reliably used as reporters of p53 activity and thus assess their suitability for use in a dual p53 cell cycle arrest/apoptosis reporter system. The gastrointestinal tract was used as a model system since it has a well defined molecular and hierarchical cell structure (reviewed in [van der Flier and Clevers, 2009]) with dramatic differences in regards to cell death susceptibility within the tissue [Marshman et al., 2001, Leibowitz et al., 2011]. In this system, cycling cells within the crypt compartment readily and rapidly undergo massive p53-dependent apoptosis, whilst cells which are arrested in $G_1$ phase of the cell cycle and migrate onto the villus rarely respond to a wide variety of apoptogenic stimuli. As it has been demonstrated in this report, this lack of apoptosis on the villi is not simply due to a lack of p53 up-regulation, since even when p53 is induced in cells on the villi in the presence of genotoxic stress, these cells remain refractory to apoptosis. We therefore also aimed to investigate the uncoupling of p53 activation from apoptosis in cells on the villi by RNA expression array analysis.

In order to develop a dual cell cycle arrest/apoptosis *p53* reporter system we planned to target p53 responsive genes using a targeted knock-in approach so that one allele of each selected gene would be replaced with a reporter gene (such as *LacZ* or florescent protein). An ideal target gene would preferably be exclusively activated by p53, invoke a specific response programme (such as cell cycle arrest or apoptosis) and would also not display any haploinsufficiency. Whilst the latter may not be completely achievable, we have set out to generate two reporter strains that would enable differential monitoring of p53 activation leading to cell cycle arrest and/or apoptotic responses.

In the case of cell cycle arrest, *p21* appears to be an ideal reporter of p53 activity in the gut as identified by both our own experiments and previously reported work on p21 expression in the intestinal epithelium following different stress stimuli [Pritchard et al., 1998,

Wilson et al., 1998]. Indeed, consistent with previous findings, p21 up-regulation was demonstrated by IHC and confirmed by cell scoring data in the crypt region of *c-Rel*$^{-/-}$ mice following exposure to 8 Gy of ionising irradiation in both the colon and small intestine (see Figure 3.1.1, Figure 3.1.2, Figure 3.1.4 and Figure 3.1.5). p21 protein was also strongly up-regulated in the crypt in response to p53 up-regulation by conditional knock-out of *Mdm2* as shown by IHC (see Figure 3.1.6) and cell scoring data (see Figure 3.1.10 and Figure 3.1.14). The up-regulation of p21 was typically greater (as indicated by a higher scoring index) than up-regulation of p53 (see Figure 3.1.8 and Figure 3.1.13). In addition, in wild-type (including *c-Rel*$^{-/-}$) animals which had received whole body irradiation, p21 also had a wider response than p53 (p21 expression was significant further along the crypt in comparison to p53). The expression of p53 coincided with the apoptosis curve in the crypt and peaked around cell positions 3-6, whilst the expression of p21 had a more bell shaped normal distribution and peaked around cell position 9-10 in the small intestine. The distribution pattern of p21 fits well with its known role as an inducer of cell cycle arrest and its pro-survival activities that generate conditions which favour repair of DNA damage rather than induction of apoptosis [Leibowitz et al., 2011, Cmielova and Rezacova, 2011]. In *Mdm2*$^{flox/flox}$ mice, p53 expression was generally increased over that of wild-type animals that had received whole body irradiation (see Figure 3.1.13) and p53 therefore had a comparable response to p21 up-regulation. Interestingly, the up-regulation of p53 and p21 in *Mdm2*$^{flox/flox}$ mice was not limited to within the crypt compartment (as observed with wild-type mice), but also extended onto the villi (see Figure 3.1.7 and Figure 3.1.16 – discussed in more detail later in this section). These experiments have demonstrated that p21 expression is induced across the entire gut, in the colonic epithelium as well as the small intestine in response to ionising radiation and an increase in p53 levels when using conditionally floxed *Mdm2* null mice. In conclusion, since p21 is essential for $G_1$ phase p53-induced cell cycle arrest and is readily up-regulated by DNA damage in the gastrointestinal tract in a p53 dependent manner ([Wilson et al., 1998] and our own data) p21 would appear to be ideal surrogate indicator of p53 activity.

*Noxa*, on the other hand, may not be an ideal reporter of p53 activity since up-regulation of Noxa neither recapitulated an apoptotic response nor was Noxa reliably induced following various stress stimuli in the small intestine. Following exposure of *c-Rel*$^{-/-}$ mice to 8

Gy of whole body ionising radiation Noxa expression did appear to accurately report p53 induction in the colon as shown by IHC (see Figure 3.1.1) and supported by cell scoring data (see Figure 3.1.4). However, in the small intestine Noxa was expressed at relatively high levels regardless of irradiation status as shown by IHC (see Figure 3.1.2 and Figure 3.1.3) and supported by cell scoring data (see Figure 3.1.5). Fei *et al.* have also shown that expression of Noxa (analysed by *in situ* hybridisation) can be independent of irradiation and p53 status in the small intestine [Fei et al., 2002], supporting the idea that Noxa may not be an ideal reporter of p53 activity in this context. Furthermore, when Noxa expression was examined in *Mdm2*$^{flox/flox}$ mice, Noxa up-regulation was dependent upon time from treatment rather than on p53 up-regulation. This Noxa up-regulation may be a side effect of the gavage technique or may be triggered by BNF itself by an unknown pathway. It is also worth mentioning here that the observed staining for Noxa could well be an indication of a problem with the specificity of the antibody (anti-Noxa Anaspec) since we have been unable to find adequate citations for this product. Nevertheless, the expression pattern we observed (relatively high background in the small intestine regardless of irradiation status) was also reported by Fei *et al.* who examined this tissue for Noxa expression by *in situ* hybridisation with and without irradiation on both a p53 wild-type and p53 null genotype [Fei et al., 2002].

The apparently p53-dependent expression of Noxa in the colon paired with high background staining for Noxa in the small intestine (without a known stimulus) is somewhat reminiscent of another BH3-only protein; Bid. Bid was also examined for suitability to act as a downstream reporter of p53 apoptotic activity, however since Bid is expressed constitutively in the small intestine (albeit in a p53-dependent fashion) [Fei et al., 2002] it would not be an appropriate reporter gene. It is interesting to note similarities between these two BH3-only proteins which both bind selectively to pro-survival Bcl-2 family members (see Figure 1.4.10) and are speculated to act as sensitizers of cell death in this tissue [Shelton et al., 2009, Ploner et al., 2008] (discussed in Section 1.4.5.3). In conclusion, since Noxa does not reliably indicate neither p53 status nor an apoptotic response, it should not be used as the counterpart to p21 in a dual cell cycle arrest/apoptosis p53 activity reporter system.

Since Noxa turned out to be less than ideal candidate gene to act as a reporter for the p53-dependent apoptotic response to DNA damage, other p53 downstream target genes

have been investigated (including *Bax*, *Bid* and *Puma* – see Section 1.4.5.3). The current literature indicates that Puma may be the best gene to compliment *p21* in our dual cell cycle arrest/apoptosis *p53* reporter system, since *Puma* is a key p53 target gene that mediates p53-induced apoptosis not just in the gut but also in other tissues, such as the spleen [Michalak et al., 2008]. We have not yet examined Puma up-regulation following γ-irradiation in detail, however others have shown this to be dependent on *p53* (at least in the GI tract) [Qiu et al., 2008, Leibowitz et al., 2011]. One obvious confounding factor in using *Puma* in a p53 activity reporter mouse is that Puma also has many p53-independent functions, including a role in oxidative stress induced apoptosis along the length of the villi [Wu et al., 2007] and during chronic colitis [Dirisina et al., 2011]. Nevertheless p53-dependent Puma-mediated apoptosis could be readily distinguished from p53-independent Puma induced apoptosis by the use of p53-null mice.

To summarise hitherto, past studies [Pritchard et al., 1998, Wilson et al., 1998] and more recent studies [Leibowitz et al., 2011] as well as our own data reaffirm that p21 is potentially an ideal reporter of p53 activation in the gut. Whilst initially there was no similarly straightforward downstream target gene for the apoptotic response to p53 activation in the gastrointestinal tract, our current literature search indicates that Puma (out of the others examined – see Sections 1.4.5) may be the best gene to compliment p21 in a dual cell cycle arrest/apoptosis p53 activity reporter system [Qiu et al., 2008, Leibowitz et al., 2011]. However, since during the early stages of this project evidence for Puma's role in p53-dependent activation of apoptosis was contradictory [Qiu et al., 2008, Fei et al., 2002] and we had yet to validate or investigate Puma expression ourselves (due to a lack of a reliable antibody), our research concentrated on developing the gene-trap *p21 lacZ* mouse in the first instance (see Section 1.5.1). The ultimate aim would be to develop a dual fluorescent apoptosis/cell cycle arrest *p53* reporter system which would have wide-reaching applications in cancer research and for studying normal development.

We envision using these mice in the first instance to examine the long standing molecular phenomenon occurring in intestinal gut epithelium, in which cells on the villi display an uncoupling of p53 activation and apoptosis [Marshman et al., 2001, Leibowitz et al., 2011, Watson and Pritchard, 2000] (see Section 1.2.6). As stated earlier this lack of apoptosis on

the villi is not simply due to a lack of p53 up-regulation, since even when p53 is induced in cells on the villi by conditional knock-out of *Mdm2* these cells do not undergo apoptosis (see Figure 3.1.17 and Section 3.1.2.3). Furthermore, p53 positive cells on the villi still failed to undergo apoptosis even when an additional stress stimulus (14 Gy whole body irradiation) was applied (see Section 3.1.3.2). Why is there this apparently black and white switch in the cells behaviour along the CVA? One possible explanation for this may be that p53 on the villi is inducing cell cycle arrest instead of apoptosis. In line with this theory, cell cycle arrest gene *p21* was up-regulated on the villi in $Mdm2^{flox/flox}$ mice (both with and without irradiation see Figure 3.1.11 and Figure 3.1.15), however it is difficult to determine whether this interpretation (p53 induces cell cycle arrest) is accurate since no similar analysis was performed for a reliable p53-responsive apoptotic gene. In instances like these, where antibodies are unreliable (as for Puma), the use of an *in vivo* p53 activity reporter system as proposed by this thesis could provide a valuable tool with which to analyse the actions and outcomes of p53 up-regulation.

The unusual up-regulation of p53 on the villi has been reported previously by another group who also used a conditional *Mdm2* knock-out system to study p53-mediated cell death in the intestinal epithelium [Valentin-Vega et al., 2008]. However, whilst we observed no increase in apoptosis along the length of the villi as a result of *Mdm2* knock-out, conversely Valentin-Vega *et al.* report a small (0.06 → 0.9 apoptotic cells/villi) but significant increase in apoptosis in the terminally differentiated cells of the villi. The reason or reasons for these two different results are investigated next. One major contributing factor might be that whilst methods used in these two reports may seem similar, the mechanism for conditional knock-out of *Mdm2* was fundamentally different between these experiments. Valentin-Vega *et al.* utilised the *VilCre* trans-gene to control activation of Cre-recombinase (and subsequent loss of *Mdm2*) rather then the CYP1A1 promoter region as in our $Mdm2^{flox/flox}$ mouse system. The impact of this is that since the *VilCre* trans-gene [Madison et al., 2002] is active throughout mouse development the transgenic mice (denoted $Mdm2^{int\Delta}$) are born deficient in *Mdm2* which resulted in abnormal gut architecture due to excessive p53-mediated cell death (this phenotype was completely rescued on a p53 null background) [Valentin-Vega et al., 2008]. Therefore the villi examined by Valentin-Vega *et al.* by their own observation were atrophied,

often inflamed, full of abnormal vacuole-like structures and had lost cell polarity which makes it difficult to compare them to villi found in a healthy, well organised adult gut. On the other hand, the CYP1A1-*Cre* trans-gene (in $Mdm2^{flox/flox}$ mice), is only induced by administration of aryl hydrocarbon compounds such as BNF [Campbell et al., 1996, Ryding et al., 2001] and therefore provides a model in which to study the effects of p53 up-regulation in morphologically normal adult gut. These fundamental structural differences may explain why Valentin-Vega *et al.* reported a significant increase in apoptosis along the length of the villus as a result of *Mdm2* knock-out whilst we do not. For instance, since the $Mdm2^{int\Delta}$ small intestine tissue is disorganised in structure it may be difficult to determine what constitutes a villi, or crypt/villus boarders may be less strict (possible given the loss of cell polarisation). In addition, as the villi are atrophied (and hence shorter) there may be bias for cross sectioning the villus tips more often and thus perhaps the increased apoptosis detected by Valentin-Vega *et al.* is simply a result of increased detection of p53-independent DICD. Finally, given the loss of the cell hierarchy the villi like protrusions in $Mdm2^{int\Delta}$ mice are unlikely to reflect true villi, therefore we are confident that in morphologically normal adult GI tract, p53 up-regulation and the apoptotic response on the villi remain uncoupled and require further investigation.

In order to investigate the differences in p53-mediated cell death along the CVA we performed an RNA expression array analysis on epithelial cell fractions enriched for either crypt or villus cells. The experimental design was to include WT mice with and without irradiation in order to determine which genes are differentially regulated along the CVA as a result of DNA damage and an $Mdm2^{flox/flox}$ treatment group in order to determine the p53 response independent of irradiation/DNA damage (outlined in Figure 3.1.17). The epithelial cell fraction collection and RNA extraction experiments were performed in collaboration with The Beatson Institute in Glasgow according to their previously optimised protocol (see Section 2.13.4). Prior to sending RNA samples for micro-array analysis, it was necessary to first check the purity and quality of the RNA and second to check whether the crypt/villus enrichment process was efficient. The initial quality control checks performed on the RNA samples, including UV spectroscopy and agarose gel electrophoresis, indicated that the RNA was of adequate purity and quality for micro-array analysis (see Table 3.1.1 and Figure

3.1.18). However, the second quality control check, which utilised QRTPCR to validate the epithelial cell extraction procedure, indicated that there may be a problem.

Crypt/villus enrichment was determined by examining the fold changes in expression of known and validated crypt- (*Lgr5* – [Barker et al., 2007, von Furstenberg et al., 2010]) or villus- (*Max* – [Mariadason et al., 2005]) specific genes. Whilst for the villus-specific gene *Max,* the enrichment protocol appeared successful (because *Max* was significantly increased in the villus fraction, p-value = 0.01), this was not the case for the crypt-specific gene *Lgr5* (see Figure 3.1.19). Contrary to the expectation *Lgr5* was also significantly enriched in the villus fraction (p-value = 0.017 – see Figure 3.1.19) most likely as a result of some contaminating crypt cells present in the villus fraction. Therefore we must conclude that the epithelial extraction protocol was unable, in our hands, to sufficiently fractionate cells along the CVA and on this decisive factor the cell extraction protocol used appeared to have failed. The reason or reasons for the failure of the enrichment process are discussed next.

Upon further investigation, it became apparent that the basic cell extraction method used in this thesis was inadequate to satisfactorily resolve epithelial cells along the CVA. The original CVA fractionation procedure developed by Weiser in 1973 for use in rats and most subsequent mouse friendly adaptations feature collection of multiple cellular fractions (5-10 – rather than just 2) over an extended time period (up to 115 minutes – rather then only 30 minutes) [Weiser, 1973, Ferraris et al., 1992, Flint et al., 1991]. These methods also included a wash step (5-15 minutes in length), the purpose of which was to remove calcium from the tissues (by chelating agents – such as EDTA) in order to reduce protein mediated cell adhesion and facilitate cell shedding [Ferraris et al., 1992]. Increasing the number of cellular fractions may provide a mechanism for better separation of crypt and villus cells since there will be less overlap/ambiguity surrounding the contents of the first (mostly villus) and last (mostly crypt) samples – although this may have the disadvantage of generating lower RNA yields per fraction. Another potential drawback might be that the extended cell collection times at 37°C could adversely affect the integrity of the RNA samples [Flint et al., 1991]. Since the length of incubation presented in these methods is a concern when extracting RNA, it is worth noting that Mariadason *et al.* have successfully used one of these methods to perform gene expression profiling along the CVA [Ferraris et al., 1992, Mariadason et al.,

2005]. This indicates that the increased length of collection time at 37°C does not appear to affect the quality of the RNA samples and hence this protocol seems compatible with our planned intention of performing RNA micro expression array analysis. Therefore, in conclusion, if the RNA expression array experiment (outlined in Figure 3.1.17) was to be repeated, the Ferraris *et al.* validated extraction procedure should be used instead [Ferraris et al., 1992].

*Potential experimental design drawbacks...*

One potential criticism of the analysis of apoptosis in this thesis is that we were relying solely on identification of the morphological characteristics of apoptosis (such as cell shrinkage, membrane blebbing and the formation of nuclear bodies [Kerr et al., 1972]) as visualised by H&E (haematoxylin and eosin) staining. This may be a concern when attempting to detect apoptosis along the length of the villi, since cells only appear morphologically apoptotic once they begin to detach from the basement membrane [Shibahara et al., 1995]. However apoptosis may have already been initiated in morphologically normal cells and therefore the total amount of cells undergoing apoptosis may be underestimated. Marshman *et al.* have investigated this possibility by comparing the traditional H&E scoring method with two other commonly used methods for identification of apoptotic cells within the gastrointestinal epithelium. These were; IHC using activated caspase-3 antibody for staining and terminal deoxynucleotidyl transferase dUTP-mediated nick end labelling (TUNEL) method [Marshman et al., 2001]. In their study quantification of apoptosis by H&E staining compared favourably with activated caspase-3 staining within both the crypt and villi. In comparison, identification of apoptosis by TUNEL staining detected twice as many positive cells within the crypt compartment and was generally unreliable for detection of apoptosis along the length of the villi. TUNEL binding may overestimate apoptosis since non-specific nicks in DNA may also occur as a result of DNA damage induced by irradiation [Marshman et al., 2001, Ansari et al., 1993]. Importantly, since scoring apoptosis by H&E staining alone was as effective as activated caspase-3 staining it is unlikely that we have underestimated the apoptosis on the villi [Marshman et al., 2001].

Another potential criticism of the experiments performed on the GI tract to investigate the p53-dependent cell death for this thesis is that these experiments were not performed using p53 null mice which would definitively confirm whether the effects observed were truly p53-dependent. However, with regards to the selection of p21 and Puma for use in the dual cell cycle arrest/apoptotic p53 activity reporter system, their p53-dependence has already been repeatedly demonstrated [Leibowitz et al., 2011, Qiu et al., 2008, Wilson et al., 1998]. The apoptosis as a result of conditional knock-out of *Mdm2* cells has also been demonstrated to be dependent on p53 [Valentin-Vega et al., 2008]. Therefore, for our purposes it was not strictly necessary to include those controls.

## 4.2 Gene-trapping

Following selection of *p21* as a suitable candidate gene to reliably indicate p53 activation in the GI tract our research was initially concentrated on developing a *p21-LacZ* reporter mouse. To accomplish this, we planned to take advantage of the gene-trapped ES cell lines available from the IGTC in the first instance because gene-trapping had the potential by-pass many of the complex and labour intensive molecular cloning stages involved in both the design and construction of DNA targeting constructs (see Section 1.5.1). The possibility of obtaining a *Puma* gene-trapped ES cell line was also investigated since according to our literature review *Puma* is a major p53 target gene for apoptosis in the GI tract [Leibowitz et al., 2011, Qiu et al., 2008] and may be the most appropriate gene to complement *p21* in our dual cell cycle arrest/apoptosis p53 activity reporter system. Generation and evaluation of the *p21-LacZ* and/or *Puma-LacZ* transgenic mouse lines would provide proof in principal that our targeted knock-in approach recapitulates an authentic report of expression in these genes. Assuming these transgenic mice respond to genotoxic stress in the expected manner we would then go on with our ultimate goal and target these loci with two different fluorescent markers to create an elegant *in vivo* system for monitoring p53-dependent programmed cell death and cell cycle arrest.

Unfortunately this relatively simple concept – to utilise the pre-targeted ES cell lines and rapidly create a proof in principal transgenic mouse strain – became a rather unproductive exercise which cost this project valuable time. Briefly, the *p21* gene-trapped ES cell line which we had selected (AM0998 – generated by SIGTR) was intrinsically flawed from the outset since the gene-trapping vector (containing β-geo) had integrated upstream of the endogenous translational initiation site. This fundamental error meant that the *LacZ* portion of the β-geo was not detectably expressed *in vitro* and furthermore even if the LacZ had been expressed, we could not expect these cells to replicate authentic activation.

At this point in the project given the unavailability of an appropriate/affordable gene-trapped ES cell line, we returned to our original plan – that is a dual fluorescent cell cycle arrest/apoptosis p53 reporter system. This would be undertaken by generating our own novel DNA targeting constructs and performing gene targeting in ES cells.

# 4.3 Generation of large DNA targeting constructs

## 4.3.1 Major obstacles

The bulk of the research project described in this thesis was spent undertaking the task of generating four separate DNA targeting constructs. As mentioned in Section 3.3.1 a molecular cloning exercise of this size is extremely labour intensive and time consuming owing to several contributing factors which are outlined below.

1) Large (4-12 kb) pieces of genomic DNA were included in the design of each gene targeting vector to be the arms of homology, however these could be;
    a. Repetitive in nature and therefore impossible to PCR (such as the *p21* right arm of homology see Section 3.3.3.7).
    b. Repetitive in nature and therefore and extremely unstable in *E. coli* (see Section 3.3.3.9).
    c. GC rich, which created problems for PCR (for example the *Puma* left arm of homology – see Section 3.3.4.1).
2) Reliance on PCR based techniques – whilst essential and a powerful mutagenesis tool – using PCR did have some drawbacks. These were;
    a. PCR required optimisation and careful primer design – which was not always straightforward (such as the *Puma* left arm of homology see Section 3.3.4.1).
    b. Sequencing had to be performed on each cloned PCR product to ensure that the DNA polymerase had not introduced any mutations.
    c. Errors in the synthesis of long oligonucleotides (see Sections 3.3.3.3 – 3.3.3.5) – resulting in incorrect incorporation of desired sequences.
3) DNA targeting constructs required many stages of sequential assembly so that failure of one step could halt progression of the whole cloning exercise until it was completed or redesigned to overcome the obstacle. This occurred at many stages of cloning and these are summarised (together with the solutions arrived at) in Table 4.3.1.

***Table 4.3.1: Cloning issues encountered during the construction of large DNA targeting constructs.***

| Cloning issues encountered | Solutions arrived at |
|---|---|
| Negative selectable marker (TK) – sequencing revealed 9 mismatches compared with the published sequence | Since these mismatches were present in the parental vector (which had been used previously in our laboratory) this was deemed suitable to use. (see Section 3.3.3.2 and Appendix D.1). |
| *p21* left arm of homology – deletion of ~ 70 bp when amplified by PCR. | Rather than amplify the *p21* left arm of homology from the BAC clone DNA in one step, we amplified it in two steps and pre-screened clones with a PCR reaction to identify clones lacking the deletion (see Section 3.3.3.3 and Figure 3.3.7). |
| *p21* left arm of homology – mutations within the primer regions. | The NLS and restriction enzyme sites were not always incorporated correctly. These were screened by sequencing (see Section 3.3.3.3) and shorter primers were designed for the subsequent cloning step. |
| *mCherry* – NLS sequence was not incorporated correctly. | Another clone was sequenced – which fortunately was identical to the expected sequence (see Section 3.3.3.4). Shorter primers were designed for the next cloning step. |
| *p21* left arm of homology fused in-frame with *mCherry* – deletion of ~ 70 bp and incorrect incorporation of primer sequences. | Many clones (~60) were pre-screened by bacterial colony PCR in order to identify 6 clones which did not contain the deletion. These 6 clones were then sequenced to check for successful incorporation of the NLS sequence and 5' & 3' restriction enzyme sites. |
| *p21* left arm of homology fused in-frame with *mCherry* – a poly A run was mutated in all clones sequenced (6 in total). | A long homopolymeric run of As within the 3 – 4 kb region of *p21* intron 1 which was 38 nt in the wild-type sequence was observed to occur in various sizes in the 6 above mention clones (36, 37 and 40 nt). One clone with 36 nt was chosen as a compromise to continue with the cloning exercise (see Section 3.3.3.5). |

| Cloning issues encountered | Solutions arrived at |
|---|---|
| Positive selectable marker (Cre/Neo$^{R}$) – sequencing revealed 3 mismatches compared with published sequence. | These 3 mismatches were not present in the mouse genomic DNA RefSeq database and therefore these clones were deemed suitable for downstream use to act as the positive selectable marker (see Section 3.3.3.6). |
| *p21* right arm of homology – PCR failed. | DNA was extremely repetitive. The right arm fragment was cloned from a suitable restriction digest fragment of a BAC clone instead (see Section 3.3.3.7). |
| *p21* right arm of homology – unstable DNA, resulting in random recombination of plasmid. | Initially this appeared to have been solved by the use of specialised *E. coli* strain MAXStbl.2 (see Section 3.3.3.7) however the problem was never fully resolved. Growing the bacteria at 27°C rather then 30°C helped reduce recombination. In order to confirm the positivity of bacterial transformants extensive screening by bacterial digests was performed to check for any loss of this ~10 kb repetitive region (see Section 3.3.3.9). |
| *p21*-mCherry final construct assembly – inefficient double digestion of FseI-PacI. | Since FseI and PacI were side by side in Vector 4 (see Appendix C.3), efficient double digest was only achieved if plasmid was digested with FseI, DNA purified, then digested with PacI. |
| *Puma* left arm of homology – difficult to PCR and restriction digest of BAC clone DNA did not appear as expected. | Long range (4-5 kb) PCR reactions were unsuccessful (see Figure 3.3.22), we then attempted to use a suitable BAC restriction digest fragment however this was also unsuccessful – since the restriction digests did not produce fragments of the expected sizes or stoichiometric ratios. In order to amplify the entire 4.6 kb left arm region, the problematic section of DNA was broken into smaller, easier to manage pieces which were then 'stitched' together by fusion PCR. 9 rounds of PCR in total – see Section 3.3.4.1. |

| Cloning issues encountered | Solutions arrived at |
|---|---|
| *Puma* left arm of homology – 30-100 bp deletion during the penultimate round of PCR | Cloning step repeated and additional clones screened until a wild-type clone was obtained (see Section 3.3.4.1). |
| *Puma* left and right arms of homology – DNA sequences did not match the RefSeq database | Multiple differences were observed (~50 in each arm of homology) which were identical between different bacterial clones – therefore these differences were assumed to be due to differences between *C57BL/6* and *129SvEv* strains rather than introduced by PCR (see Section 3.3.4.1). |
| Moving the *Mdm2*TK fragment into the yeast-E. coli shuttle vector took four attempts. | No obvious reason for failure. Using TOP10s rather than MAXstbl.2 appeared to solve the problem (see Appendix C.5). |
| Final assembly of *Mdm2* P2-Mutant DNA targeting construct – double integration of pRAYNeo$^{R}$ cassette. | Yeast DNA was retransformed into various strains of bacteria to produce the final DNA targeting construct. However, following screening of many bacterial clones (~60) which mostly contained an unknown vector – one clone was identified which had double integration of the positive selectable marker. This was rescued by using a restriction enzyme which only cut the pRAYNeo$^{R}$ once to recreate the desired targeting construct (see Section 3.3.5.6.1). |
| Final assembly of *Mdm2* P1-Null DNA targeting construct – unwanted homologous recombination events in yeast. | The unwanted homologous recombination event occurred in yeast cells due to an unanticipated additional region of homology within the shuttle vector DNA – therefore this additional region of homology was removed to increase the probability of generating the correct homologous recombination event (see Section 3.3.5.6.1). The removed region (the TK cassette) was then reintroduced once the plasmid was propagating in bacteria. |

In addition to the reasons listed above it is also important to bear in mind that each individual cloning exercise typically took a week complete (or longer if sequencing was required). This was because of multiple unavoidable overnight steps in the cloning procedure including ligation of DNA fragments, selection of transformants and outgrowth/re-growth of clones (see Figure 4.3.1). Thus realistically, if a cloning step had failed, it would not become apparent until day 4 or 5 of the experiment. In addition, the reason or reasons for failure of a cloning exercise were not always immediately obvious and therefore the solution was sometimes decidedly unforthcoming (such as during cloning of the *p21* right arm or *Puma* left arm of homology – see Sections 3.3.3.7 & 3.3.4.1). Particularly difficult stages of cloning where multiple (4-8) attempts had failed actually represents months of work and greatly contributed to the overall time taken to complete construction of the DNA targeting vectors.

Reflecting on the relative complexities of each of the cloning exercises the overall time spent generating these DNA targeting constructs was 17-25 months. The construct which took the longest time to complete was *Puma*-E2Crimson owing mainly to the difficulty in amplifying the *Puma*-left arm of homology. This is an example of how GC-rich genomic DNA and reliance on PCR techniques can drastically slow down a cloning exercise. The delay was caused since each cloned PCR product (and there were 7 in total – once we had found PCR reactions which actually produced the correct products!) required sequencing to check that the DNA polymerase had not inadvertently introduced unwanted mutations. Whilst the return of sequencing reads was usually fairly fast (2 days) not all sequencing reactions were successful (could fail on some technical level) and if clones contained mutations then additional sequencing was required which created a further delay. In addition, during the UK postal strikes in late 2009 the sequencing turnaround time (for Eurofins MWG Operon) was 2-3 weeks (if samples arrived at all) which caused major delays in cloning. Later in this project we switched to using GATC Biotech since they employed a courier service to collect sequencing samples directly (see Section 2.7.2.7).

The DNA targeting construct which took the next longest time to generate was *Mdm2* P1-Null (22 months). The major delay in this cloning exercise was associated with undesired homologous recombination events during the final vector assembly step in yeast cells (to insert the positive selectable marker – pRAYNeo$^{R}$). This resulted in a truncated plasmid

being the predominant cloning event when the DNA extracted from yeast cells was re-transformed into *E. coli* (see Section 3.3.5.6). Conversely, although the same problem was apparent during cloning of the *Mdm2* P2-Mutant gene targeting vector, purely by chance, a bacterial clone was identified which contained a rare double integration event (pRAYNeo$^R$ had inserted twice). The double integration could be rescued (see Section 3.3.5.6.1) and hence cloning for *Mdm2* P2-Mutant was completed 5 months ahead of *Mdm2* P1-Null. Indeed, cloning of the *Mdm2* P2-Mutant construct was completed in the fastest time (17 months) although since the cloning of the *Mdm2* constructs was commenced following our inventive and successful use of BAC clone restriction digests for the *p21* right arm of homology (see Section 3.3.3.7), the *Mdm2* P2-Mutant DNA targeting construct was finished after the *p21*-mCherry DNA targeting construct. Hence, the first ES cell gene targeting experiments were performed for generation of the *p21*-mCherry knock-in reporter strain.

Cloning of the *p21*-mCherry DNA targeting construct was initially completed in 18 months; however re-growth of this DNA took a further 2 months to accomplish since identification of a stable positive clone was tricky. The major cloning obstacle for generation of the *p21*-mCherry DNA targeting construct was therefore associated with the maintenance of the large (10 kb), extremely repetitive *p21* right arm of homology in *E. coli* (see Section 3.3.3.9). This is an example of how highly repetitive genomic DNA sequences can create delays in cloning, since its inherent instability made it difficult to propagate efficiently in bacteria (recombination occurred frequently which resulted in variable loss (3-8 kb) of the region). Construction of the *p21*-mCherry gene targeting vector also had its share of PCR/sequencing related idiosyncrasies, as occurred for example during cloning of the *p21* left arm of homology in-frame with mCherry (see Section 3.3.4.1). Several issues arose; including a major deletion (~70 bp), a minor deletion/addition (1-2 bp in a long A homopolymeric run) and frequent failure to successfully incorporate the 5' additional sequences during PCR mutagenesis (see Table 4.3.1). The last of these problems was probably due to the length of oligonucleotides used (48 – 61 nt) since errors are likely to accumulate with increasing length of oligonucleotide sequence (due to limitations in the synthesis procedure). Where possible we re-designed primers to be shorter and therefore circumvent this problem.

Despite the various and numerous cloning challenges encountered during this thesis, inventive redesign, use of different *E. coli* strains and persistence eventually enabled successful construction of all four desired DNA targeting constructs. As these cloning exercises proved extremely complex and time consuming we must consider whether alternative cloning methods (or combinations of same) may have finished the task more quickly and efficiently. These alternative cloning strategies are discussed next.

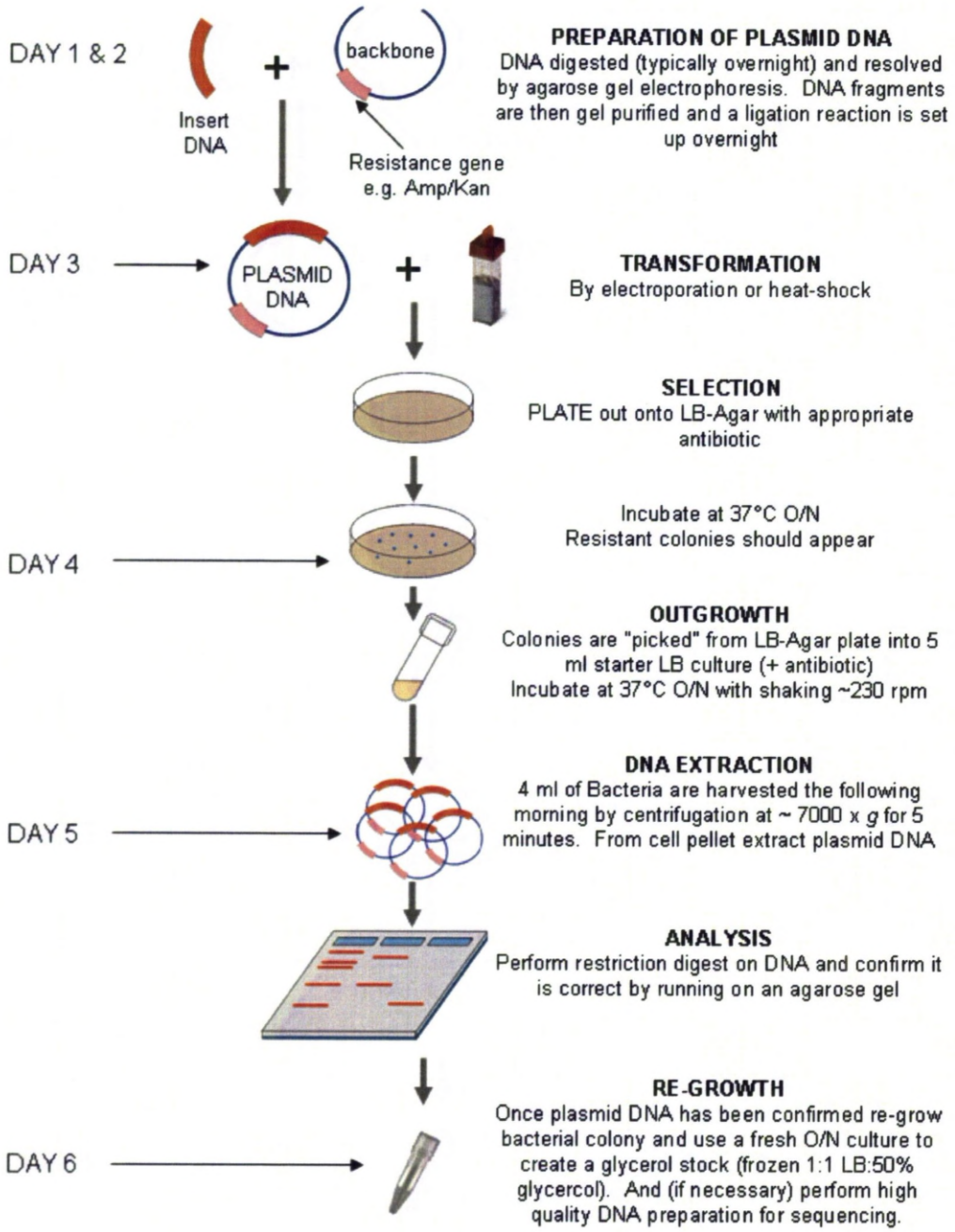


**Figure 4.3.1: Overview of a molecular cloning experiment.**

*The plasmid DNA is typically prepared using standard cloning techniques such as digestion with restriction enzyme(s) or amplification of insert DNA by PCR which could take 1-2 days depending on the complexity of the cloning exercise. The plasmid DNA with selectable marker (usually antibiotic resistance) is introduced into a suitable competent E. coli strain. Transformed bacteria are grown under selective conditions O/N on an LB-agar plate containing an appropriate antibiotic. Recombinant clones are then screened by extracting their DNA and performing a restriction digest. DNA digest patterns are examined by agarose gel electrophoresis and positive clones re-grown to generate glycerol stocks for long term storage.*

### 4.3.2 Alternative cloning strategies

The field of molecular biology is fast paced with new discoveries and technologies continuously being developed which can refine and revolutionise the basic tool-set of a molecular biologist. Molecular cloning techniques are no exception and newer, more efficient, simpler and/or more intelligent cloning procedures are constantly evolving. With the wide range of old and newer molecular cloning techniques available it is almost a certainty that the cloning exercises performed for this thesis could have been accomplished in numerous ways. Thus an important question to ask ourselves before, during and after generation of the novel DNA targeting constructs described here, is what cloning strategy/cloning techniques *should* we use(*?*), *could* we have used(*?*) and were there any *other*, potentially better methodologies to complete the same task?

Addressing the last of these questions – *are there any newer (or missed) alternative cloning strategies that could have completed the construction of the DNA targeting constructs in a radically improved way?* – In essence, at the time of writing this thesis, I think the short answer is no. None of the other commonly used molecular cloning techniques such as GATEWAY cloning, direct restriction digestion of PCR products, in gel cloning or blunt end PCR product cloning, provide a significant time or labour saving advantage over the standard/specialised techniques which were utilised for the cloning within this thesis – summarised in Table 4.3.2.

Of the newer, less routinely used cloning techniques the alternative cloning strategy with the most potential to circumvent some of the problems associated with the generation of the *p21*-mCherry and *Puma*-E2Crimson constructs is "recombineering" (recombination – mediated genetic engineering) [Ellis et al., 2001]. Briefly, recombineering exploits the recombination proteins present within bacteriophage λ to effectively allow efficient homologous recombination between very short arms of homology (~ 50 bp) in bacteria. The apparent advantage of such a cloning system is once you have an appropriate BAC clone you can in theory insert, with accuracy any desired mutational event (complete with positive selectable marker) without the need for traditional 'cut and paste' recombinant DNA techniques [Narayanan and Chen, 2011]. The resulting modified BAC clone – dubbed a BAC trans-gene (BAC-Tg) can then be used immediately as a DNA targeting construct. The

recombineering strategy therefore does have a certain appeal, particularly since generation of the arms of homology, introduction of the desired mutations and final construct assembly would be simultaneous. However, upon further inspection a variety of problems are associated this scheme – first and foremost, the use of recombination competent bacteria would have been disastrous for maintaining the *p21* right arm of homology (which included ~10 kb of extremely repetitive and unstable DNA). Second, BAC clones are typically 100-300 kb in size, thus it is highly probable that the BAC-Tg will contain additional genes and/or regulatory elements which will inevitably confound interpretation of the results due to unintended non-specific affects. Furthermore, given the size of the BAC clone and the high efficiency at which homologous recombination can take place, depending on the DNA sequence I would expect there to be a significant amount of background recombination events which, again, would confound interpretation of the results.

Whilst use of an entire BAC clone for direct cloning could be less than ideal (for the reasons detailed above) we found that restriction digestion of the BAC clone to excise particular regions of interest worked reasonably well (for example during cloning of the *Mdm2* promoter mutant DNA targeting constructs). This strategy of course has its own drawbacks – namely reliance on availability of suitable restriction enzyme sites – however on a gene-by-gene basis it could potentially be very helpful, especially when combined with homologous recombination in yeast. That is, if a suitable BAC clone fragment exists it could be inserted directly into a yeast-*E. coli* shuttle vector and then used to create the arms of homology following homologous recombination in yeast with an appropriately designed donor DNA. It is worth noting here the similarities between recombineering in bacteria and homologous recombination in yeast as cloning strategies.

Whilst it would be virtually impossible and considerably beyond the scope of this thesis to discuss every alternative cloning strategy available an effort has been made to highlight some of the more relevant molecular cloning techniques that may (or may not) have been useful. *In vitro* validation of the DNA targeting constructs is the next topic discussed below.

***Table 4.3.2: Evaluation of other commonly used cloning techniques.***

| Common cloning method | Considerations |
|---|---|
| Invitrogen GATEWAY cloning – uses specific DNA sequences and specialised enzymes to shuffle target sequences in and out of various pre-generated vectors | High start up cost – more applicable to high through-put cloning, rather than the unique and complex cloning steps involved in generation of gene targeting vectors. |
| Direct restriction digestion of PCR products – appends restriction enzyme sites during PCR then digests with those restriction enzymes and clones the fragment directly into the desired vector (no intermediate TA vector) | Restriction enzymes work with varying efficiency on terminal sections of DNA therefore an additional 10 nt cap may be required to be added to primers, which may increase non-specific products during PCR. Potential time saved may be lost if restriction enzymes are unable to cleave the DNA ends. |
| In gel cloning – performs ligation reactions within the GTG low melting temperature agarose gel. | Not attempted. No major time saving advantages since gel purification kits are fairly rapid. |
| Blunt ended PCR cloning kits – similar principal as the TA-cloning kits except for blunt ended PCR products. | Since we used Phusion DNA polymerase which created a blunt ended DNA product this kind of kit may have been beneficial – however A-tailing reactions are fairly quick and simple to perform and worked reliably in our hands (see Section 2.6.6.1). |
| Oligonucleotide directed mutagenesis of vectors – sometimes referred to as site-directed mutagenesis. A primer is designed which contains the desired point mutations and then the whole vector is amplified by a high fidelity DNA polymerase (such as Phusion). The new vector (with desired mutations) is then isolated and cloned. | Even high fidelity DNA polymerases can only amplify ~ 10 kb. Only a few point mutations in close proximity can be introduced at a time, therefore if more mutations are required multiple rounds of targeting are required. As with all PCR-based techniques any construct generated this way will require complete sequencing. |

### 4.3.3 *In vitro* validation of DNA targeting constructs

Where possible, testing of the desired gene modifications should be performed prior to ES cell gene targeting. This is because ES cell gene targeting is also an extremely labour intensive process that requires diligent care and planning during both the ES cell culture and the subsequent ES cell screening protocols. Therefore before investing considerable time and resources into an ES cell gene targeting experiment, it is essential to know that firstly, the DNA targeting construct is a full and accurate representation of the expected DNA sequence and secondly, it is desirable to know whether it is likely to produce the designed responses *in vivo*. The former was confirmed for all four DNA targeting constructs by sequencing and restriction digest mapping whilst the latter was addressed when possible by *in vitro* analysis.

For the *Mdm2* P1-Null and P2-Mutant promoter regions *in vitro* testing was essential to validate the introduced disruptions (see Section 3.3.5.2). Importantly, the modified promoter regions behaved exactly as expected – that is the *Mdm2* P1-Null promoter region had significantly reduced basal expression but equal p53-responsiveness whilst the *Mdm2* P2-Mutant promoter region had comparable basal expression but completely abrogated p53-responsiveness. These mutations would therefore be suitable for generation of transgenic mouse strains with which to study the relative contributions of the p53-independent and p53-dependent regulation of *Mdm2* (discussed further in the Section 4.4).

*In vitro* validation of the *p21*-mCherry DNA targeting construct prior to ES cell targeting was not possible since the *p21* left arm of homology (which commenced 228 bp in to *p21* intron 1) did not contain the *p21* promoter region. The murine *p21* promoter region and specifically the two p53 RE sites are located approximately 2.8 and 1.9 kb upstream of exon 1 [el-Deiry et al., 1995] and hence were not present within our gene targeting vector. We did not attempt to include the *p21* promoter region with our DNA targeting construct because that would have created a much larger *p21* left arm of homology (~ 8 kb) which was not necessary for ES cell targeting and would have been much more difficult to PCR successfully. Without the endogenous *p21* promoter region it unfortunately would not be possible to determine whether mCherry is reliably induced by p53 *in vitro* until mCherry has successfully incorporated at the *p21* locus in targeted ES cells.

However, along the same line of thought, since the *Puma*-E2Crimson DNA targeting construct does contain the endogenous *Puma* p53 REs (~110 bp upstream of exon 1 [Yu et al., 2001]) it should be possible to determine if E2Crimson is reliably induced following p53 activation *in vitro*, prior to lengthy ES cell gene targeting procedures. *In vitro* validation will be performed by co-transfection experiments of the PumaLACrimSK+ vector in p53 null MEFs with and without murine *p53*.

One final comment on the matter, each DNA targeting construct designed and created for this thesis is completely novel and totally unique – such that, even if another group attempted to create these transgenic mouse strains it would be unimaginable that they would have designed the exact same mutations and/or reached the same end result.

## 4.4 ES cell targeting

The main aim of this thesis was to generate four different transgenic mouse strains by homologous recombination in ES cells in order to study novel aspects of p53 regulation, activation and function. These strains included the *p21*-mCherry and *Puma*-E2Crimson knock-in fluorescent reporter mice which are hoped to provide valuable tools with which to monitor p53 activity *in vivo*. The study of such mice would be useful for studies where careful *in vivo* analysis of p53 activation is necessary or desired for example during the DNA damage response in the GI tract. Radiosensitivity in the GI tract is of particular relevance to cancer since radiotherapy is one of the most effective and commonly used treatments for a wide variety of cancers. However, one of the major limiting factors in radiotherapy (and chemotherapy) is unwanted cytotoxicity in highly proliferative tissues, such as the GI tract (known as GI syndrome) which can cause adverse side effects such as nausea, vomiting, diarrhoea, dehydration and in severe cases death [Qiu et al., 2010, Qiu et al., 2008, Kirsch et al., 2010]. In order to mitigate the potentially lethal GI syndrome it has been proposed to pre-treat patients undergoing radio- or chemotherapy with protective agents which either block induction of the acute apoptotic response [Burdelya et al., 2008] or promote tissue regeneration [Zhang et al., 2010]. Since the p53-dependent activation of both *Puma* and *p21* have been shown to play key roles in regulating GI syndrome [Leibowitz et al., 2011] having an *in vivo* tool with which to monitor these p53-responses in real time as proposed by this thesis would enable researchers to determine what molecular responses their treatment(s) are inducing with superior temporal and spatial detail than is currently possible. The advantages of such an *in vivo* reporter system are numerous, including;

- Real time – provides additional temporal information for acute treatment effects (might be particularly beneficial for easily accessed organs such as the skin/colon).
- Whole animal can be imaged at once – provides additional spatial information, including identification of p53-responses in unintended targets (improve traditional toxicology studies).

- Non-invasive imaging – allows for long term studies (for chronic effects of treatment(s) and/or disease progression), which ultimately permits a reduction in animal numbers since the animals can be imaged multiple times.
- More sensitive/accurate detection may be possible – since not relying on antibodies or other lengthily optimisation/visualisation procedures.
- More authentic report of p53 activity – since knock-in targeted approach uses the endogenous reporter gene locus (not affected by positional bias).
- Differential monitoring of p53 activity – demonstrate not only that p53 is activated, but which genes/responses it is attempting to elicit.

To date, no other such dual *p53* activity system exists. Thus, we envision that the fluorescent reporter mouse strains described here could find many applications in the field of cancer studies including preclinical testing of radio-protective agents, characterisation of acute/chronic p53-responses to chemotherapy and long term gene-regulation during cancer development.

The next two transgenic mouse strains we intend to generate are the *Mdm2* P1-Null and *Mdm2* P2-Mutant which will be used to answer fundamental questions relating to the p53-dependent and p53-independent regulation of *Mdm2* and ultimately addressing whether p53 mediated regulation of Mdm2 is a component of the essential negative regulation of p53. Since p53 is one of the most important tumour suppressor genes, and loss of function of p53 is considered to be a critical event in the development of almost all known cancers, involving many of the cellular responses to DNA damage (and other stress stimuli – see Section 1.4), it is not surprising that *p53* is one of the most extensively studied genes in cancer biology (see Section 1.1). However, despite considerable advances in knowledge there are still substantial gaps in this competitive field of cancer research – such as, is the *p53*-dependent up-regulation of its essential negative regulator *Mdm2* required for viability? And/or – is constitutive (p53-independent) up-regulation of basal *Mdm2* required for viability? These questions have remained unanswered for nearly 17 years, since the role of *Mdm2* as an essential negative regulator of *p53* first became apparent in 1995 [Montes de Oca Luna et al., 1995, Jones et al., 1995]. Therefore, the transgenic mice proposed for this thesis are

expected to have a significant impact in the field of cancer biology regardless of the phenotype (viable or lethal).

It is worth noting at this point – before speculating on the phenotypes of the *Mdm2* P1/P2 mutant mice – that a hypomorphic allele of *Mdm2* (~ 30% less Mdm2) resulted in mice which were smaller, with defects in lymphogenesis and had increased radiosensitivity – presumably due to increased constitutive p53 activity [Mendrysa et al., 2003]. These mice (denoted $Mdm2^{puro}$), aged normally and were resistant to tumour formation demonstrating that reduced levels of *Mdm2* can have anti-tumourigenesis properties *in vivo* [Mendrysa et al., 2006]. This study, however, cannot discriminate between the p53-dependent and p53-independent regulatory contributions to Mdm2 expression. At the other end of this extraordinarily sensitive feedback mechanism, it has been shown that a single SNP polymorphism which affects the human *MDM2* P2 promoter (T>G nucleotide 309 in intron 1) increases MDM2 protein expression by approximately 4-fold and significantly accelerated the rate of tumour onset in Li-Fraumeni patients [Bond et al., 2004]. Whilst this study indicates that increased MDM2 levels can contribute to cancer development (as evident by the high rate of *MDM2* amplification in cancers in general [Oliner et al., 1992, Nie and Tian, 2009]) it cannot however, discriminate between the p53-dependent and p53-independent regulatory contributions of MDM2 to tumourigenesis. In another relevant study, $Mdm2^{-/-}$ mice with a hypomorphic allele of p53 (denoted $p53^{515C}$) were unable to survive beyond postnatal day 13 due to a failure to cope with elevated ROS in hematopoietic cells [Abbas et al., 2010]. Thus, taken together, these studies demonstrate an overwhelming need to further investigate the relative contributions of p53-dependent and p53-independent functions of *Mdm2*. Furthermore these studies indicate that the mutations we have designed for the *Mdm2* promoter regions are likely to generate dramatic phenotypes *in vivo* with relevance to normal development, in response to genotoxic stresses and cancer susceptibility.

Following on from this, in the first instance the design of the proposed experiments involving the *Mdm2* P1-Null and P2-Mutant strains are very simple since there are only two outcomes – life or death. It is anticipated that either outcome (viable/lethal) and additional studies will provide significant insights into the p53/Mdm2 negative feedback loop. These additional experiments are discussed next.

If the genotypes of the *Mdm2* P1-Null and/or P2-Mutant lead to lethality, an important additional experiment would be to cross the heterozygote mice onto a p53 null background – thus demonstrating that lethality is as a result of de-regulated p53 activity. Further attempts could be made to rescue the lethality of these mice by intercrossing onto mice with either compromised apoptotic responses (such as $Puma^{-/-}$ or $Bax^{-/-}$) or cell cycle arrest genes (such as $p21^{-/-}$) to determine which downstream *p53* target or targets is or are responsible for the lethality[1]. Additional intercrosses to rescue lethality could include a hypomorphic p53 allele (as such $p53^{515C}$ described by [Abbas et al., 2010]) which might enable the phenotypes of such animals to be examined. In the future, for the *Mdm2* P2-Mutant it would also be interesting to determine if increased basal expression of *Mdm2* could rescue this genotype (perhaps by designing a hyperactive P1 promoter – or a more efficiently translated P1 transcript).

On the other hand, if the genotypes of the *Mdm2* P1-Null and/or P2-Mutant are viable this will give us a unique opportunity to determine – exquisitely and unequivocally – the relative p53-dependent and p53-independent contributions of *Mdm2* up-regulation in a wide variety of developmental, homeostatic control, stress induced and tumour susceptibility scenarios. This would be examined by several approaches including;

- Complete characterisation of the organs to determine any developmental issues.
- Exposure to different stress stimuli (such as γ-irradiation) to analyse p53 activity *in vivo* – including the strength and magnitude of p53 signal and up-regulation of its major downstream genes such as *p21, Puma* and *Mdm2*.
- Long term studies to establish if there is any increase/decrease in cancer formation or any affects on aging.

If the *Mdm2* P1-Null strain is viable (as I would predict) given the developmental defects apparent in the $Mdm2^{puro}$ mouse strain it would seem logical to predict that the *Mdm2* P1-Null strain might also have some developmental problems. In addition since Mdm2 basal expression is compromised the resulting animals might be more sensitive to various

[1] This is another example of where the p21-mCherry and Puma-E2Crimson p53 activity fluorescent reporter mice could be beneficial – since they could provide an authentic report of p53 activity and double knock-ins ($p21mCh^{+/+}$ and $PumaE2Crim^{+/+}$) would also compromise gene function – as might be appropriate in this instance.

genotoxic stresses due to higher basal activity of p53. This may lead to immediate problems in the neonates associated with inappropriate/excessive p53 activity in tissues, which if severe enough could result in early postnatal death (as observed in the $p53^{515C}$). If mice recover from this and/or are able to cope with the various cellular stresses then there will be long term implications regarding their susceptibility to tumour formation (which I expect would be reduced) and other late onset conditions. In addition, since there is still some controversy surrounding the effect of high p53 levels and aging (some studies indicate mice age normally [Mendrysa et al., 2006, Garcia-Cao et al., 2002] whilst others indicate premature aging [Gannon et al., 2011]) this will also be characterised.

If the *Mdm2* P2-Mutant strain is viable then this would indicate that the p53-mediated up-regulation of its own essential negative regulator, *Mdm2,* is dispensable for absolute control of p53 activity. In other words, basal levels of *Mdm2* are sufficient to keep p53 activity in check and prevent death from excessive p53 activity observed in $Mdm2^{-/-}$ mice. This would have significant implications for our understanding of the underlying biology of the p53/Mdm2 feedback loop. In this case it would then be imperative to examine the stress-responses in these mice to determine if they are able to cope with sustained p53 activity across a wide variety of tissues. Similar to the *Mdm2* P1-Null mice, the increased constitutive activity of p53 in the *Mdm2* P2-mutant mice will have further implications for their longevity, general health/development and tumour susceptibility.

In retrospect, as a novice to molecular cloning, this was an ambitious project! Notwithstanding, all four gene targeting constructs have been successfully created and ES cell targeting was performed for the *p21*-mCherry knock-in reporter and the *Mdm2* P2-Mutant transgenic strains with some promising success. In each round of ES cell targeting (despite an initial setback – see Section 3.4.1) a large number of rapidly growing, easily visible, undifferentiated ES cell colonies were obtained. Whilst time was a limiting factor to this project and therefore complete screening of these clones was not possible the initial screening by Southern blot analysis for the *Mdm2* P2-Mutant transgenic strain has already yielded positive ES cell clones (10/208 colonies were positive for integration of the self-excision positive selectable marker see Section 3.4.2). Thus we are in a very good position to

continue with the generation of the proposed mouse strains which are likely to be in high demand within the cancer biology field.

## 4.5 Future work

There are a number of obvious experiments that need to be performed and for brevity some of these are listed below:

- Screening of the *p21*-mCherry knock in reporter ES cell colonies including;
    - Southern blotting to confirm integration of mCherry and the Cre/Neo$^R$ positive selectable marker
    - Phenotypic analysis of cells to determine mCherry functionality
    - Additional Southern blotting to check that there are no additional unwanted random recombination events
- Further confirmation of the *Mdm2* P2-Mutant ES cell clones including;
    - Sequencing to unequivocally confirm the introduction of the desired point mutations.
    - Additional Southern blotting to check that there are no additional unwanted random recombination events.
- Generation of *p21*-mCherry and *Mdm2* P2-Mutant transgenic mice by blastocyst injection.
- *In vitro* validation of the Puma-E2Crimson DNA targeting construct.
- ES cell targeting with the *Mdm2* P1-Null and *Puma*-E2Crimson DNA targeting constructs and subsequent screening of ES cell clones.

# References


ABBAS, H. A., MACCIO, D. R., COSKUN, S., JACKSON, J. G., HAZEN, A. L., SILLS, T. M., YOU, M. J., HIRSCHI, K. K. & LOZANO, G. 2010. Mdm2 is required for survival of hematopoietic stem cells/progenitors via dampening of ROS-induced p53 activity. *Cell Stem Cell,* 7, 606-17.

ADAMS, D. J., QUAIL, M. A., COX, T., VAN DER WEYDEN, L., GORICK, B. D., SU, Q., CHAN, W. I., DAVIES, R., BONFIELD, J. K., LAW, F., HUMPHRAY, S., PLUMB, B., LIU, P., ROGERS, J. & BRADLEY, A. 2005. A genome-wide, end-sequenced 129Sv BAC library resource for targeting vector construction. *Genomics,* 86, 753-8.

ALIMONTI, J. B., SHI, L., BAIJAL, P. K. & GREENBERG, A. H. 2001. Granzyme B induces BID-mediated cytochrome c release and mitochondrial permeability transition. *J Biol Chem,* 276, 6974-82.

ANSARI, B., COATES, P. J., GREENSTEIN, B. D. & HALL, P. A. 1993. In situ end-labelling detects DNA strand breaks in apoptosis and other physiological and pathological states. *J Pathol,* 170, 1-8.

APPELLA, E. & ANDERSON, C. W. 2001. Post-translational modifications and activation of p53 by genotoxic stresses. *Eur J Biochem,* 268, 2764-72.

AYABE, T., ASHIDA, T., KOHGO, Y. & KONO, T. 2004. The role of Paneth cells and their antimicrobial peptides in innate host defense. *Trends Microbiol,* 12, 394-8.

BABINET, C. & COHEN-TANNOUDJI, M. 2001. Genome engineering via homologous recombination in mouse embryonic stem (ES) cells: an amazingly versatile tool for the study of mammalian biology. *An Acad Bras Cienc,* 73, 365-83.

BARKER, N. & CLEVERS, H. 2007. Tracking down the stem cells of the intestine: strategies to identify adult stem cells. *Gastroenterology,* 133, 1755-60.

BARKER, N., VAN ES, J. H., JAKS, V., KASPER, M., SNIPPERT, H., TOFTGARD, R. & CLEVERS, H. 2008. Very Long-term Self-renewal of Small Intestine, Colon, and Hair Follicles from Cycling Lgr5+ve Stem Cells. *Cold Spring Harb Symp Quant Biol.*

BARKER, N., VAN ES, J. H., KUIPERS, J., KUJALA, P., VAN DEN BORN, M., COZIJNSEN, M., HAEGEBARTH, A., KORVING, J., BEGTHEL, H., PETERS, P. J. & CLEVERS, H. 2007. Identification of stem cells in small intestine and colon by marker gene Lgr5. *Nature,* 449, 1003-7.

BERGMANN, A. 2002. Survival signaling goes BAD. *Dev Cell,* 3, 607-8.

BLATTNER, C. 2008. Regulation of p53: the next generation. *Cell Cycle,* 7, 3149-53.

BLATTNER, C., HAY, T., MEEK, D. W. & LANE, D. P. 2002. Hypophosphorylation of Mdm2 augments p53 stability. *Mol Cell Biol,* 22, 6170-82.

BOEHME, K. A., KULIKOV, R. & BLATTNER, C. 2008. p53 stabilization in response to DNA damage requires Akt/PKB and DNA-PK. *Proc Natl Acad Sci U S A,* 105, 7785-90.

BOLDIN, M. P., GONCHAROV, T. M., GOLTSEV, Y. V. & WALLACH, D. 1996. Involvement of MACH, a novel MORT1/FADD-interacting protease, in Fas/APO-1- and TNF receptor-induced cell death. *Cell,* 85, 803-15.

BOND, G. L., HU, W., BOND, E. E., ROBINS, H., LUTZKER, S. G., ARVA, N. C., BARGONETTI, J., BARTEL, F., TAUBERT, H., WUERL, P., ONEL, K., YIP, L., HWANG, S. J., STRONG, L. C., LOZANO, G. & LEVINE, A. J. 2004. A single nucleotide polymorphism in the MDM2 promoter attenuates the p53 tumor suppressor pathway and accelerates tumor formation in humans. *Cell,* 119, 591-602.

BONZON, C., BOUCHIER-HAYES, L., PAGLIARI, L. J., GREEN, D. R. & NEWMEYER, D. D. 2006. Caspase-2-induced apoptosis requires bid cleavage: a physiological role for bid in heat shock-induced death. *Mol Biol Cell,* 17, 2150-7.

BOS, J. L., FEARON, E. R., HAMILTON, S. R., VERLAAN-DE VRIES, M., VAN BOOM, J. H., VAN DER EB, A. J. & VOGELSTEIN, B. 1987. Prevalence of ras gene mutations in human colorectal cancers. *Nature,* 327, 293-7.

BOTCHKAREV, V. A., KOMAROVA, E. A., SIEBENHAAR, F., BOTCHKAREVA, N. V., SHAROV, A. A., KOMAROV, P. G., MAURER, M., GUDKOV, A. V. & GILCHREST, B. A. 2001. p53 Involvement in the control of murine hair follicle regression. *Am J Pathol,* 158, 1913-9.

BOWEN, J. M., GIBSON, R. J., KEEFE, D. M. & CUMMINS, A. G. 2005. Cytotoxic chemotherapy upregulates pro-apoptotic Bax and Bak in the small intestine of rats and humans. *Pathology,* 37, 56-62.

BOYLE, P. & FERLAY, J. 2005. Cancer incidence and mortality in Europe, 2004. *Ann Oncol,* 16, 481-8.

BRIAT, A. & VASSAUX, G. 2008. A new transgenic mouse line to image chemically induced p53 activation in vivo. *Cancer Sci,* 99, 683-8.

BRITTAN, M. & WRIGHT, N. A. 2004. Stem cell in gastrointestinal structure and neoplastic development. *Gut,* 53, 899-910.

BROOKS, C. L. & GU, W. 2006. p53 ubiquitination: Mdm2 and beyond. *Mol Cell,* 21, 307-15.

BROWN, C. Y., MIZE, G. J., PINEDA, M., GEORGE, D. L. & MORRIS, D. R. 1999. Role of two upstream open reading frames in the translational control of oncogene mdm2. *Oncogene,* 18, 5631-7.

BROWN, L., ONGUSAHA, P. P., KIM, H. G., NUTI, S., MANDINOVA, A., LEE, J. W., KHOSRAVI-FAR, R., AARONSON, S. A. & LEE, S. W. 2007. CDIP, a novel pro-apoptotic gene, regulates TNFalpha-mediated apoptosis in a p53-dependent manner. *EMBO J,* 26, 3410-22.

BRUGAROLAS, J., CHANDRASEKARAN, C., GORDON, J. I., BEACH, D., JACKS, T. & HANNON, G. J. 1995. Radiation-induced cell cycle arrest compromised by p21 deficiency. *Nature,* 377, 552-7.

BUNTING, M., BERNSTEIN, K. E., GREER, J. M., CAPECCHI, M. R. & THOMAS, K. R. 1999. Targeting genes for self-excision in the germ line. *Genes Dev,* 13, 1524-8.

BURDELYA, L. G., KRIVOKRYSENKO, V. I., TALLANT, T. C., STROM, E., GLEIBERMAN, A. S., GUPTA, D., KURNASOV, O. V., FORT, F. L., OSTERMAN, A. L., DIDONATO, J. A., FEINSTEIN, E. & GUDKOV, A. V. 2008. An agonist of toll-like receptor 5 has radioprotective activity in mouse and primate models. *Science,* 320, 226-30.

CAMPBELL, S. J., CARLOTTI, F., HALL, P. A., CLARK, A. J. & WOLF, C. R. 1996. Regulation of the CYP1A1 promoter in transgenic mice: an exquisitely sensitive on-off system for cell specific gene regulation. *J Cell Sci,* 109 ( Pt 11), 2619-25.

CANMAN, C. E., GILMER, T. M., COUTTS, S. B. & KASTAN, M. B. 1995. Growth factor modulation of p53-mediated growth arrest versus apoptosis. *Genes Dev,* 9, 600-11.

CANNON, J. S., HAMZEH, F., MOORE, S., NICHOLAS, J. & AMBINDER, R. F. 1999. Human herpesvirus 8-encoded thymidine kinase and phosphotransferase homologues confer sensitivity to ganciclovir. *J Virol,* 73, 4786-93.

CARTRON, P. F., GALLENNE, T., BOUGRAS, G., GAUTIER, F., MANERO, F., VUSIO, P., MEFLAH, K., VALLETTE, F. M. & JUIN, P. 2004. The first alpha helix of Bax plays a necessary role in its ligand-induced activation by the BH3-only proteins Bid and PUMA. *Mol Cell,* 16, 807-18.

CHANDRASEKARAN, C., COOPERSMITH, C. M. & GORDON, J. I. 1996. Use of normal and transgenic mice to examine the relationship between terminal differentiation of intestinal epithelial cells and accumulation of their cell cycle regulators. *J Biol Chem,* 271, 28414-21.

CHANG, C. J., FREEMAN, D. J. & WU, H. 2004. PTEN regulates Mdm2 expression through the P1 promoter. *J Biol Chem,* 279, 29841-8.

CHANG, T., WANG, R., OLSON, D. J., MOUSSEAU, D. D., ROSS, A. R. & WU, L. 2011. Modification of Akt1 by methylglyoxal promotes the proliferation of vascular smooth muscle cells. *FASEB J,* 25, 1746-57.

CHAVEZ-REYES, A., PARANT, J. M., AMELSE, L. L., DE OCA LUNA, R. M., KORSMEYER, S. J. & LOZANO, G. 2003. Switching mechanisms of cell death in mdm2- and mdm4-null mice by deletion of p53 downstream targets. *Cancer Res,* 63, 8664-9.

CHEN, L., WILLIS, S. N., WEI, A., SMITH, B. J., FLETCHER, J. I., HINDS, M. G., COLMAN, P. M., DAY, C. L., ADAMS, J. M. & HUANG, D. C. 2005. Differential targeting of prosurvival Bcl-2 proteins by their BH3-only ligands allows complementary apoptotic function. *Mol Cell,* 17, 393-403.

CHENG, E. H., WEI, M. C., WEILER, S., FLAVELL, R. A., MAK, T. W., LINDSTEN, T. & KORSMEYER, S. J. 2001. BCL-2, BCL-X(L) sequester BH3 domain-only molecules preventing BAX- and BAK-mediated mitochondrial apoptosis. *Mol Cell,* 8, 705-11.

CHINNAIYAN, A. M. 1999. The apoptosome: heart and soul of the cell death machine. *Neoplasia,* 1, 5-15.

CHIPUK, J. E. & GREEN, D. R. 2008. How do BCL-2 proteins induce mitochondrial outer membrane permeabilization? *Trends Cell Biol,* 18, 157-64.

CHIPUK, J. E., KUWANA, T., BOUCHIER-HAYES, L., DROIN, N. M., NEWMEYER, D. D., SCHULER, M. & GREEN, D. R. 2004. Direct activation of Bax by p53 mediates mitochondrial membrane permeabilization and apoptosis. *Science,* 303, 1010-4.

CMIELOVA, J. & REZACOVA, M. 2011. p21(Cip1/Waf1) protein and its function based on a subcellular localization. *J Cell Biochem.*

COOPERSMITH, C. M. & GORDON, J. I. 1997. gamma-Ray-induced apoptosis in transgenic mice with proliferative abnormalities in their intestinal epithelium: re-entry of villus enterocytes into the cell cycle does not affect their radioresistance but enhances the radiosensitivity of the crypt by inducing p53. *Oncogene,* 15, 131-41.

COOPERSMITH, C. M., O'DONNELL, D. & GORDON, J. I. 1999. Bcl-2 inhibits ischemia-reperfusion-induced apoptosis in the intestinal epithelium of transgenic mice. *Am J Physiol,* 276, G677-86.

COQUERET, O. 2003. New roles for p21 and p27 cell-cycle inhibitors: a function for each cell compartment? *Trends Cell Biol,* 13, 65-70.

CORY, S., HUANG, D. C. & ADAMS, J. M. 2003. The Bcl-2 family: roles in cell survival and oncogenesis. *Oncogene,* 22, 8590-607.

CREGAN, S. P., ARBOUR, N. A., MACLAURIN, J. G., CALLAGHAN, S. M., FORTIN, A., CHEUNG, E. C., GUBERMAN, D. S., PARK, D. S. & SLACK, R. S. 2004. p53 activation domain 1 is essential for PUMA upregulation and p53-mediated neuronal cell death. *J Neurosci,* 24, 10003-12.

CRYNS, V. & YUAN, J. 1998. Proteases to die for. *Genes Dev,* 12, 1551-70.

DANIAL, N. N. & KORSMEYER, S. J. 2004. Cell death: critical control points. *Cell,* 116, 205-19.

DE VRIES, A., FLORES, E. R., MIRANDA, B., HSIEH, H. M., VAN OOSTROM, C. T., SAGE, J. & JACKS, T. 2002. Targeted point mutations of p53 lead to dominant-negative inhibition of wild-type p53 function. *Proc Natl Acad Sci U S A,* 99, 2948-53.

DEGLI ESPOSTI, M. & DIVE, C. 2003. Mitochondrial membrane permeabilisation by Bax/Bak. *Biochem Biophys Res Commun,* 304, 455-61.

DENG, C. & CAPECCHI, M. R. 1992. Reexamination of gene targeting frequency as a function of the extent of homology between the targeting vector and the target locus. *Mol Cell Biol,* 12, 3365-71.

DENG, C., ZHANG, P., HARPER, J. W., ELLEDGE, S. J. & LEDER, P. 1995. Mice lacking p21CIP1/WAF1 undergo normal development, but are defective in G1 checkpoint control. *Cell,* 82, 675-84.

DIMITRIADI, M., POULOGIANNIS, G., LIU, L., BACKLUND, L. M., PEARSON, D. M., ICHIMURA, K. & COLLINS, V. P. 2008. p53-independent mechanisms regulate the P2-MDM2 promoter in adult astrocytic tumours. *Br J Cancer,* 99, 1144-52.

DIMRI, G. P., LEE, X., BASILE, G., ACOSTA, M., SCOTT, G., ROSKELLEY, C., MEDRANO, E. E., LINSKENS, M., RUBELJ, I., PEREIRA-SMITH, O. & ET AL. 1995. A biomarker that identifies senescent human cells in culture and in aging skin in vivo. *Proc Natl Acad Sci U S A,* 92, 9363-7.

DIRISINA, R., KATZMAN, R. B., GORETSKY, T., MANAGLIA, E., MITTAL, N., WILLIAMS, D. B., QIU, W., YU, J., CHANDEL, N. S., ZHANG, L. & BARRETT, T. A. 2011. p53 and PUMA

Independently Regulate Apoptosis of Intestinal Epithelial Cells in Patients and Mice With Colitis. *Gastroenterology,* 141, 1036-45.

DONEHOWER, L. A., HARVEY, M., SLAGLE, B. L., MCARTHUR, M. J., MONTGOMERY, C. A., JR., BUTEL, J. S. & BRADLEY, A. 1992. Mice deficient for p53 are developmentally normal but susceptible to spontaneous tumours. *Nature,* 356, 215-21.

DUCKWORTH, C. A. & PRITCHARD, D. M. 2009. Suppression of apoptosis, crypt hyperplasia, and altered differentiation in the colonic epithelia of bak-null mice. *Gastroenterology,* 136, 943-52.

EL-DEIRY, W. S., KERN, S. E., PIETENPOL, J. A., KINZLER, K. W. & VOGELSTEIN, B. 1992. Definition of a consensus binding site for p53. *Nat Genet,* 1, 45-9.

EL-DEIRY, W. S., TOKINO, T., VELCULESCU, V. E., LEVY, D. B., PARSONS, R., TRENT, J. M., LIN, D., MERCER, W. E., KINZLER, K. W. & VOGELSTEIN, B. 1993. WAF1, a potential mediator of p53 tumor suppression. *Cell,* 75, 817-25.

EL-DEIRY, W. S., TOKINO, T., WALDMAN, T., OLINER, J. D., VELCULESCU, V. E., BURRELL, M., HILL, D. E., HEALY, E., REES, J. L., HAMILTON, S. R. & ET AL. 1995. Topological control of p21WAF1/CIP1 expression in normal and neoplastic tissues. *Cancer Res,* 55, 2910-9.

ELLIS, H. M., YU, D., DITIZIO, T. & COURT, D. L. 2001. High efficiency mutagenesis, repair, and engineering of chromosomal DNA using single-stranded oligonucleotides. *Proc Natl Acad Sci U S A,* 98, 6742-6.

ESCOBAR, M., NICOLAS, P., SANGAR, F., LAURENT-CHABALIER, S., CLAIR, P., JOUBERT, D., JAY, P. & LEGRAVEREND, C. 2011. Intestinal epithelial stem cells do not protect their genome by asymmetric chromosome segregation. *Nat Commun,* 2, 258.

FEARON, E. R. & VOGELSTEIN, B. 1990. A genetic model for colorectal tumorigenesis. *Cell,* 61, 759-67.

FEI, P., BERNHARD, E. J. & EL-DEIRY, W. S. 2002. Tissue-specific induction of p53 targets in vivo. *Cancer Res,* 62, 7316-27.

FERRARIS, R. P., VILLENAS, S. A. & DIAMOND, J. 1992. Regulation of brush-border enzyme activities and enterocyte migration rates in mouse small intestine. *Am J Physiol,* 262, G1047-59.

FISHER, D. E. 2001. The p53 tumor suppressor: critical regulator of life & death in cancer. *Apoptosis,* 6, 7-15.

FLETCHER, J. I. & HUANG, D. C. 2008. Controlling the cell death mediators Bax and Bak: puzzles and conundrums. *Cell Cycle,* 7, 39-44.

FLINT, N., COVE, F. L. & EVANS, G. S. 1991. A low-temperature method for the isolation of small-intestinal epithelium along the crypt-villus axis. *Biochem J,* 280 ( Pt 2), 331-4.

FORRESTER, K., ALMOGUERA, C., HAN, K., GRIZZLE, W. E. & PERUCHO, M. 1987. Detection of high incidence of K-ras oncogenes during human colon tumorigenesis. *Nature,* 327, 298-303.

FREEMAN, H. J. 2008. Crypt region localization of intestinal stem cells in adults. *World J Gastroenterol,* 14, 7160-2.

FREY, U. H., BACHMANN, H. S., PETERS, J. & SIFFERT, W. 2008. PCR-amplification of GC-rich regions: 'slowdown PCR'. *Nat Protoc,* 3, 1312-7.

FRIEDRICH, G. & SORIANO, P. 1991. Promoter traps in embryonic stem cells: a genetic screen to identify and mutate developmental genes in mice. *Genes Dev,* 5, 1513-23.

FUJII, G., TSUCHIYA, R., EZOE, E. & HIROHASHI, S. 1999. Analysis of nuclear localization signals using a green fluorescent protein-fusion protein library. *Exp Cell Res,* 251, 299-306.

FUNAYAMA, R. & ISHIKAWA, F. 2007. Cellular senescence and chromatin structure. *Chromosoma,* 116, 431-40.

GANGULI, G. & WASYLYK, B. 2003. p53-independent functions of MDM2. *Mol Cancer Res,* 1, 1027-35.

GANNON, H. S., DONEHOWER, L. A., LYLE, S. & JONES, S. N. 2011. Mdm2-p53 signaling regulates epidermal stem cell senescence and premature aging phenotypes in mouse skin. *Dev Biol,* 353, 1-9.

GARCIA-CAO, I., GARCIA-CAO, M., MARTIN-CABALLERO, J., CRIADO, L. M., KLATT, P., FLORES, J. M., WEILL, J. C., BLASCO, M. A. & SERRANO, M. 2002. "Super p53" mice exhibit enhanced DNA damage response, are tumor resistant and age normally. *EMBO J,* 21, 6225-35.

GARTEL, A. L. & TYNER, A. L. 1999. Transcriptional regulation of the p21((WAF1/CIP1)) gene. *Exp Cell Res,* 246, 280-9.

GOELZ, S. E., VOGELSTEIN, B., HAMILTON, S. R. & FEINBERG, A. P. 1985. Hypomethylation of DNA from benign and malignant human colon neoplasms. *Science,* 228, 187-90.

GONZALEZ-SUAREZ, E., SAMPER, E., FLORES, J. M. & BLASCO, M. A. 2000. Telomerase-deficient mice with short telomeres are resistant to skin tumorigenesis. *Nat Genet,* 26, 114-7.

GOONESINGHE, A., MUNDY, E. S., SMITH, M., KHOSRAVI-FAR, R., MARTINOU, J. C. & ESPOSTI, M. D. 2005. Pro-apoptotic Bid induces membrane perturbation by inserting selected lysolipids into the bilayer. *Biochem J,* 387, 109-18.

GOTTLIEB, E., HAFFNER, R., KING, A., ASHER, G., GRUSS, P., LONAI, P. & OREN, M. 1997. Transgenic mouse model for studying the transcriptional activity of the p53 protein: age- and tissue-dependent changes in radiation-induced activation during embryogenesis. *EMBO J,* 16, 1381-90.

GRODEN, J., THLIVERIS, A., SAMOWITZ, W., CARLSON, M., GELBERT, L., ALBERTSEN, H., JOSLYN, G., STEVENS, J., SPIRIO, L., ROBERTSON, M. & ET AL. 1991. Identification and characterization of the familial adenomatous polyposis coli gene. *Cell,* 66, 589-600.

GROSS, A., YIN, X. M., WANG, K., WEI, M. C., JOCKEL, J., MILLIMAN, C., ERDJUMENT-BROMAGE, H., TEMPST, P. & KORSMEYER, S. J. 1999. Caspase cleaved BID targets

mitochondria and is required for cytochrome c release, while BCL-XL prevents this release but not tumor necrosis factor-R1/Fas death. *J Biol Chem,* 274, 1156-63.

GROSSMANN, J. 2002. Molecular mechanisms of "detachment-induced apoptosis--Anoikis". *Apoptosis,* 7, 247-60.

GROSSMANN, J., WALTHER, K., ARTINGER, M., RUMMELE, P., WOENCKHAUS, M. & SCHOLMERICH, J. 2002. Induction of apoptosis before shedding of human intestinal epithelial cells. *Am J Gastroenterol,* 97, 1421-8.

GU, H., ZOU, Y. R. & RAJEWSKY, K. 1993. Independent control of immunoglobulin switch recombination at individual switch regions evidenced through Cre-loxP-mediated gene targeting. *Cell,* 73, 1155-64.

HADJANTONAKIS, A. K., DICKINSON, M. E., FRASER, S. E. & PAPAIOANNOU, V. E. 2003. Technicolour transgenics: imaging tools for functional genomics in the mouse. *Nat Rev Genet,* 4, 613-25.

HAN, J., FLEMINGTON, C., HOUGHTON, A. B., GU, Z., ZAMBETTI, G. P., LUTZ, R. J., ZHU, L. & CHITTENDEN, T. 2001. Expression of bbc3, a pro-apoptotic BH3-only gene, is regulated by diverse cell death and survival signals. *Proc Natl Acad Sci U S A,* 98, 11318-23.

HANAHAN, D. & WEINBERG, R. A. 2000. The hallmarks of cancer. *Cell,* 100, 57-70.

HANSEN, J., FLOSS, T., VAN SLOUN, P., FUCHTBAUER, E. M., VAUTI, F., ARNOLD, H. H., SCHNUTGEN, F., WURST, W., VON MELCHNER, H. & RUIZ, P. 2003. A large-scale, gene-driven mutagenesis approach for the functional analysis of the mouse genome. *Proc Natl Acad Sci U S A,* 100, 9918-22.

HARPER, J. W., ADAMI, G. R., WEI, N., KEYOMARSI, K. & ELLEDGE, S. J. 1993. The p21 Cdk-interacting protein Cip1 is a potent inhibitor of G1 cyclin-dependent kinases. *Cell,* 75, 805-16.

HARRIS, S. L. & LEVINE, A. J. 2005. The p53 pathway: positive and negative feedback loops. *Oncogene,* 24, 2899-908.

HARVEY, M., SANDS, A. T., WEISS, R. S., HEGI, M. E., WISEMAN, R. W., PANTAZIS, P., GIOVANELLA, B. C., TAINSKY, M. A., BRADLEY, A. & DONEHOWER, L. A. 1993. In vitro growth characteristics of embryo fibroblasts isolated from p53-deficient mice. *Oncogene,* 8, 2457-67.

HASELKORN, T., WHITTEMORE, A. S. & LILIENFELD, D. E. 2005. Incidence of small bowel cancer in the United States and worldwide: geographic, temporal, and racial differences. *Cancer Causes Control,* 16, 781-7.

HASTY, P., RIVERA-PEREZ, J. & BRADLEY, A. 1991. The length of homology required for gene targeting in embryonic stem cells. *Mol Cell Biol,* 11, 5586-91.

HAYFLICK, L. & MOORHEAD, P. S. 1961. The serial cultivation of human diploid cell strains. *Exp Cell Res,* 25, 585-621.

HERMISTON, M. L. & GORDON, J. I. 1995. Inflammatory bowel disease and adenomas in mice expressing a dominant negative N-cadherin. *Science,* 270, 1203-7.

HILL, M. M., ADRAIN, C. & MARTIN, S. J. 2003. Portrait of a killer: the mitochondrial apoptosome emerges from the shadows. *Mol Interv,* 3, 19-26.

HOLLSTEIN, M., SIDRANSKY, D., VOGELSTEIN, B. & HARRIS, C. C. 1991. p53 mutations in human cancers. *Science,* 253, 49-53.

HONDA, R., TANAKA, H. & YASUDA, H. 1997. Oncoprotein MDM2 is a ubiquitin ligase E3 for tumor suppressor p53. *FEBS Lett,* 420, 25-7.

HUANG, D. C. & STRASSER, A. 2000. BH3-Only proteins-essential initiators of apoptotic cell death. *Cell,* 103, 839-42.

HUSSAIN, S. P. & HARRIS, C. C. 2006. p53 biological network: at the crossroads of the cellular-stress response pathway and molecular carcinogenesis. *J Nippon Med Sch,* 73, 54-64.

IJIRI, K. & POTTEN, C. S. 1983. Response of intestinal cells of differing topographical and hierarchical status to ten cytotoxic drugs and five sources of radiation. *Br J Cancer,* 47, 175-85.

INUZUKA, H., TSENG, A., GAO, D., ZHAI, B., ZHANG, Q., SHAIK, S., WAN, L., ANG, X. L., MOCK, C., YIN, H., STOMMEL, J. M., GYGI, S., LAHAV, G., ASARA, J., XIAO, Z. X., KAELIN, W. G., JR., HARPER, J. W. & WEI, W. 2010. Phosphorylation by casein kinase I promotes the turnover of the Mdm2 oncoprotein via the SCF(beta-TRCP) ubiquitin ligase. *Cancer Cell,* 18, 147-59.

ITAHANA, K., MAO, H., JIN, A., ITAHANA, Y., CLEGG, H. V., LINDSTROM, M. S., BHAT, K. P., GODFREY, V. L., EVAN, G. I. & ZHANG, Y. 2007. Targeted inactivation of Mdm2 RING finger E3 ubiquitin ligase activity in the mouse reveals mechanistic insights into p53 regulation. *Cancer Cell,* 12, 355-66.

ITTNER, L. M. & GOTZ, J. 2007. Pronuclear injection for the production of transgenic mice. *Nat Protoc,* 2, 1206-15.

IWAKUMA, T. & LOZANO, G. 2003. MDM2, an introduction. *Mol Cancer Res,* 1, 993-1000.

JACKSON, M. W. & BERBERICH, S. J. 2000. MdmX protects p53 from Mdm2-mediated degradation. *Mol Cell Biol,* 20, 1001-7.

JACKSON, R. J., ENGELMAN, R. W., COPPOLA, D., CANTOR, A. B., WHARTON, W. & PLEDGER, W. J. 2003. p21Cip1 nullizygosity increases tumor metastasis in irradiated mice. *Cancer Res,* 63, 3021-5.

JACOBS, S. B., BASAK, S., MURRAY, J. I., PATHAK, N. & ATTARDI, L. D. 2007. Siva is an apoptosis-selective p53 target gene important for neuronal cell death. *Cell Death Differ,* 14, 1374-85.

JANSSON, A. K., EMTERLING, A. M., ARBMAN, G. & SUN, X. F. 2003. Noxa in colorectal cancer: a study on DNA, mRNA and protein expression. *Oncogene,* 22, 4675-8.

JEFFERS, J. R., PARGANAS, E., LEE, Y., YANG, C., WANG, J., BRENNAN, J., MACLEAN, K. H., HAN, J., CHITTENDEN, T., IHLE, J. N., MCKINNON, P. J., CLEVELAND, J. L. & ZAMBETTI,

G. P. 2003. Puma is an essential mediator of p53-dependent and -independent apoptotic pathways. *Cancer Cell,* 4, 321-8.

JIN, X., TURCOTT, E., ENGLEHARDT, S., MIZE, G. J. & MORRIS, D. R. 2003. The two upstream open reading frames of oncogene mdm2 have different translational regulatory properties. *J Biol Chem,* 278, 25716-21.

JONES, S. N., ROE, A. E., DONEHOWER, L. A. & BRADLEY, A. 1995. Rescue of embryonic lethality in Mdm2-deficient mice by absence of p53. *Nature,* 378, 206-8.

KAMER, I., SARIG, R., ZALTSMAN, Y., NIV, H., OBERKOVITZ, G., REGEV, L., HAIMOVICH, G., LERENTHAL, Y., MARCELLUS, R. C. & GROSS, A. 2005. Proapoptotic BID is an ATM effector in the DNA-damage response. *Cell,* 122, 593-603.

KAUFMAN, M. H. & BARD, J. B. L. 1999. *The Anatomical Basis Of Mouse Development*, Academic Press.

KAUFMANN, T., TAI, L., EKERT, P. G., HUANG, D. C., NORRIS, F., LINDEMANN, R. K., JOHNSTONE, R. W., DIXIT, V. M. & STRASSER, A. 2007. The BH3-only protein bid is dispensable for DNA damage- and replicative stress-induced apoptosis or cell-cycle arrest. *Cell,* 129, 423-33.

KERR, J. F., WYLLIE, A. H. & CURRIE, A. R. 1972. Apoptosis: a basic biological phenomenon with wide-ranging implications in tissue kinetics. *Br J Cancer,* 26, 239-57.

KIM, J. Y., AHN, H. J., RYU, J. H., SUK, K. & PARK, J. H. 2004. BH3-only protein Noxa is a mediator of hypoxic cell death induced by hypoxia-inducible factor 1alpha. *J Exp Med,* 199, 113-24.

KIM, K. M. & SHIBATA, D. 2002. Methylation reveals a niche: stem cell succession in human colon crypts. *Oncogene,* 21, 5441-9.

KIM, M. R., JEONG, E. G., CHAE, B., LEE, J. W., SOUNG, Y. H., NAM, S. W., LEE, J. Y., YOO, N. J. & LEE, S. H. 2007. Pro-apoptotic PUMA and anti-apoptotic phospho-BAD are highly expressed in colorectal carcinomas. *Dig Dis Sci,* 52, 2751-6.

KIRSCH, D. G., SANTIAGO, P. M., DI TOMASO, E., SULLIVAN, J. M., HOU, W. S., DAYTON, T., JEFFORDS, L. B., SODHA, P., MERCER, K. L., COHEN, R., TAKEUCHI, O., KORSMEYER, S. J., BRONSON, R. T., KIM, C. F., HAIGIS, K. M., JAIN, R. K. & JACKS, T. 2010. p53 controls radiation-induced gastrointestinal syndrome in mice independent of apoptosis. *Science,* 327, 593-6.

KOMAROVA, E. A., CHERNOV, M. V., FRANKS, R., WANG, K., ARMIN, G., ZELNICK, C. R., CHIN, D. M., BACUS, S. S., STARK, G. R. & GUDKOV, A. V. 1997. Transgenic mice with p53-responsive lacZ: p53 activity varies dramatically during normal development and determines radiation and drug sensitivity in vivo. *EMBO J,* 16, 1391-400.

KOMAROVA, E. A., KONDRATOV, R. V., WANG, K., CHRISTOV, K., GOLOVKINA, T. V., GOLDBLUM, J. R. & GUDKOV, A. V. 2004. Dual effect of p53 on radiation sensitivity in vivo: p53 promotes hematopoietic injury, but protects from gastro-intestinal syndrome in mice. *Oncogene,* 23, 3265-71.

KORINEK, V., BARKER, N., MOERER, P., VAN DONSELAAR, E., HULS, G., PETERS, P. J. & CLEVERS, H. 1998. Depletion of epithelial stem-cell compartments in the small intestine of mice lacking Tcf-4. *Nat Genet,* 19, 379-83.

KOZAK, M. 1978. How do eucaryotic ribosomes select initiation regions in messenger RNA? *Cell,* 15, 1109-23.

KRTOLICA, A., PARRINELLO, S., LOCKETT, S., DESPREZ, P. Y. & CAMPISI, J. 2001. Senescent fibroblasts promote epithelial cell growth and tumorigenesis: a link between cancer and aging. *Proc Natl Acad Sci U S A,* 98, 12072-7.

KU, W. C., CHIU, S. K., CHEN, Y. J., HUANG, H. H. & WU, W. G. 2009. Complementary quantitative proteomics reveals that transcription factor AP-4 mediates E-box-dependent complex formation for transcriptional repression of HDM2. *Mol Cell Proteomics,* 8, 2034-50.

KUBBUTAT, M. H. & VOUSDEN, K. H. 1998. Keeping an old friend under control: regulation of p53 stability. *Mol Med Today,* 4, 250-6.

KULIKOV, R., BOEHME, K. A. & BLATTNER, C. 2005. Glycogen synthase kinase 3-dependent phosphorylation of Mdm2 regulates p53 abundance. *Mol Cell Biol,* 25, 7170-80.

LABAER, J., GARRETT, M. D., STEVENSON, L. F., SLINGERLAND, J. M., SANDHU, C., CHOU, H. S., FATTAEY, A. & HARLOW, E. 1997. New functional activities for the p21 family of CDK inhibitors. *Genes Dev,* 11, 847-62.

LAKIN, N. D., HANN, B. C. & JACKSON, S. P. 1999. The ataxia-telangiectasia related protein ATR mediates DNA-dependent phosphorylation of p53. *Oncogene,* 18, 3989-95.

LANDERS, J. E., CASSEL, S. L. & GEORGE, D. L. 1997. Translational enhancement of mdm2 oncogene expression in human tumor cells containing a stabilized wild-type p53 protein. *Cancer Res,* 57, 3562-8.

LANE, D. P. 1992. Cancer. p53, guardian of the genome. *Nature,* 358, 15-6.

LANE, D. P. & BENCHIMOL, S. 1990. p53: oncogene or anti-oncogene? *Genes Dev,* 4, 1-8.

LANE, D. P. & CRAWFORD, L. V. 1979. T antigen is bound to a host protein in SV40-transformed cells. *Nature,* 278, 261-3.

LASSUS, H., SALOVAARA, R., AALTONEN, L. A. & BUTZOW, R. 2001. Allelic analysis of serous ovarian carcinoma reveals two putative tumor suppressor loci at 18q22-q23 distal to SMAD4, SMAD2, and DCC. *Am J Pathol,* 159, 35-42.

LEIBOWITZ, B. J., QIU, W., LIU, H., CHENG, T., ZHANG, L. & YU, J. 2011. Uncoupling p53 functions in radiation-induced intestinal damage via PUMA and p21. *Mol Cancer Res,* 9, 616-25.

LETAI, A., BASSIK, M. C., WALENSKY, L. D., SORCINELLI, M. D., WEILER, S. & KORSMEYER, S. J. 2002. Distinct BH3 domains either sensitize or activate mitochondrial apoptosis, serving as prototype cancer therapeutics. *Cancer Cell,* 2, 183-92.

LEVINE, A. J. 1997. p53, the cellular gatekeeper for growth and division. *Cell,* 88, 323-31.

LI, B., CHENG, Q., LI, Z. & CHEN, J. 2010. p53 inactivation by MDM2 and MDMX negative feedback loops in testicular germ cell tumors. *Cell Cycle,* 9, 1411-20.

LI, H., ZHU, H., XU, C. J. & YUAN, J. 1998. Cleavage of BID by caspase 8 mediates the mitochondrial damage in the Fas pathway of apoptosis. *Cell,* 94, 491-501.

LI, P., NIJHAWAN, D., BUDIHARDJO, I., SRINIVASULA, S. M., AHMAD, M., ALNEMRI, E. S. & WANG, X. 1997. Cytochrome c and dATP-dependent formation of Apaf-1/caspase-9 complex initiates an apoptotic protease cascade. *Cell,* 91, 479-89.

LIANG, H. & LUNEC, J. 2005. Characterisation of a novel p53 down-regulated promoter in intron 3 of the human MDM2 oncogene. *Gene,* 361, 112-8.

LINARES, L. K., HENGSTERMANN, A., CIECHANOVER, A., MULLER, S. & SCHEFFNER, M. 2003. HdmX stimulates Hdm2-mediated ubiquitination and degradation of p53. *Proc Natl Acad Sci U S A,* 100, 12009-14.

LINDSTEN, T., ROSS, A. J., KING, A., ZONG, W. X., RATHMELL, J. C., SHIELS, H. A., ULRICH, E., WAYMIRE, K. G., MAHAR, P., FRAUWIRTH, K., CHEN, Y., WEI, M., ENG, V. M., ADELMAN, D. M., SIMON, M. C., MA, A., GOLDEN, J. A., EVAN, G., KORSMEYER, S. J., MACGREGOR, G. R. & THOMPSON, C. B. 2000. The combined functions of proapoptotic Bcl-2 family members bak and bax are essential for normal development of multiple tissues. *Mol Cell,* 6, 1389-99.

LINZER, D. I. & LEVINE, A. J. 1979. Characterization of a 54K dalton cellular SV40 tumor antigen present in SV40-transformed cells and uninfected embryonal carcinoma cells. *Cell,* 17, 43-52.

LOZANO, G. & ZAMBETTI, G. P. 2005. What have animal models taught us about the p53 pathway? *J Pathol,* 205, 206-20.

LUO, X., BUDIHARDJO, I., ZOU, H., SLAUGHTER, C. & WANG, X. 1998. Bid, a Bcl2 interacting protein, mediates cytochrome c release from mitochondria in response to activation of cell surface death receptors. *Cell,* 94, 481-90.

MADISON, B. B., DUNBAR, L., QIAO, X. T., BRAUNSTEIN, K., BRAUNSTEIN, E. & GUMUCIO, D. L. 2002. Cis elements of the villin gene control expression in restricted domains of the vertical (crypt) and horizontal (duodenum, cecum) axes of the intestine. *J Biol Chem,* 277, 33275-83.

MANSOUR, S. L., THOMAS, K. R. & CAPECCHI, M. R. 1988. Disruption of the proto-oncogene int-2 in mouse embryo-derived stem cells: a general strategy for targeting mutations to non-selectable genes. *Nature,* 336, 348-52.

MARIADASON, J. M., NICHOLAS, C., L'ITALIEN, K. E., ZHUANG, M., SMARTT, H. J., HEERDT, B. G., YANG, W., CORNER, G. A., WILSON, A. J., KLAMPFER, L., ARANGO, D. & AUGENLICHT, L. H. 2005. Gene expression profiling of intestinal epithelial cell maturation along the crypt-villus axis. *Gastroenterology,* 128, 1081-8.

MARINE, J. C. & JOCHEMSEN, A. G. 2005. Mdmx as an essential regulator of p53 activity. *Biochem Biophys Res Commun,* 331, 750-60.

MARINESCU, V. D., KOHANE, I. S. & RIVA, A. 2005. MAPPER: a search engine for the computational identification of putative transcription factor binding sites in multiple genomes. *BMC Bioinformatics,* 6, 79.

MARSH, M. N., PETERS, T. J. & BROWN, A. C. 1971. Observations of isolated enterocytes and of their subcellular components using transmission and scanning electron microscopy. *Gut,* 12, 499-508.

MARSHMAN, E., BOOTH, C. & POTTEN, C. S. 2002. The intestinal epithelial stem cell. *Bioessays,* 24, 91-8.

MARSHMAN, E., OTTEWELL, P. D., POTTEN, C. S. & WATSON, A. J. 2001. Caspase activation during spontaneous and radiation-induced apoptosis in the murine intestine. *J Pathol,* 195, 285-92.

MARTIN-CABALLERO, J., FLORES, J. M., GARCIA-PALENCIA, P. & SERRANO, M. 2001. Tumor susceptibility of p21(Waf1/Cip1)-deficient mice. *Cancer Res,* 61, 6234-8.

MARTINVALET, D., THIERY, J. & CHOWDHURY, D. 2008. Granzymes and cell death. *Methods Enzymol,* 442, 213-30.

MASON, N., ALIBERTI, J., CAAMANO, J. C., LIOU, H. C. & HUNTER, C. A. 2002. Cutting edge: identification of c-Rel-dependent and -independent pathways of IL-12 production during infectious and inflammatory stimuli. *J Immunol,* 168, 2590-4.

MAYA, R., BALASS, M., KIM, S. T., SHKEDY, D., LEAL, J. F., SHIFMAN, O., MOAS, M., BUSCHMANN, T., RONAI, Z., SHILOH, Y., KASTAN, M. B., KATZIR, E. & OREN, M. 2001. ATM-dependent phosphorylation of Mdm2 on serine 395: role in p53 activation by DNA damage. *Genes Dev,* 15, 1067-77.

MAYO, L. D., TURCHI, J. J. & BERBERICH, S. J. 1997. Mdm-2 phosphorylation by DNA-dependent protein kinase prevents interaction with p53. *Cancer Res,* 57, 5013-6.

MENDRYSA, S. M., MCELWEE, M. K., MICHALOWSKI, J., O'LEARY, K. A., YOUNG, K. M. & PERRY, M. E. 2003. mdm2 Is critical for inhibition of p53 during lymphopoiesis and the response to ionizing irradiation. *Mol Cell Biol,* 23, 462-72.

MENDRYSA, S. M., O'LEARY, K. A., MCELWEE, M. K., MICHALOWSKI, J., EISENMAN, R. N., POWELL, D. A. & PERRY, M. E. 2006. Tumor suppression and normal aging in mice with constitutively high p53 activity. *Genes Dev,* 20, 16-21.

MENDRYSA, S. M. & PERRY, M. E. 2000. The p53 tumor suppressor protein does not regulate expression of its own inhibitor, MDM2, except under conditions of stress. *Mol Cell Biol,* 20, 2023-30.

MERRITT, A. J., ALLEN, T. D., POTTEN, C. S. & HICKMAN, J. A. 1997. Apoptosis in small intestinal epithelial from p53-null mice: evidence for a delayed, p53-independent G2/M-associated cell death after gamma-irradiation. *Oncogene,* 14, 2759-66.

MERRITT, A. J., POTTEN, C. S., KEMP, C. J., HICKMAN, J. A., BALMAIN, A., LANE, D. P. & HALL, P. A. 1994. The role of p53 in spontaneous and radiation-induced apoptosis in the gastrointestinal tract of normal and p53-deficient mice. *Cancer Res,* 54, 614-7.

MERRITT, A. J., POTTEN, C. S., WATSON, A. J., LOH, D. Y., NAKAYAMA, K. & HICKMAN, J. A. 1995. Differential expression of bcl-2 in intestinal epithelia. Correlation with attenuation of apoptosis in colonic crypts and the incidence of colonic neoplasia. *J Cell Sci,* 108 ( Pt 6), 2261-71.

MEULMEESTER, E., PEREG, Y., SHILOH, Y. & JOCHEMSEN, A. G. 2005. ATM-mediated phosphorylations inhibit Mdmx/Mdm2 stabilization by HAUSP in favor of p53 activation. *Cell Cycle,* 4, 1166-70.

MEYERS, E. N., LEWANDOSKI, M. & MARTIN, G. R. 1998. An Fgf8 mutant allelic series generated by Cre- and Flp-mediated recombination. *Nat Genet,* 18, 136-41.

MICHALAK, E. M., VILLUNGER, A., ADAMS, J. M. & STRASSER, A. 2008. In several cell types tumour suppressor p53 induces apoptosis largely via Puma but Noxa can contribute. *Cell Death Differ,* 15, 1019-29.

MIDGLEY, C. A., OWENS, B., BRISCOE, C. V., THOMAS, D. B., LANE, D. P. & HALL, P. A. 1995. Coupling between gamma irradiation, p53 induction and the apoptotic response depends upon cell type in vivo. *J Cell Sci,* 108 ( Pt 5), 1843-8.

MOMPARLER, R. L., KARON, M., SIEGEL, S. E. & AVILA, F. 1976. Effect of adriamycin on DNA, RNA, and protein synthesis in cell-free systems and intact cells. *Cancer Res,* 36, 2891-5.

MONTES DE OCA LUNA, R., AMELSE, L. L., CHAVEZ-REYES, A., EVANS, S. C., BRUGAROLAS, J., JACKS, T. & LOZANO, G. 1997. Deletion of p21 cannot substitute for p53 loss in rescue of mdm2 null lethality. *Nat Genet,* 16, 336-7.

MONTES DE OCA LUNA, R., WAGNER, D. S. & LOZANO, G. 1995. Rescue of early embryonic lethality in mdm2-deficient mice by deletion of p53. *Nature,* 378, 203-6.

MOROZOVA, K. S., PIATKEVICH, K. D., GOULD, T. J., ZHANG, J., BEWERSDORF, J. & VERKHUSHA, V. V. 2010. Far-red fluorescent protein excitable with red lasers for flow cytometry and superresolution STED nanoscopy. *Biophys J,* 99, L13-5.

MUZIO, M., CHINNAIYAN, A. M., KISCHKEL, F. C., O'ROURKE, K., SHEVCHENKO, A., NI, J., SCAFFIDI, C., BRETZ, J. D., ZHANG, M., GENTZ, R., MANN, M., KRAMMER, P. H., PETER, M. E. & DIXIT, V. M. 1996. FLICE, a novel FADD-homologous ICE/CED-3-like protease, is recruited to the CD95 (Fas/APO-1) death--inducing signaling complex. *Cell,* 85, 817-27.

NAKAJIMA, W. & TANAKA, N. 2007. Synergistic induction of apoptosis by p53-inducible Bcl-2 family proteins Noxa and Puma. *J Nippon Med Sch,* 74, 148-57.

NAKANO, K. & VOUSDEN, K. H. 2001. PUMA, a novel proapoptotic gene, is induced by p53. *Mol Cell,* 7, 683-94.

NARAYANAN, K. & CHEN, Q. 2011. Bacterial artificial chromosome mutagenesis using recombineering. *J Biomed Biotechnol,* 2011, 971296.

NICHOLL, C. G., POLAK, J. M. & BLOOM, S. R. 1985. The hormonal regulation of food intake, digestion, and absorption. *Annu Rev Nutr,* 5, 213-39.

NIE, J. & TIAN, C. Y. 2009. [Progress in regulation of activity and stability of ubiquitin protein ligase MDM2]. *Yi Chuan,* 31, 993-8.

NORD, A. S., CHANG, P. J., CONKLIN, B. R., COX, A. V., HARPER, C. A., HICKS, G. G., HUANG, C. C., JOHNS, S. J., KAWAMOTO, M., LIU, S., MENG, E. C., MORRIS, J. H., ROSSANT, J.,

RUIZ, P., SKARNES, W. C., SORIANO, P., STANFORD, W. L., STRYKE, D., VON MELCHNER, H., WURST, W., YAMAMURA, K., YOUNG, S. G., BABBITT, P. C. & FERRIN, T. E. 2006. The International Gene Trap Consortium Website: a portal to all publicly available gene trap cell lines in mouse. *Nucleic Acids Res,* 34, D642-8.

O'CONNOR, M., PEIFER, M. & BENDER, W. 1989. Construction of large DNA segments in Escherichia coli. *Science,* 244, 1307-12.

ODA, E., OHKI, R., MURASAWA, H., NEMOTO, J., SHIBUE, T., YAMASHITA, T., TOKINO, T., TANIGUCHI, T. & TANAKA, N. 2000. Noxa, a BH3-only member of the Bcl-2 family and candidate mediator of p53-induced apoptosis. *Science,* 288, 1053-8.

OLINER, J. D., KINZLER, K. W., MELTZER, P. S., GEORGE, D. L. & VOGELSTEIN, B. 1992. Amplification of a gene encoding a p53-associated protein in human sarcomas. *Nature,* 358, 80-3.

OLSON, E. N., ARNOLD, H. H., RIGBY, P. W. & WOLD, B. J. 1996. Know your neighbors: three phenotypes in null mutants of the myogenic bHLH gene MRF4. *Cell,* 85, 1-4.

OLSSON, A., MANZL, C., STRASSER, A. & VILLUNGER, A. 2007. How important are post-translational modifications in p53 for selectivity in target-gene transcription and tumour suppression? *Cell Death Differ,* 14, 1561-75.

OSSINA, N. K., CANNAS, A., POWERS, V. C., FITZPATRICK, P. A., KNIGHT, J. D., GILBERT, J. R., SHEKHTMAN, E. M., TOMEI, L. D., UMANSKY, S. R. & KIEFER, M. C. 1997. Interferon-gamma modulates a p53-independent apoptotic pathway and apoptosis-related gene expression. *J Biol Chem,* 272, 16351-7.

PARANT, J., CHAVEZ-REYES, A., LITTLE, N. A., YAN, W., REINKE, V., JOCHEMSEN, A. G. & LOZANO, G. 2001. Rescue of embryonic lethality in Mdm4-null mice by loss of Trp53 suggests a nonoverlapping pathway with MDM2 to regulate p53. *Nat Genet,* 29, 92-5.

PAYNE, C. M., HOLUBEC, H., BERNSTEIN, C., BERNSTEIN, H., DVORAK, K., GREEN, S. B., WILSON, M., DALL'AGNOL, M., DVORAKOVA, B., WARNEKE, J. & GAREWAL, H. 2005. Crypt-restricted loss and decreased protein expression of cytochrome C oxidase subunit I as potential hypothesis-driven biomarkers of colon cancer risk. *Cancer Epidemiol Biomarkers Prev,* 14, 2066-75.

PAZOLLI, E. & STEWART, S. A. 2008. Senescence: the good the bad and the dysfunctional. *Curr Opin Genet Dev,* 18, 42-7.

PETITJEAN, A., MATHE, E., KATO, S., ISHIOKA, C., TAVTIGIAN, S. V., HAINAUT, P. & OLIVIER, M. 2007. Impact of mutant p53 functional properties on TP53 mutation patterns and tumor phenotype: lessons from recent developments in the IARC TP53 database. *Hum Mutat,* 28, 622-9.

PHELPS, M., DARLEY, M., PRIMROSE, J. N. & BLAYDES, J. P. 2003. p53-independent activation of the hdm2-P2 promoter through multiple transcription factor response elements results in elevated hdm2 expression in estrogen receptor alpha-positive breast cancer cells. *Cancer Res,* 63, 2616-23.

PHILLIPS, A., DARLEY, M. & BLAYDES, J. P. 2006. GC-selective DNA-binding antibiotic, mithramycin A, reveals multiple points of control in the regulation of Hdm2 protein synthesis. *Oncogene,* 25, 4183-93.

PHILLIPS, A., TEUNISSE, A., LAM, S., LODDER, K., DARLEY, M., EMADUDDIN, M., WOLF, A., RICHTER, J., DE LANGE, J., VERLAAN-DE VRIES, M., LENOS, K., BOHNKE, A., BARTEL, F., BLAYDES, J. P. & JOCHEMSEN, A. G. 2010. HDMX-L is expressed from a functional p53-responsive promoter in the first intron of the HDMX gene and participates in an autoregulatory feedback loop to control p53 activity. *J Biol Chem,* 285, 29111-27.

PIETSCH, E. C., LEU, J. I., FRANK, A., DUMONT, P., GEORGE, D. L. & MURPHY, M. E. 2007. The tetramerization domain of p53 is required for efficient BAK oligomerization. *Cancer Biol Ther,* 6, 1576-83.

PIKKARAINEN, S., KENNEDY, R. A., MARSHALL, A. K., THAM EL, L., LAY, K., KRIZ, T. A., HANDA, B. S., CLERK, A. & SUGDEN, P. H. 2009. Regulation of expression of the rat orthologue of mouse double minute 2 (MDM2) by H(2)O(2)-induced oxidative stress in neonatal rat cardiac myocytes. *J Biol Chem,* 284, 27195-210.

PLONER, C., KOFLER, R. & VILLUNGER, A. 2008. Noxa: at the tip of the balance between life and death. *Oncogene,* 27 Suppl 1, S84-92.

POTTEN, C. S. 1998. Stem cells in gastrointestinal epithelium: numbers, characteristics and death. *Philos Trans R Soc Lond B Biol Sci,* 353, 821-30.

POTTEN, C. S., BOOTH, C. & PRITCHARD, D. M. 1997a. The intestinal epithelial stem cell: the mucosal governor. *Int J Exp Pathol,* 78, 219-43.

POTTEN, C. S. & ELLIS, J. R. 2006. Adult small intestinal stem cells: identification, location, characteristics, and clinical applications. *Ernst Schering Res Found Workshop,* 81-98.

POTTEN, C. S., MERRITT, A., HICKMAN, J., HALL, P. & FARANDA, A. 1994. Characterization of radiation-induced apoptosis in the small intestine and its biological implications. *Int J Radiat Biol,* 65, 71-8.

POTTEN, C. S., OWEN, G. & BOOTH, D. 2002. Intestinal stem cells protect their genome by selective segregation of template DNA strands. *J Cell Sci,* 115, 2381-8.

POTTEN, C. S., WILSON, J. W. & BOOTH, C. 1997b. Regulation and significance of apoptosis in the stem cells of the gastrointestinal epithelium. *Stem Cells,* 15, 82-93.

PRITCHARD, D. M., JACKMAN, A., POTTEN, C. S. & HICKMAN, J. A. 1998. Chemically-induced apoptosis: p21 and p53 as determinants of enterotoxin activity. *Toxicol Lett,* 102-103, 19-27.

PRITCHARD, D. M., POTTEN, C. S., KORSMEYER, S. J., ROBERTS, S. & HICKMAN, J. A. 1999. Damage-induced apoptosis in intestinal epithelia from bcl-2-null and bax-null mice: investigations of the mechanistic determinants of epithelial apoptosis in vivo. *Oncogene,* 18, 7287-93.

PRZEMECK, S. M., DUCKWORTH, C. A. & PRITCHARD, D. M. 2007. Radiation-induced gastric epithelial apoptosis occurs in the proliferative zone and is regulated by p53, bak, bax, and bcl-2. *Am J Physiol Gastrointest Liver Physiol,* 292, G620-7.

PUTHALAKATH, H. & STRASSER, A. 2002. Keeping killers on a tight leash: transcriptional and post-translational control of the pro-apoptotic activity of BH3-only proteins. *Cell Death Differ,* 9, 505-12.

PUTHALAKATH, H., VILLUNGER, A., O'REILLY, L. A., BEAUMONT, J. G., COULTAS, L., CHENEY, R. E., HUANG, D. C. & STRASSER, A. 2001. Bmf: a proapoptotic BH3-only protein regulated by interaction with the myosin V actin motor complex, activated by anoikis. *Science,* 293, 1829-32.

QIU, W., CARSON-WALTER, E. B., LIU, H., EPPERLY, M., GREENBERGER, J. S., ZAMBETTI, G. P., ZHANG, L. & YU, J. 2008. PUMA regulates intestinal progenitor cell radiosensitivity and gastrointestinal syndrome. *Cell Stem Cell,* 2, 576-83.

QIU, W., LEIBOWITZ, B., ZHANG, L. & YU, J. 2010. Growth factors protect intestinal stem cells from radiation-induced apoptosis by suppressing PUMA through the PI3K/AKT/p53 axis. *Oncogene,* 29, 1622-32.

RAZIN, A. & RIGGS, A. D. 1980. DNA methylation and gene function. *Science,* 210, 604-10.

REESE, M. G., EECKMAN, F. H., KULP, D. & HAUSSLER, D. 1997. Improved splice site detection in Genie. *J Comput Biol,* 4, 311-23.

RIES, S., BIEDERER, C., WOODS, D., SHIFMAN, O., SHIRASAWA, S., SASAZUKI, T., MCMAHON, M., OREN, M. & MCCORMICK, F. 2000. Opposing effects of Ras on p53: transcriptional activation of mdm2 and induction of p19ARF. *Cell,* 103, 321-30.

ROBERTS, S. 1996. PCCrypts: Score. 1.0 Beta 1 ed.: Paterson Institute for Cancer Research.

ROTOLO, J. A., MAJ, J. G., FELDMAN, R., REN, D., HAIMOVITZ-FRIEDMAN, A., CORDON-CARDO, C., CHENG, E. H., KOLESNICK, R. & FUKS, Z. 2008. Bax and Bak do not exhibit functional redundancy in mediating radiation-induced endothelial apoptosis in the intestinal mucosa. *Int J Radiat Oncol Biol Phys,* 70, 804-15.

RYDING, A. D., SHARP, M. G. & MULLINS, J. J. 2001. Conditional transgenic technologies. *J Endocrinol,* 171, 1-14.

SAGE, J., MULLIGAN, G. J., ATTARDI, L. D., MILLER, A., CHEN, S., WILLIAMS, B., THEODOROU, E. & JACKS, T. 2000. Targeted disruption of the three Rb-related genes leads to loss of G(1) control and immortalization. *Genes Dev,* 14, 3037-50.

SAMBROOK, J., MACCALLUM, P. & RUSSEL, D. 2000. *Molecular Cloning: A Laboratory Manual,* Cold Spring Harbor Laboratory Press.

SAMUELS-LEV, Y., O'CONNOR, D. J., BERGAMASCHI, D., TRIGIANTE, G., HSIEH, J. K., ZHONG, S., CAMPARGUE, I., NAUMOVSKI, L., CROOK, T. & LU, X. 2001. ASPP proteins specifically stimulate the apoptotic function of p53. *Mol Cell,* 8, 781-94.

SANCHO, E., BATLLE, E. & CLEVERS, H. 2004. Signaling pathways in intestinal development and cancer. *Annu Rev Cell Dev Biol,* 20, 695-723.

SANGIORGI, E. & CAPECCHI, M. R. 2008. Bmi1 is expressed in vivo in intestinal stem cells. *Nat Genet,* 40, 915-20.

SARNA, S. K. & OTTERSON, M. F. 1989. Small intestinal physiology and pathophysiology. *Gastroenterol Clin North Am,* 18, 375-404.

SAUCEDO, L. J., MYERS, C. D. & PERRY, M. E. 1999. Multiple murine double minute gene 2 (MDM2) proteins are induced by ultraviolet light. *J Biol Chem,* 274, 8161-8.

SAVILL, J. & FADOK, V. 2000. Corpse clearance defines the meaning of cell death. *Nature,* 407, 784-8.

SAX, J. K., FEI, P., MURPHY, M. E., BERNHARD, E., KORSMEYER, S. J. & EL-DEIRY, W. S. 2002. BID regulation by p53 contributes to chemosensitivity. *Nat Cell Biol,* 4, 842-9.

SCAFFIDI, C., FULDA, S., SRINIVASAN, A., FRIESEN, C., LI, F., TOMASELLI, K. J., DEBATIN, K. M., KRAMMER, P. H. & PETER, M. E. 1998. Two CD95 (APO-1/Fas) signaling pathways. *EMBO J,* 17, 1675-87.

SCHMID, P., LORENZ, A., HAMEISTER, H. & MONTENARH, M. 1991. Expression of p53 during mouse embryogenesis. *Development,* 113, 857-65.

SCHRAMM, G., BRUCHHAUS, I. & ROEDER, T. 2000. A simple and reliable 5'-RACE approach. *Nucleic Acids Res,* 28, E96.

SCHWENK, F., BARON, U. & RAJEWSKY, K. 1995. A cre-transgenic mouse strain for the ubiquitous deletion of loxP-flanked gene segments including deletion in germ cells. *Nucleic Acids Res,* 23, 5080-1.

SERRANO, M. & BLASCO, M. A. 2001. Putting the stress on senescence. *Curr Opin Cell Biol,* 13, 748-53.

SHANER, N. C., CAMPBELL, R. E., STEINBACH, P. A., GIEPMANS, B. N., PALMER, A. E. & TSIEN, R. Y. 2004. Improved monomeric red, orange and yellow fluorescent proteins derived from Discosoma sp. red fluorescent protein. *Nat Biotechnol,* 22, 1567-72.

SHANER, N. C., STEINBACH, P. A. & TSIEN, R. Y. 2005. A guide to choosing fluorescent proteins. *Nat Methods,* 2, 905-9.

SHCHERBO, D., MURPHY, C. S., ERMAKOVA, G. V., SOLOVIEVA, E. A., CHEPURNYKH, T. V., SHCHEGLOV, A. S., VERKHUSHA, V. V., PLETNEV, V. Z., HAZELWOOD, K. L., ROCHE, P. M., LUKYANOV, S., ZARAISKY, A. G., DAVIDSON, M. W. & CHUDAKOV, D. M. 2009. Far-red fluorescent tags for protein imaging in living tissues. *Biochem J,* 418, 567-74.

SHCHERBO, D., SHEMIAKINA, II, RYABOVA, A. V., LUKER, K. E., SCHMIDT, B. T., SOUSLOVA, E. A., GORODNICHEVA, T. V., STRUKOVA, L., SHIDLOVSKIY, K. M., BRITANOVA, O. V., ZARAISKY, A. G., LUKYANOV, K. A., LOSCHENOV, V. B., LUKER, G. D. & CHUDAKOV, D. M. 2010. Near-infrared fluorescent proteins. *Nat Methods,* 7, 827-9.

SHELTON, S. N., SHAWGO, M. E. & ROBERTSON, J. D. 2009. Cleavage of bid by executioner caspases mediates feed forward amplification of mitochondrial outer membrane permeabilization during genotoxic stress-induced apoptosis in jurkat cells. *J Biol Chem.*

SHERR, C. J. 1998. Tumor surveillance via the ARF-p53 pathway. *Genes Dev,* 12, 2984-91.

SHIBAHARA, T., SATO, N., WAGURI, S., IWANAGA, T., NAKAHARA, A., FUKUTOMI, H. & UCHIYAMA, Y. 1995. The fate of effete epithelial cells at the villus tips of the human small intestine. *Arch Histol Cytol,* 58, 205-19.

SHIBATA, D., PEINADO, M. A., IONOV, Y., MALKHOSYAN, S. & PERUCHO, M. 1994. Genomic instability in repeated sequences is an early somatic event in colorectal tumorigenesis that persists after transformation. *Nat Genet,* 6, 273-81.

SHIBUE, T., SUZUKI, S., OKAMOTO, H., YOSHIDA, H., OHBA, Y., TAKAOKA, A. & TANIGUCHI, T. 2006. Differential contribution of Puma and Noxa in dual regulation of p53-mediated apoptotic pathways. *EMBO J,* 25, 4952-62.

SHIBUE, T., TAKEDA, K., ODA, E., TANAKA, H., MURASAWA, H., TAKAOKA, A., MORISHITA, Y., AKIRA, S., TANIGUCHI, T. & TANAKA, N. 2003. Integral role of Noxa in p53-mediated apoptotic response. *Genes Dev,* 17, 2233-8.

SHIBUE, T. & TANIGUCHI, T. 2006. BH3-only proteins: integrated control point of apoptosis. *Int J Cancer,* 119, 2036-43.

SHINOZAKI, T., NOTA, A., TAYA, Y. & OKAMOTO, K. 2003. Functional role of Mdm2 phosphorylation by ATR in attenuation of p53 nuclear export. *Oncogene,* 22, 8870-80.

SHIOHARA, M., EL-DEIRY, W. S., WADA, M., NAKAMAKI, T., TAKEUCHI, S., YANG, R., CHEN, D. L., VOGELSTEIN, B. & KOEFFLER, H. P. 1994. Absence of WAF1 mutations in a variety of human malignancies. *Blood,* 84, 3781-4.

SHIZUYA, H., BIRREN, B., KIM, U. J., MANCINO, V., SLEPAK, T., TACHIIRI, Y. & SIMON, M. 1992. Cloning and stable maintenance of 300-kilobase-pair fragments of human DNA in Escherichia coli using an F-factor-based vector. *Proc Natl Acad Sci U S A,* 89, 8794-7.

SHVARTS, A., STEEGENGA, W. T., RITECO, N., VAN LAAR, T., DEKKER, P., BAZUINE, M., VAN HAM, R. C., VAN DER HOUVEN VAN OORDT, W., HATEBOER, G., VAN DER EB, A. J. & JOCHEMSEN, A. G. 1996. MDMX: a novel p53-binding protein with some functional properties of MDM2. *EMBO J,* 15, 5349-57.

SIMONS, B. D. & CLEVERS, H. 2011. Stem cell self-renewal in intestinal crypt. *Exp Cell Res.*

SINICROPE, F. A., REGO, R. L., OKUMURA, K., FOSTER, N. R., O'CONNELL, M. J., SARGENT, D. J. & WINDSCHITL, H. E. 2008. Prognostic impact of bim, puma, and noxa expression in human colon carcinomas. *Clin Cancer Res,* 14, 5810-8.

SKARNES, W. C., AUERBACH, B. A. & JOYNER, A. L. 1992. A gene trap approach in mouse embryonic stem cells: the lacZ reported is activated by splicing, reflects endogenous gene expression, and is mutagenic in mice. *Genes Dev,* 6, 903-18.

SMEENK, L., VAN HEERINGEN, S. J., KOEPPEL, M., VAN DRIEL, M. A., BARTELS, S. J., AKKERS, R. C., DENISSOV, S., STUNNENBERG, H. G. & LOHRUM, M. 2008. Characterization of genome-wide p53-binding sites upon stress response. *Nucleic Acids Res,* 36, 3639-54.

SNIPPERT, H. J., VAN DER FLIER, L. G., SATO, T., VAN ES, J. H., VAN DEN BORN, M., KROON-VEENBOER, C., BARKER, N., KLEIN, A. M., VAN RHEENEN, J., SIMONS, B. D. &

CLEVERS, H. 2010. Intestinal crypt homeostasis results from neutral competition between symmetrically dividing Lgr5 stem cells. *Cell,* 143, 134-44.

SORIANO, P. 1999. Generalized lacZ expression with the ROSA26 Cre reporter strain. *Nat Genet,* 21, 70-1.

STAD, R., LITTLE, N. A., XIRODIMAS, D. P., FRENK, R., VAN DER EB, A. J., LANE, D. P., SAVILLE, M. K. & JOCHEMSEN, A. G. 2001. Mdmx stabilizes p53 and Mdm2 via two distinct mechanisms. *EMBO Rep,* 2, 1029-34.

STAMATAKI, D., HOLDER, M., HODGETTS, C., JEFFERY, R., NYE, E., SPENCER-DENE, B., WINTON, D. J. & LEWIS, J. 2011. Delta1 Expression, Cell Cycle Exit, and Commitment to a Specific Secretory Fate Coincide within a Few Hours in the Mouse Intestinal Stem Cell System. *PLoS One,* 6, e24484.

STANFORD, W. L., COHN, J. B. & CORDES, S. P. 2001. Gene-trap mutagenesis: past, present and beyond. *Nat Rev Genet,* 2, 756-68.

STOMMEL, J. M. & WAHL, G. M. 2004. Accelerated MDM2 auto-degradation induced by DNA-damage kinases is required for p53 activation. *EMBO J,* 23, 1547-56.

STOMMEL, J. M. & WAHL, G. M. 2005. A new twist in the feedback loop: stress-activated MDM2 destabilization is required for p53 activation. *Cell Cycle,* 4, 411-7.

STORCK, T., KRUTH, U., KOLHEKAR, R., SPRENGEL, R. & SEEBURG, P. H. 1996. Rapid construction in yeast of complex targeting vectors for gene manipulation in the mouse. *Nucleic Acids Res,* 24, 4594-6.

STOYKOVA, A., CHOWDHURY, K., BONALDO, P., TORRES, M. & GRUSS, P. 1998. Gene trap expression and mutational analysis for genes involved in the development of the mammalian nervous system. *Dev Dyn,* 212, 198-213.

STRACK, R. L., HEIN, B., BHATTACHARYYA, D., HELL, S. W., KEENAN, R. J. & GLICK, B. S. 2009. A rapidly maturing far-red derivative of DsRed-Express2 for whole-cell labeling. *Biochemistry,* 48, 8279-81.

STRANO, S., MUNARRIZ, E., ROSSI, M., CRISTOFANELLI, B., SHAUL, Y., CASTAGNOLI, L., LEVINE, A. J., SACCHI, A., CESARENI, G., OREN, M. & BLANDINO, G. 2000. Physical and functional interaction between p53 mutants and different isoforms of p73. *J Biol Chem,* 275, 29503-12.

STRATER, J., KORETZ, K., GUNTHERT, A. R. & MOLLER, P. 1995. In situ detection of enterocytic apoptosis in normal colonic mucosa and in familial adenomatous polyposis. *Gut,* 37, 819-25.

STRYKE, D., KAWAMOTO, M., HUANG, C. C., JOHNS, S. J., KING, L. A., HARPER, C. A., MENG, E. C., LEE, R. E., YEE, A., L'ITALIEN, L., CHUANG, P. T., YOUNG, S. G., SKARNES, W. C., BABBITT, P. C. & FERRIN, T. E. 2003. BayGenomics: a resource of insertional mutations in mouse embryonic stem cells. *Nucleic Acids Res,* 31, 278-81.

TAM, P. P. & BEDDINGTON, R. S. 1987. The formation of mesodermal tissues in the mouse embryo during gastrulation and early organogenesis. *Development,* 99, 109-26.

TANIMURA, S., OHTSUKA, S., MITSUI, K., SHIROUZU, K., YOSHIMURA, A. & OHTSUBO, M. 1999. MDM2 interacts with MDMX through their RING finger domains. *FEBS Lett,* 447, 5-9.

TAYLOR, R. C., CULLEN, S. P. & MARTIN, S. J. 2008. Apoptosis: controlled demolition at the cellular level. *Nat Rev Mol Cell Biol,* 9, 231-41.

TE RIELE, H., MAANDAG, E. R. & BERNS, A. 1992. Highly efficient gene targeting in embryonic stem cells through homologous recombination with isogenic DNA constructs. *Proc Natl Acad Sci U S A,* 89, 5128-32.

THOMAS, K. R. & CAPECCHI, M. R. 1987. Site-directed mutagenesis by gene targeting in mouse embryo-derived stem cells. *Cell,* 51, 503-12.

TIAN, H., BIEHS, B., WARMING, S., LEONG, K. G., RANGELL, L., KLEIN, O. D. & DE SAUVAGE, F. J. 2011. A reserve stem cell population in small intestine renders Lgr5-positive cells dispensable. *Nature.*

TOBY, G., LAW, S. F. & GOLEMIS, E. A. 1998. Vectors to target protein domains to different cellular compartments. *Biotechniques,* 24, 637-40.

TRUONG, A. H., CERVI, D., LEE, J. & BEN-DAVID, Y. 2005. Direct transcriptional regulation of MDM2 by Fli-1. *Oncogene,* 24, 962-9.

TSUBOUCHI, S. 1983. Theoretical implications for cell migration through the crypt and the villus of labelling studies conducted at each position within the crypt. *Cell Tissue Kinet,* 16, 441-56.

VALENTIN-VEGA, Y. A., OKANO, H. & LOZANO, G. 2008. The intestinal epithelium compensates for p53-mediated cell death and guarantees organismal survival. *Cell Death Differ,* 15, 1772-81.

VAN DER FLIER, L. G. & CLEVERS, H. 2009. Stem cells, self-renewal, and differentiation in the intestinal epithelium. *Annu Rev Physiol,* 71, 241-60.

VARESCO, L. 2004. Familial adenomatous polyposis: genetics and epidemiology. *Tech Coloproctol,* 8 Suppl 2, s305-8.

VASEY, D. B., WOLF, C. R., MACARTNEY, T., BROWN, K. & WHITELAW, C. B. 2008. p21-LacZ reporter mice reflect p53-dependent toxic insult. *Toxicol Appl Pharmacol,* 227, 440-50.

VINCZE, T., POSFAI, J. & ROBERTS, R. J. 2003. NEBcutter: A program to cleave DNA with restriction enzymes. *Nucleic Acids Res,* 31, 3688-91.

VOGELSTEIN, B. 1990. Cancer. A deadly inheritance. *Nature,* 348, 681-2.

VOGELSTEIN, B., FEARON, E. R., KERN, S. E., HAMILTON, S. R., PREISINGER, A. C., NAKAMURA, Y. & WHITE, R. 1989. Allelotype of colorectal carcinomas. *Science,* 244, 207-11.

VOGELSTEIN, B., LANE, D. & LEVINE, A. J. 2000. Surfing the p53 network. *Nature,* 408, 307-10.

VON FURSTENBERG, R. J., GULATI, A. S., BAXI, A., DOHERTY, J. M., STAPPENBECK, T. S., GRACZ, A. D., MAGNESS, S. T. & HENNING, S. J. 2010. Sorting mouse jejunal epithelial

cells with CD24 yields a population with characteristics of intestinal stem cells. *Am J Physiol Gastrointest Liver Physiol,* 300, G409-17.

VOUSDEN, K. H. 2002. Activation of the p53 tumor suppressor protein. *Biochim Biophys Acta,* 1602, 47-59.

VOUSDEN, K. H. 2006. Outcomes of p53 activation--spoilt for choice. *J Cell Sci,* 119, 5015-20.

VOUSDEN, K. H. & LU, X. 2002. Live or let die: the cell's response to p53. *Nat Rev Cancer,* 2, 594-604.

WALENSKY, L. D., PITTER, K., MORASH, J., OH, K. J., BARBUTO, S., FISHER, J., SMITH, E., VERDINE, G. L. & KORSMEYER, S. J. 2006. A stapled BID BH3 helix directly binds and activates BAX. *Mol Cell,* 24, 199-210.

WALKER, N. I., HARMON, B. V., GOBE, G. C. & KERR, J. F. 1988. Patterns of cell death. *Methods Achiev Exp Pathol,* 13, 18-54.

WATSON, A. J. & PRITCHARD, D. M. 2000. Lessons from genetically engineered animal models. VII. Apoptosis in intestinal epithelium: lessons from transgenic and knockout mice. *Am J Physiol Gastrointest Liver Physiol,* 278, G1-5.

WATSON, J. D., CAUDY, A. A., MYERS, R. M. & WITKOWSKI, J. A. 2007. Recombinant DNA - Genes and Genomes - A Short Course. *In:* COMPANY, W. H. F. A. (ed.) Third ed.: Cold Spring Harbor Laboratory Press.

WEI, C. L., WU, Q., VEGA, V. B., CHIU, K. P., NG, P., ZHANG, T., SHAHAB, A., YONG, H. C., FU, Y., WENG, Z., LIU, J., ZHAO, X. D., CHEW, J. L., LEE, Y. L., KUZNETSOV, V. A., SUNG, W. K., MILLER, L. D., LIM, B., LIU, E. T., YU, Q., NG, H. H. & RUAN, Y. 2006. A global map of p53 transcription-factor binding sites in the human genome. *Cell,* 124, 207-19.

WEI, M. C., ZONG, W. X., CHENG, E. H., LINDSTEN, T., PANOUTSAKOPOULOU, V., ROSS, A. J., ROTH, K. A., MACGREGOR, G. R., THOMPSON, C. B. & KORSMEYER, S. J. 2001. Proapoptotic BAX and BAK: a requisite gateway to mitochondrial dysfunction and death. *Science,* 292, 727-30.

WEINBERG, R. A. 2006. *The Biology Of Cancer*, Garland Science.

WEINBERG, R. A. 2007. *The Biology of Cancer*, Garland Science.

WEISER, M. M. 1973. Intestinal epithelial cell surface membrane glycoprotein synthesis. I. An indicator of cellular differentiation. *J Biol Chem,* 248, 2536-41.

WILLIAMS, A. M., PROBERT, C. S., STEPANKOVA, R., TLASKALOVA-HOGENOVA, H., PHILLIPS, A. & BLAND, P. W. 2006. Effects of microflora on the neonatal development of gut mucosal T cells and myeloid cells in the mouse. *Immunology,* 119, 470-8.

WILLIAMS, R. L., HILTON, D. J., PEASE, S., WILLSON, T. A., STEWART, C. L., GEARING, D. P., WAGNER, E. F., METCALF, D., NICOLA, N. A. & GOUGH, N. M. 1988. Myeloid leukaemia inhibitory factor maintains the developmental potential of embryonic stem cells. *Nature,* 336, 684-7.

WILLIS, S. N. & ADAMS, J. M. 2005. Life in the balance: how BH3-only proteins induce apoptosis. *Curr Opin Cell Biol,* 17, 617-25.

WILLIS, S. N., CHEN, L., DEWSON, G., WEI, A., NAIK, E., FLETCHER, J. I., ADAMS, J. M. & HUANG, D. C. 2005. Proapoptotic Bak is sequestered by Mcl-1 and Bcl-xL, but not Bcl-2, until displaced by BH3-only proteins. *Genes Dev,* 19, 1294-305.

WILLIS, S. N., FLETCHER, J. I., KAUFMANN, T., VAN DELFT, M. F., CHEN, L., CZABOTAR, P. E., IERINO, H., LEE, E. F., FAIRLIE, W. D., BOUILLET, P., STRASSER, A., KLUCK, R. M., ADAMS, J. M. & HUANG, D. C. 2007. Apoptosis initiated when BH3 ligands engage multiple Bcl-2 homologs, not Bax or Bak. *Science,* 315, 856-9.

WILSON, J. W., PRITCHARD, D. M., HICKMAN, J. A. & POTTEN, C. S. 1998. Radiation-induced p53 and p21WAF-1/CIP1 expression in the murine intestinal epithelium: apoptosis and cell cycle arrest. *Am J Pathol,* 153, 899-909.

WOLPERT, L. 1991. *The Triumph of the Embryo*, New York: Oxford University Press.

WU, B., QIU, W., WANG, P., YU, H., CHENG, T., ZAMBETTI, G. P., ZHANG, L. & YU, J. 2007. p53 independent induction of PUMA mediates intestinal apoptosis in response to ischaemia-reperfusion. *Gut,* 56, 645-54.

WU, G. S., BURNS, T. F., MCDONALD, E. R., 3RD, JIANG, W., MENG, R., KRANTZ, I. D., KAO, G., GAN, D. D., ZHOU, J. Y., MUSCHEL, R., HAMILTON, S. R., SPINNER, N. B., MARKOWITZ, S., WU, G. & EL-DEIRY, W. S. 1997. KILLER/DR5 is a DNA damage-inducible p53-regulated death receptor gene. *Nat Genet,* 17, 141-3.

WU, G. S., BURNS, T. F., MCDONALD, E. R., 3RD, MENG, R. D., KAO, G., MUSCHEL, R., YEN, T. & EL-DEIRY, W. S. 1999. Induction of the TRAIL receptor KILLER/DR5 in p53-dependent apoptosis but not growth arrest. *Oncogene,* 18, 6411-8.

WU, X. & DENG, Y. 2002. Bax and BH3-domain-only proteins in p53-mediated apoptosis. *Front Biosci,* 7, d151-6.

WYLLIE, A. H. 1980. Glucocorticoid-induced thymocyte apoptosis is associated with endogenous endonuclease activation. *Nature,* 284, 555-6.

YANG, W. C., MATHEW, J., VELCICH, A., EDELMANN, W., KUCHERLAPATI, R., LIPKIN, M., YANG, K. & AUGENLICHT, L. H. 2001. Targeted inactivation of the p21(WAF1/cip1) gene enhances Apc-initiated tumor formation and the tumor-promoting activity of a Western-style high-risk diet by altering cell maturation in the intestinal mucosal. *Cancer Res,* 61, 565-9.

YEH, Y. C., LIU, T. J., WANG, L. C., LEE, H. W., TING, C. T., LEE, W. L., HUNG, C. J., WANG, K. Y. & LAI, H. C. 2009. A standardized extract of Ginkgo biloba suppresses doxorubicin-induced oxidative stress and p53-mediated mitochondrial apoptosis in rat testes. *Br J Pharmacol,* 156, 48-61.

YEN, T. H. & WRIGHT, N. A. 2006. The gastrointestinal tract stem cell niche. *Stem Cell Rev,* 2, 203-12.

YIN, X. M. 2000. Bid, a critical mediator for apoptosis induced by the activation of Fas/TNF-R1 death receptors in hepatocytes. *J Mol Med,* 78, 203-11.

YIN, X. M. 2006. Bid, a BH3-only multi-functional molecule, is at the cross road of life and death. *Gene,* 369, 7-19.

YIN, X. M., WANG, K., GROSS, A., ZHAO, Y., ZINKEL, S., KLOCKE, B., ROTH, K. A. & KORSMEYER, S. J. 1999. Bid-deficient mice are resistant to Fas-induced hepatocellular apoptosis. *Nature,* 400, 886-91.

YU, J., ZHANG, L., HWANG, P. M., KINZLER, K. W. & VOGELSTEIN, B. 2001. PUMA induces the rapid apoptosis of colorectal cancer cells. *Mol Cell,* 7, 673-82.

ZHA, J., HARADA, H., YANG, E., JOCKEL, J. & KORSMEYER, S. J. 1996. Serine phosphorylation of death agonist BAD in response to survival factor results in binding to 14-3-3 not BCL-X(L). *Cell,* 87, 619-28.

ZHANG, H., HANNON, G. J., CASSO, D. & BEACH, D. 1994. p21 is a component of active cell cycle kinases. *Cold Spring Harb Symp Quant Biol,* 59, 21-9.

ZHANG, L., SUN, W., WANG, J., ZHANG, M., YANG, S., TIAN, Y., VIDYASAGAR, S., PENA, L. A., ZHANG, K., CAO, Y., YIN, L., WANG, W., SCHAEFER, K. L., SAUBERMANN, L. J., SWARTS, S. G., FENTON, B. M., KENG, P. C. & OKUNIEFF, P. 2010. Mitigation effect of an FGF-2 peptide on acute gastrointestinal syndrome after high-dose ionizing radiation. *Int J Radiat Oncol Biol Phys,* 77, 261-8.

ZHANG, Y. & XIONG, Y. 2001. Control of p53 ubiquitination and nuclear export by MDM2 and ARF. *Cell Growth Differ,* 12, 175-86.

ZHOU, B. B. & ELLEDGE, S. J. 2000. The DNA damage response: putting checkpoints in perspective. *Nature,* 408, 433-9.

ZHOU, J. X., LEE, C. H., QI, C. F., WANG, H., NAGHASHFAR, Z., ABBASI, S. & MORSE, H. C., 3RD 2009. IFN regulatory factor 8 regulates MDM2 in germinal center B cells. *J Immunol,* 183, 3188-94.

ZHU, J., ZHANG, S., JIANG, J. & CHEN, X. 2000. Definition of the p53 functional domains necessary for inducing apoptosis. *J Biol Chem,* 275, 39927-34.

ZINKEL, S. S. 2008. Investigation of the proapoptotic BCL-2 family member bid on the crossroad of the DNA damage response and apoptosis. *Methods Enzymol,* 442, 231-50.

ZINKEL, S. S., HUROV, K. E., ONG, C., ABTAHI, F. M., GROSS, A. & KORSMEYER, S. J. 2005. A role for proapoptotic BID in the DNA-damage response. *Cell,* 122, 579-91.

ZONG, W. X., LINDSTEN, T., ROSS, A. J., MACGREGOR, G. R. & THOMPSON, C. B. 2001. BH3-only proteins that bind pro-survival Bcl-2 family members fail to induce apoptosis in the absence of Bax and Bak. *Genes Dev,* 15, 1481-6.

# APPENDIX A OLIGONUCLEOTIDES

***Table A.1: Oligonucleotides designed for this thesis.***

*Primers are arranged alphabetically. KEY: Yellow highlight indicates the mutating nucleotides to be incorporated by the oligonucleotides at the Mdm2 P2 promoter.*

| Primer name | SEQUENCE (5'→3') | Length | GC% | $T_M$ (°C) |
|---|---|---|---|---|
| 1stPCR | AGTATCGGCCTCAGGAAGATCG | 22 | 55 | 57 |
| 2ndPCR | ATTCAGGCTGCGCAACTGTTGGG | 23 | 57 | 59 |
| AdapKpnISacII1 | GAGAGACCGCGGGTAC | 16 | 69 | 57 |
| AdapKpnISacII2 | CATGCTCTCTGGCGCC | 16 | 69 | 57 |
| AdapSpe-AclI | CTAGTAACGTTGAGAGA | 17 | 41 | 48 |
| AdapSpe-AclI | CTAGTCTCTCAACGTTA | 17 | 41 | 48 |
| CrimR+AscISalI | TCTCGTCGACAGGCGCGCCTGAGTTTGGACAAACCACA AC | 40 | 60 | 55 |
| CrimsonF | TAGCGCTACCGGACTCAGAT | 20 | 60 | 55 |
| EGFPSV40fw+RE | GAGAGAATTCACATGGTCCTGCTGGAGTTC | 30 | 50 | 60 |
| EGFPSV40Rv | GAGAACTAGTTGAGTTTGGACAAACCACAAC | 31 | 42 | 59 |
| EzrE1F | ATACTCGGGACTGCGGAGCG | 20 | 65 | 58 |
| EzrE2R | CACCCGGACGTTGATTGGCTT | 21 | 57 | 58 |
| Hprt-F | AGCTACTGTAATGATCAGTCAACG | 24 | 42 | 58 |
| Hprt-R | AGAGGTCCTTTTCACCAGCA | 20 | 50 | 58 |
| Lgr5-F | GAGTCAACCCAAGCCTTAGTATCC | 24 | 50 | 58 |
| Lgr5-R | CATGGGACAAATGCAACTGAAG | 22 | 45 | 58 |
| LoxP-Fw | ATAACTTCGTATAATGTATGCT | 22 | 27 | 51 |
| LoxP-Rv | ATAACTTCGTATAGCATACATT | 22 | 27 | 51 |
| M13-20Rv+RE | GAGAGTCGACAACACTGGCCGTCGTTTTAC | 30 | 38 | 60 |
| M2-P2regio5'-2 | TCGAGGCAGAAATACCAACC | 20 | 50 | 60 |
| M2-P2regio5'-3 | TTGTTCCGAAGCTGGAATCT | 20 | 45 | 60 |

| Primer name | SEQUENCE (5'→3') | Length | GC% | $T_M$ (°C) |
|---|---|---|---|---|
| M2-P2region3'-2 | GCTCGTCACAGAACTCTGCTT | 21 | 52 | 60 |
| MaxE1/2F | ACATCGAGGTGGAGAGCGACGC | 22 | 64 | 61 |
| MaxE2F | AGCGGGCTCACCATAATGCACT | 22 | 55 | 59 |
| MaxE3R | TGTCTAGGATTTGGGCCCGGG | 21 | 62 | 58 |
| mChEGFPfwNLS | GAGAATGGGTGCTCCTCCAAAAAAGAAGAGAAACGTAG CTCCAGTGAGCAAGGGCGAGGAG | 61 | 53 | 62 |
| mCherryRv+RE | GAGAGTCGACATTAATTCACCGTCATCACCGAAAC | 35 | 46 | 62 |
| mChNLSendF | ATGGGTGCTCCTCCAAAAAAG | 21 | 48 | 58 |
| MDM2_P2region_3' | CTGGGCCCTGATGTCATTCT | 20 | 55 | 59 |
| MDM2_P2region_5' | TAGACACAGACATGTTGGTATTG | 23 | 39 | 57 |
| mdm2-1kbF | TGGGCCCTCAAGATGACTAA | 20 | 50 | 61 |
| Mdm2-5upF1+SalI | GAGAGTCGACGTGGCGTGAGTGACTGAAAA | 30 | 53 | 60 |
| Mdm2-5upR1+XhoI | GAGACTCGAGGGTTGTGTTTACCGCTCGAA | 30 | 53 | 61 |
| Mdm2E1F1+SmaI | GAGACCCGGGGGCGCTCGTCACAGAACT | 28 | 67 | 60 |
| Mdm2E3F+HindIII | GAGA**AAGCTT**TGCAAGCACCTCACAGATTC | 30 | 47 | 60 |
| Mdm2In1F1 | AGTCCCGATCATTCCCTCTT | 20 | 50 | 60 |
| Mdm2In1R1 | AAGAGGGAATGATCGGGACT | 20 | 50 | 60 |
| Mdm2In1R1+NotI | GAGAGCGGCCGCAAGAGGGAATGATCGGGACT | 32 | 63 | 61 |
| Mdm2In1R2 | GCCCGGGTTACGAGTAGG | 18 | 67 | 60 |
| Mdm2In3F1.6kb | TGGAGAGATGGCTCAGAGGT | 20 | 55 | 60 |
| Mdm2In3F1+SmaI | GAGA**CCCGGG**TTGTGAGGATTTTAGTTATGAGAGG | 35 | 49 | 58 |
| Mdm2In3F1kb | GCCCCATTGAAGGTATCAAA | 20 | 45 | 60 |
| Mdm2In3F2.4kb | TCCACAGAAGTGGTGGTCTG | 20 | 55 | 60 |
| Mdm2In3F3.7kb | AGCTGAGGGCTGTGATTGTA | 20 | 50 | 59 |
| Mdm2In3F3kb | CTGGGCTCACTAGCTGCTTT | 20 | 55 | 60 |
| Mdm2In3R1+HindIII | GAGA**AAGCTT**AAAGCACGGATGCTTCTATGA | 31 | 42 | 60 |
| Mdm2In3R2 | GAGGGCTGGCAATATTCGT | 19 | 40 | 60 |

| Primer name | SEQUENCE (5'→3') | Length | GC% | $T_M$ (°C) |
|---|---|---|---|---|
| Mdm2In3R2+NotI | GAGA**GCGGCCGC**TGCTGAGCAGAGTGAGCAGT | 32 | 66 | 60 |
| Mdm2In4F | CAGAACTGAGGGGTGGAGAG | 20 | 60 | 60 |
| Mdm2In4F775bp | GCCGATTTCTGAGTTCAAGG | 20 | 50 | 60 |
| Mdm2PROBE-F1 | **CAAGTTCTTGTGGCAGGTTAGGGGC** | 25 | 56 | 60 |
| Mdm2PROBE-R2 | AACTCCCCGCAGAGAGCAGGAG | 22 | 64 | 60 |
| Mdm2R-2.5kb | CATTGGGGTGGGGATGGGGGA | 21 | 67 | 60 |
| Mdm2SexA1R | TGCGATAATCCAGGTTTCAA | 20 | 40 | 60 |
| Mdm2SfiIF | GCTCGTCACAGAACTCTGCTT | 21 | 52 | 61 |
| mdm2up-1.7bkF | ATCCCATGAAACTGCACACA | 20 | 45 | 60 |
| mdm2up-4kbF | GTCCTTCCCCTAGCTCATCC | 20 | 60 | 60 |
| Mdm2-up-F2 | TGCTCATGGAGACCAGAAGA | 20 | 50 | 60 |
| Mdm2upF-2.4kb | ACCCAGTTTGTGGCTTTCAC | 20 | 50 | 60 |
| Mdm2upF-3.2kb | ATGCCCTCTTCTGGTGTGTC | 20 | 55 | 60 |
| Mdm2upR-1kb | GGCCTAGTCCCCTTAACTGC | 20 | 60 | 60 |
| p21Ex2LA-Rv | CATGGTGCCTGTGGCTGAAA | 20 | 55 | 60 |
| p21Ex2LA-Rv+NLS | GAGATGGAGCTACGTTTCTCTTCTTTTTTGGAGGAGCA CCCATGGTGCCTGTGGCTGAAA | 60 | 50 | 60 |
| p21Ex3RA2-Fw | ATCCCGACTCTTGACATTGC | 20 | 50 | 57 |
| p21Ex3Rv | CTTAGCCCCCAAGACACCAT | 20 | 55 | 61 |
| p21In1+1kb | ACACCCAGTGTAGGAAGGTG | 20 | 55 | 57 |
| p21In1+1kbR | CACCTTCCTACACTGGGTGT | 20 | 55 | 57 |
| p21In1+2kb | TGTCTTCCCTTCCTTCCTCT | 20 | 50 | 58 |
| p21In1+2kbR | AGAGGAAGGAAGGGAAGACA | 20 | 50 | 58 |
| p21In1+3kb | TAGCCAAGGTAGACCCTGAA | 20 | 50 | 57 |
| p21In1+3kbR | TTCAGGGTCTACCTTGGCTA | 20 | 50 | 57 |
| p21In1+4kb | ATCACCAAGACAGCAGGGTA | 20 | 50 | 58 |
| p21In1+4kbR | TACCCTGCTGTCTTGGTGAT | 20 | 50 | 58 |

| Primer name | SEQUENCE (5'→3') | Length | GC% | $T_M$ (°C) |
|---|---|---|---|---|
| p21In1Fw1 | TCAAATAGGGAGCCCAGAGA | 20 | 50 | 60 |
| p21In1Fw2 | GTATGCTGCCACAACCACAC | 20 | 55 | 60 |
| p21In1LA-Fw | GAAGGCTTCGTTTGTTGGAG | 20 | 50 | 57 |
| p21In1LA-Fw+RE | GAGAGGCCGGCCTTAATTAAGAAGGCTTCGTTTGTTGGAG | 40 | 50 | 57 |
| p21In1mutkb | CCTGGGAGAGAGCCTTAACC | 20 | 60 | 61 |
| p21LF-300 | TAGTCCTTCCCACAGTTGGT | 20 | 50 | 57 |
| p21NLSendR | TGGAGCTACGTTTCTCTTCTTT | 22 | 41 | 57 |
| p21PROBE-F1 | AGCAGAGCTGTGGGAAGCCTGT | 22 | 59 | 60 |
| p21PROBE-R2 | CTTGTACGACAGGCAGGGAGCAT | 23 | 56 | 59 |
| p21RA10KbRv | CAGTAGGGCACAAGGGGTAA | 20 | 55 | 60 |
| p21RA12kbF | CGGGGACCAACTGTGTTAAG | 20 | 55 | 60 |
| p21RA12kbR | CCAGTTGCCAGTTCCAAAAT | 20 | 45 | 60 |
| p21RA2-Rv | CCATCGCTGAGAGAGTTCTACA | 22 | 50 | 60 |
| p21RABsrGIF | GTGATGGAGTTGTACAAT | 18 | 39 | 45 |
| p21RABsrGIR | CACTGAGAATTGTACAAC | 18 | 39 | 43 |
| P2mutant3-44 | GaTgGACAGCCGACGCCGGAgGTcTCCCAAgTTGACCAGCCCCAC | 45 | 67 | > 75 |
| P2mutant5-50 | TCCGGCGTCGGCTGTCcAtGGAGCTAAaTCCTGAtATGTCTCCAGCTGGG | 50 | 58 | > 75 |
| P2PROBE-F1 | ATCCTGATATGTCTCCAGCTGGGG | 24 | 54 | 57 |
| P2PROBE-R2 | CTGCGTCAGGGGAAGGGCTG | 20 | 70 | 59 |
| pACN1552F | ATGCATAAGGCAGGCAAGAT | 20 | 45 | 60 |
| pACN2273F | CCCGGCAAAACAGGTAGTTA | 20 | 50 | 60 |
| pACN2978F | CGGTCAGTAAATTGGACACCT | 21 | 48 | 59 |
| pACN770F | TCGTCCTGCAGTTCATTCAG | 20 | 50 | 60 |
| pACNFwAscI | GAGAGGCGCGCCTCACTATAGGGCGAATTGGAG | 33 | 61 | 59 |

| Primer name | SEQUENCE (5'→3') | Length | GC% | $T_M$ (°C) |
|---|---|---|---|---|
| pACNFwAseI | GAGAATTAATTCACTATAGGGCGAATTGGAG | 31 | 39 | 59 |
| pACNRv | TAGATCTCGAGCTCGCGAAA | 20 | 50 | 57 |
| pGT01xrRv1 | TCTAGGACAAGAGGGCGAGA | 20 | 55 | 60 |
| pGT01xrRv2 | CCTGGCCTCCAGACAAGTAG | 20 | 60 | 60 |
| pKO5527Fw+RE | GAGAGGCCGGCCTTAATTAATTTTTGTGATGCTCGTCA GG | 40 | 61 | 60 |
| PolyAF | CCCCCTGAACCTGAAACATA | 20 | 50 | 60 |
| pRAYCreF1 | AAGCTGAGCGGCAATAAAAA | 20 | 40 | 60 |
| pRAYcreF2 | AACGAAGGAAGGAGCACAGA | 20 | 50 | 60 |
| pRAYCreF3 | CGTACTGACGGTGGGAGAAT | 20 | 55 | 60 |
| pRAYCreR1 | GGGGTTTGCTCGACATTG | 18 | 55 | 60 |
| pRAYCreR3 | CCCAGCCTGCTTTTCTGTAA | 20 | 50 | 60 |
| pRAYneoF1 | AGACAATCGGCTGCTCTGAT | 20 | 50 | 60 |
| pRAYURA3F1 | GATGACAAGGGAGACGCATT | 20 | 50 | 60 |
| Primer 1 | AACTTAATGTCCTTGCTCATTAC | 23 | 35 | 55 |
| Primer 2 | TCAGTTCTGCTCACCTCTTTC | 21 | 48 | 58 |
| Primer 3 | CAATACCAACATGTCTGTGTCTA | 23 | 39 | 57 |
| Primer 4 | TTACTCCACAGAGCAGTAACC | 21 | 48 | 58 |
| Primer 5 | GTACCTTTGTATACACGGTAAAC | 23 | 39 | 57 |
| Primer 6 | GGAGAGATGGCTCAGCAATAA | 21 | 48 | 58 |
| Primer1F | GTAATGAGCAAGGACATTAAGTT | 21 | 48 | 60 |
| Puma-0.6kbR | AGGGACACACACTCCAATCC | 20 | 55 | 60 |
| Puma-1.6kbR | TCTCCAAGCCCATTTTTGAG | 20 | 45 | 60 |
| Puma129F1 | CTTTTGGGATGGGATGTCAC | 20 | 50 | 57 |
| PumaATGLARv | CATGGCGCTCCCTGGAGC | 18 | 72 | 63 |
| PumaEx1F | GTGATCCGGACACGAAGACT | 20 | 55 | 60 |
| PumaEx1LARv1n | GCAAAGGCTGCAGGATACAG | 20 | 55 | 60 |

| Primer name | SEQUENCE (5'→3') | Length | GC% | $T_M$ (°C) |
|---|---|---|---|---|
| PumaEx1R | AGTCTTCGTGTCCGGATCAC | 20 | 55 | 60 |
| PumaEx4-1F | CCAGAAATGGAGCCCAACTA | 20 | 50 | 60 |
| PumaEx4-2F | TGTGACCACTGGCATTCATT | 20 | 45 | 60 |
| PumaIn1F.3 | GCTAGTGAGACCTGGGAGGA | 20 | 60 | 59 |
| PumaIn1F.6 | GTTTGGCTCCCGAGTTTGTA | 20 | 50 | 60 |
| PumaIn1F1.2 | CCAGGCTATGTGTCATGTGG | 20 | 55 | 60 |
| PumaIn1F1.6 | TTGAGATGATGGTGGTGCAT | 20 | 45 | 60 |
| PumaIn1F2.5 | TCTGCGCTCTTCTCTGTTGA | 20 | 45 | 60 |
| PumaIn1R.3 | TCCTCCCAGGTCTCACTAGC | 20 | 60 | 59 |
| PumaIn1R.6 | TACAAACTCGGGAGCCAAAC | 20 | 50 | 60 |
| PumaIn1R1.2 | CCACATGACACATAGCCTGG | 20 | 55 | 60 |
| PumaIn1R2.5 | TCAACAGAGAAGAGCGCAGA | 20 | 50 | 60 |
| PumaIn3-1R | CCAACCAAACAAAAGGCTGT | 20 | 45 | 60 |
| PumaIn3-2F | TTAACGGCTGAGCCATCTCT | 20 | 50 | 60 |
| PumaIn3-3F | GGGCTAGTTCTGGGCATGTA | 20 | 55 | 60 |
| PumaIn3-4F | CTCTACCACCAGGGATCGAA | 20 | 55 | 60 |
| PumaIn3Fw+Neo | GAGATTTCGCGAGCTCGAGATCTATCCTCCATCTCCTT CATTGG | 44 | 50 | 57 |
| PumaIn3RAFw | TCCTCCATCTCCTTCATTGG | 20 | 50 | 57 |
| PumaLAFw1n | CTGCTGGGATTTTGTCAGGT | 20 | 50 | 57 |
| PumaLAFw2n | GCTGAATGCTCCAAGGTCTC | 20 | 55 | 60 |
| PumaRARv | CCAGAAGAGGGCATTGGATA | 20 | 50 | 57 |
| PumaRARv+RE | GAGAGTCGACCCAGAAGAGGGCATTGGATA | 30 | 53 | 57 |
| TACE-RV | ACAGCACCATTGTCCACTTG | 20 | 50 | 60 |
| TK+700bp | TACCCGAGCCGATGACTTAC | 20 | 55 | 60 |
| TK1900F | TTTATGGTTCGTGGGGGTTA | 20 | 45 | 60 |
| TK525F | CGATACCTTATGGGCAGCAT | 20 | 50 | 60 |

| Primer name | SEQUENCE (5'→3') | Length | GC% | $T_M$ (°C) |
|---|---|---|---|---|
| TKpolyAF | CTGGCACTCTGTCGATACCC | 20 | 60 | 61 |
| Villin2F | GTTTAAATTCCGGGCCAAGT | 20 | 45 | 60 |
| Villin2R | ACCCAGACTTGTGCATTTCC | 20 | 50 | 60 |

# APPENDIX B POLYMERASE CHAIN REACTIONS

***Table B.1: Polymerase chain reactions optimised and performed in this thesis***

| Forward primers(s) | Reverse primer(s) | Product size | Polymerase | Annealing temp (°C) | Extension time | Number of cycles | Additional requirements or comments | Described in Section |
|---|---|---|---|---|---|---|---|---|
| p21LF-300<br>p21In1+1kb<br>p21In1+2kb<br>p21In1+3kb<br>p21In1+4kb | 1stPCR | Unknown<br>>1919 bp | Phusion | 56 | 45 s | 30 | Screen for insertion of genetrap vector pGT01xr into p21 | 3.2.1.2.1 |
| 2ndPCR | p21In1+1kbR<br>p21In1+2kbR<br>p21In1+3kbR<br>p21In1+4kbR | Unknown<br>>151 bp | Phusion | 56 | 45 s | 30 | 2ndPCR and p21In1+4kbR produced ~ 200 bp product | 3.2.1.2.1 |

| Forward primers(s) | Reverse primer(s) | Product size | Polymerase | Annealing temp (°C) | Extension time | Number of cycles | Additional requirements or comments | Described in Section |
|---|---|---|---|---|---|---|---|---|
| p21In1Fw1<br>p21In1Fw1<br>p21In1Fw2<br>p21In1Fw2 | pGT01xrRv2<br>pGT01xrRv1<br>pGT01xrRv2<br>pGT01xrRv1 | 644 bp<br>872 bp<br>516 bp<br>744 bp | Phusion | 51 | 45 s | 30 | 5' integration site, these reactions were sent for sequencing | 3.2.1.2.1 |
| pKO5527Fw+RE | M13-20Rv+RE | 2.1 kb | Phusion | 60 | 50 s | 10 | Cloning TK cassette | 3.3.3.2 |
| p21In1LAfw | p21Ex2LARv | 4331 bp | Phusion | 60 | 1 m 55 s | 25 | Cloning *p21* left arm | 3.3.3.3 |
| p21In1LAfw+RE | p21Ex2LARv+NLS | 4381 bp | Phusion | 60 | 1 m 55 s | 25 | Cloning *p21* left arm + 5'FseI-PacI & 3'NLS | 3.3.3.3 |
| EGFPSV40fw+RE | EGFPSV40Rv | 299 bp | Phusion | 50 | 15 s | 15 | Cloning poly A signal | 3.3.3.4 |
| mChEGFPfwNLS | mCherryRv+RE | 1131 bp | Phusion | 50 | 15 s | 15 | Cloning *mCherry* + 5'NLS & 3'AseI-SalI sites | 3.3.3.4 |
| p21In1LA-Fw+RE | p21NLSendR | 4381 bp | Phusion | 60 | 1 m 55 s | 25 | 1st round fusion PCR *p21* left arm | 3.3.3.5 |
| mChNLSendF | mCherryRv+RE | 1131 bp | Phusion | 50 | 15 s | 15 | 1st round fusion PCR *mChery* | 3.3.3.5 |

| Forward primers(s) | Reverse primer(s) | Product size | Polymerase | Annealing temp (°C) | Extension time | Number of cycles | Additional requirements or comments | Described in Section |
|---|---|---|---|---|---|---|---|---|
| p21In1LA-Fw+RE | mCherryRv+RE | 5.5 kb | Phusion | 60 | 2 m 40 s | 25 | Final round fusion PCR *p21* left arm-NLS-*mCherry* | 3.3.3.5 |
| pACNFwAseI | pACNRv | 3.8 kb | Phusion | 60 | 1 m 30 s | 20 | Cloning Cre/Neo$^{R}$ – *p21* | 3.3.3.6 |
| pACNFwAscI | pACNRv | 3.8 kb | Phusion | 60 | 1 m 30 s | 20 | Cloning Cre/Neo$^{R}$ – *Puma* | 3.3.3.6 |
| p21Ex3RA2-Fw | p21Ex3Rv | 600 bp | Phusion | 50 | 30 s | 30 | Test *p21* right arm PCR | 3.3.3.7 |
| p21Ex3RA2-Fw | p21RA2-Rv | 4 kb | Phusion | 50-60 | 2 m | 30 | Attempted to PCR for *p21* right arm – failed. | 3.3.3.7 |
| p21Ex3RA2-Fw | p21RA10KbRv | 10 kb | Phusion | 50-60 | 5 m | 30 | | 3.3.3.7 |
| PumaLAFw1n<br>PumaLAFw1n<br>PumaLAFw2n<br>PumaLAFw2n | PumaEx1LARv1n<br>PumaATGLARv<br>PumaEx1LARv1n<br>PumaATGLARv | 4899 bp<br>4782 bp<br>4609 bp<br>4492 bp | Phusion | 50-60 | 1 m 55s | 30 | Attempted long range PCR for *Puma* left arm – failed. | 3.3.4.1 |
| PumaLAFw1n | Puma-1.6kbR | 629 bp | Phusion | 50-65 | 15 s | 30 | *Puma* left arm – failed. | 3.3.4.1 |
| PumaLAFw2n | Puma-1.6kbR | 339 bp | Taq | 56 | 1 m | 30 | Manual hot-start | 3.3.4.1 |
| PumaLAFw2n | PumaEx1R | 2063 bp | Phusion | 62 | 1 m 30 s | 30 | *Puma* left arm "A" | 3.3.4.1 |

| Forward primers(s) | Reverse primer(s) | Product size | Polymerase | Annealing temp (°C) | Extension time | Number of cycles | Additional requirements or comments | Described in Section |
|---|---|---|---|---|---|---|---|---|
| PumaEx1F | PumaEx1LARv1n<br>PumaIn1R2.5<br>PumaIn1R1.2 | 2645 bp<br>2203 bp<br>1445 | Phusion | 50-60 | 2 m | 30 | *Puma* left arm – failed. | 3.3.4.1 |
| PumaIn1F1.2<br>PumaIn1F1.6 | PumaIn1R2.5<br>PumaEx1LARv1n | 759 bp<br>787 bp | Taq | 56 | 1 m | 30 | Test *Puma* left arm. | 3.3.4.1 |
| PumaEx1F | PumaIn1R.6 | 798 bp | Phusion | 50-60 | 15 s | 30 | *Puma* left arm – failed. | 3.3.4.1 |
| PumaEx1F | PumaIn1R.3 | 446 bp | Phusion | 60 | 15 s | 15 | *Puma* left arm "B" Hot-start | 3.3.4.1 |
| PumaIn1F.3 | PumaIn1R.6 | 355 bp | Phusion | 60 | 15 s | 30 | *Puma* left arm "C" Hot-start, GC-rich buffer + 3% DMSO | 3.3.4.1 |
| PumaIn1F.6 | PumaIn1R1.2 | 676 bp | Phusion | 60 | 30 s | 15 | *Puma* left arm "D" Hot-start | 3.3.4.1 |
| PumaIn1F1.2 | PumaEx1LARv1n | 1132 bp | Phusion | 60 | 1 m 10 s | 15 | *Puma* left arm "E" Hot-start | 3.3.4.1 |

| Forward primers(s) | Reverse primer(s) | Product size | Polymerase | Annealing temp (°C) | Extension time | Number of cycles | Additional requirements or comments | Described in Section |
|---|---|---|---|---|---|---|---|---|
| PumaEx1F | PumaIn1R.6 | 798 bp | Phusion | 60 | 30 s | 20 | *Puma* left arm fusion PCR (B+C) "F" Hot-start, GC-rich buffer + 3% DMSO | 3.3.4.1 |
| PumaIn1F.6 | PumaEx1LARv1n | 1808 bp | Phusion | 60 | 1 m 30 s | 25 | *Puma* left arm fusion PCR (D+E) "H" Hot-start | 3.3.4.1 |
| PumaLAFw2n | PumaIn1R.6 | 2841 bp | Phusion | 60 | 1 m 30 s | 15 | *Puma* left arm fusion PCR (A+F) "G" Hot-start, GC-rich buffer + 3% DMSO | 3.3.4.1 |
| PumaLAFw2n | PumaEx1LARv1n | 4592 bp | Phusion | 60 | 2 m 20 s | 20 | *Puma* left arm fusion PCR (G+H) "I" Hot-start, GC-rich buffer + 3% DMSO | 3.3.4.1 |
| CrimsonF | CrimR+AsclSalI | 1012 bp | Phusion | 60 | 30 s | 15 | Cloning E2Crimson + 3'AscI-SalI sites. | 3.3.4.2 |
| PumaIn3RAFw | PumaRARv | 4547 bp | Phusion | 60 | 1 m 55 s | 30 | Cloning *Puma* right arm | 3.3.4.4 |

| Forward primers(s) | Reverse primer(s) | Product size | Polymerase | Annealing temp (°C) | Extension time | Number of cycles | Additional requirements or comments | Described in Section |
|---|---|---|---|---|---|---|---|---|
| PumaIn3Fw+Neo | PumaRARv+RE | 4573 bp | Phusion | 60 | 1 m 55 s | 30 | Cloning *Puma* right arm + 5'(20 bp Cre/Neo$^{R}$) & 3'SalI | 3.3.4.4 |
| Lgr5-F | Lgr5-R | 131 bp | Phusion | 64 | 30 s | 30 | Cloning the QRTPCR Lgr5 plasmid. | C.1 |
| Hprt-F | Hprt-R | 200 bp | Phusion | 60 | 30 s | 30 | Cloning the QRTPCR Hprt1 plasmid. | C.1 |
| Villin2F EzrE1F | Villin2R EzrE2R | 206 bp 164 bp | Phusion | 50-64 | 30 s | 30 | Attempted to clone Villin2 as QRTPCR plasmid, failed. | C.1 |
| MaxE1/2F | MaxE3R | 153/186 bp | Phusion | 60 | 30 s | 30 | Attempted to clone Max as QRTPCR plasmid – however two splice variants! | C.1 |

| Forward primers(s) | Reverse primer(s) | Product size | Polymerase | Annealing temp (°C) | Extension time | Number of cycles | Additional requirements or comments | Described in Section |
|---|---|---|---|---|---|---|---|---|
| MaxE2F | MaxE3R | 126 bp | Phusion | 70 | 30 s | 30 | Cloning the QRTPCR Max plasmid. | C.1 |
| Mdm2SfilF | P2mutant3-44 | 642 bp | Phusion | 55 | 15 s | 15 | 1st round fusion PCR P2-Mutant "A" | 3.3.5.4 |
| P2mutant5-50 | Mdm2SexA1R | 477 bp | Phusion | 55 | 15 s | 15 | 1st round fusion PCR P2-Mutant "B" | 3.3.5.4 |
| Mdm2SfilF | Mdm2SexA1R | 1119 bp | Phusion | 55 | 30 s | 25 | Final round fusion PCR P2-Mutant "C" | 3.3.5.4 |
| Mdm2-5upF1+SalI | Mdm2-5upR1+XhoI | 345 bp | Phusion | 55 | 15 s | 15 | Cloning the P1 5' RA | 3.3.5.5 |
| Mdm2E1F1+SmaI | Mdm2In1R1+NotI | 299 bp | Phusion | 55 | 15 s | 15 | Cloning the P1 3' RA | 3.3.5.5 |
| Mdm2E3F+HindIII | Mdm2In3R1+HindIII | 333 bp | Phusion | 55 | 15 s | 15 | Cloning the P2 5' RA | 3.3.5.5 |
| Mdm2In3F1+SmaI | Mdm2In3R2+NotI | 365 bp | Phusion | 55 | 15 s | 15 | Cloning the P2 3' RA | 3.3.5.5 |
| Mdm2E3F+HindIII<br>Mdm2In3R1+HindIII<br>Mdm2E3F+HindIII | LoxP-Rv<br>LoxP-Rv<br>Mdm2In3R1+HindIII | 415<br>-<br>333 | Phusion | 55 | 30 s | 30 | PCR screen for the orientation of "P2 5' RA" in pRAYCre. | 3.3.5.5 |

| Forward primers(s) | Reverse primer(s) | Product size | Polymerase | Annealing temp (°C) | Extension time | Number of cycles | Additional requirements or comments | Described in Section |
|---|---|---|---|---|---|---|---|---|
| Mdm2-5upF1+SalI<br>Primer3<br>Mdm2-up-F2<br>pRAYCreF1<br>Primer3<br>pRAYCreF1 | Mdm2In1R1+NotI<br>Primer4<br>pRAYCreR1<br>Mdm2In1R2<br>pRAYCreR1<br>Mdm2In3R2 | 751 bp<br>873 bp<br>676 bp<br>481 bp<br>644 bp<br>631 bp | Phusion | 60 | 30 s | 30 | P1 integration control<br>P2 integration control<br>P1 5' check<br>P1 3' check<br>P2 5' check<br>P2 3' check | 3.3.5.6 |
| Mdm2-5upF1+SalI<br>LoxP-Fw | LoxP-Rv<br>Mdm2In3R2+NotI | 427 bp<br>333 bp | Phusion | 55 | 15 s | 15 | 1st round fusion PCR for P1-Null promoter region | C.4 |
| Mdm2-5upF1+SalI | Mdm2In3R2+NotI | 726 | Phusion | 55 | 30 s | 20 | 2nd round fusion PCR for P1-Null promoter region | C.4 |
| Mdm2-5upF1+SalI<br>Mdm2In1F1 | Mdm2In1R1<br>Mdm2SexA1R | 720 bp<br>913 bp | Phusion | 60 | 30 s | 20 | 3rd round fusion PCR for "Whole P1-Null promoter" | C.4 |
| Mdm2-5upF1+SalI | Mdm2SexA1R | 1613 bp | Phusion | 60 | 1 m 10 s | 15 | Final round fusion PCR for "Whole P1-Null promoter" | C.4 |

| Forward primers(s) | Reverse primer(s) | Product size | Polymerase | Annealing temp (°C) | Extension time | Number of cycles | Additional requirements or comments | Described in Section |
|---|---|---|---|---|---|---|---|---|
| Mdm2-5upF1+SalI | Mdm2SexA1R | 1630 bp | Phusion | 55 | 1 m 10 s | 25 | Cloning WT and P2-Mutant promoter regions | C.4 |
| p21PROBE-F1 | p21PROBE-R2 | 790 bp | Phusion | 60 | 30 s | 15 | *p21* EcoNI Southern probe | C.5 |
| Mdm2PROBE-F1 | Mdm2PROBE-R2 | 378 bp | Phusion | 60 | 30 s | 15 | *Mdm2* AhdI Southern probe | C.5 |
| P2PROBE-F1 | P2PROBE-R1 | 571 bp | Phusion | 60 | 30 s | 15 | *Mdm2* P2-mutant NcoI Southern probe | C.5 |

# APPENDIX C ADDITIONAL CLONING

## *C.1 QRTPCR control plasmids*

This section describes the cloning of the control plasmids used in the QRTPCR reactions. Control plasmids contained a short (100-200 bp) PCR product derived from a cDNA of the genes of interest; *Hprt1, Lgr5* and *Max*. These products were amplified by PCR using the indicated primer pairs and whole gut cDNA as the template. The resulting PCR products were then TA-cloned into pCR2.1 and positive clones were identified by restriction digestion with EcoRI. Once the DNA sequence was confirmed these plasmids were ready for use.

***Table C.1: Summary of QRTPCR validation genes.***

| Gene | Purpose in assay | Forward primer | Reverse primer | Product size |
|---|---|---|---|---|
| *Hprt1* | House-Keeping | Hprt-F | Hprt-R | 200 bp |
| *Lgr5* | Stem cell marker | Lgr5-F | Lgr5-R | 131 bp |
| *Max* | Villus-specific | MaxE2F | MaxE3R | 126 bp |

Prior to selecting *Max* as the villus-specific gene we had initially attempted to amplify regions from *Villin2* (also known as *Ezr*). This was unsuccessful since the first product tested (using primer pair Villin2F & Villin2R ~ 206 bp) was contaminated with non-specific products. The second product (using primer pair EzrE1F & EzrE2R ~ 164 bp – these primers were designed using primerBLAST – which also scans the genomic/transcript databases for specificity) was not amplified successfully. The lack of product may be due to the fact that the second set of primers annealed ~ 3 kb from the 3' end of the Villin2 mRNA/cDNA and hence maybe the cDNA synthesis reaction had not progressed to that point. Since all specific Villin2 primers identified were localised to the 5' end of the gene it was decided to select another villus-specific gene for analysis. *Max* was chosen since it had been previously identified by another RNA expression array and had been shown to be up-regulated on the villus [Mariadason et al., 2005]. There was however one further delay in the cloning of this vector,

which was that the original primer pair for *Max* (MaxE1/2F & MaxE3R) unfortunately, did not take into account the two splice variants of *Max* and hence two different sized DNA fragments appeared when the PCR reaction was analysed by agarose gel electrophoresis. New primers were designed which were not affected by the mRNA variants.

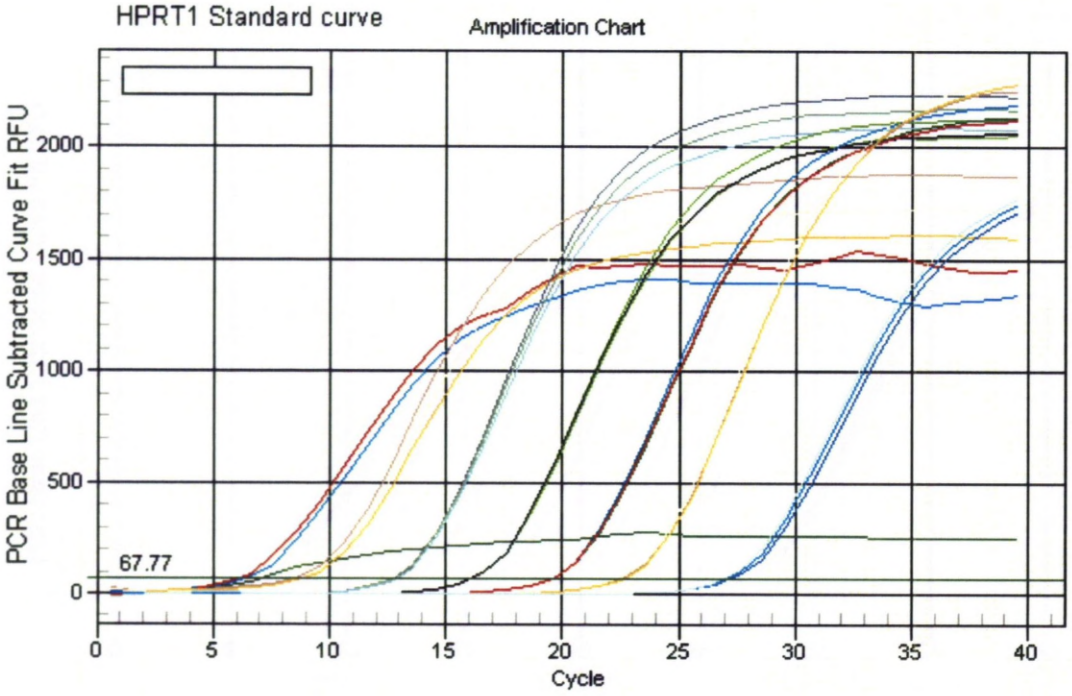


***Figure C.1: Hprt1 Standard curve.***

*Serial dilutions are spaced evenly apart, demonstrating that the technique worked in principle. The uneven lines towards the top of the chart indicate where the reaction was in plateaux phase.*

## C.2 p21 right arm of homology

This section describes the failed cloning attempts during the generation of the p21 right arm of homology.

***Table C.2: Unsuccessful cloning attempts of the p21 right arm of homology.***

| Attempt | Description | Result |
|---|---|---|
| 1st | Following digestion of BAC 262p22 clone DNA (10 µg) the EcoRV-HindIII fragment was gel purified by GENECLEAN, A-tailed and cloned into pCR-XL-TOPO. | 5 colonies – random digest pattern |
| 2nd | Following digestion of BAC clone DNA (10 µg) the EcoRV-HindII fragment was gel purified by GENECLEAN and cloned into SmaI & HindIII sites of pBluescript II SK+. | 10 colonies – random digest pattern |
| 3rd | As above except 30 µg of DNA digested and attempted to gel purify by phenol-chloroform extraction. | DNA extraction failed. |
| 4th | As above except 10 µg of DNA digested and attempted gel purified by using the genomic sized fragment protocol of the GENECLEAN kit. | No DNA after clean up. Column became blocked with cooling gel. |
| 5th | As with 2nd attempt except used the other BAC clone bmQ448e21. | BAC digest pattern did not match up! |
| 6th | As with 1st attempt except scaled up to 30 µg of DNA. | No colonies. |
| 7th | As with 2nd attempt except scaled up to 30 µg of DNA. | 12 colonies – random digest pattern. |

## *C.3 Final assembly of p21-mCherry*

This section provides a more detailed account of the final stage of cloning the *p21*-mCherry DNA targeting construct. Table C.3 summarises the various attempts made to create the ultimate p21-mCherry DNA targeting vector. Eight attempts (a-h) were made in total and several issues had to be resolved in order to complete the cloning exercise. The first issue, which accounted for two of the failed attempts (a & c) was the apparent reformation of the TK2 plasmid DNA in recombinant clones. It was not obvious how contamination with TK2 plasmid had occurred although one possible explanation might be that the pCR2.1 backbone fragment was accidentally transferred during excision of the insert fragment (TK cassette) from the agarose gel. With the backbone fragment contaminating the ligation reaction this would lead to religation of the TK2 vector and hence the resulting bacterial clones would preferentially propagate this smaller plasmid (rather than the large DNA targeting vector). This TK2 contamination problem was easily resolved; digested TK2 DNA fragments were simply separated for longer during electrophoresis and extra care was taken when excising the desired DNA fragments from gels.

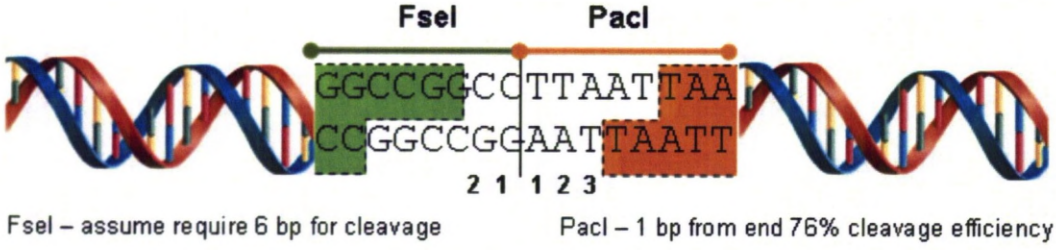


***Figure C.2: FseI and PacI restriction sites in Vector 4.***

The second problem, which accounted for another two failed cloning attempts (b & d) was incomplete double digest with restriction enzymes FseI and PacI. An incomplete digest of the parental vector meant that the desired ligation reaction could not occur and hence any rare resulting plasmids would contain random recombination (as observed in attempts b & d). Double digest with FseI and PacI was a problem in Vector 4 since these restriction sites were side by side (see Figure C.2). As a general rule, restriction enzymes typically required 6 bp of double stranded DNA from the edge of their recognition sequence in order to cleave

efficiently. Some enzymes, however (such as PacI), were more efficient at cleaving their recognition sequence and could still efficiently cut DNA with only 1 bp from the end [NEB technical reference guide]. Since PacI could still cleave 76% efficiently with only 1 bp from end, Vector 4 DNA was digested with restriction enzyme FseI first and then with PacI second. This digestion order was important because if the Vector 4 DNA was cut with PacI first, this meant FseI could not cut at all (digestion with PacI left a 3 bp margin whilst FseI required 6 bp to cleave DNA effectively). With that in mind, the cloning attempts b – d digested the backbone vector (V4) with FseI first for several hours, then fresh PacI enzyme was added (plus supplements) to the reaction to allow the second digest to occur. The second reaction with PacI was typically incubated overnight to allow complete digestion.

Despite careful planning however there were still relatively few bacterial colonies to screen using the above method and the colonies which did appear had random DNA digest patterns – which could be consistent with an incomplete double digest of parental vector (V4). Therefore to address this issue a single digest was performed on Vector 4 (using PacI), and the DNA ends were blunted to attempt unidirectional cloning (TK cassette was digested with FseI/PacI and then blunted). The resulting transformation (attempt e) produced 70+ bacterial colonies, some of which (5/72) contained evidence of the correct ligation event when screened by restriction digest with XhoI. Whilst none of the clones from this cloning attempt (e) were truly positive (for reasons discussed later), it did demonstrate that maybe the previous cloning attempts had in part failed because of inefficient double digest of the backbone vector (since the only major difference between the cloning attempts V5d and V5e was the cloning strategy: directional cloning versus unidirectional blunt ended cloning). Similar amounts of backbone and insert DNA were used in each ligation reaction and the transformation efficiencies were also similar (~1 x $10^8$ c.f.u. per µg of pUC19 DNA), however there were many more bacterial colonies using the blunt ended cloning reaction (see Table C.3). Since blunt ended cloning did not depend on double digestion of the vector backbone this may explain the increase in recombinant clones.

***Table C.3: Vector 5 (V5) final construct cloning attempts.***

| Attempt | Description | Result |
|---|---|---|
| V5a | FseI/PacI double digest in NEBuffer 4<br>50 ng of backbone to 10 ng of insert | 9 colonies<br>- TK2 vector contamination? |
| V5b | FseI digest first for several hours, then fresh PacI (+ buffers) added for digest overnight.<br>50 ng of backbone to 10 ng of insert | 1 colony<br>- Random pattern |
| V5c | As above except<br>50 ng of backbone to 250 ng of insert | 3 colonies<br>- TK2 vector contamination? |
| V5d | As above except<br>180 ng of backbone to 180 ng of insert | 4 colonies<br>- Random patterns |
| V5e | Digest with PacI only then blunt DNA ends for unidirectional cloning.<br>250 ng of backbone to 250 ng of insert | 72 colonies<br>- 5/72 had correct low molecular weight fragments but incorrect size of repetitive region |
| V5f | Digest with FseI, ethanol precipitate DNA, digest with SalI (attempt to move V4 into TK2). 50 ng backbone (TK2) to 175 ng insert | 62 colonies<br>- repetitive region was recombining |
| V5g | Digest with FseI, ethanol precipitate DNA, digest with PacI.<br>250 ng backbone to 250 ng of insert | 34 colonies<br>- repetitive region was recombining |
| V5h | As above except with re-streaked V4-3-3 DNA. *E. coli* were grown at 27°C.<br>250 ng backbone to 250 ng insert | 100 + colonies<br>3/24 appeared positive |

The next two cloning attempts (f & g – performed in parallel) therefore aimed to improve the double digest efficiency by two different methods. Attempt V5f used different restriction enzymes, FseI and SalI, which would move the main targeting construct containing 'p21 left arm-mCherry-Cre/Neo$^{R}$-p21 right arm' into the TK2 vector. It was hoped that the different enzymes would work more efficiently together. Digest was performed with FseI first

as with previous attempts (b – d) followed by an ethanol precipitation of the DNA to clean up the enzymatic reaction then the DNA was digested with SalI.

Cloning attempt V5g used the original restriction enzymes FseI and PacI however rather than just adding fresh PacI (and buffer) to the old FseI digestion reaction (in NEBuffer 4), the DNA was ethanol precipitated and a fresh reaction was set up for the second digest with PacI (in NEBuffer 1). Previously enzymatic clean up had not been performed since according the NEB technical reference guide, restriction enzymes PacI and FseI both had 100% activity in NEBuffer 4 therefore an additional clean up reaction seemed unnecessary and would result in lower DNA yields. However given the suspected problem with the double digest efficiency and that PacI was expected to cleave DNA which only had a 2 bp margin we thought using PacI's optimum buffer (NEBuffer 1) might improve the efficiency of digestion.

The unidirectional blunt ended cloning strategy was not immediately reattempted because a large number of colonies (72) had already been screened without success. Repeating the same cloning exercise therefore seemed rather futile and hence the different directional cloning strategies (f & g) detailed above were tried instead.

Both cloning attempts V5f and V5g had respectable numbers of bacterial transformants (62 and 34 respectively) indicating that the new DNA double digest methods were indeed more efficient at cleaving the backbone Vector 4. However, whilst this resolved the outstanding problem of double digest efficiency once these recombinant clones were screened (by XhoI restriction digest analysis) a separate problem was emerging. This problem was, whilst various clones contained the correct lower molecular weight fragments during XhoI restriction digest analysis, including the expected size shift (1.3 → 3.4 kb) for successful TK insertion (in e and g), the higher molecular weight fragment (~13.2 kb (e and g) or ~16.2 kb (f)) was always smaller than expected and typically appeared as multiple bands. The large molecular weight fragment contained the *p21* right arm of homology and hence it seemed likely that the repetitive region was recombining in the bacteria. This third issue accounted for three of the failed cloning attempts (e – g) and meant that due to the extreme instability of the *p21* right arm of homology within *E. coli,* varying portions of this region were lost during cloning.

The instability of this repetitive DNA region had been observed previously when the original ~10 kb EcoRV-HindIII BAC DNA digest fragment was cloned into pBluescript II SK +. This recombination problem was resolved then by using the specialised bacterial strain MAXstbl.2 to propagate the DNA. However, this time, since we were already using this strain a solution to the problem was not immediately obvious. To exacerbate the situation, when more of the penultimate Vector 4 DNA was grown and extracted from the glycerol stock, this too had the tell tale signs of recombination. Indeed only 2/10 clones picked from glycerol stock re-streak of Vector 4 appeared to keep the original size of the *p21* right arm region demonstrating once again how unstable the DNA was.

The problem with the maintenance of the unstable DNA in the *p21* right arm of homology was never completely resolved however growing the *E. coli* at 27°C (rather than 30°C as recommended by the manufacturer) helped reduce recombination enough to achieve success.

## *C.4 P1-P2 Promoter regions*

This section describes the cloning of the various *Mdm2* P1-P2 promoter regions which were used during the *in vitro* luciferase assays (see Section 3.3.5.2). These promoter regions were to contain either;

- WT (wild-type) DNA or
- P2-Mutant (containing the desired 8 point mutations) DNA or
- P1-Null (containing the DNA sequence which would remain in the genome following activation of Cre-recombinase and removal of the self-excision neomycin cassette in the first (and all subsequent) generations of *Mdm2* P1-Null transgenic mice) DNA.

The whole P1-P2 *Mdm2* promoter region (~1600 bp including 300-400 bp of upstream and downstream sequence) was cloned into pGL4.11 (a promoterless luciferase plasmid) for each promoter region. The basic method for all three luciferase plasmids was briefly; amplification of the region by PCR, TA-clone the resulting product into pCR2.1 or pCR-XL-TOPO and sequence bacterial clones which appeared positive by restriction

digestion. Once the sequence was confirmed the promoter region was then inserted in the correct orientation into pGL4.11, whereby positive clones were identified by another restriction digest.

The WT and P2-Mutant regions were cloned by performing a single PCR reaction using the primer pair Mdm2-5'upF1+SalI and Mdm2SexA1R with either the pRSMdm2TK or pRSmP2-Mutants vectors as the template DNA respectively. However, since the P1-Null region did not yet exist, in order to create the P1-Null promoter region that would appear in F1 heterozygote mice, this section of DNA was 'stitched' together from various plasmids using fusion PCR – as outlined in Figure C.3. The resulting PCR products were TA cloned into pCR-XL-TOPO and positive clones were identified by restriction digestion with EcoRV and HindIII. Once the sequence was confirmed in each clone (wholeWT-9, wholeMut-7 and wholeP1-1 – which were all conveniently in the reverse orientation within pCR-XL-TOPO) the promoter region was directionally inserted into pGL4.11 by using their common restriction sites EcoRV and HindIII. Successful insertion of the promoter region was confirmed by restriction digest with EcoRV and HindIII. These clones (WhWTluc-4, WhMUTluc-5 and WhP1Nullluc-3) then ready for the luciferase assay.

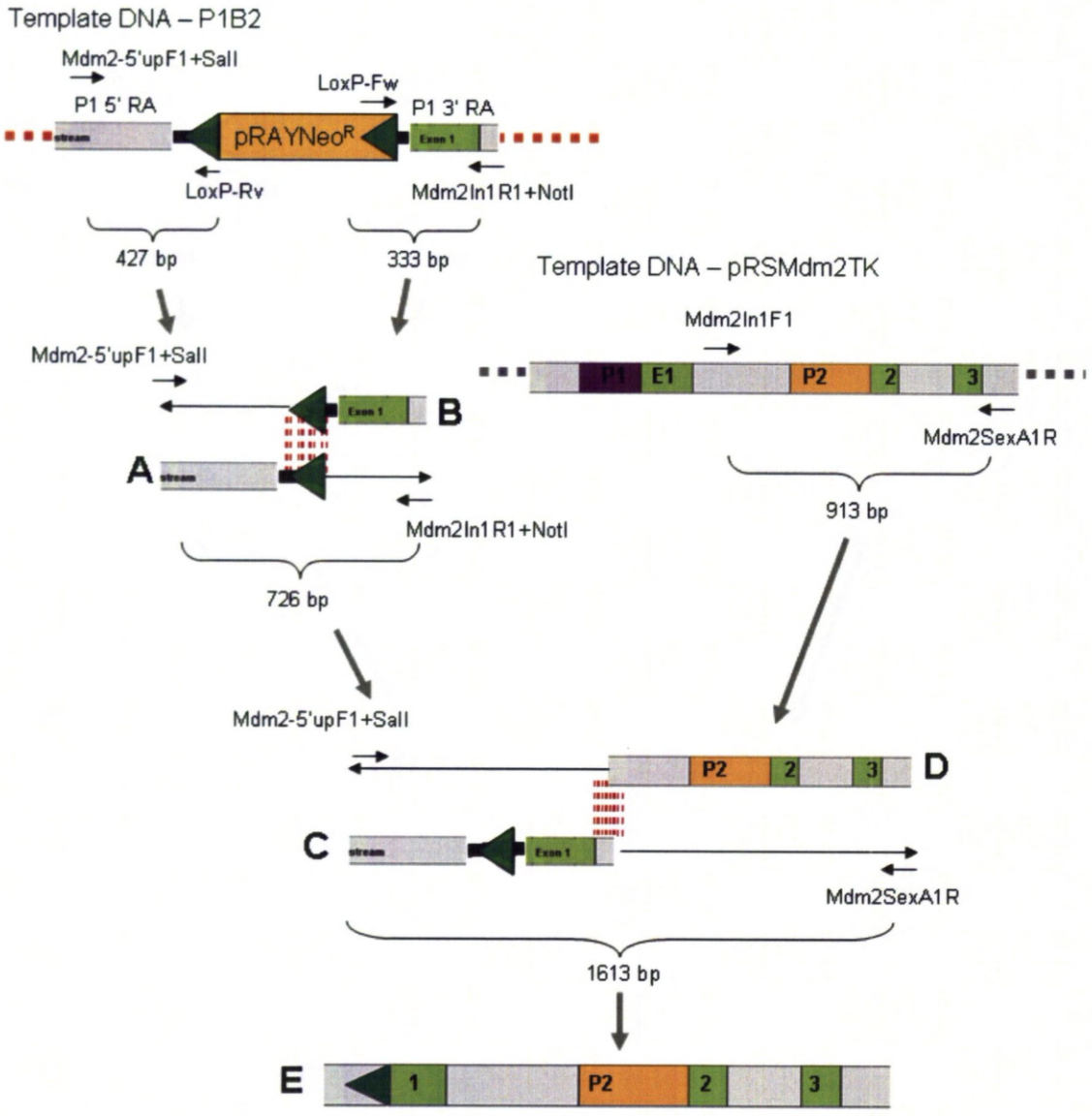


***Figure C.3: Fusion PCR of the Mdm2 P1-Null promoter region for luciferase assay.***

*Schematic diagram of each individual PCR reaction performed to construct the Mdm2 P1-Null promoter region. PCR products A & B were fused together to create product C. Product C was then TA-cloned into pCR2.1 and the resulting bacterial colonies were screened by restriction digest with SpeI before being sequenced. Once the sequence of C was confirmed it was re-amplified and used in a further fusion PCR reaction with PCR product D to produce E. E was then TA-cloned into pCR-XL-TOPO, screened by restriction digest with EcoRV & HindIII and confirmed by sequencing.*

## C.5 Mdm2 shuttle DNA construction

This section describes the failed cloning attempts during the generation of the Mdm2 shuttle vector.

***Table C.4: Cloning attempts for inserting the Mdm2TK DNA fragment into the yeast-E. coli shuttle vector pRS414.***

| Attempt | Description | Result |
|---|---|---|
| 1 | Overnight SpeI digest, followed by liquid GENECLEAN and SalI digest for 3-4 hours. 50 ng of backbone to 90 ng of insert. MAXStbl.2. | 0 colonies |
| 2 | As above except 50 ng of backbone to 225 ng of insert. | ~ 30 colonies however these grew very lumpy and DNA could not be extracted. |
| 3 | As above except 50 ng of backbone to 180 ng of insert | 0 colonies |
| 4 | As above except transformed into TOP10 bacteria | 5 colonies – all positive! |

## C.6 Generation of Southern probes

This section describes the generation of the 300-800 bp genomic specific PCR products which were used as probes for Southern blots. The primers were designed using primerBLAST (to minimise non-specific annealing of the probe) and the products were amplified by PCR using the indicated primer pairs and BAC clone DNA as the template (see Table C.5). The resulting PCR products were then TA-cloned into pCR2.1 and positive clones were identified by restriction digestion with EcoRI. The DNA sequence was confirmed and then Southern probes were prepared by digestion of the plasmid with EcoRI to excise the probe fragment from the pCR2.1 backbone. The DNA fragments were gel purified and eluted to be at ~ 50 ng/µl for radioactive labelling.

A test Southern blot was performed in order to validate the specificity of the Southern probes to ensure that they would be able to recognise the expected DNA fragments and

determine the sensitivity of each probe. Having an accurate and sensitive Southern probe was important for correct identification of potential positive ES cell colonies since there would be limited starting material and due to the nature of gene targeting experiments we could only expect 0.5 copies of the targeting construct (transgene) per cell. Both the *Mdm2* Southern probes appeared to be both specific and sensitive (able to detect 0.01 copies of the "trans-gene" and the expected genomic size fragment) however the p21-mCherry 790 bp probe was very non-specific and a new one will need to be designed for future experiments (see Figure C.4).

Copy number was calculated using the following equation; where haploid content of a mammalian genome is $3 \times 10^9$ bp and assuming 10 µg of genomic DNA available.

$$\text{Mass of trans-gene} = \left( \frac{\text{N bp trans-gene}}{3 \times 10^9 \text{ bp genomic DNA}} \right) \times 10 \text{ µg genomic DNA}$$

***Table C.5: Southern probes.***

| Construct | Restriction Enzyme | Forward primer | Reverse primer | Product size |
|---|---|---|---|---|
| *p21*-mCherry | EcoNI | p21PROBE-F1 | p21PROBE-R2 | 790 bp |
| *Mdm2* P1-Null & P2-Mutant | AhdI | Mdm2PROBE-F1 | Mdm2PROBE-R2 | 378 bp |
| *Mdm2* P2-Mutant | NcoI | P2PROBE-F1 | P2PROBE-R1 | 571 bp |

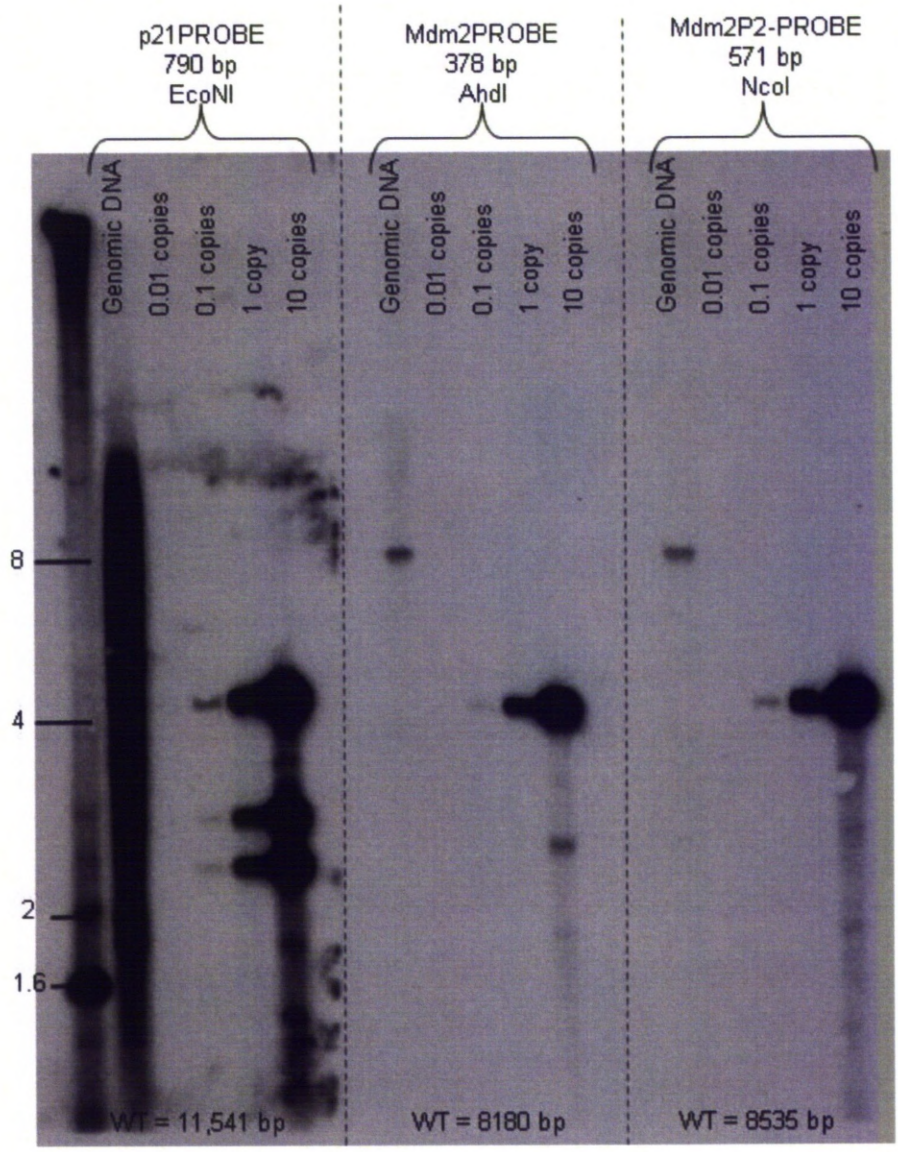


***Figure C.4: Southern probe validation.***

*2 day exposure of test Southern blot analysis for each Southern probe. 10 µg of genomic DNA was digested overnight with the indicated enzyme and run on an agarose gel with 0.01, 0.1, 1 and 10 copies of the "trans-gene" (the plasmid containing the probe). The linearised plasmid was ~ 4.4 kb in each case. The p21 probe was unable to detect a single band at 11.5 kb in the genomic DNA and instead appeared as a smear, indicating that the probe was too non-specific. Both Mdm2 probes were able to detect a single fragment of the correct size in the genomic DNA and were able to just detect 0.01 copies of the "trans-gene" (does not show up very well on this scanned copy of the film – however is much more apparent on the 8 day exposure – data not shown). Additional bands present on the 10 copies lane were from star activity of the enzyme (EcoRV) used to linearise the plasmid containing the probe.*

# APPENDIX D ALTERED SEQUENCES

## *D.1 Consensus Sequence of pKO (TK2)*

*(Sequences compared with each other and changes noted below)*
Pink = MCI Promoter, Green = TK, Orange = PolyA signal

ttttgtgatgctcgtcaggggggcggagcctatggaaaaacgccagcaacgcggccttttacggttcctgg
ccttttgcacggaccgtagagtcgagcagtgtggttttcaagaggaagcaaaaagcctctccacccaggcct
ggaatgtttccacccaatgtcgagcagtgtggttttgcaagaggaagcaaaaagcctctccacccaggcctg
gaatgtttccacccaatgtcgagcaaaccccgcccagcgtcttgtcattggcgaattggaacacgcagatgc
agtcggggcggcgcggtcccaggtccacttcgcatattaaggtgacgcgtgtggcctcgaacaccgagcgac
cctgcagcgacccgcttaacagcgtcaacagcgtgccgcacatcttggtggcgtgaaactcccgcacctctt
cggccagcgccttgtagaagcgcgtatggcttcgtaccccggccatcagcacgcgtctgcgttcgaccaggc
tgcgcgttctcgcggccatagcaaccgacgtacggcgttgcgccctcgccggcagcaagaagccacggaagt
ccgcccggagcagaaaatgcccacgctactgcgggtttatatagacggtccccacgggatggggaaaaccac
caccacgcaactgctggtggccctgggttcgcgcgacgatatcgtctacgtacccgagccgatgacttactg
gcgggtgctgggggcttccgagacaatcgcgaacatctacaccacacaacaccgccttgaccagggtgagat
atcggccgggacgcggcggtggtaatgacaagcgcccagataacaatgggcatgccttatccgtgaccga
cgccgttctggctcctcatatcgggggggaggctgggagctcacatgccccgcccccggccctcaccctcat
cttcgaccgccatcccatcgccgcccctcctgtgctacccggccgcgcgataccttatgggcagcatgacccc
ccaggccgtgctggcgttcgtggccctcatcccgccgaccttgcccggcacaaacatcgtgttgggggccct
tccggaggacagacacatcgaccgcctggccaaacgccagcgccccggcgagcggcttgacctggctatgct
gccgcgattcgccgcgtttacgggctgcttgccaatacggtgcggtatctgcagggcggcgggtcgtggcg
ggaggattgggacagctttcgggggacggccgtgccgccccagggtgccgagccccagaggcaacgcgggccc
acgaccccatatcgggacacgttatttaccctgtttcgggccccgagttgctggccccccaacggcgacct
gtacaacgtgtttgcctgggccttggacgtcttggccaaacgcctccgtcccatgcacgtctttatcctgga
ttacgaccaatcgcccgccggctgccgggacgccctgctgcaacttacctccgggatgatccagacccacgt
caccacccccaggctccataccgacgatctgcgacctggcgcgcacgtttgcacgggagatgggggaggctaa
ctgaaacacggaaggagacaataccggaaggaacccgcgctatgacggcaataaaaagacagaataaaacgc
acgggtgttgggtcgtttgttcataaacgcgggttcggtcccagggctggcactctgtcgataccccaccg
agaccccattgggggccaatacgcccgcgtttcttccttttccccaccccaccccccaagttcgggtgaaggc
ccagggctcgcagccaacgtcggggcggcaggccctgccatagccacgggccccgtgggttagggacggggt
cccccatggggaatggtttatggttcgtgggggttattattttgggcgttgcgtgggtcagtccacgactg
gactgagcagacagacccatggttttggatggcctgggcatggaccgcatgtactggcgcgacacgaacac
cgggcgtctgtggctgccaaacaccccccgacccccaaaaaccaccgcgcggatttctggcgccgccggacga
actaaacctgactacggaccggtaaaacgacggccagtgtt

Confirmed changes in order
-C, +A, A>G, A>G, C>T, T>A, +G, +C, G>C,

**Comparison of Protein Sequences (TK)**

*Protein sequence (Consensus)*
>Frame 1
MASYPGHQHASAFDQAARSRGHSNRRTALRPRRQQEATEVRPEQKMPTLLRVYIDGPHGM
GKTTTTQLLVALGSRDDIVYVPEPMTYWRVLGASETIANIYTTQHRLDQGEISAGDAAVVMTS
AQITMGMPYAVTDAVLAPHIGGEAGSSHAPPPALTLIFDRHPIAALLCYPAARYLMGSMTPQA
VLAFVALIPPTLPGTNIVLGALPEDRHIDRLAKRQRPGERLDLAMLAAIRRVYGLLANTVRYLQ
GGGSWREDWGQLSGTAVPPQGAEPQSNAGPRPHIGDTLFTLFRAPELLAPNGDLYNVFAW
ALDVLAKRLRPMHVFILDYDQSPAGCRDALLQLTSGMIQTHVTTPGSIPTICDLARTFAREMG
EAN

*Protein sequence (Original Published)*
>Frame 1
MASYPGHQHASAFDQAARSRGHSNRRTALRPRRQQEATEVRPEQKMPTLLRVYIDGPHGM
GKTTTTQLLVALGSRDDIVYVPEPMTYWRVLGASETIANIYTTQHRLDQGEISAGDAAVVMTS
AQITMGMPYTVTDAVLAPHIGGEAGSSHAPPPALTLIFDRHPIAALLCYPAARYLMGSMTPQA
VLAFVALIPPTLPGTNIVLGALPEDRHIDRLAKRQRPGERLDLAMLTAIRRVYGLLANTVRYLQ
GGGSWREDWGQLSGTAVPPQGAEPQSNAGPRPHIGDTLFTLFRAPELLAPNGDLYNVFAW

ALDVLAKRLRPMHVFILDYDQSPAGCRDALLQLTSGMIQTHVTTPGSIPTICDLARTFAREMG
EAN

*Two changes to amino acid sequence*
T133A & T232A, Threonine > Alanine, polar uncharged side chain vs. hydrophobic side chain

## *D.2 pACN self excision cassette – corrected sequence*

LoxP
HSV thymidine kinase polyA signal
Neomycin phosphotransferase
***RNA polymerase II large subunit promoter***
Cre gene with *intron from SV40*
***Testis specific angiotensin-converting enzyme promoter (tACE)***

Self-excision Neo-Cassette (consensus sequence from sequencing)
+T, -T, -A (highlighted in red)

cacctaaattgtaagcgttaatattttgttaaaattcgcgttaaatttttgttaaatcagctcatttttt
taaccaataggccgaaatcggcaaaatcccttataaatcaaaagaatagaccgagatagggttgagtgt
tgttccagtttggaacaagagtccactattaaagaacgtggactccaacgtcaaagggcgaaaaaccgt
ctatcagggcgatggcccactacgtgaaccatcaccctaatcaagtttttggggtcgaggtgccgtaa
agcactaaatcggaaccctaaagggagcccccgatttagagcttgacggggaaagccggcgaacgtggc
gagaaaggaagggaagaaagcgaaaggagcgggcgctagggcgctggcaagtgtagcggtcacgctgcg
cgtaaccaccacacccgccgcgcttaatgcgccgctacagggcgcgtcccattcgccattcaggctgcg
caactgttgggaagggcgatcggtgcgggcctcttcgctattacgccagctggcgaaaggggatgtgc
tgcaaggcgattaagttgggtaacgccagggttttcccagtcacgacgttgtaaaacgacggccagtga
attgtaatacgac***tcactatagggcgaattggag***ctcgagatctagatatcgatgaattcATAACTTCG
TATAATGTATGCTATACGAAGTTATggatctgtcgatcgacggatcgatccgaacaaacgacccaacac
ccgtgcgttttattctgtcttttattgccgatcccctcagaagaactcgtcaagaaggcgatagaagg
cgatgcgctgcgaatcgggagcggcgataccgtaaagcacgaggaagcggtcagcccattcgccgccaa
gctcttcagcaatatcacgggtagccaacgctatgtcctgatagcggtccgccacacccagccggccac
agtcgatgaatccagaaaagcggccattttccaccatgatattcggcaagcaggcatcgccatgggtca
cgacgagatcctcgccgtcgggcatgcgcgccttgagcctggcgaacagttcggctggcgcgagcccct
gatgctcttcgtccagatcatcctgatcgacaagaccggcttccatccgagtacgtgctcgctcgatgc
gatgtttcgcttggtggtcgaatgggcaggtagccggatcaagcgtatgcagccgccgcattgcatcag
ccatgatggatactttctcggcaggagcaaggtgagatgacaggagatcctgccccggcacttcgccca
atagcagccagtcccttcccgcttcagtgacaacgtcgagcacagctgcgcaaggaacgcccgtcgtgg
ccagccacgatagccgcgctgcctcgtcctgcagttcattcagggcaccggacaggtcggtcttgacaa
aaagaaccgggcgcccctgcgctgacagccggaacacggcggcatcagagcagccgattgtctgttgtg
cccagtcatagccgaatagcctctccacccaagcggccggagaacctgcgtgcaatccatcttgttcaa
tggccgatcccatattggctgcacggatc*ctgaacggcagaggttacggcagtttgtctctccccctttc*
*cgggagccaccttcttctccaaccgtcccggtcgcgctctcggcgcttctgaggagagaactggctgag*
*tgacgccctttatagattcgcccttgtgtcccgccccttcctttcccgccctccctgcgctacgggggc*
*cgcccgcaccggcctacacggagcgcgcggcggagttgttgacgctagggctccggctccctggttg*
*ggtgttctttctgacgcgacaggaggaggagaatgtTcctggtcctgtcgtcctccttttcgggtttccc*
*gtgcactcaaaccgaggacttacagaacggaggataaagttaggccatttttactcagcttcggagttc*
*aggctcatttTcagctaaagtctctcattagtatccccccacacacatcgggaaaatggtttgtcctac*
*gcatcggtaatgaaggcggggcccttcgggtcctccggagcgggttccgggggtgggggggaaggaggga*
*gggacgggacgggcctcgttcatgaatattcagttcaccgctgaatatgcataaggcaggcaagatggc*
*gcgtccaatcaattggaagtagccgttattagtggagaggccccaggacgttggggcaccgcctgtgct*
*ctagtagctttacggagccctggcgctcgatgttcagcccaagctt*ttcgcgagctcgaccgaacaaacg
acccaacacccgtgcgttttattctgtcttttattgccgctcagctttacagtgacaatgacggctgg
cgactgaatattagtgcttacagacagcactacatattttccgtcgatgttgaaatcctttctcatatg
tcaccataaatatcaaataattatagcaatcatttacgcgttaatggctaatcgccatcttccagcagg
cgcaccattgcccctgtttcactatccaggttacggatatagttcatgacaatatttacattggtccag
ccaccagcttgcatgatctccggtattgaaactccagcgcgggccatatctcgcgcggctccgacacgg
gcactgtgtccagaccaggccaggtatctctgaccagagtcatc*ctaaaatacacaaacaattagaatc*
*agtagtttaacacattatacacttaaaaattttatatttac*cttagcgccgtaaatcaatcgatgagtt

## D.3 Puma left arm of homology actual sequence

Exon 1, Exon 2, Exon 4

gctgaatgctccaaggtctctcactgtctgcagattgtccagTgtgggttattttaaatttaattgtgt
gtgagtatgTGtgtgtgtgtgtgtgtgtgtgtgtgtgtacgtgagtgtgtggacaTggacgcaggtctc
tcaggaggccaggagcatcagattcccctgAagctagggttacatatccaggcacaagatgtaggtactg
ggaacagaacacaggtccttccttgggaagagctgtaagcactcttaatcactgagttctcTccccccc
TTccccAcacttgcttcgtttttttgaaaaagatcacttgctgtgctcaaaaatgggcttggagagccgg
gcatggtggcgcacgcctttaatcccagcactcgggaggcagaggcaggaggatttctgagttcgaggc
cagcctggtctacaaagtgagttccaggacagccagggctacacacagaaaccctgtctcaaacaaaca
aacaaacaaaTaaacaaaaaagctggacagtggtggtgcatgcctttaatcccagcacttgggaggcaa
aggcaggtagatttctgagtttgaggccagcctggtctacaaactgagttccaggacaGccagggctac
acagagaaaccctgtcttgaaaaaccaaaaaaaaaaaaaggggggggggcctggaactcactatgta
actcagacagactccaaccttgcaaccacCttcctgcttCatcctctgAaagtgctgggaagacaggtg
CaagtCactGtgtttatttctttaacaagtgtcttatctcacatggctgtgtgacacccttcacagcg
ggccagtgctgggcacccataggtaagtaatatactcagtaagtttggtgacagtttgggtgagacaga
gagtctgtcaagtgccgtgagagatgtctacggcttgggaggaggaagggtcactgtttcaaaagggaa
gggaaataaatgacttttagaaaagggaaaggaaacagaaacaacagacaggatgaaatagggtgcagg
gggctgcccgggcatgtcCgtgccaggagcGcagggctgcctcttccccatttgtccagtgccagatgg
gtattacgccaggcgggccaggtgtttaagttcacgagtgtaacccgccatcaagccatttagcaggaa
cctgtctcaggagtgactttgtgagcacaggtctgggctcagtttcttctgtatgtgactggcatgttt
tgtagggtcagccagtgcagtctagtggctgtgcttcagctattgcgggtgtcagcctgagagtgctat
ttggattggagtgtgtgtccctctgaacctgccaggaagttgttctgagaaggggtcagcctttagtgt
agtgtgaatgccAtaggcatctggggacacgggtttgtgAgtcggagactgtttgaatattgtttgtgc
aactacgttttgggttgtcactgtctgtgtgtgacccagtgagccagtaagtaagataatctggatgtc
tgggtctgtgtgagctTgtgtgGccaggcccttgtccCgatgtgtatctgtgcctctggtctgactttg
tgtccctgtggctcagtcatcactgactcagtgcaccctggcgtgccagtccgttagtctgagcgtact
cctcaggtgtgggtgtgggtcccagtcagtgtgtcagtgtgtcaagcgtgtgtccggacaccctaggtc
tgggctgtccccacgctgctcctcctgcctggaccaggcctcgccccgcccctctggctgccgggaaac
cccccgcgccgaggtagggggcgcggcgcccgactgcaagccccgacttgtccccagccgcgggcgggg
ccctggcgtcacgcgggggcggggcgtgggagccagcgagaggcggggcggggcggGGCGGccgccgag
cgagcggggcccggggatctgccgggaggcctgagacgcggcatagagccacatgcgagcggggagccc
aggaggcggcggcgacaccagcaagcaagcagcagcggtgatccggacacgaagactccGgaagca
gcagcagtcactgcagttagagcagcaggagcagcagcaaggtgcctcaatagcaacccactcggcggg
cgagccctccagaaggcaaccgcccgccaccccatcgcctcctttctccggagtgttcatgcccccggg
gtgagtgagcaccccgattcccgaagctgTttacgagcggcaaggcccggagggctccctggaggaggt
gacggggtgcacgggccgataggacggtcgccttgcattcccgcagcttgtgccccagctttcatcact
gggactaaggctgggccaggcgggcgggaaggaagcacctgggactcagggcgccctgtctgggcgcac
aggtgccacagcggtctggcgggtttgtttacaaacaatggggttcgggctcgcccgcgccccctggtg
gctagtgagacctgggaggagcgtggccccgggctcgctcgagtcccccgagtcccactgcgggagggt
tggggtgggggtggcaccgaggatcggccacacccagagcgcgcgcccgccgggggcggcgacagggg
gcggcggaggctgtggctcccgcgggcgggggctgcgccccagcaacagccggttattggccccgcgcg
cgctgggcgggcggggcgggcgcacgtggcggcgtcgaggggggggGctgtgacagcggaggggcggc
ggggaccgcgcgtgcggggctgtggatctgcaggtgtctcgcctgggtgtgtgtgctcgtgtttggctc
ccgagtttgtatccctacaccgagatgttggcgtttgtcacccggaggggtgtctgcgtgagtccttgc
ccgcgtgtctgcggggtggggtgcacctgtccgtttacgggtgtgggtggccacccccccaaaccagagt
tgtatacgtgtgctcttaaggggtgaaaaggggatctgtatctgtcgcttgcctggtagtgctggtggt
ggtggtgcggacgaccggggcacttgagctgtgtttgtgtgtcgcttgagtgagctgtgttgctgtgca
ggggtctcgcccaagtgtgcgctgcgTGTGTGTGTGTGTGTGTGTGTGTGTGTGTGTGTGTGTGTGT
GTGTGTGTGTATGCGCGCGCGCGTGCTGTCTCTGGGTGTCTCCAAGACAAGCATCTGCTGTACCCAG
CTTTTGGGATGGGATGTCACCCAGTGCCTGATCGCTCGCTGGGTGACTTCTGAGCAGCAAAAGGCACAC
AAGGCACGCTGAGCATGAAGGGCTTTGGGGGTGGGGGGGATCTAGCGGGTTCAGTGCCAGCCCCTCTCT
CTGCATGCAGTGTGTGTGTGTGTGTGTGTGTGTGAAAGAGAGAGAGAGGGGGGGGTGAGAGTGAGTT
TTGGGTCTGAGGGGTTTGTCTCTGTGATCcaggctatgtgtcatgtggtgctctctctctgtagtgttt
ataccagtcacgtgaggccagtgttttctgtctctgcattaggtgtgtgtgctgctgggctctgtgtgt
gtgtgtgtgtgtgtgtgtgtgtgtgtgtgtgtgtgtgtgttttctggggctgacagttggctgtggtgt
attggggctgagagtagaggctggacctatggcttctaccagctgcggctggtgcctcccgatgtggct
gccccgcactcgaggggggatgatgtatctggatatgatgacttgtgtctatgtgtggctgttgtgtc

ccaggagctcaaagttggggCgggggtgcacattcaggtgtgttttgagatgatggtggtgcatgtgct
aaggaatagtaaggggggtgtctttgggttgtctgtgtgtatgcgggagaaacacgttgaagacttgag
tctgttgtgcttcagtgtgtgacggctgcattgtgggcgggtgagcgctggcatgtcagcagcgggtca
gtgtgagactggtgtaaatatgttgaaagggctctggatggctgtgtgtgcatgtctgtgtccccatgt
gtttctgggtgagacacctcactgggggagcgggaggggcggtaaagttggacacttctctgagttcac
tggtgtcttcccattACACACACACACACACACACACACACACACACACACACACACACACACACACAC
ACACAAACACACACACACACggttctctgacagcaccgtgtatcctgggagccccagcacccttctgc
gctcttctctgttgagaaagttctccctggcccaagccctgagagtagtaggcagttttcctggtgggt
tttgctacaaaccccagacgcagtctgtgcgcccctcaccatgtgtcccggccaggctgtccctggggt
catcccttcctgggtgggagtgacttccaggcagggtgtctgcgaggtggggtcctgcagccccccccc
ccgcagtcgccccactgacctcccgccgtgtcccgcag***gctccagggagcgccatg***gcccgcgcacgcc
aggagggcagctctccggagcccgtagagggtctagcccgcgacagtccgcgcccctcccgctcggcc
gcctgatgccctccg***ctgtatcctgcagcctttgc***

## *D.4 Puma right arm of homology, actual sequence*

tttcgcgagctcgagatctaTCCTCCATCTCCTTCATTGGTTACCACTGAGCAAATCCTAGAGACTAGG
CAAGTAGCATGGCCTGGTGGCAGCATCCCGTAATCCCACCTACTCAGGGAGGGAGAAAGAAAGTTCAAA
GCCAGCCTGGGCAACCTAGTGAGTGATATTCTGCTTCAGAAATAGTCTTTGAAGTGGCTCAGAGGATAA
AGGTGCTTGCTACCAAAACTGATGAACAGAGTTCGATTCCCAGGACCCACTTAGTAAAAGTCAAGAGTC
TAATCTTACATAGTGTTCTCTAACCTCCACATGTGCACACACAAATCCCCCCCCCCTCTCTTTCTCATA
CACACACACACACACACACACACACACACACACACACACACACACACACACACACACACACACACGTTA
ATGGTTAAGAGAACTCTTACAGAGAACCAGGGTCAGGTTCCCAGCTGACAACTGCCTGTAATTCCAGGT
CCAGGGATCCAATGCCTTCTGGTATTTGCCAGCACGTACACATTAGTTTGTTTGTTAGTTAGTTTGTTT
TTTAAAGATTTATTTATTTTATGTTTAATGAGTACACTGTTGCTGTCTTCAGACACAGGAGAAGAGGGC
ATCAGATGGTTGTGAGTCACCATGTGGTTGCTGGGATTTGAACTCAGGACCTCTGGAAGAGCAGTCAGT
GCTCTTAACGGCTGAGCCATCTCTCCAGCCCACATATTATTATTTTTTAAGTTTTATTTATTTACTTAT
TTATAATTCAGGGGAGGCTGATGTAGCTCAGTTGGTAGAGTGCTTGCCTAGGAGAGAGACACTGACCCT
TAGGTCTGTGGGTCAAGGTCACCCTCAAATACAGTTTCAGTTCCAGGACATCCTGTGCGACATGAGGTG
AGGTCTCAAAAACAGGAAGATTTTTTTCTTTTTTTTTtCTTTTGTTTTTTCGGGACAGGGTTTCTCTGTG
TAGTCCTGGCTGTCCTGCAACTCACTCTGTAGACTAGGCAAACTGGCCGGGAACTCAGAGGTTCTCTCC
TCCTGCCCTTCCCCCACTCAAGTGCTGGGCTTAAAGGTTCCACTCAGCTGAGCTTTTTTTTTTTTtAAA
ACACATGCCTGGAATCCACCAGTGAGTGGCAAAAGGTGTGGCTTAGCAGCAAACATTGTCTAGCATTAG
TCTTTTCTCCTCTTTTCTAAGAGATGGCCATCTCTGGCTTGGCCCATGTGCTGTTGTCTTCAGAGTGAA
CACCCAGGGCTCCGTGCTCCCCCTAATAGGCTAAGTATAATGATAGTGAACTCACAAGGTGGCATCCAC
CACCTCGCCCAGTTGCAAGGAGGAGGAGGGCACAGGAGGCCTGGGCTAGTTCTGGGCATGTACTCCAAT
AGGGTCATTAGCCTGACATCTTCCAAATGGATTACATTCTTCACAACCAAGAACATGAGCCCGGTGGAT
CTGCTTGGCCACATAACCAGTGGAAGGATCAAGTAAAAGCTCTCTCTCTCTCTCTCTCTCTCTCTCT
CTCTTCCGTTCTTCCTTCCTTCCTTTCTCCCTTCCTTTCTTTCTCTTTCTTTTCTTTTCTTTtctTTTc
tTTTCTTTTCTTTTCtTTTCTTTTCTTTTCTTTTCTTTCTTcCcTTcTCTCTTTCTTTCtTTCTCTCAC
TCTCCCTCCCACCCTCCCTCTcCTTCCTTCCTTCCTTCCTTCCTTCCTTCCTACCTTCCTtcCTT
CTTTCCTTCCAACACTGGCTGTCCTAGAACACACTATGTAGACCACCATGCTAGCCTTGAATTCTCAGA
GATCTGCCTGCCTCTGCCTCACAAGTTCTAAGATTAAAGATGTGAGCTACCACACCCAGCATTCTTTCT
TTCTCTCTCTCTCTCTTTCTCTCTTTCTTTTTCTCTTTTCCTTTTTTTTTtCTTTCTTTCCTTTTCTTT
CTTTTTCtTTTTTTTTTTTTTTAGGCTGGCTCTTAATAAGCTGTTCACACTGGCTTTGAACTCACTCTA
TAGCTCAGACAGGCTTTGAACTTTTGTCTTCCTGCCTCAGCCTCCTGAGTCGCTGGGATTACAGGCCTG
TGCCATCACAGAAGAAATCTAGATGCTACATCACACTTTTTCTCTACCACCAGGGATCGAACAAGAGTT
TCCCTGAAGCCAGCATTGCCAAGAGACACCTTCTCTcAGCCTTGCTGGCATGGccTGCTgTtCTcAaCC
CTCTTCCGGGgTGGTTTGAGAACTGCTTAGGCTGTCGGGCTGCTCCTTACTCTCTCTCATGTCCCAACA
GCCTTTTGTTTGGTTGGTTTGATTTTTCCAGTTAGGAGCCTGTGCTCTAGCACAAATTTAGTGAGGCAC
GCTAAGATGAGGAGTACGAGCCACCACGCCTGTCTCTCGCCTTGAGTGGGCTGCGTTTCAGCCCACCCC
TTAGAGCCCTTGTGATTCATAGGGTGTGTGTGCTAGGCTCTATGCTATGGGAATTCTGCCCCAGCCCCT
TCCCACCTAGATTGGGAGAGTGTGACGTGGTGAGTGAGGGGCTGAAAAATGGCTGGTAAGAGGGTTGCG
CACAGTTTTGGGACCGATCTCGAACCCACACCTTTTGCTCACTAACCCACTGTCTGCGGGTCCAAGCTA
ATTCCTACTTCCTCCTCTCCCCAGAGACAAGAAGAGCAGCATCGACACCGACCCTCACCCTGGAGGGTC
ATGTACAATCTCTTCATGGGACTCCTCCCCTTACCCAGGGATCCTGGAGCCCCAGAAATGGAGCCCAAC
TAGGTGCCTACACCCGCCCGGGGGACGTCGGAGACTTGGGGGGCAGGACCCCCTCCGCCTTCTGACACC

CTGGCCAGCGCGGGGGACTTTTTCTGCACCATGTAGCATACTGGACTGCCAGCCTTGCCCGTCCCAGGG
GCAGGCAAGGGATGCCACTCGAGCCCGGGCAGCCTGGGTGCACTGATGGAGATACGGACTTGGGGGGAC
CCTGGCCTCCCGAAAGCCAGGGAAGGGAGGGCTGAAGGACTCATGGTGACCGAGGGGGTGGGGACCGAG
CCGCCCGCCTCTGCCGCCCACCACCATCTCAGGAAAGGCTGCTGGTGCTGGCTGCCCGTTCCAGCTGCA
GGggGGACGCTgGGGGTGTCCCCAGTGCGCCTTCACTTTgGGCCTggCCTCAGGCCCCTgGTgCttCCC
CCCCTCCTCCTGAGGAGGGGGTCTGTGAAGAGCATATGAGCCAAACCTGACCACTAGCCTCCTGGAGCC
AGAGAATGGGGGGCGTGTGAAGGCCTTCTTAACCCAGTGCCCAGCCATCTTCCCTGAGCCGCCGGCGGG
CGGTGAACGATGCCTGCCTCACCTTCATCTGGGGGTGTCCAGGAGGGGTCCAGACTGTGAATCCTGTGC
TCTGCCCGGGACCACCCcACACCCCCAATCCCCATCCATCTCATTGCATAGGTTTAGAGAGAGCACGTG
TGACCACTGGCATTCATTTGGGGGGTGGGAGATATTGGCGGAAGCCACCCCAGCCTTAGTCCCCAGGGC
AAAGCGCTGGGGAGGAAGATGGGGAGTCAGGGAGGGGGGAAGTCTCAGAAGAGGGAGGAGTCTGGGAGC
GGGGAGGGACGGCCCAGCCTGTAAGATACTGTACATGCACTGCTGTAGATATACTGGAATGAATTTTCT
GTACATGTTTGGTTAATTTTTTTTGTACATGATTTTTGTATGTTTCCTTTTCAATAAAATCAGATTGAA
CAGTGAACACTCTTTTTGTTAGCTTTACCAGTGACAGAGCATCTGGCACTACCTGTGAGGACATGAAAG
AAACGGTGTGTGTGTGTGTGTGTGTGTGTGTGTGTGTGTGTGTGTGTGTGTGTGTGTGTGTGTGTGA
GAGAGAGAGAGAGAGAGAGAAATGGCTCAGTGGTTAAGAGCACTGACTGCTCTTCCAGAGGTCCTGAGT
TCAAATCCCAGCAACCACATGGTGGCTCACAACCATCATAATGAGATCAGACACCCTCTTCTGATATGT
CTGAAGGCAGCTACAGTGTACTTACATATAACAATAAATAAATGTAAAAAAGAGAAAGAAAGAAAGAAA
CTGGAACTTTTGGACTCTTAAGGGGCAGTCATACTAAAAGGTAAGCTAGAGGCTGGTCTGGTGGCACAG
GCCTGTCGTAGCTAGTTGGAAGGCCTGAGCAACTGAGACCCAGTCTCAGCAATGGGGAGGGGACAGGTG
GAGGGGACAGGCGGAGCGCTGGCTCAGCAGGTAGAAGTATGGGCTGTTCTTCAAGAGGATCTGCATTTA
GGTCCCAGCACCCATGCTGCAGCTCACACTCTGTAACTCAAGTTCCAGATCTGATACCTCCTGGCCTGC
GGGTACCAGGCATGTGCACAGGGCCCATTCCATGCGGACAAGGAAACCCAAAACCCCAAAAACACATAT
GCACATAAAATAGGTAAATGTGCCAGGGAGGTGGCTCAACTGTGAAGAGCACCAGCCGTTCTTCCAGAG
GTCCTGAGTTCAATTCCCAGCTACCACATGGTGGCTCACAACTATGTATAATGTTATCCAATGCCCTCT
TCTGGgtcgac